Methods in Molecular Biology 1516

Springer Protocols

Kursad Turksen *Editor*

Stem Cell Heterogeneity

Methods and Protocols

Humana Press

METHODS IN MOLECULAR BIOLOGY

Series Editor
John M. Walker
School of Life and Medical Sciences
University of Hertfordshire
Hatfield, Hertfordshire, UK

For further volumes:
http://www.springer.com/series/7651

Stem Cell Heterogeneity

Methods and Protocols

Edited by

Kursad Turksen

Ottawa Hospital Research Institute
Ottawa, ON, Canada

Humana Press

Editor
Kursad Turksen
Ottawa Hospital Research Institute
Ottawa, ON, Canada

ISSN 1064-3745 ISSN 1940-6029 (electronic)
Methods in Molecular Biology
ISBN 978-1-4939-6549-6 ISBN 978-1-4939-6550-2 (eBook)
DOI 10.1007/978-1-4939-6550-2

Library of Congress Control Number: 2016950593

Printed on acid-free paper

This Humana Press imprint is published by Springer Nature
The registered company is Springer Science+Business Media LLC New York

Preface

A long-held tenet in the stem cell field was the belief that stem cells—defined by their capacity for self-renewal and lineage developmental capacities—comprised a homogeneous population. Many studies with isolated populations of stem cells were designed and analyzed with this principle in mind. Nevertheless, with time, a variety of types of studies and data suggested that heterogeneous populations or subpopulations of stem cells exist. In this volume, I have pulled together a series of protocols that address different aspects of stem cell heterogeneity. I am very grateful to the contributors for their time and generosity in putting together their concepts and protocols.

Once again, I would like to thank Dr. John Walker, Editor in Chief of the *Methods in Molecular Biology* series, for his support and encouragement.

I am grateful to Patrick Marton, Senior Editor of the *Methods in Molecular Biology* series, for his continuous support throughout the project.

A special "thank you" goes to David Casey, Editor of the *Methods in Molecular Biology* series, for his tireless efforts and support during the final stages of the volume production.

Ottawa, ON, Canada ***Kursad Turksen***

Contents

Contributors

Elsa Abranches • *DHenrique Lab, Instituto de Medicina Molecular, Faculdade de Medicina, Universidade de Lisboa, Lisbon, Portugal; Instituto de Histologia e Biologia do Desenvolvimento, Lisbon, Portugal*

Daniel W. Allison • *Transposagen Biopharmaceuticals, Inc., Lexington, KY, USA*

Mutay Aslan • *Mass Spec. Laboratory, Department of Biochemistry, Faculty of Medicine, Akdeniz University, Antalya, Turkey*

Ena Ray Banerjee • *Immunology and Regenerative Medicine Research Laboratory, University of Calcutta, Kolkata, West Bengal, India; Department of Zoology, University of Calcutta, Kolkata, West Bengal, India*

Mirjam E. Belderbos • *Laboratory of Ageing Biology and Stem Cells, European Research Institute for the Biology of Ageing, University Medical Center Groningen, University of Groningen, Groningen, AV, The Netherlands; Department of Pediatrics, University Medical Center Groningen, Groningen, AV, The Netherlands*

Carlo Biz • *Department of Surgery, Oncology and Gastroenterology, DiSCOG, Orthopedic Clinic, University of Padova, Padova, Italy*

Aykut Bostanci • *Cancer Biology Laboratory, Department of Bioengineering, Faculty of Engineering, Ege University, Bornova, Izmir, Turkey*

David A. Brafman • *School of Biological and Health Systems Engineering, Arizona State University, Tempe, AZ, USA*

Nicholas Brookhouser • *School of Biological and Health Systems Engineering, Arizona State University, Tempe, AZ, USA*

Karolina Bukowska-Strakova • *Department of Medical Biotechnology, Faculty of Biochemistry, Biophysics and Biotechnology, Jagiellonian University, Krakow, Poland*

Leonid V. Bystrykh • *Laboratory of Ageing Biology and Stem Cells, European Research Institute for the Biology of Ageing, University Medical Center Groningen, University of Groningen, Groningen, AV, The Netherlands*

Mariana T. Cerqueira • *3B's Research Group—Biomaterials, Biodegradables, and Biomimetics, University of Minho, Headquarters of the European Institute of Excellence on Tissue Engineering and Regenerative Medicine, Guimarães, Portugal; 2-ICVS-3B's—PT Government Associate Laboratory, Braga/Guimarães, Portugal*

Hao-Chen Chang • *National Health Research Institutes, Zhunan Town, Miaoli County, Taiwan*

Ing-Ming Chiu • *National Health Research Institutes, Zhunan Town, Miaoli County, Taiwan*

Anastasia Chumakova • *Department of Cellular and Molecular Medicine, Lerner Research Institute, Cleveland Clinic, Cleveland, OH, USA*

Carmen Ciavarella • *Department of Experimental, Diagnostic and Specialty Medicine (DIMES) S.Orsola-Malpighi Hospital, University of Bologna, Bologna, Italy*

Marc Cloutier • *Recherche et Développement, Héma-Québec, Quebec, QC, Canada*

Paolo De Coppi • *Stem Cells and Regenerative Medicine Section, Developmental Biology and Cancer Programme, UCL Institute of Child Health and Great Ormond Street Hospital, London, UK*

Marina Costa • *3B's Research Group—Biomaterials, Biodegradables, and Biomimetics, University of Minho, Headquarters of the European Institute of Excellence on Tissue Engineering and Regenerative Medicine, Guimarães, Portugal; 2-ICVS-3B's—PT Government Associate Laboratory, Braga/Guimarães, Portugal*
Josh Cutts • *School of Biological and Health Systems Engineering, Arizona State University, Tempe, AZ, USA*
Bilge Debelec-Butuner • *Department of Pharmacology, Faculty of Pharmacy, Ege University, Bornova, Izmir, Turkey*
Józef Dulak • *Department of Medical Biotechnology, Faculty of Biochemistry, Biophysics and Biotechnology, Jagiellonian University, Krakow, Poland*
Caroline Eberle • *Medipan GmBH, Dahlewitz, Berlin, Germany*
Heiko Enderling • *Department of Integrated Mathematical Oncology, H. Lee Moffitt Cancer Center and Research Institute, Tampa, FL, USA*
Silvia Fittipaldi • *Department of Experimental, Diagnostic and Specialty Medicine (DIMES) S.Orsola-Malpighi Hospital, University of Bologna, Bologna, Italy*
Chiara Franzin • *Stem cells and Regenerative Medicine Laboratory, Fondazione Istituto di Ricerca Pediatrica Città della Speranza, Padova, Italy*
Piergiorgio Gamba • *Pediatric Surgery Unit, Department of Women's and Children's Health, University of Padova, Padova, Italy*
Mark R. Gilbert • *Neuro-Oncology Branch, National Cancer Institute, National Institutes of Health, NIH, Bethesda, MD, USA*
Ana M.V. Guedes • *DHenrique Lab, Instituto de Medicina Molecular, Faculdade de Medicina, Universidade de Lisboa, Lisbon, Portugal; Instituto de Histologia e Biologia do Desenvolvimento, Lisbon, Portugal*
Nur Shuhaidatul Sarmiza Abdul Halim • *Regenerative Medicine Cluster, Advanced Medical and Dental Institute (AMDI), Universiti Sains Malaysia, Kepala Batas, Penang, Malaysia*
Noor Hanis Abu Halim • *Regenerative Medicine Cluster, Advanced Medical and Dental Institute (AMDI), Universiti Sains Malaysia, Penang, Malaysia*
Björn Heindryckx • *Ghent-Fertility and Stem cell Team (G-FaST), Department for Reproductive Medicine, Ghent University Hospital, Ghent, Belgium*
Lisa Heiserich • *Medipan GmBH, Dahlewitz, Berlin, Germany*
Domingos Henrique • *DHenrique Lab, Instituto de Medicina Molecular, Faculdade de Medicina, Universidade de Lisboa, Lisbon, Portugal; Instituto de Histologia e Biologia do Desenvolvimento, Lisbon, Portugal*
Chia-Hsien Hsu • *National Health Research Institutes, Zhunan Town, Miaoli County, Taiwan*
Awad Jarrar • *Department of Cellular and Molecular Medicine, Lerner Research Institute, Cleveland Clinic, Cleveland, OH, USA*
Margot Van der Jeught • *Ghent-Fertility and Stem cell Team (G-FaST), Department for Reproductive Medicine, Ghent University Hospital, Ghent, Belgium*
Christine Jobin • *Recherche et Développement, Héma-Québec, Quebec, QC, Canada; Faculté des sciences et de génie, Biochimie, Microbiologie et Bio-informatique, Université Laval, Quebec, QC, Canada*
Alicja Jozkowicz • *Department of Medical Biotechnology, Faculty of Biochemistry, Biophysics and Biotechnology, Jagiellonian University, Krakow, Poland*
Jinkyu Jung • *Department of Stem Cell Biology, Cleveland Clinic Foundation, Cleveland, OH, USA*

Srabani Kar • *Immunology and Regenerative Medicine Research Laboratory, University of Calcutta, Kolkata, West Bengal, India*
Egi Kardia • *Regenerative Medicine Cluster, Advanced Medical and Dental Institute (AMDI), Universiti Sains Malaysia, Kepala Batas, Penang, Malaysia*
Yasuo Kitajima • *Department of Stem Cell Biology, Atomic Bomb Disease Institute, Nagasaki University Graduate School of Biomedical Sciences, Nagasaki, Japan*
Kemal Sami Korkmaz • *Cancer Biology Laboratory, Department of Bioengineering, Faculty of Engineering, Ege University, Bornova, Izmir, Turkey*
Justin D. Lathia • *Department of Cellular and Molecular Medicine, Lerner Research Institute, Cleveland Clinic, Cleveland, OH, USA; Cleveland Clinic Lerner, College of Medicine at Case Western Reserve University, Cleveland, OH, USA; Department of Molecular Medicine, Cleveland Clinic Lerner College of Medicine at Case Western Reserve University, Cleveland, OH, USA; Case Comprehensive Cancer Center, Cleveland, OH, USA*
Don-Ching Lee • *National Health Research Institutes, Zhunan Town, Miaoli County, Taiwan*
Ching-Hui Lin • *National Health Research Institutes, Zhunan Town, Miaoli County, Taiwan*
Shiying Liu • *Department of Biochemistry and Molecular Biology, University of Calgary, Calgary, AB, Canada*
Paul Macklin • *Center for Applied Molecular Medicine, University of Southern California, Los Angeles, CA, USA*
Alexandra P. Marques • *3B's Research Group—Biomaterials, Biodegradables, and Biomimetics, University of Minho, Headquarters of the European Institute of Excellence on Tissue Engineering and Regenerative Medicine, Guimarães, Portugal; 2-ICVS-3B's—PT Government Associate Laboratory, Braga/Guimarães, Portugal; 3B's Research Group, Avepark–Parque de Ciência e Tecnologia, Barco GMR, Portugal*
Guoliang Meng • *Department of Biochemistry and Molecular Biology, University of Calgary, Calgary, AB, Canada*
Kenneth Miller • *Transposagen Biopharmaceuticals, Inc., Lexington, KY, USA*
Shinjini Mitra • *Immunology and Regenerative Medicine Research Laboratory, University of Calcutta, Kolkata, West Bengal, India*
Györgyi Műzes • *Immunology Division, 2nd Department of Medicine, Semmelweis University, Budapest, Hungary*
Sonia Néron • *Recherche et Développement, Héma-Québec, Quebec, QC, Canada; Faculté des sciences et de génie, Biochimie, Microbiologie et Bio-informatique, Université Laval, Quebec, QC, Canada*
Shizuka Ogawa • *Department of Stem Cell Biology, Atomic Bomb Disease Institute, Nagasaki University Graduate School of Biomedical Sciences, Nagasaki, Japan*
Yusuke Ono • *Department of Stem Cell Biology, Atomic Bomb Disease Institute, Nagasaki University Graduate School of Biomedical Sciences, Nagasaki, Japan*
Yukiteru Ouji • *Department of Pathogen, Infection and Immunity, Nara Medical University, Kashihara, Nara, Japan*
Filiz Ozcan • *Mass Spec. Laboratory, Department of Biochemistry, Faculty of Medicine, Akdeniz University, Antalya, Turkey*
Deric M. Park • *Neuro-Oncology Branch, National Cancer Institute, National Institutes of Health, NIH, Bethesda, MD, USA*

Gianandrea Pasquinelli • *Department of Experimental, Diagnostic and Specialty Medicine (DIMES) S.Orsola-Malpighi Hospital, University of Bologna, Bologna, Italy*
Dustin W. Perry • *Transposagen Biopharmaceuticals, Inc., Lexington, KY, USA*
Martina Piccoli • *Stem cells and Regenerative Medicine Laboratory, Fondazione Istituto di Ricerca Pediatrica Città della Speranza, Padova, Italy*
Rogério P. Pirraco • *3B's Research Group—Biomaterials, Biodegradables, and Biomimetics, University of Minho, Headquarters of the European Institute of Excellence on Tissue Engineering and Regenerative Medicine, Guimarães, Portugal; 2-ICVS-3B's—PT Government Associate Laboratory, Braga/Guimarães, Portugal*
Jan Poleszczuk • *Department of Integrated Mathematical Oncology, H. Lee Moffitt Cancer Center and Research Institute, Tampa, FL, USA*
Anna Poon • *Department of Biochemistry and Molecular Biology, University of Calgary, Calgary, AB, Canada*
Mina Popovic • *Ghent-Fertility and Stem cell Team (G-FaST), Department for Reproductive Medicine, Ghent University Hospital, Ghent, Belgium*
Michela Pozzobon • *Stem cells and Regenerative Medicine Laboratory, Fondazione Istituto di Ricerca Pediatrica Città della Speranza, Padova, Italy*
Derrick E. Rancourt • *Department of Biochemistry and Molecular Biology, University of Calgary, Calgary, AB, Canada*
Mariusz Z. Ratajczak • *Stem Cell Institute at the James Graham Brown Cancer Center, University of Louisville, Louisville, KY, USA*
Rui L. Reis • *3B's Research Group—Biomaterials, Biodegradables, and Biomimetics, University of Minho, Headquarters of the European Institute of Excellence on Tissue Engineering and Regenerative Medicine, Guimarães, Portugal; 2-ICVS-3B's—PT Government Associate Laboratory, Braga/Guimarães, Portugal*
Ofer Reizes • *Department of Cellular and Molecular Medicine, Lerner Research Institute, Cleveland Clinic, Cleveland, OH, USA; Cleveland Clinic Lerner, College of Medicine at Case Western Reserve University, Cleveland, OH, USA; Department of Molecular Medicine, Cleveland Clinic Lerner College of Medicine at Case Western Reserve University, Cleveland, OH, USA; Case Comprehensive Cancer Center, Cleveland, OH, USA*
Dirk Roggenbuck • *Medipan GmBH, Berlin, Dahlewitz, Germany; Faculty of Science, Brandenburg University of Technology Cottbus-Senftenberg, Senftenberg, Germany*
Geetika Sahni • *Department of Biomedical Engineering, National University of Singapore, Singapore, Singapore*
Mohamed Samour • *Department of Cellular and Molecular Medicine, Lerner Research Institute, Cleveland Clinic, Cleveland, OH, USA; Medicine Institute, Cleveland Clinic, Cleveland, OH, USA*
Nazilah Abdul Satar • *Regenerative Medicine Cluster, Advanced Medical and Dental Institute (AMDI), Universiti Sains Malaysia, Penang, Malaysia*
Caner Saygin • *Department of Cellular and Molecular Medicine, Lerner Research Institute, Cleveland Clinic, Cleveland, OH, USA*
Gabriela Schneider • *Stem Cell Institute at the James Graham Brown Cancer Center, University of Louisville, Louisville, KY, USA*
Zachariah Payne Sellers • *Stem Cell Institute at the James Graham Brown Cancer Center, University of Louisville, Louisville, KY, USA*
Carl Simard • *Recherche et Développement, Héma-Québec, Quebec, QC, Canada*
Amar M. Singh • *Transposagen Biopharmaceuticals, Inc., Lexington, KY, USA*

Ferenc Sipos • *Immunology Division, 2nd Department of Medicine, Semmelweis University, Budapest, Hungary*
Valeriya V. Adjan Steffey • *Transposagen Biopharmaceuticals, Inc., Lexington, KY, USA*
Krzysztof Szade • *Department of Medical Biotechnology, Faculty of Biochemistry, Biophysics and Biotechnology, Jagiellonian University, Krakow, Poland*
Yi-Chin Toh • *Department of Biomedical Engineering, National University of Singapore, Singapore, Singapore; Singapore Institute for Neurotechnology (SINAPSE), National University for Singapore, Singapore, Singapore*
Luca Urbani • *Stem Cells and Regenerative Medicine Section, Developmental Biology and Cancer Programme, UCL Institute of Child Health and Great Ormond Street Hospital, London, UK*
Sharat Warrier • *Ghent-Fertility and Stem cell Team (G-FaST), Department for Reproductive Medicine, Ghent University Hospital, Ghent, Belgium*
Badrul Hisham Yahaya • *Regenerative Medicine Cluster, Advanced Medical and Dental Institute (AMDI), Universiti Sains Malaysia, Penang, Malaysia*
Masahide Yoshikawa • *Department of Pathogen, Infection and Immunity, Nara Medical University, Kashihara, Nara, Japan*
Jun Yuan • *Department of Biomedical Engineering, National University of Singapore, Singapore, Singapore*
Norashikin Zakaria • *Regenerative Medicine Cluster, Advanced Medical and Dental Institute (AMDI), Universiti Sains Malaysia, Penang, Malaysia*
Monika Zukowska • *Department of Medical Biotechnology, Faculty of Biochemistry, Biophysics and Biotechnology, Jagiellonian University, Krakow, Poland*

Methods in Molecular Biology (2016) 1516: 1–12
DOI 10.1007/7651_2016_345

Published online: 05 April 2016

Heterogeneity of Stem Cells: A Brief Overview

Györgyi Műzes and Ferenc Sipos

Abstract

Stem cells possess the extraordinary capacity of self-renewal and differentiation to various cell types, thus to form original tissues and organs. Stem cell heterogeneity including genetic and nongenetic mechanisms refers to biological differences amongst normal and stem cells originated within the same tissue. Cell differentiation hierarchy and stochasticity in gene expression and signaling pathways may result in phenotypic differences of stem cells. The maintenance of stemness and activation of differentiation potential are fundamentally orchestrated by microenvironmental stem cell niche-related cellular and humoral signals.

Keywords: Embryonic stem cells, Adult stem cells, Cancer stem cells, Induced pluripotent stem cells, Differentiation, Microenvironment

1 Introduction

Stem cells possess the extraordinary capacity of self-renewal and differentiation to various cell types, thus to form original tissues and organs. They are present in a small portion in the organism mass, but can divide via mitosis and differentiate into daughter cells, and produce more stem cells, as well. The maintenance of stemness and activation of differentiation potential are fundamentally orchestrated by microenvironmental influences, mainly the so-called stem cell niche-related cellular and humoral signals [1].

Many types of stem cells can be differentiated according to their degree of differentiation, ability of self-renewing, and sources. Stem cells can be classified to totipotent, pluripotent, multipotent, and unipotent cells according to the abundance of their plasticity. Totipotent cells like zygote, spore, or morula have the potential to generate any and all human cells, and can even give rise to an entire functional organism. Pluripotent cells, such as embryonic stem cells can procreate all tissue types, but an entire functional organism. Progenitor cells like hematopoietic stem cells and mesenchymal stem cells are multipotent cells, and can give rise to a limited range of cells within a tissue. Unipotent cells are precursor ones, with limited plasticity. In addition, regarding their origin embryonic, adult, cancer, and induced pluripotent stem cells can be distinguished [2].

2 Embryonic Stem Cells

Embryonic stem cells are pluripotent cells derived from the inner cell mass of the blastocyst. They have two peculiar properties: the ability to differentiate into all derivatives of the three primary germ layers, and, further, can propagate themselves unrestrictedly within certain circumstances [3]. After decades of investigations a fast growing list of embryonic stem cell-specific markers has been established (including Nanog, ABCG2, Oct-3/4, Oct-4A, 5T4, ALPL, E-cadherin, podocalyxin, CCR4, Rex-1, CD9, c-kit, CD30, SFRP2, CDX2, Smad2, Smad2/3, chorionic gonadotropin, Ipha chain, Cripto, SOX2, DPPA4, osteonectin, DPPA5, SSEA-1, -3, -4, FGF-4, ESGP, GCNF, STAT3, GDF-3, SUZ12, integrin alpha 6, integrin alpha 6 beta 4, TBX2, -3, -5, CD29, KLF5, TEX19, Lefty-1, -A, THAP11, TRA-1-60(R), TROP-2, LIN-28, UTF1, LIN41, ZIC3, c-Myc) [2, 4]. Though, embryonic stem cells have the potential to generate any differentiated cell types, it is necessary for being able to control their proliferation, differentiation, and to regulate their development along specific pathways. Safety of their application is also a major concern, since the risk of teratomas or other cancers may represent a serious side effect [5]. Due to these difficulties, the application of human embryonic stem cells is at present limited in vitro and in animal studies. The primordial germ line cell-derived embryonic germ cells share several characteristics of human embryonic stem cells, however, differ in important ways. Primordial germ line cells can be isolated from fetal tissue, namely the gonadal ridge within a narrow time frame [6, 7]. These cells express SSEA-1, -3, -4, TRA1-60, TRA1-81, and ALPL, and are usually interpreted as being pluripotent, nevertheless, in mice they fail to initiate teratoma formation [2, 8, 9]. Fetal stem cells, the primitive cell types found in the organs of fetuses, can differentiate into both pluripotent stem cells and hematopoietic stem cells. After birth hematopoietic stem cells correspond to fetal stem cells in the umbilical cord [10, 11]. In current medical practice, they are useful in the treatment of blood disorders, but the risk of tissue rejection is similar to those encountered in heart or kidney transplants, which may limit their clinical application [12–14].

3 Adult Stem Cells

Adult stem cells can be classified upon origin as endodermal, mesodermal, and ectodermal cells. Pulmonary epithelial, gastrointestinal tract, and pancreatic stem cells, hepatic oval cells, prostatic, testicular-, ovarian and mammary gland stem cells are all endodermal originated. Stem cells of mesodermal origin correspond to

hematopoietic, mesenchymal stroma, mesenchymal, and mesenchymal precursor stem cells, multipotent adult progenitor cells, bone marrow, fetal somatic, unrestricted somatic, and cardiac stem cells, and muscle satellite cells. Neural, skin, and ocular stem cells are of ectodermal origin [2, 15, 16]. The Cairn's theory (i.e., the immortal DNA strand hypothesis) describes a mechanism for adult stem cells to minimize genomic mutations [17]. According to this hypothesis, in adult stem cells DNA division is asymmetric, and stem cells retain a distinct template set of DNA strands over successive generations. Adult stem cells by nonrandom DNA division could transmit mutations arising from DNA replication errors onto terminally differentiating daughter cells, and thus, they may reduce the rate of accumulated mutations frequently leading to genetic disorders, like cancer [17].

Adult bone marrow comprises two types of multipotent precursor cells: the hematopoietic stem cells and the marrow stromal cells [18]. While hematopoietic stem cells can only be found in peripheral blood and umbilical cord blood, marrow stromal cells can be isolated from several other tissues, such as adipose tissue, placenta, amniotic fluid, umbilical cord blood, or fetal tissues [19, 20]. Hematopoietic stem cells can sustain the production of all blood cells, marrow stromal cells; however, they have the capacity to differentiate into osteocytes, chondrocytes, smooth muscle cells, adipocytes, and hematopoietic supportive stromal cells, as well [19, 20]. The expression of CD34, CD38, CD43, CD45RO, CD45RA, CD59, CD90, CD117, CD133, CD166, HLA-DR, and Lin are characteristic for hematopoietic stem cells. Moreover, the presence of certain metabolic markers, like rhodamine-123, Hoechst-33342, pyronin-Y, and BAAA have also been described [2, 4, 21, 22]. Marrow stromal cells can be identified by the expression of CD29, CD44, CD73, CD105, CD106, and Sca-1 [21, 22]. Adult stem cells originated from mature tissues have more limited potential as compared to embryonic or fetal stem cells. Most adult stem cells are lineage-restricted and are usually referred upon their tissue origin, such as endothelial, and mesenchymal stem cells or adipose-derived stem cells [23–25].

Besides the bone marrow, mesenchymal stem cells can also be isolated from adipose tissues, fetal liver, cord blood and, further, mobilized from peripheral blood, fetal lung, placenta, umbilical cord, dental pulp, synovial membrane, periodontal ligament, endometrium, trabecular and compact bone [26–38]. Under appropriate culture conditions, mesenchymal stem cells can differentiate into mesodermal, endodermal, and ectodermal cells. They can be applied for tissue regeneration and repair, since these cells are safe, and do not form teratoma [39–41]. Because there are no specific cell surface markers, the definition of mesenchymal stem cells seems to be rather controversial. Nowadays, they can be characterized by using a combination of cell surface markers, the ability of plastic

adherent fibroblast-like growth and functional properties. Adult human mesenchymal stem cells express several molecules, like Stro-1, CD105, CD73, CD44, CD71, CD90, ganglioside GD2, CD271, as well as ICAM-1, -2, integrins (α1,-2,-3,-5,-6,-V, β1,-3,-4), ALCAM, LFA-3, VCAM-1, and CD72 [42–49]. They also display HLA class I [50, 51]. In addition, mesenchymal stem cells lack the expression of CD11a, CD14, CD31, CD34, CD45, CD40, CD80, and CD86 [32, 48, 52, 53].

Adult stem cells play a crucial role in local tissue repair and regeneration. Upon ethic considerations separation of adult stem cells makes these cells preferable candidates for therapeutic applications like that of embryonic stem cells. Moreover, within some circumstances, adult stem cells can be achieved from an autograft, and hence, the risk of tissue rejection does not exist from a therapeutic point of view [2].

Adult stem cells are essential elements of both monolayered and stratified mammalian epithelium. Epithelium is truly multifunctional, since it can protect, secrete, and absorb, often within a single organ. The stratified skin epithelium maintains a protective barrier of the human body, defending the underlying tissues from physical and environmental stress factors, while its secretory function is mediated by sweat-releasing glands [54]. In the gastrointestinal tract, the monolayered epithelium functions not only as a barrier to ingested pathogens, but it simultaneously secretes gastric acids, mucus, proteases, and hormones for digestion [54, 55]. Moreover, it controls motility, nutrient and water uptake through differentiated absorptive cells of the villi [54, 55]. LGR proteins are 7-transmembrane G-protein-coupled receptors that function as co-receptors for Wnt [56, 57]. The non-intestinal epithelial stem cells, such as skin- and hair follicle stem cells, express all LGR proteins (LGR4, -5, -6), albeit in different regions [56, 57]. The current markers of adult intestinal stem cells depend on several conditions, like their position within the crypts, proliferation rate, and sensitivity to irradiation. Crypt base columnar cells are marked by the expression of *Lgr5, Olmf4*, *BMPR1α, PTEN, Wip1,* or Wnt-target genes, like *Ascl2, Smoc2*, and *Rnf43* [55, 58]. Additionally, *Znrf3, Troy*, and *Musashi-1* expressions are characteristic for crypt base columnar cells, as well [55, 58, 59]. Recent investigations using in vivo lineage tracing determined *Bmi1, Hopx, mTert,* and *Lrig1* as potential markers of the +4 cell population [55, 58–60].

Though extensive studies have been suggested that mature hepatocytes could serve like their own physiologic precursors, the multipotent, blast-like liver oval cells are considered as true liver-specific stem cells. These cells have been indicated to express molecular markers of adult hepatocytes and bile-duct cells (albumin, cytokeratins 7, 8, 18, 19, OV-6, A6), fetal hepatoblasts (AFP), and hematopoietic stem cells (c-kit, Sca-1, Thy-1) [61–64].

Regarding the pancreas, the candidate sources for adult pancreatic stem or progenitor cells are duct cells, the exocrine tissue, nestin+ islet-derived progenitor cells, neurogenin-3+ cells, pancreas-derived multipotent precursors, and mature β-cells. Pancreatic stem cells have the potential to differentiate into all three germ layers. Their major markers are Oct-4, nestin, c-kit, DCAMKL-1, and Pdx-1 [2, 65–67]. Although the liver along with the pancreas are much more renowned for their excess regeneration, their suitability as a practical model system to study epithelial plasticity is rather controversial since the localization of all stem cell populations has not been fully determined.

4 Cancer Stem Cells

Within the hierarchy of heterogenous cancer cell populations presumably only the subset of cancer stem cells, also termed as tumor-initiating and cancer-repopulating cells with particular capacity of self-renewal, and pluripotency exhibits direct tumor-provoking and metastatic feature, and is responsible for specific characteritics of malignant tumors, like resistance to cell death, unchecked proliferation, aggressiveness, and the common resistance to conventional therapies [68–70]. Accumulating evidence demonstrates that cancer stem cells contribute to cancer dormancy and relapse, as well [71–73]. Cancer stem cells were initially thought to originate from normal stem cells. Recent studies suggest that progenitor cells contribute to the cancer stem cell pool by genetic (like mutations or polymorphisms of tumor suppressor genes and oncogenes, different types of chromosomal alterations, microsatellite instability, etc.) and/or epigenetic (such as posttranscriptional gene expression regulation by microRNAs, promoter hypo/hypermethylation, histone acetylation, etc.) events [74–76]. However, cancer stem cells do not definitely originate from normal progenitors or stem cells. The acquisition and accumulation of genetic/epigenetic alterations can covert cancer cells as well as normal cells to a stemness state by dedifferentiation resulting finally cancer stem cells. Additionally, cell fusion between normal stem cells and somatic ones may originate cancer stem cells [77–85].

Cancer stem cells can be isolated from the tumor mass by the expression profile of specific surface antigens (e.g., CD34+ in AML, CD133+ in brain, colon, liver, lung, and prostate tumors, CD44+ in breast, pancreas, ovarial, and gastric tumors, CD138+ in multiple myeloma, or CD4+/CD25+/FoxP3+ in melanoma) [2]. Due to their longevity cancer stem cells often accumulate numerous mutations essential for malignant transformation [86]. Though cancer stem cells may arise mainly from oncogenically transformed aberrant adult stem cells, they do not inevitably exhibit all the typical characteristics [71]. Furthermore, activation of

epithelial–mesenchymal transition, a transdifferentiation mechanism in cancer cells, enables them to acquire stem cell-like properties [77]. Epithelial–mesenchymal transition might even have a special importance in early dissemination process of preinvasive tumors resulting in early disseminated tumor cells [87]. Subsequently, a second shifted phenotypic status of cancer stem cells, i.e., mesenchymal–epithelial transition may contribute to overt metastatic spreading [88]. The speculative link between cancer stem cells and cell dormancy rests especially on the realization of quiescence-induced tumor cell growth arrest. Dormant cancer stem cells are characterized mainly by a slow growth, an ability to evade host immunity, and a capability to reproduce themselves. However, the state of cancer stem cell dormancy highlights even on the plasticity of metastasis-initiating tumor cells since upon niche signals eventually they may outbreak cell cycle repression and reacquire the potential of uncontrolled proliferation, thus leading to cancer relapse [89–91]. Furthermore, cancer stem cells display an increased drug resistance capacity mainly due to high expression of ATP-binding cassette and multidrug resistance transporters [92]. In addition, cancer stem cells exhibit an inherent resistance to radiation, as well [93]. This fact is based on the lower levels of ROS and DNA damage in cancer stem cells upon radiation, as resulted from their enhanced defense antioxidant and DNA-repair capacities [91, 94].

Like normal adult stem cells, metastatic cancer stem cells could undergo dormancy in response to inhibitory microenvironmental niche signals or lacking stimulatory ones supporting the decisive role of that foreign milieu [95, 96]. As underlying mechanisms of the cancer stem cell dormancy state especially cell cycle arrest, stress-tolerance signaling, and autophagy could be implicated [97–99]. Concerning the quiescence program of stem cells dormancy signature several differentially regulated genes are involved, and determine the dormant phenotype [100, 101]. In quiescent stem cells those genes that affect the cell cycle, DNA replication, and mitochondrial functions are mainly downregulated [101]. However, this nonproliferative, quiescent phenotype of cancer stem cells with different primary tumor origin could be overcome via appreciably distinct and specific survival signals within the target organs' microenvironment [102, 103]. Tissue tropisms associated with cancer metastases clearly indicate the involvement of variant cellular and molecular mechanisms. As a hypothesis, upon releasing systemic factors carcinoma cells from primary tumors even prior to their seeding are able to establish a supportive niche within the target organ [104]. Activation of supportive niche signals related to transforming growth factor-β and their family members induces cancer stem cells to enter into a dormant state through inhibiting the capacity for their self-renewal [105, 106]. As a novel aspect, activation of autophagy by transforming growth factor-β may also

participate in its growth-inhibitory action [107]. In addition, cancer stem cells could remain dormant when stroma-derived antiproliferative factors limit their potential to outgrow [108]. Moreover, current activity of the Wnt/β-catenin and Notch signaling pathways is highly determining whether dormant cancer stem cells would be capable or not for reactivation [109, 110].

It becomes widely accepted that the tumor mass itself contains heterogeneous cancer cells and different types of stromal cells. Cell types in a cancer stem cell niche usually vary from fibroblasts, to endothelial and immune cells. These noncancer cells have been suggested to change their original features in the normal tissue/organ and to acquire a phenotype that protects cancer stem cells from anticancer therapies [111]. Cancer cells are able to recruit bone marrow derived stromal cells and surrounding tissues to construct their own microenvironment contributing to tumor initiation and progression. Moreover, cancer cells can fuse with or transdifferentiate into several types of stromal cells to favor cancer cell survival, proliferation, invasion, and metastasis. Recent data support that cancer stem cells possess a multilineage differentiation ability that is similar to normal stem cells; furthermore, they are able to transdifferentiate into vascular endothelial cells and pericytes. Various differentiated cells have been directly reprogrammed from one cell type into another by the induction of different transcription factors [80–84]. These data support that cancer stem cells obviously can generate their own pro-tumorigenic microenvironment. The direction of their cellular transformation is, in part, context-dependent, and also depends on metabolic stress conditions.

In a therapeutic point of view, it would be beneficial to include an induction of cancer stem cell differentiation before and during chemotherapies. While this induced differentiation strategy has achieved significant efficacy on blood cancer treatment, like acute promyelocytic leukemia of children, in solid tumors, however, the differentiation inducers and chemotherapeutic agents are difficult to penetrate into the tumor mass [2, 112]. The cancer stem cell transdifferentiation is also still remains elusive in many aspects, and thus, new discoveries in this area may help with developing diagnostic and therapeutic antitumor strategies, as well.

5 Induced Pluripotent Stem Cells

Induced pluripotent stem cells refer to artificially derived ones from non-pluripotent cells, typically the adult somatic cells upon inducing a forced expression of stemness-specific genes [113]. In many respects, they are similar to natural pluripotent stem cells, like embryonic stem cells. These similarities include the expression of specific stemness-related cell genes and proteins, the chromatin

methylation pattern, the doubling time, the embryoid body formation, the formation of teratomas and viable chimeras, the potency and differentiability; however, the full extent of the relation of induced pluripotent stem cells to natural ones is still being assessed [114]. The introduction of human induced pluripotent stem cells in 2007 has been cited as an important advance in stem cell research, since they may allow to obtain pluripotent stem cells without destroying embryos, the issue of graft-versus-host disease and immune rejection [115]. Induced pluripotent stem cells are already useful tools for drug development and modeling of diseases, and scientists hope to use them in transplantation medicine.

Recently studies have highlighted on the importance of microRNAs in modulation of normal and induced cellular pluripotency and reprogramming of somatic cells. This is based on findings indicating that several microRNAs can deeply affect the gene expression profile responsible for the pluripotent hallmarks of cells as well as for the somatic cell nuclear transfer [116, 117].

However, depending on the reprogramming methods used, the generation of induced pluripotent stem cells may pose significant risks that could limit their clinical application. In case of genomically altered adult cells, the expression of pro-tumorigenic genes and oncogenes may potentially be triggered. However, there exist such techniques that could remove oncogenes after the induction of pluripotency, and even the generation of induced pluripotent stem cells without any genetic alteration of the adult stem cells is possible (protein-induced pluripotent stem cells), the medical use of these cells needs further investigations [118–121].

References

1. Morrison SJ, Spradling AC (2008) Stem cells and niches: mechanisms that promote stem cell maintenance throughout life. Cell 132:598–611
2. Hui H, Tang Y, Hu M, Zhao X (2011) Stem Cells: General Features and Characteristics. Ali Gholamrezanezhad (ed). Stem Cells in Clinic and Research; ISBN: 978-953-307-797-0. InTech. http://www.intechopen.com/books/stem-cells-in-clinicand-research/stem-cellsgeneral-features-and-characteristics.
3. Damdimopoulou P, Rodin S, Stenfelt S et al (2015) Human embryonic stem cells. Best Pract Res Clin Obstet Gynaecol. doi:10.1016/j.bpobgyn.2015.08.010
4. Stem Cell Basics. In Stem Cell Information [World Wide Web site]. Bethesda, MD: National Institutes of Health, U.S. Department of Health and Human Services, 2015 Available at http://stemcells.nih.gov/info/basics/Pages/Default.aspx
5. Grinnemo KH, Sylvén C, Hovatta O et al (2008) Immunogenicity of human embryonic stem cells. Cell Tissue Res 331:67–78
6. Ledda S, Bogliolo L, Bebbere D et al (2010) Characterization, isolation and culture of primordial germ cells in domestic animals: recent progress and insights from the ovine species. Theriogenology 74:534–543
7. Kakegawa R, Teramura T, Takehara T et al (2008) Isolation and culture of rabbit primordial germ cells. J Reprod Dev 54:352–357
8. Roach S, Cooper S, Bennett W et al (1993) Cultured cell lines from human teratomas: windows into tumour growth and differentiation and early human development. Eur Urol 23:82–87
9. Shamblott MJ, Axelman J, Littlefield JW et al (2001) Human embryonic germ cell

derivatives express a broad range of developmentally distinct markers and proliferate extensively in vitro. Proc Natl Acad Sci U S A 98:113–118

10. Lee MW, Jang IK, Yoo KH et al (2010) Stem and progenitor cells in human umbilical cord blood. Int J Hematol 92:45–51
11. Lee ES, Bou-Gharios G, Seppanen E et al (2010) Fetal stem cell microchimerism: natural-born healers or killers? Mol Hum Reprod 16:869–878
12. Navarrete C, Contreras M (2009) Cord blood banking: a historical perspective. Br J Haematol 147:236–245
13. Harari-Steinberg O, Pleniceanu O, Dekel B (2011) Selecting the optimal cell for kidney regeneration: fetal, adult or reprogrammed stem cells. Organogenesis 7:123–134
14. Biazar E (2014) Use of umbilical cord and cord blood-derived stem cells for tissue repair and regeneration. Expert Opin Biol Ther 14:301–310
15. Wabik A, Jones PH (2015) Switching roles: the functional plasticity of adult tissue stem cells. EMBO J 34:1164–1179
16. Tsimbouri PM (2015) Adult stem cell responses to nanostimuli. J Funct Biomater 6:598–622
17. Cairns J (1975) Mutation selection and the natural history of cancer. Nature 255:197–200
18. Lagasse E, Connors H, Al-Dhalimy M et al (2000) Purified hematopoietic stem cells can differentiate into hepatocytes in vivo. Nat Med 6:1229–1234
19. Herzog EL, Chai L, Krause DS (2003) Plasticity of marrow-derived stem cells. Blood 102:3483–3493
20. Yagi H, Soto-Gutierrez A, Kitagawa Y et al (2010) Bone marrow mesenchymal stromal cells attenuate organ injury induced by LPS and burn. Cell Transplant 19:823–830
21. Quesenberry PJ, Goldberg LR, Dooner MS (2015) Concise reviews: a stem cell apostasy: a tale of four H words. Stem Cells 33:15–20
22. Bone Marrow (Hematopoietic) Stem Cells. In Stem Cell Information [World Wide Web site]. Bethesda, MD: National Institutes of Health, U.S. Department of Health and Human Services, 2011. Available at http://stemcells.nih.gov/info/Regenerative_Medicine/pages/2006chapter2.aspx
23. Barrilleaux B, Phinney DG, Prockop DJ et al (2006) Review: ex vivo engineering of living tissues with adult stem cells. Tissue Eng 12:3007–3019
24. Gimble JM, Katz AJ, Bunnell BA (2007) Adipose-derived stem cells for regenerative medicine. Circ Res 100:1249–1260
25. Feisst V, Meidinger S, Locke MB (2015) From bench to bedside: use of human adipose-derived stem cells. Stem Cells Cloning 8:149–162
26. Zuk PA, Zhu M, Ashjian P et al (2002) Human adipose tissue is a source of multipotent stem cells. Mol Biol Cell 13:4279–4295
27. Zhang HJ, Miao ZC, He ZP et al (2005) The existence of epithelial-to-mesenchymal cells with the ability to support hematopoiesis in human fetal liver. Cell Biol Int 29:213–219
28. Tondreau T, Meuleman N, Delforge A et al (2005) Mesenchymal stem cells derived from CD133-positive cells in mobilized peripheral blood and cord blood: proliferation, Oct4 expression, and plasticity. Stem Cells 23:1105–1112
29. Zheng CL, Yang SG, Guo ZX et al (2009) Human multipotent mesenchymal stromal cells from fetal lung expressing pluripotent markers and differentiating into cell types of three germ layers. Cell Transplant 18:1093–1109
30. Fukuchi Y, Nakajima H, Sugiyama D et al (2004) Human placenta-derived cells have mesenchymal stem/progenitor cell potential. Stem Cells 22:649–658
31. Sarugaser R, Lickorish D, Baksh D et al (2005) Human umbilical cord perivascular (HUCPV) cells: a source of mesenchymal progenitors. Stem Cells 23:220–229
32. Lu LL, Liu YJ, Yang SG et al (2006) Isolation and characterization of human umbilical cord mesenchymal stem cells with hematopoiesis-supportive function and other potentials. Haematologica 91:1017–1026
33. Huang GT, Gronthos S, Shi S (2009) Mesenchymal stem cells derived from dental tissues vs. those from other sources: their biology and role in regenerative medicine. J Dent Res 88:792–806
34. Hermida-Gomez T, Fuentes-Boquete I, Gimeno-Longas MJ et al (2011) Quantification of cells expressing mesenchymal stem cell markers in healthy and osteoarthritic synovial membranes. J Rheumatol 38:339–349
35. Park JC, Kim JM, Jung IH et al (2011) Isolation and characterization of human periodontal ligament (PDL) stem cells (PDLSCs) from the inflamed PDL tissue: in vitro and in vivo evaluations. J Clin Periodontol 38:721–731

36. Schwab KE, Hutchinson P, Gargett CE (2008) Identification of surface markers for prospective isolation of human endometrial stromal colony-forming cells. Human Reprod 23:934–943
37. Sakaguchi Y, Sekiya I, Yagishita K et al (2004) Suspended cells from trabecular bone by collagenase digestion become virtually identical to mesenchymal stem cells obtained from marrow aspirates. Blood 104:2728–2735
38. Zhu H, Guo ZK, Jiang XX et al (2010) A protocol for isolation and culture of mesenchymal stem cells from mouse compact bone. Nat Protoc 5:550–560
39. Wang Y, Han ZB, Ma J et al (2012) A toxicity study of multiple-administration human umbilical cord mesenchymal stem cells in cynomolgus monkeys. Stem Cells Dev 21:1401–1408
40. Wang Y, Zhang Z, Chi Y et al (2013) Long-term cultured mesenchymal stem cells frequently develop genomic mutations but do not undergo malignant transformation. Cell Death Dis 4:e950
41. Zhaoa Q, Renb H, Hana Z (2015) Mesenchymal stem cells: immunomodulatory capability and clinical potential in immune diseases. J Cell Immunother. doi:10.1016/j.jocit.2014.12.001
42. Simmons PJ, Torok-Storb B (1991) Identification of stromal cell precursors in human bone marrow by a novel monoclonal antibody, STRO-1. Blood 78:55–62
43. Barry FP, Boynton RE, Haynesworth S et al (1999) The monoclonal antibody SH-2, raised against human mesenchymal stem cells, recognizes an epitope on endoglin (CD105). Biochem Biophys Res Commun 265:134–139
44. Barry F, Boynton R, Murphy M et al (2001) The SH-3 and SH-4 antibodies recognize distinct epitopes on CD73 from human mesenchymal stem cells. Biochem Biophys Res Commun 289:519–524
45. Martinez C, Hofmann TJ, Marino R et al (2007) Human bone marrow mesenchymal stromal cells express the neural ganglioside GD2: a novel surface marker for the identification of MSCs. Blood 109:4245–4248
46. Xu J, Liao WB, Gu DS et al (2009) Neural ganglioside GD2 identifies a subpopulation of MSC in human umbilical cord. Cell Physiol Biochem 23:415–424
47. Majumdar MK, Keane-Moore M, Buyaner D et al (2003) Characterization and functionality of cell surface molecules on human mesenchymal stem cells. J Biomedical Sci 10:228–241
48. Pittenger MF, Mackay AM, Beck SC et al (1999) Multilineage potential of adult human mesenchymal stem cells. Science 284:143–147
49. Majumdar MK, Thiede MA, Mosca JD et al (1998) Phenotypic and functional comparison of cultures of marrow-derived mesenchymal stem cells (MSCs) and stromal cells. J Cell Physiol 176:57–66
50. Le Blanc K, Tammik C, Rosendahl K et al (2003) HLA expression and immunologic properties of differentiated and undifferentiated mesenchymal stem cells. Exp Hematol 31:890–896
51. Zhao Q, Ren H, Li X et al (2009) Differentiation of human umbilical cord mesenchymal stromal cells into low immunogenic hepatocyte-like cells. Cytotherapy 11:414–426
52. Klyushnenkova E, Mosca JD, Zernetkina V et al (2005) T cell responses to allogeneic human mesenchymal stem cells: immunogenicity, tolerance, and suppression. J Biomed Sci 12:47–57
53. Weiss ML, Anderson C, Medicetty S et al (2008) Immune properties of human umbilical cord Wharton's jelly-derived cells. Stem Cells 26:2865–2874
54. Blanpain C, Horsley V, Fuchs E (2007) Epithelial stem cells: turning over new leaves. Cell 128:445–458
55. Tan S, Barker N (2015) Epithelial stem cells and intestinal cancer. Semin Cancer Biol 32:40–53
56. Vries RG, Huch M, Clevers H (2010) Stem cells and cancer of the stomach and intestine. Mol Oncol 4:373–384
57. Barker N, Bartfeld S, Clevers H (2010) Tissue-resident adult stem cell populations of rapidly self-renewing organs. Cell Stem Cell 7:656–670
58. Pirvulet V (2015) Gastrointestinal stem cell up-to-date. J Med Life 8:245–249
59. Sipos F, Műzes G (2015) Injury-associated reacquiring of intestinal stem cell function. World J Gastroenterol 21:2005–2010
60. Buczacki SJ, Zecchini HI, Nicholson AM et al (2013) Intestinal label-retaining cells are secretory precursors expressing Lgr5. Nature 495:65–69
61. Newsome PN, Hussain MA, Theise ND (2004) Hepatic oval cells: helping redefine a paradigm in stem cell biology. Curr Top Dev Biol 61:1–28
62. Shafritz DA, Oertel M, Menthena A et al (2006) Liver stem cells and prospects for

liver reconstitution by transplanted cells. Hepatology 43:S89–S98
63. Sekine S, Gutiérrez PJ, Lan BY et al (2007) Liver-specific loss of beta-catenin results in delayed hepatocyte proliferation after partial hepatectomy. Hepatology 45:361–368
64. Verhulst S, Best J, van Grunsven LA et al (2015) Advances in hepatic stem/progenitor cell biology. EXCLI J 14:33–47
65. Marty-Santos L, Cleaver O (2015) Progenitor epithelium: sorting out pancreatic lineages. J Histochem Cytochem 63:559–574
66. May R, Sureban SM, Lightfoot SA et al (2010) Identification of a novel putative pancreatic stem/progenitor cell marker DCAMKL-1 in normal mouse pancreas. Am J Physiol Gastrointest Liver Physiol 299: G303–G310
67. Yang JH, Lee SH, Heo YT et al (2010) Generation of insulin-producing cells from gnotobiotic porcine skin-derived stem cells. Biochem Biophys Res Commun 397:679–684
68. Reya T, Morrison SJ, Clarke MF et al (2001) Stem cells, cancer, and cancer stem cells. Nature 414:105–111
69. Sell S (2010) On the stem cell origin of cancer. Am J Pathol 176:2584–2594
70. Kreso A, Dick JE (2014) Evolution of the cancer stem cell model. Cell Stem Cell 14:275–291
71. Gupta PB, Chaffer CL, Weinberg RA (2009) Cancer stem cells: mirage or reality? Nat Med 15:1010–1012
72. Wang Z, Ouyang G (2012) Periostin: a bridge between cancer stem cells and their metastatic niche. Cell Stem Cell 10:111–112
73. Pattabiraman DR, Weinberg RA (2014) Tackling the cancer stem cells—what challenges do they pose? Nat Rev Drug Discov 13:497–512
74. Krivtsov AV, Twomey D, Feng Z et al (2006) Transformation from committed progenitor to leukaemia stem cell initiated by MLL-AF9. Nature 442:818–822
75. Huntly BJ, Shigematsu H, Deguchi K et al (2004) MOZ-TIF2, but not BCR-ABL, confers properties of leukemic stem cells to committed murine hematopoietic progenitors. Cancer Cell 6:587–596
76. Huang Z, Wu T, Liu AY et al (2015) Differentiation and transdifferentiation potentials of cancer stem cells. Oncotarget 6:39550–39563
77. Mani SA, Guo W, Liao MJ et al (2008) The epithelial-mesenchymal transition generates cells with properties of stem cells. Cell 133:704–715
78. Friedmann-Morvinski D, Bushong EA, Ke E et al (2012) Dedifferentiation of neurons and astrocytes by oncogenes can induce gliomas in mice. Science 338:1080–1084
79. Scaffidi P, Misteli T (2011) In vitro generation of human cells with cancer stem cell properties. Nat Cell Biol 13:1051–1061
80. Ricci-Vitiani L, Pallini R, Biffoni M et al (2010) Tumour vascularization via endothelial differentiation of glioblastoma stem-like cells. Nature 468:824–828
81. Wang R, Chadalavada K, Wilshire J et al (2010) Glioblastoma stem-like cells give rise to tumour endothelium. Nature 468:829–833
82. Soda Y, Marumoto T, Friedmann-Morvinski D et al (2011) Transdifferentiation of glioblastoma cells into vascular endothelial cells. Proc Natl Acad Sci U S A 108:4274–4280
83. Cheng L, Huang Z, Zhou W et al (2013) Glioblastoma stem cells generate vascular pericytes to support vessel function and tumor growth. Cell 153:139–152
84. Liu AY, Ouyang G (2013) Tumor angiogenesis: a new source of pericytes. Curr Biol 23: R565–R568
85. Amamoto R, Arlotta P (2014) Development-inspired reprogramming of the mammalian central nervous system. Science 343:1239882
86. Marjanovic ND, Weinberg RA, Chaffer CL (2013) Cell plasticity and heterogeneity in cancer. Clin Chem 59:168–179
87. Klein CA (2010) Framework models of tumor dormancy from patient-derived observations. Curr Opin Genet Dev 21:42–49
88. Brabletz T (2012) To differentiate or not—routes towards metastasis. Nat Rev Cancer 12:425–436
89. Allan AL, Vantyghem SA, Tuck AB et al (2006) Tumor dormancy and cancer stem cells: implications for the biology and treatment of breast cancer metastasis. Breast Dis 26:87–98
90. Meacham CE, Morrison SJ (2013) Tumour heterogeneity and cancer cell plasticity. Nature 501:328–337
91. Wang SH, Lin SY (2013) Tumor dormancy: potential therapeutic target in tumor recurrence and metastasis prevention. Exp Hematol Oncol 2:29
92. Donnenberg VS, Meyer EM, Donnenberg AD (2009) Measurement of multiple drug resistance transporter activity in putative cancer stem/progenitor cells. Methods Mol Biol 568:261–279

93. Rich JN (2007) Cancer stem cells in radiation resistance. Cancer Res 67:8980–8984
94. Diehn M, Cho RW, Lobo NA et al (2009) Association of reactive oxygen species levels and radioresistance in cancer stem cells. Nature 458:780–783
95. Li L, Clevers H (2010) Coexistence of quiescent and active adult stem cells in mammals. Science 327:542–545
96. Sneddon JB, Werb Z (2007) Location, location, location: the cancer stem cell niche. Cell Stem Cell 1:607–611
97. Ranganathan AC, Adam AP, Zhang L et al (2006) Tumor cell dormancy induced by p38(SAPK) and ER-stress signaling: an adaptive advantage for metastatic cells? Cancer Biol Ther 5:729–735
98. Lamb R, Lisanti MP, Clarke RB et al (2014) Co-ordination of cell cycle, migration and stem cell-like activity in breast cancer. Oncotarget 5:7833–7842
99. Lara-Padilla E, Caceres-Cortes JR (2012) On the nature of the tumor-initiating cell. Curr Stem Cell Res Ther 7:26–35
100. Kleffel S, Schatton T (2013) Tumor dormancy and cancer stem cells: two sides of the same coin? Adv Exp Med Biol 734:145–179
101. Cheung TH, Rando TA (2013) Molecular regulation of stem cell quiescence. Nat Rev Mol Cell Biol 14:329–340
102. Joyce JA, Pollard JW (2009) Microenvironmental regulation of metastasis. Nat Rev Cancer 9:239–252
103. Suzuki M, Mose ES, Montel V et al (2006) Dormant cancer cells retrieved from metastasis-free organs regain tumorigenic and metastatic potency. Am J Pathol 169:673–681
104. Psaila B, Lyden D (2009) The metastatic niche: adapting the foreign soil. Nat Rev Cancer 9:285–293
105. Yamazaki S, Iwama A, Takayanagi S et al (2009) TGF-beta as a candidate bone marrow niche signal to induce hematopoietic stem cell hibernation. Blood 113:1250–1256
106. Wakefield LM, Hill CS (2013) Beyond TGFbeta: roles of other TGFbeta superfamily members in cancer. Nat Rev Cancer 13:328–341
107. Suzuki HI, Kiyono K, Miyazono M (2010) Regulation of autophagy by transforming growth factor-β (TGFβ) signaling. Autophagy 6:645–647
108. Kobayashi A, Okuda H, Xing F et al (2011) Bone morphogenetic protein 7 in dormancy and metastasis of prostate cancer stem-like cells in bone. J Exp Med 28:2641–2655
109. Vermeulen L, De Sousa E, Melo F et al (2010) Wnt activity defines colon cancer stem cells and is regulated by the microenvironment. Nat Cell Biol 12:468–476
110. Sikandar SS, Pate KT, Anderson S et al (2010) NOTCH signaling is required for formation and self-renewal of tumor-initiating cells and for repression of secretory cell differentiation in colon cancer. Cancer Res 70:1469–1478
111. Kise K, Kinugasa-Katayama Y, Takakura N (2015) Tumor microenvironment for cancer stem cells. Adv Drug Deliv Rev. doi:10.1016/j.addr.2015.08.005
112. Wang ZY, Chen Z (2000) Differentiation and apoptosis induction therapy in acute promyelocytic leukaemia. Lancet Oncol 1:101–106
113. Thomson JA, Itskovitz-Eldor J, Shapiro SS et al (1998) Embryonic stem cell lines derived from human blastocysts. Science 282:1145–1147
114. Ying QL, Nichols J, Chambers I et al (2003) BMP induction of Id proteins suppresses differentiation and sustains embryonic stem cell self-renewal in collaboration with STAT3. Cell 115:281–292
115. Okita K, Ichisaka T, Yamanaka S (2007) Generation of germline-competent induced pluripotent stem cells. Nature 448:313–317
116. Wang Y, Baskerville S, Shenoy A et al (2008) Embryonic stem cell-specific microRNAs regulate the G1-S transition and promote rapid proliferation. Nat Genet 40:1478–1483
117. Bao X, Zhu X, Liao B et al (2013) MicroRNAs in somatic cell reprogramming. Curr Opin Cell Biol 25:208–214
118. Huangfu D, Osafune K, Maehr R et al (2008) Induction of pluripotent stem cells from primary human fibroblasts with only Oct4 and Sox2. Nat Biotechnol 26:1269–1275
119. Martin GR (1981) Isolation of a pluripotent cell line from early mouse embryos cultured in medium conditioned by teratocarcinoma stem cells. Proc Natl Acad Sci U S A 78:7634–7638
120. Sivakumar M, Dineshshankar J, Sunil PM et al (2015) Stem cells: an insight into the therapeutic aspects from medical and dental perspectives. J Pharm Bioallied Sci 7:S361–S371
121. Guillot PV (2015) Induced pluripotent stem (iPS) cells from human fetal stem cells. Best Pract Res Clin Obstet Gynaecol. doi:10.1016/j.bpobgyn.2015.08.007

Methods in Molecular Biology (2016) 1516: 13–46
DOI 10.1007/7651_2016_347

Published online: 05 April 2016

Establishment and Characterization of Naïve Pluripotency in Human Embryonic Stem Cells

Sharat Warrier, Mina Popovic, Margot Van der Jeught, and Björn Heindryckx

Abstract

Mouse embryonic stem cells are known to represent the naïve state of pluripotency, while human embryonic stem cells typically represented the primed state of pluripotency, characterized by a higher drift toward differentiation and some other disadvantages. Here we describe an efficient method for rapid, transgene free induction of the naïve pluripotent state in human by applying a novel combination of small molecules and growth factors in the culture medium (2i, LIF, basic fibroblast growth factor, ascorbic acid, and forskolin). Conversion of primed human embryonic stem cells towards the naive pluripotent state should be confirmed by a detailed characterization of the cells, as described in this chapter.

Keywords: Naïve pluripotency, Human embryonic stem cells, Mouse embryonic fibroblasts, Karyotyping, Immunostaining, Quantitative real-time PCR

1 Introduction

Despite their common traits of self-renewal and pluripotency, embryonic stem cells (ESCs) can differ substantially in transcriptional profile, epigenetic profile, morphology, and culture requirements, especially between different species. It has become clear that pluripotency is not a fixed state, but exists in at least two different forms, being the naïve and primed pluripotent state [1, 2]. Their difference lies in their origin as well as the specific culture conditions applied. While naïve mouse ESCs (mESCs) are derived from preimplantation stage blastocysts, primed mouse epiblast stem cells (mEpiSC) originate from postimplantation stage embryos [3, 4]. Moreover, the derivation of naïve mESCs from nonpermissive mice strains is mostly only successful in presence of the small molecules PD0325901 and CHIR99021 (known as the 2 inhibitor or 2i condition), inhibiting the Mitogen-Activated Protein Kinase (Erk1/2) and Glycogen Synthase Kinase 3β (GSK3β) pathways respectively [1, 5]. Although derived from the preimplantation blastocyst stage, human ESCs (hESCs) represent the primed state of pluripotency. For clinical applications, the derivation of hESCs in

the naïve state of pluripotency is of great interest, as this type of cells will open new opportunities for patient-specific, disease-relevant research.

There are three possible routes to achieve the naïve pluripotent state in humans: directly from preimplantation embryos, by reprogramming somatic cells, and by conversion of established primed hESCs. To date, different groups have reported various culture conditions (with or without transfection) for the establishment of naïve hESCs [6–14], but only limited successes have been obtained thus far for the direct derivation of naïve hESC lines from the preimplantation stage in human [7, 13]. The growing number of studies reporting new culture conditions enabling successful conversion of primed hESCs towards the naïve state implies that multiple routes can lead to the induction of naïve pluripotency in hESCs both at molecular and epigenetic level [14, 15]. Remarkably, the golden combination of 2i, together with leukemia inhibitory factor (LIF) and/or basic fibroblast growth factor (bFGF) seems to be indispensable for promoting the naïve state in hESCs.

We recently described a fast and reproducible new method to induce the naïve state of pluripotency in hESCs by introducing a novel combination of small molecules and growth factors in the culture medium (2i, LIF, basic fibroblast growth factor, ascorbic acid, and forskolin), without the need for transgene induction [14].

2 Materials

2.1 Tissue Culture

1. CD1 mice (*see* **Note 1**).
2. Surgical scissors.
3. Dissecting forceps.
4. 23G hypodermic needles.
5. 1 mL, 200 μL, 100 μL, 20 μL, 2 μL micropipettes.
6. 1 mL, 200 μL, 20 μL, 10 μL micropipette tips.
7. 60 mm Tissue culture treated dishes.
8. 12-well, 6-well culture plates.
9. Center-well culture plates.
10. 15 and 50 mL conical centrifuge tubes.
11. T25 (25 cm^2 surface area) and T75 (75 cm^2 surface area) tissue culture treated flasks with filter cap.
12. 2, 5, 10 mL plastic disposable pipettes.
13. Pipette controller.
14. 9 in., glass Pasteur pipettes. Sterilize at 140 °C for 4 h.
15. 0.2 μm disposable syringe filter units.

16. 10 mL disposable syringes.
17. 200, 500, and 1500 μL collection tubes.
18. 250 and 500 mL disposable filter units.
19. 2 mL cryovials.
20. 1 °C cryovial freezing container.
21. Vacuum aspirator for tissue culture.
22. Benchtop tissue culture centrifuge.
23. Stereomicroscope.
24. Inverted tissue culture microscope.
25. Water bath.
26. Hemocytometer.
27. Oven for heat sterilization.
28. Liquid nitrogen.
29. Liquid nitrogen storage tank.
30. Glass beads (*see* **Note 2**).
31. CO_2 humidified incubator with N_2 source.
32. Dulbecco's phosphate buffered saline, calcium and magnesium free (DPBS), 1× liquid. Store at 4 °C.
33. 0.05 and 0.25 % trypsin–EDTA (1×, vol/vol). Store at 4 °C.
34. 200 mM L-glutamine. Store at −20 °C.
35. Penicillin–streptomycin (P/S, 10,000 U/mL). Store at −20 °C.
36. Dulbecco's Modified Eagle Medium (DMEM), high glucose. Store at 4 °C.
37. Dimethyl sulfoxide (DMSO). Store at room temperature in the dark (*see* **Note 3**).
38. Heat-inactivated fetal bovine serum (FBS): Prior to use, incubate FBS for 30 min at 56 °C (*see* **Note 4**).
39. MEF culture medium: Add 50 mL heat inactivated FBS, 5 mL L-glutamine and 5 mL of penicillin–streptomycin to 450 mL DMEM, vacuum-filter. Store at 4 °C for up to 2 weeks.
40. MEF freezing medium: Add 20 % heat inactivated FBS and 20 % DMSO to 60 % DMEM (*see* **Note 5**).
41. Trypan blue solution, 0.4 % (*see* **Note 6**).
42. 70 % ethanol (vol/vol) in sterile water.
43. Gelatine, 0.1 % (wt/vol): Dissolve 500 mg of gelatine in 500 mL of sterile water. Incubate in water bath at 37 °C overnight to ensure gelatine is thoroughly dissolved. Vacuum-filter. Store at 4 °C for up to 4 months.

44. 1× PBS: Dilute 50 mL of 10× PBS in 450 mL sterile filtered water. Store at room temperature.
45. Mitomycin C from *Streptomyces caespitosus* solution: Dissolve 2 mg of Mitomycin C in 2 mL 1× PBS. Add solution to 200 mL of DMEM. Vacuum-filter. Store 8 mL aliquots at −20 °C.
46. KnockOut DMEM (KO-DMEM). Store at 4 °C.
47. KnockOut serum replacement. Store at −20 °C.
48. MEM nonessential amino acids (100×). Store at 4 °C.
49. β-mercaptoethanol (*see* **Note** 7). Store at 4 °C.
50. Bovine serum albumin (BSA). Store at 4 °C.
51. Basic fibroblast growth factor (bFGF): Spin down the vial. Dissolve the lyophilized powder in 500 μL 5 mM TRIZMA® HCl. Add 500 μL 1× PBS and 0.1 % BSA (wt/vol). Ensure the lyophilized powder has completely dissolved before aliquoting in 5 μL volumes. Store at −20 °C.
52. PD 0325901: Spin down the vial and reconstitute by dissolving in 2.071 mL of DMSO. For a 1 μM concentration, add 1 μL/mL of medium. Store at −20 °C.
53. CHIR 99021: Spin down vial and reconstitute by dissolving in 860 μL DMSO. For a 3 μM concentration, add 0.6 μL/mL of medium. Store at −20 °C.
54. Leukemia inhibitory factor, human, 1000 U (LIF): Add 1 μL/mL of medium. Store at 4 °C.
55. L-Ascorbic acid, 50 ng/mL: Weigh 0.005 g and dissolve in 100 mL of water. Store at 4 °C for up to 2 weeks.
56. Forskolin: Dissolve 10 mg forskolin in 2.436 μL DMSO. For a 10 μM concentration add 1 μL/mL of medium. Store at −20 °C.
57. Y27634 (ROCKi): Dissolve 5 mg Y27634 in 1.56 mL DMSO. For a 10 μM concentration add 1 μL/mL of medium. Store at −20 °C.
58. hESC Media: 1× KO-DMEM, 20 % KOSR, 1 % MEM nonessential amino acids, 1 % penicillin–streptomycin, 0.1 mM L-glutamine, 0.1 mM β-mercaptoethanol, and 4 ng/mL of bFGF. For 200 mL: To 160 mL of 1× KO-DMEM, add 40 mL KOSR, 2 mL MEM nonessential amino acids, 2 mL penicillin–streptomycin, 2 mL L-glutamine, 400 μL β-mercaptoethanol, and 16 μL of bFGF. Store at 4 °C for up to 2 days.
59. Naïve Conversion Medium (NCM): 1× KO-DMEM, 20 % KOSR, 1 % MEM-NEAA, 1 % P/S, 0.1 mM L-glutamine, 0.1 mM β-mercaptoethanol, 12 ng/mL bFGF, 1 μM PD 0325901, 3 μM CHIR 99021, 10 μM forskolin, 50 ng/mL

L-ascorbic acid, and 1000 U human LIF. For 10 mL: to 10 mL hESC medium, add 2.4 μL bFGF, 10 μL PD 0325901, 6 μL CHIR 99021, 10 μL forskolin, and 10 μL LIF. Store at 4 °C for up to 2 days.

60. Slow freezing medium, hESC medium or NCM: 10 % DMSO, supplemented with 1 μM Y27634. For 10 mL, add 10 μL Y27634 to 10 mL hESC medium. Make prior to freezing and use immediately.
61. Thawing medium: hESC Medium or NCM, supplemented with 1 μM Y27634. For 10 mL, add 10 μL Y27634 to 10 mL hESC medium. Store at 4 °C for up to 2 days.
62. Collagenase (0.1 % wt/vol): Dissolve 0.1 g of collagenase in 100 mL KO-DMEM. Vacuum-filter-sterilize, aliquot and store at −20 °C.

2.2 Karyotyping

1. Measuring flask.
2. Sterile deionized water.
3. 500 mL and 1 L glass screw cap bottle.
4. Fume hood.
5. Dark glass bottle.
6. Magnetic stirrer with heating plate.
7. Magnetic stirrer bars.
8. Heating plate.
9. Oven.
10. Parafilm.
11. Whatmann filter N°1.
12. Glass Slide Holder.
13. Styrofoam Box.
14. Ice blocks.
15. Versene Solution.
16. Colcemid solution: Dissolve colcemid in Hanks Balanced Salt Solution with Phenol Red at 10 μg/mL concentration. Make 1 mL aliquots and store at 4 °C (*see* **Note 8**).
17. 95 % Hypotonic solution: For 1 L, dissolve 9.5 g of sodium citrate (0.05625 M) in 800 mL deionized water. Stir on a magnetic stirrer for at least 30 min. Transfer the solution to a measuring flask and add sterile deionized water to make up to 1 L. Seal the flask with Parafilm and gently mix the solution. Filter the solution into a sterilized 1 L bottle with a screw cap. Store at 37 °C.

18. HCl, 0.1 M: Add 25 mL of 1 M HCl to 225 mL sterile deionized water in a glass screw cap bottle. Store at room temperature for 1 day (*see* **Note 9**).
19. Fixative: methanol–glacial acetic acid, >99 % in a 3:1 ratio (*see* **Note 10**). Store at −20 °C.
20. Phosphate buffer (PB) (pH ± 6.8): For 500 mL, weigh 2.96625 g of $Na_2HPO_4{\cdot}2H_2O$ and 2.2675 g KH_2PO_4. Dissolve in 400 mL of sterile deionized water in a 500 mL glass screw cap bottle. Stir on a magnetic stirrer for at least 30 min. Transfer the solution to a measuring flask and add sterile deionized water to make up volume to 500 mL. Seal with Parafilm and mix the solution gently. Store at room temperature for up to 2 weeks.
21. Saline sodium citrate buffer (SSC): For 250 mL, in a 500 mL glass screw cap bottle, dissolve 2.19 g of NaCl and 1.105 g of $C_6H_5Na_3{\cdot}2H_2O$ (Trisodium citrate) in 250 mL of sterile deionized water. Store at room temperature for up to 2 weeks.
22. Leishman stock solution: For 50 mL, weigh 0.1 g of Leishman's stain (Eosin-Methylene blue). Working in a fume hood, dissolve the powder in 50 mL methanol. Stir on a magnetic stirrer for at least 2 days at room temperature. Working in a fume hood, filter the solution over a double Whatmann filter N°1 into a dark screw cap glass bottle. Store at room temperature for up to 2 weeks in the dark.
23. Leishman working solution: Dilute the Leishman stock solution in phosphate buffer in a 1:3 ratio. Add 50 mL Leishman stock solution to 150 mL PB. Store at room temperature. Make fresh each time and use immediately.
24. 5 % Trypsin stock solution: Dissolve 0.1 g of Difco™ Trypsin 250 in 2 mL sterile deionized water. Make 85 µL aliquots and store at −20 °C for up to 6 months.
25. Trypsin working solution: Add 10 µL of trypsin from the above prepared aliquots to 100 mL of phosphate buffer (pH 6.8) in a glass slide holder. Mix well. Store at 37 °C for 1 day.

2.3 Alkaline Phosphatase Assay for Pluripotency

We apply the protocol as suggested by the manufacturer for the Alkaline Phosphatase Staining Kit II, Stemgent.

1. Phosphate Buffered Saline with Tween® 20 (PBST) solution: add 5 µL Tween® 20 to 10 mL 1× PBS in a 15 mL conical tube to make a final concentration of 0.05 %. Mix thoroughly and store at room temperature.
2. Alkaline Phosphatase substrate solution: for one well of a 6-well culture plate, mix 0.5 mL of Solution A and 0.5 mL of Solution B in a 15 mL conical tube. Incubate at room temperature for 2 min and add Solution C (*see* **Note 11**).

2.4 Immunocytochemistry Assay for Pluripotency

1. Glass coverslips, round 13 mm.
2. Center-well organ culture dish (*see* **Note 12**).
3. 4-well tissue culture plate.
4. Magnetic stirrer with heating plate.
5. Magnetic stirrer bars.
6. Glass beaker.
7. pH meter with probe.
8. Aluminum foil.
9. Parafilm.
10. Plastic box with lid.
11. Glass microscope slides.
12. Glass slide staining dish.
13. Lint-free microscope and slide tissue paper.
14. Coverslip sealant.
15. 4 % paraformaldehyde (PFA): Add 150 mL of 1× PBS to a glass beaker and heat to 60 °C while gently stirring on a magnetic stirrer for about 15 min. Cover the beaker with aluminum foil. Weigh 8 g of PFA (*see* **Note 13**). Add PFA to the heated 1× PBS solution and continue stirring gently at 60 °C. Gradually add 1 M Sodium Hydroxide (NaOH) dropwise with a pipette until the solution becomes clear (*see* **Note 14**). Once PFA has dissolved, cool the solution for approximately 1 h at room temperature.
16. Calibrate pH meter as per manufacturer's instructions. Adjust the pH of the PFA solution to pH 6.9 by adding 1 M HCl. Bring the solution to a final volume of 200 mL with 1× PBS. Store aliquots at −20 °C.
17. Permeability Solution: 0.1 % Triton X in 1× PBS (vol/vol). Add 10 μL of Triton X to 10 mL of 1× PBS (*see* **Note 15**). Mix well to ensure Triton X is dissolved in solution. Store at 4 °C for 1 week.
18. Blocking solution: 0.05 % Tween® 20 (vol/vol), 1 % bovine serum albumin (BSA) (wt/vol) in 1× PBS (*see* **Note 16**). Weigh 0.1 g of BSA and dissolve in 10 mL 1× PBS. Add 5 μL Tween (*see* **Note 17**). Store at 4 °C for 1 week.
19. Primary Antibodies: The antibody combination includes two nuclear markers (*see* **Note 17**). The primary antibody is Oct3-4 (mouse monoclonal IgG) with Nanog (rabbit polyclonal IgG) (*see* **Note 18**). Prepare antibody dilutions in blocking solution, as per manufacturer's instructions. Store as per manufacturer's instructions.

20. The corresponding fluorescence-conjugated secondary antibodies include donkey anti-Mouse IgG polyclonal (Excitation 495 nm, Emission 519 nm) and donkey anti-rabbit polyclonal (Excitation 590 nm, Emission 617 nm) (*see* **Note 19**). Prepare antibody dilutions in blocking solution, as per manufacturer's instructions. Store as per manufacturer's instructions.
21. Mounting medium, Vectashield® containing 4′,6-diamidino-2-phenylindole (DAPI) (*see* **Note 20**): DAPI is a convenient nuclear counterstain as it binds to DNA. It has an absorption maximum at 358 nm and fluoresces blue at an emission maximum of 461 nm.
22. Fluorescence microscope with appropriate fluorophore filters.

2.5 Quantitative Real-Time PCR

1. DNA LoBind tubes.
2. PCR cabinet with UV source.
3. Vortex.
4. Mini-centrifuge.
5. Crushed ice.
6. TRIzol® (Life Technologies).
7. RNeasy mini kit for RNA extraction. Note: For our experiments we use (QIAGEN). However, depending on preference, other commercially available kits are also suitable.
8. RNAse away (Life Technologies).
9. Rnase-free DNase Set (QIAGEN).
10. Vivacon columns (Sartorius).
11. iSCript™ Advanced cDNA synthesis kit for RT-qPCR (Bio-Rad).
12. Qubit 2.0 fluorometer (Life Technologies).
13. Qubit ssDNA kit.
14. Qubit Assay tubes.
15. DEPC-treated water.
16. iTaq™ Universal SYBR® Green Supermix.
17. iTaq™ Universal Probes Supermix.
18. 6-FAM-probe (*see* Table 1).
19. Assays of interest (*see* Table 1).

Table 1
Overview of the housekeeping genes, primer sequences, and kits used for quantitative real-time PCR

Housekeeping genes		Primer sequences	Kit used
GAPDH	Glyceraldehyde-3-phosphate dehydrogenase	*F*: AGCCTCAAGATCAGCAATG *R*: ATGGACTGTGGTCATGAGTCCTT	iTaq™ Universal Probes Supermix
Probe	6-FAM-probe	CCAACTGCTTAGCACCCCTGGCC	
B2M	β-2-microglobulin	*F*: TGCTGTCTCCATGTTTGATGTATCT *R*: TCTCTGCTCCCCACCTCTAAGT	iTaq™ Universal SYBR Green Supermix
RPL13A	Ribosomal protein L13A	*F*: CCTGGAGGAGAAGAGGAAAGAGA *R*: TTGAGGACCTCTGTGTATTTGTCAA	
Pluripotency assay		Primer sequences	Kit used
OCT4	Octamer-binding transcription factor 4/POU5F1	Hs01895061_u1 (Taqman® gene expression assay)	iTaq™ Universal Probes Supermix
NANOG	Homeobox protein NANOG	Hs02387400_g1 (Taqman® gene expression assay)	
KLF4	Kruppel-like factor 4	*F*: TACCAAGAGCTCATGCCACC *R*: CGCGTAATCACAAGTGTGGG	iTaq™ Universal SYBR Green Supermix
KLF2	Kruppel-like factor 2	*F*:CACACAGGTGAGAAGCCCTA *R*:GCACAGATGGCACTGGAATG	
ZFP42	Zinc finger protein	*F*:CAGTCCAGCAGGTGTTTGCT *R*: TGGCTCATGTTTTCCTGCCT	
PECAM1	Platelet/endothelial cell adhesion molecule 1	*F*: GAGCATATACTGGTCGCCCC *R*: TGAGTCTAGGTCGGGGAGTG	
DPPA3	Developmental pluripotency associated 3	*F*: CCGATGGACCCATCACAGTT *R*:ATTTGAGAGGCCCCTGAATCG	
XIST	X (inactive)-specific transcript	*F*: AATGACTGACCACTGCTGGG *R*: GTGTAGGTGGTTCCCCAAGG	
ESRRB	Estrogen-related receptor beta	*F*: GCCATGATGGAAAATGCCCC *R*: CCAGAGATGCTTTCCCTGGC	

3 Methods

All procedures are to be carried out at room temperature in a laminar flow cabinet, unless otherwise specified. Ensure to use aseptic tissue culture techniques throughout. Ensure that all solutions are prepared using tissue culture/embryo grade reagents and water (endotoxin free). All incubations should be performed in a humidified incubator at 37 °C, 5 % CO_2 in hypoxic conditions, 5 % O_2.

3.1 Mouse Embryonic Fibroblast (MEF) Isolation (See Note 21)

1. Purchase 12 days pregnant CD1 mice (*see* **Note 22**). Embryos should be harvested between gestational day 12.5 and 14.5.
2. Incubate fresh T75 tissue culture flasks with 20 mL of MEF culture medium.
3. Sacrifice pregnant female mice (*see* **Note 23**) at approximately day 13.5 of gestation.
4. Use dissecting forceps and scissors to carefully remove uterine horns and transfer into 60 mm tissue culture dish.
5. Dissect embryos from the uterus (*see* **Note 24**).
6. Transfer embryos to fresh 60 mm tissue culture dish and wash with 1–2 mL of DPBS.
7. Carefully cut away embryo head and liver with scissors (*see* **Note 25**).
8. Remove all blood clots from embryo and wash with 1–2 mL of DPBS.
9. Transfer remaining tissues into fresh 60 mm tissue culture dish.
10. Finely mince the tissue with needles (*see* **Note 26**).
11. Add 2 mL of 0.25 % trypsin–EDTA.
12. Incubate at 37 °C for 10 min, manually shaking one to two times (*see* **Note 27**).
13. Inactivate trypsin–EDTA by adding equal volume of MEF culture medium (2 mL).
14. Collect the cell suspensions in a 15 mL conical tube and pellet cells by centrifugation at 1000 × *g* for 5 min.
15. Carefully take off the supernatant and resuspend cells in 1 mL MEF medium.
16. Seed cells into prepared T75 flasks. Place in incubator. This is regarded as passage 0 (*see* **Note 28**).
17. Culture cells until flask is confluent (*see* **Note 29**).
18. Change medium after first day and every alternate day thereafter.

3.2 MEF Passaging

1. Incubate fresh T75 tissue culture flasks with 20 mL of MEF culture medium.
2. Pre-warm 0.25 % trypsin–EDTA to room temperature.
3. Remove the medium from the MEF culture flask and wash with calcium, magnesium free DPBS (*see* **Note 30**).
4. Remove DPBS and add 3 mL of 0.25 % trypsin–EDTA to cover the entire culture flask surface.
5. Incubate for 5 min.
6. Lightly tap the bottom of the flask (*see* **Note 31**).
7. Neutralize the trypsin by adding an equal volume of MEF culture medium (6 mL).
8. Wash the flask wall with MEF culture medium to remove any remaining cells.
9. Transfer to a 15 mL conical tube and centrifuge at 1000 × *g* for 5 min.
10. Resuspend the pellet in 2 mL of MEF culture medium.
11. Seed cells into prepared T75 flasks, now regarded as passage 1 (*see* **Note 32**).
12. Culture cells until flask is confluent (takes approximately 3 days).
13. Repeat steps for another two passages, i.e., passage 3.

3.3 MEF Freezing

For greater convenience and time-efficiency, freeze large stocks of MEFs at passage 3 (*see* **Note 33**). This will eliminate the need of coordinating MEF preparations with hESC manipulations.

1. Repeat **steps 2–7** of the MEF passaging protocol.
2. Count cells using a hemocytometer (use 10 μL of cell suspension and 10 μL of trypan blue).
3. Calculate amount of MEF freezing medium required at 3×10^6 cells/mL.
4. Centrifuge suspension at 1000 × *g* for 5 min.
5. Add MEF freezing medium dropwise (*see* **Note 34**).
6. Mix gently.
7. Dispense into cryovials in 1 mL aliquots.
8. Place vials in liquid nitrogen vapor for 1 h (*see* **Note 35**).
9. Store vials at −80 °C overnight and transfer to a liquid nitrogen storage tank (*see* **Note 36**).
10. Thaw one vial for confirmation of cell viability (*see* **Note 37**).

3.4 MEF Thawing

1. Incubate fresh T75 tissue culture flasks with 20 mL of MEF culture medium.
2. Thaw cells by placing cryovials in a 37 °C water bath until few ice crystals remain.
3. Disinfect vial with 70 % ethanol.
4. Transfer thawed MEFs dropwise into a conical tube containing 12 mL of MEF culture medium (*see* **Note 38**).
5. Centrifuge at 1000 × *g* for 5 min (*see* **Note 39**).
6. Carefully remove supernatant and resuspend pellet in 2 mL of MEF culture medium and mix thoroughly to ensure single cell suspension.
7. Transfer MEF suspensions to preprepared T75 culture flasks and incubate.
8. Culture until cells reach confluency (3–4 days) (*see* **Note 40**).

3.5 MEF Inactivation and Feeder Layer Seeding

3.5.1 Mitomycin C Treatment

1. Ensure MEFs have reached confluency.
2. Pre-warm Mitomycin C solution to 37 °C.
3. Remove MEF-medium and add Mitomycin C. Use 8 mL Mitomycin C solution per T75 flask.
4. Incubate for 2.5–3 h at 37 °C (*see* **Note 41**).

3.5.2 Gelatine Coating

1. Cover the entire culture surface a T25 flask with 0.1 % gelatine solution (*see* **Note 42**).
2. Incubate for 1 h at room temperature.

3.5.3 MEF Seeding

1. Pre-warm 0.25 % trypsin–EDTA, calcium and magnesium free DPBS and MEF culture medium to room temperature.
2. Remove Mitomycin C solution (*see* **Note 43**) and wash two times with 10 mL DPBS.
3. Trypsinize as if passaging (*see* **steps 2–9** of Sect. 3.2).
4. Resuspend the pellet in 4 mL of MEF culture medium.
5. Count cells using a hemocytometer (use 10 μL of cell suspension and 10 μL of trypan blue).
6. Calculate final concentration of MEFs required depending on the surface area of the culture vessel, at 2.5×10^4 cells per 1 cm^2 in 1 mL volume of MEF medium.
7. Aspirate remaining liquid gelatine from the coated culture vessel.
8. Add appropriate volume of diluted MEF solution into each gelatine-coated culture vessel.
9. Incubate overnight prior to use (*see* **Notes 44** and **45**).

3.6 Manual Passage of hESCs

1. Check freshly prepared MEF feeder flask for attachment.
2. Incubate hESC medium at room temperature (*see* **Notes 46** and **47**).
3. Prepare a phase contrast microscope by wiping the complete working surface with 70 % ethanol (vol/vol) and place it in a laminar flow.
4. Refresh the freshly prepared MEF fed flask with the equilibrated hESC medium and incubate at 37 °C.
5. Prepare a 23G needle by bending it at a 65°–90° angle (*see* **Note 48**).
6. Observe the hESC culture under the microscope to select the undifferentiated colonies for passage.
7. Aspirate the spent medium in the hESC flask and refresh with freshly prepared hESC medium.
8. Using the prepared needle, cut the colonies horizontally and vertically to make a checkered pattern of appropriate size (*see* Fig. 1).
9. Scrape the sections of colonies gently without scratching the plastic underneath the colonies (*see* **Note 48**).
10. Swirl the culture dish, in a circular motion and transfer the cut colonies using a P200 pipette into the freshly prepared MEF flask.
11. Observe attachment after 24 h and change half the volume of spent medium in the flask with freshly prepared medium (*see* **Note 49**).
12. Culture for 4–6 days (*see* **Note 50**) until cells reach confluency. Then passage onto a freshly prepared MEF feeder flask.

3.7 Enzymatic Passage of hESCs

1. Check freshly prepared MEF flask for attachment.
2. Prepare an inverted phase contrast microscope by disinfecting all surfaces with 70 % ethanol (vol/vol).
3. Equilibrate DPBS (calcium, magnesium free), hESC medium and an aliquot of collagenase to room temperature (*see* **Note 47**).
4. Check for confluency of hESCs and prevalence of any differentiated colonies (s*ee* **Note 50**).
5. Discard the spent MEF medium from the new MEF prepared flask and refresh with an appropriate volume of hESC medium (*see* **Note 49**) and incubate at 37 °C.
6. Rinse the cells with calcium, magnesium free DPBS (*see* **Note 30**) and discard.
7. Add an appropriate volume of 0.1 % collagenase gently. Incubate at 37 °C for 5–6 min (*see* **Note 51**).

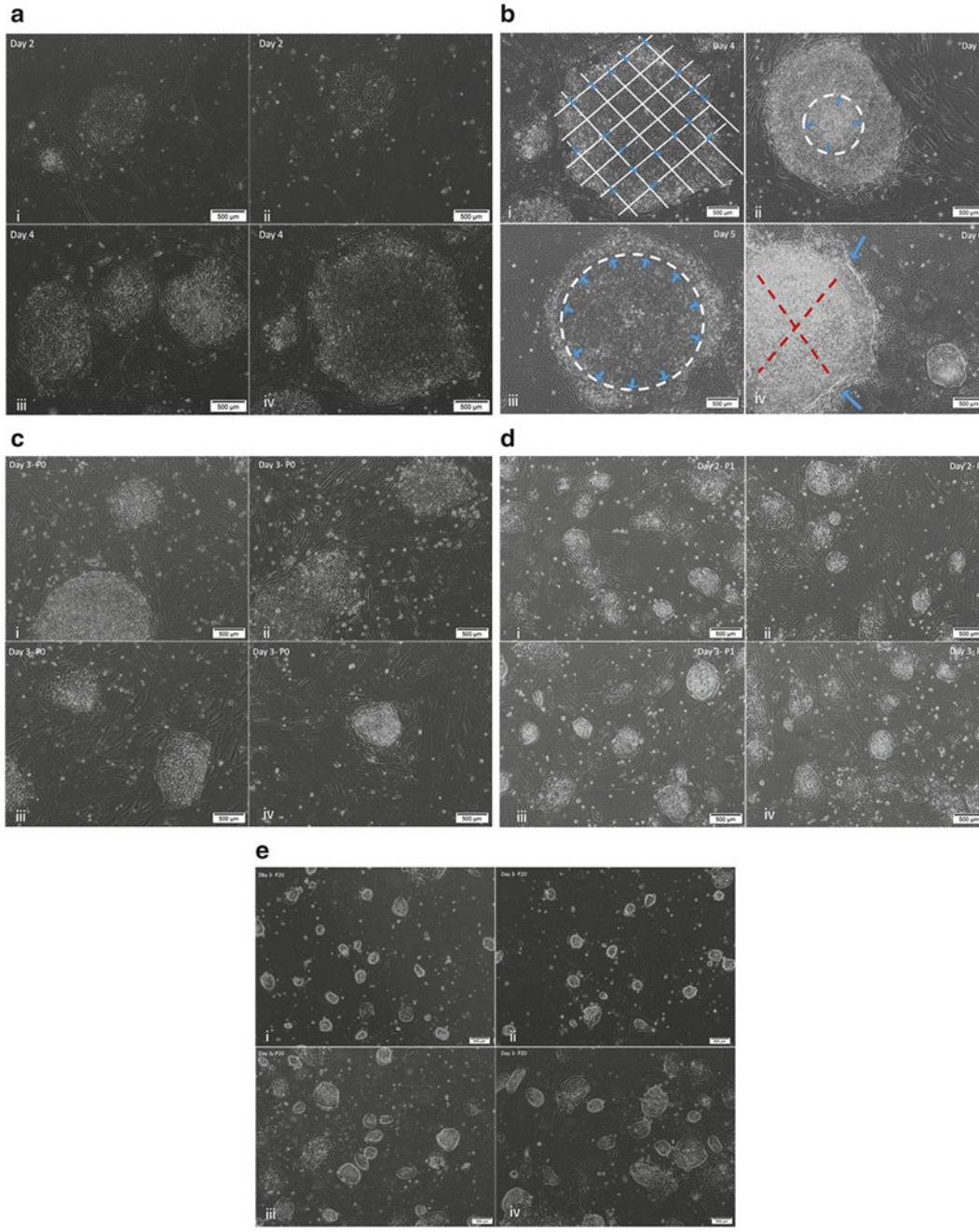

Fig. 1 Primed and naïve hESC morphology in naïve conversion medium (NCM). (**a**) (*i*, *ii*) Early colonies 2 days post splitting using collagenase on MEFs. (*iii*, *iv*) Well defined colonies 4 days post splitting using collagenase on MEFs. The colonies are now ready for the next passage. (**b**) (*i*) Manual passage of primed hESCs using a 23G needle or stem cell cutting tool. (*ii*) Primed hESC colony differentiating at the center. (*iii*) Primed hESC colony differentiating at the edges. (*iv*) *Red cross* indicates differentiated colony for excision. *Blue arrows* indicate direction for cutting the colony. (**c**) P0 hESC colonies in NCM condition on day 3 post splitting using collagenase. (**d**) P1, Mixed population of domed and flat colonies post single cell passaging of P0 cultures using trypsin. (**e**) Late passage well-defined domed naïve hESCs in NCM culture condition

8. Observe the colonies under the microscope. Once cell-cell contact seems diminished, add sterilized glass beads to culture flask to break the colonies into smaller fragments.
9. Neutralize the collagenase with double the volume of hESC medium and collect the cell suspension in a 15 mL conical tube.
10. Centrifuge at 200 × *g* for 5 min. Aspirate and discard the spent medium.
11. Gently resuspend the cell pellet in 2 mL hESC medium.
12. Transfer an appropriate volume of the resuspended cell suspension to the freshly prepared MEF flask.
13. Gently shake the flask to evenly distribute the cells clumps and incubate at 37 °C (*see* **Note 52**).
14. Refresh the flask with half the volume of hESC medium after 24 h. Culture for 4–6 days until cells reach confluency (*see* **Note 50**).

3.8 Naïve hESC Conversion of Primed hESCs

1. To start conversion, check if parental primed hESC culture flask is confluent and manually cut out any differentiated colonies (*see* **Note 48**).
2. Passage enzymatically using 0.1 % collagenase (*see* **Note 51**).
3. Aspirate MEF medium from the freshly prepared MEF culture flask and replace with naïve conversion medium (NCM). Incubate at 37 °C.
4. Resuspend cell pellet after centrifugation in 2 mL NCM. Transfer an appropriate volume of cell suspension into the new MEF feeder flask (*see* **Note 52**).
5. Observe attachment, refresh half the volume after 24 h and everyday thereafter (*see* **Note 53** and Fig. 1c).

3.9 Passaging Naïve hESCs

1. The primed cells cultured in NCM will be ready to passage within 5–6 days post plating (*see* **Note 53**).
2. Check for confluent cultures, aspirate spent medium and wash with calcium, magnesium free DPBS.
3. Add an appropriate volume of 0.05 % trypsin–EDTA (vol/wt) to cover the cell culture surface and incubate at 37 °C for 5 min (*see* **Note 54**).
4. Using a P200 pipette, triturate the cells to ensure single cell population and neutralize the trypsin–EDTA using double the volume of NCM (*see* **Note 55**).
5. Collect the neutralized cell suspension in a 15 mL conical tube and centrifuge at 200 × *g* for 5 min.

6. Aspirate the spent medium and resuspend in 2 mL NCM. Using the P200 pipette resuspend the cells to further ensure a single cell population.
7. Distribute the cells into a freshly prepared MEF feeder flask.
8. The culture can then be passaged every 3–4 days (*see* **Notes 56** and **57** and Fig. 1d, e).

3.10 Cryopreservation of Naïve and Primed hESCs

1. Label and annotate cryovials with relevant information (*see* **Note 58**). Prechill the tubes at 4 °C.
2. Prepare hESC freezing medium.
3. Change the medium in the hESC culture flask with hESC freezing medium and incubate at 37 °C for 1 h.
4. Manually cut out any differentiated colonies (*see* Steps).
5. Split the cells as mentioned above enzymatically or manually and centrifuge at 200 × *g* for 5 min (*see* **Note 59**).
6. Aliquot 1 mL freezing medium into prechilled cryovials.
7. Resuspend the cells in 1 mL hESC medium or NCM with ROCKi.
8. Distribute cells in the prechilled cryovials containing freezing medium (s*ee* **Note 60**).

3.11 Thawing of hESCs

1. Equilibrate 12 mL hESC thaw media or NCM with ROCKi at room temperature in a 15 mL conical tube.
2. Aspirate MEF medium from MEF feeder 6-well plate and wash with calcium, magnesium free DPBS.
3. Aspirate the calcium, magnesium free DPBS and replace with 2 mL hESC medium (with 4 ng/mL bFGF and 10 μM ROCKi) and incubate at 37 °C.
4. Select a cryovial of frozen hESCs from the liquid nitrogen tank and place it on a prechilled rack.
5. To thaw, incubate vial in a prewarmed water bath (37 °C), until only a small ice crystal is observed.
6. Disinfect the vial and transfer the contents to the 15 mL conical tube (*see* **Note 61**).
7. Centrifuge the cell suspension at 200 × *g* for 5 min.
8. Aspirate the spent medium gently, without disturbing the pellet of hESCs.
9. Resuspend the pellet in 2 mL thawing medium.
10. Transfer the 2 mL cell suspension to the freshly prepared MEF plated culture plate. Gently swirl the plate in a figure-eight to evenly distribute the clumps of cells (s*ee* **Note 52**).

11. After 24 h, observe if the cells have attached and refresh the medium with an appropriate volume of hESC medium (without ROCKi, 2 mL/well of a 6-well plate). Feed the cells daily with fresh medium.
12. Once confluent colonies are observed (*see* **Note 62**), passage the colonies manually to freshly prepared MEF prepared culture flasks.

3.12 Karyotyping Naïve and Primed hESCs

3.12.1 Arresting Cell Cycle at Metaphase

1. Culture hESC until confluency in a T25 flask at the desired passage number.
2. Add 8 μL of 10 μg/mL Colcemid to 5 mL hESC medium or NCM and store at room temperature (*see* **Note 8**).
3. Aspirate the spent medium from the culture flask and wash twice with 1× PBS.
4. Replace with 5 mL Colcemid containing medium.
5. Incubate for 16 h at 37 °C.

3.12.2 Producing Single Cell Populations

1. Set water bath at 37 °C.
2. Collect the Colcemid solution from the culture flask using a 5 mL pipette in a 15 mL conical tube. Wash the cells with 2 mL Versene and transfer the Versene to the same 15 mL conical tube.
3. Incubate the cell culture in 2 mL 0.05 % trypsin–EDTA for 5 min at 37 °C (*see* **Note 63**).
4. Neutralize the trypsin using the collected medium (with Versene). Transfer cell suspension to the 15 mL conical tube and centrifuge for 10 min at 122 × *g* (*see* **Note 64**).

3.12.3 Fixation of the Cells

1. Aspirate the supernatant and add 8 mL hypotonic solution (*see* **Note 65**).
2. Resuspend the pellet by titrating, using a 1000 μL tip and incubate for 20 min at 37 °C.
3. Add ±2 mL fixative using a glass pipette and vortex thoroughly (*see* **Note 66**).
4. Incubate for 10 min at room temperature.
5. Centrifuge for 10 min at 122 × *g*.
6. Aspirate the fixative to a waste tube, using a glass pipette.
7. Repeat **steps 1–3** three times (*see* **Note 66**).
8. Meanwhile, annotate a new 15 mL conical tube for storage (*see* **Note 64**).
9. Transfer the fixative to a waste tube, using a glass pipette.
10. Resuspend the pellet in 2–8 mL fixative and transfer the fixed cells to the new 15 mL conical tube.

11. Store the fixed cell suspension at −20 °C for at least 1 h, preferably overnight.
12. Clean required number of microscope slides with detergent, then deionized water and place them in a slide rack at −20 °C (*see* **Note 67**). Perform this a few hours before commencing with the protocol.
13. Switch-on the humidity chamber at least 15 min prior to use.
14. Prepare fresh fixative solution.
15. Centrifuge the chilled tubes with fixed samples from the −20 °C freezer for 10 min at 122 × *g* and place them in a precooled ice box or on crushed ice.
16. Place the cleaned and chilled glass slides in a Styrofoam box with ice blocks.
17. Working in a fume hood, aspirate the supernatant from the sample tubes and leave the tube inverted on a paper towel for any residual fixative to leak out.
18. Add 400 μL fresh fixative and triturate the cell pellet using a P200 pipette.
19. Humidify a microscope slide by breathing on it. Hold it vertically, apply 10 μL of the suspension at the top of a microscope slide and let it spread out. Dry the slide on a heating plate.
20. Check the dilution of the suspension and the spread of the chromosomes on a phase-contrast microscope (*see* **Note 68**).
21. To improve the contrast and sharpness of the bands incubate the slides in a black slide box or rack at 65 °C for 24 h or for longer incubation periods at 37 °C (*see* **Notes 69** and **70**).

3.12.4 G-Banding

1. Set an oven at 100 °C and another oven at 90 °C for drying the slides (*see* **Note 71**).
2. Incubate the prepared slides for 10 min at 100 °C and then let the slides cool to room temperature.
3. Incubate the slides in 0.1 M HCl at room temperature.
4. Rinse the slides thoroughly three times in deionized water.
5. Dry the slides for 3–5 min in a 90 °C incubator and then let the slides cool to room temperature.
6. Once cooled incubate the slides in SSC solution for 10 min in a water bath at 55 °C.
7. Rinse thoroughly three times with deionized water and dry the slides in a 90 °C oven for 5 min.
8. While drying the slides, pre-warm 100 mL phosphate buffer in a glass slide holder at 37 °C in a warm water bath.

9. Just before use, add 10 μL trypsin stock solution to the phosphate buffer and mix well. Incubate the slides in the trypsin–-phosphate buffer solution for 5–8 s at 37 ° C (*see* **Note 72**).
10. Dry the slides for 5 min at 90 °C.
11. Working in a fume hood, stain the prepared microscope slide with Leishman working solution for 2–3 min (*see* **Note 73**).
12. Wash off the staining solution with tap water, check the quality of the bands with a light microscope.
13. View the slide at 1000× for further detailed observations (*see* **Note 74**).
14. Repeat **steps 13–16** until the required banding and staining quality is acquired (*see* **Note 75**).
15. Visualization: search for metaphase spreads on the prepared slides (*see* **Note 76**).

3.13 Alkaline Phosphatase Staining Assay for Pluripotency

We use the Alkaline Phosphatase Staining Kit II from Stemgent. For ease of observation we culture hESCs in 6-well or 12-well culture plates.

1. Aspirate the spent culture medium from a culture well of a 6-well plate containing cells and rinse with 2 mL 1× PBST solution.
2. Incubate the cells in 1 mL Fix solution provided in the kit. Incubate at room temperature for 3–5 min (*see* **Note 77**).
3. Without allowing the wells to dry, aspirate the fixative and rinse the well with 2 mL 1× PBST solution.
4. Aspirate the 1× PBST solution and incubate the cells in 1.5 mL of freshly prepared AP Substrate solution. Wrap the plate in aluminum foil. Incubate the cells at room temperature for 8–15 min (*see* **Note 78**).
5. After assessing appropriate incubation period, aspirate the AP Substrate Solution and rinse the stained culture well twice with 2 mL 1× PBST solution.
6. Add 2 mL 1× PBS and observe under an inverted phase contrast microscope. A red or purple stain indicates alkaline phosphatase expression. The plate can be stored at 4 °C.

3.14 Immunocytochemistry for Pluripotency

3.14.1 Preparation of MEF Feeder Cells on Glass Coverslips (See Note 79)

1. Following thawing (as per Sect. 3.4), treat MEF cultures with Mitomycin C (as per Sect. 3.5.1).
2. Prior to Gelatine coating, wash 13 mm coverslips in 70 % ethanol for 5 min and wash the coverslips twice in 0.1 % gelatine (*see* **Notes 80** and **81**).
3. Add 0.5 mL of 0.1 % gelatine to the center well of four organ culture dishes.

4. Place the washed coverslip into the well.
5. Incubate for 1 h at room temperature.
6. Perform remaining steps as per MEF seeding protocol (Sect. 3.5.3).
7. Culture hESCs as per Sects. 3.6–3.9 (*see* **Note 82**)

3.14.2 Cell Fixation

1. Fill 3× 4-well tissue culture plate (*see* **Note 83**) with 500 µL of 1× PBS.
2. Fill additional 4-well tissue culture plate with 0.5 % PFA.
3. Using forceps, carefully transfer coverslips using into first 4-well culture dish, 1 per well.
4. Keep coverslips in 1× PBS for 5 min.
5. Repeat **steps 3** and **4** for second 1× PBS 4-well culture dish.
6. Transfer coverslips to 4 % PFA for 20 min at room temperature for fixation (*see* **Note 84**).
7. Transfer to third 1× PBS filled 4-well culture dish.
8. If required, wrap dish in Parafilm and store at 4 °C in 1× PBS (*see* **Note 85**).

3.14.3 Staining with Primary Antibodies

1. Calculate total volume of primary antibody solution based on number of coverslips × 50 µL, i.e., 200 µL for four coverslips and dilution recommended by manufacturer (*see* **Note 86**).
2. Prepare primary antibody solution (*see* **Note 86**).
3. Fill 4× 4-well culture dishes with 500 µL of 1× PBS solution.
4. Fill 1× 4-well culture dish with permeability solution.
5. Fill 1× 4-well culture dish with blocking solution.
6. Transfer each coverslip to first 4-well dish and keep in 1× PBS for 5 min.
7. Repeat process with second and third 1× PBS 4-well culture dish.
8. Transfer coverslips to permeability solution wells for 8 min at room temperature (*see* **Note 87**).
9. Transfer coverslips to 1× PBS dish for 5 min.
10. Transfer to blocking solution wells for 1 h at room temperature (*see* **Note 88**).
11. Cut a 5 cm × 10 cm piece of Parafilm and press to borders of a plastic box, place damp tissue paper around the edges of the box to maintain moisture (*see* **Note 89**).
12. Aliquot 3× 50 µL drops of primary antibody solution and 1× 50 µL drop of blocking solution onto Parafilm. Ensure box is level.

13. Reverse three coverslips (culture surface facing downwards) onto primary antibody solution drops and one coverslip onto the blocking solution—negative control (*see* **Note 90**).
14. Cover box with lid and store at 4 °C overnight.

3.14.4 Staining with Secondary Antibodies

1. Calculate total volume of secondary antibody solution based on number of coverslips and dilution recommended by manufacturer (*see* **Note 86**). Work in the dark and cover secondary antibody solution with foil.
2. Fill 6× 4-well culture dishes with 1× PBS.
3. Transfer coverslips to first 1× PBS 4-well culture dish for 5 min. Ensure to reinvert coverslips with culture surface facing upwards.
4. Repeat washing step by transferring coverslips to second and then third 1× PBS culture dish for 5 min each.
5. Prepare fresh Parafilm, as per **step 11** of Sect. 3.14.3.
6. From this step forward samples should be protected from light (*see* **Note 91**). Aliquot 4× 50μL drops of secondary antibody solution on Parafilm.
7. Invert coverslips (culture surface facing downwards) onto secondary antibody drops.
8. Incubate for 1 h at room temperature. Keep sample box level and in the dark.
9. Clean microscope glass slides with 100 % ethanol in glass slide staining dish.
10. Wipe slides with lint free slide tissue and air dry.
11. Transfer coverslips to 1× PBS 4-well culture dish for 5 min. Ensure to reinvert slides (culture surface facing upwards).
12. Repeat twice with fresh 1× PBS 4-well culture dish.
13. Make 15 μL Vectashield with DAPI drops on glass slides (*see* **Note 92**).
14. Reverse coverslips onto drops, culture surface facing downwards (*see* **Note 93**). Place the coverslip on an angle and slowly release to avoid air bubbles.
15. Turn on the fluorescent microscope (*see* **Note 94**) and allow to warm up for several minutes prior to use.
16. Place the slides on the microscope and use a 10× phase-contrast objective lens in bright field mode to focus on the cells.
17. Change the filter for fluorescence accordingly to visualize stained cells.

18. Allow slides to dry, aspirate any remaining mounting medium and seal after 2 days with coverslip sealant (*see* **Note 95**). Store at 4 or −20 °C.

3.15 Naïve Pluripotency Gene Expression Analysis

3.15.1 RNA Isolation and Reverse Transcription (See Note 96)

For RNA extraction we apply a combination of TRIzol® reagent and RNeasy Mini kit (Qiagen). We concentrate the cDNA using Vivacon 500 spin columns (Sartorius). Complementary DNA (cDNA) was synthesized using the iScript Advanced cDNA Synthesis kit (Bio-Rad).

1. Passage cells as suggested for primed hESCs and naïve hESCs.
2. Aspirate the supernatant after centrifugation and resuspend the cell pellet in 1 mL cold TRIzol® reagent in a fume hood.
3. Lyse the cells in TRIzol® by vigorously titrating the cell pellet.
4. Freeze lysed cell sample at −80 °C.
5. Cool the centrifuge to 4 °C.
6. Thaw frozen samples (in TRIzol®) to room temperature for 5 min promoting complete dissociation of nucleoproteins.
7. Add 200 µL of chloroform per mL of TRIzol®.
8. Homogenize the samples by vortexing for 10–15 s.
9. Incubate at room temperature for 2–3 min.
10. Centrifuge at 12000 × *g* for 15 min at 4 °C (*see* **Note 97**).
11. Meanwhile, label RNeasy Mini columns and new DNA LoBind tubes. Place the RNeasy Mini columns on the DNA LoBind tubes.
12. Transfer the upper colorless aqueous phase with RNA to fresh DNA LoBind tubes (±450 µL).
13. Add an equal volume of cold 70 % ethanol (±450 µL) and mix by pipetting gently.
14. Transfer up to 700 µL to an RNeasy Mini column and centrifuge for 15 s at 8000 × *g* (*see* **Note 98**).
15. Discard the eluent.
16. If the volume is greater than 700 µL, repeat **step 14**.
17. Discard the eluent and add 350 µL of RW1 buffer to the column.
18. Centrifuge for 15 s at 8000 × *g* and discard the eluent.
19. Prepare DNase incubation mix by adding 10 µL DNase I stock solution to 70 µL RDD buffer. Mix gently by pipetting. Do not vortex (*see* **Note 99**).
20. Add 80 µL of DNase I incubation mix immediately on each column membrane (*see* **Notes 99** and **100**).
21. Incubate for 15 min at room temperature.

22. During the 15 min incubation, prepare fresh collection tubes in a tray with crushed ice.
23. Add 350 µL of RW1 buffer again on the column and centrifuge for 15 s at ≥8000 × *g*.
24. Discard the eluent.
25. Place RNeasy Mini columns in new DNA LoBind tubes on ice.
26. Add 500 µL of RPE buffer diluted in ethanol to the column.
27. Centrifuge for 15 s at ≥8000 × *g* and discard the eluent.
28. Repeat **step 2** and centrifuge for 2 min at ≥8000 × *g*.
29. Discard the eluent and centrifuge again for 1 min at 4 °C at 15000 × *g* to dry the membrane.
30. Meanwhile annotate and prepare new DNA LoBind tubes.
31. Place the columns on the new DNA LoBind tubes.
32. Add 40 µL of RNase-free water to the column membrane and incubate on ice for 2–3 min.
33. Centrifuge for 1 min at ≥8000 × *g* or 15000 × *g*.
34. RNA can now be frozen at −80 °C.
35. Transfer RNA solution into the Vivacon® columns carefully without touching the membrane.
36. Centrifuge at 4 °C for 15 min at 5000 × *g*.
37. Meanwhile thaw the iScript™ Advanced cDNA synthesis kit on ice.
38. Invert the column into a new collection tube and centrifuge at 4 °C for 2 min at 2500 × *g*.
39. Check RNA volume using a P20 pipette and transfer the RNA into a 500 µL DNA LoBind tube (*see* **Note 101**).
40. Add 8 µL of the iScript™ mix to the 500 µL tube containing the concentrated RNA (*see* **Note 102**).
41. Add 2 µL of the iScript™ Reverse Transcriptase enzyme (*see* **Note 102**).
42. Add appropriate volume of Nuclease free water to make the final volume up to 40 µL.
43. Incubate the reaction mix in a thermal cycler using the program, 30 min at 42 °C and 5 min at 85 °C.
44. Prepared cDNA can be frozen at −20 °C.
45. For cDNA concentration determination, ensure all Qubit® reagents are equilibrated to room temperature before use. Work in a relatively dark work space.
46. Prepare Qubit® working solution in a 15 mL conical tube by mixing 1 µL Qubit® reagent and 199 µL Qubit® buffer per sample (*see* **Note 103**).

47. For the standards, distribute 190 μL Qubit® working solution to two Qubit® assay tubes and 10 μL Standards 1 and 2 from the kit respectively, making a final volume of 200 μL.
48. For measuring the cDNA concentration in the sample, distribute 199 μL Qubit working solution to Qubit® assay tube and mix 1 μL of cDNA sample, making a final volume of 200 μL.
49. Vortex all the assay tubes for 2–3 s and incubate at room temperature for 2 min.
50. Measure the standards 1 and 2 respectively first on the Qubit® 2.0 Fluorometer, followed by the samples.

3.15.2 Quantitative Real-Time PCR

1. Thaw the iTaq™ Universal SYBR® Green Supermix, iTaq™ Universal Probes Supermix, gene expression assays of interest and probe if required on ice (*see* Table 1).
2. Dilute the sample cDNA for each gene to a concentration of 10 ng per reaction (*see* **Note 104**).
3. For each reaction of the triplicate, add 200 nM forward primer, 300 nM reverse primer, probe if required, iTaq™ Supermix with or without SYBR Green, depending on the assay of choice, diluted to a final volume of 15 μL using DEPC-treated water.
4. To this mix, add 5 μL diluted cDNA at 10 ng concentration.
5. Pipette 20 μL of cDNA reaction mix, in triplicates per sample, in each well of a qPCR plate.
6. Seal the plate with associated plastic adhesive seal.
7. Cover the plate with aluminum foil.
8. Centrifuge the plate at 3 × *g* for 5 min to collect the cDNA reaction mix at the bottom.
9. Set up qPCR program, 2 min at 96 °C before 45 cycles of 15 s at 95 °C followed by 1 min at 60 °C (*see* **Note 105**).

4 Notes

1. Any mouse strain is suitable as an embryo source. However, inbred mice may produce less embryos per mating compared to outbred strains.
2. Ensure to sterilize glass beads in order to avoid culture contamination. To ensure the glass beads are sterile before use, we treat with 1 M HCl overnight. The HCl is then neutralized with 1 M NaOH. Rinse under running tap water for at least 2 h. Then rinse with sterile water at least four times. Air dry the beads overnight in a laminar flow. Sterilize at 140 °C for 4 h.

3. DMSO is hazardous and toxic. Ensure to handle using personal protective equipment as per product Materials and Data Safety Sheet. Dispose of in accordance with environmental control regulations.
4. Prior to heat inactivation, FBS should be stored at −20 °C in small enough volumes to only thaw and inactivate the amount required. Heat inactivation will eradicate mycoplasmas and other microorganisms, however due to its nutrient rich serum content, storage of larger volumes at 4 °C may support the growth of other contaminants, such as fungi. Furthermore, frequent freeze thaw cycles should be avoided as they may denature critical protein components.
5. Make medium just prior to freezing and use immediately.
6. Trypan Blue is hazardous, toxic and carcinogenic. When handling wear personal protective equipment at all times, as per product Material and Safety Data Sheet and dispose of in accordance with environmental control regulations.
7. β-Mercaptoethanol is hazardous, toxic and corrosive. Handle the compound under a fume hood using personal protective equipment, as per product Materials and Data Safety Sheet. Dispose of in accordance with environmental control regulations.
8. Colcemid depolymerizes microtubules, inhibits spindle formation in the metaphase and also affects the condensation of chromosomes. Hence, the concentration used and incubation period is very crucial. Short incubations could lead to inadequately condensed chromosomes and over exposure would lead to very condensed short chromosomes. Colcemid is highly toxic and possibly mutagenic on skin contact, inhalation and ingestion. Handle the compound under a fume hood using personal protective equipment, as per product Materials and Data Safety Sheet.
9. HCL 0.1 M hydrolyzes disulfide bridges in chromosomal proteins. When handling wear personal protective equipment at all times, as per product Material and Safety Data Sheet and dispose of in accordance with environmental control regulations.
10. Methanol is highly toxic on ingestion, irritating on inhalation and eye contact. In severe cases, it can also cause blindness. Glacial acetic acid is corrosive on contact, ingestion and inhalation can cause irritation. Both are flammable. When handling wear personal protective equipment at all times, as per product Material and Safety Data Sheet and dispose of in accordance with environmental control regulations.
11. Use the Alkaline phosphatase substrate solution within 30 min of preparation.

12. For upscaling, 4-well culture dishes or 12-well culture dishes may also be utilized for culture of hESCs on coverslips and subsequent fixation and immunostaining.
13. Paraformaldehyde is very hazardous in case of skin or eye contact and should not be inhaled. When handling wear personal protective equipment at all times, as per product Material and Safety Data Sheet and dispose of in accordance with environmental control regulations.
14. We recommend adjusting the pH to allow for the paraformaldehyde to dissolve in solution. This method is preferable to heating the solution, as high temperatures may lead to the formation of formic acid, resulting in high background staining.
15. Triton X is very viscous, pipette slowly and following aspiration hold the pipette tip in solution for a few seconds to ensure appropriate volume remains in pipette.
16. The BSA takes time to dissolve. Ensure it is thoroughly dissolved prior to use.
17. Similarly, to Triton X, Tween® 20 is viscous. Follow same technique for accurate pipetting volume (*see* **Note 15**).
18. This combination of primary antibodies evades the need for large cell numbers, while also circumventing cross-reactions between the secondary antibodies. When using multiple primary antibodies, it is critical that they are from different species or alternatively distinct isotypes.
19. When choosing a secondary antibody ensure that it matches the primary antibody. Primary and respective secondary antibody should be from the same species and of the same isotype. When using multiple primary and secondary antibody combination, in order to differentiate the markers, it is critical that the secondary antibody fluorophores emit within different color ranges.
20. We recommend using a mounting media that contains agents that minimize photo-bleaching. Commercially available mounting media containing a nuclear counterstain in solution aid convenience.
21. MEF cultures may also be acquired commercially. Such MEFs may be of benefit for new researchers in the field or for cultures at a smaller scale.
22. Pregnant mice at a specific gestational day can be purchased. We order these mice from Iffa-Credo.
23. Sacrifice of mice should be performed rapidly and humanly by cervical dislocation, with the excretion of pressure to the neck and quick dislocation of the spinal column.

24. The embryos should be weighed and/or measured to ensure that they are at the predicted gestational stage.
25. The brain and dark red organ tissues (i.e., liver) can be used for DNA or RNA extraction, however should not be used for MEF generation.
26. Mincing the tissue too excessively may reduce the cell yield. Ensure embryos are small enough to be aspirated into a 5 or 10 mL pipette.
27. Prolonged exposure of tissue to trypsin should be avoided, as cells may lyse. For optimal results do not process more than five embryos at a time. Ensure all flasks and media are prepared prior to trypsinization.
28. Seed approximately one embryo per T75 flask.
29. Cells will typically grow to confluency in 2–5 days. Monitor cell density by using an inverted microscope.
30. Washing cells removes any traces of serum that may inhibit the action of trypsin.
31. Taping the flask should release all the cells from the culture surface. A loose cell layer is generally visible to the naked eye. If cells do not readily detach, incubate flask for a further 1–2 min.
32. Typically, one confluent T75 flask can be split into two or three T75 flasks.
33. MEFs may also be frozen at passage 1, however will require culture for another 2 passages prior to inactivation, to ensure a pure cell population.
34. This technique will ensure maximum cell survival post thaw.
35. The liquid nitrogen vapor will decelerate the freezing process, allowing cells to maintain viability. Vials should not be snap-frozen in liquid nitrogen.
36. Vials can be stored at −80 °C for several months and in liquid nitrogen long term.
37. It is also good practice to check cultures for Mycoplasma using a PCR-based method or commercially available Mycoplasma Detection Kits.
38. Only add a maximum of two cryovials per 12 mL of MEF medium, i.e., per conical tube.
39. This ensures the removal of cryoprotectant from the culture.
40. Monitor cell density carefully. Culture of passage 3 MEFs beyond confluency may hinder complete inactivation.
41. The duration of the Mitomycin C treatment is critical. Insufficient timing will enable further MEF proliferation, while excessive exposure to Mitomycin C will compromise the MEF culture.

42. Any type of tissue culture flask or dish may be used for MEF seeding, depending on hESC culture requirements. Volume of gelatine solely depends on tissue culture surface area.
43. Mitomycin C is a DNA synthesis inhibitor and is highly toxic. All solutions containing Mitomycin C traces should be handled safely. When handling wear personal protective equipment at all times, as per product Material and Safety Data Sheet and dispose of in accordance with environmental control regulations.
44. If not using MEF dishes within 24 h of inactivation, refresh MEF culture media to remove any unattached/lysed cells.
45. For optimal results ensure to utilize MEF dishes within 2–3 days' post seeding.
46. An aliquot of bFGF is stable for about 3–5 days at 4 °C.
47. Always equilibrate all media and reagents to room temperature before use. To reduce the osmotic stress on the cells, we always add cells to any medium as drops while gently swirling the conical tube. Be careful not to make bubbles while resuspending. To ensure optimum sized primed hESC colonies, we utilize 5 mL pipettes. If the colonies are too small, poor attachment and cell death is observed. Overcrowding of the new flask after passaging leads to premature differentiation. While aspirating be gentle and always be careful not to aspirate the cell pellet itself.
48. When manually passaging, we use a sterilized forceps to bend the needle of choice. If the plastic in the culture flask is also scratched, selectively transfer only the colonies, as the clumps of cells tend to attach to the strands of plastic. Ensure to also change needle as there might be plastic attached to the needle itself. For manual cutting of sections of hESC colonies *see* Fig. 1b.
49. In a 6-well culture plate we usually feed 2 mL medium per well, a T12.5 culture flask with 2.5 mL medium and a T25 culture flask with 5 mL medium.
50. After thawing a vial of cryopreserved primed hESCs, if the colonies are small or under developed, cut manually for the first five passages until confluent cultures are observed. For ease of manual passaging we always thaw onto 6 well plates and maintain for at least five passages after thawing. We use a P200 to transfer the colonies at this stage. Once confluent cultures are observed, we switch to enzymatic passaging and larger culture formats such as T25 culture flasks as required. The number of days the culture requires to reach confluency usually differs as proliferation rate may differ between cell lines, from 5 to 10 days.

51. Post collagenase treatment, the colonies should appear to have shrunken. The colonies would appear to develop holes, edges of the colonies would appear to round up and pull away from the plate. The colonies should not have completely detached or be floating.
52. To ensure well distributed cell populations, if using a 6-well culture plate, gently swirl the plate in a figure-eight. If using T25 or 12.5 tissue culture flask formats, gently shake the flask. When observing under 10× magnification, we aim at observing three to four clumps of cells. The volume of cell suspension always depends on the size of the cell pellet.
53. We consider this passage 0 (P0). The attached colonies should start showing the initiation of the domed-opaque morphology rather than the typical flat epithelial like morphology observed in the primed pluripotent state (*see* Fig. 1c). These transient converted cells can now be efficiently passaged as single cells with little or no cell loss in the absence of ROCKi. We did not observe any major effect of ROCKi during the naïve conversion process.
54. Trypsin is very harsh and should be used in very low concentrations. Enzymatic passage is known to be attributed as one of the causes for the genomic instability of hESC. We use about 500–1000 μL per well of a 6-well culture plate.
55. It is important to ensure the cell suspension consists of single cells as any clumps of cells will flatten out and attain a flat epithelial like morphology. Repeated titrating using a P200 pipette post trypsinization usually breaks the clumps of cells. Ensure no bubbles are made while titrating as presence of bubbles will lead to cell death.
56. If prevalence of a larger number of domed colonies versus flat colonies is observed, using a 23G needle or a stem cell cutting tool manually cut out the flat colonies leaving behind only the domed colonies for passaging enzymatically. For ease of manual passaging, we prefer to culture in 6-well or 12-well culture plates.
57. If prevalence of a few domed colonies and increased flat morphology representative of a primed morphology is observed, cut out the domed colonies using a 25G needle and incubate in 50 μL drop of 0.05 % trypsin–EDTA (vol/vol) on a 35 mm petri dish at 37 °C on a heating plate. Triturate the cells using a pulled glass pipette. Neutralize the trypsin–EDTA using NCM and transfer the drop to a freshly prepared culture well.
58. Make sure to annotate the cell line, passage number and any other details required on the cryovial before cryopreservation when freezing or disinfecting the vial when thawing.

59. Clonal passaging of primed hESCs, in our hands, can be attained using 0.05 % trypsin–EDTA (vol/wt) but requires the addition of ROCKi to the medium to improve adhesion to the feeder layer. The ROCKi can be omitted from the medium 24 h' post passaging when refreshing the passaged culture flask.
60. We usually freeze about one to two million cells per cryovial. We annotate the name of the cell line, culture medium, pluripotency status, passage number and the date of freezing.
61. When the water bath is used to warm media or to thaw vials, always disinfect using 70 % ethanol (vol/vol). Ensure the water bath is cleaned regularly.
62. Confluent primed hESC colonies are usually observed anywhere between 6 and 12 days. The naïve hESCs reach confluency in a shorter period of time due to their shorter doubling time. We have also observed the older the cryopreserved vial the longer it takes for the first colonies to arise.
63. Ensure the cells have detached or incubate for another minute or 2.
64. Ensure the annotated tubes are clear and protected from smudge. Ensure to use separate glass pipettes for each tube to prevent contamination between samples.
65. Use the same batch of products and solutions prepared for samples involved in a single experiment to ensure there is no batch variation. Always prepare the hypotonic solution and fixative fresh the day before or on the day of use itself.
66. When adding fixative, the volume depends on the turbidity of the suspension. The preferred color to be observed is opaque white but slightly transparent. If the pellet has changed color to yellow or is too large, resuspend once again in 8 mL of fixative, centrifuge for 7 min at 500 $\times$ *g* and discard the fixative. If the cell suspension was stored for long, centrifuge for 5 min at 3500 $\times$ *g* and discard the fixative. Resuspend in fresh fixative until the right turbidity is acquired.
67. The glass slides need to be dust and grease free. Thoroughly clean with detergent and deionized water.
68. A good chromosomal spread should encompass only a few overlapping chromosomes. Conversely, the chromosomes should not be over spread, in order for the correct metaphase to be readily determined. For the banding to be clearly visible, chromosomes should not be encompassed within the cytoplasm and long chromosomes should be well distributed. Short chromosomes spread more readily, however it is more difficult to visualize the bands and vice versa if the chromosomes are long.

69. To obtain ideal chromosomal spreads certain factors need to be taken into consideration. The time required for drying the slides with chromosomal spreads usually depends on the temperature, which should ideally be maintained between 20 and 25 °C and humidity should be maintained at approximately 55–75 %. If the slides are dried too rapidly, increased overlap of the spreads and presence of cytoplasm is observed. If the rate of drying is too slow, overspreading is observed due to excessive breaking of the nuclear membrane and may lead to rolled up chromosomes due to evaporation of the drops of fixative.
70. If large overlapping chromosomes are observed, add 45 % acetic acid and in extreme cases 99 % acetic acid can also be used. If the suspension is too concentrated, dilute with a few drops of fixative or increase the humidity. If this leads to overspreading, add fixative once again, centrifuge, discard the supernatant and resuspend in a reduced volume of fixative in reduced humidity.
71. A hair dryer can also be used in place of the second oven at 90 °C.
72. Trypsin will partially digest the chromosomal proteins, which leads to banding of the chromosomes.
73. For the next steps, a prepared microscope slide is tested for optimal staining time, while the others are drying. Staining time differs between different batches of Leishman's working solution.
74. When viewing slides at 1000× magnification always use a drop of immersion oil.
75. If the chromosomes are still too moist and have swollen, the prepared microscope slides can be placed at 65, 80 or 90 °C from 1 to 6 h. With extreme problems with banding, slides can be placed at 65 °C overnight.
76. We use the metaphase finder software, RELOSYS. The karyogram is developed using the software Ikaros 3. We usually check multiple karyograms of each sample to determine the banding pattern for any abnormalities
77. We usually incubate the cells for a maximum of 3–4 min when staining naïve hESCs and 5 min when staining primed hESCs. Excessive fixation will lead to loss of alkaline phosphatase activity.
78. Usually 8 min suffices for naïve hESCs and about 10–15 min for primed hESCs. Observe the color change closely after 5 min of incubation and terminate the reaction immediately when the color turns bright to inhibit nonspecific staining.
79. We highly recommend using coverslips for culturing hESCs for immunostaining. Although staining may be performed directly

on the surface of the culture well, staining coverslips will not only preserve antibodies, but also prevent samples from drying out. Furthermore, the careful transfer of coverslips from one solution to the next will reduce the damage to hESC colonies, which may be caused by the change in surface tension that occurs when one solution is entirely removed and replaced with another.

80. At this stage, handle coverslips with sterile forceps to prevent culture contamination.
81. Alternatively, coverslips may be sterilized by UV irradiation treatment for 15 min.
82. Allow sufficient time in culture for the hESCs to completely adhere to the MEF feeder layer on the coverslips. This will prevent cells from detaching during the staining protocol.
83. Alternatively, center-well organ culture dishes or 12-well culture dishes may be used, depending on experimental design and at the convenience of the researcher.
84. Fixation can also be performed at 4 °C overnight for a maximum of 24 h.
85. For optimum staining results, avoid extended storage of coverslips, i.e., longer than 1 month.
86. As an example for four coverslips and two antibodies with 1:200 dilutions, use the following calculations 4×50 μL $= 200$ μL therefore, (2.5 + 2.5 (each antibody)) in 200 μL = 5 μL (antibodies) + 195 μL (blocking solution).
87. The cell membrane must be made permeable to allow the antibody to enter the cell, as the antigen of interest is located within the cell. If using a surface antigen, skip permeabilization step.
88. Treatment of cells with a blocking agent prevents nonspecific binding of the antibody.
89. Moistened tissue paper is used to prevent coverslips from drying out during the incubation. Ensure not to wet the paper too much however, as it may lead to condensation at the edge of the coverslip, which may draw off the antibody solution.
90. The use of suitable controls is critical for accurate interpretation of immunostaining results. Ensure to include a negative control in all experiments, using blocking solution with no primary antibody. Further controls, such as tissue type, absorption, or isotype matched controls (for monoclonal primary antibodies) may also be employed to verify the primary antibody staining specificity.
91. Following treatment with secondary antibody, it is critical to avoid exposure of samples to light, in order to prevent photobleaching of the fluorophore.

92. Aliquot Vectashield + DAPI with pipette. Ensure to first dry any mounting medium residue on a paper tissue to prevent excess of DAPI stain solution on slide. This will avoid coverslips from sliding and potentially causing damage to the hESC samples.
93. It is useful to dab off excess 1× PBS from the edge of the slide on a paper towel.
94. Alternatively, a confocal microscope may also be used.
95. Nail polish may also be used.
96. Place tips, pipettes, DNA LoBind tubes and PCR grade tubes (200 μL) under the UV lamp (6000 J/cm^2). Open tip boxes when placed under the UV lamp. Always work with PCR grade filter tips. Use RNAse free water (DEPC-treated water) and DNAse. During RNA isolation preferably work on crushed ice.
97. After centrifugation two phases will be observed. The upper colorless phase consists of the RNA and the white ring separating the colorless phase and the lower red phase is the DNA. For the rest of the protocol we use the RNeasy mini kit (Qiagen). Be very careful while pipetting not to transfer any of the DNA.
98. When using the RNeasy and Vivacon® columns be extra careful not to touch the membrane with the pipette tip. When using DNAse, place the drop directly on the membrane.
99. Production of DNase I stock solution: dissolve the DNase I powder in 550 μL RNase-free water. Gently mix, do not vortex and aliquot in 500 μL tubes at varying volumes.

    Store at −20 °C.
100. Pipette directly on the membrane itself since the volume is low and would not function appropriately unless directly pipetted on the membrane itself.
101. Approximately 13 μL of concentrated RNA should be observed in the collection tube.
102. Solutions and reagents from the kit are viscous so be careful not to make bubbles.
103. Keep in mind the two standards.
104. Always work with technical triplicates to asses for technical errors and for relevant biological information with biological replicates.
105. When applicable, an additional heating step from 60 to 95 °C was added to obtain melting curves.

References

1. Nichols J, Smith A (2009) Naïve and primed pluripotent states. Cell Stem Cell 4:487–492
2. Nichols J, Smith A (2011) The origin and identity of embryonic stem cells. Development 138:3–8
3. Brons IG, Smithers LE, Trotter MW et al (2007) Derivation of pluripotent epiblast stem cells from mammalian embryos. Nature 448:191–195
4. Tesar PJ, Chenoweth JG, Brook FA et al (2007) New cell lines from mouse epiblast share defining features with human embryonic stem cells. Nature 448:196–199
5. Ying QL, Wray J, Nichols J et al (2008) The ground state of embryonic stem cell self-renewal. Nature 453:519–523
6. Chan YS, Goke J, Ng JH et al (2013) Induction of a human pluripotent state with distinct regulatory circuitry that resembles preimplantation epiblast. Cell Stem Cell 13:663–675
7. Gafni O, Weinberger L, Mansour AA et al (2013) Derivation of novel human ground state naïve pluripotent stem cells. Nature 504:282–286
8. Gu Q, Hao J, Zhao XY et al (2012) Rapid conversion of human ESCs into mouse ESC-like pluripotent state by optimizing culture conditions. Protein Cell 3:71–79
9. Hanna J, Cheng AW, Saha K et al (2010) Human embryonic stem cells with biological and epigenetic characteristics similar to those of mouse ESCs. Proc Natl Acad Sci U S A 107:9222–9227
10. Takashima Y, Guo G, Loos R et al (2014) Resetting transcription factor control circuitry toward ground-state pluripotency in human. Cell 158:1254–1269
11. Theunissen TW, Powell BE, Wang H et al (2014) Systematic identification of culture conditions for induction and maintenance of naïve human pluripotency. Cell Stem Cell 15:471–487
12. Valamehr B, Robinson M, Abujarour R et al (2014) Platform for induction and maintenance of transgene-free hiPSCs resembling ground state pluripotent stem cells. Stem Cell Rep 2:366–381
13. Ware CB, Nelson AM, Mecham B et al (2014) Derivation of naïve human embryonic stem cells. Proc Natl Acad Sci U S A 111:4484–4489
14. Duggal G, Warrier S, Ghimire S et al (2015) Alternative routes to induce naïve pluripotency in human embryonic stem cells. Stem Cells 33 (9):2686–2698
15. Van der Jeught M, O'Leary T, Duggal G et al (2015) The post-inner cell mass intermediate: implications for stem cell biology and assisted reproductive technology. Hum Reprod Update 21(5):616–626

Methods in Molecular Biology (2016) 1516: 47–56
DOI 10.1007/7651_2016_322

Published online: 01 April 2016

An Effective and Reliable Xeno-free Cryopreservation Protocol for Single Human Pluripotent Stem Cells

Guoliang Meng, Anna Poon, Shiying Liu, and Derrick E. Rancourt

Abstract

Efficient cryopreservation of human pluripotent stem cells (hPSCs) in chemically defined, xeno-free conditions is highly desirable for medical research and clinical applications such as cell-based therapies. Here we present a simple and effective slow freezing–rapid thawing protocol for the cryopreservation of feeder-free, single hPSCs. This cryopreservation protocol involves the supplementation of 10 % dimethyl sulfoxide (DMSO) and 10 μM Rho-associated kinase inhibitor Y-27632 into two types of xeno-free, defined media supplements (Knockout Serum Replacement and TeSR2). High post-thaw cell recovery (~90 %) and cell expansion (~70 %) can be achieved using this protocol. The cryopreserved single cells retain the morphological characteristics of hPSCs and differentiation capabilities of pluripotent stem cells.

Keywords: Human pluripotent stem cells, Cryopreservation, Chemically defined, Xeno-free, Slow freezing, Rapid thawing, Dimethyl sulfoxide, Rho-associated kinase inhibitor

1 Introduction

Human embryonic stem cells (hESCs) can give rise to derivatives of all three germ layers and offer great potential for cell therapy and regenerative medicine [1–3]. There are currently over a thousand of hESC lines available for research (International Stem Cell Registry). However, the majority of these cell lines have been either directly or indirectly exposed to animal materials such as mouse fibroblasts (MEFs), bovine serum, and porcine-derived trypsin during their derivation, propagation, and cryopreservation [4, 5]. The presence of nonhuman or xenogenic proteins poses the risks of eliciting immune reaction and transmitting infectious agents (e.g., prions) and microbes (e.g., viruses) to human patients. In order to realize the full clinical potential of stem cells, it is highly desirable to maintain cells in xeno-free defined (XFD) media devoid of nonhuman derivatives. While there are emerging xeno-free culture systems that support hESC derivation and expansion [6–12], only a limited number of protocols exist for xeno-free cryopreservation of hESCs. In addition, the freezing media reported in some of these protocols contain animal-derived products, and thus are not xeno-free [13–15].

Here we describe a simple and effective hESC cryopreservation protocol that utilizes a slow freezing–rapid thawing procedure respectively to cryopreserve hESCs that are in single cells dissociated from hESC colonies. This protocol involves commercially available xeno-free reagents including dimethyl sulfoxide (DMSO), Rho-associated kinase inhibitor (ROCKi) Y-27632, and defined xeno-free media supplements, Knockout Serum Replacement (KSR) and TeSR2. DMSO helps preserve cell integrity by preventing ice crystal formation during the slow freezing step [16], and ROCKi serves as an anti-apoptotic reagent that has also been shown to help maintain the undifferentiated state of hESCs [17]. We tested the effects of different concentrations of DMSO and ROCKi on cryopreserving hESCs. We found 10 % DMSO and 10 μM ROCKi in either KSR or TeSR2 consistently yield high numbers of viable cells (~90 %) recovered after freeze/thaw procedure, and majority of these cells (~70 %) expand and form colonies. We cryopreserved, cultured, and passaged different hESC lines (H1 and H9) for prolonged periods using the XFD culture system described in this protocol. The hESCs at different passages had normal karyotypes and retained their pluripotent properties as assessed by expression of genes that are characteristic to hESCs and their ability to form teratomas containing derivatives of all three germ layers.

In addition to hESCs, our protocol is also effective for the cryopreservation of human induced pluripotent stem cells (hiPSCs; data not shown). Our chemically defined and xeno-free cryopreservation protocol may be employed as a reliable and cost-effective platform for the large-scale banking of hESCs (and hiPSCs) to meet the ongoing demand of cells for present/future research and clinical applications.

2 Materials

2.1 Reagents

1. KnockOut™ Serum Replacement XenoFree (KSR-XF, Life Technologies, cat no. 12618-012).
2. TeSR2 5× supplement (TeSR2-S, Stemcell Technologies, cat no. 05862).
3. Poly-D-lysine (PDL, Millipore, cat no. A-003-E).
4. HEScGRO basal medium (Millipore, cat no. SCM021).
5. Basic fibroblast growth factor (bFGF) (human animal-free recombinant; Millipore, Cat no. GF003AF).
6. ROCKi, Y-27632 (PeproTech, cat no. SM-1293823-A).
7. Accutase cell detachment solution (Stemcell Technologies, cat no. 07920).
8. DMEM/F12 + GlutaMax (Life Technologies, cat no. 10565-018).

9. Dimethyl sulfoxide (DMSO, Sigma, cat no. D2650).
10. Distilled water (Life Technologies, cat no. 15230-162).
11. DPBS (Life Technologies, cat no. 14190-144).

2.2 Cell Lines

1. hESC line, H1 (WiCell Research Institute, Madison, WI, USA; Karyotype: 46, XY; Passage 30).
2. hESC line, H9 (WiCell Research Institute, Madison, WI, USA; Karyotype: 46, XX; Passage 27).

2.3 Disposables

1. Pasteur pipette, glass, cotton plugged (5.3/4″) (Sigma, cat no. 14672-410).
2. 15 mL conical tubes (multiple brands).
3. 50 mL conical tubes (multiple brands).
4. 35 mm culture dishes (Nunc).
5. Millex-GP Syringe Filter Unit, 0.22 μm. (Millipore, cat no. SLGP033RS).
6. 5, 10 and 25 mL plastic disposable pipettes (multiple brands).
7. Nunc cryotube internal thread, 1.0 mL (Sigma, cat no. V7509-500EA).
8. 2, 20, 200, 1000 μL pipette tips (multiple brands).
9. 5, 10, and 30 mL syringes (multiple brands).

2.4 Equipment

1. Pipet aid (Drummond Scientific, cat no. 4-000-101).
2. Micropipettes (2, 20, 200, and 1000 μL) (Gilson).
3. Mr. Frosty freezing container (Thermo Fisher Scientific, cat no. 5100-0001).
4. Centrifuge (MSE, MISTRAL 1000).
5. Inverted phase-contrast microscopes (OLYMPUS 1X70; MOTIC, CHINA).
6. Dissecting stereomicroscope (LEICA MZ12).
7. Class II biosafety cabinet for tissue culture (THE BAKER COMPANY).
8. Tissue culture incubator (SANYO).
9. Water bath (VWR Scientific).
10. Hemacytometer (Fisher Scientific).
11. Liquid nitrogen tank (Taylor-Wharton).

2.5 Reagent Setup

1. ROCKi Y-27632: Dissolve 5 mg Y-27632 in 1.485 mL water to give a 10 mM stock solution. Aliquot and store at −80 °C.
2. XFD hESC culture medium: Supplement HEScGRO basal medium with 100 ng/mL basic fibroblast growth factor (bFGF) and 10–15 μM ROCKi, Y-27632 (Fig. 1; *see* **Note 1**).

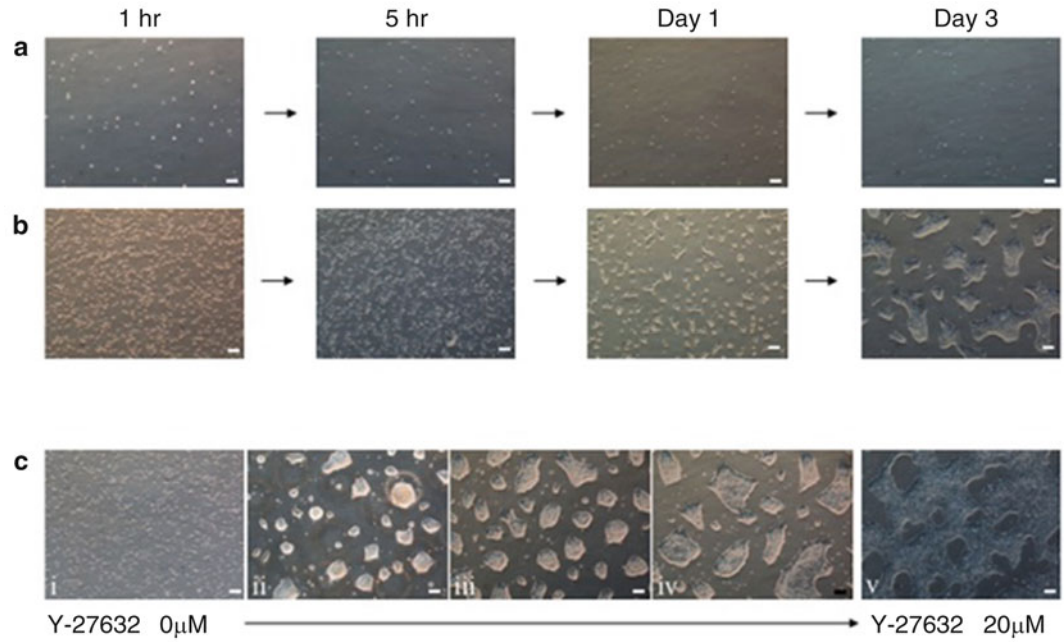

Fig. 1 Formation of hESC colonies from different seeding densities and Y-27632 concentrations. (**a**) No hESC colonies formed at low seeding density (1×10^3 cells/cm^2): One hour (h) after plating, single cells evenly attached to the culture dish surface. At 5 h, the cells failed to aggregate. No colonies were observed at the end of Day 1 and Day 3 of cell culture. (**b**) Formation of hESC colonies at high seeding density (3×10^4 cells/cm^2): One hour after plating, the single cells evenly attached to the culture dish surface. At 5 h, the cells migrated towards each other and formed aggregates. After Day 1 of cell culture, small colonies were formed. At Day 3, bigger colonies were present and ready for passaging or cryopreservation. (**c**) The effect of different concentrations of Y27632 on hESC colony formation (day 3): (*i*) 0 μM; (*ii*) 2.5 μM; (*iii*) 5.0 μM; (*iv*) 10 μM; (*v*) 20 μM

3. XFD freezing media: Supplement KnockOut™ Serum Replacement XenoFree or TeSR2 with 10 % DMSO and 10 μM ROCKi Y-27632.

2.6 Preparation of PDL-Coated Dishes

1. Dilute PDL to 20 μL/mL with distilled water.
2. Treat 35 mm culture dishes with diluted PDL.
3. Incubate plates with PDL for at least 5 h or overnight.
4. Wash plates with DPBS three times before use.

3 Methods

3.1 Culture of hESCs

Culture hESCs on PDL-coated 35-mm dishes in XFD medium and passage cells every 3–4 days as previously described [8]. Briefly, dissociate hESCs into single cells with Accutase, collect cells by centrifugation, resuspend cells with culture medium, and then evenly divide cells into culture dishes at a density of

1.5–2.5 × 10^5 cells/mL. Each 35 mm culture dish contains approximately 3–5 × 10^5 cells/dish in 2 mL of culture medium. Change culture medium every day until hESCs are ready for cryopreservation (usually on the third or fourth day of cell culture).

3.2 Cryopreservation of hESCs

1. Culture cells to the exponential phase in 35 mm dishes (*see* **Note 2**).
2. Remove the culture medium from the dishes and wash cells with 2 mL of DMEM/F12.
3. Add 0.7 mL of pre-warmed Accutase to each 35 mm culture dish.
4. Incubate the culture dishes in a CO_2 incubator at 37 °C for 5–7 min (*see* **Note 3**).
5. Add 1 mL culture medium into each dish. Using a micropipette with 1000 μL filter tip, gently pipette medium several times to dissociate hESC colonies into single cells.
6. Transfer the cell suspension from each dish into a 15 mL conical tube.
7. Wash the culture dishes with 1 mL of culture medium. Transfer medium into the conical tube.
8. Top the conical tube off with a total of 7 mL culture medium. Centrifuge the tube at 250 × g for 4 min.
9. Discard the supernatant and resuspend the cell pellet in 1.5 mL of the cold freezing medium.
10. Aliquot 1.5 mL of cell suspension into three cryovials.
11. Place cryovials immediately into a Nalgene Mr. Frosty freezing container and store the container in −80 °C freezer overnight.
12. Transfer the cryovials into a liquid nitrogen tank for long-term storage.

3.3 Thawing of hESCs

1. Prepare PDL-coated 35 mm dishes according Sect. 2.6.
2. Add 2 mL culture medium to each dish and incubate the dishes in a 37 °C incubator.
3. Remove a cryovial from the liquid nitrogen tank and immediately place the cryovial onto a float rack in the 37 °C water bath.
4. Quickly thaw the cells by gently swirling the cryovial in the water bath until only a small fraction of ice remains in the vial (*see* **Note 4**).
5. Spray and wipe the exterior of the cryovial with 70 % ethanol to sterilize the surface before bringing the cryovial into the culture hood/biological safety cabinet.
6. Transfer the cell suspension to a 15 mL conical tube. Add XFD culture medium (the culture medium to freezing medium volume ratio is 10:1) dropwise to the cell suspension in the conical tube.

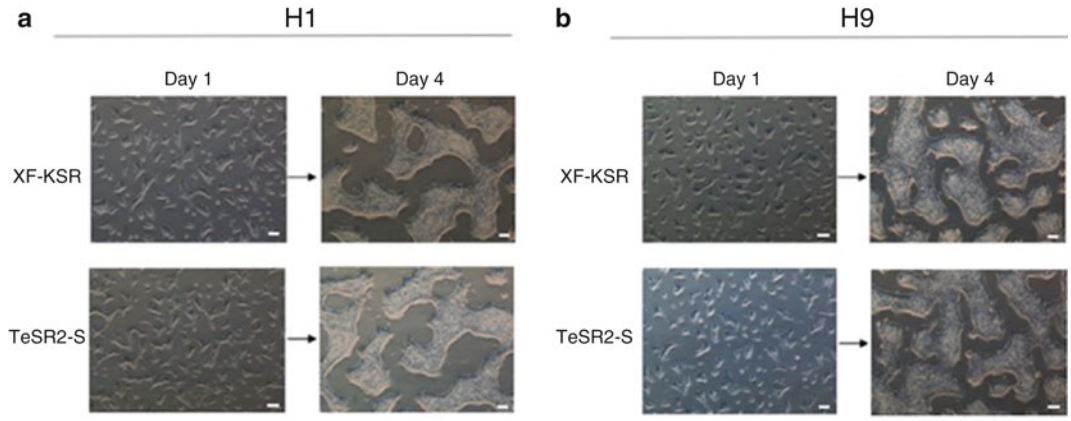

Fig. 2 Comparison between two different freezing media on hESC growth in the XFD culture system. Two hESC cell lines H1 (**a**) and H9 (**b**) cryopreserved in two freezing media (KSR-XF and TeSR2-S), thawed, and grown in the XFD culture system. Representative microphotographs of post-thawed hESCs on Day 1 and Day 4 of cell culture

7. Collect the cells by centrifugation at 250 × *g* for 4 min.
8. Gently remove the supernatant without disturbing the cell pellet.
9. Resuspend the cells in culture medium and evenly divide them into PDL-treated dishes at the density of 1.5–2.5 × 10^5 cells/mL (Fig. 1; *see* **Note 5**).
10. Culture cells in a humidified 37 °C, 5 % CO_2 incubator. Monitor cell growth and change culture medium daily (Fig. 2; *see* **Notes 6**).

3.4 Characterization of hESCs

Evaluate post-thawed hESCs for hallmarks of pluripotency after long-term culture. The protocols below assess hESCs for genetic stability, pluripotent marker expression, in vitro and in vivo differentiation into the three germ layers (Fig. 3).

1. G-banded karyotyping: Incubate cells with 0.1 μg/mL of colcemid at 37 °C for 1 h, then trypsinize, resuspend, and incubate cells in 75 mM KCl for 20 min at room temperature. Fix cells with 3:1 methanol: glacial acetic acid and drop cells onto slides to make chromosome spreads. Allow the slides to dry and then bake the slides for 90 min at 80 °C. Treat slides with 0.05 % trypsin for 30 s to 1 min, and then stain slides with Giemsa and Leishman's solution. Analyze at least 10 metaphase spreads for each hESC samples.
2. Immunocytochemistry of pluripotency markers: Fix hESC colonies with 4 % paraformaldehyde for 15 min at room temperature, wash three times with PBS, then permeabilize with 0.1 % Triton-X 100 in 0.1 M phosphate-buffered saline (PBS) for 15 min at room temperature. Wash cells three times with

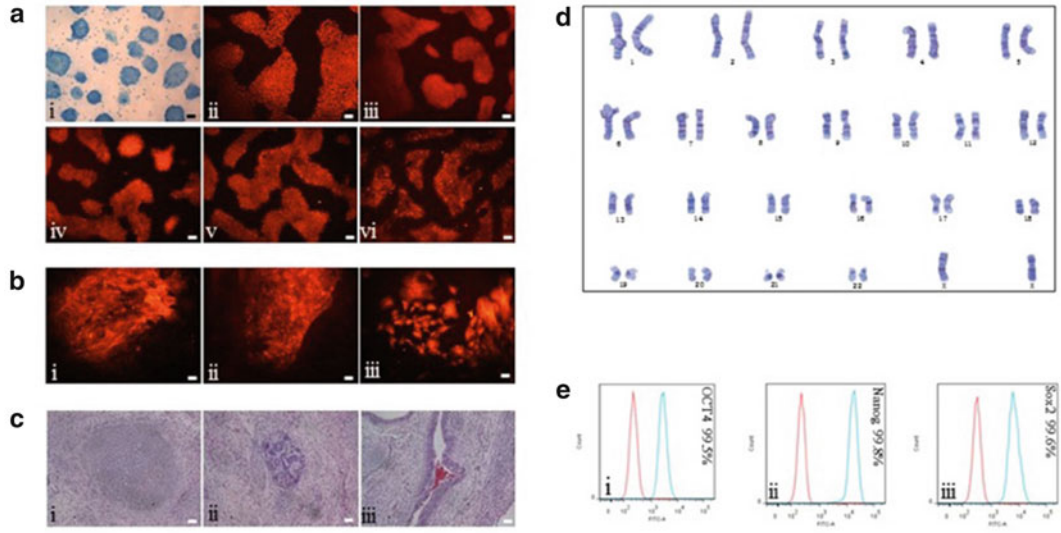

Fig. 3 Characterization of hESCs cryopreserved in KSR-XF and grown in the XFD culture system. (**a**) Immunofluorescence staining of (*i*) alkaline phosphatase and pluripotency markers, (*ii*) OCT4, (*iii*) Nanog, (*iv*) SSEA-4, (*v*) TRA-1–60, and (*vi*) TRA-1–81. (**b**) Immunofluorescence staining of in vitro hESC-derived tissues containing all three germ layers stained with (*i*) mesoderm marker: smooth muscle actin, (*ii*) endoderm marker: α-fetoprotein, (*iii*) ectoderm marker: β-tubulin III. (**c**) H & E staining of in vivo hESC-derived tissues containing all three germ layers including (*i*) cartilage of the mesoderm lineage, (*ii*) neural clusters of the ectoderm lineage, and (*iii*) gland cells from the endoderm lineage. (**d**) Karyotype of post-thawed H9 hESCs (46, XX). (**e**) FACS analysis of post-thawed H9 hESCs showed high (≥99 %) expression of pluripotency markers (*i*) Oct4, (*ii*) Nanog, and (*iii*) SSEA-4

PBS and block with 10 % normal goat serum in PBS for 60 min at room temperature. Incubate cells with primary antibodies: OCT4 (sc5279, Santa Cruz), SSEA-4 (ES cell characterization kit, SCR001, Millipore), TRA-1-60 (ES cell characterization kit, SCR001, Millipore), TRA-1-81 (ES cell characterization kit, SCR001, Millipore) at 1:100 dilution, and Nanog (PA5-20889, Invitrogen) at 1:50 dilution and 4 °C overnight. The next day, wash cell samples three times with PBS, and then incubate samples with the appropriate secondary antibodies, Alexa Fluor 546 goat anti-mouse IgG (H + L) (1:100; Invitrogen) and Alexa Fluor 594 donkey anti-rabbit IgG (H + L) (1:200, Invitrogen) for 2 h at room temperature.

3. Flow cytometric analysis of hESCs: Dissociate hESC colonies into single cells with 0.25 % Trypsin–EDTA and stain cells with the following antibodies against pluripotency markers: anti-OCT4 (Alexa Fluor 488 conjugated, Millipore), Anti-Nanog (N-terminus-Alexa Fluor 488 conjugated, Millipore), and Anti-SOX-2 (FITC conjugate, Millipore). Mouse IgG1 Alexa Fluor 488, rabbit IgG Alexa Fluor 488, and mouse IgG2b

FITC serve as respective isotope controls. Analyze stained samples with a fluorescence-activated cell sorting machine.

4. Differentiation of hESCs into the three germ layers: For in vitro differentiation, mechanically detach Day 3 cultured hESC colonies and culture hESCs in 60-mm agar-coated tissue culture dishes (Nunc) containing the differentiation medium. After 8–10 days in culture, the hESC aggregates should generate cystic embryoid bodies (EBs). Transfer the EBs onto gelatin-coated 4-well plates (Nunc) and culture the EBs for an additional 4–6 days. Analyze the differentiated cell types with immunohistochemistry using monoclonal antibodies against β-tubulin III (ectoderm; 1:400; Sigma T8660), smooth muscle actin (mesoderm; 1:200; Sigma A5228), α-fetoprotein (endoderm; 1:400; Sigma A8452), and secondary antibody Alexa Fluor 546 goat anti-mouse (1:200; Invitrogen). For in vivo differentiation, dissociate hESC clumps with 1 mg/ml collagenase IV (Invitrogen), centrifuge, and resuspend cells in the HEScGRO basal medium. Inject cell clumps into the rear leg of 6- to 8-week-old severe combined immunodeficient (SCID) mice ($2–3 \times 10^6$ cells/injection). Sacrifice mice 10–12 weeks post-injection. Remove teratomas at injection site, fix tissues with 4 % paraformaldehyde, and embed tissues in paraffin. Prepare 5 μm-thick paraffin sections with a microtome, stain sections with hematoxylin and eosin (H & E), and examine stained sections under a bright-field microscope.

4 Notes

1. It is imperative to supplement the culture and freezing media with ROCKi, Y-27632. From our years of experience culturing different lines of hESCs and hiPSCs, Y-27632 (10–15 μM) effectively maintains hESCs in the undifferentiated state. The hESCs cryopreserved with the freezing media described in this protocol can also be grown in other culture systems, such as the Matrigel/mTeSR1 system and the Vitronectin/Essential 8 system.
2. The exponential phase of a hESC line can be determined by plotting out a growth curve. Both H1 and H9 cell lines reach 70–80 % confluence when they are in the exponential phase. Other hESC lines that vary in their proliferation properties may exhibit differences in the exponential phase.
3. To ensure maximum recovery of cells without much damage, add 10 μM Y-27632 to Accutase before use and minimize Accutase exposure time to the cells. Treatment time required to generate viable single cells may vary among different hESC

lines. Optimal Accutase exposure time should be determined for each cell line.

4. To minimize damage to the frozen cells during thawing, it is imperative to promptly defrost the cryovial containing the frozen cells in a 37 °C water bath. Remove the cryovial from the water bath when majority of the cells have been thawed with a little bit of ice remaining in the cryovial.
5. After cell plating, the process of colony formation encompasses 4 steps: single cell attachment, migration, aggregation, and proliferation. At the density of 1.5–2.5 $\times$ 10^5 cells/mL (equivalent to 3–5 $\times$ 10^4 cells/cm^2), most cells participate in colony formation where small hESC colonies start appearing in the dish as early as day 2 in cell culture. These colonies should be large enough for passaging and freezing Day 3–4 in cell culture. However, at low density of cells (1–2 $\times$ 10^3 cells/cm^2), none or only a few colonies tend to form after cell plating.
6. In this culture system, hESCs tend to expand rapidly in vitro which may lead to unwanted spontaneous differentiation. Monitor the cells every day and perform subculture in Day 3–4 post thawing and plating.

Acknowledgements

This work was supported by a CIHR Regenerative Medicine Team Grant FRN 27639.

References

1. Thomson JA, Itskovitz-Eldor J, Shapiro SS, Waknitz MA, Swiergiel JJ, Marshall VS, Jones JM (1998) Embryonic stem cell lines derived from human blastocysts. Science 282:1145–1147
2. Trounson A, Pera M (2001) Human embryonic stem cells. Fertil Steril 76:660–661
3. Klimanskaya I, Rosenthal N, Lanza R (2008) Derive and conquer: sourcing and differentiating stem cells for therapeutic applications. Nat Rev Drug Discov 7:131–142
4. Meng G, Liu S, Krawetz R, Chan M, Chernos J, Rancourt DE (2008) A novel method for generating xeno-free human feeder cells for human embryonic stem cell culture. Stem Cells Dev 17:413–422
5. Chen HF, Chuang CY, Shieh YK, Chang HW, Ho HN, Kuo HC (2009) Novel autogenic feeders derived from human embryonic stem cells (hESCs) support an undifferentiated status of hESCs in xeno-free culture conditions. Hum Reprod 24:1114–1125
6. Melkoumian Z, Weber JL, Weber DM, Fadeev AG, Zhou Y, Dolley-Sonneville P, Yang J, Qiu L, Priest CA, Shogbon C, Martin AW, Nelson J, West P, Beltzer JP, Pal S, Brandenberger R (2010) Synthetic peptide-acrylate surfaces for long-term self-renewal and cardiomyocyte differentiation of human embryonic stem cells. Nat Biotechnol 28:606–610
7. Rajala K, Lindroos B, Hussein SM, Lappalainen RS, Pekkanen-Mattila M, Inzunza J, Rozell B, Miettinen S, Narkilahti S, Kerkelä E, Aalto-Setälä K, Otonkoski T, Suuronen R, Hovatta O, Skottman H (2010) A defined and Xeno-free culture method enabling the establishment of clinical-grade human embryonic, induced pluripotent and adipose stem cells. PLoS One 5(4):e10246
8. Meng G, Liu S, Rancourt DE (2012) Synergistic effect of medium, matrix, and exogenous factors on the adhesion and growth of human pluripotent stem cells under defined, xeno-free conditions. Stem Cells Dev 21:2036–2048

9. Tannenbaum SE, Turetsky TT, Singer O, Aizenman E, Kirshberg S, Ilouz N, Gil Y, Berman-Zaken Y, Perlman TS, Geva N, Levy O, Arbell D, Simon A, Ben-Meir A, Shufaro Y, Laufer N, Reubinoff BE (2012) Derivation of xeno-free and GMP-grade human embryonic stem cells—platforms for future clinical applications. PLoS One 7:e35325
10. Marinho PA, Vareschini DT, Gomes IC, Paulsen Bda S, Furtado DR, Castilho Ldos R, Rehen SK (2013) Xeno-free production of human embryonic stem cells in stirred microcarrier systems using a novel animal/human-component-free medium. Tissue Eng Part C Methods 19:146–155
11. Fan Y, Hsiung M, Cheng C, Tzanakakis ES (2014) Facile engineering of xeno-free microcarriers for the scalable cultivation of human pluripotent stem cells in stirred suspension. Tissue Eng Part A 20:588–599
12. Rodin S, Antonsson L, Niaudet C, Simonson OE, Salmela E, Hansson EM, Domogatskaya A, Xiao Z, Damdimopoulou P, Sheikhi M, Inzunza J, Nilsson AS, Baker D, Kuiper SY, Blennow E, Nordenskjöld M, Grinnemo KH, Kere J, Betsholtz C, Hovatta O, Tryggvason K (2014) Clonal culturing of human embryonic stem cells on laminin-521/E-cadherin matrix in defined and xeno-free environment. Nat Commun 5:3195
13. Richards M, Fong CY, Tan S, Chan WK, Bongso A (2004) An efficient and safe xeno-free cryopreservation method for the storage of human embryonic stem cells. Stem Cells 22:779–789
14. Holm F, Ström S, Inzunza J, Baker D, Strömberg AM, Rozell B, Feki A, Bergström R, Hovatta O (2010) An effective serum- and xeno-free chemically defined freezing procedure for human embryonic and induced pluripotent stem cells. Hum Reprod 25:1271–1279
15. T'Joen V, Cornelissen R (2012) Xeno-free plant-derived hydrolysate-based freezing of human embryonic stem cells. Stem Cells Dev 21:1716–1725
16. Imaizumi K, Iha M, Nishishita N, Kawamata S, Nishikawa S, Akuta T (2016) A simple and efficient method of slow freezing for human embryonic stem cells and induced pluripotent stem cells. Methods Mol Biol 1341:15–24
17. Mollamohammadi S, Taei A, Pakzad M et al (2009) A simple and efficient cryopreservation method for feeder-free dissociated human induced pluripotent stem cells and human embryonic stem cells. Hum Reprod 24:2468–2476

Methods in Molecular Biology (2016) 1516: 57–89
DOI 10.1007/7651_2016_343

Published online: 05 April 2016

Clonal Analysis of Cells with Cellular Barcoding: When Numbers and Sizes Matter

Leonid V. Bystrykh and Mirjam E. Belderbos

Abstract

Cellular barcoding is a recently rediscovered tool to trace the clonal output of individual cells with genetically distinct and heritable DNA sequences. Each year a few dozens of papers are published using the cellular barcoding technique. Those publications largely focus on mutually related issues, namely: counting cells capable of clonal proliferation and expansion, monitoring clonal dynamics in time, tracing the origin of differentiated cells, characterizing the differentiation potential of stem cells and similar topics. Apart from their biological content, claims and conclusions, these studies show remarkable diversity in technical aspects of the barcoding method and sometimes in major conclusions. Although a diversity of approaches is quite usual in data analysis, deviant handling of barcode data might directly affect experimental results and their biological interpretation. Here, we will describe typical challenges and caveats in cellular barcoding publications available so far.

Keywords: Barcode, Clone, Sequencing, Barcode clonal analysis, Stem cells, Hematopoiesis

1 Introduction

The term "barcode" ("bar code" or "bar-code") most likely comes from the 1952 patent by IBM of the universal product code, which was printed on the label of the commercial product and looked like a set of stripes and therefore soon named the "bar code." In biology, two different categories of barcodes circulate at this time. The first category of sequences named barcodes are relatively short genomic sequences from evolutionary preserved DNA loci, which are sufficiently old and variable in different species. These loci are used as unique tags for species and to measure degree of evolutionary distance between species. The cytochrome C oxidase gene is a well-known example of this type of barcode. Another kind of barcode is a synthetic DNA sequence. Two kinds of this barcode sequence are currently in use: one category are made by design (i.e., a defined set of sequences made by certain rules) in order to assist multiplexed sequencing protocols, for instance Illumina sequencing indexes. The design of this barcode category can be quite elaborate in terms of implementation, recognition, and protection from errors. Another category of synthetic barcodes

discussed here is made by random chemistry. These barcodes are relatively cheap and simple in design and production. They are used for vector libraries, microbial population studies, and recently for clonal studies in multicellular organisms. A considerable part of studies using such barcodes is dedicated to clonal analysis of hematopoiesis [1–7], although other primary cells have also been used, for instance brain cells [8–10] or mammary stem cells [11], as well as cell lines [10, 12, 13].

No matter what cells are used, the major principles of for designing a cellular barcoding experiment and analyzing results are supposed to be the same. In the current review, we describe major parameters in making a barcoded vector library, describe critical steps, and peculiarities of treating experimental data and reporting them. Not every paper provided a fully detailed description of the experimental protocols. Therefore, we are limited in this review to the level of our understanding and our interpretation of the data, which might be different from original view of the authors.

2 Barcoded Library Design

2.1 Vectors

Successful integration of barcode DNA into the host cell genome begins with the choice of an efficient vector and with the protocol for ligating barcodes into this vector. Currently, retroviral and lentiviral vectors are the most popular, mostly due to their high degree of transduction efficiency and the availability of well-standardized protocols. Transposon-driven barcoding can be used as a potential alternative to viral vectors in the future, yet this method has not reached a sufficient degree of transduction efficiency.

Usually, the position of the integration site for the barcode is at the 3′-end of GFP (or any other fluorescent protein marker) and at the 5′-end to the flanking 3′-LTR. This is supposedly a safe place: Thus far, no adverse effects of barcode integration on host cell function have been reported. In theory, placing the barcode to the very end of the viral part of the vector could potentially be more useful, especially when combining the barcoding technique with integration site (IS) analysis. In that case, the IS and barcode could be read in one sequence. This would simplify the analysis and quantification at the same time.

2.2 Barcode Design

In the context of this review, a cellular barcode is defined as a synthetic DNA sequence of predetermined length, consisting of (semi-)random nucleotides. It can be of different length and style, and it can be combined with nonrandom nucleotide sequences. An overview of recently used barcodes is presented in Table 1. Note, here we use the IUPAC notation for DNA sequences. The simplest

Table 1
Overview of barcode structures in literature

Structure	Code	Example	Length	Max. variation	Retrieval	Notes	Reference
Random	N27	TAGAACCGGATAGATACGATCGAACCC TACTAACACGTAATACACTTGGAAACC TAGTTTTTGCCATAACGGCCGTCCGGG	27	1.80144E+16	By flanking sequences only	Variable GC%, no direct ligation into the vector	[3, 14]
Restricted random	$(SW)_{12}$	CTCAGTCTGTCACAGAGTCACAGA CTCTGTCACACAGTGTGAGAGTCT GAGTCAGACTGACTGACAGACTCA	24	16777216	Flanking sequences, regular expressions	Constant GC%, no direct ligation into the vector, imperfect repeats	[9]
Restricted random	$(SW)_{15}$	GTCTGTCTGTCACACTGTGAGTGAGAGACT GACAGAGTCTGTCACAGTGTGTGACACTGT CAGTGAGACACAGTCTCACTGACTCTGTGT	30	1073741824	Flanking sequences, regular expressions	Constant GC%, no direct ligation into the vector, imperfect repeats	[13]
Complex restricted random	$((N)_8\text{-}(SW)_5)_5\text{-}N_8$	GCGCGCAG.GACTCTGTGA.TGGAGACG.C ACTGACACTTACTATTC.CTGTCTGAGT. TCGTGTAG.GAGTCTCACTGGCCTCAC. GACTGAGTCT.TTGAACCC	98	2.17781E+40	Flanking sequences, regular expressions	Variable GC%, no direct ligation into the vector, less imperfect repeats	[1]
Semi-random	AANNATCNN GATSSAAANNG GTNNAACNNTG	AAGTATCGTGATTTAAAAAGGTGAAACAGTG AAGGATCCAGATAAAAATGGGTATAACGGTG AAAAATCTGGATTAAAAGGGGTTCAACCGTG	31	4194304	Flanking sequences, regular expressions, motif search	Variable GC%, direct ligation into the vector	[2]

(continued)

Table 1
(continued)

Structure	Code	Example	Length	Max. variation	Retrieval	Notes	Reference
Semi-random	TANNCAGNNAT CNNCTTNN CGANNGGA NNCTANNCT TNNGA	TACCCAGTAATCACCTTATCGAATGGACTCTATCCTTCAGA TAAGCAGTCATCACCTTGTCGATCGGAGCCTAGTCTTGCGA TAAACAGGTATCATCTTAACGAGCGGATGCTAGGCTTGCGA	41	4294967296	Flanking sequences, regular expressions, motif search	Variable GC%, direct ligation into the vector	[17]
Semi-random	GGNNNACNNNG TNNNCGNNNT ANNNCANNNT GNNNGA	GGCGCACCGCGTCGCCGCCATAACTCAAAATGAACGA GGGAGACTAGGTGCCCGAAATACCTCATGTTGCTCGA GGTCGACTTCGTTACCGCTGTATAGCACTCTGGGAGA	37	4.39805E+12	Flanking sequences, regular expressions, motif search	Variable GC%, direct ligation into the vector	[4]

barcode consists solely of random nucleotides, symbolically written as $(N)_x$, where N stands for any of the four bases: A, C, G, T and x for the number of bases. This type, $(N)_{27}$ was used in some hematopoietic studies [3, 14].

Several studies used a variation of the completely random barcode, applying certain restrictions to the variable positions. For example, Golden et al. used a 24-base sequence of strong and weak bases $(SW)_{12}$, where S stands for a strong bases (C or G) and W is a weak base (A or T) [10]. A similar, but longer, barcode was recently used, $(WS)_{15}$ [13]. Schepers et al. also restricted certain positions to weak or strong bases, but mixed this with completely random positions $((N)_8\text{-}(SW)_5)_5\text{-}N_8$ [1]. This barcode type was originally designed for hybridization arrays, and was later also analyzed by sequencing [15]. The major advantage of the random SW-pattern is the reasonably constant GC-ratio. This might be useful for hybridization assays and give some advantage in PCR amplification. A disadvantage of fully random and partially restricted barcodes is that they require PCR amplification before they can be ligated to the vector, otherwise big wobbles formed by strand mismatches will be eliminated by the DNA repair system. Also, periodic SW structures tend to form simple repeats. These repeats are known to be prone to small indels (insertion or deletion) [16]. Not surprisingly, it was revealed in some publications [8].

We introduced a semi-random barcode, which consists of a constitutive backbone combined with variable positions, e.g., AANNATCNNGATSSAAANNGGTNNAACNNTG [2]. The same or a modified version was used by others [6, 17]. Later we introduced more backbones [4]. The semi-random barcode has several advantages over fully random barcodes. First, its recognizable signature facilitates barcode retrieval in multiplexed sequencing data. Second, a semi-random barcode can be ligated directly to the vector without prior PCR reaction. Third, different barcode backbones can be combined in different parts of experiments and followed separately as they can be discriminated in the sequencing data.

2.3 Making a Barcode Library

The next step after selection of the vector and barcode structure is production of the barcode library. One example of a protocol for production of a barcode library was published recently [18]. However, in literature, several different strategies for producing a barcode library have been used. These strategies can be classified based upon the use of PCR amplification prior to vector ligation, and on the use of bacterial cloning (Fig. 1):

1. Barcodes can be amplified by PCR prior to ligation into the vector of choice (Fig. 1a). This approach has the advantage of eliminating wobbles due to DNA mismatches, but also harbors the risk of decreasing library complexity and introducing PCR bias.

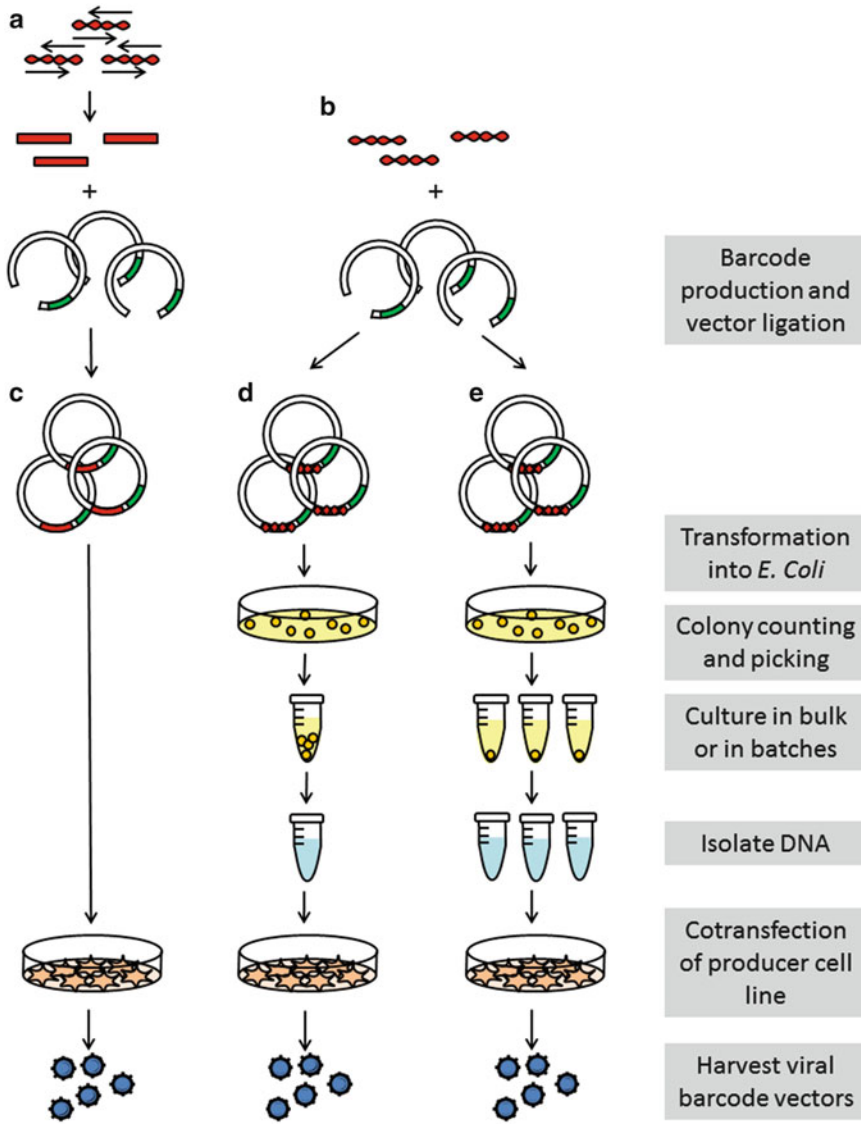

Fig. 1 Summary of protocols for production of a barcode library. (**a**) First, the barcode linker is made of two (semi-)random oligonucleotides, which form imperfect DNA duplexes. Prior to ligation into the vector, PCR is used to amplify barcodes into perfectly matching DNA double strands. (**b**) Alternatively, imperfect DNA duplexes are ligated into the vector directly, without previous PCR amplification. (**c**) Subsequently, the ligated barcode vector is used to transduce the viral packaging cell line. (**d**, **e**) Alternatively, ligated vector products can be subcloned in *E. coli*. Batches of colonies (**d**) or individual colonies (**e**) are selected and used to generate library stocks and to assess library complexity. Barcoded vector DNA can be used for transduction of the packaging cell line and generation of barcoded viral particles

2. Barcodes can be ligated directly into the vector (Fig. 1b). Note that this is only possible with semi-random barcodes, as the fixed barcode positions allow for sufficient stability for later barcode amplification.

Subsequently, three approaches for production and amplification of the library have been reported:

1. No cloning (Fig. 1c): Barcoded vectors are used directly for transduction of the packaging cell line and generation of viral particles, which are subsequently used for transduction of cells of interest [3, 13].
2. Partial cloning (Fig. 1d): Competent *E. coli* are transformed with freshly barcode ligated vector, and grown on plates. Colonies are harvested and DNA is isolated in bulk, which is used for production of viral particles and consequently to transduce the cells of interest [11]. Library complexity is assessed by transduction of a cell line, or by (re-)plating an aliquot of *E. coli* to test the number of uniquely labeled colonies [12].
3. Complete cloning (Fig. 1e): This strategy resembles strategy 2, with the exception that *E. coli* colonies are cultured as single colonies or small batches from which vector DNA is isolated [1, 2, 10].

Obviously, the first protocol (Fig. 1c) is the shortest and the easiest. It is likely to contain the maximal diversity of barcodes since it is not limited to any subsequent selection step (although PCR and restriction step will decrease it). One disadvantage is that a relatively small amount of vector DNA is produced. This kind of library allows little room for experimental analysis and validation of its content. There is also a risk of losing some part of the library during the transduction protocol, and estimation of the actual library size and composition is difficult.

The second protocol (Fig. 1d) allows to assess the approximate size of the vector library, since every *E. coli* colony can be counted. Hypothetically every colony carries only one barcode sequence. This protocol also generates more vector DNA since every colony contains millions of identical vector copies. With more DNA in the collected library, one can perform more experiments using the same library and therefore allow its validation.

The third approach is the most laborious (Fig. 1e), but renders the highest library quality. One of the unaddressed issues in the first two strategies of library production is that the ligation of the barcode into the vector is not perfect. Two kinds of problems are persistently detected: the first is empty vectors with no barcode inserted (first reported by Golden et al. [10]), the second is concatemers, insertion of multiple barcode copies into a single vector (regularly

observed by us). Although the fraction of each aberration can be small, it still can be a source of unaccountable clones in the library and in the experiment, and therefore decrease the accuracy of library size counting. To address these issues, we and others commonly culture *E. coli* cells in batches of 1–10 colonies [1, 2, 10, 18]. Every batch of *E. coli* is inspected for empty vectors and concatemers by PCR and gel electrophoresis, and only those preps that pass quality control are pooled into the final library. Although this step is time consuming, this protocol theoretically provides the best quality of the barcode library, yet likely of a smaller size.

3 Validation of the Library

A substantial amount of uncertainty in experimental barcoding protocols resides in the assessment of size of the barcode library. Current literature provides a broad range of examples how the used libraries were confirmed regarding their size and skewing properties. Generally, those validation strategies are quite diverse and do not follow common standards (actually, no standards for library production and validation are yet available). To our understanding, published protocols can be ordered based upon their degree of certainty for the reported library size (from higher to lower).

1. All barcoded vectors are cloned individually in *E. coli*, each colony is stored separately as stock. Each individual *E. coli* stock (representing one barcode) is used separately for DNA isolation and sequencing. The entire library is countable, all sequences are defined. The process of barcode identification in the experiment is reduced to the search for identical barcodes in the library. See for example the protocol by Schepers et al., and by Naik et al. [1, 5].
2. The library is cloned in *E. coli*. Colonies are cultured in small batches (2–50 colonies per batch). Each batch is sequenced separately to produce a list of barcodes most likely present in the library (library sizes varied from 200 to 800 barcodes). Subsequently, barcodes from experimental data are compared to the barcodes in the library. The count is probabilistic. This was our strategy through the publications from Gerrits et al. [2] to Verovskaya et al. [4, 19].
3. The library is transduced into *E. coli*. Colonies are counted and the library size is deduced from this number [6]. This count is even more approximate compared to the above since it has no correction for the efficiency of barcode integration and other aberrations.

4. The library is partially cloned into *E. coli* or a cell line, and partially sequenced to deduce the total size of the library [13, 17]. By deduction, library sizes were claimed of two million barcodes (actually 4 libraries of 5×10^5 barcodes each) [17], and 10^7 barcodes [13]. With this version more assumptions are taken for approximation. Note that direct count of such size libraries is hardly possible.
5. No subcloning in *E. coli* is performed. The ligated vector is used directly for transduction of the packaging cell line. The library size is deduced from deep sequencing data [3, 14]. This is probably the least certain way of library size assessment. A major challenge in this strategy is to discriminate sequencing noise from true barcode calls.

Obviously, there is a dilemma between labor investment, library size design, and precision of the library size assessment. Once a library of individual barcode preps is fully cloned and sequenced per barcode, the subsequent data analysis is relatively straightforward [5]. However, producing a highly complex library from individual barcode preps is time-consuming and barely feasible by hand, yet well affordable by automation. For example, to make a barcode library of 100,000 barcodes, one would have to culture *E. coli* batches and isolate DNA 274 preps per day nonstop for a whole year. Robotic library production is an attractive alternative to the manual library production, allowing for a high-quality library of high complexity. However, until this will become possible, we have to rely on less effort- and time-consuming protocols, yet reliable enough regarding library design and validation. One commonly used alternative is culturing and sequencing of sub-libraries [2, 4, 19]. This strategy saves labor effort over individual barcode sequencing, and still keeps track of the sequence information.

3.1 Library Sequencing

Currently most of the studies are done with the libraries where exact sequence information is not known. Several strategies can be used to maximize reliability of barcode identification, using statistical approaches in sequence data analysis to minimize the risk of false-positive calls and consequently overestimation of library size. Note that the total number of unique barcode sequences in raw data can be thousands of times higher than the real number of barcodes subjected for sequencing.

3.2 Skewing

Ideally, a well-mixed barcode library consists of a set of barcodes of equal frequency. This simple assumption is frequently used in the simulation scripts. In reality, this is not the case. It is not surprising although. It is like assuming for the sake of theory all humans being equal, while finding in reality that every person is different. So far, all reported libraries show substantial skewing: some barcodes in the library are more abundant, whereas others are present at low

frequencies [2, 3, 13]. This skewing is an intrinsic result of technical limitations during library production, which can be further aggravated by in vitro culturing [12]. This issue is particularly relevant in the case of stable retroviral and especially lentiviral vector-producing cell lines. In principle, these cell lines allow for the stable production of viral particles, and are therefore considered a renewable source for the library. However, it is currently unknown whether the libraries produced by these cell lines would retain their quality and complexity over time.

Overall, skewing creates additional limitations on estimation of the library size. More details are provided in Experimental Design, chapter Counting Barcodes, and Appendix. In short, greater skewing reduces the actual library size. Shannon index can be used to correct skewing.

3.3 Are Big Libraries Better Than Small?

Reported library sizes vary from a few hundred (our group) to thousands [1, 6], hundreds of thousands [3, 17], and even millions [13].

One can assume that bigger libraries are universally better than smaller libraries. However, several problems arise when dealing with extraordinarily big library sizes. First, as we explained above, the sizes of the biggest libraries reported are more deduced than validated. Second, it is difficult to avoid skewing. This eventually decreases the effective size of the library. Third, the packaging cell line for viral production might limit the actual number of barcodes, especially when the library is big and became close to the cell numbers used for transfection. Fourth, big libraries are more difficult to handle for sequencing. As an Illumina single lane run currently provides about 150 million reads, sequencing a library of one million barcodes will have an average sequencing depth of only 150 reads per barcode per lane. When we approach library sizes of ten million barcodes, then the sequencing depth will only cover 15 reads per barcode. Obviously, if not enough depth is used, many barcodes will be missing and the actual library size will be artificially decreased. Interestingly, all big libraries used until now were not fully sequenced [3, 13, 17]. Consequently, barcode retrieval and analysis of sequencing results becomes more problematic, since no reference to the library can be made.

Fifth, when dealing with samples of high clonal complexity, the high number of barcodes with relatively few reads will complicate signal–noise discrimination. As mentioned previously, it is possible to analyze the complexity of bigger libraries by repetitive sequencing of either the library itself or of cell samples transduced with the library. However, for very big libraries, this becomes a massive effort. In our data with mid-size libraries we can easily discriminate noise if major barcodes are sequenced up to

1000 times and more. For a library with one million barcodes a sequencing depth of a 1000 reads per barcode will be expensive and computationally challenging.

4 Experimental Design

So far we discussed library size and related issues. A relatively big size of the library is necessary to uniquely label each (stem) cell with a unique barcode. The choice of barcode library and its complexity also depends on the experimental question and corresponding design. Experimental designs found in the literature can be roughly split in two categories:

1. Use a big library to monitor a small number of clonogenic (stem) cells ("classic barcoding").
2. Use a small library to test with a large number of clonogenic cells, usually cell lines ("clonal screening").

The rationale for those two designs is quite clear. The first case is a typical cellular barcoding experiment, where we try to uniquely label few active stem cells. Unique labeling of each (stem) cell requires a relatively big size of the library. As an empirical rule, the ratio between the number of clone forming cells and the number of barcodes must be at least 1:100 or more. The uniqueness of barcoding can be predicted more exactly using a binomial distribution function and/or a random model (see Appendix).

The second case is known for screening tests with libraries of vectors carrying some active factors and using positive selection protocol as the end goal [13, 20, 21]. Obviously, there can be some cases in-between of those extremes.

4.1 Classic Cellular Barcoding

Multiple papers dedicated to tracing clonal activity of hematopoietic and other stem cells have used a rather uniform experimental design, which we therefore call "classic." (Although the barcoding design is relatively recent, it inherits features of other label tracing experiments in biology and other disciplines, which has a long history.) In this design, a barcode library of high complexity is used to mark a limited number of clonogenic (stem) cells. The high abundance of barcodes over target cells limits the risk that multiple cells are marked with the same barcode. This probability can be predicted by binomial statistics [2, 3], or computed by a random model (with various extra options to account for skewing). An advantage of the random model is that it allows for correction for library skewing, thereby potentially providing a more realistic prediction of the proportion of uniquely labeled cells.

This strategy was recently used to follow the clonality of hematopoietic stem cells, T-cells, mammary gland cells or other cells are studied [2, 4, 7, 22]. In addition to stem cell monitoring, classic cellular barcoding design has also been applied for labeling DNA sites with unique molecular identifiers (UMIs), and for random genome integration [23].

This design is also applicable to clonal analysis of cell lines, when strict selective conditions are used [13]. Although initially multiple cells may be labeled by the same barcode, stringent selection will result only in a small number of surviving clones, which are most likely labeled uniquely.

A different example: barcoding cell lines [12] violate the rule of unique barcoding and therefore fall out of this category.

4.2 Libraries for Clonal Competition

Some experimental designs employ a collection of vectors for the competition studies in vivo or in vitro. Since all vectors in the collection are different in CDS, iRNA, or miRNA they carry, the cloned component also plays a role of the barcode. Surely, those vectors can be also barcoded. Although the general concept looks simple, there is one serious caveat in such designs. Opposite to the cellular barcoding where we use big libraries to mark a modest number of stem cells, the competition study implies that each barcode in the library has to be tested in the targeted stem cells. Therefore, their roles are reversed: for instance, testing a library of 500 miRNAs in hematopoietic stem cells of mice needs at least 5000 stem cells to ensure that approximately 95 % of cells with one type of barcoded vector at least once. This obviously requires a considerable amount of stem cells. To our knowledge, we account approximately 2–5 stem cells per million of whole bone marrow transduced with barcoded vector library. So, for a reliable competition study, we will need to use one to two billion bone marrow cells. This is practically impossible for several reasons. First, venous injection of more than ten million cells into a mouse has a high risk of causing pulmonary embolism. Second, the number of cells needed greatly exceeds the estimated size of the murine bone marrow niche size, which is approximately 450 million cells [24]. Therefore, accommodating two billion cells in mouse recipient will be highly unlikely to succeed. If too few cells are transplanted, the outcome of the screen will be quite stochastic, needless to say there will be not much reproducibility between different publications. Not surprisingly, therefore, such screens are usually performed with cell lines or onco-transformed primary cells [20], where a number of clone forming cells is practically unlimited [21]. Bhang et al., performed similar experiment using an unusually big library [13]. Although this does not influence the outcome (a small number of barcodes were positively selected), the use of a big library for such a clonal selection experiment is likely excessive.

5 Identification of Barcodes by Sequencing

After the library is made and the barcoding experiment is performed, all experimental samples undergo sequencing. Deep sequencing of the PCR amplified barcode locus is the method of choice, as it is both exact and quantitative, reporting the relative frequency of all barcodes in a certain sample. However, preparation of samples for deep sequencing is a time-consuming process, and some elements of analysis can be done faster using Sanger sequencing.

5.1 Sanger Sequencing

Sanger sequencing of the barcode locus can be used as a relatively quick (yet less quantitative) method to assess the number of barcodes in a given sample (Fig. 2). Details are explained in the Appendix.

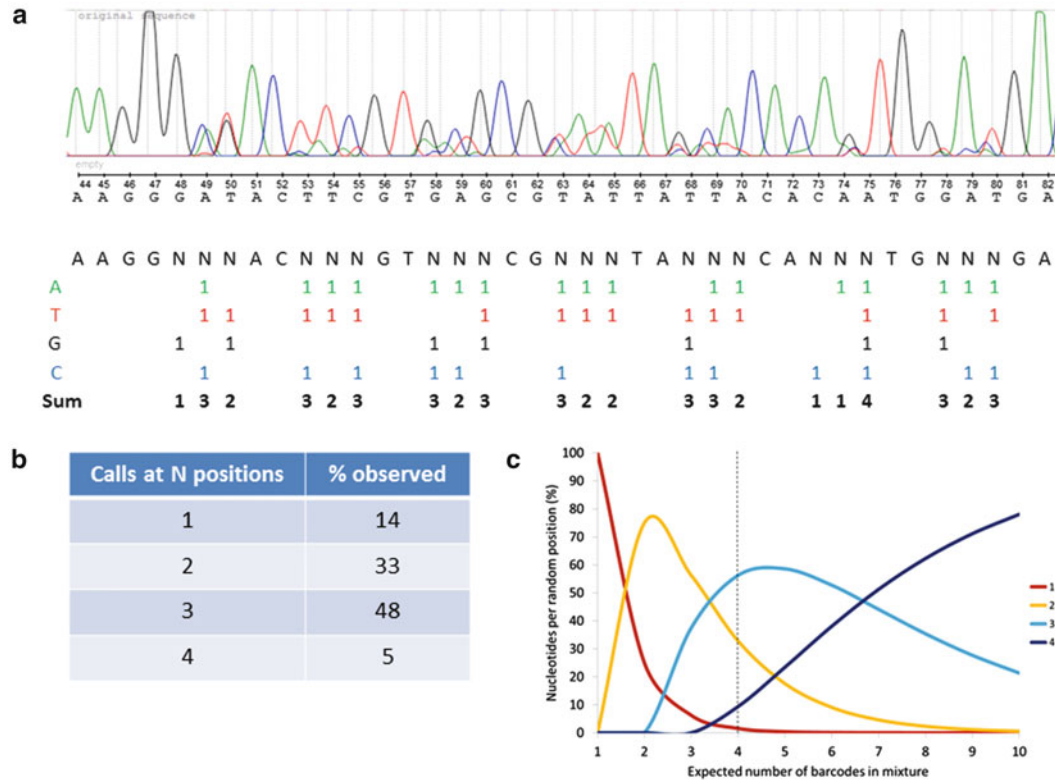

Fig. 2 Analysis of barcode complexity by Sanger sequencing. (**a**) DNA from an experimental sample is isolated and sent for Sanger sequencing. The number of base calls (peaks on the chromatogram) at each random position of the barcode are counted. In this example, a mix was made of four individually prepared barcodes. (**b**) Subsequently, the number of calls at the random positions is expressed as a fraction of the total number of random nucleotides. In this example, one single peak is observed at 3/21 random positions = 14 %. (**c**) The resulting percentages can be plotted in a nomogram, which predicts the number of barcodes in the mixture, which in this case is 4

Briefly, the complexity of the sample can be roughly assessed by counting the number of single, double, triple and quadruple peaks at each variable position of the barcode. In case we see all variable positions in the barcode represented by all 4 bases, the expected complexity must be high (>10 clones), therefore the sample is a candidate for deep sequencing. If, however, the Sanger read reveals no or few extra signals in the variable positions, it indicates that only a few barcodes contribute to the sample, which can be called oligoclonal. Whenever clonality of the sample is low, there is little need for using deep sequencing. Instead, the sample can be cloned into *E. coli* and individual colonies can be prepped and sequenced by Sanger sequencing (multiple per sample, depending on the number of expected barcodes). This might sound as a low-resolution option, however, it might be time-saving and useful as an alternative internal control for barcode identification in deep sequencing data: the chromatogram in Sanger sequencing must generally agree with the results and frequencies of barcodes after deep sequencing.

5.2 Deep Sequencing

Deep sequencing, usually in multiplexed format, is the major method for barcode sequencing which was used in practically all current publications. Barcode analysis of deep sequencing results generally requires two essential filtering steps: (1) filtering of PCR noise, and (2) pooling of similar barcodes. Depending on the experiment, additional steps may be needed. Failure of adequate data analysis may result in false identification of an extraordinarily high number of barcodes, and/or in the false impression of stochastic clonal behavior.

The only limitation of deep sequencing is that it needs multiplexing of samples. To do so, we and others use specially tagged amplification primers [2, 4, 19], others used Illumina indexes [6], some authors used library tags [3]. Note that tagged primers allow the maximal degree of multiplexing.

The number of samples that can be combined into one sequencing run depends on the number of expected barcodes and on the sequencing depth. When working with mid-sized libraries and biological objects of low to moderate clonality (2–100 barcodes), we can save sequencing costs by multiplexing 100 to 500 samples in one sequencing run on Illumina single lane (150 million reads). This will result in sequencing sets of a few thousands to one million reads per sample, which provides good accuracy in barcode quantification. However, if we deal with an experiment where we expect approximately a million barcodes in a sample, multiplexing is not an option anymore and each sample will need to be sequenced individually to ensure sufficient depth (see the paragraph above on "Are big libraries better than small?").

a

Barcode pool	Total reads	Unique reads
2	51347	1304
7	48625	1563
14	131705	3995
20	26337	1145

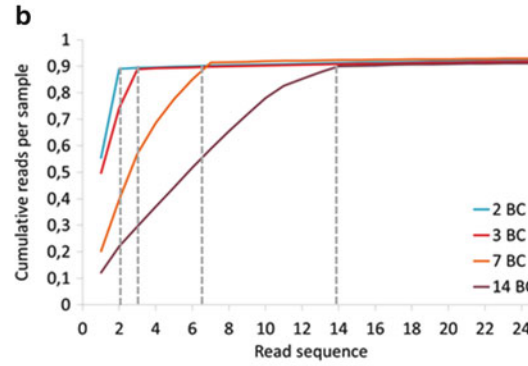

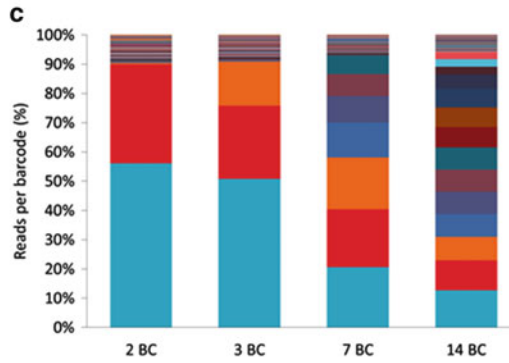

Fig. 3 Determining the threshold for noise removal. Barcodes were mixed at equimolar concentrations in pools of 2, 3, 7 and 14 barcodes. Deep sequencing was performed on an Illumina platform (HiSeq 2500). (**a**) Total reads and unique reads per sample. Note that the number of unique reads is many times higher than the true number of barcodes in the sample. (**b**) Visual impression of the barcode composition in each sample. Data were truncated to the top 250 unique reads. (**c**) Cumulative plot of barcode frequencies in all samples. Note the sharp change of the curve when all true barcodes have been counted. The tail of the curve consists of minor barcode reads, likely generated by sequencing and PCR errors

5.3 Noise Filtering by Frequency

The first step in analysis of deep sequencing results of a barcode experiment is signal to noise discrimination. It is known that deep sequencing generates plenty of noise: The number of unique reads is usually thousands times higher than the true number of barcodes (Fig. 3). These "false positive" reads may complicate barcode retrieval and result in the false identification of barcodes.

In conventional genome sequencing data, a single unique sequence mutation in a single read is always considered as noise, and thus ignored. Only when the read frequency surpasses a certain threshold, the mutation is considered significant. This is usually included in the conventional packages to detect and analyze SNP and small indels (for instance SAMtools [25] or GATK [26]). In case of barcodes, the conventionally used packages for deep sequencing analysis are not applicable. However, the concept is the same: a single unique read is more likely to be sequencing noise rather than a true barcode, and should not be taken as significant. Actually, two reads are still barely significant.

Binomial statistics predicts that at least five observations are needed to claim significantly different from zero ($P < 0.05$).

Noise filtering is relatively easy when the number of clones (barcodes) is small. In samples with a limited number of barcodes, each barcode has a substantial number of reads. When plotting the read frequencies of the barcodes ordered from large to small, a considerable drop of frequencies will mark the transition from true barcodes to background noise. In a cumulative frequency scale, the curve will noticeably bend at the turning point, indicating the change from high frequencies (true barcodes) to very low frequencies of barcodes (false) (Fig. 3).

However, in samples with a high number of barcodes, the difference between minor barcodes and noise by frequency is less obvious, and noise filtering becomes more cumbersome. Generally, noise filtering by sequence frequency can be applied for very low frequency reads only. A more powerful approach is filtering by sequence similarity, as described below.

5.4 Noise Removal Based on Sequence Similarity

Raw deep sequencing data commonly show massive amounts of barcode sequences that only differ in one nucleotide. These differences are likely due to PCR- and sequencing errors, as (1) deep sequencing of known (combinations of) individual barcodes also produces many sequences highly related to the original barcode; and (2) the abundance of small differences between these barcodes contrasts with the predicted distances by binomial models. Therefore, strategies are needed for the identification of similar barcodes, and subsequent removal of such satellites and pooling their read frequencies.

Note that the chance of finding two highly similar barcodes in one experiment can be precalculated, based on the number of possible barcodes and on the size of the library (see Appendix). For every used library we might know in advance how likely we can get barcode pairs different by one, two or three bases. Technically, it is desirable to calculate this parameter for every published library [18], as this in part determines the threshold for similarity of barcodes in a sample (and subsequent pooling of barcode read frequencies).

If the library is made in a such a way that it became highly unlikely to have a barcode pair different by one base, we assume that all found barcodes different by one base are due to sequencing errors, so we can merge all those barcodes into one cluster with the major barcode as the hub element (Fig. 4).

In current publications, substantial variation exists in the used cutoff for sequence similarity, ranging from a (Hamming) distance of 1–3 nucleotides. This might be acceptable, provided that it is supported by theoretical or experimental evidence. Unfortunately, the rationale for establishing the noise threshold is often not well explained. As we explained above, authors are supposed to use

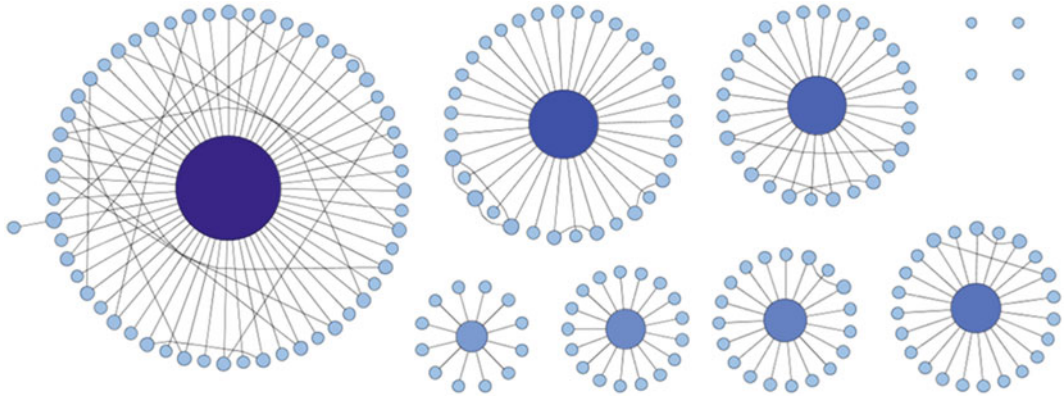

Fig. 4 Clustering analysis of barcode deep sequencing results. A barcode mixture of seven barcodes was sequenced. The raw barcode sequencing file was truncated by removing single reads, the 200 most abundant barcodes were used for similarity analysis. Subsequent clustering based on Hamming distance ($D = 1$) reveals seven major clusters, each with a substantial number of satellite sequences which only differ in one base pair. Out of 200 sequences, only four sequences cannot be assigned to one of the major clusters. Graphical representation was made using the yED software program (www.yworks.com/yed)

some statistically sound computational model which will predict the likely distance ($D_{\min}$) in the used library and compare it with sequencing data.

Distance analysis is a feasible option for small- to mid-size libraries. However, with increasing library size, those measurements become increasingly computationally intensive. In a set of 100 barcodes, a little less than 5000 pairwise comparisons have to be made. In a set of one million barcodes the number of comparisons will be approximately 5×10^{11}. Moreover, the real library is always skewed to some degree, and it causes further discrepancies between predicted (Poisson statistics) and expected events. Therefore, we probably need a compromise between library size and our real needs for unique barcoding in the real system.

5.5 Additional Filtering Steps

Depending on the situation, at least two more filtering steps could be suggested. One is applicable when all barcodes in the library are sequenced. In this case, every barcode in the sample can be validated for its presence in the library. If not present, it can be discarded as a false read. Another filtering step is based on biological significance, focusing on dominant barcodes and removing small clones. For instance, in hematopoietic studies, it is frequently suggested that a true stem cell must contribute at least up to 0.5 % of the cell content in the blood, and otherwise can be ignored [4, 27]. This simple rule allows for considerable reduction in the barcodes reported. Technically, if the 0.5 % threshold for barcode contribution is used, we cannot report more than 200 active stem cells per blood sample (as $200 = 1/0.05$, this paradoxical conclusion was pointed to one of us by Ingmar Glauche).

Nevertheless, some authors reported much bigger numbers of stem cells in blood per sample [14]. Note, these are disputable thresholds, which might vary depending on the concept and opinion of the author.

5.6 Accounting for Distribution Bias in Counting Barcodes

We might think that counting clones is as easy as counting any other physically defined items, like snooker balls on the table or mice in a cage. It is not quite so. The problem is the variable size of barcode clones, which makes their counting a bit more complicated.

Usually, in a set of barcoded clones, there is a limited number of big clones and thousands of small clones. Therefore, just telling "we have found 5000 clones in a blood sample 6 weeks after transplant" is not sufficient to understand the clonal contribution of the stem cells. It is possible that out of those 5000 hypothetical clones, only three major clones contribute to the 80 % of all mature blood cells and the next 20 clones add up to the 99 % of all blood contribution. In some settings, it may be informative to mention the remaining 4977 barcodes contributing to the remaining 1 % of the blood, yet these will be mostly obscure.

This dilemma reminisces a well-known Pareto principle and some other inequality measures, like the Gini index. Here, however, we will apply another approach, namely the Shannon information index, to correct for inequality of barcode clone sizes (see details of the calculations in the Appendix).

Let's consider an extreme case of raw sequence data of a mix of two barcodes preps (used in Fig. 3). Suppose we do not know the real number of barcodes in this sample. If we just count the number of unique raw reads in the sample after deep sequencing, we will count 470 barcodes. Two things are apparent, although. One is the considerable amount of skewing. Using the Shannon information index correction on raw data, not more than five barcodes in the sample are suggested. The second feature is the unusually high number of barcodes with a Hamming distance of 1–3 bases. (Fig. 5). If we consequently, remove these minor similar barcodes (in this case barcodes with 1 base difference), the list will be reduced to 83 barcodes. Subsequent Shannon correction further reduces the predicted sample complexity to no more than three barcodes. Although this is not exactly two expected barcodes, three barcodes is quite close to the right answer. Surely it is much better than the possible alternative suggestion of 470 barcodes (all unique), or 83 distance-corrected barcodes. Altogether, Shannon correction would be a useful tool to deal with barcode skewing in biological samples, as well as in barcode libraries reported earlier (Fig. 6) [2, 3, 13].

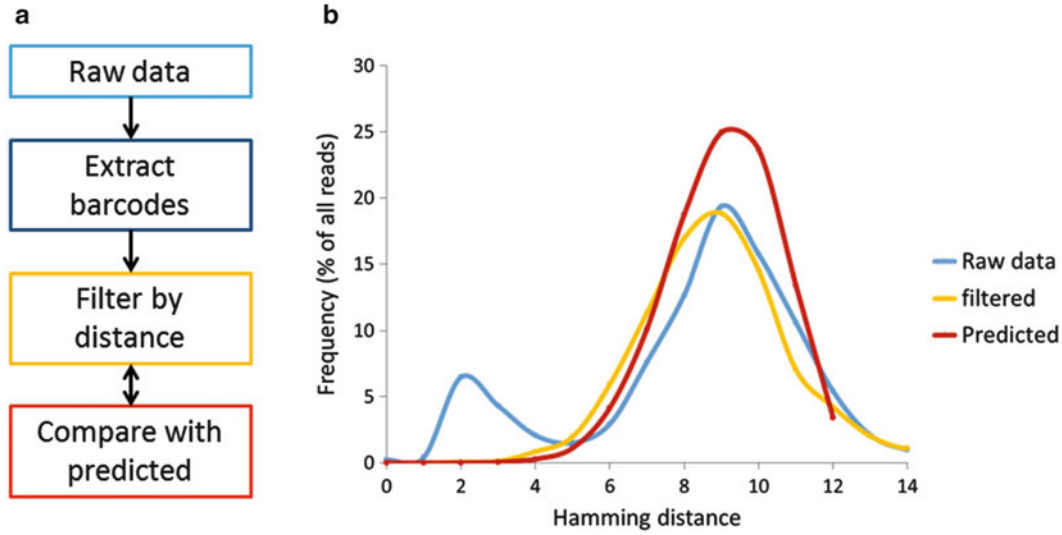

Fig. 5 Stepwise filtering of barcode deep sequencing results. (**a**) Essential steps in checking and processing barcode sequencing data. (**b**) Importance of noise filtering. In this example, two barcodes were mixed at equimolar ratios. Frequencies of barcodes were plotted as raw (unfiltered) data, filtered data (Hamming distance >1) and predicted distances (see Appendix for details on prediction of barcode distances). Note the unusually high frequencies of similar barcodes (Hamming distance 1–3) in the raw data, which likely represent sequencing errors

a

	Distribution			
	Equal	Linear	Fibonacci	Exp.
	1	1	1	2
	1	2	1	4
	1	3	2	8
	1	4	3	16
	1	5	5	32
	1	6	8	64
	1	7	13	128
	1	8	21	256
	1	9	34	512
	1	10	55	1024
Shannon index	**2.30**	**2.15**	**1.70**	**1.38**
Equitability index	**1.00**	**0.93**	**0.74**	**0.60**
Complexity	**10**	**9**	**5**	**4**

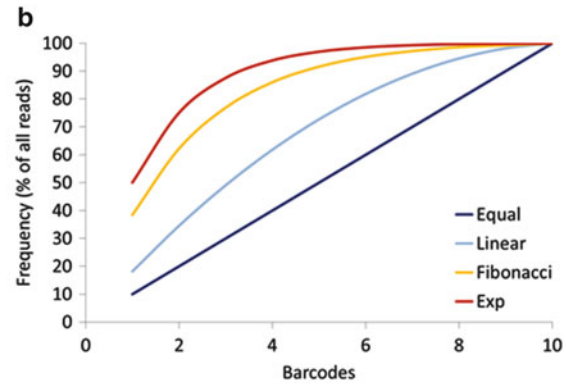

Fig. 6 Shannon correction to estimate skewing of barcode distribution. The example considers four sets of ten barcodes, each with a different distribution: equal, or skewed to different degrees (linear, Fibonacci, exponential). For each set, the Shannon index and the equitability index as shown in the Appendix. Although the number of barcodes in each set is similar, their unequal distribution will result in different estimated complexities

5.7 Resolution of Barcoding

There is one more point of confusion in recent literature, which needs to be clarified. Some authors seem to equate size of the library and/or sequencing depth with the resolution of the barcoding method. Indeed, the library size imposes a potential limit on the theoretical maximum of the detected barcodes. A small library or low coverage in sequencing might limit the resolution of barcoded clone discovery. However, the major problem of current publications on cellular barcoding is likely the correct reporting of barcodes and their sizes and numbers. In this context, resolution of a barcoding experiment has a meaning of correctness (or precision) of the barcode calling. It generally relies on two parameters common for many other methods, namely sensitivity and specificity. A barcoding experiment typically deals with the dilemma of detecting the maximum of truly present barcodes in the sample, while also rejecting most of the false barcodes (such as irrelevant sequences, mutated sequences, contaminating sequences etc., details in the Appendix). This aspect of resolution, which is only marginally dependent on the library size, is not yet well studied, neither documented in the barcoding literature. In fact, it requires an experiment with upfront known barcode sequences and testing protocols of their recovery from noisy sequencing data.

6 Recent Developments and Future Directions

6.1 Alternative Methods for Clonal Analysis

As technical progress continues, we might expect further improvement and/or replacement of cellular barcoding by some superior method or combination of methods for assessment of clonality.

A potential alternative for clonal analysis of (retro)virally transduced stem cells is (and was) the retroviral integration site analysis. Noteworthy, the barcoding method appeared as a simplified alternative to the retroviral integration site analysis, which is also used to label and count retrovirally transduced stem cells. Since restriction of the genomic DNA is prone to biases [28], the nonrestrictive analysis might prevail (by for instance total shredding and genomic DNA sequencing). As can be witnessed from the current literature, a restriction-free version of this method [29] keeps progressing in time [30, 31]. A potential improvement in the barcoding method includes the use of fully designed libraries instead of those generated by random synthesis [28, 32, 33]. Such schemes already exist, and with improving technical tools they might be implemented in the future. Implementing defined libraries will simplify barcode counts and improve the method's resolution significantly.

Multicolored barcoding is another method for clonal analysis (introduced nearly decade ago). It is usually done by either multiple vector transduction (RGB mouse [17]) or with a Cre-LoxP cassette (brainbow mouse [34]). This approach keeps inspiring authors to explore combinatorial limits with Cre-LoxP system and reach

higher degree of fidelity and complexity [35, 36]. Obviously, there might be improvement in resolution and discrimination of colors and their combinations. Although the recombination/excision system is more complicated in terms of combinatorial equality of occurring chances, when properly implemented, it may become closer to the long desired in vivo barcoding without retroviral or lentiviral transduction.

6.2 Mutation-Based Clonal Studies

Another alternative for barcodes as clonal markers are (combinations of) naturally occurring genetic mutations. Some authors follow mutations of naturally unstable simple repeats, which allows tracing clonal evolution at the single cell level [16, 37–39]. Those repeat regions, also known as microsatellites, have also been used to study cancer evolution [39, 40], although other somatic mutations, especially in cancer-associated genes, are more preferential in cancer studies [40–42]. Some authors use more stable somatic mutations [43]. In this case, the resolution is lowered to follow the clonality of different organs. The list of publications on clonal cancer evolution is steadily increasing in last years and needs more dedicated space than we have in this manuscript. Obviously, we can expect more data, claims and controversies in this field in coming years.

One might think of combining clonal data from different kinds of studies, or assume that one type of clonal study would replicate in others while using different techniques. To the contrary, direct comparison of those data is problematic. The major issue is conceptual and technical differences. Compare for instance philosophy and algorithms used for clonality in cancer, single-cell simple repeats analysis and barcoding. They are fundamentally different.

In cancer we expect gradual and progressive appearance of unique detectable mutations, some might reach clonal domination, some will fluctuate, some will come and go. We generally take the hypothesis of unique nonrecurrent origin of those mutations. The used algorithms behind those data will try to explain dynamics and distribution of those mutations in time by linking detected mutations gradually accumulating in time to the minimal number of clones, defined as unique combination of mutations per each cell. Therefore, it will likely generate a tree-like network connecting clones with different sets of mutations, and the branches will gradually increase in numbers in time (proportional to the increasing number of detected mutations in a given population of cells). In case of simple repeats dynamics, we do not expect either unique or driving mutation. Therefore, correlation between cancer clone progression and satellite mutation can be only occasional. Note that both approaches are not aimed on the counting of leukemic stem cells. In fact, they cannot be used for such counting. To the contrary, cellular barcoding is blind to the genetic drift and it marks all stem cells at one time point uniquely. Therefore, it is possible that the same population analyzed by those methods might look

like highly polyclonal according to one assay and rather monoclonal or oligoclonal by the other. Obviously, an exciting challenge for the future will be the attempt to combine those methods in one study, and we already witness the beginning of such discussions in recent literature [44].

Acknowledgements

We kindly acknowledge Erik Zwart, Evgenia Verovskaya, and Tilo Buschmann for their critical review, comments, and suggestions. M. Belderbos was supported by personal grants from the University Medical Center Groningen, the European Research Institute for the Biology of Ageing and the Dutch Cancer Society.

Appendix: Background and Examples of Data Analysis

Probability of Unique Barcoding

To tag each target cell with a unique barcode, the number of barcodes needs to be in excess of the number of target cells. Here, we illustrate how to calculate whether the library size is sufficiently big compared to the potential number of barcoded cells. If we ignore the inequality of barcodes present in the library (ideally they should be all equal, yet most of the times the library is skewed, see below for how to deal with this), then the probabilities can be calculated by filling numbers into the binomial distribution model

If n is the library size and k is the number of barcoded cells, then the approximate probability of having each cell uniquely barcoded is as follows:

$$P(k,n) = \begin{array}{l}\text{binom.dist}(\text{hits} = 1,\ \text{trials} = k,\\ \qquad \text{probability of hit} = 1/n,\ \text{cumulative} = \text{true})\end{array} \tag{1a}$$

This can be presented as a formula:

$$P(k,n) = \left(\frac{n!}{k!(n-k)!}\right) P^k (1-P)^{n-k} \tag{1b}$$

Example:

Suppose we have a library of 500 barcodes (n) and we aim to barcode 50 stem cells uniquely (k). What is our risk of having two stem cells labeled with the same barcode?

In this case:

$$1 - P(50,500) = \begin{array}{l}1 - \text{binom.dist}(\text{hits} = 1,\ \text{trials} = 50,\\ \qquad \text{probability of hit} = 1/500,\\ \qquad \text{cumulative} = \text{true}) = 0.004597188\end{array}$$

Therefore, this is a relatively safe experimental design (<0.5 % chance of having a pair of cells identically labeled). Note: this is not the same as calculating the probability of having at least one pair of barcodes equal (a.k.a. "birthday paradox," the probability of having identically labeled pair cells at least once in entire set). Such a probability is quite high. Here, we count the probability of having equal barcodes among other paired combinations. This equation will be used for analyzing barcode sequencing data below.

How to Estimate Approximate Number of Barcodes from Reading a Crude PCR Barcode SANGER Chromatogram

The number of barcodes in a sample can be approximated by analysis of the Sanger chromatogram (Fig. 2). This can be done by prediction models in different ways. The easiest way is to use a random generator and to count the probabilities of appearance of a single, double, triple, or quadruple peak at each of the variable positions of the barcode, depending on number of trials called (n). A pseudo code would look like:

My barcode mix = n

MaxIterations = 1000

For i in range(0,MaxIterations):

  For j in range(0, n):

    Repeat take random(A, C, G, T)

  Count frequency of single, double, triple, quadruple bases

Collect and report all frequencies

An example of the counts by random is as follows:

Frequencies of base calls, *N*				
BC mix	**1**	**2**	**3**	**4**
1	1000	0	0	0
2	240	760	0	0
3	65	557	378	0
4	17	320	572	91
5	2	177	605	216
6	1	70	568	361
7	0	53	428	519
8	0	36	350	614
9	0	13	303	684
10	0	8	230	762

Where BC mix stands for numbers of barcodes in the mixture (in columns). The frequencies of base calls are shown for each kind (single peak, double peak etc.)

Another, more accurate approach is to count all possible combinations of base calls depending on number of trials, as follows:

	Frequencies of base calls, *N*			
BC mix	**1**	**2**	**3**	**4**
1	1	0	0	0
2	4	12	0	0
3	4	36	24	0
4	4	84	144	24
5	4	180	600	240
6	4	372	2160	1560
7	4	756	7224	8400
8	4	1524	23184	40824
9	4	3060	72600	186480
10	4	6132	223920	818520

Both approaches can be programmed and they give equivalent results.

Major Properties of Barcode Libraries

There are three major parameters in barcoding to check and analyze: (1) the total number of barcodes (in the library and in experimental data); (2) the randomness of barcodes regarding their sequence, and (3) the evenness of barcodes in the sample (in the library and in experimental data). The effective library size is directly affected by the randomness of synthesis: The less randomly it is made, the less barcodes will be in the library. Evenness (uniformity) of barcodes also affect the effective size of the library: with less evenness the effective size will decrease. Finally, randomness of sequences is connected to the observed and expected distances between barcodes. Below, we present the minimal computational background to estimate these parameters.

Randomness

Poisson and binomial distributions are good in predicting uniqueness of barcoding by random sequences, and they are good in estimating maximal sizes of libraries and clones. Whenever possible, it is important to report how random the chemical synthesis of the used barcodes was. Sanger sequencing of *E.coli* clones is preferential because it is free from sequencing errors. Deep sequencing data are acceptable if sequencing noise is convincingly (adequately) removed.

Skewing

Skewing is a massively ignored aspect of the effective size of the vector library. It can be approached from the perspective of information theory. In an ideal library of evenly distributed frequencies of items, we have the maximal Shannon diversity index, H_{sh}. If items are not equal then we can calculate the diversity indexes in two different ways. One is Shannon diversity index:

$$H_{\mathrm{sh}} = \sum p_i \times \mathrm{Ln}(p_i) \tag{2}$$

where p_i is the probability value for every barcode on the list. If the barcode frequencies are equal then $p_i = 1/N$, where N is the number of all barcodes. If those frequencies are not equal, then for every barcode, the p_i value will be a fraction of the frequency for the i-th barcode reads divided by total reads for all barcodes. Corrected barcode numbers by those parameters (C_{b}) will be:

$$C_{\mathrm{b}} = \exp(H_{\mathrm{sh}}) \tag{3}$$

This information content however will decrease upon increased skewing. Too small frequencies present in the library will have progressively fewer contributions to the whole library. This can be directly estimated by measuring the mentioned above indexes. An example is already given in Fig. 6.

A nearly identical solution to the Shannon correction can be done using the information index (in bits of information):

$$\mathrm{IB} = \sum p_i \times \mathrm{Log}_2(p_i) \tag{4}$$

And correction will be done as following:

$$C_{\mathrm{b}} = 2^{\mathrm{IB}} \tag{5}$$

The result is identical to the Shannon index described above.

For skewing, the equitability index can be used, which is a Shannon index divided by the total number of reported barcodes.

$$\mathrm{Eq} = H_{\mathrm{Sh}}/\mathrm{Ln}(N) \tag{6}$$

Consider the example presented in Fig. 6. The table displays four data sets ten barcodes, with either equal frequencies or different degrees of inequality. Next to the table is the normalized cumulative frequency plot.

For equal barcodes, the cumulative frequency line is diagonal. More unequal sets deviate further from diagonal. If we calculate the Shannon diversity index for each set and then take the correction for Shannon index as in Eq. 3, it will suggest ten barcodes for the equal set (as we might expect), nine barcodes for linear set, and five and four for the remaining two. Although each set consists of ten

barcodes, inequality of barcodes reduces their effective set size. From the plot (Fig. 6b), it becomes clear that the information content correction is roughly similar to the number of barcodes in the cumulative 95 % of barcode reads. The advantage of Shannon index correction compared to the % threshold approach is that it is correcting for the library size without any additional assumptions. In other words, it is not bound to the taste and preferences of the analyst.

Note that such cumulative plot also illustrates a degree of inequality which, when inversed, is also known as the Lorenz curve (if plotted from smallest to biggest barcodes cumulatively). Data closer to the diagonal are more equal to each other, and the other way around.

Skewing parameter varies from Eq = 1, if barcodes are equal, while approaching zero with increased skewing. For the power function, Eq = 0.6.

Distances Between Barcodes

The distance between barcodes is defined as the number of different bases between a pair of barcodes. For instance, the 6-mers AAATTG and AACTTC differ by 2 bases. If we take into account substitutions only, this will be referred to the Hamming distance ($D_H = 2$). As a simple guide for assessment of randomness we can rely on the fact that a probability for a certain number of similar bases in two randomly selected barcodes, $S_{ki,kj}$, with the length of **I** bases follows a binomial distribution.

$$P(S_{ki,kj}) = \text{binom.dist}(S_{ki,kj}, \text{length} = I, \text{probability} = 0.25, \text{cumulative} = \text{false}) \tag{7a}$$

or as an equation (suggested by Tilo Buschmann):

$$P(d(S_i, S_j) = d) = \binom{l}{d} \times \left(\frac{1}{4}\right)^{d} \times \left(\frac{3}{4}\right)^{l-d} \tag{7b}$$

The similarity degree between two randomly chosen barcodes is equal to the difference in barcode length, Len(BC) and the Hamming distance (D_H), therefore:

$$P(\text{Len(BC)} - D_H) = P(S_{ki,kj}) \tag{8}$$

The distribution consequently predicts that if you take for instance any random pair of 12-base words or compare any randomly picked word to the full library set, the most likely and frequent distance will be 9–10 bases, as shown in the table below:

Similarity	D_{min}	P
0	12	0.031676352
1	11	0.126705408
2	10	0.232293248
3	9	0.258103609
4	8	0.193577707
5	7	0.103241444
6	6	0.04014945
7	5	0.011471272
8	4	0.002389848
9	3	0.000354052
10	2	3.54052E-05
11	1	2.14577E-06
12	0	5.96046E-08

Likewise, any randomly picked barcode compared to the full set of barcodes of the same length follows exactly the same distribution. This approach was used for the random simulation on the Fig. 5.

Example:

Let's take for example the raw sequencing data of the mixture of two barcodes used for Fig. 5. There are 468 unique barcodes in this file. Suppose we do not know how many true barcodes are in the file. We can only assume that with more true barcodes we will have a better fit to what is expected by random simulation. As explained above, a truly random set of barcodes shows a (transformed) binomial distribution of distances upon random sampling of the set. We can do random sampling of the given set using a custom script of an approximate structure like the following pseudo code:

```
Import Distance Package (See Below in the Protocol)
Read the source file
Repeat 1000 × N times:
    Take random barcode1, barcode2
    If barcode1 not equal to barcode2:
        Measure distance
        Add result to the array of distances
Report all distances frequencies
```

Data for this particular case are shown in Fig. 5b. It is clear that the raw set of 2 barcodes contains an unusually high number of distances 1–3. Therefore, it disagrees with the hypothesis of the random set. One obvious explanation is that the set is contaminated with false barcodes, likely generated by sequencing errors. Therefore, this set requires filtering by small distances.

Resolution of Barcode Detection

Let's define our barcodes as:

True positive: barcodes which are really present in the library, sequence confirmed.

True negative: barcodes detected in the sample not present in the library, have obscure origin, and likely originate from PCR errors or likewise, rejected by the method.

False negative: barcodes which are present in the library, but rejected by the method.

False positive: barcodes which are false barcode, but accepted by the method.

Sensitivity is defined as the fraction of true positive barcodes to the sum of true positive and false negative, whereas specificity is defined as a fraction of the false positive in the sample to the sum of true negative and false positive barcodes.

$$\text{Sensitivity} = \frac{\text{true\_positives}}{(\text{true\_positives} + \text{false\_negatives})} \tag{9}$$

The denominator here is all barcodes in the library

$$\text{Specificity} = \frac{\text{true\_negatives}}{(\text{true\_negatives} + \text{false\_positives})} \tag{10}$$

The denominator in this formula is the sum of all false reads in the data.

The estimation of sensitivity can be illustrated by filtering of the sequencing data from the sample based on one of the parameters, like using the minimal distance or read frequency. As a reference we can take the barcode library, validated by repetitive resequencing of the batch.

To summarize: the resolution of the method is a measure of its performance regarding sensitivity and specificity. A claim of high resolution is equivalent to the claim of the best possible detection of the barcodes in the sample and the best possible separation of true and false barcodes.

Protocol for Converting Raw Deep Sequencing Data into Sets of Barcodes

Here, we provide a pipeline for retrieval of barcodes from deep sequencing data.

Step 1. Import raw data.

The raw sequencing data from an Illumina HiSeq2500 machine are a collection of per-cycle bcl base-call files. These bcl files are converted to compressed FATSQ.gz files with bcl2FATSQ (https://support.illumina.com/downloads/bcl2FATSQ_conversion_software_184.html). A sample sheet, provided by the researcher/operator, lets the software assign reads to samples, and samples to projects, provided that Illumina multiplex primers where used. After this de-multiplexing, the FATSQ (2) files are available to download through a file transfer protocol (FTP) server (this can be arranged differently, depending on the local organization). For further data processing, a workstation with at least 32 Gb memory and 1 Tb hard drive space is advised. Note that all the steps can be performed on systems using Linux, Windows, or Mac OS, however a minimal of 8 Gb RAM and 250 Gb hard drive space is recommended.

Step 2. Data compression.

Multiplex barcode sequencing data (FATSQ format) ranges in file size between 1 and 50 Gb. Depending on the operational system, this can be a challenge. To ease downstream analysis, we compress the data with the following steps.

1. Remove low quality reads; depending on the sequencer, the data will use an encoding scheme for example Illumina 1.8+-. Using the quality line for each read, one can filter on a predetermined cutoff value. This could be the total read quality value or a minimal quality value for the first x number of base pairs.
2. Collapse reads; remove redundant FATSQ lines 1, 3, and 4. Thereafter, collapse reads and add their frequency, see example below.

   AACCTT
   AACCTT
   AAGGTT

   After collapsing data:

   AACCTT 2
   AAGGTT 1
3. Remove single reads; After collapsing the FATSQ data, all reads with a frequency of one are removed. Note, these singles hold minimal biological value and needlessly increase the volume of the dataset.

   By compressing FATSQ files one can reduce the size with 99 %.

Step 3. Barcoded samples.

After data compression, all sequencing reads are further demultiplexed into samples. Note that initial sequencing data are split into separate files based on the Illumina indexes. For this purpose, we use special primers with variable tags (8–9 nt long) for amplifying the barcoded region of individual samples. By using unique sample tags and adjacent part of the primer, totally 13 nt in length of every read is tested for exact matching. For every sample marked with unique primer tag, a (text/csv/tsv) file is generated that lists the unique reads within this sample, and their frequencies. In principle, more sophisticated tag-extraction protocols could be used. However, since the tag is positioned at the very beginning of the sequencing read, and sequencing quality is likely the best out of entire read, more sophisticated algorithms will be more time consuming and provide little improvement in retrieved numbers of reads per sample.

Step 4. Converting lists or read into lists of barcodes.

So far, entire sequencing reads were collected into multiple separate files. Each of the reads supposedly contains a barcode. Depending on the type of barcodes, multiple search strategies are possible; exact match, regular expressions or motif search (probably along with multiple different options). We routinely use MOODS (Motif Occurrence Detection Suite [45] in BioPerl or Python custom script. First, the barcode sequence ("the backbone") is transformed into a position-weight matrix. Second, MOODS searches for any similarity to the barcode sequence. The threshold for similarity is empirically established to such level, that in every read no more than one barcode is detected. Usually it tolerates multiple mismatches in the barcode backbone. Small indels on the side of the barcode will be tolerated, too. However, indels in the center of the barcode will deteriorate the discovery of the barcode. To circumvent this problem, an algorithm with gapped motif search must be implemented. For this, the GLAM2 tool (or a similar algorithm) might be used [46, 47]. For each sample, a file with unique barcodes and their frequency is generated.

Step 5. Compression of barcode lists.

The barcode list generated in the previous step is largely redundant, containing multiple identical barcodes, which must be merged, as well as their frequencies. Moreover, usually all minor barcodes with minimal distance of 1 base can be eliminated (and their frequencies added to the major similar barcode, see Fig. 4). We routinely use a custom script. Two distances can be employed, Levenshtein (which takes into account both SNPs and indels) or Hamming (SNP only). In Python and Perl, the Levenshtein package can be used for both types of distances (https://pypi.python.org/pypi/python-Levenshtein/). Several packages are available in

R, such as Stringdist [48] and DNABarcodes [4]. Both packages are able to measure different kinds of distances, including the ones mentioned above. Note that the routinely used threshold by Hamming distance=1 is arbitrary and chosen for simplicity of theoretical considerations. Other distances can be used too, provided they are well justified.

After this step the barcode lists per sample can be used for analysis. Depending on the details of the experiment some other cutoffs can be used. For instance, steps like the 0.5 % biologically meaningful cutoff might be introduced here.

Usually, the end product is made by assembly of the individual samples into a table, representing each particular experiment. We routinely use a custom script for this purpose. From this table the dynamics of each individual barcode can be followed.

References

1. Schepers K, Swart E, van Heijst JWJ et al (2008) Dissecting T cell lineage relationships by cellular barcoding. J Exp Med 205:2309–2318. doi:10.1084/jem.20072462
2. Gerrits A, Dykstra B, Kalmykowa OJ et al (2010) Cellular barcoding tool for clonal analysis in the hematopoietic system. Blood 115:2610–2618, doi: 10.1182/blood-2009-06-229757; 10.1182/blood-2009-06-229757
3. Lu R, Neff NF, Quake SR, Weissman IL (2011) Tracking single hematopoietic stem cells in vivo using high-throughput sequencing in conjunction with viral genetic barcoding. Nat Biotechnol 29:928–933. doi:10.1038/nbt.1977
4. Verovskaya E, Broekhuis MJC, Zwart E et al (2013) Heterogeneity of young and aged murine hematopoietic stem cells revealed by quantitative clonal analysis using cellular barcoding. Blood 122:523–532. doi:10.1182/blood-2013-01-481135
5. Naik SH, Schumacher TN, Perié L (2014) Cellular barcoding: a technical appraisal. Exp Hematol 42:598–608. doi:10.1016/j.exphem.2014.05.003
6. Cheung AMS, Nguyen LV, Carles A et al (2013) Analysis of the clonal growth and differentiation dynamics of primitive barcoded human cord blood cells in NSG mice. Blood 122:3129–3137. doi:10.1182/blood-2013-06-508432
7. Brugman MH, Wiekmeijer A-S, van Eggermond M et al (2015) Development of a diverse human T-cell repertoire despite stringent restriction of hematopoietic clonality in the thymus. Proc Natl Acad Sci U S A 112: E6020–E6027. doi:10.1073/pnas.1519118112
8. Harwell CC, Fuentealba LC, Gonzalez-Cerrillo A et al (2015) Wide dispersion and diversity of clonally related inhibitory interneurons. Neuron 87:999–1007. doi:10.1016/j.neuron.2015.07.030
9. Golden JA, Cepko CL (1996) Clones in the chick diencephalon contain multiple cell types and siblings are widely dispersed. Development 122:65–78
10. Golden JA, Fields-Berry SC, Cepko CL (1995) Construction and characterization of a highly complex retroviral library for lineage analysis. Proc Natl Acad Sci U S A 92:5704–5708
11. Nguyen LV, Cox CL, Eirew P et al (2014) DNA barcoding reveals diverse growth kinetics of human breast tumour subclones in serially passaged xenografts. Nat Commun 5:5871. doi:10.1038/ncomms6871
12. Porter SN, Baker LC, Mittelman D, Porteus MH (2014) Lentiviral and targeted cellular barcoding reveals ongoing clonal dynamics of cell lines in vitro and in vivo. Genome Biol 15: R75. doi:10.1186/gb-2014-15-5-r75
13. Bhang HC, Ruddy DA, Krishnamurthy Radhakrishna V et al (2015) Studying clonal dynamics in response to cancer therapy using high-complexity barcoding. Nat Med 21:440–448. doi:10.1038/nm.3841
14. Wu C, Li B, Lu R et al (2014) Clonal tracking of rhesus macaque hematopoiesis highlights a distinct lineage origin for natural killer cells. Cell Stem Cell 14:486–499. doi:10.1016/j.stem.2014.01.020
15. Gerlach C, Rohr JC, Perié L et al (2013) Heterogeneous differentiation patterns of

individual CD8+ T cells. Science 340:635–639. doi:10.1126/science.1235487

16. Chapal-Ilani N, Maruvka YE, Spiro A et al (2013) Comparing algorithms that reconstruct cell lineage trees utilizing information on microsatellite mutations. PLoS Comput Biol 9, e1003297. doi:10.1371/journal.pcbi.1003297
17. Cornils K, Thielecke L, Hüser S et al (2014) Multiplexing clonality: combining RGB marking and genetic barcoding. Nucleic Acids Res 42, e56. doi:10.1093/nar/gku081
18. Bystrykh LV, de Haan G, Verovskaya E (2014) Barcoded vector libraries and retroviral or lentiviral barcoding of hematopoietic stem cells. Methods Mol Biol 1185:345–360. doi:10.1007/978-1-4939-1133-2_23
19. Verovskaya E, Broekhuis MJC, Zwart E et al (2014) Asymmetry in skeletal distribution of mouse hematopoietic stem cell clones and their equilibration by mobilizing cytokines. J Exp Med 211:487–497. doi:10.1084/jem.20131804
20. Kolfschoten IGM, van Leeuwen B, Berns K et al (2005) A genetic screen identifies PITX1 as a suppressor of RAS activity and tumorigenicity. Cell 121:849–858. doi:10.1016/j.cell.2005.04.017
21. Adams BD, Guo S, Bai H et al (2012) An in vivo functional screen uncovers miR-150-mediated regulation of hematopoietic injury response. Cell Rep 2:1048–1060. doi:10.1016/j.celrep.2012.09.014
22. Nguyen LV, Pellacani D, Lefort S et al (2015) Barcoding reveals complex clonal dynamics of de novo transformed human mammary cells. Nature. doi:10.1038/nature15742
23. Akhtar W, de Jong J, Pindyurin AV et al (2013) Chromatin position effects assayed by thousands of reporters integrated in parallel. Cell 154:914–927. doi:10.1016/j.cell.2013.07.018
24. Colvin GA, Lambert J-F, Abedi M et al (2004) Murine marrow cellularity and the concept of stem cell competition: geographic and quantitative determinants in stem cell biology. Leukemia 18:575–583. doi:10.1038/sj.leu.2403268
25. Li H, Handsaker B, Wysoker A et al (2009) The sequence alignment/map format and SAMtools. Bioinformatics 25:2078–2079. doi:10.1093/bioinformatics/btp352
26. McKenna A, Hanna M, Banks E et al (2010) The genome analysis toolkit: a MapReduce framework for analyzing next-generation DNA sequencing data. Genome Res 20:1297–1303. doi:10.1101/gr.107524.110
27. Dykstra B, Olthof S, Schreuder J et al (2011) Clonal analysis reveals multiple functional defects of aged murine hematopoietic stem cells. J Exp Med 208:2691–2703, doi: 10.1084/jem.20111490; 10.1084/jem.20111490
28. Bystrykh LV (2012) Generalized DNA barcode design based on Hamming codes. PLoS One 7:e36852. doi:10.1371/journal.pone.0036852
29. Kim S, Kim N, Presson AP et al (2010) High-throughput, sensitive quantification of repopulating hematopoietic stem cell clones. J Virol 84:11771–11780. doi:10.1128/JVI.01355-10
30. Kim S, Kim N, Presson AP et al (2014) Dynamics of HSPC repopulation in nonhuman primates revealed by a decade-long clonal-tracking study. Cell Stem Cell 14:473–485. doi:10.1016/j.stem.2013.12.012
31. Gabriel R, Kutschera I, Bartholomae CC et al. (2014) Linear amplification mediated PCR–localization of genetic elements and characterization of unknown flanking DNA. J Vis Exp. e51543. doi: 10.3791/51543
32. Xu Q, Schlabach MR, Hannon GJ, Elledge SJ (2009) Design of 240,000 orthogonal 25mer DNA barcode probes. Proc Natl Acad Sci 106:2289–2294. doi:10.1073/pnas.0812506106
33. Buschmann T, Bystrykh LV (2013) Levenshtein error-correcting barcodes for multiplexed DNA sequencing. BMC Bioinformatics 14:272. doi:10.1186/1471-2105-14-272
34. Livet J, Weissman TA, Kang H et al (2007) Transgenic strategies for combinatorial expression of fluorescent proteins in the nervous system. Nature 450:56–62. doi:10.1038/nature06293
35. Wei Y, Koulakov AA (2012) An exactly solvable model of random site-specific recombinations. Bull Math Biol 74:2897–2916. doi:10.1007/s11538-012-9788-z
36. Peikon ID, Gizatullina DI, Zador AM (2014) In vivo generation of DNA sequence diversity for cellular barcoding. Nucleic Acids Res 42, e127. doi:10.1093/nar/gku604
37. Ally D, Ritland K, Otto SP (2008) Can clone size serve as a proxy for clone age? An exploration using microsatellite divergence in Populus tremuloides. Mol Ecol 17:4897–4911. doi:10.1111/j.1365-294X.2008.03962.x
38. Mock KE, Rowe CA, Hooten MB et al (2008) Clonal dynamics in western North American aspen (Populus tremuloides). Mol Ecol 17:4827–4844. doi:10.1111/j.1365-294X.2008.03963.x

39. Naxerova K, Brachtel E, Salk JJ et al (2014) Hypermutable DNA chronicles the evolution of human colon cancer. Proc Natl Acad Sci U S A 111:E1889–E1898. doi:10.1073/pnas.1400179111
40. Shlush LI, Chapal-Ilani N, Adar R et al (2012) Cell lineage analysis of acute leukemia relapse uncovers the role of replication-rate heterogeneity and microsatellite instability. Blood 120:603–612. doi:10.1182/blood-2011-10-388629
41. Mullighan CG (2013) Genomic characterization of childhood acute lymphoblastic leukemia. Semin Hematol 50:314–324. doi:10.1053/j.seminhematol.2013.10.001
42. Ding L, Ley TJ, Larson DE et al (2012) Clonal evolution in relapsed acute myeloid leukaemia revealed by whole-genome sequencing. Nature 481:506–510, doi: 10.1038/nature10738; 10.1038/nature10738
43. Behjati S, Huch M, van Boxtel R et al (2014) Genome sequencing of normal cells reveals developmental lineages and mutational processes. Nature 513:422–425. doi:10.1038/nature13448
44. Blundell JR, Levy SF (2014) Beyond genome sequencing: lineage tracking with barcodes to study the dynamics of evolution, infection, and cancer. Genomics 104:417–430. doi:10.1016/j.ygeno.2014.09.005
45. Korhonen J, Martinmäki P, Pizzi C et al (2009) MOODS: fast search for position weight matrix matches in DNA sequences. Bioinformatics 25:3181–3182. doi:10.1093/bioinformatics/btp554
46. Bailey TL, Boden M, Buske FA et al (2009) MEME SUITE: tools for motif discovery and searching. Nucleic Acids Res 37:W202–W208. doi:10.1093/nar/gkp335
47. Bailey TL, Johnson J, Grant CE, Noble WS (2015) The MEME suite. Nucleic Acids Res 43:W39–W49. doi:10.1093/nar/gkv416
48. van der Loo MPJ (2014) The stringdist package for approximate string matching. R J 6:111–122

Methods in Molecular Biology (2016) 1516: 91–99
DOI 10.1007/7651_2016_361

Published online: 03 June 2016

Analysis of Cell Cycle Status of Murine Hematopoietic Stem Cells

Krzysztof Szade*, Karolina Bukowska-Strakova*, Monika Zukowska, Alicja Jozkowicz, and Józef Dulak

Abstract

Hematopoietic stem cells (HSC) act as paradigmatic tissue-specific adult stem cells. While they are quiescent in steady-state conditions, they enter the cell cycle and proliferate in stress conditions and during tissue regeneration. Therefore, analysis of cell cycle status of HSC is crucial for understanding their biology. However, due to low number of HSC in tissue and need to use many surface markers for their identification, analysis of their cycle status is technically complicated. Here, we presented our simple strategy to analyze cell cycle of strictly defined LKS $CD48^{-}CD150^{+}CD34^{-}$ HSC, together with Ki67 and DAPI staining by flow cytometry.

Keywords:: Hematopoietic stem cells, Cell cycle phase, Quiescence, Dormancy, Proliferation, Ki67, Flow cytometry, Activation, G0, G1

1 Introduction

Adult stem cells are often characterized as quiescent cells that in steady-state conditions rarely proliferate and enter active cell cycle phases [1]. Nevertheless, small subset of stem cells do proliferate and self-renew their population. Their activation and proliferation changes in stress conditions and during tissue regeneration [1]. Moreover, stem cells isolated from several different genetically modified mouse models show the aberrant balance between quiescence and activation [2]. Therefore checking what fraction of stem cells enter the cell cycle and proliferate is important when investigating the function and heterogeneity of stem cells.

Cell cycle and proliferation analyzes are among the most common types of analysis done by flow cytometry [3]. They are based on stoichiometric binding of fluorescent dye to DNA. When these dyes are used together with other markers such us Ki67, flow cytometry allows to distinguish G0, G1, S, and G2/M cell cycle

*Author contributed equally with all other contributors.

phases at the single-cell level [3]. Apart from Ki67, also labeling of RNA in viable cells by pyronin Y was used together with DNA dyes to distinguish the cell cycle phases [3].

However, these methods which are in most cases relatively simple and well established, become more complicated when analyzing adult stem cells isolated from tissues. This is caused by small number of adult stem cells in the tissues and necessity to use several fluorescent dyes for proper identification. The spectral properties of several fluorescent dyes used simultaneously limit the ability to apply additionally dyes needed for cell cycle analysis. Especially, the broad emission spectrum of pyronin makes its use with other dyes difficult. Additionally, the labeling of intracellular antigens requires fixation and permeabilization of cells. Fixating agents may affect the fluorescent dyes, particularly the tandem dyes, what impedes the proper identification of rare stem cells. To omit these problems, more complicated protocol was proposed, that involved sorting of additionally labeled carrier cells [4]. Nevertheless, this protocol remains also more cumbersome to apply.

Here, we share our method to analyze cell cycle status of hematopoietic stem cells (HSC). For HSC identification we used several surface markers (Lineage, c-Kit, Sca-1, CD48, CD150, CD34) and to distinguish cell cycle phases we applied DAPI and Ki67. We showed how to fix the cells for Ki67 labeling to sustain the properties of fluorescent dyes. This method allows for analysis of cell cycle status in fully-phenotyped HSC without either additional sorting of cells or use the carrier cells.

2 Materials

2.1 Staining Whole Murine Bone Marrow

1. A centrifuge for 15 ml conical tubes and 5 ml FACS tubes with cooling option.
2. Cell strainer—40 μm Becton Dickinson (BD).
3. Antibodies used in the protocol are listed in Table 1 (**Note 1**).
4. Staining buffer: 2 % fetal bovine serum (FBS, cell culture grade) in phosphate-buffered saline (PBS) without addition of calcium and magnesium ions. Add 1 ml of FBS to 49 ml of PBS in 50 ml conical tube.
5. 20 μg/ml DAPI dissolved in distilled water: dissolve 2 mg of DAPI in 1 ml of distilled water and then add 10 μl of the stock to 990 μl of distilled water to obtain 20 μg/ml solution.

2.2 Fixation and Permeabilization

1. 1× FACS lysing solution: dilute 10× FACS Lysing solution (BD, cat. 349202) in distilled water. Volume of 3 ml of 1× solution is needed per sample.
2. BD IntraSure Kit (cat. 641776). While planning experiment, take into consideration that the protocol uses double volume of reagents comparing to manufacturer's protocol.

Table 1
Antibodies used in the presented protocol

Antigen	Dye	Clone	Company
CD11b	PE	M1/70	BD
Gr-1	PE	RB6-8C5	BD
Ter119	PE	TER119	BD
B220	PE	RA3-6B2	BD
CD3	PE	17A2	BD
c-Kit	APC-eFluor780	BM8	eBioscience
Sca-1	PE-Cy7	D7	BD
CD48	PerCP-Cy5.5	HM-48-1	Biolegend
CD150	APC	TC15-12F12.2	Biolegend
CD34	AlexaFluor700	RAM34	eBioscience
Ki67	AlexaFluor488	B56	BD

Table 2
Configuration of flow cytometry used in the study

Laser	Chanel	Mirror	Filter
405 nm	DAPI	–	450/20
488 nm	FITC PerCP-Cy.5.5	505 635	530/30 685/35
561 nm	PE PE-Cy7	– 750	585/15 780/60
640 nm	APC Alexa Fluor 700 APC-eFluor780	– 690 750	670/14 730/45 780/60

2.3 Flow Cytometry

In the presented protocol we use the BD LSR Fortessa cytometer with configuration described in Table 2.

3 Methods

3.1 Labeling the Surface Antigens of Whole Bone Marrow Cells

Prepare a single-cell suspension of whole murine bone marrow (isolation of murine bone marrow was described in [5]). Do not lyse the red blood cells at this step. Cool down the centrifuge to 4 °C and perform all steps on ice.

Table 3
Mix of antibodies used to stain surface antigens

Antibody	Per one sample
CD11b-PE	1 μl
Gr-1-PE	1 μl
Ter119-PE	1 μl
B220-PE	1 μl
CD3-PE	1 μl
c-Kit-APC-eFluor780	2 μl
Sca-1-PE-Cy7	2 μl
CD150-APC	2 μl
CD48-PerCP-Cy5.5	2 μl
CD34-FITC	2 μl
Total mix per sample:	15 μl

1. Filter the single-cell suspension of whole murine bone marrow through 40 μm strainer.
2. Centrifuge at 600 × *g* for 10 min, 4 °C.
3. Suspend the cells in 3 ml of ice-cold staining buffer.
4. Calculate the concentration of cell suspension (**Note 2**).
5. Uptake the volume with 1×10^7 cells from each sample. Prepare additional samples for controls and compensations (**Note 3**). Centrifuge all samples at 600 *g* for 10 min, 4 °C.
6. Suspend the samples in total volume of 85 μl (**Note 4**).
7. Prepare the mix according to Table 3 (include reserve). Add 15 μl of mix to each sample. Make sure that whole suspension is on the bottom of the fax tube and mix thoroughly by pipetting.
8. Incubate for 20 min on ice in darkness. Do not wash the cells, but directly proceed to the next step.

3.2 Fixation, Permeabilization, and Ki67 Labeling

Fixation and permeabilization is done using the BD Intrasure Kit with modified protocol (**Note 5**).

1. Add 200 μl of Reagent A to cell suspension with antibodies and mix by vortexing.
2. Incubate for 5 min at room temperature (RT) in the darkness.
3. Add 1 ml of 1× BD FACS lysing solution and directly mix by pipetting. Add additional 2 ml of 1× BD FACS lysing solution and vortex to mix (**Note 6**).
4. Incubate for 10 min at RT in darkness.

5. Centrifuge at 800 × *g*, for 5 min (**Note 7**).
6. Prepare the dilution of Ki67 antibody (*see* Table 1) in Reagent B for all samples (with reserve). Add 5 μl of Ki67 to 95 μl of Reagent B per sample.
7. Remove the supernatant, add 100 μl of mix of Reagent B and Ki67 antibody and mix by pipetting.
8. Incubate for 45 min at RT.
9. Wash with 2 ml of staining buffer and centrifuge at 800 × *g* for 5 min.

3.3 DAPI Labeling and Collection of Samples

1. Discard supernatant. Suspend the cells in 150 μl of PBS. Add 5 μl of 20 μg/ml DAPI to each sample and incubate in darkness for 10 min at RT.
2. Add 150 μl of PBS to each sample. Samples are ready to be collected.
3. Set the linear scale on channel in which DAPI signal will be collected. Set the voltage so that in the stain sample the main G0/G1 peak localizes around channel 50 (Fig. 1) (**Note 8**). Set the remaining parameters and collect the compensation controls.
4. Given that long term HSC (LT-HSC) are very rare population collect 4×10^6 cells to be sure that you have enough events in LT-HSC gate. Gate HSC and analyze their cell cycle status according to the Figs. 1 and 2. Note that even if the high number of cells is acquired, number of cells in LT-HSC gate is not enough to distinguish between S, G2, and M phases. Therefore we gate together proliferating cells as in S/G2/M phases.

4 Notes

1. We propose the set of antibodies that allows identification of LT-HSC. However, depending on possessed equipment and flow cytometry configuration this set could be further improved or expanded. The presented protocol gave us satisfactory results, but we are aware that using CD34 antibody conjugated with Alexa Fluor700 dye and CD150 antibody conjugated with APC is suboptimal. If the expanded cytometer configuration is available one may check if other dyes will provide better separation of analyzed populations, e.g. dyes excited with 405 nm laser and emitting in red spectrum. However, the potential other dyes that presented in the protocol have to be checked for compatibility with fixation method presented in the article.

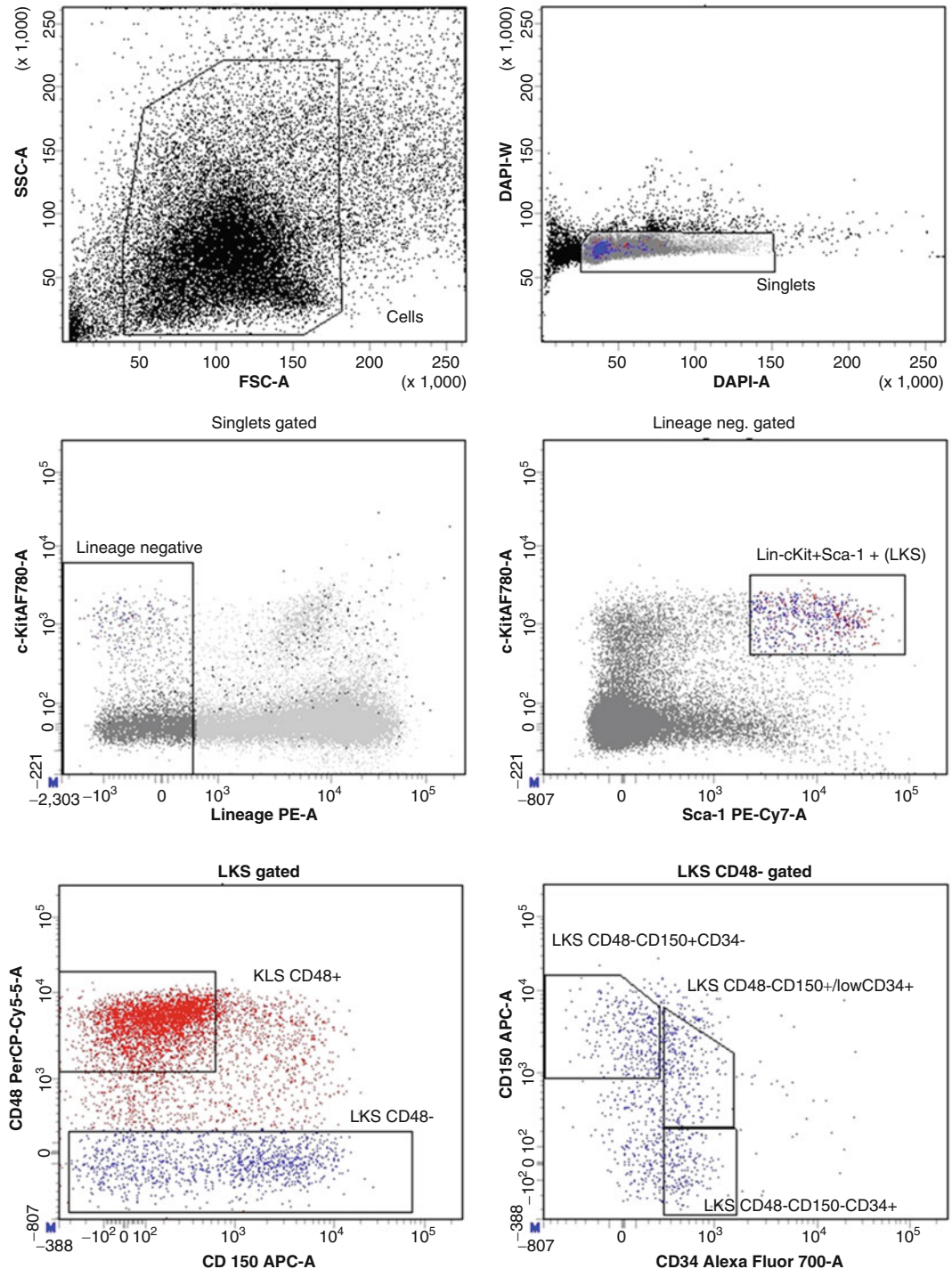

Fig. 1 Gating strategy to distinguish LT-HSC (defined as LKS $CD48^{-}CD150^{+}CD34^{-}$ from other populations)

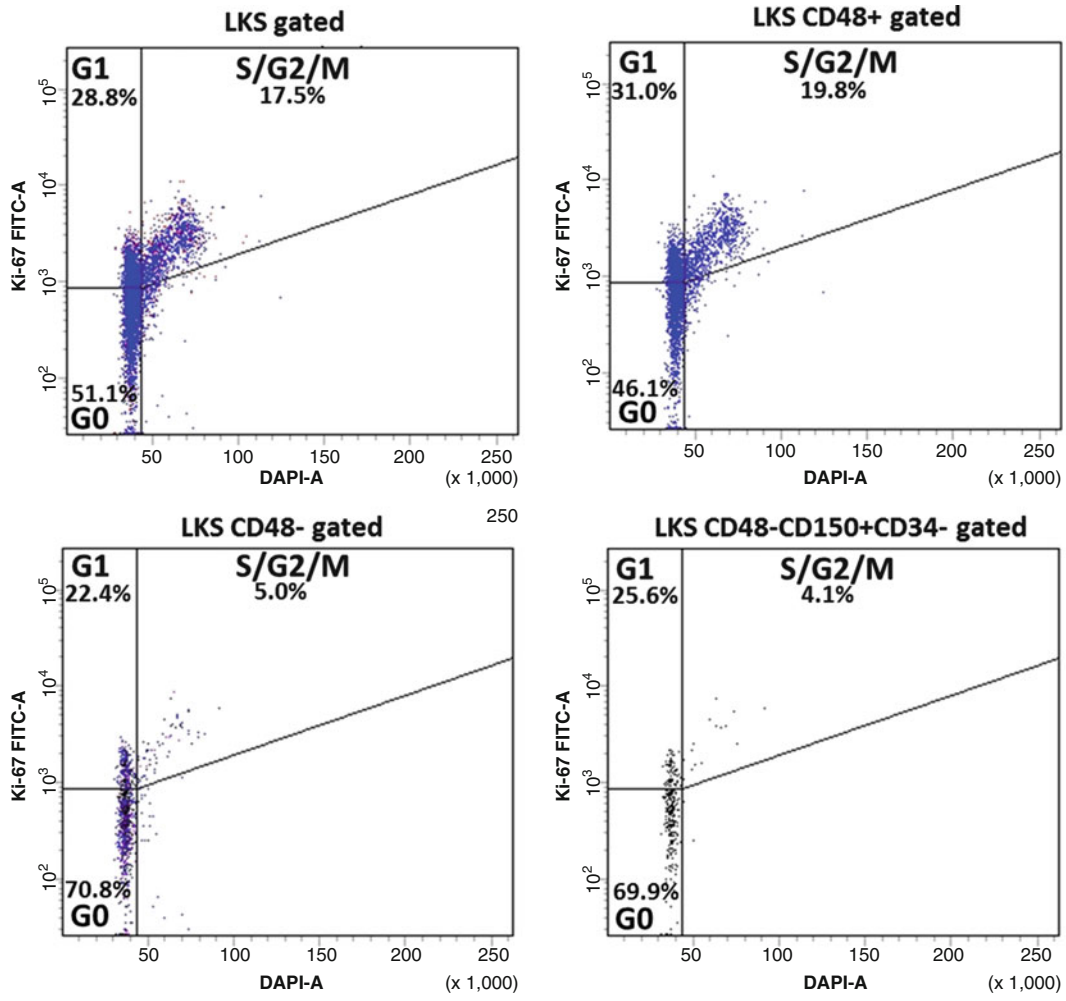

Fig. 2 Exemplary results of cell cycle analysis from different gated populations. Note the higher number of proliferating cells when gates include progenitors cells (LKS, LKS CD48$^+$) in contrast to gates enriched in quiescent stem cells

Additionally, other markers could be used to isolate LT-HSC: endothelial protein C receptor (EPCR) [6], TEK tyrosine kinase (Tie-2) [7] and endoglin (CD105) [8].

2. We use the automated MUSE cell counter to calculate cell concentration. If the standard method of cell counting is to be used, we advise the Turk's solution for cell counting. For preparing the dilution of cell suspension for counting, estimate the total number of whole bone marrow cells from adult mice from both femurs and tibias to be approximately 3–7 $\times$ 10^7 cells.
3. For proper cell identification by flow cytometry we suggested several control tubes. First of all, the single stained compensation samples should be included in the analysis. It is worth to

note that fixation may affect some of the dyes (especially the tandem dyes), therefore it is recommended to make the compensation controls that are fixed in the same way as samples.

Given that the analysis involved several dyes we also use the Fluorescence-Minus-One (FMO) controls. The FMO control is done by staining all the antigens except the one for which the control is made. We find reasonable to make FMO for all dyes, at least when the analysis is made for the first time, as these controls guide the correct gating and cell identification. The matched isotype control is recommended as long as being used in the same concentration as the proper antibody and has the same dye to antibody ratio. Otherwise the isotype control may be misleading. Therefore, we suggest using the isotype control provided from the same company as the particular antibody is provided.

4. Take into consideration the volume of pellet itself. It is reasonable to add at the beginning a lower volume of staining buffer e.g. 50 μl, then check the volume of cell suspension and fill the remaining amount of the buffer to obtain the final volume of 85 μl.
5. The use of IntraSure reagents in the presented protocol differs from manufacturer recommendation. Originally, the IntraSure kit was dedicated to stain 1×10^6 cells. However, this number of cells is not enough to obtain reasonable number of LT-HSC in the subsequent cell cycle analysis. Therefore we modified the protocol for initial number of 1×10^7 cells and increased volume of used reagents.
6. In order to fix all cells uniquely and avoid cell clumps, mix the cell suspension immediately after adding the first part of fixation buffer. Adding 3 ml of fixation buffer without proper mixing may result in non-optimal cell fixation.
7. After fixation the cells can be centrifuged with higher acceleration with no damage to the cells. Additionally, the cells after fixation do not pellet as well as the nonfixed cells and the higher centrifugation speed helps to avoid losing the pellet during discarding the supernatant.
8. Even if you set the voltage in DAPI channel to place main G0/G1 peak around channel 50 in one sample, it might be slightly different in the next samples due to some variation in cell number in the tube. Therefore, we suggest to adjust the gate on DAPI intensity in each sample in blinded fashion, so that the gate is set just after the main G0/G1 peak (Fig. 1).

Acknowledgments

The research was supported by grants: HARMONIA (NCN2015/18/M/NZ3/00387) granted to Alicja Jozkowicz by Polish National Science Centre and PRELUDIUM (NCN2013/11/N/NZ3/00956) granted to Krzysztof Szade by Polish National Science Centre. The Faculty of Biochemistry, Biophysics, and Biotechnology of Jagiellonian University is a partner of the Leading National Research Centre (KNOW) supported by the Ministry of Science and Higher Education.

References

1. Bryder D, Rossi DJ, Weissman IL (2006) Hematopoietic stem cells: the paradigmatic tissue-specific stem cell. Am J Pathol 169:338–346. doi:10.2353/ajpath.2006.060312
2. Rossi L, Lin KK, Boles NC et al (2012) Less is more: unveiling the functional core of hematopoietic stem cells through knockout mice. Cell Stem Cell 11:302–317. doi:10.1016/j.stem.2012.08.006
3. Shapiro HM (2003) Parameters and probes. In: Practical flow cytometry, 4th edn. Wiley, New Jersey
4. Mayle A, Luo M, Jeong M, Goodell MA (2013) Flow cytometry analysis of murine hematopoietic stem cells. Cytometry A 83A:27–37. doi:10.1002/cyto.a.22093
5. Szade K, Zukowska M, Jozkowicz A, Dulak J (2016) Measuring ATP concentration in a small number of murine hematopoietic stem cells. Methods Mol Biol. doi: 10.1007/7651_2016_358
6. Balazs AB, Fabian AJ, Esmon CT, Mulligan RC (2006) Endothelial protein C receptor (CD201) explicitly identifies hematopoietic stem cells in murine bone marrow. Blood 107:2317–2321. doi:10.1182/blood-2005-06-2249
7. Arai F, Hirao A, Ohmura M et al (2004) Tie2/angiopoietin-1 signaling regulates hematopoietic stem cell quiescence in the bone marrow niche. Cell 118:149–161. doi:10.1016/j.cell.2004.07.004
8. Chen CZ, Li M, De Graaf D et al (2002) Identification of endoglin as a functional marker that defines long-term repopulating hematopoietic stem cells. Proc Natl Acad Sci 99:15468

Methods in Molecular Biology (2016) 1516: 101–119
DOI 10.1007/7651_2016_356

Published online: 23 April 2016

Dissecting Transcriptional Heterogeneity in Pluripotency: Single Cell Analysis of Mouse Embryonic Stem Cells

Ana M.V. Guedes, Domingos Henrique, and Elsa Abranches

Abstract

Mouse Embryonic Stem cells (mESCs) show heterogeneous and dynamic expression of important pluripotency regulatory factors. Single-cell analysis has revealed the existence of cell-to-cell variability in the expression of individual genes in mESCs. Understanding how these heterogeneities are regulated and what their functional consequences are is crucial to obtain a more comprehensive view of the pluripotent state.

In this chapter we describe how to analyze transcriptional heterogeneity by monitoring gene expression of *Nanog*, *Oct4*, and *Sox2*, using single-molecule RNA FISH in single mESCs grown in different cell culture medium. We describe in detail all the steps involved in the protocol, from RNA detection to image acquisition and processing, as well as exploratory data analysis.

Keywords:: Stem cells, Pluripotency, Heterogeneity, Transcription, Single-molecule FISH, Stochastic gene expression

1 Introduction

Pluripotency is defined as the capacity of cells to differentiate into any cell type from each of the primary embryonic germ layers, while being able to maintain a pool of undifferentiated cells. The maintenance of pluripotent mouse Embryonic Stem cells (mESCs) in culture requires the coordinated activity of a complex Pluripotency Transcription Network in which the transcription factors Nanog, Oct4, and Sox2 play a central role [1–4].

Traditionally, the pluripotent state was viewed as being homogeneous and characterized by a specific genetic signature. This view has been replaced by the notion that the pluripotent state is highly heterogeneous and dynamic, comprising variable expression of both pluripotency genes and lineage-affiliated genes [5–8]. The discovery that expression of several pluripotency regulators fluctuates over time and the possibility that pluripotent stem cells might exist in multiple interconvertible states (associated with variable capacities of self-renewal and differentiation) [5, 9–11] highlight the dynamic nature of the pluripotent transcriptional program, which might be a fundamental feature of pluripotency. Moreover, it has been shown that different levels of expression of some

pluripotency genes, such as *Rex1*, *Dppa3*, *Prdm14*, or *Nanog*, has a functional impact in pluripotency and results in different propensities of cells to differentiate [12–14].

The variability observed in mESC cultures has been proposed to reflect two different features: (1) stochastic fluctuations or "noise" in gene expression, resulting from the inherent randomness of the biochemical processes associated with transcription and translation; and (2) the presence of multiple functional states that coexist and show different gene expression patterns and variable correlations between a set of genes [15]. However, the biological significance of this variability is yet to be understood.

In order to dissect mESC heterogeneity, single cell approaches are vital [16, 17], since analysis of individual cells usually leads to more accurate representations of variations between cells when compared with the averages typically obtained by bulk measurements. One of the most adequate methods to perform single cell analysis is single-molecule RNA FISH (smFISH) [18–21]. This technique is based on in situ hybridization followed by microscopy analysis, and has the advantage of providing accurate integer counts of mRNA molecule numbers in individual cells [17, 20]. smFISH uses a set of short fluorophore-labeled oligonucleotides that hybridize with the target mRNA, resulting in the presence of large number of fluorophores bound to an individual mRNA, providing enough fluorescent signal to be detected as a diffraction-limited spot [19, 22].

Several studies on single cell analysis of transcriptional heterogeneity in mESCs have been published recently. While some of them attempt to characterize gene expression profiles of several pluripotency markers, in cells subject to different environmental signals and perturbations [15, 23, 24], others focus on the analysis of specific genes, such as *Nanog* [15, 25, 26] and how their heterogeneity is modulated.

In this chapter, we describe how to perform single cell transcriptional analysis in mESCs by smFISH. We describe the workflow used to perform multiplex smFISH in mESCs, from cell culture and fixation (Section 3.1), to probe design and preparation (Sections 3.2 and 3.3), and hybridization with RNA in cultured cells (Section 3.4). In addition, we describe the procedures for image acquisition (Section 3.5) and processing (Section 3.6), as well as exploratory data analysis (Section 3.7). As an example, we characterize the expression of the pluripotency regulators *Nanog*, *Oct4*, and *Sox2* with the objective of getting a better understanding of their heterogeneity, dynamics and interactions. We show a comparative analysis in cells grown in ground state conditions (2i/LIF), in conventional Serum/LIF, and upon early events of non-directed differentiation induced by LIF withdrawal (Serum). This simplistic

analysis offers further evidence for the stochastic nature of gene expression in the pluripotent state, and indicates that mRNA transcription in mESCs is a noisy process, probably as a result of the uniquely permissive chromatin environment found in mESCs [27].

2 Materials

2.1 Equipment

1. Cell culture hood.
2. 37 °C CO_2 incubator.
3. Standard wide-field fluorescence microscope (in this case a Zeiss Axiovert) equipped with:
   (a) Mercury or metal-halide lamp;
   (b) Filter sets appropriate for the fluorophores selected (Table 1);
   (c) Cooled CCD or EMCCD camera;
   (d) High numerical aperture (>1.3) 100× objective;
   (e) Motorized XY stage to acquire multiple positions;
   (f) Motorized *Z*-stack acquisition;
   (g) Controlling computer and software able to do multi-position acquisition.
4. External storage for data files.
5. Computer for data processing analysis.
6. MATLAB software with image processing toolbox.
7. RStudio software for data analysis [28].

2.2 Reagents and Materials

Prepare all solutions under sterile conditions, in a laminar flow hood class II.

2.2.1 mESC Culture

All mESC culture procedures were performed according to what has been described by Pezzarossa et al. [29]. Here we provide a brief description of reagents and materials needed for mESC culture and advise consulting [29] for more details.

Table 1
Optical filters required for smFISH protocol

	Exitation	Beam splitter	Emission	Supplier
Alexa594	590DF10	610DRLP	630/DF30	Omega
Cy5	640/30	660	700/75	Chroma
TMR	546/10	560	580/30	Chroma
Dapi	365/12	395	>397	Zeiss

Details for excitation, beam splitter, and emission filters for all the channels needed in the protocol. Suppliers are also provided

1. Cell line: E14tg2a, a non-modified cell line derived from 129/Ola mice blastocysts (a kind gift from Austin Smith's lab, University of Cambridge, UK).
2. Cell culture medium: For the experiments described in this chapter we have used Serum/LIF, 2i/LIF, and Serum medium.
   (a) *Serum/LIF medium*: mix the following components to make 250 ml of medium; filter-sterilize and supplement with 2 ng/ml of Leukemia inhibitory factor (LIF) prior to use.
      - 200 ml of 1× Glasgow Modified Eagle's medium—GMEM (GIBCO);
      - 2 ml of 200 mM glutamine (100×, GIBCO);
      - 2 ml of 100 mM Na pyruvate (100×, GIBCO);
      - 2 ml of 100× nonessential amino acids (GIBCO);
      - 2 ml of 100× penicillin–streptomycin solution (GIBCO);
      - 200 μL of 0.1 M 2-mercaptoethanol (Sigma);
      - 20 ml of heat inactivated ES screened fetal bovine serum (Hyclone, cat.no. SH30070.03ES).
   (b) *2i/LIF medium*: commercial iStem medium [30] (Cellartis). Supplement with 2 ng/ml LIF prior to use (home-made iStem may also be used).
   (c) *Serum medium*: same composition as Serum/LIF medium but without supplementing with LIF prior to use.
3. Other reagents/materials:
   - 0.1 % gelatine diluted from 2 % (Sigma) in tissue culture grade H_2O.
   - 0.1× trypsin solution: mix 5 ml of 2.5 % trypsin (GIBCO), 0.5 ml of heat-inactivated chicken serum, 0.1 ml of 0.5 M EDTA, and PBS to 50 ml to prepare a 1× trypsin solution. Dilute the 1× trypsin solution with PBS to prepare 0.1× working solution.
   - 6-well multi-well tissue culture dish (Nunc, cat.no. 140675).
   - 60-mm tissue culture dishes (Nunc, cat.no. 150288).

2.2.2 Cell Fixation

Prepare solutions with ribonuclease free ultrapure water in a fume hood. Perform sample handling in a fume hood.

1. 37 % formaldehyde (Sigma, cat. no. 252549).
2. 1× PBS.
3. 70 % Ethanol.

2.2.3 Hybridization and Washing

Prepare solutions with ribonuclease free ultrapure water in a fume hood. Perform sample handling in a fume hood.

1. Hybridization buffer: 1 g of dextran sulfate (Sigma, cat.no. D8906), 1 ml of formamide (Ambion, cat.no. AM-9342), 1 ml of 20× SSC and ultrapure ribonuclease free H_2O up to 10 ml. Store at −20 °C in 500 µl aliquots.
2. Probe sets specific for the genes to be detected, labeled with appropriate fluorophores (Stellaris RNA FISH Biosearch Technologies) (**Note 1**).
3. TE buffer: 10 mM Tris, 1 mM EDTA pH = 8.
4. Washing buffer: 5 ml of 20× SSC, 5 ml of formamide, 500 µl of 10 % Triton and ultrapure ribonuclease free H_2O up to 50 ml. Store at room temperature.
5. DAPI (Sigma).

2.2.4 Cell Mounting

1. Equilibration buffer: 850 µl of H_2O, 100 µl of 20× SSC, 40 µl of 10 % glucose, 10 µl of Tris 1 M pH 8, 10 µl of 10 % Triton. Prepare fresh.
2. Glucose oxidase (Sigma cat.no G2133): prepare aliquots of stock solution (37 mg/ml). Dilute stock to 3.7 mg/ml in 50 mM of Sodium Acetate. Store at −20 °C and use shortly after thawing.
3. Catalase (Sigma cat.no C-3515). Store at 4 °C. Vortex thoroughly before using.
4. Anti-fade buffer: 100 µl of Equilibration buffer, 1 µl of 3.7 mg/ml glucose oxidase, 1 µl of catalase. Always prepare fresh.
5. Glass slides 76 × 26 × 1 mm.
6. #1 glass coverslips 18 × 18mm or 50 × 24 mm.
7. Dow corning high vacuum silicone grease (Sigma cat.no Z273554).
8. Precision tweezers.
9. Stereoscope with bottom lighting.

3 Methods

3.1 Cell Culture

Perform all cell manipulations under sterile conditions in a laminar-flow cell culture hood (class II). All mESC culture procedures were performed according to what has been described by Pezzarossa et al. [29]. Here we provide a brief description and advise consulting [29] for a more detailed description.

1. Perform routine cell passaging and expansion in Serum/LIF medium, on gelatin-coated dishes, and incubate cells at 37 °C in a 5 % (v/v) CO_2 incubator.
2. Passage cells every other day at a cell density of 3×10^4 cells/cm^2.
3. Perform cell dissociation using 0.1× trypsin and incubating for 2 min at 37 °C.
4. Plate mESCs in the conditions to be tested (Serum/LIF, 2i/LIF or Serum—as described in Section 2.2.1). Plating of one to three 60-mm Nunc dishes usually provides sufficient cells to perform several smFISH experiments (**Note 2**).

3.1.1 Cell Fixation

1. Two days after cell plating, harvest the cells cultured in Serum/LIF, 2i/LIF, and Serum medium (or other tested conditions).
2. Dissociate cells by trypsinization and ensure a good single resuspension.
3. Wash cells with 1× PBS and spin cells down (4 min, 165 × *g*-force).
4. Resuspend thoroughly in 4.5 ml of 1× PBS and add 500 μl of 37 % Formaldehyde, ensuring proper homogenization by pipetting up and down.
5. Incubate cells for 10 min at RT.
6. Spin cells down (4 min, 165 × *g*-force), remove supernatant and wash cells twice with 1× PBS.
7. Resuspend in a desired volume of 70 % ethanol for permeabilization during at least 2 h and store at 4 °C (**Note 3**).

3.2 Probe Design (Custom Stellaris® FISH Probes)

The probe set sequences used in the described experiments (for Nanog, Oct4, and Sox2) are shown in Table 2.

1. Select the sense strand of the target sequence for the design of complementary oligonucleotide probes (**Note 4**).
2. Proceed to probe designing using Stellaris® FISH Probe Designer (Biosearch Technologies Inc., Petaluma, CA) available at www.biosearchtech.com/stellarisdesigner.
3. Select the fluorophores to be coupled with the probe set—Alexa594, Cy5 or TMR fluorophores (or the equivalents CAL Fluor® Red 610, Quasar® 670 or Quasar® 570, respectively) (Biosearch Technologies, Inc.) (**Note 5**).
4. Follow the website instructions for ordering the probe sets.

3.3 Preparation of Probe Stocks

1. Spin down the lyophilized pooled probes sets, blend and dissolve in the appropriate volume of TE buffer to create a probe stock of 100 μM.

Table 2
Oligo sequences for each probe set used (Nanog, Oct4, and Sox2)

Gene	Nanog	Oct4	Sox2
Probe set	aaatcagcctatctgaaggc	tgagaaggcgaagtctgaag	ccgtctccatcatgttatac
Oligos	cagaaagagcaagacaccaa	aggttcgaggatccacccag	tccgggctgttcttctggtt
	gaagtcagaaggaagtgagc	tggaggcccttggaagctta	ataccatgaaggcgttcatg
	actcagtgtctagaaggaaa	tgagcctggtccgattccag	ttctcctgggccatcttacg
	ggttttaggcaacaaccaaa	acatggggagatccccaata	atctccgagttgtgcatctt
	cgagggaagggatttctgaa	tccctccgcagaactcgtat	tcggacaaaagtttccactc
	cacactcatgtcagtgtgat	aacctgaggtccacagtatg	ttataatccgggtgctcctt
	cagaactaggcaaactgtgg	aacttgggggactaggccca	tcatgagcgtcttggttttc
	ttcccagaattcgatgcttc	tcaggctgcaaagtctccac	ggaagcgtgtacttatcctt
	aaaaactgcaggcattgatg	tgctttccactcgtgctcct	tagctgtccatgcgctggtt
	agcaagaatagttctcggga	tcagaggaggttccctctga	ttgctccagccgttcatgtg
	cagagcatctcagtagcaga	ttctccaacttcacggcatt	tcctgcatcatgctgtagct
	gaagaggcaggtcttcagag	tttcatgtcctgggactcct	tgcatcggttgcatctgtgc
	tgggactggtagaagaatca	aactgttctagctccttctg	tcatggagttgtactgcagg
	tcaggacttgagagcttttg	tcttctgcttcagcagcttg	ttcatgtaggtctgcgagct
	cttgttctcctcctcctcag	tgggtgtaccccaaggtgat	agtaggacatgctgtaggtg
	gagaacacagtccgcatctt	aaagagaacgcccagggtga	ttgaccacagagcccatgga
	ctgtccttgagtgcacacag	tggtctggctgaacaccttt	tgggaggaagaggtaaccac
	tgaggtacttctgcttctga	aaggcctcgaagcgacagat	aggtacatgctgatcatgtc
	gagagttcttgcatctgctg	catgttcttaaggctgagct	tgggccatgtgcagtctact
	atagctcaggttcagaatgg	ttcctccacccacttctcca	agtgtgccgttaatggccgt
	gaaaccaggtcttaacctgc	gaaggttctcattgttgtcg	aaaatctctcccccttctcca
	ttgcacttcatcctttggtt	gtctccgatttgcatatctc	cccaattcccttgtatctct
	tcaaccactggtttttctgc	tagttcgctttctcttccgg	tactctcctctttttgcacc
	ttctgaatcagaccattgct	cacctcacacggttctcaat	ctgcggagatttttttttcct
	gatactccactggtgctgag	tcagaaacatggtctccaga	tttttccgcagctgtcgttt
	ggatagctgcaatggatgct	atctgctgtagggagggctt	aatttggatgggattggtgg
	cagatgcgttcaccagatag	aagctgattggcgatgtgag	tagtcggcatcacggttttt
	aagttgggttggtccaagtc	gaaccacatccttctctagc	gaagtcccaagatctctcat
	gtctggttgttccaagttgg	cgccggttacagaaccatac	ctgtacaaaaatagtccccc
	aaagtcctccccgaagttat	acttgatcttttgcccttct	tatacatggtccgattcccc

(continued)

Table 2
(continued)

Gene	Nanog	Oct4	Sox2
	ctgcaactgtacgtaaggct	cttctcgttgggaatactca	gcgtagtttttttcctccag
	caaatcactggcagagaagt	ggtgtccctgtagcctcata	cctaacgtaccactagaact
	tagtggcttccaaattcacc	agaggaaaggatacagcccc	aagacttttgcgaactccct
	ctaaaatgcgcatggctttc	atagcctggggtgccaaagt	ccggagtctagctctaaata
	ataattccaaggcttgtggg	gtgtggtgaagtgggggctt	ctgtacaaaagttgcttgca
	tggagtcacagagtagttca	tcaggaaaagggactgagta	gattgccatgtttatctcga
	agatgttgcgtaagtctcat	aacagagggaaaggcctcgc	caagaacccttttcctcgaaa
	gctttgccctgactttaagc	atgggagagcccagagcagt	aagctgcagaatcaaaaccc
	tttggaagaaggaaggaacc	gctggtgcctcagtttgaat	ccttgtttgtaacggtccta
	caaatcactggcagagaagt	ttgccttggctcacagcatc	ccagtacttgctctcatgtt
	tagtggcttccaaattcacc	aaagctccaggttctcttgt	aacaagaccacgaaaacggt
	ctaaaatgcgcatggctttc	ccctcctcagtaaaagaatt	acaatctagaacgtttgcct
	ataattccaaggcttgtggg	ccacccctgttgtgctttta	gatatcaacctgcatggaca
	tggagtcacagagtagttca	agcttctttccccatcccac	gggtaggattgaacaaaagc
	agatgttgcgtaagtctcat	ctcctgatcaacagcatcac	cggaaaataaaagggggggaa
	gctttgccctgactttaagc	aatgatgagtgacagacagg	ccaataacagagccgaatct
	tttggaagaaggaaggaacc	gtgtgtcccagtctttattt	tatacatggattctcggcag

2. Rehydrate oligonucleotides for 30 min at room temperature, protect from light and vortex to ensure proper homogenization.
3. Store probe stocks at −20 °C, protected from light (**Note 6**).
4. Prepare working dilution, by adding 2 μl of probe stock to 38 μl of TE buffer for a final concentration of 5 μM (1:20 dilution) and mixing thoroughly (**Note 7**).
5. Store working stocks at −20 °C and protect from light when handling.

3.4 smFISH in Cells in Suspension

A schematic representation of the steps involved here is depicted in Fig. 1a.

1. Spin down 200 μl of fixed cells in ethanol (2 min, 165 × *g*-force) (**Note 8**).
2. Remove supernatant and wash in 850 μl of Wash buffer (**Note 9**).

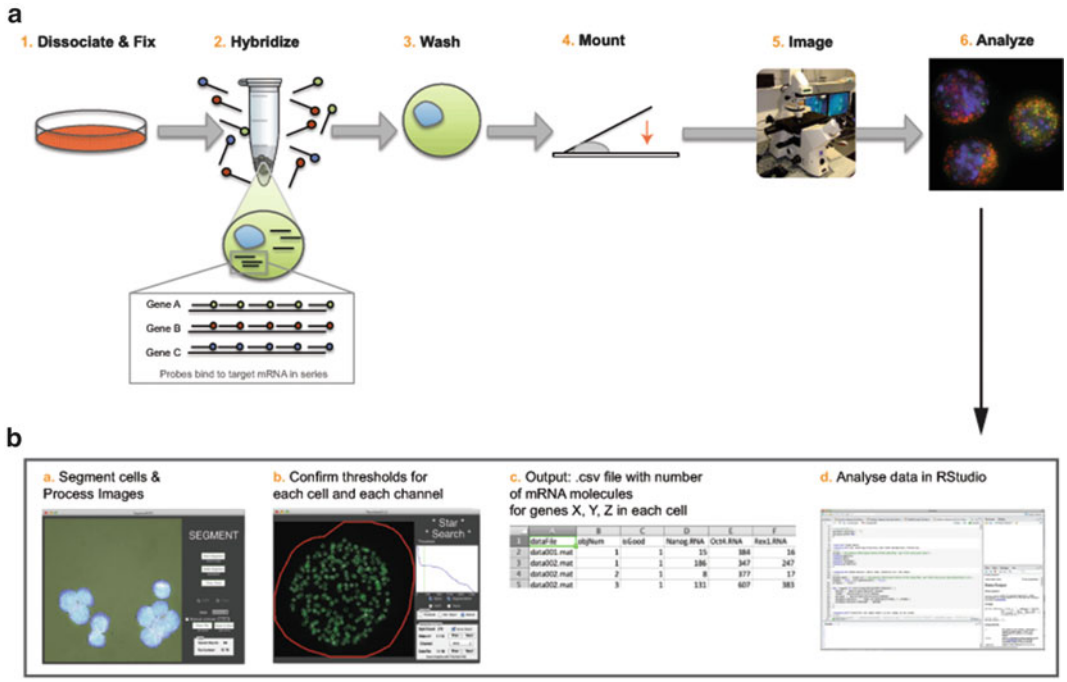

Fig. 1 Representation of the smFISH protocol workflow. (**a**) Key steps involved in the protocol of smFISH for mESCs. (**b**) Key steps involved in image processing and data analysis of data generated by smFISH

3. Prepare the hybridization mix by adding 1 μl of the working dilutions of each of the desired probes to 100 μl of hybridization buffer (approximate final probe concentration of 50 nM).
4. Spin cells down (2 min, 165 × *g*-force), remove Wash buffer, and resuspend the pellet in 100 μl hybridization mix, mixing thoroughly and vortexing (**Note 10**).
5. Protect from light, seal the tube to prevent evaporation, and incubate overnight in a 37 °C oven.
6. On the following morning, add 850 μl of Wash buffer and spin down (2 min, 165 × *g*-force).
7. Remove supernatant, add 850 μl of Wash buffer and incubate for 30 min at room temperature.
8. Spin cells down (2 min, 165 × *g*-force).
9. Remove supernatant, add 850 μl of Wash buffer supplemented with 1 μl of 1 mg/ml DAPI solution, and incubate for 30 min at room temperature.
10. Prepare fresh Equilibration buffer.
11. Spin cells down (2 min, 165 × *g*-force), remove supernatant and wash with 850 μl of Equilibration buffer.
12. Spin cells down (2 min, 165 × *g*-force) and resuspend pellet in 10 μl of Anti-fade buffer (**Notes 11** and **12**).

13. Proceed to mounting (**Note 13**):
    (a) Place 5 μl of cell suspension on a clean glass microscope slide (**Note 14**).
    (b) Check cell density under the stereoscope and remove any cell clumps that will prevent proper smashing (**Note 15**). Add a few microliters of Anti-fade buffer whenever cell density is too high.
    (c) Use a #1 cover glass with the help of precision tweezers to spread cell solution and apply pressure gently over the surface of the cover glass (**Note 16**).
    (d) Wipe excess liquid with tissue paper while pressing gently with the tweezers.
    (e) While observing through the stereoscope lens, press the coverslip until cells are properly smashed (**Note 17**).
    (f) Seal cover glass using silicone grease to prevent liquid evaporation (**Note 18**).
    (g) Proceed to imaging.

3.5 Image Acquisition

1. At least 30 min before starting the acquisition turn ON the microscope setup.
2. Place a drop of immersion oil on the objective.
3. Position the slide in the microscope and allow the temperature to stabilize for 30 min (**Note 19**).
4. Choose an area with good cell density and focus using the DAPI channel (**Note 20**).
5. Test signal intensity for each channel and define the exposure time for each of the fluorophores (it ranges from 1 to 5 s) and for DAPI (usually few milliseconds) (**Notes 21** and **22**).
6. Select and record the positions to be imaged. Avoid marking the same position twice by starting from left and moving to right down (**Note 23**).
7. For each position, set the lower plane of the *Z*-stack, allow the software to define the distance between planes (usually 0.3 μM is enough) and the number of optical sections needed to span the vertical extent of the cell (usually 20–30 sections).
8. Use the acquisition software to prepare a protocol (*macros*) that allows automate running through the list of recorded positions and, in each position, goes to the lower plane, takes the defined optical sections with the defined exposure time for each channel and saves the *Z*-stack as a .tiff image format.
9. Begin imaging acquisition.

10. At the end of the acquisition, before beginning data analysis, review the images to check for the quality of the acquisition (**Note 24**).

3.6 Image Processing

Here we describe the procedures for Image Processing using custom software written in Matlab. This software has been developed in Arjun Raj's Laboratory [19, 22, 31] and is publicly available at https://bitbucket.org/arjunrajlaboratory/rajlabimagetools/wiki/Home, with a worked out example. A schematic representation of the workflow of Image processing is also available in Fig. 1b.

1. Segment cells using DAPI channel and a RNA fluorophore channel in order to be able to properly define cytoplasm and cell boundaries.
2. Process the images.
3. Review the automatic threshold performed by the software for each cell and each acquired RNA channel. Adjust if needed (**Note 25**).
4. Exclude cells that don't have proper RNA signal or that have autofluorescent dirt.
5. Save the output data as a .csv file, including the number of mRNA molecules in each channel for each cell.
6. Back up original raw data images and create a database with .csv files (**Note 26**).
7. Import .csv files for RStudio and proceed to statistical analysis and graphical representation of the observed data.

3.7 Data Analysis

A series of different statistical analysis and graphical representations can be performed with the acquired data using different software. Here we report a list of the most common statistics using R, a programming language for statistical computing and graphics. We have taken advantage of RStudio [32], an integrated development environment for R [28], and ggplot2, a data visualization and plotting package developed for R [33].

In this section, we use data obtained when performing triple labeling with Nanog, Oct4, and Sox2 probes in mESCs grown in Serum/LIF, 2i/LIF, or Serum conditions.

3.7.1 Distribution Analysis

A histogram graphical representation of the obtained data for each gene is crucial as the first approach during the exploratory analysis. It allows not only to understand the shape of data distribution but also to get an estimate of the probability distribution of mRNA molecules per cell (Fig. 2). Alternatively, boxplots or violin plots can be used.

Analysis of the histograms obtained in the described experiments shows that the distribution of *Nanog*, *Oct4*, and *Sox2* mRNA

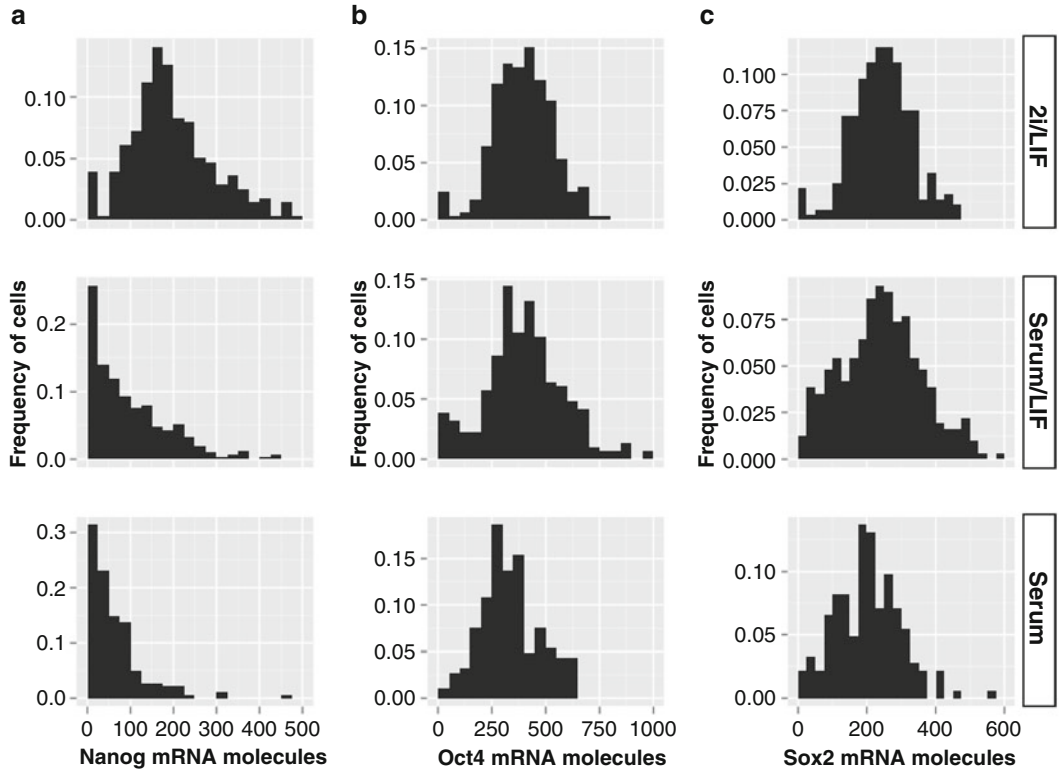

Fig. 2 Histogram representation of mRNA distributions from Nanog, Oct4, and Sox2 in single cells grown in different culture conditions (Serum/LIF, 2i/LIF, and Serum). (**a**) Histogram representation showing the distribution of Nanog mRNA molecules per cell for cells grown in 2i/LIF, Serum/LIF, and Serum. Bin-width = 25. (**c**) Same as (**a**) for Oct4 mRNA. Bin-width = 50. (**c**) Same as (**a**) for Sox2 mRNA. Bin-width = 25

molecules per cell is extremely variable, ranging from 0 molecules per cell to 500, 1000 and 600 mRNA molecules, respectively (Fig. 2). It can also be observed that the shape of the distributions is variable between genes and conditions. The shape of the distributions is a good indication of how the gene's transcription is regulated [17]. Poissonian distributions are suggestive of a one-state model, in which transcription is always ON. Non-Poissonian or long tailed distributions indicate a two-state model of transcription, in which the promoter alternates between ON and OFF states in a pulsatile manner [18, 19]. Regarding *Nanog*, the distribution of mRNAs/cell in 2i/LIF conditions shows a reasonable approximation to a Poisson, with few cells expressing very low or very high numbers of transcripts, whereas in Serum/LIF the distribution shows a long exponential tail, with a substantial number of cells having very few mRNA molecules. In Serum conditions, a reduction in the number of cells expressing high and intermediate levels of *Nanog* and an increase in the low-*Nanog* expressing cells is

observed, comparatively to the trend observed in Serum/LIF conditions. In the case of *Oct4* and *Sox2*, the shape of the mRNAs/cell distribution does not vary greatly within the different culture conditions. In all cases, the distributions show a good approximation to a bell-shaped distribution, with few cells expressing very low or high levels of *Oct4* or *Sox2*.

Overall, the high heterogeneity in *Nanog*, *Oct4*, and *Sox2* mRNA expression between mESCs points out to a bursty transcription, characterized by long periods of gene inactivity and sporadic pulses of transcription.

3.7.2 Descriptive Analysis

Several statistical measurements can be extracted from the distributions of mRNA molecules per cell that describe the distribution, and can give information about the transcription of the genes under study. In Table 3, we have summarized mean, standard deviation, median, minimum and maximum values, as well as Fano factor (FF), coefficient of variation (CV), and the total number of cells analyzed. Measurements such as FF (defined as the ratio between the variance and the mean) and CV (defined as the ratio between the standard deviation and the mean) are a good measure of heterogeneity and noise in gene expression [18, 19].

In the case of *Nanog*, it can be observed that when cells are passed from Serum/LIF to 2i/LIF there is an increase in the average number of transcripts/cell from 96 ± 89 to 195 ± 99. This increase is not due to a change in the distribution range of *Nanog* expression, reflecting instead an alteration in the balance between cells expressing high or low levels of *Nanog* mRNA (Fig. 2a). Upon LIF withdrawal (Serum conditions), the average value in transcripts per cell drops, as expected, from 96 ± 89 to

Table 3
Statistical measurements extracted from mRNA distributions

Gene	Medium	Mean ± sd	Median	Min–max	FF	CV	*N*
Nanog	2i/LIF	195 ± 99	178.5	4–504	50.2	0.5	278
	Serum/LIF	96 ± 89	70.5	0–443	81.7	0.9	312
	Serum	65 ± 73	44	0–511	81.9	1.1	183
Oct4	2i/LIF	395 ± 136	396	0–762	47.2	0.3	278
	Serum/LIF	398 ± 181	394	5–971	82.3	0.5	312
	Serum	335 ± 135	316	1–627	54.6	0.4	183
Sox2	2i/LIF	242 ± 87	238.5	0–466	31.4	0.4	278
	Serum/LIF	242 ± 117	240.5	0–599	57	0.5	312
	Serum	202 ± 94	203	7–561	44.1	0.5	183

Statistical measurements of Nanog, Oct4, and Sox2 mRNA distributions from cells grown in different cell culture medium (same data used to plot the histograms depicted on Fig. 2). Values are represented in the form of number of transcripts. FF stands for Fano factor, CV for coefficient of variation, and *N* for number of cells analyzed

65 ± 73, since *Nanog* expression is known to be downregulated upon differentiation. In the case of *Oct4* and *Sox2*, there is less variation between culture conditions. This is reflected in the CV values for *Oct4* and *Sox2*, which are close to 0.5 in all the analyzed conditions. On the contrary, the CV in *Nanog* expression is 0.5 only in 2i/LIF and increases to 0.9 in Serum/LIF and 1.1 in Serum, reflecting the increase in variability between cells in these two conditions.

Additionally, we can have an estimation of noise strength using the FF measure. High values indicate deviation from that predicted for a normal Poissonian distribution, in which FF is equal to 1. It can be observed that *Nanog*, *Oct4*, and *Sox2* have FF values much higher than 1 in all tested conditions, thus suggesting that transcription of these genes is noisy in pluripotent cells, occurring in transcriptional bursts.

3.7.3 Correlational Analysis

Correlations between mRNA molecule numbers in each cell can be calculated whenever double or triple stainings are performed. The best graphical representation of correlations between two genes is the scatter plot (Fig. 3). To obtain a statistical measure of the correlation, the Spearman correlation coefficient can be used, since is does not assume a normal distribution of the data. The correlation analysis between the three analyzed genes shows that *Sox2* and *Nanog* have a moderate to strong correlation in all culture conditions ($0.4 \leq r \leq 0.79$) (Fig. 3a), whereas *Oct4* and *Sox2* show moderate to strong correlation in 2i/LIF and Serum/LIF ($0.4 \leq r \leq 0.79$) and weak correlation in Serum ($0.2 \leq r \leq 0.39$) (Fig. 3b). The correlation between *Oct4* and *Nanog* expression is also variable between culture conditions (Fig. 3c). While in 2i/LIF most cells express high levels of both genes and the correlation is strong ($r = 0.57$), in Serum/LIF this correlation is weaker ($r = 0.4$) mostly due to the presence of two subpopulations of cells (one expressing high levels of both genes and another with low levels of *Nanog* and varying levels of *Oct4*), further decreasing in Serum conditions ($r = 0.27$).

To explore the correlation between the three genes, scatter plots can be used, coloring cells according to the expression levels of the third gene. This can be achieved by classifying cells as high- or low-expressing by the definition of a cut-off (Fig. 3c). The definition of a cutoff results from graphical interpretation and depends on the ability to distinguish two subpopulations of cells. The use of this graphical representation depicted in Fig. 3c shows that most low-*Sox2* cells in 2i/LIF also express low levels of *Oct4* and *Nanog*, while in Serum/LIF and Serum cells with low *Sox2* levels express low levels of *Nanog* but varying levels of *Oct4*.

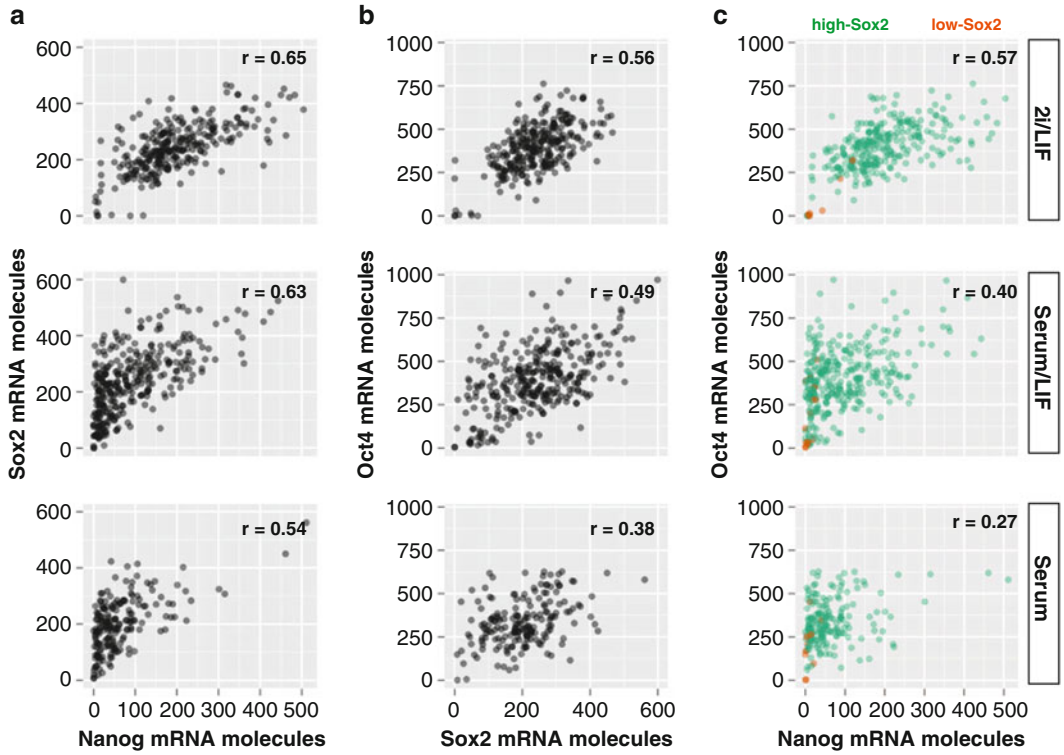

Fig. 3 Correlations between Nanog, Oct4, and Sox2 mRNA molecules in single cells. (**a**) smFISH analysis of Nanog versus Sox2 cells grown in 2i/LIF, Serum/LIF, and Serum. Each dot represents one single cell and the transparency of the dots was used to avoid over-plotting. For each graph, the Spearman correlation coefficient (*r*) is depicted. (**b**) Same as (**a**) for Sox2 versus Oct4. (**c**) Same as (**a**) for Nanog versus Oct4. Sox2 Level is color-coded as high (>50 transcripts—*green*) or low (<50 transcripts—*orange*)

4 Notes

1. Probe sets can be ordered directly labeled with the desired fluorophore or labeled in house and purified using high-pressure liquid chromatograph (HPLC) [34].
2. The amount of cells to fix is dependent on the experimenter objectives but should take into consideration that a considerable fraction of cells is lost during the protocol due to the high number of centrifugation steps.
3. Cells can be stored in 70 % ethanol, at 4 °C, for long periods of time without RNA degradation. The volume used to resuspend cells is dependent on the number of cells fixed and should ensure high concentration of cells (1 ml per 3×10^6 cells).
4. Go to the UCSC genome browser and select the species and gene of interest. Click on the RefSeq version of the gene and, if no preference exists for a specific isoform, select the one covering the largest shared common sequence between isoforms.

Finally, select the Genomic Sequence option and search for the coding sequence (CDS). If this region is not sufficient to design enough probes, the 3′ and 5′ UTR regions can be added.

5. Other fluorophores can be used and are available on the website. When using other fluorophores, compatibility has to be confirmed and proper filter sets have to be available.
6. Probe stocks should be exposed to a minimum of freeze/thaw cycles to prevent degradation.
7. Other dilutions can be tested if hybridization efficiency needs to be optimized (e.g., 1:10,1:20,1:50,1:100).
8. The volume of cells to use is variable. The volume is defined by the minimum needed to be able to have a detectable pellet and to account for cell loss during the various centrifugation steps of the protocol. Additionally, attention should be given to the type of microcentrifuge tubes used, because they can negatively influence the pellet formation and, consequently, the efficiency of the protocol.
9. In all centrifugations with Wash buffer, the pellets are very delicate and easily detach from the tubes, leading to loss of cells. In order to prevent this, do not remove all the supernatant.
10. When preparing the hybridization mix for several samples, take into account its high viscosity and always prepare extra volume.
11. The volume to resuspend cells is variable and depends on the pellet size. High concentration of cells is preferred for mounting.
12. Anti-fade solution is only needed when working with photosensitive-labeled probes (e.g., Cy5). This solution acts as an oxygen scavenging system, preventing photobleaching [35]. When only Alexa 594 and TMR labeled probes are being used, resuspend cells directly into 2× SSC.
13. Alternatively, cells can be kept at 4 °C until mounting, but imaging should always be performed within 24–48 h, due to rapid signal degradation.
14. Make sure that the coverslips and slides are very clean since any dust will prevent proper cell mounting.
15. Be aware of the time spent in the mounting procedure. Long periods of time in the stereoscope may lead to heating of the sample and consequent evaporation of the small volume of cell suspension.
16. This is the most critical step in the protocol for signal quality. For acquisition of good fluorescence signal, cell thickness needs to be reduced (ideally to 2–5 μm) and the formation of air bubbles should be avoided. Practicing several times is strongly

advised in order to prevent over or under smashing. Over smashing of cells leads to loss of cell integrity and precludes proper cell segmentation, whereas under smashing leads to bad quality signal. Note that, when cells are not smashed, pressing the coverslip with the tweezers leads to an evident increase in cell surface area; when this increase stops, smashing is optimal.

17. Liquid evaporation leads to loss of signal quality, especially when using Cy5 labeled probes. The air that enters leads to increase in oxygen content and photobleaching, preventing glucose oxidase and catalase efficient action.
18. Do dot seal the cover glass with nail polish, since it leads to autofluorescence, thereby preventing proper RNA detection.
19. This step allows temperature to stabilize between all microscope components and sample, preventing thermal drift, which may consequently result on fluctuations in the *Z*-axis.
20. Cell density is an important parameter to consider in this step: cell density should be high in order to acquire several cells per image field, but not too high since this hampers the subsequent steps of image processing.
21. RNA signals are very dim and can only be seen through the CCD camera, and not directly in the eyepieces.
22. In some cases, acquisition of a channel with transmitted light may be important, since it facilitates identification of the borders of the cells in the posterior segmentation steps.
23. Before starting the full experiment, run a test acquisition with few positions in order to confirm that the setup is working correctly. Note that each position can be done individually, in the case of absence of XY stage. However this increases considerably the labor time spent at the microscope.
24. In this step, images that were acquired out of focus should be eliminated. Also, check if there are image fields with bad signal due to drying or presence of autofluorescence dirt and eliminate then from further analysis.
25. Cells with a well-defined threshold present a clear plateau between the background signal and the RNA signal in the histogram showing the cell's fluorescence intensity distribution (a representative histogram is shown in Fig. 1b, section b). In the case of a non-clear threshold, find a cell which has a clear signal and in which the threshold shows a defined plateau, and fix that contrast and threshold value (by not automatically adjusting the *x* axis) to all cells.
26. The database should include information on the quality of data in each channel for each experiment as well as the probe acquired in each channel. Always check for differences between same probe sets labeled with different fluorophores.

Acknowledgments

This work was supported by Fundação para a Ciência e Tecnologia, Portugal [SFRH/ BPD/78313/2011 to E.A., SFRH/BD/80191/ 2011 to A.M.V.G. and PTDC/SAUOBD/100664/2008].

References

1. Niwa H (2007) How is pluripotency determined and maintained? Development 134:635–646
2. Boyer LA et al (2005) Core transcriptional regulatory circuitry in human embryonic stem cells. Cell 122:947–956
3. Young RA (2011) Control of the embryonic stem cell state. Cell 144:940–954
4. Kuijk EW et al (2008) Differences in early lineage segregation between mammals. Dev Dyn 237:918–927
5. Chambers I et al (2007) Nanog safeguards pluripotency and mediates germline development. Nature 450:1230–1234
6. Abranches E, Bekman E, Henrique D (2013) Generation and characterization of a novel mouse embryonic stem cell line with a dynamic reporter of Nanog expression. PLoS One 8: e59928
7. Abranches E et al (2014) Stochastic NANOG fluctuations allow mouse embryonic stem cells to explore pluripotency. Development 141:2770–2779
8. Torres-Padilla M-EE, Chambers I (2014) Transcription factor heterogeneity in pluripotent stem cells: a stochastic advantage. Development 141:2173–2181
9. Kalmar T et al (2009) Regulated fluctuations in nanog expression mediate cell fate decisions in embryonic stem cells. PLoS Biol 7:e1000149
10. MacArthur BD et al (2012) Nanog-dependent feedback loops regulate murine embryonic stem cell heterogeneity. Nat Cell Biol 14:1139–1147
11. Hayashi K, Lopes SM, Tang F, Surani MA (2008) Dynamic equilibrium and heterogeneity of mouse pluripotent stem cells with distinct functional and epigenetic states. Cell Stem Cell 3:391–401
12. Singh AM, Hamazaki T, Hankowski KE, Terada N (2007) A heterogeneous expression pattern for Nanog in embryonic stem cells. Stem Cells 25:2534–2542
13. Toyooka Y, Shimosato D, Murakami K, Takahashi K, Niwa H (2008) Identification and characterization of subpopulations in undifferentiated ES cell culture. Development 135:909–918
14. Yamaji M et al (2013) PRDM14 ensures naive pluripotency through dual regulation of signaling and epigenetic pathways in mouse embryonic stem cells. Cell Stem Cell 12:368–382
15. Singer Z et al (2014) Dynamic heterogeneity and DNA methylation in embryonic stem cells. Mol Cell 55:319–331
16. Eldar A, Elowitz MB (2010) Functional roles for noise in genetic circuits. Nature 467:167–173
17. Raj A, van Oudenaarden A (2008) Nature, nurture, or chance: stochastic gene expression and its consequences. Cell 135:216–226
18. Raj A, van Oudenaarden A (2009) Single-molecule approaches to stochastic gene expression. Annu Rev Biophys 38:255–270
19. Raj A, van den Bogaard P, Rifkin SA, van Oudenaarden A, Tyagi S (2008) Imaging individual mRNA molecules using multiple singly labeled probes. Nat Methods 5:877–879
20. Raj A, Peskin CS, Tranchina D, Vargas DY, Tyagi S (2006) Stochastic mRNA synthesis in mammalian cells. PLoS Biol 4:e309
21. Etzrodt M, Endele M, Schroeder T (2014) Quantitative single-cell approaches to stem cell research. Cell Stem Cell 15:546–558
22. Raj A, Tyagi S (2010) Detection of individual endogenous RNA transcripts in situ using multiple singly labeled probes. Meth Enzymol 472:365–386
23. Kumar R et al (2014) Deconstructing transcriptional heterogeneity in pluripotent stem cells. Nature 516:56–61
24. Faddah DA et al (2013) Single-cell analysis reveals that expression of nanog is biallelic and equally variable as that of other pluripotency factors in mouse ESCs. Cell Stem Cell 13:23–29
25. Hansen CH, van Oudenaarden A (2013) Allele-specific detection of single mRNA molecules in situ. Nat Methods 10:869–871
26. Miyanari Y, Torres-Padilla M-EE (2012) Control of ground-state pluripotency by allelic regulation of Nanog. Nature 483:470–473
27. Gaspar-Maia A, Alajem A, Meshorer E, Ramalho-Santos M (2011) Open chromatin in pluripotency and reprogramming. Nat Rev Mol Cell Biol 12:36–47

28. Core Team RCTR (2013) R: a language and environment for statistical computing. R Foundation for Statistical Computing, Vienna, Austria
29. Pezzarossa A, Guedes A, Henrique D, Abranches E (2015) Imaging pluripotency time-lapse analysis of mouse embryonic stem cells. Embryonic Stem Cell Protocols, Volume 1341 of the series Methods in Molecular Biology pp 87–100
30. Ying Q-LL et al (2008) The ground state of embryonic stem cell self-renewal. Nature 453:519–523
31. Raj A, Tyagi S (2009) Imaging individual mrna molecules using multiple singly labeled probes, US Patent App. 13/062. http://www.google.com/patents/US20120129165
32. RStudio Team (2015) RStudio: Integrated Development for R. RStudio, Inc., Boston, MA, http://www.rstudio.com/
33. Wickham H (2009) ggplot2: elegant graphics for data analysis. Springer, New York
34. Batish M, Raj A, Tyagi S (2011) Single molecule imaging of RNA in situ. Methods Mol Biol 714:3–13
35. Aitken C, Marshall A, Puglisi J (2008) An oxygen scavenging system for improvement of dye stability in single-molecule fluorescence experiments. Biophys J 94:1826–1835

Methods in Molecular Biology (2016) 1516: 121–144
DOI 10.1007/7651_2016_357

Published online: 23 April 2016

Generation of Regionally Specific Neural Progenitor Cells (NPCs) and Neurons from Human Pluripotent Stem Cells (hPSCs)

Josh Cutts, Nicholas Brookhouser, and David A. Brafman

Abstract

Neural progenitor cells (NPCs) derived from human pluripotent stem cells (hPSCs) are a multipotent cell population capable of long-term expansion and differentiation into a variety of neuronal subtypes. As such, NPCs have tremendous potential for disease modeling, drug screening, and regenerative medicine. Current methods for the generation of NPCs results in cell populations homogenous for pan-neural markers such as SOX1 and SOX2 but heterogeneous with respect to regional identity. In order to use NPCs and their neuronal derivatives to investigate mechanisms of neurological disorders and develop more physiologically relevant disease models, methods for generation of regionally specific NPCs and neurons are needed. Here, we describe a protocol in which exogenous manipulation of WNT signaling, through either activation or inhibition, during neural differentiation of hPSCs, promotes the formation of regionally homogenous NPCs and neuronal cultures. In addition, we provide methods to monitor and characterize the efficiency of hPSC differentiation to these regionally specific cell identities.

Keywords: Human pluripotent stem cells, Neural progenitor cells, Neurons, Anterior–posterior patterning, Disease modeling, Drug screening, Regenerative medicine

1 Introduction

Neurodegenerative diseases including Alzheimer's disease (AD), Parkinson's disease (PD), amyotrophic lateral sclerosis (ALS), Huntington's disease (HD), and spinal muscular atrophy (SMA) currently affect approximately seven million Americans [1]. The already large burden these diseases have on families and the economy will continue to grow with the increasing proportion and size of the aged population, with costs for Alzheimer's disease and other dementias estimated to rise from $226 billion in 2015 to more than $1 trillion in 2050 [2]. Unfortunately, the etiology and pathophysiology of these devastating diseases remains incompletely understood limiting current therapeutic options to mainly palliative in nature.

Although the pathology of these diseases remains elusive, distinctive hallmarks include the degeneration of regionally specific neurons [3]. For example, AD largely affects neurons in the cortex,

hippocampus, and amygdala [4]. By comparison, PD results in the dysfunction of dopaminergic neurons in the substantia nigra of the midbrain [5] while ALS affects motor neurons in the hindbrain and spinal cord [6]. Because the cognitive and motor decline that is associated with these specific CNS diseases is due to the loss or dysfunction of specific neuronal subtypes, the ability to generate neuronal cultures of specific identity is critical in using hPSC-derived neurons to model and potentially treat neurodegenerative diseases.

Studies in model organisms, such as flies, worms, zebrafish, and mice have provided important insights into the role of a variety of signaling pathways in early neural development and patterning. From these studies, a general model for neural patterning has been proposed in which naïve ectodermal cells acquire an initial anterior neural identity through BMP antagonism and a subsequent WNT signaling gradient is responsible for inducing specific regional identities in these anterior cell types [7, 8]. Further examination of neural patterning in model organisms has led to the conclusion that a gradient of WNT signaling specifies neural cell identity along the anterior–posterior (A/P) axis. Specifically, loss-of-function studies in mice demonstrate that WNT-deficient embryos display posterior truncation (i.e., midbrain, hindbrain, and spinal cord structures fail to develop properly) with a significant expansion of the forebrain compartment [9–15]. On the other hand, gain-of-function in which the WNT pathway is ectopically activated leads to suppression of anterior fates and expansion of posterior neural markers [8, 16–20].

Here, we describe a recently published neural differentiation protocol based on the modulation of TGF-β and WNT signaling that allows for the differentiation of hPSCs into NPCs with specific A/P regional identity [21]. These regionally specified NPCs can be expanded and subsequently differentiated into cortical, midbrain dopaminergic, or spinal motor neurons. Overall, these differentiation methods will aid in the translation of these cell types for disease modeling, drug screening, and regenerative medicine therapies.

2 Materials

2.1 Equipment and Supplies

1. Biological Safety Cabinet.
2. CO_2 incubator with humidity and gas controls to maintain a stable environment of 37 °C, >95 % humidity, and 5 % CO_2.
3. Water bath set at 37 °C.
4. Benchtop cell culture centrifuge.
5. Orbital shaker (incubator safe).
6. Pipet Controller.

7. Serological pipettes (5, 10, and 25 ml).
8. 10-, 20-, 200-, and 1000-μl micropipettes.
9. 10-, 20-, 200-, and 1000-μl micropipette tips.
10. Tissue culture treated polystyrene dishes: 6-well, 12-well, and 24-well and 100 mm.
11. Ultra-low attachment 6-well multi-well plates (Bioexpress., cat. no. T-3326-1).
12. 1.5 ml microcentrifuge tubes.
13. Polystyrene conical tubes: 15- and 50-ml.
14. Hemacytometer.
15. Inverted light microscope with 4× and 10× phase objectives.
16. Polyethylene cell lifter (Corning Inc., cat.no. 3008).
17. Biospec Nano (Shimadzu Biotech) or comparable spectrophotometer.
18. C1000 Touch Thermal Cycler with 384 well reaction module (Biorad cat.no. 1851138).

2.2 Stock Solutions and Reagents

1. Essential 8™ animal protein free, defined, feeder-independent medium for maintenance of undifferentiated, human ESCs and iPSCs (Thermo Fisher Scientific, Cat. No. A1517001).
2. Dulbecco's Modified Eagle Medium/Nutrient Mixture F-12 (DMEM/F-12; Life Technologies, cat.no. 11320-033).
3. Dulbecco's Modified Eagle Medium (DMEM; Life Technologies, cat no. 11965-118).
4. 100× N-2 supplement (Life Technologies; cat.no. 17502-048).
5. 50× B-27 serum-free supplement (Life Technologies, cat.no. 17504-044).
6. Penicillin–Streptomycin (P/S) 5000 U/ml (Life Technologies; cat.no. 15070-063). Make aliquots of 5 ml and store at −20 °C.
7. GlutaMAX™ supplement (Life Technologies; cat.no. 35050-061). Make aliquots of 5 ml and store at −20 °C.
8. Phosphate-Buffered Saline (PBS), pH 7.4 (Life Technologies, cat.no. 10010023).
9. StemPro® Accutase® cell dissociation reagent (Life Technologies, cat.no. A1110501). Make aliquots of 5 ml and store at −20 °C.
10. Matrigel™, Growth Factor Reduced (BD Biosciences, cat.no. 354230). Make aliquots per lot instructions and store at −20 °C.
11. Rho-associated protein kinase inhibitor (ROCKi, Y-27632; EMD Millipore, cat.no. SCM075). Dissolve in DMSO at a

concentration of 5 mM. Make aliquots of 50 μl in 1.5 ml microcentrifuge tubes and store at −20 °C. Protect from light. A final concentration of 5 μM will be used for the first day after passaging hPSCs and the first day of embryoid body (EB) formation.

12. Human recombinant Noggin (R&D Systems, cat.no. 6057-NG). Reconstitute in sterile, distilled water at a concentration of 200 μg/ml. Make aliquots of 25 μl in 1.5 ml microcentrifuge tubes and store at −20 °C. A final concentration of 50 ng/ml will be used during NPC generation.
13. Dorsomorphin dihydrochloride (DM; Tocris Biosciences, cat. no. 3093). Dissolve in DMSO at a concentration of 25 mM. Make aliquots of 10 μl in 1.5 ml microcentrifuge tubes and store at −20 °C. A final concentration of 0.5 μM will be used during NPC generation.
14. Human recombinant bFGF (Life Technologies, cat.no. PHG6014). Reconstitute in sterile, distilled water at a concentration of 30 μg/ml. Make aliquots of 50 μl in 1.5 ml microcentrifuge tubes and store at −20 °C. A final concentration of 30 ng/ml will be used to culture and expand NPCs.
15. Human recombinant EGF (R&D Systems, cat.no. 236-EG). Reconstitute in sterile, distilled water at a concentration of 30 μg/ml. Make aliquots of 50 μl in 1.5 ml microcentrifuge tubes and store at −20 °C. A final concentration of 30 ng/ml will be used to culture and expand NPCs.
16. Human recombinant BDNF (R&D Systems, cat.no. 248-BD-005). Reconstitute in sterile, distilled water at a concentration of 20 μg/ml. Make aliquots of 25 μl in 1.5 ml microcentrifuge tubes and store at −20 °C. A final concentration of 20 ng/ml will be used during the 4 weeks of neuronal differentiation.
17. Human recombinant GDNF (R&D Systems, cat.no. 212-GD). Reconstitute in sterile, distilled water at a concentration of 20 μg/ml. Make aliquots of 25 μl in 1.5 ml microcentrifuge tubes and store at −20 °C. A final concentration of 20 ng/ml will be used during the 4 weeks of neuronal differentiation.
18. *N*-[(3,5-Diflurophenyl)acetyl-]-L-alanyl-2-phenyl]gylcine-1,1-dimethlethyl ester (DAPT) γ-secretase inhibitor (Tocris Biosciences; cat.no. 2634). Dissolve in DMSO at a concentration of 5 mM. Make aliquots of 50 μl and store at −20 °C. A final concentration of 1.0 μM will be used during the 4 weeks of neuronal differentiation.
19. N6, 2′-O-Dibutyryladenosine 30, 50-cyclic monophosphate sodium salt (db-cAMP; Sigma, cat.no. D0260). Dissolve in sterile, distilled water at a concentration of 25 mM. Make aliquots of 1.0 ml and store at −20 °C. A final concentration

of 0.5 mM will be used during the 4 weeks of neuronal differentiation.

20. Poly-L-ornithine 10 mg/ml solution (PLO; Sigma, cat.no. P4957). Make aliquots of 1.0 ml in 1.5 ml microcentrifuge tubes and store at 4 °C.
21. Laminin (LN) from Engelbreth-Holm-Swarm murine sarcoma basement membrane, 1 mg/ml solution (Sigma, cat.no. L2020). Make aliquots of 1.0 ml in 1.5 ml microcentrifuge tubes and store at −20 °C.
22. N6-[2-[[4-(2,4-Dichlorophenyl)-5-(1H-imidazol-2-yl)-2-pyrimidinyl]amino]ethyl]-3-nitro-2,6-pyridinediamine (CHIR 98014) glycogen synthase kinase-3 (GSK-3) inhibitor (Sigma-Aldrich, cat.no. SML1094-5MG). Dissolve in DMSO at a concentration of 10 mM. Make aliquots of 50 μl and store at −20 °C.
23. *N*-(6-Methyl-2-benzothiazolyl)-2-[(3,4,6,7-tetrahydro-4-oxo-3-phenylthieno[3,2 d]pyrimidin-2-yl)thio]-acetamide (IWP2) WNT inhibitor (Stemgent, cat.no. 04-0034). Dissolve in DMSO at a concentration of 5 mM. Make aliquots and store at −20 °C.
24. Nucelospin RNA Isolation Kit (Macherey-Nagel, cat. no. 740955.25).
25. TaqMan® Gene Expression Mastermix (Life Technologies, cat. no. 4369016).
26. β-Mercaptoethanol (Life Technologies, cat. no. 21985-023).
27. Ethyl alcohol, pure, Molecular Biology Grade (Sigma, cat. no. E7023-500 ml).
28. Nuclease Free Water (Life Technologies, cat. no. AM9939).
29. BD Cytofix™ Fixation Buffer (BD Biosciences, cat. no. 554655).
30. BD Phosflow™ Perm Buffer III (BD Biosciences, cat. no. 558050).
31. Taqman® Gene Expression Assays (*see* Table 1).
32. Primary and Secondary Antibodies (*see* Table 2).
33. Hoechst 33342 10 mg/ml (Life Technologies, cat. no. H3570).

2.3 Medium

1. Neural Base Medium (NBM). Combine 500 ml Dulbecco's Modified Eagle Medium/Nutrient Mixture F-12 (DMEM/F-12; Life Technologies, cat.no. 11320-033), 5 ml 50× B27 Supplement, 2.5 ml 100× N2 Supplement, 5 ml GlutaMAX, and 5 ml P/S.
2. Neural Induction Medium (NIM). In a 50 ml conical tube, combine 50 ml NBM, 12.5 μl of 200 μg/ml Noggin, and 1 μl

Table 1
Taqman® gene expression assays used for qPCR

Gene	Taman® gene expression assay
18s	Hs99999901_s1
CTIP2 (BCL11B)	Hs00256257_m1
CUX1	Hs00738851_m1
DLX2	Hs00269993_m1
EMX1	Hs00417957_m1
EN1	Hs00154977_m1
FOXG1	Hs01850784_s1
GATA2	Hs00231119_m1
GATA3	Hs00231122_m1
HOXA2	Hs00534579_m1
HOXB4	Hs00256884-m1
HOXB6	Hs00980016_m1
LMX1A	Hs00892663_m1
LMX1B	Hs00158750_m1
MNX1 (HB9)	Hs00907365_m1
NURR1 (NR4A2)	Hs00428691_m1
PITX3	Hs01013935_g1
SATB2	Hs00392652_m1
SIX3	Hs00193667_m1
TH	Hs00165941_m1

of 25 μM Dorsomorphin. The medium can be stored at 4 °C for up to 2 weeks.

3. Neural Expansion Medium (NEM). In a 50 ml conical tube, combine 50 ml NBM, 15 μl of 100 μg/μl FGF, and 15 μl of 100 μg/μl EGF. The medium can be stored at 4 °C for up to 2 weeks.
4. Neural Differentiation Medium (NDM). In a 50 ml conical tube, combine 50 ml Neural Base Medium, 50 μl of 20 ng/ml BDNF, 50 μl of 20 ng/ml GDNF, 10 μl of 5 mM DAPT, and 1.0 ml of 25 mM db-cAMP. The medium may be stored at 4 °C for up to 2 weeks.

Table 2
Primary and secondary antibodies used for immunofluorescence

Antibody	Vendor	Catalog #	Concentration used
Goat anti-SOX2	Santa Cruz	SC-17320	1:50
Goat anti-OTX2	R&D Systems	AF1979	1:200
Mouse anti-B3T	Fitzgerald	10R-T136A	1:1000
Mouse anti-MNX1	DSHB	81.5C10	1:100
Mouse anti-SOX1	BD	560749	1:10
Rabbit anti-FOXG1	Abcam	AB18259	1:100
Rabbit anti-HOXB4	Abcam	AB76093	1:10
Rabbit anti-LMX1A	Abcam	AB139726	1:100
Rabbit anti-NURR1	Millipore	AB5778	1:200
Rabbit anti-TBR1	Abcam	AB31940	1:200
Alexa 647 Donkey Anti-Goat	Life Technologies	A-21447	1:200
Alexa 647 Donkey Anti-Rabbit	Life Technologies	A-31573	1:200
Alexa 647 Donkey Anti-Mouse	Life Technologies	A-31571	1:200
Alexa 546 Donkey Anti-Goat	Life Technologies	A-11056	1:200
Alexa 546 Donkey Anti-Rabbit	Life Technologies	A-10040	1:200
Alexa 546 Donkey Anti-Mouse	Life Technologies	A-10036	1:200
Alexa 488 Donkey Anti-Goat	Life Technologies	A-11055	1:200
Alexa 488 Donkey Anti-Rabbit	Life Technologies	A-21206	1:200
Alexa 488 Donkey Anti-Mouse	Life Technologies	A-21202	1:200

3 Methods

An overview of the protocol for generation, expansion, and neuronal differentiation of regionally specific NPCs is presented in Fig. 1a. Although this protocol can be modified to generate NPCs of any A/P regional identity, we present methods to generate NPCs of (1) forebrain/cortical, (2) midbrain, and (3) hindbrain/spinal cord identity. These NPCs can be expanded and subsequently differentiated into (1) cortical, (2) midbrain GABAergic or dopaminergic, and (3) hindbrain or spinal motor neurons, respectively.

Undifferentiated hPSCs are grown in feeder-free conditions on Matrigel™-coated plates. Undifferentiated hPSCs are directed to the neural lineage through the stepwise formation of embryoid bodies (EBs; Fig. 1b left panel) and neuroepithelial-like rosettes

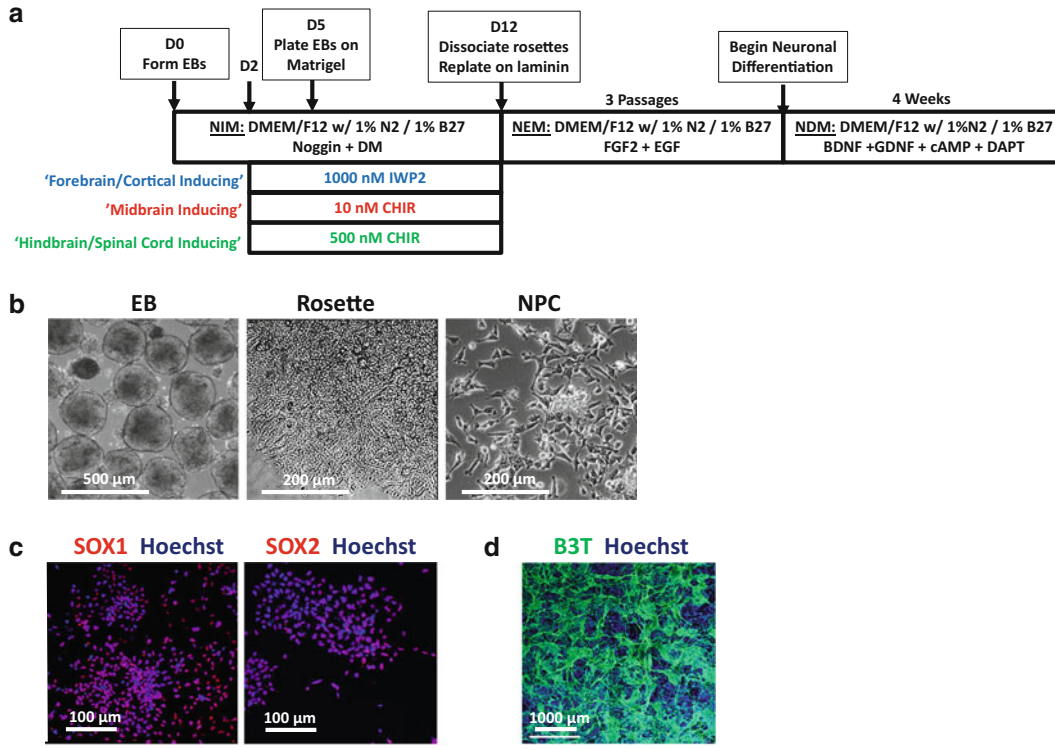

Fig. 1 Generation of regionally specific NPCs and neurons through exogenous manipulation of WNT signaling. (**a**) Outline of protocol to generation regionally specific NPCs and neurons from hPSCs. (**b**) Phase contrast images of EBs (*left panel*), neural rosettes (*center panel*), and NPCs (*right panel*). (**c**) Immunofluorescent analysis of NPC cultures for pan-neural markers SOX1 and SOX2. (**d**) Immunofluorescent analysis of neuronal cultures for pan-neuronal marker B3T. Figure and legend adapted with permission from [21]

(Fig. 1b center panel) in the presence of the TGF-β/BMP antagonists Noggin and Dorsomorphin. Patterning of these cells to specific A/P identities is achieved by fine tuning the level of WNT signaling activity through treatment of differentiating cultures with IWP2 (a small molecule that acts on PORCN to block WNT processing and secretion; [22] or increasing concentration of CHIR 98104 (CHIR; a potent inhibitor of GSK-3β and activator of the WNT pathway). Neural rosettes are enzymatically dissociated and replated on laminin (LN)-coated plates to form NPCs (Fig. 1b right panel). NPCs derived from this can be maintained as proliferative, multipotent SOX1+SOX2+ (Fig. 1c) cells in the presence of FGF2 and EGF on LN-coated plates. Subsequent differentiation of NPCs to B3T+ neurons (Fig. 1d) is achieved through the withdrawal of FGF2 and EGF and addition of BDNF, GDNF, db-cAMP, and DAPT. NPC and neuronal cell populations can be characterized by qPCR and immunofluorescence.

3.1 Maintenance of hPSCs in Feeder Free Conditions

1. hPSCs are maintained in feeder-free conditions on Matrigel™ coated 100 mm plates with E8 culture medium.
2. Prior to passaging hPSCs prepare a working solution of Matrigel™ by thawing one aliquot of Matrigel™ on ice (*see* **Note 1**).
3. Make a 1:25 dilution of Matrigel™ in cold DMEM in a 50 ml conical. The working solution of Matrigel™ should be maintained on ice and can be stored at 4 °C for up to 2 weeks.
4. Coat a 100 mm dish with 5 ml of Matrigel™ working solution per dish in a tissue culture hood and transfer to 37 °C incubator for 20 min (*see* **Note 2**).
5. Warm E8, DMEM, and Accutase® solution in 37 °C water bath.
6. Aspirate medium from 100 mm plate of 75 % confluent hPSCs and add 5 ml of Accutase®.
7. Incubate the plate in a CO_2 incubator for 5 min. After 5 min check cell dissociation under microscope to determine if additional incubation is required for cell detachment.
8. Add 5 ml of DMEM medium to the plate.
9. Using a 10 ml serological pipette, gently wash off the remaining cells and transfer the cell suspension to a 15 ml conical tube
10. Centrifuge the conical tube at 200 × *g* for 5 min.
11. Aspirate the supernatant and resuspend the cells in 5 ml E8 + 5 μl ROCKi. Gently pipette up and down 3–4 times with a 1000 μl pipette to break up any visible cell clumps.
12. Take 10 μl of the cell suspension to perform a cell count using a hemacytometer (*see* **Note 3**).
13. Using the cell count from the hemacytometer calculate the volume of cell suspension needed for 1.2×10^6 cells.
14. In a separate 15 ml conical add 9 ml E8, 9 μl ROCKi and the volume of cell suspension equivalent to 1.2×10^6 cells (*see* **Note 4**).
15. Aspirate Matrigel™ solution from previously coated 100 mm plate (*see* **Note 5**).
16. Add the cell suspension to the Matrigel™ coated plate.
17. Place the plate in the CO_2 incubator. Gently move the plate in several quick horizontal and vertical motions to disperse cells evenly across the cell culture surface.
18. Change the medium daily by aspirating the old medium and adding 10 ml fresh E8 (*see* **Note 6**). After 2–3 days, bright colonies should appear. hPSCs need to be passaged when the colonies begin to merge and the culture reaches approximately 75–80 % confluency, which typically occurs 3–4 days after passaging (*see* **Note 7**).

3.2 Formation and Growth of EBs

1. Warm Neural Induction Medium (NIM), DMEM, and Accutase® in a 37 °C water bath.
2. Aspirate E8 medium from healthy, 75–80 % confluent hPSC grown in a 100 mm plate.
3. Add 5 ml of Accutase® solution and incubate in the CO_2 incubator at 37 °C for 5 min. Observe under the microscope to determine if additional incubation is required for cell detachment.
4. Add 5 ml of warmed DMEM to the plate.
5. Using a 10 ml serological pipette gently wash off the remaining attached cells until the plate is clear.
6. Gently triturate the cell suspension until all noticeable cell clumps are broken up.
7. Transfer the cell suspension to a 15 ml conical tube.
8. Take 10 μl of the cell suspension to perform a cell count using the hemocytometer.
9. Centrifuge the conical tube at 200 × *g* for 5 min.
10. Aspirate the supernatant and resuspend the cells in NIM such that the final concentration of cells is 5.0×10^5 cells/ml (*see* **Note 8**).
11. Add 4 ml of cell suspension per well to an ultra-low attachment 6-well plate. A total of 2×10^6 cells will be present in each well.
12. Add 4 μl of 5 mM ROCKi per well of EBs.
13. Place the plate on an orbital shaker inside a CO_2 incubator. Set the shaker speed at 95 RPM.
14. After 24 h, examine the cells under the microscope. Small clusters of cells should be visible (Fig. 1b left panel). Do not change the medium.
15. After 48 h carefully aspirate approximately ½ (2 ml) of the medium from each well using a 5 ml serological pipette (*see* **Note 9**).
16. Add 2 ml of NIM to each well. Add the appropriate amount of IWP2 or CHIR so that the *final concentration* is as follows: (*see* **Notes 10** and **11**).
    (a) Forebrain/Cortical Induction: 1000 nM IWP2.
    (b) Midbrain Induction: 10 nM CHIR.
    (c) Hindbrain/Spinal Cord Induction: 500 nM CHIR.
17. Place the plate back on the orbital shaker inside a CO_2 incubator.
18. Continue to remove ½ (2 ml) of medium and replace with 2 ml fresh NIM each day. Add the appropriate amount of IWP2 or CHIR so that the final concentrations are the same as stated in **Step 16.**

3.3 EB Plating and Formation of Neural Rosettes

1. After 5 days of EB growth, plate EBs on Matrigel™ coated plates to induce formation of neural rosettes (Fig. 1b center panel).
2. Prior to plating EBs prepare a working solution of Matrigel™ by thawing one aliquot of Matrigel™ on ice.
3. Make a 1:25 dilution of Matrigel™ in cold DMEM in a 50 ml conical (*see* **Note 1**).
4. Coat each well of a 6-well tissue culture plate with 1.5 ml of Matrigel™ working solution per well. Incubate in a CO_2 incubator at 37 °C for 20 min (*see* **Note 2**).
5. Warm NIM in a 37 °C water bath.
6. Aspirate Matrigel™ solution from each well (*see* **Note 5**).
7. Add 4 ml of NIM. Add the appropriate amount of IWP2 or CHIR so that the *final concentration* is as follows:
   (a) Forebrain/Cortical Induction: 1000 nM IWP2.
   (b) Midbrain Induction: 10 nM CHIR.
   (c) Hindbrain/Spinal Cord Induction: 500 nM CHIR.
8. Using a 1000 μl pipette carefully aspirate 75 % of the medium from wells with EBs. Carefully transfer EBs to Matrigel™ coated wells. One well of EBs should be split equally to two Matrigel™ coated wells.
9. Quickly place the plate in the CO_2 incubator at 37 °C. Gently move the plate in several quick horizontal and vertical movements to evenly disperse the EBs (*see* **Note 12**).
10. After 24 h, carefully examine the cells under the microscope. EBs should have settled and adhered to the plate. Do not change the medium (*see* **Note 13**).
11. After 48 h, carefully remove ½ (2 ml) of the medium from each well using a 1000 μl pipette and replace 2 ml fresh NIM with patterning factors:
    (a) Forebrain/Cortical Induction: 1000 nM IWP2.
    (b) Midbrain Induction: 10 nM CHIR.
    (c) Hindbrain/Spinal Cord Induction: 500 nM CHIR.
12. Place plate back inside a CO_2 incubator. Changes of half of the medium should be made daily. After 3 days, the EBs should spread out on the Matrigel™ substrate and neural rosette structures should be visible (Fig. 1b center panel).

3.4 Generation, and Expansion of NPCs

1. After 7 days of culture, rosettes should be dissociated and replated onto poly-L-ornithine/Laminin (PLO/LN) coated plates.

2. To make PLO/LN coated plates make a 400 ng/ml working solution of poly-L-ornithine (PLO) by combining 2 ml 0.01 % PLO with 48 ml DPBS.
3. Coat a 100 mm dish with 10 ml of the PLO working solution at 37 °C for 4 h.
4. After 4 h of incubation, aspirate the PLO working solution and wash the PLO-coated 100 mm plates three times with 10 ml of PBS.
5. Thaw an aliquot of laminin (LN) on ice. Prepare a 4 μg/ml working solution of LN by adding 400 μl of 0.5 mg/ml LN to 50 ml of sterile PBS in a 50 ml conical tube.
6. Coat the PLO-coated 100 mm plate with 10 ml of LN working solution and incubate at 37 °C for 4 h (*see* **Note 14**).
7. Aspirate the LN working solution and rinse the plates one time with 10 ml of PBS.
8. Warm DMEM, Neural Expansion Medium (NEM) and Accutase® solution in a 37 °C water bath.
9. Gently aspirate NIM from the day 7 rosette cultures.
10. Add 1 ml of Accutase® to each well and incubate in the CO_2 incubator at 37 °C for 10 min. After 10 min, gently tap the sides of the plate against a solid surface to ensure complete cell dissociation (*see* **Note 15**).
11. Using a 10 ml serological pipette, gently wash off the remaining attached cells until the plate is clear.
12. Gently pipette the cell suspension until visible cell clumps are broken up.
13. Transfer the cell suspension to a 15 ml conical with 10 ml warm DMEM and centrifuge the tube at 200 × *g* for 5 min.
14. Resuspend the cells in the appropriate amount of NEM medium with ROCKi at 5 μM so that the final cell concentration is approximately 1–2 × 10^6 cells/ml (*see* **Note 3**).
15. Take 10 μl of the cell suspension to perform a cell count using the hemocytometer.
16. In a separate 15 ml conical tube add 9 μl ROCKi, 9 ml of fresh NEM, and cell suspension to equal 1.1 × 10^6 cells.
17. Aspirate PBS from PLO/LN coated plates and add the approximately 10 ml cell suspension onto a PLO/LN coated plate.
18. Place the plate in the CO_2 incubator. Gently move the plate in several quick horizontal and vertical motions to disperse the cells evenly across the cell culture surface.
19. Change the medium every other day by aspirating the old medium and adding 10 ml of fresh NEM.

20. Once the cells reach confluency they should be Accutase®. passaged at a density of $2.0 \times 10^4/cm^2$ onto new PLO/LN coated plates which typically occurs every 5–7 days. After 2–3 passages, NPCs should have a morphology as displayed in Fig. 1b right panel.

3.5 Characterization of NPCs

NPCs can be characterized using qPCR (Fig. 2a) and immunofluorescent staining (Fig. 2b). NPCs of all A/P regional identities should express high levels of the pan neural markers SOX1, SOX2, and NESTIN (Fig. 1c). NPCs of forebrain cortical identity should express high levels of FOXG1, DLX2, SIX3, and OTX2 (blue cluster in Fig. 2a). Midbrain-specified NPCs should express high levels of LMX1A and EN1 (red cluster in Fig. 2a) while hindbrain/spinal cord-specified NPCs should express high levels of HOXA2 and HOXB4 (green cluster in Fig. 2a).

3.5.1 Characterization of NPCs by qPCR

1. After three passages, NPCs can be characterized by qPCR analysis for pan neural markers and regionalized markers.
2. Warm DMEM and Accutase® solution in a 37 °C water bath.
3. Aspirate NEM from passage 3 NPC cultures.
4. Add 5 ml of Accutase® solution to each 100 mm plate and incubate in the CO_2 incubator for 5 min. After 5 min, gently tap the sides of the plate against a solid surface to ensure complete cell dissociation.
5. Observe under the microscope to determine if additional incubation is needed.
6. Using a 10 ml serological pipette, gently wash off the remaining attached cells with 5 ml of warmed DMEM until the plate is clear (*see* **Note 15**).

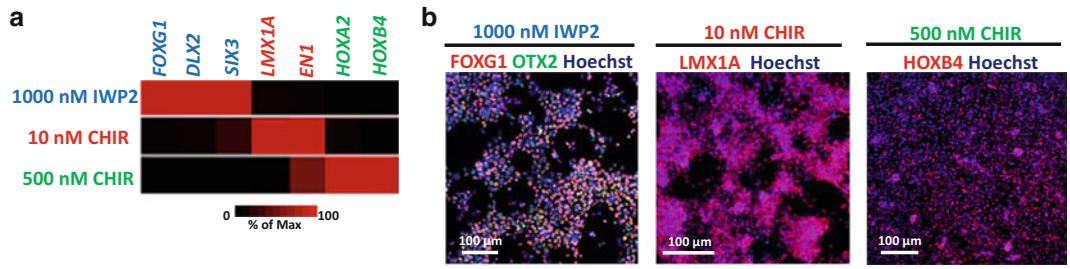

Fig. 2 Characterization of regionally specific NPCs. (**a**) Gene expression analysis of NPCs generated from hPSCs in the presence of 1000 nM IWP2, 10 nM CHIR, and 500 nM CHIR. The data are displayed in a heatmap where black corresponds to minimum expression levels and red corresponds to maximum levels. For each gene analyzed, the expression levels were normalized to the sample with the highest expression level. Primers used for gene expression analysis are listed in Table 1. (**b**) Immunofluorescent analysis of NPC cultures generated from hPSCs in the presence of 1000 nM IWP2, 10 nM CHIR, and 500 nM CHIR. Antibodies used for immunofluorescent analysis are listed in Table 2. Figure and legend adapted with permission from [21]

7. Gently pipette the cell solution into a 15 ml conical and spin down at 200 × *g* for 5 min.
8. Aspirate the supernatant and freeze the cell pellet at −80 °C or proceed directly with RNA isolation protocol with the Machery Nagel kit as described below.
9. Add 350 µl Buffer RA1 and 3.5 µl β-mercaptoethanol to each sample tube. Vortex vigorously.
10. Filtrate the lysate by placing the NucleoSpin® filter (purple ring) in a collection tube and applying the mixture to the filter. Centrifuge for 1 min at 11,000 × *g*.
11. Discard the NucleoSpin® filter and add 350 µl ethanol (70 %) to the lysate. Mix by pipetting up and down five times.
12. For each sample take one NucleoSpin® RNA column (light blue ring) placed in a Collection Tube. Pipette the sample lysate up and down 2–3 times and load the lysate to the column. Centrifuge for 30 s at 11,000 × *g*. Following centrifugation place the column in a new collection tube (2 ml).
13. Add 350 µl Membrane Desalting Buffer (MDB) and centrifuge at 11,000 × *g* for 1 min to dry the membrane.
14. Prepare DNAse reaction mixture in a sterile 1.7 ml eppendorf tube. For each isolation add 10 µl reconstituted rDNase (*see* **Notes 16** and **17**) to 90 µl Reaction Buffer for rDNase. Mix by gently flicking the tube. Apply 95 µl DNase reaction mixture onto the center of the silica membrane and incubate at room temperature for 15 min.
15. Add 200 µl Buffer RAW2 to the column and centrifuge for 30 s at 11,000 × *g*. Following centrifugation place the column in a new collection tube (2ml).
16. Add 600 µl Buffer RA3 to the column and centrifuge for 30 s at 11,000 × *g*. Aspirate flow through and place column back into the collection tube (*see* **Note 18**).
17. Add 250 µl Buffer RA3 to the column and centrifuge for 2 min at 11,000 × *g*.
18. Place the column in a nuclease free collection tube (1.5 ml) and elute the RNA in 20 µl RNase-free H_2O at 11,000 × *g* for 1 min.
19. Following RNA isolation check RNA quality and concentration using a Biospec Nano. Prior to analysis, blank the Biospec Nano by placing 1 µl of nuclease free H_2O on the pedestal and selecting "Blank."
20. Following blanking, pipette 1 µl of RNA on pedestal and click "Measure." Record values for concentration, 260/280, and 260/230 (*see* **Note 19**).

21. Using the previously measured concentration of RNA, calculate the volume of RNA equivalent to 1000 ng.
22. In 0.2 μl PCR tubes prepare the following volumes for each sample: 4 μl iScript RT Supermix, 1000 ng of RNA (volume previously calculated), and nuclease free water to 20 μl volume.
23. Place the 0.2 μl PCR tubes in a thermal cycler and run for 5 min at 25 °C, 20 min at 46 °C, and 1 min at 95 °C.
24. Following reverse transcription, cDNA may be stored at −80 °C or used directly to perform RT-qPCR.
25. Prepare the 384 well qPCR plate as follows.
26. In order to prepare a master mix for each sample of cDNA to be analyzed. First calculate the number of wells required for each sample (x) by multiplying the number of genes to be analyzed by 3 (for 3 technical replicates/sample of cDNA) (*see* **Note 20**). Add 3 to this number to account for residual volume losses ($y = x + 3$).
27. Take the number calculated in **step 27** (y) and multiply it by the following values to determine the volumes to add to a 1.7 ml eppendorf tube in order to prepare cDNA sample master mixes (*see* **Note 21**).
    (a) TaqMan® Gene Expression Mastermix: 5(y) μl.
    (b) cDNA: 0.1(y) μl.
    (c) Nuclease free H_2O: 4.4(y) μl.
28. Add 9.5 μl of sample master mix to each well (*see* **Note 23**).
29. Add 0.5 μl of primer for a gene to each well. Primers used for qPCR analysis are listed in Table 1. Include an endogenous reference gene such as 18S (*see* **Note 23**).
30. Once the plate is fully loaded, seal with optical cover being careful not to touch the surface of the optical cover (*see* **Note 24**).
31. Spin down the 384 well plate at 200 × *g* for 1 min.
32. Load the 384 well plate into the thermal cycler and run for 10 min at 95 °C, then 40 cycles (15 s at 95 °C, 1 min at 60 °C).
33. Following completion, use to Ct values to calculate relative fold changes in gene expression using the $2^{-\Delta\Delta CT}$ method [23].

3.5.2 Characterization of NPCs by IF Staining

1. After three passages, NPCs can be characterized by immunofluorescent (IF) staining.
2. Warm DMEM, NEM, and Accutase® solution in a 37 °C water bath.
3. Aspirate NEM from passage 3 NPC cultures.

4. Add 5 ml of Accutase® solution to each 100 mm plate and incubate in the CO_2 incubator for 5 min. After 5 min, gently tap the sides of the plate against a solid surface to ensure complete cell dissociation (*see* **Note 15**).
5. Observe under the microscope to determine if additional incubation and tapping is required.
6. Add 5 ml warmed DMEM medium to the plate.
7. Using a 10 ml serological pipette, gently wash off the remaining attached cells until the plate is clear.
8. Gently pipette the cell solution up and down until all visible cell clumps are broken up.
9. Transfer the cell suspension to a 15 ml conical tube.
10. Centrifuge the tube at 200 × *g* for 5 min.
11. Resuspend the cells in the appropriate amount of NEM medium so that the final cell concentration is about 1.0–2.0 × 10^6 cells/ml (*see* **Note 3**).
12. Take 10 μl of the cell suspension to perform a cell count using the hemacytometer.
13. Dilute cell suspension in NEM such that the final cell concentration is 1.0 × 10^5 cells/ml.
14. Into three wells of a PLO/LN coated 24-well plate add 1.0 ml of cell suspension.
15. Place the plate back inside a CO_2 incubator.
16. After 24 h, aspirate the NEM medium from each well.
17. Wash each well twice with 1 ml of sterile PBS.
18. Fix the NPCs by adding 1 ml of Fixation Buffer to each well. Incubate the cells in Fixation Buffer for 10 min at room temperature.
19. Aspirate the Fixation Buffer and wash each well twice with 1 ml of sterile PBS.
20. Incubate the primary antibodies overnight at 4 °C. See Table 2 for list of antibodies. Antibodies should be diluted in PBS to concentrations listed in Table 2.
21. Aspirate the primary antibodies and wash each well twice with 1 ml of sterile PBS.
22. Incubate the secondary antibodies for 1 h at room temperature in the dark. See Table 2 for list of antibodies. Antibodies should be diluted in PBS to concentrations listed in Table 2.
23. Aspirate the secondary antibodies and wash each well twice with 1 ml of sterile PBS.

24. Add 0.5 ml of Hoechst 3342 (1:5000 dilution in PBS) to each well to counterstain nuclei. Incubate for 10 min a room temperature in the dark.
25. Aspirate the Hoechst 3342 and ash each well twice with 1 ml of sterile PBS.
26. Image NPCs using a fluorescent microscope.

3.6 Differentiation of NPCs to Neurons

1. Warm DMEM, Neuronal Differentiation Medium (NDM) and Accutase® solution in a 37 °C water bath.
2. Aspirate NEM from passage 3 NPC cultures.
3. Add 5 ml of Accutase® solution to each plate and incubate in the CO_2 incubator for 5 min. After 5 min, gently tap the sides of the plate against a solid surface to ensure complete cell dissociation.
4. Observe under the microscope to determine if additional incubation and tapping is required.
5. Add 5 ml of warmed DMEM medium to the plate.
6. Using a 10 ml serological pipette, gently wash off the remaining attached cells.
7. Gently pipette the cell suspension up and down until all visible cells clumps are broken up.
8. Transfer the cell suspension to a 15 ml conical tube.
9. Centrifuge the tube at 200 × *g* for 5 min.
10. Aspirate the supernatant and resuspend the cells in the appropriate amount of NDM medium so that the final cell concentration is 1.0–2.0 × 10^6 cells/ml (*see* **Note 3**). Carefully pipette the cell suspension up and down 2–3 times with a 10 ml serological pipette until all cell aggregates are broken up.
11. Take 10 μl of the cell suspension to perform a cell count using the hemocytometer.
12. Dilute the cell suspension to 1.5 × 10^5 cells/ml with NDM.
13. Add 1.5 ml of cell suspension to each well of a 12-well PLO/LN coated plate.
14. Place the plate in the CO_2 incubator. Gently move the plate in several quick horizontal and vertical motions to disperse the cells evenly across the cell culture surface.
15. Change the medium every other day by aspirating the old medium and adding 2 ml of fresh NDM per well.
16. After 4 weeks in NDM cells should acquire a neuronal morphology.

3.7 Characterization of Neurons

Resultant neuronal cultures can be characterized using qPCR (Fig. 3a) and immunofluorescent staining (Fig. 3b). Neuronal cultures should express high levels of the pan-neural markers MAP2 and B3T. Neurons generated from forebrain/cortical specified NPCs should express high levels of markers such as CTIP2, CUX1, EMX1, FOXG1, SATB2, and TBR1 (blue cluster in Fig. 3a). By comparison, midbrain specified NPCs will generate neurons with a midbrain GABAergic or dopaminergic phenotype (red cluster in Fig. 3a) while neurons generated from hindbrain/spinal cord biased NPCs will express high levels of markers association with a hindbrain and spinal motor neuron phenotype (green cluster in Fig. 3a).

3.7.1 Characterization of Neurons by qPCR

1. Neurons can be characterized by qPCR analysis for pan neuronal markers and A/P-related neuronal markers.
2. Warm DMEM and Accutase® solution in a 37 °C water bath.
3. Aspirate NDM from neuronal cultures.
4. Add 0.5 ml of Accutase® solution to each well of a 12 well plate and incubate in the CO_2 incubator for 5 min. After 5 min, gently tap the sides of the plate against a solid surface to ensure complete cell dissociation.
5. Observe under the microscope to determine if additional incubation is needed.
6. Using a 1000 µl pipette, gently wash off the remaining attached cells with warmed DMEM until the plate is clear (*see* **Note 15**).
7. Gently pipette the cell solution into a 15 ml conical and spin down at 200 × *g* for 5 min.

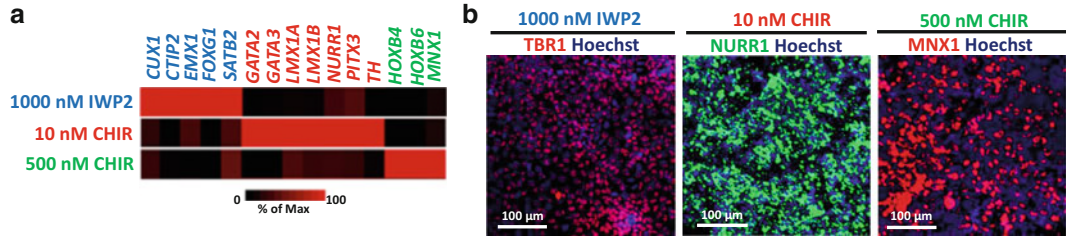

Fig. 3 Characterization of regionally specific neurons. (**a**) Gene expression analysis of neurons differentiated from NPCs generated from hPSCs in the presence of 1000 nM IWP2, 10 nM CHIR, and 500 nM CHIR. The data are displayed in a heatmap where black corresponds to minimum expression levels and red corresponds to maximum levels. For each gene analyzed, the expression levels were normalized to the sample with the highest expression level. Primers used for gene expression analysis are listed in Table 1. (**b**) Immunofluorescent analysis of neurons differentiated from NPCs generated from hPSCs in the presence of 1000 nM IWP2, 10 nM CHIR, and 500 nM CHIR. Antibodies used for immunofluorescent analysis are listed in Table 2. Figure and legend adapted with permission from [21]

8. Aspirate the supernatant and freeze the cell pellet at −80 °C or proceed directly with RNA isolation protocol in Machery Nagel kit described below.
9. Add 350 µl Buffer RA1 and 3.5 µl β-mercaptoethanol to each sample tube. Vortex vigorously.
10. Filtrate the lysate by placing a NucleoSpin® filter (purple ring) in a collection tube and applying mixture to the filter. Centrifuge for 1 min at 11,000 × *g*.
11. Discard the NucleoSpin® filter and add 350 µl ethanol (70 %) to the lysate. Mix by pipetting up and down five times.
12. For each sample take one NucleoSpin® RNA column (light blue ring) placed in a Collection Tube. Pipette the sample lysate up and down 2–3 times and load the lysate to the column. Centrifuge for 30 s at 11,000 × *g*. Following centrifugation place the column in a new collection tube (2 ml).
13. Add 350 µl Membrane Desalting Buffer (MDB) and centrifuge at 11,000 × *g* for 1 min to dry the membrane.
14. Prepare DNAse reaction mixture in a sterile 1.7 ml eppendorf tube. For each isolation add 10 µl reconstituted rDNase (*see* **Notes 16** and **17**) to 90 µl Reaction Buffer for rDNase. Mix by flicking the tube. Apply 95 µl DNase reaction mixture onto the center of the silica membrane and incubate at room temperature for 15 min.
15. Add 200 µl Buffer RAW2 to the column and centrifuge for 30 s at 11,000 × *g*. Following centrifugation place the column in a new collection tube (2ml).
16. Add 600 µl Buffer RA3 to the column and centrifuge for 30 s at 11,000 × *g*. Aspirate flow through and place column back into the collection tube (*see* **Note 18**).
17. Add 250 µl Buffer RA3 to the column and centrifuge for 2 min at 11,000 × *g*.
18. Place the column in a nuclease free collection tube (1.5 ml) and elute the RNA in 20 µl RNase-free H_2O at 11,000 × *g* for 1 min.
19. Following RNA isolation check RNA quality and concentration using a Biospec Nano. To do this, first blank the Biospec Nano by placing 1 µl of nuclease free H_2O on the pedestal and selecting "Blank."
20. Following blanking, place 1 µl of RNA on pedestal and click "Measure." Record values for concentration, 260/280, and 260/230 (*see* **Note 19**).
21. Calculate the required volume of RNA required for the reverse transcription reaction. Using the previously measured

concentration of RNA calculate the volume of RNA equivalent to 1000 ng.

22. In 0.2 µl PCR tubes prepare the following volumes for each sample: 4 µl iScript RT Supermix, 1000 ng of RNA (volume previously calculated), and nuclease free water to 20 µl volume.
23. Place the 0.2 µl PCR tubes in a thermal cycler and run for 5 min at 25 °C, 20 min at 46 °C, and 1 min at 95 °C.
24. Following reverse transcription cDNA may be stored at −80 °C or used directly to perform RT-qPCR.
25. Prepare the 384 well qPCR plate as follows.
26. In order to prepare a master mix for each sample of cDNA to be analyzed. First calculate the number of wells required for each sample (x) by multiplying the number of genes to be analyzed by 3 (for 3 technical replicates/sample of cDNA) (*see* **Note 20**). Add 3 to this number to account for pipetting losses ($y = x + 3$).
27. Take the number calculated in **step 27** (y) and multiply it by the following values to determine the volumes to add to a 1.7 ml Eppendorf tube in order to prepare cDNA sample master mixes (*see* **Note 21**).
    (a) TaqMan® Gene Expression Mastermix: 5(y) µl.
    (b) cDNA: 0.1(y) µl.
    (c) Nuclease free H_2O: 4.4(y) µl.
28. Add 9.5 µl of sample master mix to each well (*see* **Note 22**).
29. Add 0.5 µl of primer for a gene to each well. Primers used for qPCR analysis are listed in Table 1. Include an endogenous reference gene such as 18S (*see* **Notes 22** and **23**).
30. Once the plate is fully loaded, seal with optical cover being careful not to touch the surface of the optical cover (*see* **Note 24**).
31. Spin down the 384 well plate at 200 × *g* for 1 min.
32. Load the 384 well plate into the thermal cycler and run for 10 min at 95 °C, then 40 cycles (15 s at 95 °C, 1 min at 60 °C).
33. Following completion, use to Ct values to calculate relative fold changes in gene expression using the $2^{-\Delta\Delta CT}$ method [23].

3.7.2 Characterization of Neurons by IF Staining

1. Fix neurons by adding 1.5 ml of Fixation Buffer to each well. Incubate the cells in Fixation Buffer for 10 min at room temperature
2. Aspirate the Fixation Buffer and wash each well twice with 2 ml of sterile PBS.

3. Permeabilize cells by adding 1.5 ml of Perm Buffer to each well. Incubate the cells in Perm Buffer for 30 min at room temperature.
4. Aspirate the Perm Buffer and wash each well twice with 2 ml of sterile PBS.
5. Add 1.5 ml of primary antibodies and incubate overnight at 4 °C. See Table 2 for list of antibodies. Antibodies should be diluted in PBS to concentrations listed in Table 2.
6. Aspirate the primary antibodies and wash each well twice with 2 ml of sterile PBS.
7. Add 1.5 ml of secondary antibodies and incubate for 1 h at room temperature in the dark. See Table 2 for list of antibodies. Antibodies should be diluted in PBS to concentrations listed in Table 2.
8. Aspirate the secondary antibodies and wash each well twice with 1 ml of sterile PBS.
9. Add 0.5 ml of Hoechst 3342 to each well to counterstain nuclei. Incubate for 10 min at room temperature in the dark.
10. Aspirate the Hoechst 3342 and wash each well twice with 1 ml of sterile PBS.
11. Image neurons using a fluorescent microscope.

4 Notes

1. Matrigel™ aliquots and working solution should be kept on ice during thawing.
2. If not used within 24 h the culture plate should be sealed with Parafilm™ to avoid evaporation of Matrigel™ working solution. Culture plates can be sealed with Parafilm™ and stored at 4 °C for up to 1 week after coating. Prior to using stored Matrigel™ coated plates, allow the plates to equilibrate at room temperature for 15 min.
3. The dynamic range of the hemacytometer is 5.0×10^5–2.0×10^6 cells/ml. If the cell suspension is not in this range additional E8 medium may need to be added to obtain an accurate cell count.
4. hPSCs can be grown and maintained in other tissue culture plate sizes (e.g., multi-well dishes). Cells should be plated in these formats at a density of approximately $9.0 \times 10^3/cm^2$. Ideal seeding densities for different hPSC lines will vary and may need to be determined empirically.
5. Aspirate Matrigel™ solution immediately prior to seeding cells. Do not allow the Matrigel™ coated surfaces to dry out.

6. Do not add ROCKi. ROCKi is only added during passaging to aid in hPSC survival.
7. If the colonies are passaged too late, then colonies will begin to display signs of differentiation. Differentiated cells develop a fibroblast-like morphology and can be removed using manual dissection techniques prior to passaging.
8. Optimal cell density for EB formation may be hPSC line dependent. When working with a new cell line determine the optimal cell density will need to be empirically determined.
9. Use caution when aspirating medium as not to disturb the EBs in suspension.
10. Do not add ROCKi. ROCKi is added on the first day of EB formation to aid cell survival.
11. Optimal concentrations for CHIR 98014 and IWP2 may be hPSC line dependent. When working with a new cell line determine optimal concentrations empirically.
12. Failure to evenly disperse the EBs throughout the cell culture surface may result in aggregation of EBs into the center of the well and hinder the ability neural rosettes to form.
13. Do not move the plate prior to 24 h to allow for sufficient time for the EBs to settle and adhere. On average, approximately 5–10 % of the EBs will be of cystic or nonuniform shape and will not attach to the Matrigel™ coated plates.
14. If not used immediately, the PLO/LN culture plates should be sealed to avoid evaporation of laminin working solution. Culture plates can be sealed with Parafilm™ and stored at −20 °C.
15. Complete dissociation from the cell culture surface may require the use of a cell lifter.
16. Lyophilized rDNase should be initially stored at 4 °C. To aliquot rDNase, add indicated volume of nuclease free H_2O indicated (on the vial) to the vial and incubate at room temperature for 1 min. Gently swirl the vial to completely dissolve rDNAse. Be careful not to mix rDNase vigorously as it is sensitive to mechanical agitation. Dispense aliquots at 10 μl and store at −20 °C.
17. rDNase is sensitive to mechanical agitation, be careful not to mix vigorously.
18. Make sure residual buffer is washed away with Buffer RA3.
19. RNA quality can be assessed by examining the A_{260}/A_{280}, a ratio between 1.8 and 2.0 is acceptable. A ratio below 1.8 could indicate protein contamination which can lower reaction efficiency in downstream applications.
20. qPCR experiments should be carried out in three technical replicates.

21. Components of the TaqMan® Gene Expression Mastermix can settle during storage, so gently mix prior to use. However, do not vortex or mix vigorously to prevent the formation of bubbles which can impact fluorescence readings.
22. It is critical to not dispense to the second stop to avoid the formation of bubbles which would interfere with fluorescence readings.
23. A reference gene is required to analyze data using the $2^{-\Delta\Delta CT}$ method. For addition information on the selection of reference genes the reader should consult previous publications [24].
24. Use the tabs delineated with perforations to handle the optical covers to prevent fingerprints on the optical cover. Use a square plastic installing tool provided with the covers to smooth down the cover, especially along the four edges at the top of the plate, to prevent evaporation in reaction wells during PCR cycles.

References

1. Lunn JS, Sakowski SA, Hur J, Feldman EL (2011) Stem cell technology for neurodegenerative diseases. Ann Neurol 70(3):353–361
2. Alzheimer's Association (2015) Alzheimer's disease facts and figures. Alzheimers Dement. 11(3):332–384
3. Jucker M, Walker LC (2013) Self-propagation of pathogenic protein aggregates in neurodegenerative diseases. Nature 501(7465):45–51
4. Castellani RJ, Rolston RK, Smith MA (2010) Alzheimer disease. Dis Mon 56(9):484–546
5. Damier P, Hirsch EC, Agid Y, Graybiel AM (1999) The substantia nigra of the human brain. II. Patterns of loss of dopamine-containing neurons in Parkinson's disease. Brain 122(Pt 8):1437–1448
6. Thomsen GM, Gowing G, Svendsen S, Svendsen CN (2014) The past, present and future of stem cell clinical trials for ALS. Exp Neurol 262 (Pt B):127–137
7. Elkouby YM, Frank D. (2010) Wnt/β-Catenin Signaling in Vertebrate Posterior Neural Development. San Rafael (CA): Morgan & Claypool Life Sciences. Available from: https://www.ncbi.nlm.nih.gov/books/NBK53460/
8. Kiecker C, Niehrs C (2001) A morphogen gradient of Wnt/beta-catenin signalling regulates anteroposterior neural patterning in Xenopus. Development 128(21):4189–4201
9. Augustine K, Liu ET, Sadler TW (1993) Antisense attenuation of Wnt-1 and Wnt-3a expression in whole embryo culture reveals roles for these genes in craniofacial, spinal cord, and cardiac morphogenesis. Dev Genet 14 (6):500–520
10. Augustine KA, Liu ET, Sadler TW (1995) Interactions of Wnt-1 and Wnt-3a are essential for neural tube patterning. Teratology 51 (2):107–119
11. McMahon AP, Joyner AL, Bradley A, McMahon JA (1992) The midbrain-hindbrain phenotype of Wnt-1-/Wnt-1-mice results from stepwise deletion of engrailed-expressing cells by 9.5 days postcoitum. Cell 69(4):581–595
12. Liu P, Wakamiya M, Shea MJ, Albrecht U, Behringer RR, Bradley A (1999) Requirement for Wnt3 in vertebrate axis formation. Nat Genet 22:361–365
13. Lekven AC, Thorpe CJ, Waxman JS, Moon RT (2001) Zebrafish wnt8 encodes two wnt8 proteins on a bicistronic transcript and is required for mesoderm and neurectoderm patterning. Dev Cell 1(1):103–114
14. Erter CE, Wilm TP, Basler N, Wright CV, Solnica-Krezel L (2001) Wnt8 is required in lateral mesendodermal precursors for neural posteriorization in vivo. Development 128 (18):3571–3583
15. Glinka A, Wu W, Onichtchouk D, Blumenstock C, Niehrs C (1997) Head induction by simultaneous repression of Bmp and Wnt signalling in Xenopus. Nature 389(6650):517–519
16. Ciani L, Salinas PC (2005) WNTs in the vertebrate nervous system: from patterning to neuronal connectivity. Nat Rev Neurosci 6 (5):351–362

17. McGrew LL, Lai CJ, Moon RT (1995) Specification of the anteroposterior neural axis through synergistic interaction of the Wnt signaling cascade with noggin and follistatin. Dev Biol 172(1):337–342
18. McGrew LL, Hoppler S, Moon RT (1997) Wnt and FGF pathways cooperatively pattern anteroposterior neural ectoderm in Xenopus. Mech Dev 69(1–2):105–114
19. Hamilton FS, Wheeler GN, Hoppler S (2001) Difference in XTcf-3 dependency accounts for change in response to beta-catenin-mediated Wnt signalling in Xenopus blastula. Development 128(11):2063–2073
20. Darken RS, Wilson PA (2001) Axis induction by wnt signaling: target promoter responsiveness regulates competence. Dev Biol 234 (1):42–54
21. Moya N, Cutts J, Gaasterland T, Willert K, Brafman DA (2014) Endogenous WNT signaling regulates hPSC-derived neural progenitor cell heterogeneity and specifies their regional identity. Stem Cell Rep 3 (6):1015–1028
22. Chen B, Dodge ME, Tang W, Lu J, Ma Z, Fan C-W et al (2009) Small molecule-mediated disruption of Wnt-dependent signaling in tissue regeneration and cancer. Nat Chem Biol 5 (2):100–107
23. VanGuilder HD, Vrana KE, Freeman WM (2008) Twenty-five years of quantitative PCR for gene expression analysis. Biotechniques 44 (5):619–626
24. Hellemans J, Vandesompele J (2014) Selection of reliable reference genes for RT-qPCR analysis. Methods Mol Biol 1160:19–26

Methods in Molecular Biology (2016) 1516: 145–152
DOI 10.1007/7651_2015_315

Published online: 19 February 2016

Isolation and Culture of Embryonic Stem Cells, Mesenchymal Stem Cells, and Dendritic Cells from Humans and Mice

Srabani Kar, Shinjini Mitra, and Ena Ray Banerjee

Abstract

Stem cells are cells capable of proliferation, self-renewal, and differentiation into specific phenotypes. They are an essential part of tissue engineering, which is used in regenerative medicine in case of degenerative diseases. In this chapter, we describe the methods of isolating and culturing various types of stem cells, like human embryonic stem cells (hESCs), human umbilical cord derived mesenchymal stem cells (hUC-MSCs), murine bone marrow derived mesenchymal stem cells (mBM-MSCs), murine adipose tissue derived mesenchymal stem cells (mAD-MSCs), and murine bone marrow derived dendritic cells (mBMDCs). All these cell types can be used in tissue engineering techniques.

Keywords: Stem cells, Embryonic stem cells (ESCs), Undifferentiated cells, Lineage specific differentiation, Embryoid body (EB), Mesenchymal stem cells (MSCs), Umbilical cord (UC), Bone marrow derived mesenchymal stem cells (BM-MSCs), Adipose derived mesenchymal stem cells (AD-MSCs), Bone marrow derived dendritic cells (BMDCs)

1 Introduction

Stem cells are undifferentiated cells capable of proliferation, self-renewal, and differentiation towards specific phenotypes. The differentiation of cells is controlled by a variety of cues, including the various mechanical forces at play in their surrounding microenvironments. In particular, the nature of the substrate on which these cells lie and its innate stiffness are known to be important in determining cell fate.

Tissue engineering is an interdisciplinary field that applies the principles and methods of bioengineering, material science, and life sciences toward the assembly of biological substitutes that will restore, maintain, and improve tissue functions or a whole organ following damage either by disease or traumatic processes [1].

The general principle of tissue engineering lies on four factors—scaffold (three-dimensional tissue structures that guide the organization, growth, and differentiation of cells), extracellular matrix or ECM (that can provide the optimal conditions for cell

adhesion, growth and differentiation, by controlling environmental factors) [2], growth factors (soluble peptides capable of binding cellular receptors and producing permissive or preventive cellular response towards differentiation and/or proliferation of cells) [3], and cells (viable cells, that are non-immunogenic, highly proliferative, easy to harvest, and pluripotent, with the ability to differentiate into a variety of cell types with specialized functions) [2, 4–8].

The main success in the field of in vitro tissue engineering has come from the use of primary cells. However, this strategy has limitations, because of the invasive nature of cell collection and the potential for cells to be in a diseased state. Therefore, attention has become focused upon the use of stem cells, including embryonic stem (ES) cells, bone marrow mesenchymal stem cells (BM-MSCs), and umbilical cord-derived mesenchymal stem cells (UC-MSCs). Feeder cells provide conducive environments for growth of many stem cell lines. However, there remains the chance of contamination with xenogenic materials. So to prevent that, feeder-free systems for growing stem cells are being developed [9].

Also known as human pluripotent stem cells, human embryonic stem cells (hESCs) are derived from human embryos or human fetal tissues. They are self-replicating, and are also known to develop into cells and tissues of the three primary germ layers called the ectoderm, mesoderm, and endoderm (the primary layers of cells in the embryo from which all tissues and organs develop). Human ESCs have been used in a tissue engineering format to induce differentiation and amplification into the desired type of cell. In this chapter, we show how to induce hESCs to differentiate into the non-ciliated squamous epithelial cells present in the lung.

Mesenchymal stem cells (MSCs) are multipotent stromal cells that have the ability to differentiate into a variety of cell types, including osteoblasts or bone cells, chondrocytes or cartilage cells, and adipocytes or fat cells. MSCs do not differentiate into hematopoietic cells. They can be derived from bone marrow or other non-marrow tissues, such as adipose tissue, adult muscle, corneal stroma, or dental pulp of baby. MSCs have the capability to regenerate different tissues, but not the capacity to reconstitute entire organs. The most primitive form of MSC can be isolated from the umbilical cord (UC) tissue, namely Wharton jelly, and the umbilical cord blood. Wharton jelly contains a higher concentration of MSCs than UC blood, whereas the UC blood is a source of hematopoietic stem cells. The UC MSCs have more primitive properties than adult MSCs obtained later in life, which makes them a good source of MSCs for clinical application [10].

Dendritic cells are antigen-presenting cells (APCs) which play a critical role in the regulation of the adaptive immune response. Also referred to as professional APCs, they have the ability to induce a primary immune response in resting, naïve T lymphocytes. DCs are

capable of capturing antigens, processing them, and presenting them on the cell surface along with appropriate co-stimulation molecules. Dendritic cells can be isolated from mouse spleen and other mouse tissues, as well as from human tissues [11].

2 Materials

2.1 Cells

1. Undifferentiated human embryonic stem cells (hESCs).
2. Mesenchymal stem cells isolated from mice bone marrow (BM-MSCs), adipose tissue (AD-MSCs), and human umbilical cord (UC-MSCs).
3. Dendritic cells from mice bone marrow (BMDCs).

2.2 Culture Medium

1. Embryonic stem cell (ESC) conditioned medium: Knockout Dulbecco's modified Eagle medium (KO-DMEM), 20 % knockout serum replacement (KOSR), 1 mM sodium pyruvate, 0.1 mM β-mercaptoethanol (β-ME), 0.1 mM minimum essential medium (MEM), 1 % nonessential amino acids (NEAA), 1 mM L-glutamine, and 2 ng/ml basic fibroblast growth factor (bFGF).
2. Embryoid body (EB) medium: KO-DMEM, 20 % KOSR, 20 % non-heat inactivated fetal calf serum (FCS), 1 % NEAA, 1 mM L-glutamine, and 0.1 mM β-ME.
3. Small Airways Growth Medium (SAGM): small airways basal medium, 30 μg/ml bovine pituitary extract, 5 μg/ml insulin, 0.5 μg/ml hydrocortisone, 0.5 μg/ml gentamicin sulfate–amphotericin B, 0.5 mg/ml bovine serum albumin (BSA), 10 μg/ml transferrin, 0.5 μg/ml epinephrine, and 0.5 ng/ml recombinant human epidermal growth factor (rhEGF).
4. Bronchiolar Epithelium Growth Medium (BEGM): bronchiolar epithelial basal medium, 30 μg/ml bovine pituitary extract, 5 μg/ml insulin, 0.5 μg/ml hydrocortisone, 0.5 μg/ml gentamicin sulfate–amphotericin B, 0.1 ng/ml retinoic acid, 10 μg/ml transferrin, 6.5 ng/ml triiodothyronine, 0.5 μg/ml epinephrine, and 0.5 ng/ml rhEGF.
5. Growth medium: DMEM, 10 % fetal bovine serum (FBS), 1 % penicillin–streptomycin (Pen-Strep).
6. Freezing medium: 90 % DMEM + FBS, 10 % dimethyl sulfoxide (DMSO).
7. Adipose tissue derived MSC (AD-MSC) culture medium: DMEM, 20 % FBS.
8. Bone marrow derived dendritic cell (BMDC) medium: RPMI-1640, 10 % FBS, 20 mM Pen-Strep.

2.3 Buffers and Reagents

1. Dispase solution: 1.2 U/ml dispase dissolved in Ca^{2+}- and Mg^{2+}-free phosphate buffered saline (PBS), 10 % ESC-qualified fetal bovine serum (FBS).
2. DMSO neutralizing medium: DMEM, 10 % FBS.
3. Cell detachment solution (pH 8.0): 0.05 % trypsin, 0.5 mM EDTA.
4. Adipose tissue digestion solution: 1× PBS, 2 % BSA, 2 mg/ml collagenase A.
5. Recombinant murine granulocyte macrophage colony stimulating factor (rmGM-CSF): 1000 ng/ml rmGM-CSF stock.
6. 1× phosphate buffered saline (PBS) (pH 7.4): 137 mM NaCl, 2.7 mM KCl, 10 mM Na_2HPO_4, 1.8 mM KH_2PO_4.
7. Hanks' balanced salt solution (HBSS) (pH 7.0): 1.26 mM $CaCl_2$, 5.33 mM KCl, 0.44 mM KH_2PO_4, 0.50 $MgCl_2 \cdot 6H_2O$, 0.41 $MgSO_4 \cdot 7H_2O$, 138 mM NaCl, 4 mM $NaHCO_3$, 0.30 Na_2HPO_4, 5.60 mM glucose, 0.03 mM phenol red.

2.4 Instruments

1. Humidified CO_2 incubator, at 37 °C, 5 % CO_2
2. Biosafety cabinet
3. Centrifuge
4. Centrifuge tubes
5. Tissue culture plates (10 mm, 60 mm, 90 mm)
6. 40 μm nylon mesh filter

3 Methods

3.1 Culture and Differentiation of Human Embryonic Stem Cells (hESCs)

3.1.1 Expansion of hESCs

1. Plate primary mouse embryonic fibroblast (MEF) feeder cells, prepared from timed pregnant CF-1 female mice (day 13.5 of gestation), in conditioned medium, in 6-well 10 mm tissue culture plates (*see* **Note 1**).
2. Incubate the cells in a humidified 5 % CO_2 incubator at 37 °**C**.
3. After growth, γ-irradiate the MEF cells with 3000 rads for 5 min, to stop differentiation of MEF cells (*see* **Note 2**).
4. Plate the hESCs on the γ-irradiated MEF feeder cells in ESC conditioned medium, and incubate in a humidified 5 % CO_2 incubator at 37 °**C**.

3.1.2 Embryoid Body Formation

1. Treat colonies with well-defined boundaries and minimum differentiation, with dispase solution at 37 °**C**, till the ESC colonies nearly detach from the plates.

2. Wash the colonies off the plates, then wash twice with ESC conditioned medium without bFGF.
3. Resuspend the cells in EB medium, and transfer to ultra-low attachment tissue culture plates.
4. Grow for 4 days at 37 °**C**.

3.1.3 Generation of Non-ciliated Pulmonary Epithelial Cells

1. Transfer EBs to tissue culture plates after dispase digestion.
2. Culture EBs for 12 days in SAGM or BEGM (Refresh medium every other day).
3. From the day 12 culture in SAGM or BEGM, flow sort the alveolar epithelium cells on the basis on surface expression of SP-C and AQP-5.
4. Grow the flow sorted SP-C^+ and $AQP5^+$ cells in SAGM or BEGM for 4 days.

3.2 Isolation and Culture of Human Umbilical Cord Mesenchymal Stem Cells (hUC-MSCs)

1. Collect human umbilical cord from hospitals (*see* **Note 3**), and store in DMSO at −80 °**C**, in 50 ml centrifuge tubes.
2. On the day of the experiment, thaw the tube to 37 °**C** quickly, till only a few ice crystals remain.
3. Wash the cord in DMSO-neutralizing medium and transfer to petri dish containing 7 ml of the growth medium.
4. Squeeze out the inner contents of the cord into the medium using forceps and scalpel.
5. Chop the remaining cord into small sections using surgical blades and place them in 20 ml growth medium in a 90 mm tissue culture plate (*see* **Note 1**).
6. Add the inner contents of the cord into the plate containing the sections and incubate at 37 °C, with 5 % CO_2 for 5 days. Keep undisturbed for 3 days, then check under microscope for adherent cells. Continue incubation till 5 days.
7. Once cells become confluent, they can be passaged, after detachment with trypsin–EDTA, or frozen and stored in cryovials, containing freezing medium.

3.3 Isolation of Murine Bone Marrow Derived Mesenchymal Stem Cells (mBM-MSCs)

1. Collect femur and tibia from mice in growth medium, and remove the flesh and muscles (*see* **Notes 4** and **5**).
2. Under a biosafety cabinet, cut the ends of the bones and flush the contents of the bone with growth medium, into sterile centrifuge tubes.
3. Plate 5×10^4 cells in tissue 60 mm culture plates (*see* **Note 1**), in growth medium, for 3 h at 37 °**C**, with 5 % CO_2.
4. Remove non-adherent cells carefully after 3 h and add fresh medium.

5. When the cells become confluent, treat with 0.5 ml of 0.25 % trypsin–EDTA for 2 min at room temperature (25 °**C**), to get a purified population of BM-MSCs.

3.4 Isolation of Murine Adipose Tissue Derived MSCs (mAD-MSCs)

1. Isolate inguinal adipose tissue from 12- to 14-week-old BALB/c mice (*see* **Notes 4** and **5**).
2. Digest in adipose tissue digestion solution for 15–20 min.
3. Filter through 40 μm nylon filter mesh, centrifuge at 500 × *g* for 5 min, and resuspend pellet in AD-MSC growth medium.
4. Plate 5×10^4 cells in 60 mm tissue culture plates (*see* **Note 1**) and incubate at 37 °C with 5 % CO_2.
5. Change medium every 2 days, and passage after cells reach 80–90 % confluence.

3.5 Isolation of Murine Bone Marrow Derived Dendritic Cells (mBMDC)

1. Collect femur and tibia from mice in growth medium, and remove the flesh and muscles (*see* **Notes 4** and **5**).
2. Under a biosafety cabinet, cut the ends of the bones and flush the contents of the bone with growth medium, into sterile centrifuge tubes.
3. Dilute the BM suspension in HBSS to a final volume of 20 ml. disintegrate any clumps formed by vigorous pipetting.
4. Centrifuge the suspension at 250 × *g* for 8 min. Remove the supernatant and resuspend the pellet in HBSS.
5. Wash the cells twice in HBSS at 250 × *g* for 8 min each.
6. After the second wash, resuspend the cells in BMDC medium to a cell concentration of 10×10^6 cells/ml.
7. Add 9.6 ml of the BMDC medium to a sterile 90 mm petri dish. To it, add 0.2 ml of the cell suspension and 0.2 ml of rmGM-CSF stock (to get a final concentration of 20 ng/ml).
8. Gently swirl the petri dish to mix uniformly and incubate at 37 °**C**, with 5 % CO_2 and 95 % humidity, for 3 days.
9. Add 10 ml of fresh medium with 20 ng/ml rmGM-CSF every 3 days.
10. Harvest the primary BMDCs from the petri dish, by collecting the non-adherent cells by gently pipetting them with the culture medium.
11. Collect the cell suspension carefully into centrifuge tubes. Discard the adherent cells, which are mainly macrophages
12. Centrifuge the cell suspension at 250 × *g* for 8 min and resuspend in BMDC medium at a required concentration.

4 Notes

1. Treat all tissue culture plates with 0.1 % gelatin for better adherence of cells. Treat plates with gelatin overnight at room temperature. Discard the gelatin, air-dry the plates in a laminar airflow hood for 45 min, and then expose them to UV for 30 min.
2. To stop differentiation of MEF feeder cells (Section 3.1.1), mitomycin C (at a final concentration of 10 μg/ml) for 2–3 h at 37 °**C** can be used instead of γ-irradiation.
3. Collection of human umbilical cord should be done with the consent of the patients.
4. Animal sacrifices should be done ethically.
5. All animal handling should be done with proper protective gear, and under the laminar airflow hood.

Acknowledgements

The authors wish to acknowledge Department of Biotechnology (Government of India) for funding the research work on BJNhem 19 and 20. Further the fellowship for SK was provided by Science and Engineering Research Board (Government of India). The work on H7 was undertaken by ERB in Professor William R. Henderson Jr.'s lab with funding from NIH and under his tutelage. The authors would like to acknowledge collaborators whose intellectual input have been instrumental in mentoring stem cell research in the ERB lab, namely Professors Thalia Papayannopoulou and Charles E. Murry, experts in stem cell biology, the former in hematopoiesis and the latter in cardiomyocyte differentiation.

References

1. Langer R, Vacanti JP (1993) Tissue engineering. Science 260(5110):920–926
2. Naughton GK (2002) From lab bench to market: critical issues in tissue engineering. Ann N Y Acad Sci 961:372–385
3. Whitaker MJ, Quirk RA, Howdle SM, Shakesheff KM (2001) Growth factor release from tissue engineering scaffolds. J Pharm Pharmacol 53:1427–1437
4. Knight MA, Evans GR (2004) Tissue engineering: progress and challenges. Plastic Reconstruct Surg 114:26E–37E
5. Fuchs JR, Nasseri BA, Vacanti JP (2001) Tissue engineering: a 21st century solution to surgical reconstruction. Ann Thorac Surg 72:577–591
6. Shieh SJ, Vacanti JP (2005) State-of-the-art tissue engineering: from tissue engineering to organ building. Surgery 137:1–7
7. Stock UA, Vacanti JP (2001) Tissue engineering: current state and prospects. Annu Rev Med 52:443–451
8. Koh CJ, Atala A (2004) Therapeutic cloning and tissue engineering. Curr Top Dev Biol 60:1–15

9. Denning C, Allegrucci C, Priddle H et al (2006) Common culture conditions for maintenance and cardiomyocyte differentiation of the human embryonic stem cell lines, BG01 and HUES-7. Int J Dev Biol 50:27–37
10. Banerjee ER (2014) Perspectives in regenerative medicine. Springer, India
11. Madaan A, Verma R, Singh AT, Jain SK, Jaggi M (2014) A stepwise procedure for isolation of murine bone marrow and generation of dendritic cells. J Biol Methods 1(1):e1

Methods in Molecular Biology (2016) 1516: 153–169
DOI 10.1007/7651_2016_324

Published online: 14 April 2016

Decoding the Epigenetic Heterogeneity of Human Pluripotent Stem Cells with Seamless Gene Editing

Amar M. Singh, Dustin W. Perry, Valeriya V. Adjan Steffey, Kenneth Miller, and Daniel W. Allison

Abstract

Pluripotent stem cells exhibit cell cycle-regulated heterogeneity for trimethylation of histone-3 on lysine-4 (H3K4me3) on developmental gene promoters containing bivalent epigenetic domains. The heterogeneity of H3K4me3 can be attributed to Cyclin-dependent kinase-2 (CDK2) phosphorylation and activation of the histone methyltransferase, MLL2 (KMT2B), during late-G1. The deposition of H3K4me3 on developmental promoters in late-G1 establishes a permissive chromatin architecture that enables signaling cues to promote differentiation from the G1 phase. These data suggest that the inhibition of MLL2 phosphorylation and activation will prevent the initiation of differentiation. Here, we describe a method to seamlessly modify a putative CDK2 phosphorylation site on MLL2 to restrict its phosphorylation and activation. Specifically, by utilizing dimeric CRISPR RNA-guided nucleases, RFNs (commercially known as the NextGEN™ CRISPR), in combination with an excision-only piggyBac™ transposase, we demonstrate how to generate a point mutation of threonine-542, a predicted site to prevent MLL2 activation. This gene editing method enables the use of both positive and negative selection, and allows for subsequent removal of the donor cassette without leaving behind any unwanted DNA sequences or modifications. This seamless "donor-excision" approach provides clear advantages over using single stranded oligo-deoxynucleotides (ssODN) as donors to create point mutations, as the use of ssODN necessitate additional mutations in the donor PAM sequence, along with extensive cloning efforts. The method described here therefore provides the highest targeting efficiency with the lowest "off-target" mutation rates possible, while removing the labor-intensive efforts associated with screening thousands of clones. In sum, this chapter describes how seamless gene editing may be utilized to examine stem cell heterogeneity of epigenetic marks, but is also widely applicable for performing precise genetic manipulations in numerous other cell types.

Keywords: Heterogeneity, Pluripotent stem cells, CRISPR, TALEN, piggyBac, MLL2, CDK2

1 Introduction

Several tools and methodologies have been developed for creating site-specific genetic modifications to cells in culture or in vivo. These include Zinc Finger Nucleases (ZFNs), Transcription Activator-Like Effector Nucleases (TALENs), and Clustered Regularly Interspaced Short Palindromic Repeats (CRISPR)/Cas9 [1]. By using these nucleases with a donor template, homology directed repair (HDR) may occur, facilitating the ability to create knock-in mutations. Creating single point mutations, however, is more

challenging, but may be accomplished through the use of single-stranded oligo-deoxynucleotides (ssODN) as the donor, or through the subsequent removal of a donor plasmid. To use the ssODN approach, the nuclease and guide RNA vectors, along with the ssODN is co-transfected into cells, such that the ssODN serves as the donor to facilitate HDR. Mutations in the PAM sequence on the ssODN donor are needed to prevent the recutting from Cas9 [2], which therefore leaves behind unwanted mutations in the genome. Furthermore, due to the lack of selection, a few thousand clones are typically needed for screening to find a cell with the correct modification. As an alternative approach, a donor plasmid containing a drug-selectable marker may be used, which reduces the need to screen 1000s of clones, to just 100–200 clones. The selection cassette may then be subsequently removed by employing Cre recombinase or piggyBac™ transposase. Like the ssODN approach, utilizing a Cre/loxP system following HDR, will leave behind unwanted DNA sequences in the genome, which may be detrimental to the future studies. Importantly, unlike all other approaches, the use of a piggyBac™ transposase following HDR leaves a genetic modification that is seamless, and therefore completely free from any additional genetic modifications. To prevent the reincorporation of the donor cassette randomly into the genome following its removal, an excision-only piggyBac™ transposase (PBx) may be utilized [3]. This "donor-excision" approach with PBx therefore provides the most robust, efficient, and precise genetic modification strategy available.

One of the major pitfalls with the CRISPR technology is the high likelihood of "off-target" mutations [4]. Dimeric CRISPR RNA-guided nucleases (RFNs, marketed as NextGEN™ CRISPRs by Transposagen) was developed as a method to overcome this weakness [5, 6]. Multiple studies that have utilized this technology have found that RFNs, compared to conventional CRISPR/Cas9, offers the ability to edit the genome with far fewer "off-target" mutations [5–7]. RFNs in combination with donor excision by PBx therefore provides the best methodology for performing genetic modifications, and is well suited for studying stem cell heterogeneity.

Multiple, overlapping layers of heterogeneity at the epigenetic, transcript and protein levels have been observed in pluripotent stem cell (PSC) populations [8]. Two underlying, and potentially inter-dependent, causes have been identified that contribute to this heterogeneity; that is, (1) the stochastic activity of signaling networks and (2) the position of a cell within the cell cycle [8]. Stochastic activity of FGF/ERK and WNT/GSK3β signaling networks, in both mouse and human PSCs, is thought to promote heterogeneity of pluripotency factors and/or differentiation factors [9–14]. Some of the factors heterogeneously expressed in PSCs include Nanog [15–18], Rex1 [19], Gata6 [15, 20], and Sox17

[20], just to name a few. Conversely, inhibition of FGF/ERK and WNT/GSK3β pathways reduce heterogeneity of developmental factors and contribute to the establishment of a naïve PSC ground-state [21].

During the cell cycle of human PSCs, developmental factors, such as GATA6 and SOX17, exhibit weak induction during G1, which rapidly subsides as the cells progress into S phase, indicating that heterogeneity of developmental factors is cell cycle-regulated [20]. Furthermore, these findings support the initial observations made by Mummery and colleagues many years ago, that stem cells initiate their differentiation from the G1 phase [22]. Additional studies have also corroborated these findings that human PSCs initiate their differentiation from the G1 phase [20, 23–25]. Why G1 serves as a "Differentiation Induction Point" has remained unclear, but this may explain why PSCs have an unusual cell cycle structure consisting of a truncated G1 and a larger percentage of cells in S phase [26]. In this scenario, S phase serves to protect the pluripotent state and prevent unwarranted differentiation. One potential explanation for the "G1-Differentiation Induction Point" model is that the epigenetic status and chromatin structure established directly following mitosis is more amenable to activation by signaling factors [8]. This therefore establishes a rationale for why epigenetic heterogeneity may exist.

Recent work has shown that 5-hydroxymethylcytosine (5hmC), an epigenetic modification associated with the demethylation of genes, is heterogeneous and cell cycle-dependent at some loci in hPSCs, including developmental genes such as GATA6 [20]. Interestingly, trimethylation of lysine-4 on histone-3 (H3K4me3) is also cell-cycle dependent at bivalent domains (those domains containing both H3K4me3 active marks and H3K27me3 repressive marks) of developmental gene promoters, but not at bivalent domains on metabolic gene promoters [27]. The cell cycle-regulation of H3K4me3 establishes cell cycle-regulated enhancer–promoter looping interactions, which controls the transcriptional activation of developmental genes such as GATA6 and SOX17. These data also indicate that chromatin architecture is dynamic and cell cycle-regulated, and therefore heterogeneous within a population of PSCs. Unlike H3K4me3, H3K27me3 appears to be stable at bivalent domains during the course of the cell cycle, indicating that the regulation of the enzymes controlling H3K4 methylation at developmental gene promoters is responsible for this epigenetic heterogeneity [27].

MLL2 (KMT2B) is considered to be the major histone methyltransferase that controls H3K4me3 at bivalent developmental genes in PSCs [28, 29], and was found to be phosphorylated by CDK2 [27]. This phosphorylation by CDK2 directly controls the ability of MLL2 to specifically bind to genes during late G1 and to modulate their transcript levels. Suppression of CDK2 or MLL2

activity with small molecule inhibitors reduced H3K4me3 levels and blocked the cell cycle-regulated expression of developmental transcripts, thereby reducing heterogeneity within stem cell cultures [27]. Overall these data indicate that heterogeneity of epigenetic marks, such as H3K4me3, are directly regulated by the cell cycle machinery. These data also suggest that preventing MLL2 phosphorylation would block cell cycle-regulated heterogeneity of developmental transcripts, and also potentially the induction of differentiation from G1 [27]. Here, we describe how this hypothesis can be examined using seamless gene editing with RFNs and PBx.

2 Materials

2.1 Cell Culture Reagents

1. mTesr1 medium, Stem Cell Technologies, #05850.
2. Matrigel, Corning, #354230.
3. Rock inhibitor (Y27632), Stem Cell Technologies, #72304.
4. Thiazovivan, LC Laboratories, #T-9753.
5. CHIR99021, LC Laboratories, #C-6556.
6. SB431542, SellectChem, #S1067.
7. PD325901, LC Laboratories, #P-9688.
8. Puromycin, Life Technologies, #A1113803.
9. Ganciclovir, Sigma, #G2536.
10. Accutase, Stem Cell Technologies, #07920.
11. Dulbeccos phosphate buffered saline (Ca++/Mg++ Free), Life Technologies, #14190-144.
12. DMEM/F-12, Life Technologies, #10565-018.
13. Sterile 5, 10, and 25 ml serological pipets, and 10, 200, and 1000 μl pipet tips.
14. Sterile 96-, 24-, 12-well, 35, 60, and 100 mm cell culture-treated plates.
15. Sterile 15 and 50 ml conical tubes and sterile 1.5 ml microcentrifuge tubes.
16. 12 × 75 mm, 5 ml polystyrene round-bottom tubes with cell-strainer caps.
17. P3 Primary Cell 4D-Nucleofector Kit, Lonza, #V4XP-3012.
18. Cyrostor CS10, Stem Cell Technologies, #07930.

2.2 Molecular Biology Reagents

1. QuickExtract DNA extraction kit, Epicentre, #QE09050.
2. PCR Purification Kit, Qiagen, #28104.
3. Gel Extraction Kit, Qiagen #28704.

4. GoTaq Polymerase, Promega, #M7102.
5. TOPO TA PCR Kit, Life Technologies, #450071.
6. Molecular Grade Agarose, VWR, #97062.
7. Ethidium Bromide, Sigma, #E1510.
8. TAE buffer for electrophoresis (50×), Fisher Scientific, #BP1332500.
9. Sterile 5, 10 and 25 ml serological pipets, and 10, 200 and 1000 μl pipet tips.
10. MLL2 donor piggyBac™ plasmid, PBx and RFNs (NextGEN™ CRISPRs) for MLL2, Transposagen Biopharmaceuticals, #FF-GEK.
11. XTN™ TALENs for MLL2, Transposagen Biopharmaceuticals, #Verified XTN™ TALEN.
12. Protein G Dynabeads, ThermoFisher Scientific, #10003D.
13. KAPA SYBR FAST qPCR master mix, KAPA Biosystems, #KK4406.
14. MaXtract High Density, Qiagen, #129056.

3 Methods

We have established a methodology for performing seamless gene editing that utilizes both positive and negative selection, which provides the most robust genetic modification system available (Fig. 1). By pairing this system with RFNs, we have devised a highly precise and efficient genetic modification strategy that can be utilized in nearly any cell type. Unlike conventional CRISPR, RFNs do not suffer from high off-target mutation rates [5, 6]. Furthermore, this system is particularly useful in iPSCs, as these cells have a low single-cell cloning efficiency and a relatively low transfection efficiency, which often makes genetic modifications more cumbersome and difficult [1, 2]. Performing genetic modifications using RFNs with donor excision by PBx is well suited for studies that examine epigenetic heterogeneity of stem cells, and here we describe how to use this system to modify a putative CDK2 phosphorylation site on MLL2. Previous work has shown that the inhibition of CDK2 with a small molecule leads to a loss of threonine phosphorylation on MLL2 in hPSCs [27]. Since CDK2 phosphorylation typically occurs at the consensus sequence, (K/R)(S/T)*PX(K/R), where the * represents a phosphorylated serine or threonine, and X represents any amino acid [30], the threonine phosphorylation sites on MLL2 can be easily predicted. The MLL2 sequence consists of 2715 amino acids, but contains only two putative threonine phosphorylation sites at T176 and T542. In the following sections we describe a method to create a T542A

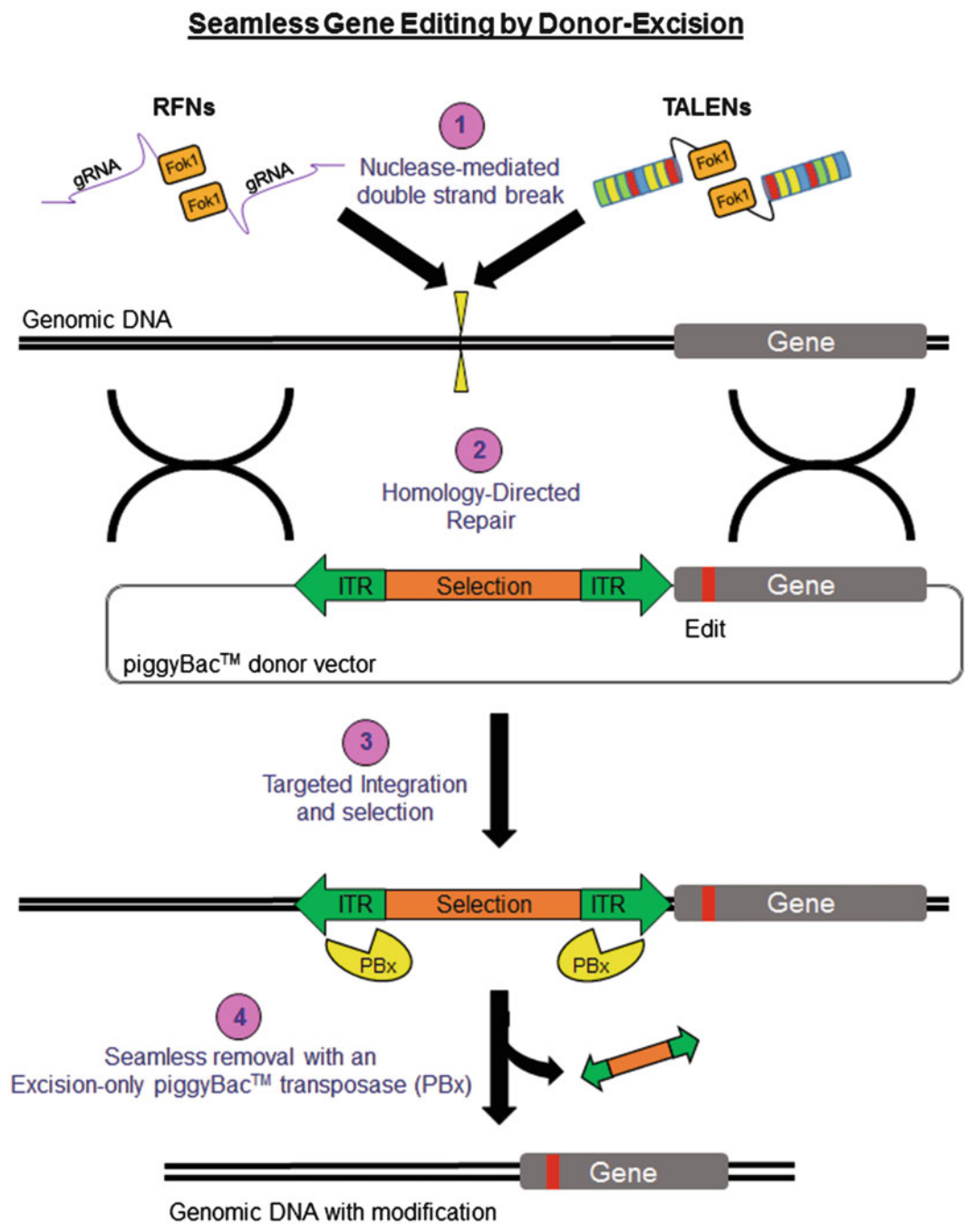

Fig. 1 Seamless gene editing using RFNs and PBx. A model depicting the steps necessary to perform precise genetic modifications using donor excision. Following the transfection of the donor piggyBac™ cassette and RFNs, cells are positively selected using puromycin to isolate those cells that have undergone homology-directed repair. Next, cells are transfected with an excision-only piggyBac™ transposase (PBx), to remove the targeting cassette. Finally, those cells that have removed the cassette are selected with ganciclovir (negative selection), leaving behind only those cells having the desired gene edit

mutation on MLL2 by seamless gene editing, which is anticipated to reduce MLL2 activity and G1-linked heterogeneity of H3K4me3 on developmental gene promoters, such as GATA6 and SOX17. We also provide a protocol to validate the reduction of MLL2 binding and H3K4me3 levels at GATA6 and SOX17 promoters in the genetically modified clone.

3.1 Design of Donor Construct, RFNs, and TALENs

1. Download the MLL2/KMT2B genomic sequence from the UCSC Genome Bioinformatics website including approximately 10 kb upstream and downstream from the T542 modification.
2. Identify a TTAA sequence within 200 bp from the modification, with the closest proximity being preferable. Since no nearby TTAA sites are present, a silent mutation may be used to enable PBx excision. For MLL2, we created a silent mutation at I540, changing the "ATC" to an "ATT," thereby establishing the TTAA sequence necessary for piggyBac™ excision (Fig. 2).
3. Design left and right homology arms of approximately 750 bp flanking the TTAA and the mutation (T542A; an ACA to GCC).
4. The donor arms can be synthesized from an external provider and cloned into the donor plasmid using conventional cloning approaches.
5. RFNs for MLL2 can be designed and purchased from an external provider (Fig. 2) (*see* **Note 1**).

3.2 Passaging, Transfection, and Selection of Targeting Constructs

1. Add fresh mTesr1 medium containing Y27632 Rock inhibitor (10 μM, final) to iPSCs to be transfected and incubate for 3 h in a 37 °C incubator with 5 % CO_2 (*see* **Note 2**).
2. Aspirate medium from cells and add 2 ml of Accutase for a 60 mm dish, incubate at 37 °C for approximately 5 min, or until cells are dislodged.
3. Triturate cell suspension using a 5 ml pipet and transfer to a 15-ml tube, containing 2 ml of DPBS, and centrifuge at 100×*g* for 4 min.
4. Resuspend cells in 2 ml of fresh medium and perform a cell count using a hemocytometer.
5. Aliquot 1 million cells for each nucleofection sample, GFP control, donor-only vector, and donor with RFNs, and centrifuge cells as above (*see* **Note 3**).
6. Resuspend cell pellet in 100 μl of Lonza P3 Buffer and add 4 μg of total DNA for each sample (the ratio gRNA plasmids to nuclease should be 5:1).

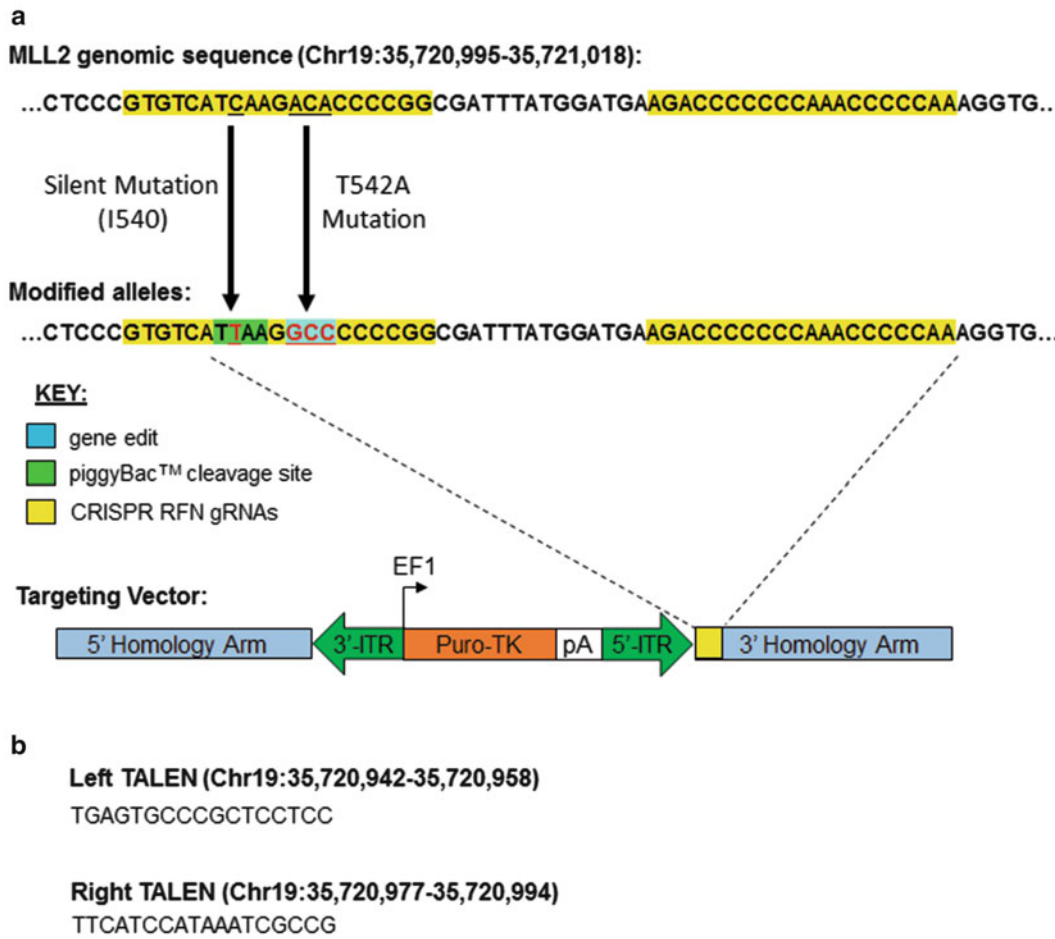

Fig. 2 Plasmid design of the MLL2 targeting vector, RFNs, and TALENs. (**a**) MLL2 genomic sequence is shown and the site to be modified, along with the sequences that may be used to generate the guide RNAs for RFNs. To facilitate the excision with PBx, a silent, single base-pair mutation is made generating a TTAA. (**b**) The sequences are shown that can be used to generate TALENs

7. Perform nucleofection using Lonza 4D-Nucleofector using program CB-150.
8. Following nucleofection, quickly transfer cells to a previously prepared Matrigel-coated 24-well plate containing medium with Rock inhibitor, (*see* **Note 4**) and return to incubator.
9. After 24 h, examine cells for viability and transfection efficiency by GFP using a fluorescent microscope.
10. On day 2, if the cells are confluent, passage the cells to a 6-well plate using Accutase as outlined above.
11. Begin puromycin selection on day 5, using a final concentration of 0.2 μg/ml (*see* **Note 5**).

12. Select the cells with puromycin for 7–10 days with daily medium changes. Passaging may be necessary if dense cell colonies appear.
13. Once numerous colonies have appeared, passage to expand cells and freeze the modified pool.
14. Collect approximately 100,000 cells and store the cell pellet in the −20 °C for subsequent targeting validation (*see* Section 3.5).

3.3 Single-Cell Cloning

1. In preparation for single-cell cloning by fluorescent activated cell sorting (FACS), passage cells using Accutase as described in Section 3.2, steps 2–4.
2. Prepare a cell suspension of 1–2 million cells per ml in a 2 ml volume, and pass through a flow cytometry tube with a cell strainer cap. Keep cells on ice.
3. Prepare 100 ml of mTesr1 medium containing the SMC4 cocktail of inhibitors, consisting of 5 μM of Thiazovivan, 1 μM of CHIR99021, 2 μM SB431542, and 0.5 μM of PD325901.
4. Aspirate medium from ten 96-well plates that have been pre-coated with MEFs and add 100 μl of mTesr1-SMC4 medium to each well.
5. Using a BD MoFlo or similar instrument, perform FACS with a 100 μm tip at 4 °C with 25 psi, and sort cells 1 cell/well into the 96-well plate. Cells should be gated on forward scatter and side scatter. Repeat this step to prepare a total of 10 96-well plates. Return plates to incubator.
6. Change medium on the 10 96-well plates daily for 7 days, include SMC4 for the first 3 days.
7. On day 7, screen each well of the 96-well plates for those that have a single colony and mark positive wells. Ideal colonies should have a typical iPSC morphology. Using this approach we typically obtain a single-cell cloning efficiency of 20 %.

3.4 Clone Consolidation, Replica Plating, and Freezing

1. To consolidate clones, aspirate medium from all wells of one 96-well plate containing clones needed to be consolidated.
2. Add 25 μl of Accutase/DPBS (50:50 mix) to those wells that have a single iPSC colony. Incubate for 5 min at 37 °C, until cells are detached.
3. Aspirate supernatant from a Matrigel-pre-coated plate, and add 100 μl of mTesr1 with Rock inhibitor to each well.
4. Once cells are dislodged, add 75 μl of fresh medium with Rock inhibitor to each well, mix by pipetting and transfer the cell suspension to a new well of the 96-well plate.
5. Centrifuge plate at 100×*g* for 4 min.

6. Gently aspirate supernatant, leaving a small volume behind so not to disturb the cell. Add 100 μl of fresh medium containing Rock inhibitor and return plate to incubator.
7. Repeat steps 1–6 as needed to consolidate all 10 96-well plates into 2–3 96-well plates.
8. Incubate and change medium daily until colonies of sufficient size have developed (approximately 5–7 days).
9. To begin replica plating and freezing, prepare two Matrigel-coated 96-well plates and a 500 μl freezing plate on ice, for each plate of consolidated clones.
10. Aspirate medium from 96-well plate with clonal cell colonies. Add 25 μl of Accutase/DPBS (50:50 mix) and incubate at 37 °C for 5 min.
11. Add 125 μl of fresh medium with Rock inhibitor to each well using a multichannel pipet and mix gently—using a new tip for each well.
12. Aspirate Matrigel from each 96-well plate and add 100 μl of medium with Rock inhibitor to each well.
13. Using a multichannel pipet, transfer 50 μl of cells from the old 96-well plate to each of the new 96-well plates and to the freezing plate, using a new pipet tip for each well.
14. Return the two new 96-well plates to the incubator and culture for 3–5 days, changing medium daily. One plate will be used for maintenance and the other will be used for targeting validation. The plate for targeting analysis can be washed in DPBS and stored dry at −20 °C for analysis.
15. To the remaining freezing plate, add 150 μl of freezing medium (Cryostor CS10) to the freezing plates and mix gently. Label and wrap plate in Parafilm. Store plate in a Styrofoam box in a −80 °C freezer.
16. To recover frozen clones, the freezing plate can be placed in a 37 °C water bath for 1–2 min, until it is 50 % thawed. Next, 300 μl of fresh medium with Rock inhibitor can be added gently to the wells of interest. The cell suspension should then be added to a Matrigel-coated 24-well plate containing 500 μl of medium with Rock inhibitor, incubated at 37 °C and cultured until colonies appear.

3.5 Targeting Identification and Validation

1. To validate successfully targeted clones, either from cell pool prior to single-cell cloning (3.2) or consolidated plates (3.4), 5′ and 3′ junction primers should be developed that span the MLL2 donor arms. Our junction primers sequences are:

   Forward (5′arm): CGTGTCAGCTCTTCCCTGTT

   Reverse: (5′arm): GACCGATAAAACACATGCGTCA

Forward (3′arm): GCAAACCCGTTGCGAAAAAG

Reverse (3′arm): GACCACACTCACCGGC

Expected amplicon sizes are 1448 bp for the 5′-arm and 1417 bp for the 3′-arm. Additional primers can also be developed to provide further validation.

2. To determine if a clone has monoallelic or biallelic targeting, endogenous primers spanning the insertion site should be used. The absence of a band of 2.3 kb, but present at 6.8 kb denotes biallelic targeting, while the presence of a bands at 2.3 kb and 6.8 kb is indicative of monoallelic targeting. The endogenous primer sequences are F-GTTGCCGAATGTGTTCTGTGT; R-GAAAGGCAGGTTCTGAGGGT.
3. To isolate genomic DNA, use the QuickExtract DNA Extraction Kit. Begin by adding 100 μl to each well of the 96-well plate, previously stored at −20 °C.
4. Briefly vortex plate for 10–15 s and incubate for 6 min at 65 °C.
5. Briefly vortex plate for 10–15 s and incubate for 2 min at 98 °C. Samples may be stored at −20 °C, until you are ready to proceed with PCR.
6. Prepare PCR reactions as follows in 96-well plate format.

   2 μl of genomic DNA sample (from step 4 above).

   12.5 μl GoTaq Mix.

   2.5 μl each Forward primer (10 μM stock).

   2.5 μl each Reverse primer (10 μM stock).

   2.5 μl molecular grade water.
7. Perform PCR using the following program:

   Step 1: 95 °C, 2 min.

   Step 2: 95 C, 30 s.

   Step 3: 55 C, 30 s.

   Step 4: 72 C, 1 min.

   Step 5: Repeat steps 2–4, 34 times.

   Step 5: 72 C, 5 min.
8. Analyze PCR products by performing gel electrophoresis with 5 μl of sample, using a 1 % ethidium bromide stained agarose gel and visualize by UV light.
9. PCR products should be excised from the gel with a scalpel, and DNA should be extracted using the Qiagen Gel Extraction Kit. Any remaining PCR products can be purified using the Qiagen PCR Purification kit and stored in −20 °C.
10. PCR products should be cloned into a TOPO TA Vector (Life Technologies) and transformed in *E. coli* (DH5a or similar).

11. Following TOPO cloning of PCR products, sequencing should be performed to confirm that the cells have the correct modification of interest. These results can then be used to identify correctly modified clones.

3.6 Excision of Targeting Construct

1. To excise the targeting construct from the identified clones and leaving behind only the mutation in MLL2, a transfection with an excision-only piggyBac™ transposase (PBx) should be performed. Follow steps 1–10, Section 3.2, using 4 μg of PBx plasmid.
2. After 2 days following transfection, begin ganciclovir treatment to select for those cells that have excised the donor construct using 5 μg/ml ganciclovir (*see* **Note 6**). Maintain under ganciclovir treatment for 1–2 weeks with daily medium changes (*see* **Note 7**).
3. Confirm the excision of the donor plasmid by performing PCR as described in Section 3.5, using primers that span the edited bases.

3.7 Validation of MLL2 Binding Deficiency and Reduced H3K4me3 by Chromatin Immunoprecipitation-Quantitative PCR (ChIP-qPCR)

1. Expand hPSCs from the MLL2-modified line and parental cell line by culturing in 100 mm Matrigel-coated plates.
2. Passage and count cells as described in Section 3.2, and centrifuge ten million cells of each PSC population.
3. Gently resuspend cell pellet in 1 ml of freshly prepared 1 % methanol-free formaldehyde, and incubate on a rotary shaker for 5 min at room temperature.
4. Add 50 μl of 2.5 M glycine to the cell suspension, mix gently, and place on rotary shaker for 5 min at room temperature.
5. Add 10 ml of DPBS to the cell suspension, mix gently, and pellet cells by centrifugation.
6. Aspirate supernatant. Cells may be flash-frozen in liquid nitrogen and stored at −80 °C.
7. Prepare magnetic beads for ChIP assay. Aliquot 200 μl of Protein G-DynaBeads into three 1.5 ml tubes, and add 1 ml of blocking solution (0.05 % BSA in DPBS), invert, place on magnetic tube rack and aspirate supernatant. Repeat this process two more times. Add 100 μl of blocking solution to the beads, and add 20 μg of MLL2 antibody to the first tube, 20 μg of H3K4me3 to the second tube, and 20 μg of IgG control antibody to the third tube. Incubate overnight at 4 °C on a tube rotator. Following incubation, wash 3× in 1 ml of blocking solution and resuspend magnetic beads in 100 μl of blocking solution. Keep on ice.
8. Thaw cell pellets for both cell lines on ice and add 1 ml of cold lysis buffer 1 (50 mM Hepes–KOH, pH 7.5, 140 mM NaCl,

1 mM EDTA, 10 % glycerol, 0.5 % NP-40, 0.25 % Triton X-100 with 1× protease inhibitors), and resuspend cell pellet. Incubate at 4 °C on a tube rotator for 10 min. Pellet cells by centrifugation at 1350 × *g* for 5 min at 4 °C and aspirate supernatant.

9. Add 1 ml of room temperature lysis buffer 2 (10 mM Tris–HCl, pH 8.0, 200 mM NaCl, 1 mM EDTA, pH 8.0, 0.5 mM EGTA, pH 8.0 with 1× protease inhibitors) and resuspend cell pellet. Incubate at room temperature for 10 min on a tube rotator. Pellet nuclei by centrifugation at 1350 × *g* for 5 min at 4 °C and aspirate supernatant.
10. Add 1 ml of cold lysis buffer 3 (10 mM Tris–HCl, pH 8.0, 100 mM NaCl, 1 mM EDTA, pH 8.0, 0.5 mM EGTA, pH 8.0, 0.1 % sodium deoxycholate, 0.5 % N-lauroylsarcosine, with 1× protease inhibitors) to nuclei on ice, and gently resuspend pellet.
11. Perform sonication of each sample using a Covaris S2 Sonicator for 8 min (peak power 140, cycle/burst 200, duty factor 5) at 4 °C (*see* **Note 8**), and transfer to a new 1.5 ml tube.
12. Add 100 µl of 10 % Triton X-100 in water to the sonicated cell suspensions, mix by inversion, and centrifuge at 13,000 × *g* for 10 min at 4 °C.
13. Transfer supernatant to a fresh tube and remove 50 µl as the Input for each sample, store at 4 °C.
14. Aliquot the remaining sample for each condition into 3 tubes (~300 µl) labeled as IgG, H3K4me3, and MLL2.
15. Add 50 µl of the appropriate antibody–bead mixture to each tube and place on tube rotator at 4 °C for overnight incubation.
16. Wash cells 3× in 1 ml of ice-cold RIPA buffer (50 mM Hepes–KOH, pH 7.6, 500 mM LiCl, 1 mM EDTA, pH 8.0, 1 % NP40, 0.7 % sodium deoxycholate) on magnetic tube rack.
17. Wash cells 1× in 1 ml of ice-cold TE buffer (10 mM Tris–HCl, 1 mM EDTA, pH 8.0) with 50 mM NaCl.
18. Pellet beads by centrifugation 950 × *g* for 3 min at 4 °C, and using a 20 µl pipet tip carefully remove any residual buffer.
19. Add 210 µl of elution buffer (50 mM Tris–HCl, pH 8.0, 10 mM EDTA, 1 % Sodium Dodecyl Sulfate).
20. Incubate at 65 °C for 15 min, mix by gentle vortexing every 3 min.
21. Centrifuge beads at 16,000 × *g* for 1 min and transfer supernatant to a new tube for each sample, and incubate at 65 °C overnight.

22. Add 150 μl of elution buffer to the Input sample and incubate at 65 °C overnight.
23. Add 200 μl of TE to each sample, along with 4 μl of 20 mg/ml RNAse A, and incubate at 37 °C for 2 h.
24. Add 7 μl $CaCl_2$ stock solution (300 mM $CaCl_2$, 10 mM Tris–HCl, pH 8.0), along with 4 μl of 20 mg/ml proteinase K, and incubate at 55 °C for 30 min.
25. Add 400 μl of phenol–chloroform–isoamyl alcohol to each sample, mix by vortexing, and transfer to a pre-spun MaXtract High Density 2.0 ml tube (Qiagen).
26. Centrifuge at 16,000 × *g* for 5 min at room temperature and collect the aqueous supernatant.
27. Precipitate the DNA by adding 16 μl of 500 mM NaCl, 6 μl of 5 mg/ml glycogen, and 880 μl of Ethanol.
28. Mix by inversion and incubate overnight at −80 °C.
29. Centrifuge at 20,000 × *g* for 10 min at 4 °C, and carefully aspirate supernatant.
30. Add 500 μl of 70 % ethanol, gently vortex to resuspend DNA pellets, centrifuge and aspirate again.
31. Allow DNA pellets to dry for 10 min at room temperature (with the lid open), and then add 100 μl of molecular grade water.
32. Analyze 2 μl of Input samples on an Agilent Bioanalyzer or similar device, to confirm that the peak of sonicated DNA samples is within the 200–500 bp size range.
33. Perform qPCR of ChIP DNA samples by adding 2 μl of DNA sample, to 5 μl of SYBR Fast qPCR master mix (KAPA Biosystems), 1 μl of Forward and Reverse primers each (10 μM stock), 0.2 μl ROX (High or Low depending on your Real-Time PCR instrument), and 0.8 μl molecular grade water for each sample. Prepare reactions in technical triplicate.
34. Target genes for examining heterogeneity may include genes such as GATA6 and SOX17. See Singh et al. for primer sequences [27].
35. Perform qPCR on a ViiA™ Real-Time PCR instrument or similar device, and calculate results based on percentage of Input. First adjust input to reflect amount of sample used for immunoprecipitation (50 μl Input, 350 μl IP, a 1/7 dilution). Log base 2 of 7=2.8. CT INPUT–2.8=Adjusted INPUT CT value. Next, calculate the average of the Adjusted INPUT CT values from the technical triplicate. Finally, calculate the percentage of Input for each sample, 100*2^(CT Adjusted INPUT – CT of the sample). An average and standard deviation may also be calculated.

4 Notes

1. As an alternative approach to using RFNs, TALENs may be utilized (Fig. 2). Like the RFN platform, TALENs also offer significantly reduced off-target efficiency compared to traditional CRISPR technologies. Furthermore, the development of additional reagents facilitates targeting to different genomic sequences, therefore providing increased "design density" and likelihood of success.
2. Prior to performing transfections, cells should be passaged as single cells 2–3 times, using Accutase with medium containing Rock inhibitor. This transition is imperative for sufficient survival for nucleofection of single cells.
3. Prior to performing Nucleofection, an optimization should be performed comparing transfection efficiencies with different programs, along with a comparison to lipofection. We have found that different iPSC lines may have different transfection efficiencies, and in some cases lipofection can out-perform nucleofection.
4. Matrigel aliquots should be prepared on ice, and diluted in cold DMEM/F-12 medium. Aliquots should be stored at −20 °C. A final dilution of 1:200 should be used for coating plates, and incubated at 37 °C for at least 30 min. Matrigel-coated plates may be used for up to 1–2 weeks, unless they have dried out.
5. A kill curve for puromycin should be performed prior to transfections. The ranges to test should be untreated, 0.05, 0.1, 0.25, 0.5, and 1.0 μg/ml. Both the number of live cells and cell viability (% of live to dead cells) should be calculated. We typically find that selection of PSCs to be in the range of 0.1–0.25 μg/ml.
6. Once stable cell lines are generated with the piggyBac™ donor vector, these cells should be used for a ganciclovir kill curve. The typical range of ganciclovir is 1–50 μg/ml. Due to the efficiency of PBx, it should be estimated that 60–80 % of transfected cells will die, along with un-transfected cells, from ganciclovir treatment.
7. As an optional method, a GFP reporter can be included between the homology arms of the donor plasmid, under an EF1 promoter. Upon PBx nucleofection, those cells that have excised the piggyBac™ cassette, may be isolated by FACS.
8. Prior to sonication, an optimization should be performed to determine the best sonication conditions such that the peak of DNA fragments is within 200–500 bp. We recommend changing the length of time from 6 to 12 min.

References

1. Singh AM, Adjan Steffey VV, Yeshi T, Allison DW (2015) Gene editing in human pluripotent stem cells: choosing the correct path. J Stem Cell Regen Biol 1:1–5. doi:10.15436/2741-0598.15.004
2. Hendriks WT, Jiang X, Daheron L, Cowan CA (2015) TALEN- and CRISPR/Cas9-mediated gene editing in human pluripotent stem cells using lipid-based transfection. Curr Protoc Stem Cell Biol 34:5B.3.1–5B.3.25. doi:10.1002/9780470151808.sc05b03s34
3. Li X, Burnight ER, Cooney AL et al (2013) piggyBac transposase tools for genome engineering. Proc Natl Acad Sci U S A 110:E2279–E2287. doi:10.1073/pnas.1305987110
4. Koo T, Lee J, Kim JS (2015) Measuring and reducing off-target activities of programmable nucleases including CRISPR-Cas9. Mol Cell 38:475–481. doi:10.14348/molcells.2015.0103
5. Guilinger JP, Thompson DB, Liu DR (2014) Fusion of catalytically inactive Cas9 to FokI nuclease improves the specificity of genome modification. Nat Biotechnol 32:577–582. doi:10.1038/nbt.2909
6. Tsai SQ, Wyvekens N, Khayter C et al (2014) Dimeric CRISPR RNA-guided FokI nucleases for highly specific genome editing. Nat Biotechnol 32:569–576. doi:10.1038/nbt.2908
7. Hara S, Tamano M, Yamashita S et al (2015) Generation of mutant mice via the CRISPR/Cas9 system using FokI-dCas9. Sci Rep 5:11221. doi:10.1038/srep11221
8. Singh AM (2015) Cell cycle-driven heterogeneity: on the road to demystifying the transitions between "poised" and "restricted" pluripotent cell states. Stem Cells Int 2015:219514. doi:10.1155/2015/219514
9. Ying Q-L, Wray J, Nichols J et al (2008) The ground state of embryonic stem cell self-renewal. Nature 453:519–523. doi:10.1038/nature06968
10. Marks H, Kalkan T, Menafra R et al (2012) The transcriptional and epigenomic foundations of ground state pluripotency. Cell 149:590–604. doi:10.1016/j.cell.2012.03.026
11. Price FD, Yin H, Jones A et al (2013) Canonical Wnt signaling induces a primitive endoderm metastable state in mouse embryonic stem cells. Stem Cells 31:752–764. doi:10.1002/stem.1321
12. Singh AM, Reynolds D, Cliff T et al (2012) Signaling network crosstalk in human pluripotent cells: a Smad2/3-regulated switch that controls the balance between self-renewal and differentiation. Cell Stem Cell 10:312–326. doi:10.1016/j.stem.2012.01.014
13. Davidson KC, Adams AM, Goodson JM et al (2012) Wnt/β-catenin signaling promotes differentiation, not self-renewal, of human embryonic stem cells and is repressed by Oct4. Proc Natl Acad Sci U S A 109:4485–4490. doi:10.1073/pnas.1118777109
14. Blauwkamp TA, Nigam S, Ardehali R et al (2012) Endogenous Wnt signalling in human embryonic stem cells generates an equilibrium of distinct lineage-specified progenitors. Nat Commun 3:1070. doi:10.1038/ncomms2064
15. Singh AM, Hamazaki T, Hankowski KE, Terada N (2007) A heterogeneous expression pattern for Nanog in embryonic stem cells. Stem Cells 25:2534–2542. doi:10.1634/stemcells.2007-0126
16. Chambers I, Silva J, Colby D et al (2007) Nanog safeguards pluripotency and mediates germline development. Nature 450:1230–1234. doi:10.1038/nature06403
17. Hatano S-Y, Tada M, Kimura H et al (2005) Pluripotential competence of cells associated with Nanog activity. Mech Dev 122:67–79. doi:10.1016/j.mod.2004.08.008
18. Kalmar T, Lim C, Hayward P et al (2009) Regulated fluctuations in nanog expression mediate cell fate decisions in embryonic stem cells. PLoS Biol 7, e1000149. doi:10.1371/journal.pbio.1000149
19. Toyooka Y, Shimosato D, Murakami K et al (2008) Identification and characterization of subpopulations in undifferentiated ES cell culture. Development 135:909–918. doi:10.1242/dev.017400
20. Singh AM, Chappell J, Trost R et al (2013) Cell-cycle control of developmentally regulated transcription factors accounts for heterogeneity in human pluripotent cells. Stem Cell Rep 1:532–544. doi:10.1016/j.stemcr.2013.10.009
21. Davidson KC, Mason EA, Pera MF (2015) The pluripotent state in mouse and human. Development 142:3090–3099. doi:10.1242/dev.116061
22. Mummery CL, van den Brink CE, de Laat SW (1987) Commitment to differentiation induced by retinoic acid in P19 embryonal carcinoma cells is cell cycle dependent. Dev Biol 121:10–19
23. Sela Y, Molotski N, Golan S et al (2012) Human embryonic stem cells exhibit increased propensity to differentiate during the G1 phase prior to phosphorylation of retinoblastoma

protein. Stem Cells 30:1097–1108. doi:10.1002/stem.1078

24. Pauklin S, Vallier L (2013) The cell-cycle state of stem cells determines cell fate propensity. Cell 155:135–147. doi:10.1016/j.cell.2013.08.031
25. Chetty S, Pagliuca FW, Honore C et al (2013) A simple tool to improve pluripotent stem cell differentiation. Nat Methods 10:553–556. doi:10.1038/nmeth.2442
26. Singh AM, Dalton S (2009) The cell cycle and Myc intersect with mechanisms that regulate pluripotency and reprogramming. Cell Stem Cell 5:141–149. doi:10.1016/j.stem.2009.07.003
27. Singh AM, Sun Y, Li L et al (2015) Cell-cycle control of bivalent epigenetic domains regulates the exit from pluripotency. Stem Cell Rep 5:323–336. doi:10.1016/j.stemcr.2015.07.005
28. Hu D, Garruss AS, Gao X et al (2013) The Mll2 branch of the COMPASS family regulates bivalent promoters in mouse embryonic stem cells. Nat Struct Mol Biol 20:1093–1097. doi:10.1038/nsmb.2653
29. Denissov S, Hofemeister H, Marks H et al (2014) Mll2 is required for H3K4 trimethylation on bivalent promoters in embryonic stem cells, whereas Mll1 is redundant. Development 141:526–537. doi:10.1242/dev.102681
30. Morgan DO (1997) Cyclin-dependent kinases: engines, clocks, and microprocessors. Annu Rev Cell Dev Biol 13:261–291. doi:10.1146/annurev.cellbio.13.1.261

Methods in Molecular Biology (2016) 1516: 171–181
DOI 10.1007/7651_2016_325

Published online: 01 April 2016

Stencil Micropatterning for Spatial Control of Human Pluripotent Stem Cell Fate Heterogeneity

Jun Yuan*, Geetika Sahni*, and Yi-Chin Toh

Abstract

Human pluripotent stem cells (hPSCs) have the intrinsic ability to differentiate and self-organize into distinct tissue patterns, although this requires the presentation of spatial environmental cues, i.e., biochemical and mechanical gradients. Cell micropatterning technologies potentially offer the means to spatially control stem cell microenvironments and organize the resultant differentiation fates. Here, we describe stencil micropatterning as a simple and robust method to generate hPSC micropatterns for controlling hPSC differentiation patterns. hPSC micropatterns are specified by the geometries of the cell stencil through-holes, which physically confine the locations where the underlying extracellular matrix and hPSCs can access and attach to the substrate. This confers the unique capability of stencil micropatterning to work with a variety of culture substrates and extracellular matrices for optimal hPSC culture. We present the detailed steps of stencil micropatterning to successfully generate hPSC micropatterns, which can be used to investigate how spatial polarization of cell adhesion results in cell fate heterogeneity.

Keywords: Human pluripotent stem cells, Cell micropatterning, Stencil, Differentiation fate, Spatial organization, Tissue patterning, Embryonic development

1 Introduction

Human pluripotent stem cells (hPSCs), including embryonic stem cells (hESCs) and induced pluripotent stem cells (hiPSCs), are widely exploited in regenerative medicine as well as experimental modeling of normal and diseased organogenesis because of their differentiation potential into cell lineages of all three germ layers [1, 2]. The differentiation fates of hPSCs are highly sensitive to local environmental factors that can modulate autocrine or paracrine signalings [1] as well as mechanotransduction processes [3–5]. Cell micropatterning encompasses a set of techniques that have been developed to spatially organize the geometry and location of a cell population in order to control the local cellular microenvironment, such as cell–cell interactions [6] and cell–matrix interactions [3]. In the context of hPSCs, cell micropatterning has been

*Author contributed equally with all other contributors

employed to gain significant insights into how niche-dependent autocrine signaling modulates hESC pluripotency-differentiation decisions [7] and organization into early embryonic differentiation patterns [6]. 2D and 3D micropatterned hPSCs have been used to control the colony size, which in turn influenced differentiation decisions into the three germ layers [8, 9]. We have employed hPSC micropatterns to modulate the extent of cell–cell and cell–matrix interactions within a hPSC colony to probe how crosstalk between integrin and E-cadherin-mediated adhesions can give rise to cell fate heterogeneity [10]. The demonstrations from the above reports open new avenues towards the application of micropatterned hPSCs as experimental models for drug toxicity screening for developmental diseases [11], to study the effect of growth factors and hormones during tissue or organ development, and to unravel the formation of tissue patterns.

A myriad of cell micropatterning techniques have been developed as reviewed by Falconnet et al. [12] but only a handful, such as micro-contact printing [7, 8, 13], microwell culture [14, 15], and photopatterning [6] have been successfully implemented with hPSCs. The challenge with micropatterning hPSCs lies in their vulnerability and a stringent requirement of specific extracellular matrices (ECM) and growth conditions for cell attachment and survival. For 2D hPSC patterns, micro-contact printing is one of the most common methods to generate hPSC micropatterns on tissue culture and glass substrates [13]. The method can be used to pattern Laminin and Matrigel®, although it typically requires a two-step coating process aided by poly-D-lysine, and needs specific inert atmospheric and humidity conditions to make stable ECM micropatterns for hPSCs to attach on [6, 13]. The foremost consideration of every micropatterning method is whether the surface modification regime can generate hPSC-adhesive ECM patterns at the desired geometrical resolution while minimizing unspecific cell attachment to the surrounding areas.

Here, we report the use of stencil micropatterning as a robust method to generate hPSC micropatterns without additional surface

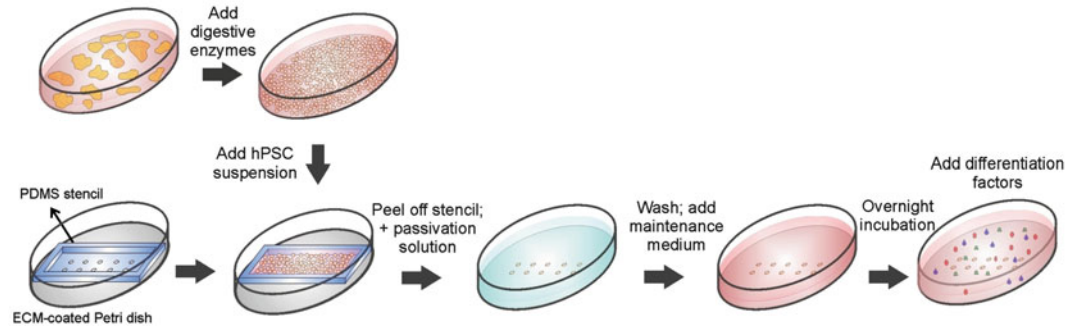

Fig. 1 Schematic representation of the workflow to micropattern hPSC colonies and induce differentiation

modification prior to ECM coating (Fig. 1). The cell stencil comprises of a thin membrane, e.g., polydimethylsiloxane (PDMS) sheet, with micron to millimeter size through-holes sealed onto a cell culture substrate to physically contain ECM coatings and subsequently seeded hPSCs. As stencil patterning works by physically restraining the location where hPSCs can access and attach directly to the underlying ECM coated substrate, this method is compatible with various substrates that can support hPSC cultures. The only requirement is that the choice of stencil material can form a reversible seal with the substrate. These substrates include conventional tissue culture polystyrene (TCPS) [16], ligand conjugated substrates [17], as well as elastomeric substrates with tunable stiffness (e.g., PDMS) [18]. This method also allows coating of different ECM, such as Vitronectin, Laminin, and Matrigel® to allow for proper attachment and differentiation of hPSCs. Therefore, as compared to other cell micropatterning techniques, stencil patterning confers the unique capability to adopt optimized ECM–substrate configurations for a specific hPSC line to ensure optimal cell–matrix adhesion, survival and differentiation.

2 Materials

2.1 PDMS Stencils

1. Polydimethylsiloxane (PDMS) sheets: 120–150 μm and 2 mm thick.
2. CO_2 laser cutter.
3. Uncured Sylgard® 184 PDMS: Weigh out 10:1 of PDMS prepolymer and curing agent and mix thoroughly by stirring. Degas in a vacuum chamber for 30 min to remove bubbles. Use the uncured PDMS within 1 h after preparation before it polymerizes.

2.2 Matrigel® Coating on Stenciled Substrate

1. 70 % analytical grade ethanol.
2. Oxygen plasma system.
3. Dulbecco's Modified Eagle Medium: Nutrient Mixture F-12 (DMEM/F12).
4. 1.5× hESC qualified Matrigel® solution: Prepare aliquots of hESC-qualified Matrigel® according to the Certificate of Analysis and store at −20 °C. Ensure that each aliquot yields 1× hESC-qualified Matrigel® solution when diluted in 25 mL of DMEM/F12 according to manufacturer's product sheet. Add one aliquot of Matrigel® into 16.7 mL of DMEM/F12 to make 1.5× Matrigel® solution. Keep all the 1.5× Matrigel® solution on ice to prevent gelation (*see* **Note 1**).

2.3 Cell Harvesting and Seeding Onto Stenciled Substrate

1. Accutase™ solution.
2. hPSC maintenance medium for feeder free hPSC cultures (e.g., mTeSR1).
3. 5 mM stock Y27632 (ROCK inhibitor) solution: Reconstitute 1 mg of ROCK inhibitor (ROCKi) in 591 μL of sterile ultrapure water, aliquot into 50 μL per tube and store in the dark at −20 °C (*see* **Note 2**).
4. hPSC maintenance medium supplemented with 10 μm ROCKi: Dilute 2 μL stock ROCKi solution per mL of hESC maintenance medium. Prepare fresh solution for each patterning experiment.

2.4 Passivation of Stenciled Substrate

1. Passivation solution: 0.5 % Poloxamer 407 (Pluronic F127) in DMEM/F12. Weigh out 5 g of Pluronic F127 powder and dissolve into 100 mL of ultrapure water to prepare the 5 % Pluronic F127 stock solution. Sterilize the 5 % Pluronic F127 solution using a 0.2 μm syringe filter. Store at room temperature. For subsequent use, prepare fresh 0.5 % Pluronic F127 in DMEM/F12 by diluting 5 % Pluronic F127 stock solution.

3 Methods

3.1 Design and Fabrication of PDMS Stencils

1. Design the stenciling sheet with through-holes of the desired geometry and size (e.g., 1000 μm circles) and the stencil gasket using computer-aided design software [10].
2. Laser-cut the stenciling sheet and gasket on 120–150 μm and 2 mm thick PDMS sheets respectively using a CO_2 laser-cutter [10] (*see* **Note 3**).
3. Bond the PDMS gasket with the PDMS stenciling sheet using liquid uncured PDMS and bake at 60 °C for 3–4 h to assemble the PDMS stencil (*see* **Note 4**).
4. Trim off the excessive part of the PDMS stenciling sheet to obtain the final PDMS stencil for micropatterning (Fig. 2).
5. Sterilize the PDMS stencil by autoclaving at 120 °C for 30 min and drying in an oven before use (*see* **Note 5**).

3.2 ECM Coating on Stenciled Substrate

1. Seal a PDMS stencil onto a selected culture substrate (e.g., 60 mm Petri dish) by dispensing a small amount of 70 % analytical grade ethanol in ultrapure water sufficient to wet the surface of the culture substrate, and placing the stencil on top.
2. Place the culture substrate and the stencil inside a biosafety cabinet overnight to allow the ethanol to evaporate completely.
3. Check that the stencil forms a good seal with the culture substrate to prevent leakages of ECM coating solution

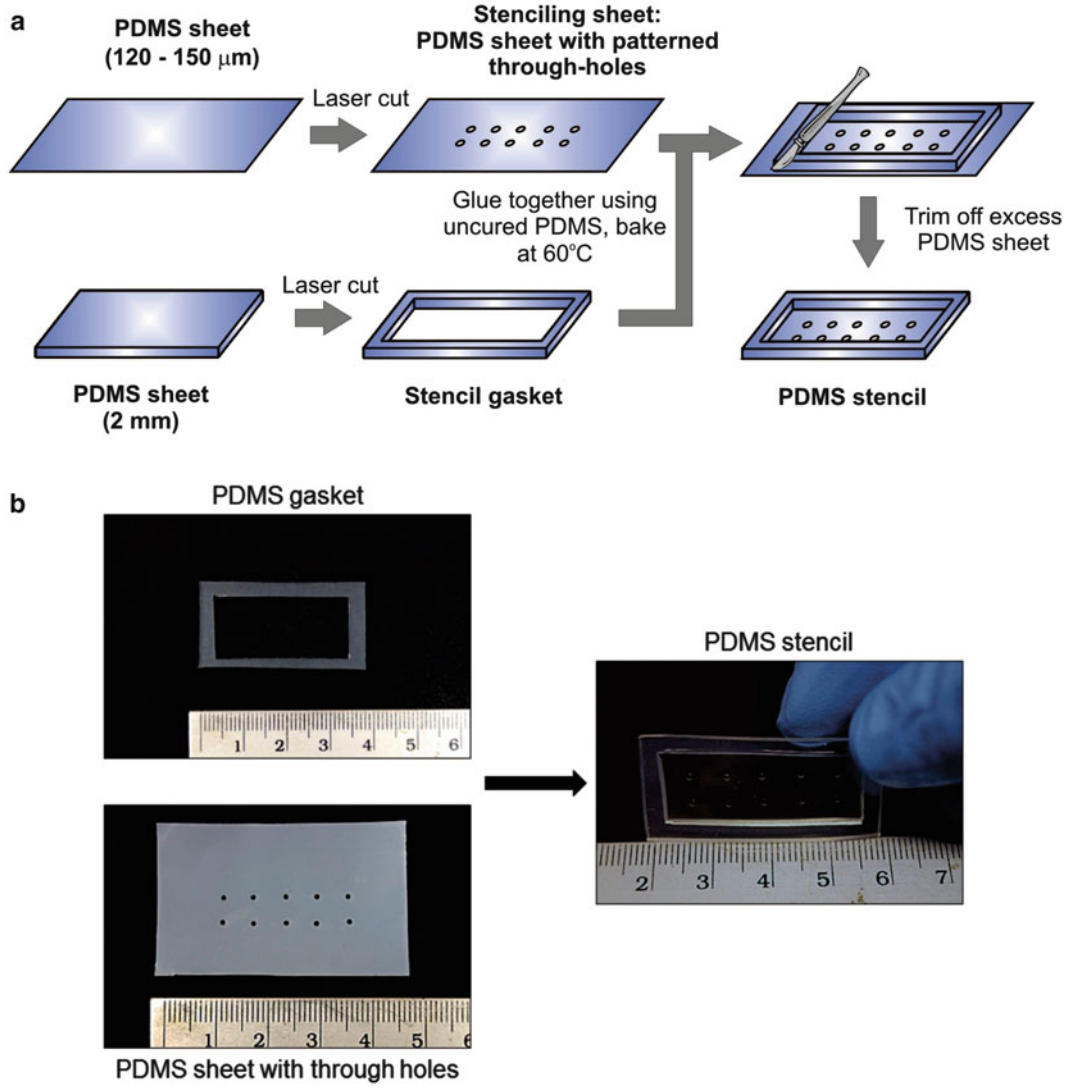

Fig. 2 Generation of PDMS stencil for micropatterning. (**a**) Schematic representing the critical steps in stencil fabrication. A 127 μm thick PDMS sheet was laser-cut to produce the designed patterns, and another 2 mm thick PDMS sheet was laser-cut to produce the gasket. These two components were bonded together with uncured PDMS to assemble the stencil. (**b**) Images showing assembly of the components to form a PDMS stencil with 1 mm circular through-holes

(*see* **Note 6**). Store the stenciled substrate under sterile conditions until it is ready for ECM coating and cell seeding.

4. Prior to ECM coating, treat the stenciled substrate with 100 W O_2 plasma for 90 s. This facilitates surface wetting and prevents air bubble formation in the micropattern through-holes upon the addition of ECM coating solution. To ensure sterility, only expose the stenciled substrate inside the plasma chamber prior to plasma treatment, and quickly transfer into a sterile container after completion of the plasma treatment.

5. Add a suitable volume of 1.5× hESC-qualified Matrigel® solution to cover the whole stencil. Seal the stenciled substrate in an airtight container to prevent the ECM solution from drying out, and incubate for 5 h at 37 °C before use.

3.3 Cell Seeding onto Stenciled Substrate

1. Examine hPSC colonies grown under feeder free conditions and remove differentiated regions using a vacuum aspirator (*see* **Note 7**).
2. Wash twice with 2 mL DMEM/F12 per well of 6-well plate.
3. Add 1 mL of Accutase™ per well of 6-well plate and incubate at 37 °C for 8 min (*see* **Note 8**). Tap the plate gently to detach all colonies from substrate.
4. Rinse each well with at least 4 mL of DMEM/F12 per 1 mL of Accutase™ and collect the cell suspension into a 15 mL conical tube.
5. Centrifuge the cell suspension at 200 × *g* for 3 min at room temperature.
6. Aspirate to remove the supernatant and add 400 μL of hPSC maintenance medium supplemented with ROCKi to resuspend the cells (*see* **Note 9**). Pipette the cell suspension up and down three times gently to break clumps into single cells.
7. Mix the single cell suspension well and dilute 10 μL of cell samples into 190 μL of DMEM/F12 (1:20 dilution). Use a hemocytometer to determine the cell density in the stock cell suspension.
8. Calculate the required cell seeding density for a given stencil (*see* **Note 10**). We have experimentally determined the cell seeding density required to obtain a confluent monolayer of single hESCs is approximately 4444 cells/mm^2. Thus, a stencil with an area of 450 mm^2 and seeding volume of 400 μL will require a cell suspension to be at a density of two million cells/400 μL.
9. Dilute the stock cell suspension to the required seeding density (*see* **step 8**) with hPSC maintenance medium supplemented with ROCKi.
10. Add a designated volume of cell suspension containing the required number of cells into each stencil and leave the culture substrate undisturbed in a biosafety cabinet for 5 min at room temperature to allow cells to settle (*see* **Note 11**).
11. Transfer the culture substrate into incubator and incubate for 1 h to allow for cell attachment. Take care to keep the substrate level during the transfer process so that cells remain as a monolayer on the stenciled substrate (*see* **Note 11**).

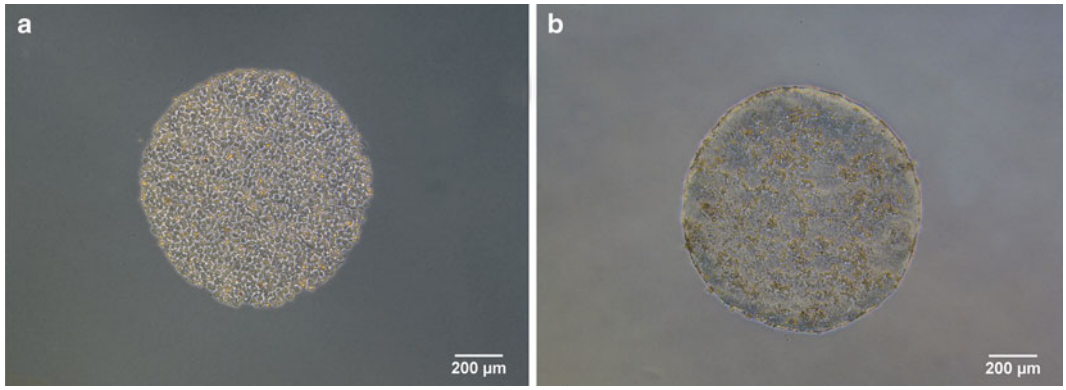

Fig. 3 Micropatterned H9 hESC colonies (1000 μm *circles*) on Matrigel® coated tissue culture polystyrene (TCPS) substrate. Microscopic images of hESC micropattern colony (**a**) immediately after the removal of PDMS stencils, and (**b**) after overnight incubation prior to the addition of differentiation medium

3.4 Stencil Removal and Passivation of Unpatterned Substrate

1. Examine the stenciled substrate under a microscope to check if cells are properly attached onto the underlying substrate.
2. Aspirate away cell suspension from the stencil.
3. Add sufficient volume of passivation solution to the area surrounding the stencil so that the passivation solution can cover the entire culture substrate (e.g., 2 mL/60 mm Petri dish).
4. Use a pair of autoclaved forceps to gently peel off the stencil (*see* **Note 12**). Swirl the passivation solution around as the stencil is peeled off to prevent the cells from drying out.
5. Incubate the micropatterned cells in passivation solution for 10 min at 37 °C (*see* **Note 13**).
6. Aspirate away the passivation solution. Wash three times with DMEM/F12.
7. Add appropriate volume of hPSC maintenance medium supplemented with ROCKi. Visually inspect the micropatterned cells in the culture substrate to ensure that the cell monolayer remains intact (Fig. 3a). Incubate at 37 °C overnight.
8. After overnight incubation, inspect the hPSC micropatterns again to ensure that there is no cell detachment or formation of bald spots devoid of cells (Fig. 3b). Remove the hPSC maintenance medium supplemented with ROCKi (*see* **Note 9**). Wash once with DMEM/F12 and add the desired differentiation medium.

4 Notes

1. The 1.5× hESC-qualified Matrigel® solution should be kept on ice during the coating step. Unused 1.5× hESC-qualified Matrigel® solution can be stored at 4 °C for up to 1 week for subsequent cell micropatterning experiments.

2. Use aluminum foil to cover the ROCKi tube to avoid light exposure when handling ROCKi.
3. CO_2 laser cutters are suitable for the direct fabrication of micropattern through-holes >1000 μm. The resolution of laser cutting is dependent on the spot size of the laser beam and the precision of the mechanical stage controlling the path of the laser beam. For conventional CO_2 laser cutters, we found that it can produce circular or curved features with good fidelity but not geometries with sharp corners (e.g., square). If small or sharp features are desired, the through-holes in the stenciling sheet can be fabricated by molding PDMS on a microfabricated silicon template containing reliefs of the micropatterns [19]. The challenge of the molding method is to produce micro-size through-holes in thin PDMS sheets with no residual PDMS over the silicon template reliefs. Several strategies have been developed to address this problem as described by Li et al. [19].
4. The stenciling sheet should be flat and free of dust when bonded to the gasket in order to prevent leakages from the stencil. This can be achieved by using Magic™ Tape to secure the stenciling sheet onto a clean, flat surface and using a transparency film to protect it from dust. To bond the gasket with the stenciling sheet, a thin and uniform layer of uncured PDMS can be applied on one of the gasket faces with a cotton swab before placing it onto the stenciling sheet. Excessive uncured PDMS can result in buckling of the stenciling sheet after the PDMS polymerizes, which may compromise the sealing of the stencil to the culture substrate, causing ECM and cell solution to leak from the stencil through-holes.
5. After autoclaving, the stencils should be thoroughly dried in an oven to ensure that they can form a good seal with the culture substrate.
6. Check the seal by examining for the presence of air bubbles between the stencil and the culture substrate.
7. To achieve efficient differentiation, the quality of the hPSC culture is very critical. The hPSC colonies should be harvested at 70–80 % confluence for micropatterning experiments, with the majority of colonies showing undifferentiated hPSC morphology while removing the differentiated areas. Differentiated cell areas can be identified by the loss of typical hPSC morphology, e.g., loss of rounded, tightly packed epithelial morphology, high nucleus/cytoplasm ratio with prominent nucleoli. Over-confluent hPSC cultures usually cause spontaneous differentiation, and if the differentiated areas are not removed prior to cell seeding, the differentiated cells will disrupt normal differentiation pattern formation. Typically, a 70–80 % confluent hPSC culture on a 6-well plate can yield approximately 1.5–2 million single cells.

8. When harvesting hPSC colonies as single cell suspension, the over-treatment with Accutase™ should be avoided as this often results in cell death after overnight incubation even if the cells can attach initially. Experimentally, 8 min of Accutase™ treatment is optimal for the H9 hESC line cultured in our lab, although it is recommended to optimize the treatment time separately for different cell lines.
9. When hPSCs are maintained and seeded as single cells, it is critical to add appropriate concentration of ROCKi to the maintenance medium to ensure that the hPSCs survive and can attach on the stenciled substrate. However, extended incubation with ROCKi may prevent the establishment of normal cell–cell and cell–matrix interaction, and therefore, ROCKi should be removed before the commencement of differentiation experiments.
10. The cell seeding density plays a critical role in generating a confluent monolayer of cells with defined cell–cell and cell–matrix adhesions. Cell seeding density is calculated based on the average cell size, stencil surface area and cell seeding volume, and then optimized experimentally. A low cell seeding density often results in poor patterning fidelity. Given their epithelial nature, hPSCs have a strong tendency to aggregate and grow as colonies. Therefore, when there are insufficient cells within the micropattern, the attached cells will aggregate resulting in "bald spots" within the micropattern. Conversely, an overly high cell seeding density will cause over-crowding of cells in the micropatterns. This results in multiple cell layers being formed, especially at the periphery of the micropattern.
11. After cell seeding, it is important that cells settle down and subsequently attach onto the stenciled substrate as a monolayer. This can be achieved by dispensing the cell suspension in the middle of the stencil and leaving the substrate undisturbed for 5 min in the biosafety cabinet to allow the cells to settle. The culture substrate can be checked under the microscope to visualize for the formation of a confluent cell carpet on the stencil. During the transfer of the stenciled substrate from the biosafety cabinet to the microscope and incubator, utmost care must be taken to keep the substrate level to prevent aggregation of the cells. Any shaking or stirring of the substrate should be avoided as it does not help with distributing the cells uniformly.
12. To remove the stencil after sufficient incubation, a curved forceps with blunt ends is advisable to be used to peel off the stencil from the substrate. The stencil should be peeled off in a single and gentle action to avoid any distortion of the micropatterns.

13. When passivating the area of substrate surrounding the micropatterns with 0.5 % Pluronic F127, long treatment time should be avoided due to its cytotoxic behavior. For individual hPSC lines, we recommend that the treatment time be optimized to ensure there is no cytotoxic effects on the cells.

Acknowledgements

This work is supported by NUS start-up grant (R-397-000-192-133) and ETPL Gap Fund (R-397-000-198-592). G.S. is an NUS Research scholar. The authors would like to thank Dr. Jiangwa Xing for her technical support on cell micropatterning. The authors have no competing financial interests.

References

1. Graf T, Stadtfeld M (2008) Heterogeneity of embryonic and adult stem cells. Cell Stem Cell 3(5):480–483. doi:10.1016/j.stem.2008.10.007
2. S-i N, Goldstein RA, Nierras CR (2008) The promise of human induced pluripotent stem cells for research and therapy. Nat Rev Mol Cell Biol 9(9):725–729. doi:10.1038/nrm2466
3. Guilak F, Cohen DM, Estes BT, Gimble JM, Liedtke W, Chen CS (2009) Control of stem cell fate by physical interactions with the extracellular matrix. Cell Stem Cell 5(1):17–26. doi:10.1016/j.stem.2009.06.016
4. Dalby MJ, Gadegaard N, Oreffo RO (2014) Harnessing nanotopography and integrin-matrix interactions to influence stem cell fate. Nat Mater 13(6):558–569. doi:10.1038/nmat3980
5. Joddar B, Ito Y (2013) Artificial niche substrates for embryonic and induced pluripotent stem cell cultures. J Biotechnol 168 (2):218–228. doi:10.1016/j.jbiotec.2013.04.021
6. Warmflash A, Sorre B, Etoc F, Siggia ED, Brivanlou AH (2014) A method to recapitulate early embryonic spatial patterning in human embryonic stem cells. Nat Methods 11 (8):847–854. doi:10.1038/nmeth.3016
7. Peerani R, Rao BM, Bauwens C, Yin T, Wood GA, Nagy A, Kumacheva E, Zandstra PW (2007) Niche-mediated control of human embryonic stem cell self-renewal and differentiation. EMBO J 26(22):4744–4755. doi:10.1038/sj.emboj.7601896
8. Lee LH, Peerani R, Ungrin M, Joshi C, Kumacheva E, Zandstra P (2009) Micropatterning of human embryonic stem cells dissects the mesoderm and endoderm lineages. Stem Cell Res 2 (2):155–162. doi:10.1016/j.scr.2008.11.004
9. Hwang Y-S, Chung BG, Ortmann D, Hattori N, Moeller H-C, Khademhosseini A (2009) Microwell-mediated control of embryoid body size regulates embryonic stem cell fate via differential expression of WNT5a and WNT11. Proc Natl Acad Sci 106 (40):16978–16983. doi:10.1073/pnas.0905550106
10. Toh Y-C, Xing J, Yu H (2015) Modulation of integrin and E-cadherin-mediated adhesions to spatially control heterogeneity in human pluripotent stem cell differentiation. Biomaterials 50:87–97. doi:10.1016/j.biomaterials.2015.01.019
11. Xing J, Toh YC, Xu S, Yu H (2015) A method for human teratogen detection by geometrically confined cell differentiation and migration. Sci Rep 5:10038. doi:10.1038/srep10038
12. Falconnet D, Csucs G, Grandin HM, Textor M (2006) Surface engineering approaches to micropattern surfaces for cell-based assays. Biomaterials 27(16):3044–3063. doi:10.1016/j.biomaterials.2005.12.024
13. Bauwens CL, Peerani R, Niebruegge S, Woodhouse KA, Kumacheva E, Husain M, Zandstra PW (2008) Control of human embryonic stem cell colony and aggregate size heterogeneity influences differentiation trajectories. Stem Cells 26(9):2300–2310. doi:10.1634/stemcells.2008-0183
14. Khademhosseini A, Ferreira L, Blumling Iii J, Yeh J, Karp JM, Fukuda J, Langer R (2006) Co-culture of human embryonic stem cells

with murine embryonic fibroblasts on microwell-patterned substrates. Biomaterials 27(36):5968–5977. doi:10.1016/j.biomaterials.2006.06.035

15. Mohr JC, de Pablo JJ, Palecek SP (2006) 3-D microwell culture of human embryonic stem cells. Biomaterials 27(36):6032–6042. doi:10.1016/j.biomaterials.2006.07.012
16. Mei Y, Saha K, Bogatyrev SR, Yang J, Hook AL, Kalcioglu ZI, Cho SW, Mitalipova M, Pyzocha N, Rojas F, Van Vliet KJ, Davies MC, Alexander MR, Langer R, Jaenisch R, Anderson DG (2010) Combinatorial development of biomaterials for clonal growth of human pluripotent stem cells. Nat Mater 9(9):768–778. doi:10.1038/nmat2812
17. Melkoumian Z, Weber JL, Weber DM, Fadeev AG, Zhou Y, Dolley-Sonneville P, Yang J, Qiu L, Priest CA, Shogbon C, Martin AW, Nelson J, West P, Beltzer JP, Pal S, Brandenberger R (2010) Synthetic peptide-acrylate surfaces for long-term self-renewal and cardiomyocyte differentiation of human embryonic stem cells. Nat Biotechnol 28(6):606–610. doi:10.1038/nbt.1629
18. Evans ND, Minelli C, Gentleman E, LaPointe V, Patankar SN, Kallivretaki M, Chen X, Roberts CJ, Stevens MM (2009) Substrate stiffness affects early differentiation events in embryonic stem cells. Eur Cell Mater 18(1e13d):13e14
19. Li W, Xu Z, Huang J, Lin X, Luo R, Chen CH, Shi P (2014) NeuroArray: a universal interface for patterning and interrogating neural circuitry with single cell resolution. Sci Rep 4:4784. doi:10.1038/srep04784

Methods in Molecular Biology (2016) 1516: 183–193
DOI 10.1007/7651_2016_349

Published online: 07 April 2016

Visualizing the Functional Heterogeneity of Muscle Stem Cells

Yasuo Kitajima, Shizuka Ogawa, and Yusuke Ono

Abstract

Skeletal muscle stem cells are satellite cells that play crucial roles in tissue repair and regeneration after muscle injury. Accumulating evidence indicates that satellite cells are genetically and functionally heterogeneous, even within the same muscle. A small population of satellite cells possesses "stemness" and exhibits the remarkable ability to regenerate through robust self-renewal when transplanted into a regenerating muscle niche. In contrast, not all satellite cells self-renew. For example, some cells are committed myogenic progenitors that immediately undergo myogenic differentiation with minimal cell division after activation. Recent studies illuminate the cellular and molecular characteristics of the functional heterogeneity among satellite cells. To evaluate heterogeneity and stem cell dynamics, here we describe methods to conduct a clonal analysis of satellite cells and to visualize a slowly dividing cell population.

Keywords: Muscle stem cells, Satellite cells, Functional heterogeneity, Slow-dividing cells, Clonal analysis, Single cell analysis

1 Introduction

Experiments conducted to understand stem cell biology typically acquire data that represent the average of an entire cell population. Indeed, the dynamics and functions of minor cell populations may be masked by the major cell population [1]. Single-cell analysis precisely characterizes a functionally heterogeneous population of stem cells.

Muscle stem cells, called satellite cells, which are located between the basal lamina and sarcolemma of myofibers [2], play important roles in muscle growth, hypertrophy repair, and regeneration in adults. Satellite cells, which are mitotically quiescent in healthy adult muscle, express the paired-box transcription factor Pax7. Satellite cells are swiftly activated in response to stimuli such as muscle injury to become myoblasts that express the myogenic regulatory factor MyoD and then extensively proliferate. The majority of satellite cells downregulate Pax7 expression, maintain MyoD levels, and undergo myogenic differentiation to produce new myonuclei. In contrast, other satellite cells maintain Pax7

levels, downregulate MyoD expression, return to a quiescent state, and then self-renew to replenish the stem cell pool [3, 4].

Accumulating evidence suggests that satellite cells are functionally heterogeneous [5–13]. Individual analysis of cloned satellite cells is required to determine if all satellite cells possess stem cell functions. Our previous clonal analysis demonstrates that proliferative ability varies widely among satellite cell clones isolated from the same myofiber of the mouse extensor digitorum longus (EDL) muscle [9]. Importantly, analysis of individual clones reveals a positive correlation between the number of self-renewing $Pax7^{+ve}$-$MyoD^{-ve}$ cells and colony size, indicating that some cells possess "stemness" such as the remarkable ability to expand the cell population that is associated with an enhanced ability to self-renew. In contrast, approximately 20 % of the satellite cells in the EDL muscle completely committed to myogenic differentiation after several days in vitro, revealing that some cells are a non-stem cell population that does not self-renew and only generates myonuclei [9].

Subpopulations of satellite cells proliferate slowly and exhibit stem cell phenotypes [5, 8, 14]. The relationship between the cell cycle and functional heterogeneity of cultured satellite cells was studied using the fluorescent lipophilic dye PKH26 [14]. The results of this study show that the vast majority of satellite cells are low PKH26-retaining ($PKH26^{low}$) "fast-dividing" cells. Importantly, high PKH26-retaining ($PKH26^{high}$) "slow-dividing" cell - derived self-renewed cells efficiently form secondary myogenic colonies after passage, while the $PKH26^{low}$ fast-dividing cell-derived self-renewed cells rapidly commit to myogenic differentiation after a few cycles of cell division. Consequently, the slow-dividing cell population retains long-term self-renewal ability, and the fast-dividing cell population is depleted after several passages in vitro. Thus, slow-dividing cells represent a minority population that may retain stem cell-like properties [8, 14].

In this chapter, we describe methods for performing a clonal analysis of satellite cells and for visualizing a slow-dividing cell population to evaluate heterogeneity and stem cell dynamics.

2 Materials

2.1 Myofiber Isolation and Cell Culture

1. Dulbecco's modified Eagle's medium (DMEM), high glucose, GlutaMAX™, Pyruvate (Gibco, Cat No 10569).
2. Penicillin and streptomycin solution (× 100) (Wako, Cat No 168-23191).
3. Collagenase type I (Worthington, Cat No 4197).
4. Bovine serum albumin (BSA) (Sigma, Cat No A9418).
5. Matrigel, growth factor reduced (Corning, Cat No 354230).

6. Trypsin–EDTA solution 0.25 % (Sigma, Cat No T4049).
7. Chick embryo extract, Ultrafiltrate (CEE), 20 ml (US Biological, Cat No C3999).
8. Fetal bovine serum (FBS) (Gibco, Cat No 10437-028).
9. Microfuge tubes, 1.5 ml (BD, Cat No AM12400).
10. Centrifuge tubes with skirt, 25 ml (IWAKI, Cat No 2362-025).
11. Culture plates: 96-well plate (Nunc, Cat No167008), 6-well plate (Nunc, Cat No 164008) and 384-well plate (Nunc, Cat No 142761).
12. Pasteur pipettes (IWAKI, Cat No IK-PAS-9P)
13. Diamond pen (AS ONE, Cat No 6-539-05).
14. Rubber pipette bulbs, 1.5 ml (Capital Analytical, Cat No PM310031C).
15. Deep petri dishes (φ 50 × 20.3H mm) (Sterilin, Cat No 124).
16. 0.45 μm syringe filters, yellow (Sartorius, Cat No 17598).
17. Dissection microscope (Zeiss, Cat No Stemi2000C).

2.2 Immunostaining and PKH26 Staining

1. 4 % paraformaldehyde (PFA) (Nacalai, Cat No 09154-85).
2. Goat serum (Sigma, Cat No G9023).
3. Triton X-100 (Sigma, Cat No T8787).
4. Tween 20 (Sigma, Cat No P9416).
5. Mouse anti-Pax7 antibody (Santa Cruz, Cat No sc-81648).
6. Rabbit anti-MyoD antibodiy (Santa Cruz, Cat No sc-304).
7. The mouse anti-MyHC (MF20) antibody (R&D Systems, Cat No MAB4470).
8. Alexa Fluor 488 goat anti-mouse IgG antibody (Molecular Probe, Cat No A-11001).
9. Alexa Fluor 546 anti-rabbit IgG antibody (Molecular Probe, Cat No A-11035).
10. Vectashield mounting Medium containing 4,6-diamidino-2-phenylindole (DAPI) (Vector Laboratories, Cat No H-1200).
11. PKH26 Red Fluorescent Cell Linker Midi Kit (Sigma, Cat No MIDI26).

3 Methods

All procedures are performed using sterile technique in a biological safety cabinet (BSC).

3.1 Culture of Satellite Cell Clones

3.1.1 Preparation

1. Prepare DMEM containing 1 % of each penicillin and streptomycin.
2. Filter 5 % BSA in PBS through a sterile syringe filter (0.45-μm pore hydrophilic PVDF membrane). Inactivate the BSA solution at 60 °C for 60 min.
3. To prevent isolated individual myofibers from adhering to the petri dishes, rinse them with the 5 % BSA solution, and remove the excess. Add 6–8 ml of DMEM per dish and place the dishes in an incubator (37 °C, 5 % CO_2) before use.
4. Using a diamond pen, inscribe a circle on glass Pasteur pipettes, and break the pipette at the circle to create pipette openings with diameters of 1.5-mm (small) or 10-mm (large).
5. Polish the cut ends of the Pasteur pipettes with a burner to prevent injuring the fibers. Fit the heat-polished Pasteur pipettes with a rubber bulb, and coat the inside of the pipettes with the 5 % BSA solution to prevent the myofibers from adhering.
6. Immediately before dissection, prepare 1 ml of 0.2 % collagenase type I solution in DMEM per EDL muscle, and in the BSC, sterilize the collagenase solution using a sterile syringe fitted with a 0.4-μm filter (*see* **Note 1**).
7. In the BSC, filter-sterilize the collagenase/DMEM using a sterile syringe described above, and for each muscle, add 2 ml of collagenase solution to a 25-ml tube. Place the tube in a 37 °C water bath or incubator.
8. Dilute Matrigel to 1 mg/ml in DMEM containing 1 % each of penicillin and streptomycin on ice. Aliquots of diluted Matrigel can be stored at 4 °C for up to 2 weeks or at −20 °C for longer term.

3.1.2 Isolation of the EDL Muscle from the Hindlimb

1. This protocol is a modified version of the original method [15]. Sacrifice 8-week-old C57BL6 male mice using cervical dislocation, and carefully dissect the EDL muscle (Fig. 1a) (*see* **Note 2**). Spray the hindlimbs with 70 % ethanol, and remove the skin from the leg musculature. Fasten the mouse to a dissecting board using hypodermic needles inserted through the forelimb and contralateral hindlimb that will be dissected. Cut all tendons of the EDL and *tibialis anterior* (TA) muscles on the dorsal side of the paw, and carefully remove the muscles (*see* **Note 3**).
2. Place the isolated EDL muscle into a 25-ml tube containing the collagenase solution (Fig. 1b) and incubate for approximately 90 min at 37 °C in an atmosphere containing 5 % CO_2, and gently shake the tube every 15 min. The appropriate time depends on the size of the muscle and activity of the collagenase. Enzymatic digestion is finished when the muscle appears slightly swollen, indicating that several individual myofibers are separated from the edge of the muscle.

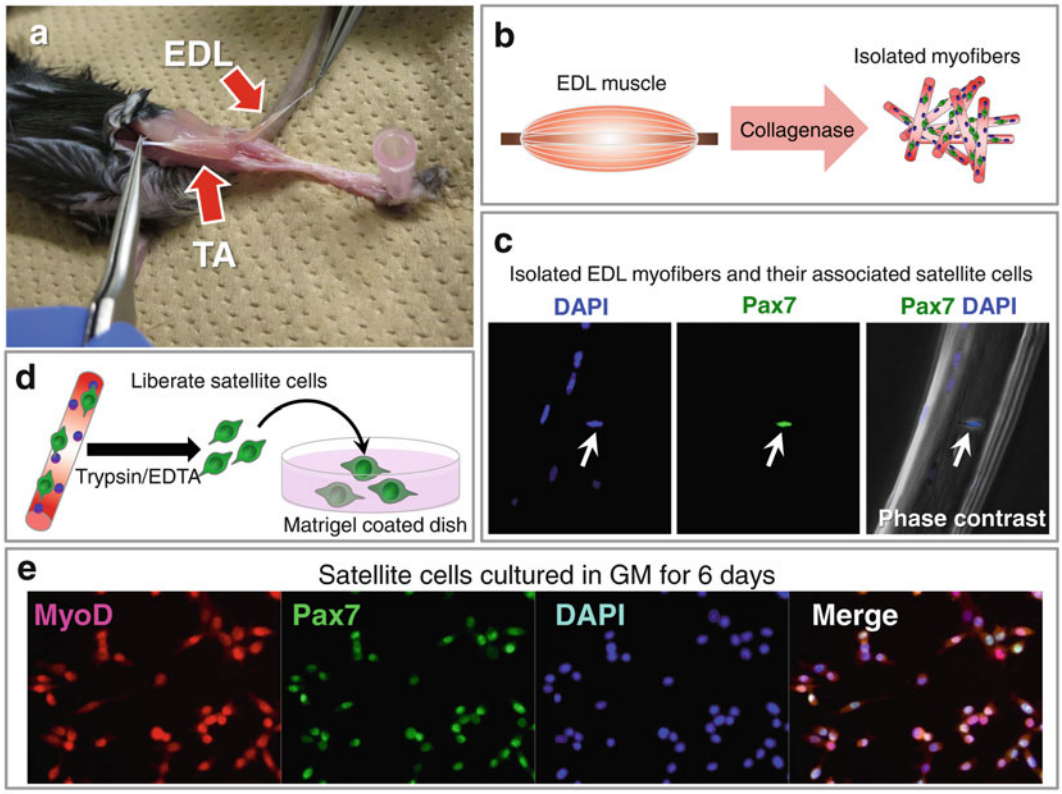

Fig. 1 Isolation of satellite cells from EDL myofibers. (**a**) Dissection and isolation of EDL muscles from mice. The image shows partially removed TA and EDL muscles. (**b**) Disaggregated myofibers prepared from collagenase-treated TA and EDL muscles. (**c**) Freshly isolated EDL myofibers and their associated satellite cells are immediately fixed and reacted with an anti-Pax7 antibody. (**d**) Digestion of myofibers to liberate the associated satellite cells for culture in the Matrigel-coated dishes. (**e**) Immunohistochemical analysis of Pax7 and MyoD expression by isolated satellite cells cultured in GM for 6 days

3. To prevent myofibers from adhering to the petri dishes, coat the inside with 5 % BSA.
4. Place the digested muscle into a petri dish containing DMEM to remove excess collagenase from the tube, and incubate the muscle at 37 °C 5 % CO_2 incubator for 30 min (*see* **Note 4**).
5. To dissociate the muscle into individual myofibers (Fig. 1c), use the large diameter of the Pasteur pipette rinsed with 5 % BSA to triturate the soaked muscle approximately ~50 times until it disaggregates, as observed using a stereoscopic dissecting microscope.
6. To further dissociate bulk myofibers into individual myofibers, use the small diameter of a Pasteur pipette rinsed with 5 % BSA to triturate the muscle 2–3 times and remove the hypercontracted dead myofibers, tendons, vessels, and other debris. Wash the dissociated myofibers with DMEM. The number of washes depends on the amount of debris.

7. Using the small diameter of a Pasteur pipette, collect the isolated noncontractile individual myofibers (Fig. 1c). It is important to determine that the myofibers are free of associated endothelium, motor neurons, and other contaminants.

3.1.3 Clonal Culture

To analyze their functional heterogeneity, the satellite cells are further dissociated from the isolated myofibers to determine their phenotypes and proliferative ability. If *Pax7-CreERT2* [16] and *Rosa26-YFP* mouse lines [17] are available, the tamoxifen-induced *Pax7*-expressing (YFP-labeled) satellite cell population of *Pax7-CreERT2;Rosa26-YFP* mice can be obtained using FACS sorting. This protocol is designed to clone satellite cells isolated from a single myofiber (Fig. 2).

1. To partially digest the myofiber and liberate the associated satellite cells (Fig. 1d), collect three clean isolated myofibers containing approximately 12 satellite cells into a 1.5 ml microtube (*see* **Note 5**). Remove the excess DMEM.

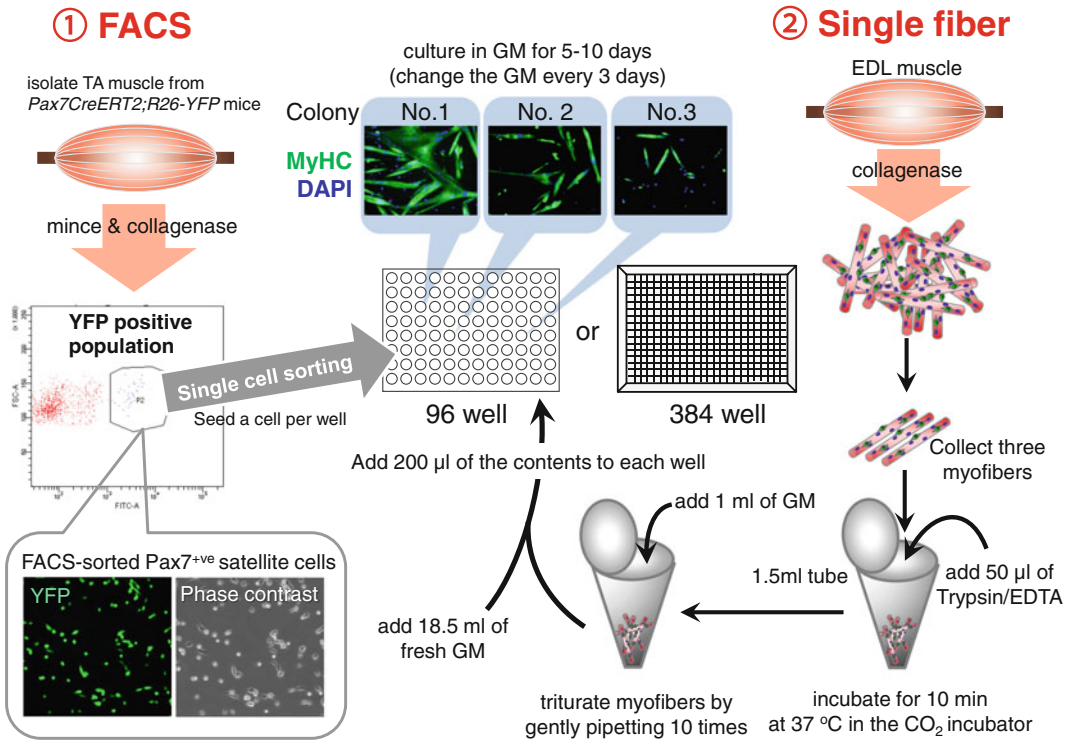

Fig. 2 Clonal culture of satellite cells. Clonal culture is performed to evaluate the heterogeneity of the satellite cell population, and two different methods for the isolation of satellite cells are shown as follows: (1) Using *Pax7-CreERT2;Rosa26-YFP* mice, the tamoxifen-induced *Pax7+* (YFP-labeled) satellite cell population sorted using FACS are seeded in a 96-well plate (or a 384-well plate) diluted so that each well contains a single cell. (2) Satellite cells are enzymatically dissociated from isolated myofibers and plated in a 96-well plate (or a 384-well plate) at clonal density

2. Dissociate satellite cells from myofibers by adding 50 µl of 0.125 % trypsin–EDTA solution and incubate for 10 min at 37 °C in the CO_2 incubator.
3. After trypsinization, add 1 ml of growth medium (GM) containing GlutaMax DMEM, 30 % FBS, 1 % chicken embryo extract, and 1 % penicillin–streptomycin.
4. To release the satellite cells associated with a myofibre, triturate the trypsinized myofibers by gently pipetting 10 times using a 1-ml pipet.
5. Place the contents of the tube into a 25-ml centrifuge tube, add 18.5 ml of fresh GM, and mix well.
6. Add 200 µl of the contents at clonal density to each well of a 96-well plate (*see* **Note 6**) and culture in GM for 5–10 days at 37 °C in the CO_2 incubator (*see* **Note 7**). Change the GM every 3 days.
7. After 5–10 days of culture, fix and react the satellite cell-derived colonies with anti-Pax7 and anti-MyoD antibodies to visualize activated/proliferating, self-renewing, and committed cells as described in the next section.

3.1.4 Immunostaining

Immunofluorescence staining of the clonal cells is performed using anti-Pax7 and anti-MyoD antibodies after 5–10 days of culture (Fig. 1e). To visualize immune complexes, dilute the primary and secondary antibodies in washing buffer containing 0.025 % Tween 20/PBS.

1. To fix the plated satellite cells to the 96-well slides, remove the medium and add 100 µl of 4 % PFA for 10 min. Gently wash the cells at least three times with 100-µl PBS to remove PFA.
2. To block nonspecific binding of the antibodies and permeabilize the cells, add 50 µl of blocking/permeabilizing solution containing 5 % goat-serum and 0.3 % Triton X-100/PBS to the cells for 20 min at room temperature. Remove the solution and wash the cells once with 0.025 % Tween 20/PBS.
3. Incubate the cells with the primary antibodies (mouse anti-Pax7 antibody, diluted 1:100 and rabbit anti-MyoD antibody, diluted 1:400) at 4 °C overnight.
4. Wash the cells 3 times with 100 µl of 0.025 % Tween 20/PBS, and detect the primary antibodies using the appropriate species-specific secondary antibodies conjugated to Alexa Fluor tags (Alexa Fluor 488-conjugated goat anti-mouse IgG antibody, diluted 1:400, and Alexa Fluor 546-conjugated anti-rabbit IgG antibody, diluted 1:400). Incubate the cells with the secondary antibodies with gentle agitation in the dark for 60 min at room temperature.

5. Wash the cells at least three times with 100 µl of 0.025 % Tween 20/PBS and mount the cells in Vectashield mounting medium containing DAPI diluted in PBS.
6. View the samples using a fluorescence microscope. Samples are stable for at least 2 weeks at 4 °C.

3.2 Identification of Slow-Dividing Cells

PKH26 is a stable red fluorescent dye that is used for in vitro cell-tracking applications. One of the most common uses of PKH26 is proliferation analysis based on dye dilution. The daughter cells fluoresce with an intensity of approximately 50 % of that of the parental cell [14]. Thus, slowly dividing cells are indirectly identified according to the intensity of PKH26 fluorescence (Fig. 3).

1. According to procedure Sect. 3.1.2, partially digest the freshly isolated myofibers to liberate the associated satellite cells. Collect 300–400 isolated myofibers into a 25-ml tube and allow them to settle to the bottom of the tube (approximately 5 min).

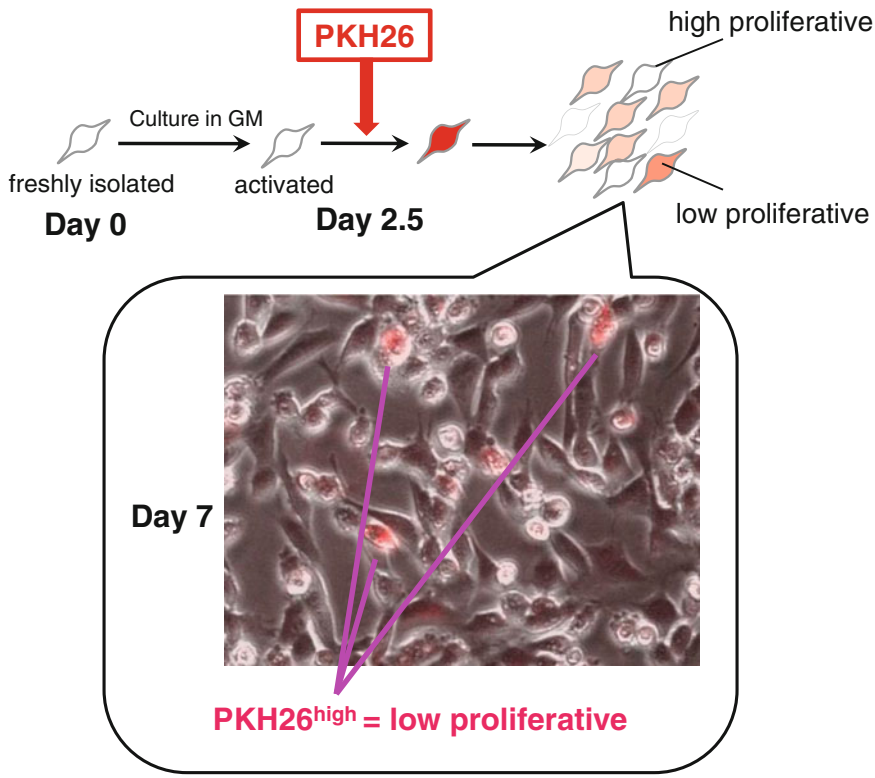

Fig. 3 A slow-dividing cell population present in activated satellite cells. To monitor the cell cycle, the membranes of activated satellite cells are labeled with the fluorescent dye PKH26 2.5 days after isolation. PKH26-labeled cells are maintained in growth medium to stimulate proliferation for 4.5 days (7 days after isolation). A typical image shows that the vast majority of activated satellite cells are $PKH26^{low}$ fast-dividing cells, whereas $PKH26^{high}$ slow-dividing cells are observed as a minority population 4.5 days after staining

2. Remove excess DMEM and add 250 μl of 0.125 % trypsin–EDTA to dissociate satellite cells from myofibers, and incubate for 10 min (37 °C, 5 % CO_2).
3. After trypsinization, add 9.75 ml of GM to inhibit trypsin activity.
4. Triturate the trypsinized myofibers by pipetting them gently 20 times using a 1 ml pipet.
5. Plate the contents into a Matrigel-coated 6-well plate (100–200 myofibers per well) and culture the myofibers in GM for 2.5 days in the incubator (37 °C, 5 % CO_2).
6. After 2.5 days, trypsinize and collect the satellite cells, label them with PKH26, according to the manufacturer's instructions, and change the GM every day thereafter.
7. After 4.5 days (7 days after isolation), the vast majority of satellite cells are $PKH26^{low}$ fast-dividing cells, while the others are $PKH26^{high}$ slow-dividing cells. $PKH26^{low}$ and $PKH26^{high}$ populations can be sorted using FACS according to the fluorescence intensity of PKH26. The behaviors of the $PKH26^{low}$- and $PKH26^{high}$-cells can be analyzed using time-lapse imaging.

4 Notes

1. The collagenase preparation should be analyzed before use, because its activity differs among lots.
2. Dissect the EDL muscle as soon as possible after sacrificing the animal. This will ensure that the muscle is healthy and will facilitate dissection.
3. Handle only the tendon of the TA and EDL muscles using forceps to avoid damaging and reducing the number of viable myofibers after collagenase digestion.
4. Continue the collagenase digestion if the muscle does not become clearly separated.
5. EDL myofibers harbor an average of four satellite cells per myofiber [18], and it is therefore possible to isolate 20 satellite cells from five myofibers. It is important to note that the number of satellite cells per EDL myofiber may vary.
6. The contents of the tube are mixed and plated evenly in a Matrigel-coated 96-well plate so that the entire surface area (30.72 cm^2) is used per 3 myofibers that contain approximately 12 satellite cells (0.32 cm^2 per well × 96 wells). Cells should be plated so that wells will contain a single cell. Two separated colonies are infrequently present in a single well and should be treated as having arisen from separate satellite cells.

7. The proliferative potential among satellite cell clones from the same EDL muscle after 10 days of culture varies widely from approximately 2500 cells (11–12 doublings) to 50 cells (5–6 doublings) [9]. Cells in small colonies are counted directly using a microscope. In contrast, images of entire large colonies are acquired, and cells are counted from images displayed on a computer monitor or using ImageJ software.

Acknowledgements

The authors thank Daiki Seko for the image shown in Fig. 1a. This work was supported by the Special Coordination Funds for Promoting Science and Technology from the Japan Science and Technology Agency (JST), a Grant-in-Aid for Challenging Exploratory Research (Research Project Number 25560338) and a Grant-in-Aid for Young Scientists A (Research Project Number 15H05368) from the Japan Society for the Promotion of Science (JSPS), and the Ichiro Kanehara Foundation.

References

1. Hoppe PS, Coutu DL, Schroeder T (2014) Single-cell technologies sharpen up mammalian stem cell research. Nat Cell Biol 16 (10):919–927. doi:10.1038/ncb3042
2. Mauro A (1961) Satellite cell of skeletal muscle fibers. J Biophys Biochem Cytol 9:493–495
3. Zammit PS, Partridge TA, Yablonka-Reuveni Z (2006) The skeletal muscle satellite cell: the stem cell that came in from the cold. J Histochem Cytochem 54(11):1177–1191
4. Wang YX, Dumont NA, Rudnicki MA (2014) Muscle stem cells at a glance. J Cell Sci 127 (21):4543–4548
5. Schultz E (1996) Satellite cell proliferative compartments in growing skeletal muscles. Dev Biol 175(1):84–94
6. Kuang S, Kuroda K, Le Grand F, Rudnicki MA (2007) Asymmetric self-renewal and commitment of satellite stem cells in muscle. Cell 129 (5):999–1010
7. Rocheteau P, Gayraud-Morel B, Siegl-Cachedenier I, Blasco MA, Tajbakhsh S (2012) A subpopulation of adult skeletal muscle stem cells retains all template DNA strands after cell division. Cell 148(1–2):112–125
8. Chakkalakal JV, Jones KM, Basson MA, Brack AS (2012) The aged niche disrupts muscle stem cell quiescence. Nature 490(7420): 355–360
9. Ono Y, Boldrin L, Knopp P, Morgan JE, Zammit PS (2010) Muscle satellite cells are a functionally heterogeneous population in both somite-derived and branchiomeric muscles. Dev Biol 337(1):29–41
10. Tanaka KK, Hall JK, Troy AA, Cornelison DD, Majka SM, Olwin BB (2009) Syndecan-4-expressing muscle progenitor cells in the SP engraft as satellite cells during muscle regeneration. Cell Stem Cell 4(3):217–225
11. Day K, Shefer G, Shearer A, Yablonka-Reuveni Z (2010) The depletion of skeletal muscle satellite cells with age is concomitant with reduced capacity of single progenitors to produce reserve progeny. Dev Biol 340(2):330–343
12. Ogawa R, Ma Y, Yamaguchi M, Ito T, Watanabe Y, Ohtani T, Murakami S, Uchida S, De Gaspari P, Uezumi A, Nakamura M, Miyagoe-Suzuki Y, Tsujikawa K, Hashimoto N, Braun T, Tanaka T, Takeda S, Yamamoto H, Fukada S (2015) Doublecortin marks a new population of transiently amplifying muscle progenitor cells and is required for myofiber maturation during skeletal muscle regeneration. Development 142(1):51–61
13. Sacco A, Doyonnas R, Kraft P, Vitorovic S, Blau HM (2008) Self-renewal and expansion of single transplanted muscle stem cells. Nature 456(7221):502–506

14. Ono Y, Masuda S, Nam HS, Benezra R, Miyagoe-Suzuki Y, Takeda S (2012) Slow-dividing satellite cells retain long-term self-renewal ability in adult muscle. J Cell Sci 125 (Pt 5):1309–1317. doi:10.1242/jcs.096198
15. Moyle LA, Zammit PS (2014) Isolation, culture and immunostaining of skeletal muscle fibres to study myogenic progression in satellite cells. Methods Mol Biol 1210:63–78. doi:10.1007/978-1-4939-1435-7_6
16. Lepper C, Fan CM (2010) Inducible lineage tracing of Pax7-descendant cells reveals embryonic origin of adult satellite cells. Genesis 48(7):424–436. doi:10.1002/dvg.20630
17. Srinivas S, Watanabe T, Lin CS, William CM, Tanabe Y, Jessell TM, Costantini F (2001) Cre reporter strains produced by targeted insertion of EYFP and ECFP into the ROSA26 locus. BMC Dev Biol 1:4
18. Ono Y, Urata Y, Goto S, Nakagawa S, Humbert PO, Li TS, Zammit PS (2015) Muscle stem cell fate is controlled by the cell-polarity protein Scrib. Cell Rep 10(7):1135–1148. doi:10.1016/j.celrep.2015.01.045

Methods in Molecular Biology (2016) 1516: 195–204
DOI 10.1007/7651_2016_321

Published online: 01 April 2016

Isolation and Expansion of Muscle Precursor Cells from Human Skeletal Muscle Biopsies

Chiara Franzin, Martina Piccoli, Luca Urbani, Carlo Biz, Piergiorgio Gamba, Paolo De Coppi, and Michela Pozzobon

Abstract

One of the major issues concerning human skeletal muscle progenitor cells is represented by the efficient isolation and in vitro expansion of cells retaining the ability to proliferate, migrate and differentiate once transplanted. Here we describe a method (1) effective in obtaining human muscle precursor cells both from fresh and frozen biopsies coming from different muscles, (2) selective to yield cells uniformly positive for CD56 and negative for CD34 without FACS sorting, (3) reliable in maintaining proliferative and in vitro differentiative capacity up to passage 10.

Keywords: Human muscle precursor cells, Skeletal muscle biopsy, CD56, Enzymatic digestion, Human muscle cell primary culture

1 Introduction

Two main approaches are currently employed for the obtainment of myogenic precursor cells, namely single fiber isolation, firstly described by Rosenblatt and colleagues [1] and applied also for human samples [2], and whole muscle enzymatic digestion with different adaptations [3,4]. The first method allows to get a virtually pure population of activate satellite cells but is a quite complex procedure, starting from the muscle collection which has to provide myofibers preserved in their length, whereas the second one is more simple and fast but yields a mixed cell population and usually need further passages such as preplating or fluorescence-activated cell sorting [5,6]. In terms of surface antigen expression, different proteins have been investigated to better define the precursor cells in human muscle; however, so far the literature is quite unanimous in identifying the cells restricted to a myogenic fate in the $CD56^{+}CD34^{-}$ population [7,8].

Here we describe a protocol to efficiently isolate and expand in culture human muscle precursor cells from different skeletal muscles through a whole muscle digestion method without the need of further cell processing. This is possible following the

combination of (1) careful biopsy collection and cleaning, (2) double enzymatic digestion, (3) defined medium composition and appropriate plastic ware. This method allows obtaining homogeneous $CD56^{+}CD34^{-}$ cell population that maintains proliferative and in vitro differentiative capacity up to passage 10. Moreover, although other improvements mainly regarding culture conditions are needed in the perspective of a future possible clinical application, we defined a freezing procedure that does not affect cell isolation and characteristics.

2 Materials

2.1 Culture Media and Plastic Ware

1. Prepare the Collagenase I 0.2 % (w/v) solution: weigh 200 mg of lyophilized collagenase from *Clostridium histolyticum* for general use, Type I (Sigma Aldrich) and resuspend with 2 mL of DMEM (1×) 1 g/L glucose (+) L-glutamine (+) pyruvate (GIBCO, Thermo Fisher Scientific), then add 98 mL of DMEM. Filter the solution through a 0.22 μm filter and stock single-use aliquots at −20 °C.
2. Trypsin 0.05 % with EDTA and phenol red (GIBCO, Thermo Fisher Scientific).
3. Red blood cell lysis buffer: Auto Lyse Plus (Biosource).
4. Washing medium: DMEM (1×) 1 g/L glucose (+) L-glutamine (+) pyruvate containing 20 % fetal bovine serum (FBS) (GIBCO, Thermo Fisher Scientific) and 1 % penicillin/streptomycin (pen/strep) (GIBCO, Thermo Fisher Scientific).
5. Proliferation medium: DMEM (1×) 1 g/L glucose (+) L-glutamine (+) pyruvate containing 20 % FBS, 10^{-6} M dexamethasone (Sigma Aldrich), 10 ng/mL recombinant mouse FGF basic protein (R&D Systems), 10 μg/mL insulin (Insuman Rapid 100UI/mL, Sanofi Aventis) and 1 % pen/strep.
6. Differentiation medium: MEM alpha (1X), (+) L-glutamine, (+) ribonucleosides, (+) deoxyribonucleosides, (−) ascorbic acid (GIBCO, Thermo Fisher Scientific) containing 2 % horse serum (GIBCO, Thermo Fisher Scientific), 10 μg/mL insulin, and 1 % pen/strep.
7. Freezing medium: 70 % FBS, 10 % DMEM (1×) 4.5 g/L glucose (+) L-glutamine (+) pyruvate (GIBCO, Thermo Fisher Scientific), 20 % dimethyl sulfoxide.
8. Non-Tissue Culture Treated (NTC) Plate, polystyrene, flat bottom: 96-well, 24-well, and 6-well plates (Falcon, Corning). Use these plates for cell expansion and proliferating cell characterization.

9. Non-Tissue Culture Treated (NTC) polystyrene petri dishes, 100×20 mm and 150×25 mm (Falcon, Corning). Use these plates for cell expansion.
10. Tissue Culture Treated (TC) Plate, polystyrene, flat bottom: 24-well plates (Falcon, Corning). Use these plates for myogenic differentiation.

2.2 Flow Cytometry Analysis

1. Tubes or other supports suitable for your cytometer.
2. Antibodies anti-human antigens: CD34-FITC clone 581, CD56-PE clone B159, 7-aminoactinomycin D (7AAD) (all from BD Pharmigen). Isotype controls: mouse IgG1-FITC (IOTest Immunotech), PE mouse anti-human Igk (BD Pharmigen).

2.3 Immunofluorescence Analysis

1. Routine reagents: 4 % paraformaldehyde (PFA) for fixation, 0.5 % Triton X-100 in phosphate-buffered saline (PBS) for permeabilization, 10 % horse serum in PBS for saturation, 1 % bovine serum albumin (BSA) in PBS for antibodies dilution, 4′,6-diamidino-2-phenylindole (DAPI) fluorescence mounting medium for nuclei counterstaining.
2. Proliferating cell characterization. Primary antibodies: monoclonal rabbit IgG anti-human Ki-67 clone SP6 (Novusbio), monoclonal mouse IgG_1 anti-human PAX7 clone PAX7 (R&D systems), polyclonal rabbit IgG anti-human MYOD clone M318 (Santa Cruz Biotechnology), polyclonal rabbit IgG anti-human MYF5 clone C20 (Santa Cruz Biotechnology). Secondary antibodies: chicken anti-rabbit IgG (H + L) Alexa Fluor® 594 conjugate (Thermo Fisher Scientific), goat anti-mouse IgG (H + L) Alexa Fluor® 594 conjugate (Thermo Fisher Scientific).
3. Differentiated cell characterization. Primary antibody: monoclonal mouse IgG_{2B} anti-human Myosin Heavy Chain clone MF20 (R&D systems). Secondary Antibody: goat anti-mouse IgG (H + L) Alexa Fluor® 594 conjugate (Thermo Fisher Scientific).

3 Methods

3.1 Cell Isolation

1. Carry the muscle biopsy (*see* **Note 1**, Figs. 1 and 2) in sterile saline from operating theater to the laboratory cell processing room (*see* **Note 2**).
2. Transfer the sample on a petri dish using disposable sterile plastic pincers and quickly rinse it with Betadine® or similar products and PBS.

Muscle type	N° of samples
Biceps	2
Deltoid	3
Extensor forearm	2
Flexor carpi	2
Flexor longus pollicis	1
Flexor hallucis longus	3
Peroneus	14
Pronator teres	2
Quadriceps rectus femoralis	3
Sovraspinatus muscle	3
Tibialis	4
Triceps	1
Vastus lateralis	2

Fig. 1 Muscle sources. Biopsies were obtained from different skeletal muscles, as highlighted in *pink* in the illustration; the number of samples analyzed for each muscle is shown in the table

3. Transfer the sample in a clean petri dish and carefully remove visible vasculature, connective tissue, and potential adipose tissue (*see* **Note 3**).
4. Divide the muscle in pieces weighting up to 500 mg (*see* **Note 4**) and treat every piece separately.
5. Mince the sample in very small pieces (1–2 mm^3) using two disposable sterile scalpels.
6. Cover minced sample with 3 mL of 0.2 % (w/v) Collagenase I in a well of 6-well plate and incubate for 90 min at 37 °C.
7. Transfer the digestion product in a 15 mL conical centrifuge tube, add 10 mL of washing medium and homogenate with serological pipette, then centrifuge at 300 × *g* for 10 min.
8. Take out the supernatant and resuspend the pellet with 2 mL of 0.05 % Trypsin–EDTA, transfer in a well of 6-well plate and incubate for 60 min at 37 °C.

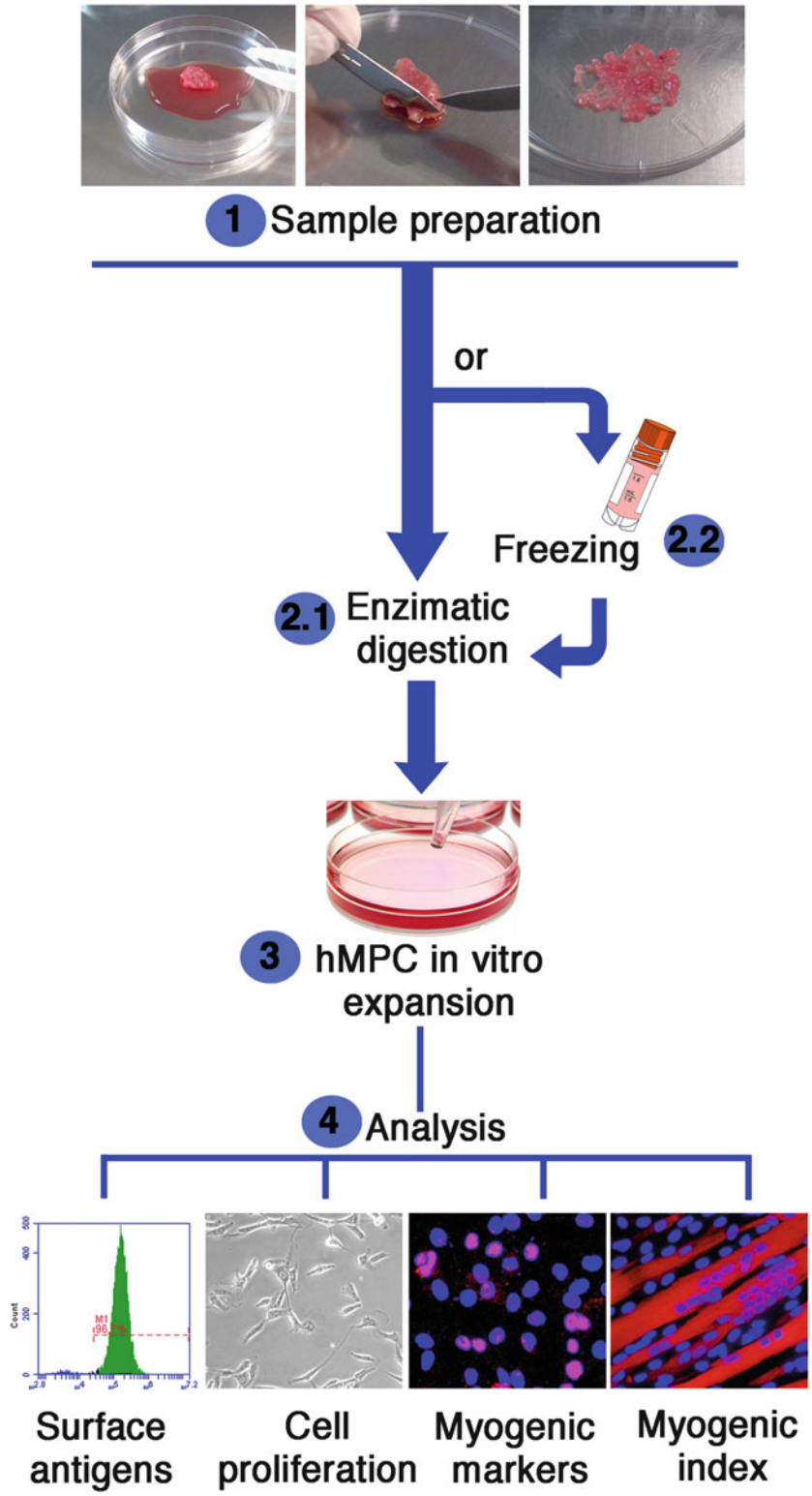

Fig. 2 Method outline. After washing and removal of non-muscle tissue (1) samples are directly subject to enzymatic digestion (Sect. 2.1) or frozen for later use (Sect. 2.2). Isolated cells are cultured for several passages (3) and characterized in terms of surface antigen expression, proliferation, myogenic marker expression, and myogenic index (4)

9. Transfer the digestion product in a 15 mL conical centrifuge tube, add 10 mL of washing medium and homogenate with serological pipette, then filter twice the cell suspension first through 70 μm and then 40 μm cell strainers. Centrifuge at 300 × *g* for 10 min.
10. Resuspend the pellet in 3 mL red blood cell lysis buffer for 5 min, add 10 mL of washing medium and centrifuge at 300 × *g* for 10 min.
11. Resuspend the pellet in 2 mL of proliferation medium and seed cells in a well of 6-well NTC plate.
12. Refresh proliferation medium after 48–72 h (*see* **Note 5**). Usually attached cells appear after 5–7 days from enzymatic digestion (*see* **Note 6**).

3.2 Sample Freezing

1. Transfer minced sample obtained at **step 5** of Sect. 3.1 in a 2 mL cryovial and add 1 mL of freezing medium.
2. Proceed with slow cooling protocol as for cell samples and store in liquid nitrogen (*see* **Note 7**).

3.3 Sample Thawing

1. Take out sample from liquid nitrogen and thaw in water bath at 37 °C.
2. Transfer sample in a 15 mL conical centrifuge tube, add 10 mL of washing medium and centrifuge at 300 × *g* for 10 min.
3. Proceed with **step 6** of Sect. 3.1.

3.4 Cell Expansion

1. Take out the medium from the well or dish and wash twice with PBS. Add the appropriate volume of 0.05 % Trypsin–EDTA (300 μL for wells of 6-well plate, 1 mL for 100×20 mm dishes, 2 mL for 150×25 mm dishes) and incubate for 5–10 min at 37 °C.
2. Add washing medium, collect detached cells and centrifuge at 300 × *g* for 10 min. Remove the supernatant, resuspend cell pellet in proliferation medium and seed cells on a suitable NTC well or dish. Usually around 1×10^5 cells in a 100×20 mm dish and 2.5×10^5 cells in a 150×25 mm dish are seeded. We recommend never exceeding the 60–70 % of confluence. In our experience cells maintain unaltered characteristics up to passage 10.

3.5 Cell Characterization

1. Doubling time analysis (Fig. 3a): seed 1×10^4 cells for each well of 24-well NTC plate in proliferation medium, after 48 h detach cells by trypsin treatment and proceed with counting. Consider at least three wells separately. Calculate the doubling time (*g*) using the following equation $g = 48\text{ h} \times [\log 2/\log (N_{48h}/N_0)]$ in which *g* is the generation (or doubling) time during the logarithmic phase of the growth curve, N_{48h} is the

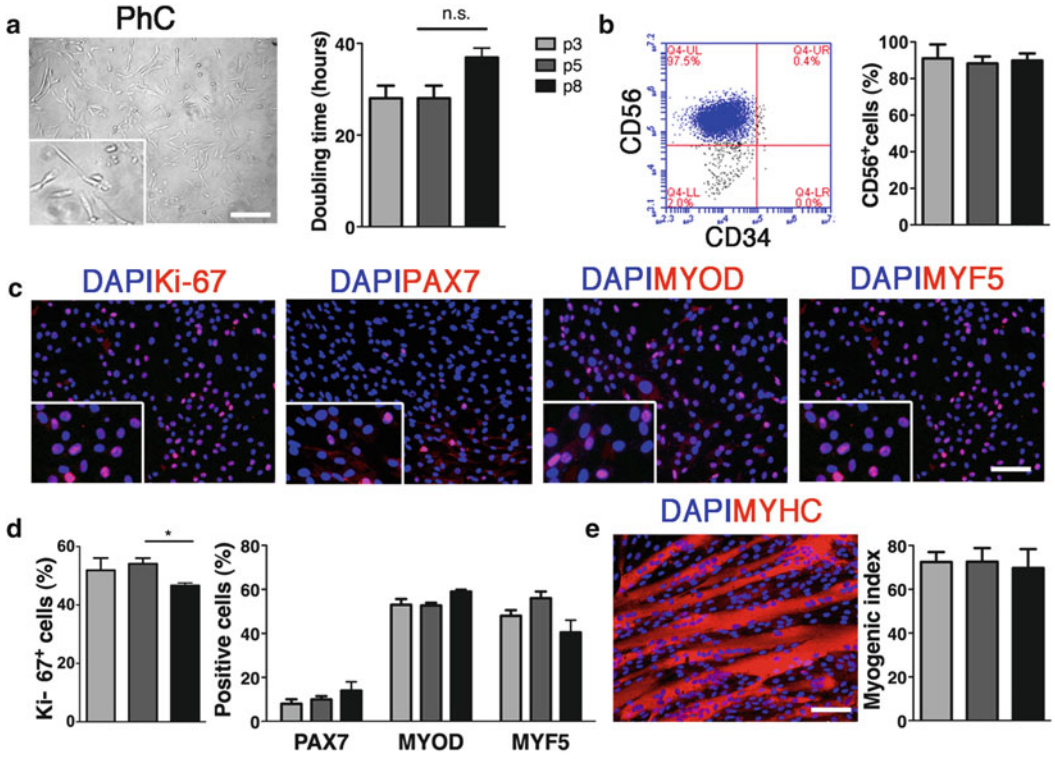

Fig. 3 Cell characterization. (**a**) Representative image of cell appearance in culture at phase contrast microscope (scale bar = 100 μm) and bar graph of doubling time calculated at different passages. (**b**) Representative dot-plot of expanded cells (passage 5) analyzed for the expression of CD56 and CD34 and bar graph of CD56 expression at different passages. (**c**) Representative pictures of Ki-67 and myogenic markers expression (passage 5) (scale bar = 100 μm). (**d**) Percentage of cells positive for Ki-67 and myogenic markers at different passages (at least five fields for each independent experiment). (**e**) Representative picture of myosin heavy chain staining (passage 5) (scale bar = 100 μm) and myogenic index calculation at different passages (at least five fields for each independent experiment)

cell number at 48 h after seeding and N_0 is the cell number at time 0 [9].

2. Flow cytometry analysis (Fig. 3b): detach cells by trypsin treatment and proceed with incubation using antibodies described in Sect. 2.2. Usually we observe more than 90 % of CD56 positive cells and no cells positive for CD34.
3. Immunofluorescence analysis of proliferating cells (Fig. 3c, d): seed 5×10^3 cells for each well of 96-well NTC plate in proliferation medium, after 48 h take out the culture medium, wash twice with PBS and fix cells by incubation with 4 % PFA at 4 °C for 10 min. Proceed with the immunostaining protocol using the antibodies described in the **item 2** of Sect. 2.3.

4. Myogenic differentiation and myogenic index evaluation (Fig. 3e): seed 1.5×10^4 cells for each well of 24-well TC plate in proliferation medium and let cells proliferate for 48 h, then take out the medium and add differentiation medium. After 48 h refresh differentiation medium and after other 48 h take out the medium, wash twice with PBS and fix cells by incubation with 4 % PFA at 4 °C for 10 min. Proceed with the immunostaining protocol using the antibodies described in the **item 3** of Sect. 2.3. Calculate the myogenic index defined as the number of nuclei residing in cells containing three or more nuclei divided by the total number of nuclei [10]. Consider at least five fields at 20× magnification for each sample.

4 Notes

1. We experienced efficient isolation and expansion of muscle precursor cells starting from biopsies obtained from different adult skeletal muscle listed in Fig. 1. We also applied our method to pediatric abdominal muscle biopsies and derived muscle precursor cells with similar features to those observed in cells of adult origin (described in Fig. 3).
2. If it is not possible to process the biopsy immediately after surgery it can be maintained in sterile saline at 4 °C not longer than 24 h.
3. We considered biopsies from adult healthy subjects aged from 25 to 60 years undergoing scheduled orthopedic operations or surgery after trauma, with muscle being virtually free of ectopic adipose tissue deposition that is instead present during aging or in some pathological condition [11].
4. For samples weighting less than 200 mg adjust reagent volumes and plastic ware as following:
   - 1.5 mL of 0.2 % Collagenase I in a well of 24-well plate (**step 6** of Sect. 3.1)
   - 1 mL of 0.05 % Trypsin–EDTA in a well of 24-well plate (**step 8** of Sect. 3.1)
   - Avoid incubation with red blood cells lysis buffer (**step 10** of Sect. 3.1)
   - Seed cells in 1 mL of proliferation medium in a well of 24-well NTC plate (**step 11** of Sect. 3.1)

   In case of small samples attached cells could appear slightly later (7–10 days).
5. Despite of washing and filtering procedures it is possible to still observe cell and fiber debris at this stage, we thus recommend taking out medium and washing cells with PBS or washing medium before adding fresh proliferation medium.

6. If attached cells appear before 5 days, it is possible that fibroblasts overcame the proliferation of myogenic cells. This may occur despite the careful removal of connective tissue from biopsies and an accurate muscle sample collection during surgery can help in avoiding this inconvenience. Although the large and granular appearance of fibroblasts is easily distinguishable from the elongated and thin shape of myogenic cells, we recommend performing flow cytometry analysis at earlier passage as possible to evaluate the percentage of CD56 positive cells.
7. In our experience there are not differences between freshly processed and frozen/thawed biopsies, apart a possible delay in the appearance of attached cells.
8. Both adult and pediatric biopsies were taken after approval by local ethical committee and informed consent acceptance by patients (Prot N. 2682P and 3030P, Azienda Ospedaliera di Padova).

Acknowledgements

This work has been funded by Fondazione Istituto di Ricerca Città della Speranza (Grant number 12/01) and CARIPARO-IRP Ricerca Pediatrica Program (Grant number 13/04). Luca Urbani and Paolo De Coppi are supported by GOSH and NIHR (RP-2014-04-046).

References

1. Rosenblatt JD, Lunt AI, Parry DJ, Partridge TA (1995) Culturing satellite cells from living single muscle fiber explants. In Vitro Cell Dev Biol Anim 31(10):773–779. doi:10.1007/BF02634119
2. De Coppi P, Milan G, Scarda A, Boldrin L, Centobene C, Piccoli M, Pozzobon M, Pilon C, Pagano C, Gamba P, Vettor R (2006) Rosiglitazone modifies the adipogenic potential of human muscle satellite cells. Diabetologia 49 (8):1962–1973. doi:10.1007/s00125-006-0304-6
3. Agley CC, Rowlerson AM, Velloso CP, Lazarus NR, Harridge SD (2013) Human skeletal muscle fibroblasts, but not myogenic cells, readily undergo adipogenic differentiation. J Cell Sci 126(Pt 24):5610–5625. doi:10.1242/jcs.132563, jcs.132563 [pii]
4. Gaster M, Kristensen SR, Beck-Nielsen H, Schroder HD (2001) A cellular model system of differentiated human myotubes. APMIS 109(11):735–744
5. Jankowski RJ, Haluszczak C, Trucco M, Huard J (2001) Flow cytometric characterization of myogenic cell populations obtained via the preplate technique: potential for rapid isolation of muscle-derived stem cells. Hum Gene Ther 12(6):619–628. doi:10.1089/104303401300057306
6. Xu X, Wilschut KJ, Kouklis G, Tian H, Hesse R, Garland C, Sbitany H, Hansen S, Seth R, Knott PD, Hoffman WY, Pomerantz JH (2015) Human satellite cell transplantation and regeneration from diverse skeletal muscles. Stem Cell Rep 5(3):419–434. doi:10.1016/j.stemcr.2015.07.016, S2213-6711(15)00222-2 [pii]
7. Bareja A, Holt JA, Luo G, Chang C, Lin J, Hinken AC, Freudenberg JM, Kraus WE, Evans WJ, Billin AN (2014) Human and mouse skeletal muscle stem cells: convergent and divergent mechanisms of myogenesis. PLoS One 9(2):e90398. doi:10.1371/journal.pone.0090398, PONE-D-13-42782 [pii]

8. Pisani DF, Dechesne CA, Sacconi S, Delplace S, Belmonte N, Cochet O, Clement N, Wdziekonski B, Villageois AP, Butori C, Bagnis C, Di Santo JP, Kurzenne JY, Desnuelle C, Dani C (2010) Isolation of a highly myogenic CD34-negative subset of human skeletal muscle cells free of adipogenic potential. Stem Cells 28 (4):753–764. doi:10.1002/stem.317
9. Scarda A, Franzin C, Milan G, Sanna M, Dal Pra C, Pagano C, Boldrin L, Piccoli M, Trevellin E, Granzotto M, Gamba P, Federspil G, De Coppi P, Vettor R (2010) Increased adipogenic conversion of muscle satellite cells in obese Zucker rats. Int J Obes (Lond) 34 (8):1319–1327. doi:10.1038/ijo.2010.47, ijo201047 [pii]
10. van der Velden JL, Schols AM, Willems J, Kelders MC, Langen RC (2008) Glycogen synthase kinase 3 suppresses myogenic differentiation through negative regulation of NFATc3. J Biol Chem 283(1):358–366. doi:10.1074/jbc.M707812200, M707812200 [pii]
11. Vettor R, Milan G, Franzin C, Sanna M, De Coppi P, Rizzuto R, Federspil G (2009) The origin of intermuscular adipose tissue and its pathophysiological implications. Am J Physiol Endocrinol Metab 297(5):E987–E998. doi:10.1152/ajpendo.00229.2009, 00229.2009 [pii]

Methods in Molecular Biology (2016) 1516: 205–217
DOI 10.1007/7651_2016_358

Published online: 03 May 2016

Measuring ATP Concentration in a Small Number of Murine Hematopoietic Stem Cells

Krzysztof Szade*, Monika Zukowska*, Alicja Jozkowicz, and Jozef Dulak

Abstract

The metabolism of quiescent adult stem cells differs from the metabolism of differentiated cells. The metabolic processes are tightly regulated and their alterations disturb function of stem cells. One of the indicators of metabolic status of cells is the ATP level. While the method of measuring the ATP levels has been known for many years, estimating ATP levels in small population of defined stem cells isolated directly from the tissue has remained challenging. Here, we show our method of measuring the ATP levels in hematopoietic stem cells sorted from murine bone marrow. We used magnetic sorting as well as cell sorter and adopted the commonly used bioluminescence-based detection kits in described protocol. Our strategy allows to measure ATP levels in 1000 highly purified HSC.

Keywords: Hematopoietic stem cells, ATP, Metabolism, Cell sorting

1 Introduction

Adult stem cells renew tissues and sustain homeostasis of the organism throughout lifetime [1]. They constitute the reservoir of regeneration potential. Therefore, it is evolutionarily understandable that tissue-specific adult stem cells remain in quiescent state that protects from cell cycling-induced damages [2, 3]. This quiescence is characterized by distinctive metabolic state [4]. It was shown that adult stem cells are more dependent on glycolytic metabolism in contrast to oxidative metabolism of proliferating and differentiated effector cells [4, 5].

Alteration of cell metabolism is often linked to changed levels of cellular ATP, as it was shown in hematopoietic stem cells (HSC) [5]. HSC actively suppress influx of pyruvate into mitochondrial oxidation pathway and favor the glycolytic transformation of pyruvate into lactate [5]. If the pathways suppressing pyruvate influx into mitochondria are inhibited it results in altered metabolic homeostasis and reduced cellular ATP levels [5]. Therefore, measuring ATP levels may be an important indication of metabolic

* Author contributed equally with all other contributors.

status of stem cells, e.g., when analyzing the metabolism of cells in gene-knockout models.

Here, we show how to measure ATP levels in HSC. The method of the ATP detection based on bioluminescent luciferase reaction that we applied in our protocol was already described in the 1980s [6]. However, the main problem when measuring ATP in HSC is the low number of these cells and complicated protocol of their isolation. This makes the standard method of ATP detection more challenging in case of HSC and other rare stem cell populations. Therefore, in this work we describe in detail the experimental setup for isolation, sorting, and subsequent measurement of ATP levels in 1000 sorted HSC, using commercially available bioluminescence-based kit with a modified protocol.

We showed that obtained results are consistent with previous work where numbers of HSC used for analysis were at least ten times higher [5].

2 Materials

2.1 Isolation of Mouse Bone Marrow Cells

1. Surgical instruments and other supplies: scissors, bone crusher, two blunt-nosed thumb forceps, 1 ml syringes with 25G needle, 3 cm diameter petri dishes.
2. Staining buffer: 2 % fetal bovine serum (FBS, cell culture grade) in phosphate-buffered saline (PBS) without addition of calcium and magnesium ions. Add 1 ml of FBS to 49 ml of PBS in 50 ml conical tube. 50 ml of staining buffer allows to flush bone marrow from 4 to 5 mice. Keep on ice during the isolation.

2.2 Staining of Bone Marrow Cells

1. 10× red blood cell (RBC) lysis buffer (according to [7]): 1.5 M NH_4Cl, 100 mM $NaHCO_3$, 10 mM disodium EDTA in distilled water. Dissolve 80.2 g NH_4Cl, 8.4 g $NaHCO_3$, 3.7 g EDTA in 900 ml of distilled water. Adjust pH to 7.4 with HCl/NaOH and complete up to 1000 ml with distilled water (**Note 1**). 10× stock solution is stable for 6 months at 4 °C. Dilute the stock solution ten times with distilled water to obtain working solution.
2. A centrifuge for 15/50 ml conical tubes and 5 ml FACS tubes with cooling option.
3. 40 μm nylon strainer (BD).
4. Antibodies used in the protocol are listed in Table 1 (**Note 2**). Prepare the 100× stock of 20 μg/ml of DAPI in distilled water.

Table 1
Panel of antibodies used in the protocol

Antigen	Dye	Clone	Company
CD11b	PE	M1/70	BD
Gr-1	PE	RB6-8C5	BD
Ter119	PE	TER119	BD
B220	PE	RA3-6B2	BD
CD3	PE	17A2	BD
c-Kit	APC-eFluor780	BM8	eBioscience
Sca-1	PE-Cy7	D7	BD
CD48	PerCP-Cy5.5	HM-48-1	Biolegend
CD150	APC	TC15-12F12.2	Biolegend
CD34	FITC	RAM34	BD

Table 2
Laser and filter configuration on MoFlo XDP cell sorter used for HSC isolation

Laser (nm)	Chanel	Mirror	Filter
488	FITC (FL-1) PE (FL-2) PerCP-Cy.5.5 (FL-4) PE-Cy7 (FL-5)	505 LP 560 LP 650 LP 720 LP	529/28 575/25 670/30 785/62
355	UV (FL-6)	506 SP	457/50
642	APC (FL-8) APC-eFluor780 (FL-10)	695 SP 740 LP	670/30 785/62

Dilute the 100× DAPI stock directly in staining buffer as described in the protocol.

2.3 Depletion by Magnetic-Activated Cell Sorting (MACS)

1. LS MACS columns (Miltenyi Biotec) together with MACS Midi Separator (**Note 3**).
2. MACS buffer: 2 mM EDTA, 0.5 % BSA in PBS, 0.09 % azide, sold as ready to use autoMACS running buffer (Miltenyi Biotec).
3. Anti-PE magnetic beads (Miltenyi Biotec) to deplete lineage cells stained as described in the protocol.

2.4 Cell Sorting

1. In the described strategy we use MoFlo XDP cell sorter (Becton Dickinson) with Smart Sampler and 355 nm (100 mW), 488 nm (200 mW), and 642 nm (100 mW) lasers together with filter configuration presented in Table 2 (**Note 4**).

2. Inside the sorting chamber use polypropylene FACS tubes instead of polystyrene tubes to avoid electrostatic charges.

2.5 Measuring ATP Concentration

1. Described protocol is based on ATP Bioluminescence Assay Kit HS II (Roche, cat. no. 11 699 709 001) and adapted to measure ATP in small number of sorted cells.
2. Dilution buffer is provided in the kit and is ready-to-use. It can be stored at 4 °C.
3. Luciferase Reagent: Dissolve powder provided in the kit in 10 ml of dilution buffer, without stirring or shaking. Incubate for 5 min at 4 °C. For homogenous solution mix by carefully rotating the bottle. Prepared luciferase reagent may be stored at −20 °C. Each freeze/thaw cycle reduces the luciferase activity, therefore aliquot the reagent and avoid refreezing.
4. ATP standard: Dissolve powder provided in the kit in dilution buffer to obtain final concentration of 10 mg/ml (16.5 mM). For example add 960 μl of Dilution Buffer to 9.60 mg ATP. Solution is stable for at least 4 weeks when stored at −20 °C, 1 week at 4 °C and 8 h on ice.
5. Cell Lysis Reagent: Cell lysis reagent is provided in the kit and is ready-to-use. It is stored at 4 °C.
6. 70 % ethanol: for 50 ml mix 36.5 ml of 96 % ethanol with 13.5 ml distilled water. Prepare fresh solution before use.
7. We used Tecan Infinite M200 Pro plate reader to measure the luminesce signal (**Note 5**).

3 Methods

Isolation and staining of bone marrow cells have to be performed on ice to block cell metabolism and prevent degradation of ATP. Cool down centrifuge and all the reagents, except the RBC lysis buffer.

3.1 Isolation of Murine Bone Marrow

1. Euthanize mice according to guidelines of your local ethical committee on animal research.
2. Dissect both tibias and femurs without opening of the bone marrow cavity of the bones (**Note 6**). Clean the bones from remaining muscle tissue with scissors and sterile swabs. Put the bones into 1 ml of ice cold staining buffer in petri dish and keep them on ice until next flushing step.
3. While keeping the bones with the forceps cut the ends of the bones from both sides with scissors or bone crusher (**Note 7**).
4. Aspirate the ice-cold staining buffer into the syringe with mounted needle, insert the needle into open end of the bone, and flush the bone marrow into 15 ml tube placed on ice.

Repeat the flushing several times from both ends of the bone until bone is clear with no remaining marrow. This is usually achieved with 5–10 ml of staining buffer. Keep the flushed bone marrow on ice until next steps.

3.2 Lysis of RBC Cells

1. Warm 1× RBC lysis solution to room temperature.
2. Filter the flushed bone marrow through a 40 μm nylon strainer into 15 or 50 ml conical tubes.
3. Centrifuge samples at 600 × *g* for 10 min at 4 °C.
4. Discard the supernatant and suspend the pellet in 1 ml of 1× RBC lysis buffer by pipetting several times. Then add next 1 ml of 1× RBC lysis buffer (**Note 8**). Incubate at room temperature for 7 min.
5. Add 10 ml of PBS and centrifuge at 600 × *g* for 10 min at 4 °C.
6. Discard the supernatant and suspend the pellet in total volume of 100 μl of ice-cold MACS supplemented with 2 % FBS (**Note 9**). Transfer 95 μl of cell suspension to 5 ml FACS tube.

3.3 Depletion of Lineage Committed Cells (Notes 10 and 11)

1. Prepare the antibody mix to stain lineage antigens according to Table 3. When preparing mix calculate the final volume for one sample more than the actual number of samples. Avoid exposing to direct light. Add 5 μl of the mix to each FACS tube. Stain for 20 min on ice in darkness.
2. Add 2 ml of MACS buffer to each tube and centrifuge at 600 × *g* for 10 min at 4 °C.
3. Discard the supernatant and resuspend cell pellet in final volume of 80 μl of MACS buffer. Add 20 μl of anti-PE magnetic beads. Incubate for 15 min on ice in darkness.
4. Wash samples with 2 ml of MACS buffer and centrifuge at 600 × *g* for 10 min at 4 °C.
5. During the centrifugation place the columns in magnetic MACS Midi Separator (**Note 12**). Prime the columns with

Table 3
Mix of antibodies for lineage antigens

Antibody	Per one sample (μl)
CD11b-PE	1
Gr-1-PE	1
Ter119-PE	1
B220-PE	1
CD3-PE	1
Total mix per sample	5

Table 4
Mix of antibodies used to distinguish HSC

Antibody	Per one sample (μl)
c-Kit-APC-eFluor780	2
Sca-1-PE-Cy7	2
CD150-APC	2
CD48-PerCP-Cy5.5	2
CD34-FITC	2
DAPI	1
Total mix per sample	11

3 ml of MACS buffer, wait until the whole volume passes through the column and discard the effluent.

6. After centrifugation discard the supernatant and suspend cells in 500 μl of MACS buffer.
7. Place a 15 ml conical tube under the column in ice bucket to collect the cell suspension.
8. Filter the cell suspension by 40 μm nylon strainer directly to column. Wait until whole volume passes through the column and apply 3 ml of MACS buffer to wash the column. Collect the effluent to the same tube. Repeat washing twice. Columns can be discarded (**Note 13**).
9. Centrifuge collected cells at 600 × *g* for 10 min at 4 °C, discard the supernatant and suspend the pellet in final volume of 90 μl of staining buffer. Prepare antibody mix according to Table 4. Add 11 μl of antibody mix to each sample and incubate for 20 min on ice in darkness.
10. Add 2 ml of PBS and centrifuge at 600 × *g* for 10 min at 4 °C. Discard supernatant and suspend cells in 400 μl of staining buffer. Transfer to 1.5 ml Eppendorf tubes (**Note 14**). Cells are ready for sort.

3.4 Cell Sorting (Note 15)

1. Prepare Eppendorf tubes with 23 μl of dilution buffer (**Note 16**).
2. Gate the LT-HSC and additional populations if wanted (e.g., short-term HSC-ST-HSC, and multipotent progenitors-MPP) according to the Fig. 1. Sort 1000 cells to 1.5 ml Eppendorf tubes containing 23 μl of dilution buffer (**Notes 17** and **18**).

3.5 Preparing Tecan Plate Reader Injection System

1. Remove the injector from carrier slot and place it into the service position in injector box.

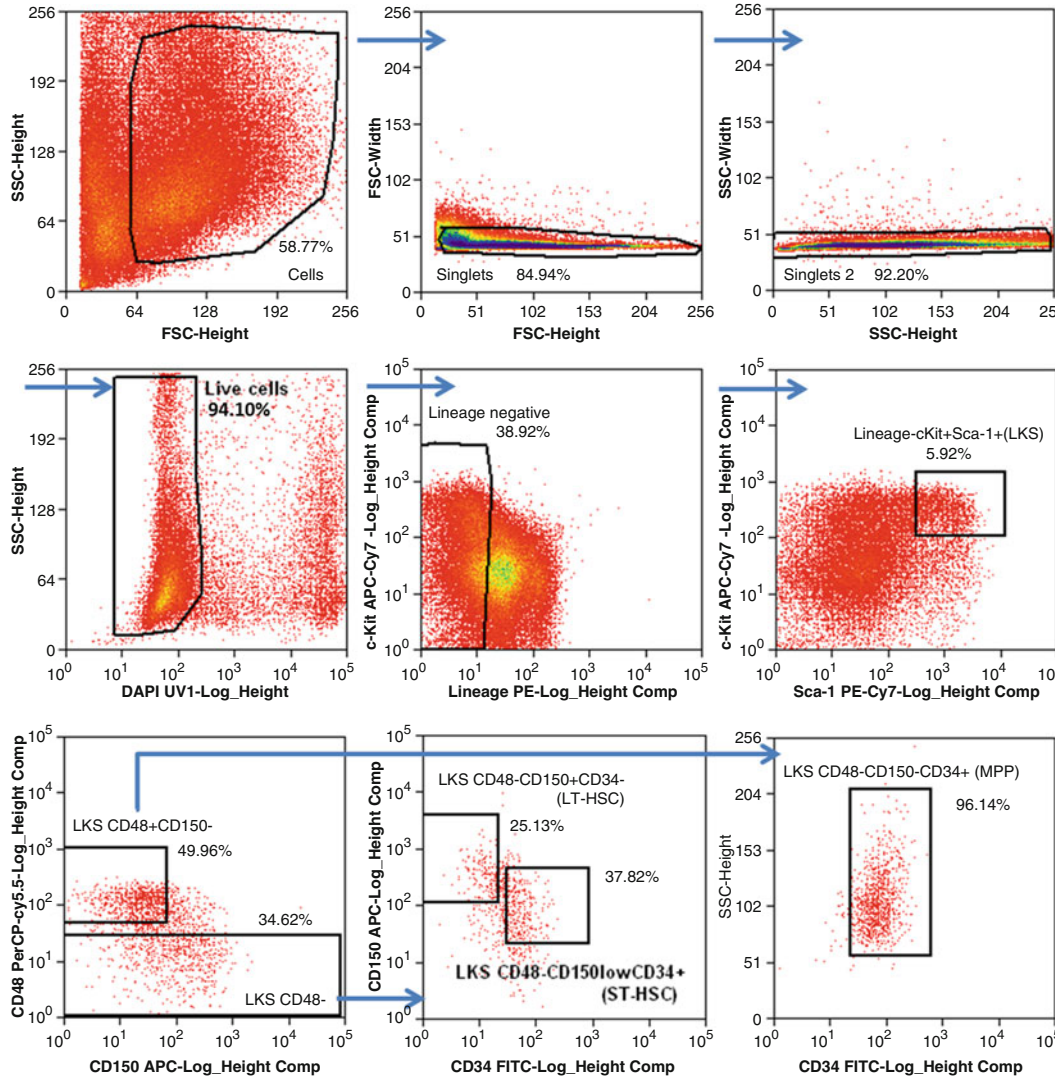

Fig. 1 Gating scheme of murine LT-HSC, ST-HSC and MPP populations from murine bone marrow

2. Place empty container under the injector. Fill storage bottles with distilled water, place the tubing in the bottles and wash the system.
3. Remove distilled water and wash the system with 70 % ethanol.
4. Prime the pumps with 70 % ethanol for 30 min, with syringes fully lowered.
5. Wash the system with 70 % ethanol.
6. Wash the system with distilled water.
7. Prime syringes with distilled water, leave it for storage.
8. Clean the end of injector needles with cotton swab soaked in 70 % ethanol.

Table 5
Tecan settings to measure bioluminescence signal

Parameter	Value
Injection volume	50 µl/s
Speed	100 µl/s
Refill speed	100 µl/s
Wait (time)	2 s
Attenuation	None
Integration time	10 s
Settle time	0 s

9. Remove distilled water from chosen pump (A or B).
10. Add prepared luciferase reagent solution to appropriate storage bottle.
11. Prime the pump with luciferase reagent.
12. Using iControl software set the reader for well-wise luminescence measurements and chose appropriate injection needle (A or B). Prepare the protocol of bioluminescence measurement according to Table 5.

3.6 Preparing ATP Standard Serial Dilutions

1. Dilute 16.5 mM ATP standard solution in dilution buffer to obtain 1 µM concentration.
2. Add diluted ATP standard solution from **step 1** to three Eppendorf tubes, 30 µl each. They will serve as the highest concentration of ATP standard curve. Keep prepared solution on ice.
3. Prepare 18 Eppendorf tubes, each containing 27 µl of dilution buffer. Mark them from 10^{-7} to 10^{-12} (6 dilutions × 3 repetitions).
4. Take 3 µl from sample prepared in **step 2**. and add it to the first Eppendorf marked 10^{-7}.
5. Pipette thoroughly and repeat action by taking 3 µl from Eppendorf 10^{-7} and adding them to the one marked 10^{-8}.
6. Repeat this till you reach Eppendorf marked 10^{-12}. From dilution 10^{-12} discard 3 µl.
7. Repeat **steps 5–7** with the rest of marked Eppendorf tubes.
8. Prepare additional three Eppendorf tubes for blank controls, each containing 27 µl of dilution buffer.

3.7 Cell Lysis

1. Add 27 μl of cell lysis reagent to each sample, ATP standard dilutions and blank solutions.
2. Incubate samples for 5 min, RT.

3.8 Measuring ATP Signal

1. Transfer 50 μl from each sample to the black 96-well plate.
2. Immediately, start the measurement on plate reader with previously set protocol (Table 5) based on adding 50 μl of luciferase reagent solution to all of the samples by automated injection and read the signal from each well 2 s after substrate is added.
3. After measurement, backflush the rest of luciferase reagent and aliquot it into Eppendorf tubes. Store in −20 °C. Wash the injection system (**steps 2–11** in part: *Preparing Tecan plate reader injection system*).
4. To calculate ATP concentration subtract the blank values from raw data and calculate results from a log-log plot of the ATP standard curve (exemplary standard curve shown in Fig. 2). Divide received value by the number of cells in a given sample to obtain normalized ATP concentration per single cell (*see* Fig. 3).

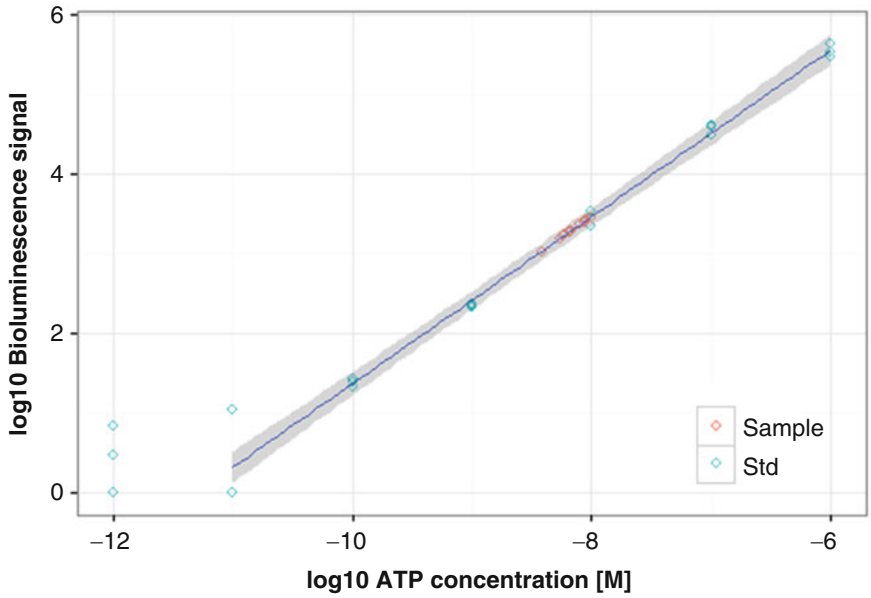

Fig. 2 Exemplary standard curve for calculating ATP concentrations. Points for standard curve shown in blue, points for measured samples with 770–1000 sorted cells (LT-HSC, ST-HSC, and MPP) shown in red. Usually, the 10^{-12} dilution of the standard curve is below the detection limit and is discarded. Note that the signal from sorted samples is located in the middle of the standard curve range what minimize the error when calculating ATP concentration

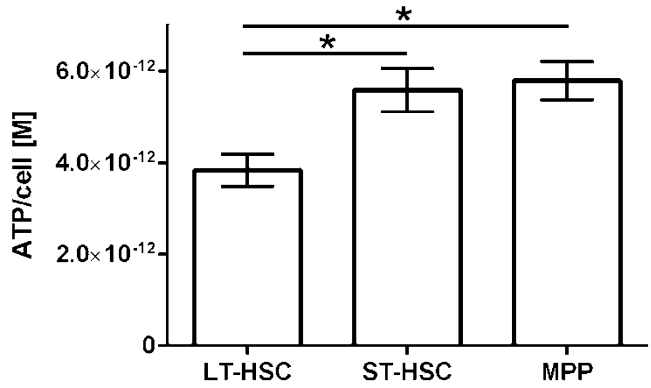

Fig. 3 Typically obtained values of ATP concentration per cell in LT-HSC, ST-HSC and MPP. Note the lower levels of ATP in LT-HSC in comparison to ST-HSC and MPP cells what is consistent with previous report [5]. Mean ± SEM from 6 to 7 measurements per group from two independent experiments

4 Notes

1. Store the RBC lysis buffer as 10× stock solution and prepare fresh 1× working solution before use. The 1× working solution is not stable under longer storage. This buffer was initially proposed for human blood cells [7], but in our hands it works properly also on murine bone marrow and blood cells.
2. Our antibodies panel enables to use a strategy based on MACS columns and MoFlo XDP cell sorter to isolate long term repopulating HSC (LT-HSC) defined as Lineage$^-$c-Kit$^+$Sca-1$^+$CD48$^-$CD150$^+$CD34$^-$. Other antibodies can be used depending on what antibodies sets and cell sorter configuration are available. However, each combination has to be optimized. Please note that fluorochrome used for lineage labeling is next used for depletion on MACS columns. Other markers could be additionally used to isolate LT-HSC: endothelial protein C receptor (EPCR) [8], TEK tyrosine kinase (Tie-2) [9], and endoglin (CD105) [10].
3. LS columns are dedicated for positive selection; however, in our protocol we used them for negative selection of Lineage$^+$ cells. The LD columns are dedicated for depletion and they deplete even weakly stained cells, but they also decrease the total yield of cells in comparison to LS columns. Given that we used magnetic depletion only as a presort before the crucial isolation by cell sorter, we prefer LS columns to obtain maximal number of LT-HSC.
4. Other cell sorters or configuration of lasers and filters can be used; however, each combination has to be verified for optimal cell sorting. Having opportunity to use more laser lines and detectors allows to decrease compensation between selected

channels and increase number of markers possible to detect. The 355 nm UV laser is used for depletion of dead $DAPI^{high}$ cells. Instead, the 405 nm violet laser can be used. Eventually, if either of these lasers are available, gating out the $DAPI^{high}$ events is not absolutely crucial, as the presented method of isolation results in over 90 % of viable $DAPI^{neg/low}$ cells in LT-HSC gate.

In our hands the 25 mW red diode mounted in some of the MoFlo XDP instruments is not sufficient to provide proper separation of populations shown in the protocol when using APC, Alexa 700 and APC-eFluor 780 dyes. We do recommend to use 642 nm 100 mW laser with separate line with beam shaping optics for satisfactory results.

5. Other plate reader that have option to inject substrate into well of 96-well plate with subsequent readout within given time (1–2 s) can be used.
6. The bones should be dissected within 5–10 min after euthanasia.
7. Cut off the minimal parts of the bones' ends to minimize the loss of bone marrow, but yet big enough to open the bone marrow cavity and insert the 25G needle.
8. It is important to immediately suspend the pellet by pipetting. Adding the RBC lysis buffer onto pellet without proper suspending may result in excessive cell clumps.
9. Take into consideration that some residual volume always remains in the tube after supernatant is discarded, therefore check what volume is left and add the buffer to obtain final volume of 100 μl. To reduce residing volume use the Pasteur pipette attached to aspiration pump rather than inverting the tube up-side down.
10. The depletion of lineage positive cells on MACS, before the separation by cell sorter, is not obligatory. However, depletion of lineage positive cells, that constitute the majority of bone marrow cells, increase the speed, purity and efficiency of subsequent cell sorting of rare cell populations such as hematopoietic stem cells. Therefore we suggest magnetic depletion before cell sort.
11. Cells are stained with set of antibodies for lineage committed cells which are conjugated with PE dye for subsequent depletion of lineage positive cells. We recommend to first stain the cells for lineage antigens, and then perform the depletion with anti-PE magnetic beads and then stain for other antigens. Staining for all antigens together followed by MACS depletion is not recommended, as anti-PE beads may bind also PE-Cy7

tandem dye what leads to the loss of cells stained with Sca-1-PE-Cy7 antibody.

12. When analyzing bone marrow from several mice, we recommend to use three Midi Separators simultaneously or Quadro Separator to speed up the process.
13. In case one wants to analyze also the lineage positive cells, remove the columns from the separator, place over new collection tube, add 5 ml MACS buffer to the column and flush using the plunger provided with columns.
14. Transferring the cell suspension to 1.5 ml Eppendorf tube helps to sort maximal volume possible when sorting on MoFlo XDP with Smart Sampler. In case one uses other cell sorter this may not be necessary.
15. It is crucial to have the sorter well calibrated and drop delay very stable during the sort. We use the "Purify" mode with 1.0 drop envelope settings on MoFlo XPD cell sorter. Make sure that the deflected streams hits the surface of 23 μl dilution buffer placed in 1.5 ml buffer. When using MoFlo sorter, place the Eppendorf tubes on top of 5 ml polypropylene FACS tubes that are placed in the two middle positions in the FACS tubes' rack. This makes the way of deflected stream shorter and decreases the chance that the sorted drop will not reach the dilution buffer.
16. In our hands sorting of 1000 cells to 23 μl of dilution buffer results in final volume of ~27 μl. However, this may vary when a different sorter is used. Therefore, it is reasonable to check how much volume is added to the sample when 1000 cells are sorted to achieve final volume of 27 μl after the sort.
17. If possible, keep the same number of sorted cells between samples. We recommend 1000 cells per sample. By sorting 1000 cells it is possible to have duplicate or even triplicate from one 8–12-week-old mice (older mice have more LT-HSC and therefore even more samples can be sorted). You can measure ATP signal from smaller number of cells and afterwards normalize the signal to number of sorted cells but we do not advise going below 500 cells.
18. It is advised to perform this step right before measurements as to not leave luciferase reagent in room temperature for too long. For priming, choose the lowest volume possible.

Acknowledgments

The research was supported by the following grants: HARMONIA (NCN 2015/18/M/NZ3/00387) granted to Alicja Jozkowicz by Polish National Science Centre and PRELUDIUM (NCN 2013/

11/N/NZ3/00956) granted to Krzysztof Szade by Polish National Science Centre. The Faculty of Biochemistry, Biophysics, and Biotechnology of Jagiellonian University is a partner of the Leading National Research Centre (KNOW) supported by the Ministry of Science and Higher Education.

References

1. Bryder D, Rossi DJ, Weissman IL (2006) Hematopoietic stem cells: the paradigmatic tissue-specific stem cell. Am J Pathol 169:338–346. doi:10.2353/ajpath.2006.060312
2. Weissman IL (2000) Stem cells: units of development, units of regeneration, and units in evolution. Cell 100:157–168
3. Wilson A, Laurenti E, Oser G et al (2008) Hematopoietic stem cells reversibly switch from dormancy to self-renewal during homeostasis and repair. Cell 135:1118–1129. doi:10.1016/j.cell.2008.10.048
4. Suda T, Takubo K, Semenza GL (2011) Metabolic regulation of hematopoietic stem cells in the hypoxic niche. Cell Stem Cell 9:298–310. doi:10.1016/j.stem.2011.09.010
5. Takubo K, Nagamatsu G, Kobayashi CI et al (2013) Regulation of glycolysis by Pdk functions as a metabolic checkpoint for cell cycle quiescence in hematopoietic stem cells. Cell Stem Cell 12:49–61. doi:10.1016/j.stem.2012.10.011
6. Kricka LJ, Wienhausen GK, Hinkley JE, De Luca M (1983) Automated bioluminescent assays for NADH, glucose 6-phosphate, primary bile acids, and ATP. Anal Biochem 129:392–397
7. McCoy JP (2001) Handling, storage, and preparation of human blood cells. Curr Protoc Cytom Chapter 5:Unit 5.1. doi: 10.1002/0471142956.cy0501s00
8. Balazs AB, Fabian AJ, Esmon CT, Mulligan RC (2006) Endothelial protein C receptor (CD201) explicitly identifies hematopoietic stem cells in murine bone marrow. Blood 107:2317–2321. doi:10.1182/blood-2005-06-2249
9. Arai F, Hirao A, Ohmura M et al (2004) Tie2/angiopoietin-1 signaling regulates hematopoietic stem cell quiescence in the bone marrow niche. Cell 118:149–161. doi:10.1016/j.cell.2004.07.004
10. Chen CZ, Li M, De Graaf D et al (2002) Identification of endoglin as a functional marker that defines long-term repopulating hematopoietic stem cells. Proc Natl Acad Sci 99:15468

Methods in Molecular Biology (2016) 1516: 219–226
DOI 10.1007/7651_2016_362

Published online: 02 June 2016

Growth Factor-Free Pre-vascularization of Cell Sheets for Tissue Engineering

Marina Costa*, Rogério P. Pirraco*, Mariana T. Cerqueira, Rui L. Reis, and Alexandra P. Marques

Abstract

The therapeutic efficacy of tissue-engineered constructs is often compromised by inadequate inosculation and neo-vascularization. This problem is considered one of the biggest hurdles in the field and finding a solution is currently the focus of a great fraction of the research community. Many of the methodologies designed to address this issue propose the use of endothelial cells and angiogenic growth factors, or combinations of both, to accelerate neo-vascularization after transplantation. However, an adequate solution is still elusive. In this context, we describe a methodology that combines the use of the stromal vascular fraction (SVF) isolated from adipose tissue with low oxygen culture to produce pre-vascularized cell sheets as angiogenic tools for Tissue Engineering. The herein proposed approach takes advantage of the SVF angiogenic nature conferred by adipose stem cells, endothelial progenitors, endothelial and hematopoietic cells, and pericytes and further potentiates it using low oxygen, or hypoxic, culture. Freshly isolated nucleated SVF cells are cultured in hyperconfluent conditions under hypoxia ($pO_2 = 5$ %) for up to 5 days in medium without extrinsic growth factors enabling the generation of contiguous sheets as described by the cell sheet engineering technique. Flow cytometry and immunocytochemistry allow confirming the phenotype of the different cell types composing the cell-sheets as well the organization of the $CD31^+$ cells in branched and highly complex tube-like structures. Overall, a simple and flexible approach to promote growth factor-free pre-vascularization of cell sheets for tissue engineering (TE) applications is described.

Keywords: Cell sheets, Vascularization, Hypoxia, Stromal vascular fraction, Adipose tissue, Growth factor-free

1 Introduction

TE approaches using complex and robust designed constructs demand the development of a vascular tree capable of sustaining an efficient supply of oxygen and nutrients required by the transplanted cells. The most common strategies designed to architect robust networks of vessel-like structures prior to implantation involve delivery of angiogenic growth factors and/or culture of endothelial cells [1–7]. However, these strategies are compromised

*Author contributed equally with all other contributors.

by delayed formation and maturation of the newly formed blood vessels. Additionally, but not less important, an adequate source of endothelial cells to be used in such strategies remains elusive. In this context, SVF of the adipose tissue may be considered an extremely valuable tool due to its intrinsic angiogenic potential. A cocktail of angiogenic populations of cells is easily obtained after enzymatic digestion of an expendable and abundant tissue obtained from abdominoplasty or liposuction surgical procedures. These include, among others, endothelial and hematopoietic cells, mesenchymal and endothelial progenitors, pericytes, fibroblasts, and pre-adipocytes [8]. As previously reported [9], the endothelial progenitors and mural cells in this heterogeneous isolate possess the potential to spontaneously reassemble in capillary-like network in vitro. Since SVF cells are thought to reside in the adipose tissue in a confined hypoxic microenvironment ranging from 2 to 8 % of oxygen supply [10], the modulation of oxygen concentrations may be a way to control the spontaneous formation of capillary-like networks.

Moreover, most of stem cell niches hold highly hypoxic conditions with oxygen concentrations considerably lower than the atmospheric values, which contributes for cells to maintain some basic properties such as stemness and proliferative rate [11]. Upon stress oxygen conditions, cellular metabolic activities are mainly regulated by hypoxia-inducible factors (HIFs) [11]. These factors, when stabilized by the lack of dioxygen, regulate the transcription of several genes that induce glycolysis, erythropoiesis, and angiogenesis, being ultimately promoters of angiogenesis [11–13]. Severe hypoxic conditions (<0.1 % O_2) have been shown to increase the production of VEGF-A and angiogenin (ANG) in human adipose-derived stem cells (hASCs) [14]. Increased VEGF secretion by hASCs was also demonstrated under prolonged cultures in hypoxic conditions improving its pro-angiogenic potential [15] to levels similar to those achieved with the addition of angiogenic growth factors [16]. Nevertheless, due to the association of uncontrolled angiogenesis with pathological conditions [17, 18], the balance between the delivery and release of angiogenic growth factors must be well-controlled suggesting that hypoxic conditioning may avoid the need to use of these extrinsic factors.

TE strategies are not only conditioned by an insufficient vascularization but also by potential host response to scaffolding biomaterials [19]. Cell sheet engineering, which involves cell culture in a temperature-responsive polymer until confluence is reached and then the spontaneous detachment, by temperature lowering, of the cells within their own extracellular matrix that acts as a natural scaffold has been proposed as an alternative approach [20]. Strategies using single cell sheets for the treatment cornea and esophagus, and stacked homotypic and heterotypic cell sheets as 3D constructs for repairing cartilage, periodontium and myocardium-damaged

tissues [21] are currently under clinical trials. Thus, merging this highly promising TE concept and hypoxic conditioning that better mimic tissue microenvironments, with the potential of SVF cells, allowed proposing a methodology to obtain highly angiogenic and pre-vascularized cell sheets capable of promoting neo-vascularization of TE constructs without the use of extrinsic growth factors.

2 Materials

2.1 Labware

(*see* **Note 1**)

Beakers (Labbox, Cat. No. BKL3-500-006)

Pipettes (Corning, Cat. No. P8250)

Falcon conical centrifuge tubes (Fisher Scientific, Cat. No. 05-539-13)

Nylon mesh strainer (Cole-Parmer, Cat. No. TW-06786-12)

Forceps (RSG, Cat. No. 311.105)

Cell strainers of 100 μM pore size (Corning, Cat. No. 352360)

15.6 mm diameter 24-well culture sterile plates (Corning, Cat. No. 353047)

Flow cytometry tubes (BD Falcon, Cat. No. 352054)

UP cell 35 mm dishes (VWR, Cat. No. 174904)

2.2 Reagents

Dulbecco's Phosphate-buffered saline (D-PBS) (Life Technologies, Cat. No. 21600)

Phosphate-buffered saline (PBS) (Sigma, Cat. No. P4417)

Collagenase, from *Clostridium histolyticum* (Sigma, Cat. No. C6885)

Distilled water (DiH_2O)

Ammonium Chloride (Merck, Cat. No. 1.01145.1000)

Potassium bicarbonate (Sigma, Cat. No. 237205)

Ethylenediaminetetraacetic acid (EDTA) (Sigma, Cat. No. E6758)

α – MEM medium (Life Technologies, Cat. No. 12000)

Sodium Bicarbonate (Sigma, Cat. No. S5761)

Fetal bovine serum (FBS) (Life Technologies, Cat. No. 10270)

Antibiotic/antimycotic solution (Life Technologies, Cat. No. 15240)

Methylene blue 0.05 wt% in H_2O (Sigma Aldrich, Cat. No. 319112)

Acetic acid (VWR, Cat. No. 20104.334)

CD105 – FITC (Bio-Rad, Cat. No. MCA1557F)

CD73 – PE (BD Biosciences, Cat. No. 550257)

CD90 – APC (BD Biosciences, Cat. No. 559869)

CD45 – FITC (BD Biosciences, Cat. No. 555482)

CD34 – PE (BD Biosciences, Cat. No. 555822)

CD31 – APC (R&D Systems, Cat. No. FAB3567A)

DRAQ5 – (eBioscience, Cat. No. 65-0880-92)

Formaldehyde (VWR, Cat. No. ALFA33314K2)

10 % Neutral Buffered Formalin (Thermo Scientific, Cat. No. 5701)

Triton X-100 (Sigma, Cat. No. X100)

Bovine serum albumin (BSA) (Amresco, Cat. No. 0332)

Rabbit anti-human-mouse CD31 (Abcam, Cat. No. ab28364)

Mouse anti-human CD146 (Abcam, Cat. No. ab24577)

Donkey anti-rabbit 488 (Invitrogen, Cat. No. A21206)

Donkey anti-mouse 594 (Invitrogen, Cat. No. A21203)

4′,6-diamidino-2-phenylindole (DAPI) (Sigma, Cat. No. D9564)

2.3 Reagents Setup

1. Collagenase solution: Make a 0.05 % collagenase type II solution in PBS and filter (0.22 μm pore size).
2. Red blood cells lysis buffer: prepare a 154 mM of ammonium chloride, 10 mM of potassium bicarbonate and 0.1 mM of ethylenediaminetetraacetic acid (EDTA) solution in 1 L of distilled water, filter (0.22 μm pore size) and store at 4 °C.
3. α-MEM medium: Supplement the medium with 10 % of fetal bovine serum and 1 % antibiotic/antimycotic solution, filter (0.22 μm pore size) and store at 4 °C.
4. Cell's counting solution: make a 3 % acetic acid solution in methylene blue 0.05 wt% in H_2O.
5. Acquisition buffer: make a 1 % formaldehyde solution in PBS, filter (0.22 μm pore size) and store it at room temperature (RT).
6. Permeabilization solution: make a 0.2 % triton X-100 solution in PBS
7. Blocking solution: make a 3 % BSA solution in PBS.
8. Dilution solution: prepare a 1 % BSA solution in PBS.
9. CD31 and CD146 working solutions: Dilute 1:50 rabbit anti-human-mouse CD31 and 1:100 mouse anti-human CD146 in dilution solution.
10. Alexa 488 and Alexa 594 working solutions: Dilute 1:500 secondary donkey anti-rabbit 488 and 1:500 secondary donkey anti-mouse 594 in dilution solution.
11. DAPI working solution: Dilute 1:1000 4′,6-diamidino-2-phenylindole (DAPI) in dilution solution.

3 Methods

3.1 Isolation of SVF Cells from Human Adipose Tissue (See Note 1)

1. Transfer Lipoaspirate to a beaker.
2. Wash the adipose tissue with PBS thrice, removing, by pipetting, the blood fraction which deposits on the bottom.
3. Incubate the adipose fraction with collagenase solution at 37 °C for at least 30 min and up to 45 min, under agitation at 160 rpm, until the tissue is sufficiently digested.
4. Remove remnants of connective tissue and blood vessels by filtering digested tissue with a nylon mesh strainer with the assistance of forceps.
5. Centrifuge the digested suspension at 800 × *g*, 4 °C, for 10 min.
6. Discard the supernatant.
7. Incubate the obtained SVF with a red blood cells' lysis buffer for 10 min at RT to lyse erythrocytes.
8. Restore the osmotic equilibrium with the same volume of α – MEM medium.
9. Centrifuge the cell suspension at 300 × *g*, for 5 min, at RT.
10. Resuspend the red blood cells-free SVF in α – MEM medium.
11. Filter the cell suspension with a 100 μm nylon mesh cell strainer.

3.2 Cell Counting and Plating

1. Incubate 20 μl of cell suspension with 180 μl of the cell's counting solution (*see* **Note 2**),
2. Plate 1.05×10^5 nucleated cells/cm^2 in a UP cell 35 mm dish.

3.3 Hypoxic Conditions (pO_2 = 5 %) of Culture

1. Place the plates in a hypoxia modular incubator chamber.
2. Keep the atmosphere humidified by placing a petri dish containing sterile water inside the chamber.
3. Flush it for 6 min with a mixture of 5 % O_2, 5 % CO_2 and 90 % N_2 (*see* **Note 3**).
4. Close all the valves immediately after the flush.
5. Place the hypoxic chamber in the incubator at 37 °C.
6. After 5 and 8 days of culture prepare cells for posterior characterization.

3.4 Analysis

(*see* **Note 4**)

3.4.1 Flow Cytometry (Fig. 1)

1. Pipette 2 μl of each fluorochrome-conjugated antibody, in a flow cytometer tube.
2. Add 100 μl of the cell suspension containing 1×10^5 cells to each tube.

		CELLULAR SURFACE EXPRESSION MARKERS					
Days of culture	Condition	CD105 (%)	CD73 (%)	CD90 (%)	CD45 (%)	CD34 (%)	CD31 (%)
Day 0		20.7	12.3	95.7	12.0	71.4	45.6
Day 5	Hypoxia	93.0	72.5	99.3	4.5	15.0	19.3

Mesenchymal markers Hematopoietic markers Endothelial marker

Fig. 1 Cellular surface expression of mesenchymal markers (CD105, CD73, CD90) and of the hematopoietic (CD45, CD34) and endothelial (CD31) markers determined by flow cytometry for one representative sample

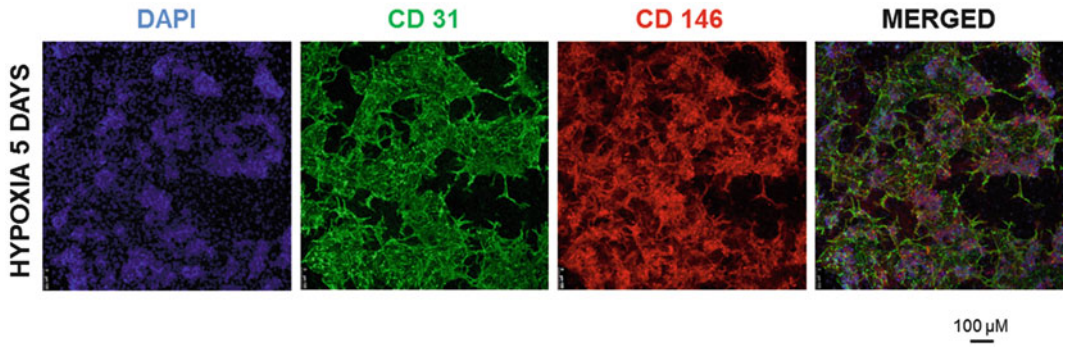

Fig. 2 Representative images of the organization of CD31 (*green*) and CD146 (*red*) expressing cells within the cell sheet after 5 days of culture under hypoxic conditions. Nuclei are shown in *blue*

3. Vortex the tubes.
4. Incubate in the dark during 20 min at RT.
5. Wash thoroughly with PBS.
6. Centrifuge at 350 × *g*, RT, for 5 min.
7. Resuspend cells in acquisition buffer.
8. Acquire data in a flow cytometer.

3.4.2 Immunocytochemistry (Fig. 2)

1. Fix SVF cells in 10 % formalin immediately after each time point, for 30 min.
2. Wash cells with PBS thrice.
3. Incubate cells with a permeabilization solution for 10 min.
4. Wash cells with PBS thrice.
5. During 30 min incubate cells with a blocking solution.
6. Wash cells with PBS thrice.
7. Perform an overnight incubation with CD31 and CD146 working solution.
8. Wash cells with PBS thrice.

9. Incubate cells with Alexa 488 and Alexa 594 working solution for 1 h.
10. Counterstain cell's nuclei with DAPI working solution for 5 min.
11. Analyze results in a fluorescence microscope.

4 Notes

1. All labware was sterilized prior use.
2. For discerning the cells of interest (nucleated) among all erythrocytes and debris, a cell counting solution was used.
3. Flush a second time after 10 min if the amount of culture plates is high.
4. As the SVF includes non-nucleated cells and debris it is advisable the use of DRAQ5 to gate only nucleated cells.

References

1. Li L, Pan S, Ni B et al (2014) Improvement in autologous human fat transplant survival with SVF plus VEGF-PLA nano-sustained release microspheres. Cell Biol Int 38:962–970
2. Perets A, Baruch Y, Weisbuch F et al (2003) Enhancing the vascularization of three-dimensional porous alginate scaffolds by incorporating controlled release basic fibroblast growth factor microspheres. J Biomed Mater Res 65A:489–497
3. Kawamoto A, Asahara T, Losordo DW (2002) Transplantation of endothelial progenitor cells for therapeutic neovascularization. Cardiovasc Radiat Med 3:221–225
4. Kalka C, Masuda H, Takahashi T et al (2000) Transplantation of ex vivo expanded endothelial progenitor cells for therapeutic neovascularization. Proc Natl Acad Sci U S A 97:3422–3427
5. Yamaguchi J, Kusano KF, Masuo O et al (2003) Stromal cell-derived factor-1 effects on ex vivo expanded endothelial progenitor cell recruitment for ischemic neovascularization. Circulation 107:1322–1328
6. Sanz L, Santos-Valle P, Alonso-Camino V et al (2008) Long-term in vivo imaging of human angiogenesis: critical role of bone marrow-derived mesenchymal stem cells for the generation of durable blood vessels. Microvasc Res 75:308–314
7. Santos MI, Unger RE, Sousa RA et al (2009) Crosstalk between osteoblasts and endothelial cells co-cultured on a polycaprolactone-starch scaffold and the in vitro development of vascularization. Biomaterials 30:4407–4415
8. Planat-Benard V, Silvestre J-S, Cousin B et al (2004) Plasticity of human adipose lineage cells toward endothelial cells: physiological and therapeutic perspectives. Circulation 109:656–663
9. Koh YJ, Koh BI, Kim H et al (2011) Stromal vascular fraction from adipose tissue forms profound vascular network through the dynamic reassembly of blood endothelial cells. Arterioscler Thromb Vasc Biol 31:1141–1150
10. Ivanovic Z (2009) Hypoxia or in situ normoxia: the stem cell paradigm. http://www.ncbi.nlm.nih.gov/pubmed/19160417
11. Haque N, Rahman MT, Abu Kasim NH et al (2013) Hypoxic culture conditions as a solution for mesenchymal stem cell based regenerative therapy. Sci World J. 2013;2013: 632972. doi: 10.1155/2013/632972
12. Lin Q, Yun Z (2015) The hypoxia-inducible factor pathway in adipocytes: the role of HIF-2 in adipose inflammation and hypertrophic cardiomyopathy. Front Endocrinol 6:1–7
13. Karuppagounder SS, Ratan RR (2012) Hypoxia-inducible factor prolyl hydroxylase inhibition: robust new target or another big bust for stroke therapeutics? J Cereb Blood Flow Metab 32:1347–1361
14. Hsiao ST, Lokmic Z, Peshavariya H et al (2013) Hypoxic conditioning enhances the angiogenic paracrine activity of human adipose-derived stem cells. Stem Cells Dev 22:1614–1623

15. Rasmussen JG, Frøbert O, Pilgaard L et al (2011) Prolonged hypoxic culture and trypsinization increase the pro-angiogenic potential of human adipose tissue-derived stem cells. Cytotherapy 13:318–328
16. Bhang SH, Cho SW, Lim JM et al (2009) Locally delivered growth factor enhances the angiogenic efficacy of adipose-derived stromal cells transplanted to ischemic limbs. Stem Cells 27:1976–1986
17. Carmeliet P (2005) VEGF as a key mediator of angiogenesis in cancer. Oncology 69:4–10. doi:10.1159/000088478
18. Hu B, Cheng S-Y (2009) Angiopoietin-2: development of inhibitors for cancer therapy. Curr Oncol Rep 11:111–116
19. Karp JM, Sock G, Teo L (2009) Review mesenchymal stem cell homing: the devil is in the details. Stem Cell 4:206–216
20. Yamato M, Okano T (2004) Cell sheet engineering. http://linkinghub.elsevier.com/retrieve/pii/S1369702104002342
21. Owaki T, Shimizu T, Yamato M et al (2014) Cell sheet engineering for regenerative medicine: current challenges and strategies. http://www.ncbi.nlm.nih.gov/pubmed/24964041

Methods in Molecular Biology (2016) 1516: 227–241
DOI 10.1007/7651_2016_329

Published online: 01 April 2016

In Vitro Culture of Human Hematopoietic Stem Cells in Serum Free Medium and Their Monitoring by Flow Cytometry

Marc Cloutier, Christine Jobin, Carl Simard, and Sonia Néron

Abstract

Hematopoietic stem cells can be isolated from human blood cells trapped in leukoreduction systems. The leukoreduction systems filters or chambers are usually discarded from routine blood or platelet donations in blood banks around the world. These CD34+ cells are a good source of normal stem cells and can be used as models to characterize the blood stem cells before and after culture in vitro. This chapter contains detailed methodologies for the isolation of stem cells from peripheral blood, the culture of these cells in a medium exempt of animal proteins and for the flow cytometry analysis of the resulting cell population for the characterization of their differentiation

Keywords: Adult CD34+ cells, Hematopoietic progenitors, Stem cell expansion, Animal protein free medium, Flow cytometry, Multiparametric methods, SPADE

1 Introduction

For cellular therapy involving reconstitution of hematopoietic system, the main sources of hematopoietic stem cells are mobilized peripheral blood, bone marrow, and cord blood.

The $CD34^+$ cell dose necessary for successful engraftment varies greatly in those three sources. Bone marrow stem cells were the first to be used for regenerative medicine in 1999 [1]. Bone marrow $CD34^+$ doses are highly variable ranging from 0.07 to 19×10^6 cells/kg [2] (*see* **Note 1**). In fact, it is strictly related to the volume that can be collected from the donors. Conversely, mobilized peripheral $CD34^+$ cells are used at $2.5–11 \times 10^6$ $CD34^+$ cells/kg [3] and cord blood optimal number is equal or higher than 0.6×10^6 CD34+ cells/kg [4]. Although the cell dose required when using cord blood is the lowest, the small number of hematopoietic stem cells per cord blood unit limits their use to children or low weight patients (<40 Kg) [5, 6]. For this reason, expansion of $CD34^+$ cells from cord blood is intensely studied to extend their utilization to adult patients.

Hematopoietic stem cells are present in very low proportions in peripheral blood of healthy adults. In average, 0.01–0.06 % of circulating leukocytes are $CD34^+$ cells, giving about 1×10^3 to 4×10^3 CD34+ cells per mL of blood [7, 8]. Blood $CD34^+$ cells can be obtained in greater amounts by collecting larger volumes of blood (400–500 mL), or by recovering the cells trapped into leukoreduction filters [9] or leukoreduction chambers [10]. The interest in these leukoreduction systems is that thousands of them are generated and discarded each day in blood banks around the world. Consequently, several groups interested in promoting the use of peripheral $CD34^+$ cells in cell therapy are working on their ex vivo expansion to increase their numbers [11–14].

Routine platelet donations generate leukoreduction units, which contain up to 3×10^6 $CD34^+$ cells [14] that can be isolated following standard Ficoll centrifugation and positive selection with magnetic beads. The $CD34^+$ cells are then cultured using a home-made medium containing no animal proteins except for human albumin [14, 15]. The use of a culture medium for which all components are defined, allows minimizing undesired influences on the study of the $CD34^+$ cells.

For the fine characterization of the culture product, we use six to eight phenotypical markers. As a first step, 2-dimensional analysis was used to see the major populations. For the analysis of heterogeneity, we use the software SPADE (Spanning tree progression of density normalized events) available at the Cytobank platform (Cytobank Inc., http://www.cytobank.org) [16, 17].

1.1 Overview of the Chapter

The one-step culture method proposed in this chapter enables the expansion of adult $CD34^+$ cells recovered from peripheral blood. The important point is that these $CD34^+$ cells are collected from blood from healthy individuals in absence of mobilization. These $CD34^+$ cells can thus be obtained from normal blood collection or isolated from leukoreduction systems, which are normally discarded following routine blood product donations in blood banks. The $CD34^+$ cells are directly isolated using a commercially available magnetic positive selection kit targeting $CD34^+$ cells. This chapter also includes the formulation of a custom designed culture medium, which is free from animal protein. This medium can be easily prepared from commercially available components providing a complete knowledge of the constituent and freedom to remove an element or add a substitute. This medium is also functional in atmospheric and physiologic oxygen levels (8 % and less).

The cytokine cocktail proposed here was chosen to minimize the progression of $CD34^+$ cells into erythroid lineage. Nevertheless, we reported that the bias was still present in the resulting cultured cells after 8–12 cultures days confirming the knowledge that the circulating $CD34^+$ cells are already committed to generate red blood cells progenitors [14]. The flow cytometry analysis

procedures are detailed with clones, antibodies and fluorochrome. This information provide a good starting point to assess the heterogeneity of the $CD34^+$ cells directly in blood and after the expansion phase. This chapter also offers valuable information to understand value of the Cytobank tool SPADE, which might appear complex at first, but is indispensable for multiparametric analyses.

2 Materials

2.1 Preparation of Blood Mononuclear Cells and Isolation of CD34+ Cells

Peripheral $CD34^+$-enriched cells are used in this method as a starting source of hematopoietic stem cells and multipotent progenitors. $CD34^+$ cells from other sources can also be used. CD34+ cells can be enriched by any means available. The details provided below describe the technique of positive immunomagnetic purification currently used in our laboratory.

1. Ficoll-Hypaque (1.077 g//mL) isotonic solution (Ficoll-Paque™ PLUS, GE Healthcare, Baie d'Urfé, QC, Canada) for the isolation of MNC from peripheral blood.
2. LeucoSep™ centrifuge tubes (Greiner Bio-One, Monroe, NC, USA).
3. Rinse solution: 10 % Anticoagulant-citrate-dextrose (ACD).
4. A complete EasySep™ separation unit (Stem Cell Technologies, Vancouver, BC, Canada).
5. EasySep™ Human CD34 Positive Selection Kit (Stem Cell Technologies).
6. Cryopreservation medium: 40 % fetal bovine serum (Life Technologies, Burlington, ON, Canada) and 10 % Dimethylsulfoxide (DMSO, Sigma-Aldrich) in Iscove's modified Dulbecco medium (IMDM, Life Technologies).
7. 15- and 50-mL polypropylene centrifuge tubes (Falcon Becton Dickinson Labware, Franklin Lakes, NJ, USA).
8. 2-mL cryotubes (VWR International, Mississauga, ON, Canada).
9. Hank's balanced salt solution (HBSS, Life Technologies)–10 % anticoagulant citrate-dextrose (ACD, Baxter Healthcare Corp., Deerfield, IL, USA).
10. 0.4 % trypan blue solution (Invitrogen).
11. Automated cell counter or hemacytometer (Hausser Scientific, Horsham, PA, USA).
12. CoolCell LX freezing system (Biocision, Mill Valley, CA, USA).
13. Thawing solution: PBS with 50 % fetal bovine serum (FBS, Life Technologies).
14. PBS with 1 mM EDTA and 4 % human serum albumin (HSA, CSL Behring, Ottawa, ON, Canada)

2.2 $CD34^+$ Cells Proliferation

1. Enriched $CD34^+$ cells in suspension, obtained following the procedure in Section 3.1.
2. Human recombinant cytokines (SCF, Flt-3L, TPO, IL-6, IL-3 (Peprotech, Rocky Hill, NJ, USA)). Aseptically reconstitute each cytokine at 10 μg/mL in PBS–1 % HSA. Mix and dissolve well before aliquoting. Store at −35 °C and avoid multiple freezing-thawing.
3. Animal protein-free medium: 10 μg/mL insulin (Life Technologies), 20 μg/mL LDL (Stem Cell Technologies), 200 μg/mL holo-transferrin (BD Biosciences, San Jose, CA, USA), 250 μg/mL HSA, 100 μM Trolox (Sigma-Aldrich) and 0.125 % chemically defined lipid mixture 1 (Sigma-Aldrich) in IMDM. Cytokine supplementation: 10 ng/mL SCF, 25 ng/mL Flt-3L, 30 ng/mL TPO, 20 ng/mL IL-3.
4. 0.4 % trypan blue solution (Life Technologies).
5. Automated cell counter or hemocytometer (Hausser Scientific).
6. 6-well and 24-well cell culture microplates (Costar, Corning Inc., Corning, NY, USA, or Becton Dickinson labware).
7. 25 and 75 cm^2 cell culture T-flasks (Corning Inc or any other manufacturer).
8. 15 and 50 mL polypropylene centrifuge tubes (Falcon).

2.3 Detection and Quantification of Progenitors

1. Methylcellulose-based medium Methocult™ Optimum H4034 (Stem Cell Technologies.
2. 6-well cell culture microplates (Costar, Corning Inc., Corning, NY, USA, or Becton Dickinson labware).
3. Sterile polypropylene centrifuge tubes (Falcon).
4. 0.4 % trypan blue solution (Life Technologies).
5. Automated cell counter or hemacytometer (Hausser Scientific).
6. Vortex.
7. Inverted microscope for colony counting.
8. Incubator set at 37 °C with 5 % CO_2 in air and ≥95 % humidity.

2.4 Flow Cytometry

1. 7-amino-actinomycin D (7-AAD, Beckman Coulter Inc., Mississauga, ON, Canada).
2. Anti-mouse Igκ negative control compensation particles (BD Biosciences).
3. Stem Cell Enumeration Kit (BD Biosciences).
4. Fluorochrome-coupled human antibodies from BD Biosciences, Miltenyi (San Diego, Ca, USA) and eBiocience (San Diego, CA, USA), *see* Table 1.

Table 1
List of antibodies used for the phenotyping of the cells

Panel	Marker	Fluorochrome	Detector[a]	Clone	Supplier
Multipotent	CD45	FITC	FL1	HI30	BD Biosciences
	CD34	PE	FL2	581	BD Biosciences
	CD133	APC	FL5	293C3	Miltenyi Biotec
	CD38	Efluor 450	FL7	HB7	eBioscience
	CD90	Brillant violet 510	FL8	5E10	BD Biosciences
Progenitors	CD45RA	FITC	FL1	HI100	BD Biosciences
	CD123	PE	FL2	6H6	eBioscience
	CD71	PE-Cy7	FL4	OKT9	eBioscience
	CD135	APC	FL5	4G8	BD Biosciences
	CD45	APC-H7	FL6	2D1	BD Biosciences
Differentiated	CD33	FITC	FL1	HIM3-4	BD Biosciences
	CD235a	PE	FL2	HIR2	BD Biosciences
	CD13	PE-Cy7	1.1.1 FL4	1.1.2 WM15	BD Biosciences
	CD14	APC	FL5	M5E2	BD Biosciences
	CD41a	Brillant Violet 421	FL8	HIP8	BD Biosciences
All panels	Dead cells	7-AAD	FL3	NA	Beckman Coulter or BD Biosciences

[a]Detectors are given only as indication and these are settings for a flow cytometer CyFLOW ML (Partec, Germany)
7-AAD (7-aminoactinomycin D)

5. Flow cytometers (Partec CyFlow ML flow cytometer, Swedesboro, NJ, USA and BD Biosciences Accuri C6).
6. Centrifuge microtubes, 1.5 mL (Axygen Scientific, Union City, CA, USA).
7. 5 mL polystyrene FACS tubes (Sarstedt AG & Co., Nümbrecht, Germany).
8. FCS Express 5 software (De Novo Software, Thornhill, ON, Canada).
9. SPADE software (Cytobank, http://www.cytobank.org/).

3 Methods

3.1 Preparation of Mononuclear Cells

This method describes how to use leukoreduction chamber. However it can also be used with any sources of peripheral blood CD34+ cells. Blood samples present in leukoreduction chambers are kept stored at room temperature until process (*see* **Note 2**). Peripheral blood mononuclear cells from leukoreduction chambers are isolated on a Ficoll-Hypaque density gradient and cryopreserved.

1. Prepare a HBSS-10 % ACD solution (*see* **Note 3**). This solution will be used to extract the blood from the leukoreduction

chambers and to wash the cells. This solution can be prepared the day before and stored at room temperature.

2. Prepare two LeucoSep™ tubes per blood sample: add 15 mL Ficoll-Hypaque per LeucoSep tube and centrifuge at 1000 × *g*, 1 min at room temperature.
3. Leukoreduction chambers preparation:
   (a) Attach the chamber to a support, larger ring downward.
   (b) Clean the chamber with alcohol swabs.
   (c) Cut both the upper and the lower tube segments with sterile scissors, starting with the upper segment.
   (d) Place a 50 mL centrifuge tube underneath the chamber.
   (e) Place a 60 mL syringe coupled to a 22½ needle into the top opening and fill it with 40 mL HBSS-10 % ACD.
   (f) Slowly push the solution through the chamber using the piston.
4. Divide the blood-HBSS-ACD solution into the two LeucoSep™ tubes prepared in **step 2** above.
5. Centrifuge for 8 min, at 1000 × *g* without brakes, at room temperature.
6. After centrifugation, recover the interface in a separate 50 mL centrifuge tube and add HBSS-10 % ACD solution to bring to 50 mL. Take a sample for a cell count.
7. Centrifuge for 6 min at 230 × *g* at room temperature.
8. Count the cells using a hemocytometer or an automatic cell counter.
9. Resuspend the pellet with cold cryopreservation medium (4 °C) (*see* **Note 4**) at a density of approximately 100 × 10^6 cells/mL.
10. Prepare 1 mL aliquots of the suspension into cryotubes.
11. Place the cryotubes in a Coolcell container and place the container at −80 °C for approximately 18 h before transferring the cryotubes into liquid nitrogen.

3.2 Magnetic Labeling and CD34⁺ Cell Separation

$CD34^+$-enriched cells can be obtained by several means. Many commercial kits are available for this purpose. The protocol described here was developed with $CD34^+$ cells isolated from thawed MNC by positive selection using the EasySep™ human CD34 positive selection kit (Stem Cell Technologies) following manufacturer's instructions.

1. Thaw cryopreserved MNC in a 37 °C water bath. Do not let the sample thaw completely. Remove from the water bath as soon as it gets slushy (*see* **Note 5**).
2. Slowly transfer cells into 15 mL cold PBS–50 % FBS (*see* **Note 6**).

3. Centrifuge for 6 min at 230 × *g* at room temperature.
4. Remove the supernatant and resuspend the pellet in PBS containing 1 mM EDTA and 4 % HSA.
5. Take a sample to count the cells and assess viability.
6. Complete the volume to a cellular density of 5×10^7 cells/mL.
7. Purify The $CD34^+$ population using the EasySep™ human CD34 positive selection kit following manufacturer's instructions.
8. Following purification, cells can be aliquoted and cryopreserved or cultured.

3.3 Ex Vivo Expansion of $CD34^+$-Enriched Cells

Cells are cultured in the animal protein-free medium described in Section 2.2. This is a basic medium allowing the proliferation of primitive stem cells with a minimum of differentiation. However, we recommend running tests with various cytokine cocktails depending on the objective of the research (*see* **Note 7**).

Cultures are usually performed in 24-well tissue culture plates with volumes ranging from 0.7 to 1.0 mL. We recommend using only the central wells and to fill the peripheral wells with either basic medium without cytokine, or with PBS in order to avoid evaporation, which would lead to density overestimation. The cultures can also be performed in other types of plates or flasks by keeping the same volume-to-culture surface ratio.

Cultures were performed at standard (18 %) and physiological oxygen level, namely 8 % O_2 [18, 19] (*see* **Note 8**). When using oxygen tensions lower than standard culture conditions (18 % O_2), culture medium should be pre-equilibrated in the incubator set at the desired oxygen tension at least 4 h to overnight [18, 20]. It is critical to limit the exposure to atmospheric O_2, thus, the periods out of the incubator should be kept to a minimum.

1. Resuspend the cells in culture medium to seed them at a density of 1×10^5 cells/mL.
2. Harvest a sample to measure the cell density and viability either with a hemocytometer or automatic cell counter.
3. Incubate at 5 % CO_2 and at the standard (18 %) or physiologic (8 %) oxygen tension.
4. The cells are usually cultured 7–10 days.
5. Flow cytometry (Section 3.4) and cell counts are usually performed on days 0, 4 and 7 to assess cell differentiation and expansion.
6. After each cell harvest, count the cells and assess viability by trypan blue 0.4 % (v/v) exclusion or using an automated cell counter.

7. After 4 days, gently mix the cell suspension by pipetting up and down. After cell count, add fresh culture medium to reach 5×10^5 cells/mL
8. At the end of the culture, harvest cells by mixing the cultures thoroughly. For low volume cultures, use P1000 micropipette and perform 10–15 gentle ups and downs. For larger cultures, use a serological 5 or 10 mL serological pipette.

3.4 Culture Analysis

For a quantitative monitoring and phenotypic determination of the purified and cultured cells, flow cytometry is used (*see* Section 3.4.1) while the various progenitors populations can be measured using colony assays (*see* Section 3.4.2).

3.4.1 Flow Cytometry

Phenotypical analysis by flow cytometry is carried out using different panels aiming at identifying different targets. For a quantitative determination of the $CD34^+$ cell population in the isolate or in the culture, cells are stained and analyzed following the ISHAGE protocol [21, 22]. Three more antibody panels are also used in order to better characterize the population in the culture. These panels aim at identifying multipotent, progenitor or differentiated cells. The panels are presented in Table 1. We also present an alternative for an objective assessment of cellular heterogeneity from single-cell measurements using SPADE (Section 3.4.1.3).

Determination of $CD34^+$ Cells Concentrations and Proportions

Absolute numbers of CD34+ cells in the freshly purified cell suspension or in the culture can be obtained by flow cytometry using the guidelines for the ISHAGE protocol [21].

1. Add 20 μL of the anti-CD34 PE/anti-CD45 FITC mix and 20 μL of 7-AAD in a Trucount tube (Stem Cell Enumeration Kit).
2. Sample 100 μL of the cell suspension and transfer into the Trucount tube. Alternatively, cells can be diluted in culture medium or PBS to a final volume of 100 μL.
3. Incubate for 20 min at room temperature away from light.
4. Add 360 μL PBS.
5. Acquire data on a flow cytometer as soon as possible as the cells are not fixed.
6. Analyze data following the basic gating system illustrated in Fig. 1.
7. The $CD34^+$ cell concentration (cells/μL) in the cell suspension:
   CD34+ concentration:

$$\frac{(\text{events in P3} \times \#\text{ beads per } \mu\text{L} \times \text{dilution factor})}{\#\text{ beads measured}}$$

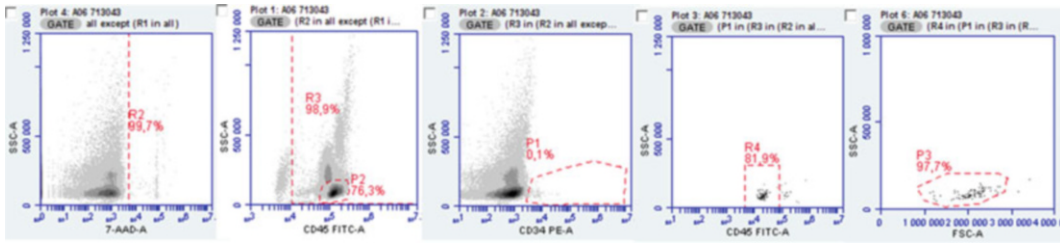

Fig. 1 Gating strategy adapted from the ISHAGE guidelines. $CD34^+$ cells are obtained with the P3 gate. R2 identifies the viable cells while R3 identifies leukocytes among the viable cells. Gate P1 identifies $CD34^+$ cells among viable leukocytes. Percentage of viable CD34+ cells is obtained by dividing the number of cells in the P3 region by the number of events in the R3 region

Flow Cytometry Analysis of CD34 Phenotypes

Three panels are used in order to characterize the cell suspensions at various steps in the process. The panels and antibodies listed in Table 1 are used to discriminate the cells according to three classifications: multipotent, progenitor, or differentiated cells.

For each panel, we prepared the test tube, one negative control with cells only (no antibody), five tubes for fluorescence minus one (FMO) controls and one FMO tube with all antibodies except 7-AAD. In the FMO control tubes, all antibodies, except the one of interest, are added to the cells [23]. Thus, when all three panels are performed, 22 tubes are prepared: 1 negative control, 3 test tubes, and 18 FMO controls (*see* **Note 9**).

1. Gently suspend the cells into suspension and transfer the proper number of cells into test tubes (*see* **step 5**). Complete the volume to 100 μL with PBS or culture medium.
2. Add the antibodies according to Table 1 and following the manufacturer's instructions for the volume to be used per 10^6 cells.
3. Incubate 30 min in the dark at room temperature.
4. Wash the cell/antibody mixture by adding 1 mL of PBS buffer. Centrifuge at 1000 × *g* for 5 min. Discard the supernatants and suspend the cell pellets in 0.5 mL of PBS buffer.
5. Proceed to flow cytometry without further delay. For the staining of cryopreserved PBMCs, a minimum of 400 viable CD45lowCD34+ events are acquired in a threshold gate. For the staining of cultured cells, a minimum of 50,000 viable cells are acquired.
6. Compensation beads are also analyzed on the flow cytometers, with the same acquisition settings are for the cells, in order to eliminate the fluorescence overlap when analyzing the acquisition data. Compbeads are stained with antibodies conjugated with each individual fluorochrome used. At this step antibodies can be different from the one used in the panels since only fluorochrome molecules are important for compensation.

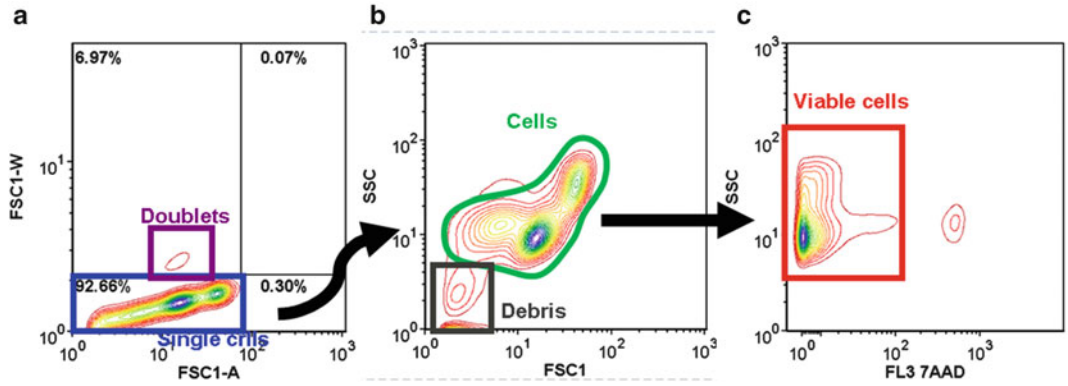

Fig. 2 Gating strategy for the elimination of (**a**) doublet, (**b**) debris and (**c**) dead cells

Compensation beads provide distinct positive and negative populations for which the emission of fluorescence in non specific channels can be eliminated by an algorithm included in the FCS Express software.

7. Analyze the data using FCS Express.
   This software allows a quick two-dimensional analysis, that is to say the analysis of two markers at a time, and allows a hierarchy of regions that fit together in order to specifically target cell populations. Unstained samples, or negative controls, allow the visualization of the autofluorescence levels of the cells. FMO controls are used to distinguish positive events from negative ones and to position the quadrants.
   (a) Prepare a compensation file using the compensation beads data. Apply the compensation on the data files.
   (b) Doublets are excluded according to their FSC-W/FSC-A ratio (Fig. 2a).
   (c) Debris are excluded by delimiting a region in a FSC/SSC histogram as shown in Fig. 2b.
   (d) Among the remaining events, dead cells are also excluded by selecting events negative for 7-AAD (Fig. 2c).
   (e) Proceed to 2D analysis using the FMO controls in order to determine positivity.

SPADE Analysis

Two-D analysis of cytometry data is a powerful tool to characterize cells. However, when many markers are used or when rare events are searched, the task can be tedious. SPADE (Spanning Tree Progression of Density Normalized Events) is an algorithm to analyze and visualize high-dimensional cytometry data [16, 17]. It is included in Cytobank and, alternatively, is also available as a Bioconductor package or a stand-alone program from Peng Qiu's website (http://pengqiu.gatech.edu/software/SPADE2/) (*see* **Note 10**).

SPADE is useful to assess the heterogeneity of the culture and compare it between conditions. SPADE will cluster cells in nodes based on the relative expression of all markers selected for the analysis. Based on their similarities, these nodes will be linked and take the form of a branched tree. Each node is filled with a color representing the intensity of a parameter in function of a defined color scale. The tree can be visualized according to various parameters including the numbers of cell, median fluorescence intensity or the ratio with a control. The number of links between the nodes is proportional to their differences. Or, in other words, the farther apart the nodes are on the tree, the most different they are. The size of the nodes is proportional to their number of events. Thus, by comparing the forms of the trees and the size of the nodes generated under different conditions, it's easy to view how similar or dissimilar the cultures are. In addition, the appearance of new, unexpected, subpopulations will be obvious. These subpopulations would often have been missed by traditional analysis unless looking specifically for them.

By selecting a group of data files as reference for baseline expression, the relative expressions of the markers can also be evaluated and compared. The nodes will then be colored with different hues based on the relative level of expression of the selected markers, as presented in Jobin et al. [14].

3.4.2 Detection and Quantification of Progenitors

The methocult Optimum H4034 (Stem Cell technologies) medium is an in vitro functional assay for enumerating multipotential and lineage committed hematopoietic progenitor cells of cultured cells or cells from other sources (*see* **Note 11**). This semisolid methylcellulose medium contains the cytokines required to allow individual progenitor cells to produce colony forming units (CFU). Progenitor cells of different lineages and maturational stages produce colonies that can be distinguished according to differences in phenotypical traits (size, morphology and cellular disposition and composition): Burst Forming Unit-Erythroid (BFU-E), CFU-erythroid (CFU-E), CFU-granulocyte-macrophage (CFU-GM) and CFU-granulocytes-erythroid-macrophage-megakaryocyte (CFU-GEMM). The number of colonies provides an assessment of the number of viable and functional CFUs in the sample.

1. Freshly isolated $CD34^+$ cells or the cultured cells are gently resuspended.
2. $CD34^+$ cells are counted as described in Section 3.4.1.1.
3. The methylcellulose medium is seeded according to the manufacturer's instructions in 35 mm petri dislos.
4. Two to three different concentrations are plated in order to obtain an optimal range between 25 and 75 colonies per well

after 14 days of incubation. We have found that plating 250 and 500 $CD34^+$ cells tend to produce the most reliable and consistent results.

5. After 14 days of incubation at 37 °C, 5 % CO_2 in air, using a microscope with the proper magnification adjusted on the colony size as CFU-GM and CFU-GEMM tend to be larger. The total number of CFUs is counted according to the manufacturer's instructions.

4 Notes

1. Indications for bone marrow doses are not related to the number of CD34+ cells but to the total nucleated cell (TNC) number. An estimation of about 4×10^8 TNC/kg is usually considered according to a yield of about 0.22×10^8 cells per mL of bone marrow. However, the limiting factor in such transplantation is the maximal volume of bone marrow which can be harvested from the donor. According to the standard of the Foundation for the Accreditation of Cellular Therapy (FACT), clinicians have to enumerate the $CD34^+$ cells, but consider the TNC value to calculate the dose to be received by their patient.
2. When needed, shipping of blood samples has to be done at room temperature. Shipping on ice or at 4 °C could impair the efficiency of Ficoll separation because of platelets aggregation. Large volumes of blood, such as collection bag, can be rapidly cooled at 22 °C by using phase 22 cooling packs as described elsewhere [24]. After collection, blood samples or leukoreduction systems are stable for up to 24 h.
3. Blood samples, in tubes, collection bags, leukoreduction filters and leukoreduction chambers are all supplemented with anticoagulant solutions. It is crucial to maintain the proportion of anticoagulant between 10 % and 12.5 % during the first steps of preparation to optimize the recovery yield.
4. We have used fetal bovine serum in our freezing medium. However, expansion of CD34 cells for cellular therapy production necessitates avoiding components of animal origin. Serum free medium containing DMSO are already used in cord blood banks for the cryopreservation and can be purchased from Alanza Inc (Thornhill, ON, Canada; www.alanzainc.com) or Wak-Chemie (Cryosure-DEX40,WakChemie Medical GMBH, Germany, email: info@wak-chemie.com).
5. Peripheral blood mononuclear cells (PBMC) can be used after the Ficoll step or stored frozen before isolation of the CD34+ cells. Cord blood mononuclear cells can also be stored frozen

and prepared using a DNase A treatment to remove aggregates. This treatment is not recommended for thawed PBMC. In fact, we have tried to add DNase and it has been a source of problems including reduced recovery of PBMC and impairment of CD34+ cells isolation.

6. We have experienced agglutination between beads and cells with the EasySep™ Human CD34 Positive Selection Kit. For this reason, we did not follow manufacturer's instructions regarding the addition of FBS but we have used PBS supplemented with 1 % human albumin and 1 mM EDTA. This modification was also supported by Koizumi's study [25].
7. Long-R3-Insulin-like growth factor (Sigma-Aldrich) can be added to the culture medium. We have tested 15 ng/mL and observed no difference for the progression of CD34+ cells in vitro.
8. To test oxygen levels closer to that of a human body, namely 8 % pO2 we have used culture incubators controlling both CO_2 and oxygen levels, namely Heracell 150i (Thermo Scientific). To verify stability of culture conditions when the door were opened in our routine monitoring of the cells. These incubators have been qualified to operate at 5 % O_2 but could not be qualified for 3 % O_2. The period before to reach equilibrium after opening the doors was too long.
9. Flow cytometry controls such as FMO are often omitted because of a restricted amount of cells. However, since FMO are only used to position the quadrant and establish the positivity, a smaller number of cells can be used to make sure the test tube contains enough events to be analyzed. Often, 2000–5000 events will be enough for a FMO control.
10. At first, SPADE software can appear complex, but we can reassure that SPADE can be used by anyone who is able to understand the basis of flow cytometry. We strongly encourage reading the guide on the use of SPADE in Cytobank. This guide is freely available from the Cytobank website at (http://www.cytobank.org/pdf/fluidigmtutorial_pbmc_2014_digitalcopy.pdf). A tutorial video can also be seen on Youtube video (https://www.youtube.com/watch?v=Cpe_0cxD7_Y). ViSNE, like SPADE is a tool allowing to map flow cytometry data into two dimensions which are calculated by using all parameters assigned to each individual cells [26]. A guide to use this application is available on Cytobank website (http://www.cytobank.org/pdf/visne_tutorial-quickguide-digitalcopy.pdf).
11. The enumeration of BFU-E, CFU-E, CFU-GM, and CFU-GEMM can be eased by consulting the Colony culture medium and scoring procedures section in the Atlas of human hematopoietic colonies. The atlas is available at Stem cell technologies Inc. (http://www.stemcell.com).

Acknowledgement

C.J. owned a BMP-Innovation-Research Scholarship in a practice environment.

References

1. Webb S (2013) Banking on cord blood stem cells. Nat Biotechnol 31:585–588
2. Bittencourt H, Rocha V, Chevret S, Socie G, Esperou H, Devergie A, Dal Cortivo L, Marolleau JP, Garnier F, Ribaud P, Gluckman E (2002) Association of CD34 cell dose with hematopoietic recovery, infections, and other outcomes after HLA-identical sibling bone marrow transplantation. Blood 99:2726–2733
3. Remberger M, Torlen J, Ringden O, Engstrom M, Watz E, Uhlin M, Mattsson J (2015) The effect of total nucleated and CD34+ cell dose on outcome after allogeneic hematopoietic stem cell transplantation. Biol Blood Marrow Transplant 21:889–893
4. Castillo N, Garcia-Cadenas I, Barba P, Martino R, Azqueta C, Ferra C, Canals C, Sierra J, Valcarcel D, Querol S (2015) Post-thaw viable CD45(+) cells and clonogenic efficiency are associated with better engraftment and outcomes after single cord blood transplantation in adult patients with malignant diseases. Biol Blood Marrow Transplant 21:2167–2172
5. Pineault N, Abu-Khader A (2015) Advances in umbilical cord blood stem cell expansion and clinical translation. Exp Hematol 43:498–513
6. Fares I, Chagraoui J, Gareau Y, Gingras S, Ruel R, Mayotte N, Csaszar E, Knapp DJ, Miller P, Ngom M, Imren S, Roy DC, Watts KL, Kiem HP, Herrington R, Iscove NN, Humphries RK, Eaves CJ, Cohen S, Marinier A, Zandstra PW, Sauvageau G (2014) Cord blood expansion. Pyrimidoindole derivatives are agonists of human hematopoietic stem cell self-renewal. Science 345:1509–1512
7. Anderlini P, Korbling M (1997) The use of mobilized peripheral blood stem cells from normal donors for allografting. Stem Cells 15:9–17
8. Herbein G, Sovalat H, Wunder E, Baerenzung M, Bachorz J, Lewandowski H, Schweitzer C, Schmitt C, Kirn A, Henon P (1994) Isolation and identification of two CD34+ cell subpopulations from normal human peripheral blood. Stem Cells 12:187–197
9. Peytour Y, Villacreces A, Chevaleyre J, Ivanovic Z, Praloran V (2013) Discarded leukoreduction filters: a new source of stem cells for research, cell engineering and therapy? Stem Cell Res 11:736–742
10. Néron S, Thibault L, Dussault N, Cote G, Ducas E, Pineault N, Roy A (2007) Characterization of mononuclear cells remaining in the leukoreduction system chambers of apheresis instruments after routine platelet collection: a new source of viable human blood cells. Transfusion 47:1042–1049
11. Peytour Y, Guitart A, Villacreces A, Chevaleyre J, Lacombe F, Ivanovic Z, Praloran V (2010) Obtaining of CD34+ cells from healthy blood donors: development of a rapid and efficient procedure using leukoreduction filters. Transfusion 50:2152–2157
12. Duchez P, Chevaleyre J, Brunet de la Grange P, Vlaski M, Boiron JM, Wouters G, Ivanovic Z (2013) Cryopreservation of hematopoietic stem and progenitor cells amplified ex vivo from cord blood CD34+ cells. Transfusion 53:2012–2019
13. Dietz AB, Bulur PA, Emery RL, Winters JL, Epps DE, Zubair AC, Vuk-Pavlovic S (2006) A novel source of viable peripheral blood mononuclear cells from leukoreduction system chambers. Transfusion 46:2083–2089
14. Jobin C, Cloutier M, Simard C, Neron S (2015) Heterogeneity of in vitro-cultured CD34+ cells isolated from peripheral blood. Cytotherapy 17:1472–1484
15. Néron S, Roy A, Dumont N, Dussault N (2011) Effective in vitro expansion of CD40-activated human B lymphocytes in a defined bovine protein-free medium. J Immunol Methods 371:61–69
16. Bendall SC, Simonds EF, Qiu P, Amir el AD, Krutzik PO, Finck R, Bruggner RV, Melamed R, Trejo A, Ornatsky OI, Balderas RS, Plevritis SK, Sachs K, Pe'er D, Tanner SD, Nolan GP (2011) Single-cell mass cytometry of differential immune and drug responses across a human hematopoietic continuum. Science 332:687–696
17. Qiu P, Simonds EF, Bendall SC, Gibbs KD Jr, Bruggner RV, Linderman MD, Sachs K, Nolan GP, Plevritis SK (2011) Extracting a cellular hierarchy from high-dimensional cytometry data with SPADE. Nat Biotechnol 29:886–891

18. Wenger RH, Kurtcuoglu V, Scholz CC, Marti HH, Hoogewijs D (2015) Frequently asked question in hypoxia research. Hypoxia 3:35–43
19. Jez M, Rozman P, Ivanovic Z, Bas T (2015) Concise review: the role of oxygen in hematopoietic stem cell physiology. J Cell Physiol 230:1999–2005
20. Newby D, Marks L, Lyall F (2005) Dissolved oxygen concentration in culture medium: assumptions and pitfalls. Placenta 26:353–357
21. Sutherland DR, Anderson L, Keeney M, Nayar R, Chin-Yee I (1996) The ISHAGE guidelines for CD34+ cell determination by flow cytometry. International Society of Hematotherapy and Graft Engineering. J Hematother 5:213–226
22. Keeney M, Chin-Yee I, Weir K, Popma J, Nayar R, Sutherland DR (1998) Single platform flow cytometric absolute CD34+ cell counts based on the ISHAGE guidelines. International Society of Hematotherapy and Graft Engineering. Cytometry 34:61–70
23. Roederer M (2001) Spectral compensation for flow cytometry: visualization artifacts, limitations, and caveats. Cytometry 45:194–205
24. Thibault L, Beausejour A, Jacques A, Ducas E, Tremblay M (2014) Overnight storage of whole blood: cooling and transporting blood at room temperature under extreme temperature conditions. Vox Sang 106:127–136
25. Koizumi K, Sawada K, Sato N, Yamaguchi M, Nishio M, Tarumi T, Takano H, Fukada Y, Ieko M, Yasukouchi T, Sekiguchi S, Koike T (1999) Large scale purification of human blood CD34(+) cells using a nylon-fiber syringe system and immunomagnetic microspheres. Cytotherapy 1:319–327
26. Amir el AD, Davis KL, Tadmor MD, Simonds EF, Levine JH, Bendall SC, Shenfeld DK, Krishnaswamy S, Nolan GP, Peer D (2013) viSNE enables visualization of high dimensional single-cell data and reveals phenotypic heterogeneity of leukemia. Nat Biotechnol 31:545–552

Methods in Molecular Biology (2016) 1516: 243–255
DOI 10.1007/7651_2016_327

Published online: 10 April 2016

Aerosol-Based Cell Therapy for Treatment of Lung Diseases

Egi Kardia, Nur Shuhaidatul Sarmiza Abdul Halim, and Badrul Hisham Yahaya

Abstract

Aerosol-based cell delivery technique via intratracheal is an effective route for delivering transplant cells directly into the lungs. An aerosol device known as the MicroSprayer® Aerosolizer is invented to transform liquid into an aerosol form, which then can be applied via intratracheal administration for drug delivery. The device produces a uniform and concentrated distribution of aerosolized liquid. Using the capability of MicroSprayer® Aerosolizer to transform liquid into aerosol form, our group has designed a novel method of cell delivery using an aerosol-based technique. We have successfully delivered skin-derived fibroblast cells and airway epithelial cells into the airway of a rabbit with minimum risk of cell loss and have uniformly distributed the cells into the airway. This chapter illustrates the application of aerosol device to deliver any type of cells for future treatment of lung diseases.

Keywords: Airway epithelial cells, Skin-derived fibroblast, Aerosol delivery, Cell-based therapy, MicroSprayer® Aerosolizer

1 Introduction

The route of therapeutic cell delivery to the target organ, i.e., the lungs, must be very effective in the sense that the technique should be very specific and direct to the target region of the lungs. For this purpose, the application of intratracheal aerosol-based delivery technique is an effective way to deliver transplant cells directly into the lungs to treat patients with lung-related diseases. Intratracheal administration of cells using MicroSprayer® Aerosolizer (PennCentury Inc.) is based on the technology of this device which has tiny jewel components in the very tip of it and the liquid which contain the transplant cells is forced through to produce aerosol by hydraulic pressure [1]. This device also produces a uniform and concentrated distribution of aerosolized liquid. There are many bioactive materials and live viruses, gene therapy viral vectors that have been put through the MicroSprayer which are remains viable. Unlike nebulizers and inhalers used in animal models that being respired in the usual sense, the formulation of aerosols has been designed to consist of small spherical droplets or particles that can penetrate into the airways or lungs periphery,

which then can lead to an optimum delivery of the transplant cells to the lungs. The local administration permits the transplanted cells to be localized directly into the lungs, which makes intratracheal administration a more reliable and efficient. This method also offer significant preclinical and clinical advantages compared with other types of delivery, as indicated by the survival of cells without any sign of stress following aerosolization in vitro [1]. An in vivo approach using aerosolized cell-based therapy might results in a good cell distribution in lungs and provides the evidence that the cells are able to engraft on the site of injured epithelium. For the application of intratracheal aerosol-based cell delivery technique using animal as a model, rabbits are large enough to allow the Microsprayer be easily inserted into tracheal. In large animal models, tracheal diameters and wall thickness is comparable with that of human than in small animal models [2]. In addition, rabbit is phylogenetically closer to primates than are rodents, easy to handle, and readily available, making them a good model for investigating lung related disease [3]. Taken together, this technique allows direct targeting of the lung for clinical intervention and also provides a site-specific source to release therapeutic proteins and/or other cellular products of interest by the retained cells. This technique also have a great impact on the application of cell-based therapy, as it offers advantages over other routes of cell delivery including intravenous, intrapulmonary, and intraoral delivery [4–6]. Although this technique is not described specific cell types of the airway stem cell to be used in aerosol-based cell therapy, it is known the fact that the heterogeneous population of airway epithelial cells resides in tracheobronchial tree of the lungs contribute equally to the potential of lung-epithelial-tissue-specific stem cells that responsible for lung regeneration and repair. Therefore, isolation of specific cell types (tissue specific stem cells) as a source of cells for an aerosol-based cell therapy is highly recommended.

2 Materials

2.1 For Trachea Collection

1. Adult New Zealand white rabbit (weight 2.31 ± 0.33 kg) (*see* **Note 1**).
2. Centrifuge tubes 15 ml.
3. A sterilized instrument pack consisting of the following items: a pair of surgical scissors, two scalpel, blades, two forceps, 3 ml syringe, one 25 G needle, drapes, and sterile gloves.
4. 70 % ethanol.
5. 1× phosphate buffered saline (PBS).
6. Pentobarbital.

2.2 For Isolation of Airway Epithelial Cells (AECs)

1. Tissue culture supplies including petri dish, 25 cm^2 culture flask, and 15 ml centrifuge tubes.
2. A sterilized instrument pack consisting of the following items: two scalpel, blades, and two forceps.
3. Hemocytometer counting chamber.
4. 0.4 % trypan blue solution.
5. Cell strainer with 70 μm mesh.
6. MACSmix™ tube rotator.
7. Minimal essential medium (MEM) free Ca^{2+} Mg^{2+} dissociation solution. This solution contains (100 ml stock): 100 ml sterile dH_2O, 0.37 g $NaHCO_3$, 0.4 g KCl, 0.012 g NaH_2PO_4, 1 μl Fe $(NO_3)_3$ (*see* **Note 2**), 0.01 g sodium pyruvate, 1.2 ml penicillin and streptomycin. The pH of the solution is adjusted to 7.5 in room air with a few drops of concentrated HCl. Then, it is filter-sterilized using 0.22 μm membrane filter. This solution can be stored for months at 4 °C, and −20 °C for long term storage.
8. Pronase.
9. Deoxyribonuclease I (DNase I).
10. 0.25 % trypsin–EDTA.
11. Fetal bovine serum (FBS).
12. Bronchiole Epithelial Growth Medium (BEGM™). BEGM™ is a kit for airway epithelial cells culture. Preparation: add 200 μl bovine pituitary extract, 50 μl hydrocortisone, 50 μl human epidermal growth factor, 50 μl epinephrine, 50 μl transferrin, 50 μl insulin, 50 μl retinoic acid, 50 μl triiodothyronine, and 50 μl gentamycin (comes with the kit) into 500 ml Bronchiole Epithelial Basal Medium (*see* **Note 3**).
13. Red blood cell lysis buffer.
14. Collagen type IV from human placenta, acid soluble. Use a ratio of 5 mg collagen with 50 ml deionized water and 100 μl glacial acetic acid. Stir moderately on a magnetic stirrer at 37 °C until collagen strands are dissolved. The time required for the collagen to dissolve varies. Fifteen to twenty minutes is usually sufficient. Filter-sterilize using 0.22 μm membrane filter. This solution can be stored for months at 4 °C, and −20 °C for long term storage.

2.3 For Skin Collection

1. Adult New Zealand white rabbit (weight 2.31 ± 0.33 kg).
2. 15 and 50 ml centrifuge tubes.
3. A sterilized instrument pack consisting of the following items: a pair of surgical scissors, two scalpel, blades, two forceps, 3 ml syringe, one 25 G needle, drapes, and sterile gloves.

4. Electric clipper vacuum.
5. 70 % ethanol.
6. 1× PBS.
7. Pentobarbital.

2.4 For Skin-Derived Fibroblast Cells (SFCs) Isolation

1. Tissue culture supplies including petri dish, 25 cm^2 culture flask, and 15 ml centrifuge tubes.
2. A sterilized instrument pack consisting of the following items: two scalpel, blades, and two forceps.
3. Hemocytometer counting chamber.
4. 0.4 % trypan blue solution.
5. Cell strainer with 70 μm mesh.
6. MACSmix™ tube rotator.
7. Dispase.
8. 0.25 % trypsin–EDTA.
9. FBS.
10. Dulbecco's Modified Eagle's Medium (DMEM). DMEM is purchased as a premade medium. Preparation: add 5 ml FBS, 0.5 ml gentamycin into 45 ml DMEM to make a complete growth medium.
11. Red blood cell lysis buffer.

2.5 For Aerosol Delivery

1. Tissue culture supplies including 25 cm^2 culture flask, and 15 ml centrifuge tubes.
2. Forceps.
3. Rectal thermometer.
4. MicroSprayer® Aerosolizer Model IA-1B (*see* Fig. 1).

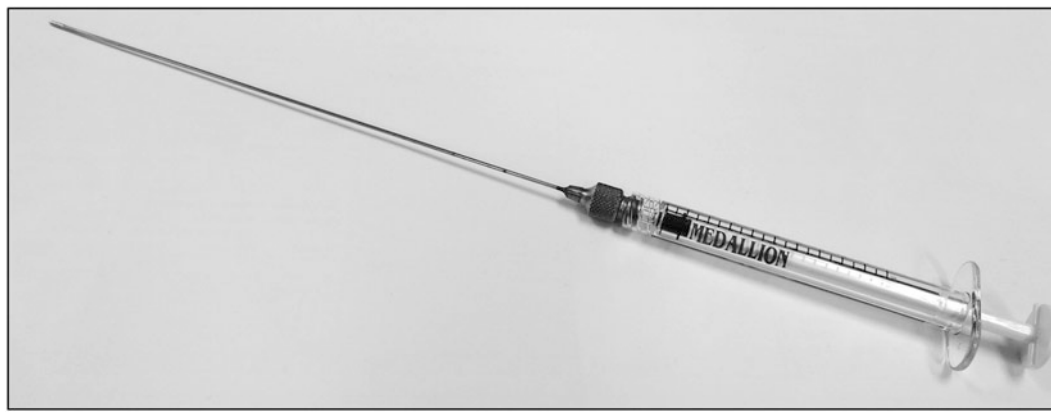

Fig. 1 MicroSprayer® Aerosolizer - Model IA-1B is a device that can transform a liquid into an aerosol form

5. 1 ml polycarbonate syringe (custom-made to fit the Micro-Sprayer® Aerosolizer Model IA-1B) (Penn-Century Inc.).
6. Hemocytometer counting chamber.
7. 0.4 % trypan blue solution.
8. FBS.
9. BEGM™.
10. DMEM.
11. 0.05 and 0.25 % trypsin–EDTA.
12. Endotracheal tube with 7–8 cm length and 2.5 mm diameter.
13. KY Jelly.
14. Eye ointment (Methachlor).
15. Ketamine.
16. Xylazine.

3 Methods

3.1 Trachea Collection

1. Place 10 ml of ice-cold 1× PBS in a 15 ml centrifuge tube.
2. Euthanize the animal with overdose pentobarbital (*see* **Notes 4** and **5**).
3. Open the abdomen by midline incision and exsanguinate the rabbit by cutting the major abdominal arteries.
4. Expose the thoracic cavity by trimming away the diaphragm, cut along the sternum, and maximize access to the lungs by carefully fracturing the ribs.
5. Expose and excise the trachea between the larynx and the bifurcation into the main stem bronchi.
6. Trim off the extraneous fat and connective tissue. Transfer the trachea into a centrifuge tube filled with ice-cold 1× PBS.

   Continue the next procedure under a biosafety cabinet.

3.2 AECs Culture Medium and Substrate Preparation

1. Prepare a collagen-coat culture flask (*see* Section 2.2, **step 14** and **Note 6**).
2. Coat-collagen onto the culture flask surface inside a BSC.
3. Remove the excessive liquid collagen from surface and air-dry the culture flask for overnight.
4. The collagen improves cell attachment efficiency and proliferation.
5. Prepare dissociation medium (medium must be freshly prepared). On the day of use, dissolve pronase and DNase I into the previously prepared stock of MEM free Ca2+ Mg2+

(*see* Section 2.2, **step 7**). In the MEM solution, dissolve 0.034 g pronase and 0.004 g DNase I per 20 ml. Stir to dissolve enzymes and then add 0.2 ml penicillin and streptomycin. Filter-sterilize using 0.22 μm membrane filter.

3.3 Isolation of AECs

1. Transfer the trachea into a petri dish filled with 1× PBS (*see* Fig. 2a).
2. Rinse trachea with 70 % ethanol for a few seconds and followed by 1× PBS for a few seconds.
3. Remove the larynx and all fat tissue surrounding the trachea.
4. Cut the trachea into 1 × 1 cm pieces (*see* Fig. 2b) and transfer them into a 15 ml centrifuge tube.
5. Add 10 ml dissociation medium (*see* Section 3.2, **step 5**) into the centrifuge tube.
6. Place the tube in the MACS mix tube rotator, and store it for 24 h at 4 °C (*see* **Note 7** and Fig. 3).
7. Collect the tissue suspension into a new 15 ml centrifuge tube using cell strainer and place the trachea pieces into a petri dish.
8. Hold the pieces of trachea with a pair of forceps and gently scrape off the epithelial cell layer with a sterile scalpel blade (*see* **Note 8**).
9. Collect the scrapings into the 15 ml centrifuge tube and add 0.25 % trypsin–EDTA.
10. Incubate for 10 min at 37 °C.
11. To end dissociation, add 10 % (v/v) FBS to the dissociation solution. Invert the tube several times to agitate the cell suspension.
12. Filter cell suspension through a 70 μm cell strainer.

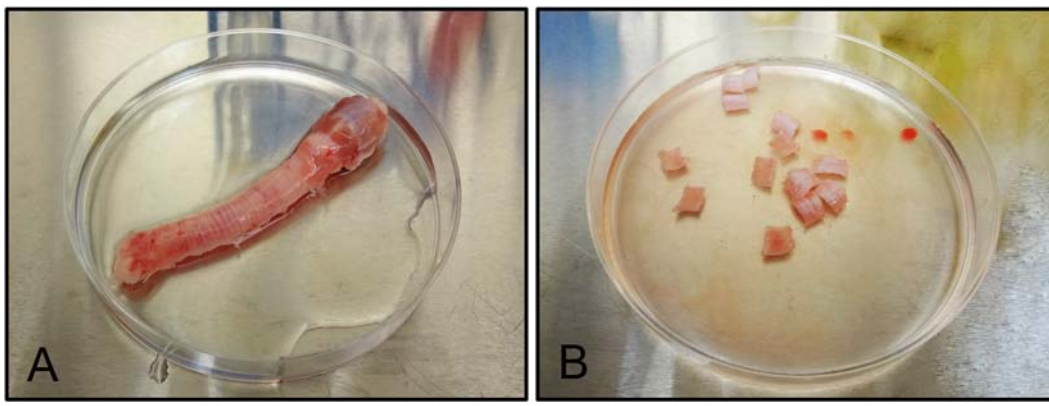

Fig. 2 (**a**) The trachea collected was washed and placed in cold 1x PBS, (**b**) then the trachea was excised into smaller pieces

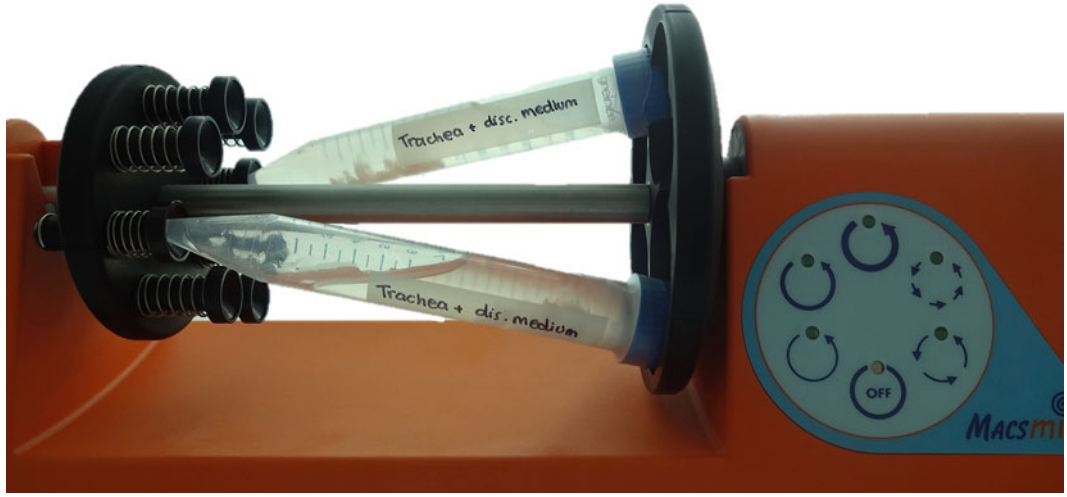

Fig. 3 MACSmix™ tube rotator. The trachea pieces were submerged in dissociation medium and incubated for 24 h at 4 °C

13. Centrifuge the filtrate at 300×*g* for 5 min.
14. Discard supernatant and reconstitute the cell pellet in 1× PBS.
15. Centrifuge the suspension at 300×*g* for 5 min.
16. Discard supernatant and add 1 ml red lysis buffer to remove red blood cells. Repeat this step if red blood cells still present.
17. Centrifuge the suspension cells at 300×*g* for 5 min and reconstitute the cell pellet in BEGM™. Pass the cells several times with the pipette to ensure adequate separation.
18. Observe the isolated cells under a microscope (*see* **Note 9**) and count the total number of cells using a hemocytometer
19. Seed the isolated tracheal epithelial cell suspension onto a collagen-coat 25 cm^2 culture flask at a density of 10^5 cells.
20. Maintain the cells in a humidified incubator with 5 % CO_2 at 37 °C.
21. 24 h post initial seeding, aspirate the BEGM™.
22. Gently wash the adhered cells with 1× PBS and add BEGM™.
23. Change the medium every 2–3 days. Split the cells when 90 % confluent (*see* **Note 10**).

3.4 Skin Collection

1. Place 10 ml of ice-cold 1× PBS in a 50 ml centrifuge tube.
2. Euthanize the animal with overdose pentobarbital (*see* **Notes 4** and **5**).
3. Shave fur from the abdomen with electric clippers.

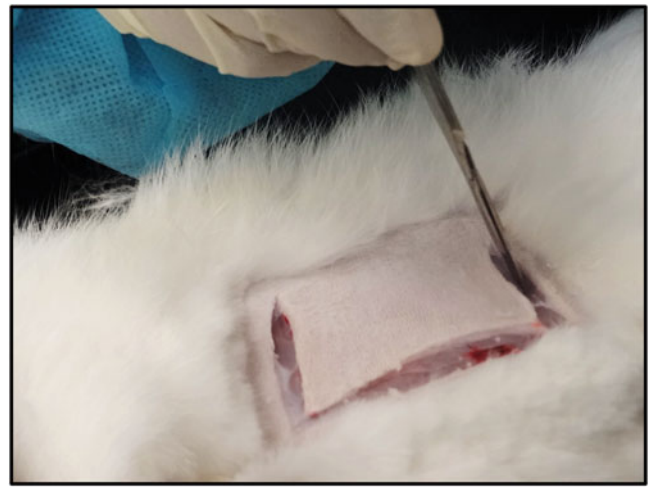

Fig. 4 Incision of rabbit abdomen skin. The fur of the abdomen was shaved with electric clippers

4. Make an incision with a scalpel to collect the exposed skin (*see* Fig. 4).
5. Transfer the trachea into a centrifuge tube filled with ice-cold 1× PBS.
6. Continue the next procedure under a biosafety cabinet.

3.5 SFCs Culture Medium and Suspension Preparation

1. Prepare dissociation medium (medium must be freshly prepared). On the day of use, dissolve 80 mg dispase in 100 ml 1× PBS. Stir to dissolve enzymes and filter-sterilize using 0.22 μm membrane filter.

3.6 Isolation of SFCs

1. Transfer the skin into a petri dish filled with 1× PBS.
2. Rinse skin with 70 % ethanol for a few seconds and followed by 1× PBS for a few seconds.
3. Remove the excessive fat tissue surrounding the skin.
4. Lay the skin onto the bottom of a clean dish, with the dermis facing down.
5. Excise the skin into 1 × 1 cm pieces and transfer them into a 15 ml centrifuge tube.
6. Add 10 ml dissociation medium (*see* Section 3.5, **step 1**) into the centrifuge tube.
7. Place the tube in the MACS mix tube rotator, and store it for 24 h at 4 °C (*see* **Note 7**).
8. Discard the tissue suspension and place the skin pieces into a petri dish.
9. Separate the epidermis away from the dermis using a sterile forceps and discard it.

10. Collect the dermis into the 15 ml centrifuge tube and add 0.25 % trypsin–EDTA.
11. Incubate for 10 min at 37 °C.
12. To end dissociation, add 10 % (v/v) FBS to the dissociation solution. Invert the tube several times to agitate the cell suspension.
13. Filter cell suspension through a 70 μm cell strainer.
14. Centrifuge the filtrate at 300×*g* for 5 min.
15. Discard supernatant and reconstitute the cell pellet in 1× PBS.
16. Centrifuge the suspension at 300×*g* for 5 min.
17. Discard supernatant and add 1 ml red lysis buffer to remove red blood cells. Repeat this step if red blood cells still present.
18. Centrifuge the suspension cells at 300×*g* for 5 min and reconstitute the cell pellet in complete DMEM. Pass the cells several times with the pipette to ensure adequate separation.
19. Observe the cell colonies under a microscope and count the total number of cells using a hemocytometer.
20. Seed the isolated fibroblast cells suspension onto a 25 cm^2 culture flask at a density of 10^5 cells.
21. Maintain the cells in an incubator with 5 % CO_2 at 37 °C.
22. Twenty-four hours post initial seeding, aspirate the DMEM.
23. Gently wash the adhered cells with 1× PBS and add DMEM.
24. Change the medium every 2–3 days. Split the cells when 90 % confluent.

3.7 In Vitro Aerosolization

1. Prepare cell culture with confluency at 90 %.
2. Aspirate the growth medium and wash with 1× PBS.
3. Aspirate the 1× PBS and add 0.05 % trypsin–EDTA into AECs culture and 0.25 % trypsin–EDTA into SFCs culture to harvest the cells.
4. Incubate for 5 min at 37 °C. Prolong incubation time if cells are still attached onto the culture flask.
5. Transfer the cells into a 15 ml centrifuge tube. To end dissociation, add 10 % (v/v) FBS to the dissociation solution. Invert the tube several times to agitate the cell suspension.
6. Centrifuge at 1500 rpm for 5 min.
7. Count the total number of cells using a hemocytometer.
8. Transfer the 1 ml of cell solution (10^5 cells/ml) to a polycarbonate syringe.
9. Add 4 ml of complete BEGM™ for AECs and DMEM for SFCs into a culture flask.

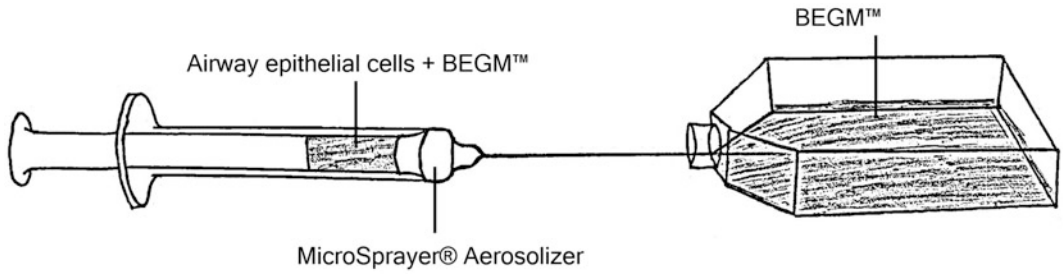

Fig. 5 Schematic diagram of in vitro aerosolization. The tubing of MicroSprayer was inserted into the culture flask to deliver the cells

10. Insert the tubing of MicroSprayer into the culture flask and push the plunger with a firm constant pressure (*see* Fig. 5).
11. Bubbles will form as a result of aerosolization and debris from cells can be found in the medium when observed microscopically.
12. Maintain the cells in an incubator with 5 % CO_2 at 37 °C.
13. Observe cell growth daily until confluent.

3.8 AECs Aerosolization and Transplantation

1. Prepare cell culture with confluency at 90 %.
2. Aspirate the growth medium and wash with 1× PBS.
3. Aspirate the 1× PBS and add 0.05 % trypsin–EDTA into AECs culture and 0.25 % trypsin–EDTA into SFCs culture to harvest the cells.
4. Incubate for 5 min at 37 °C. Prolong incubation time if cells are still attached onto the culture flask.
5. Transfer the cells into a 15 ml centrifuge tube. To end dissociation, add 10 % (v/v) FBS to the dissociation solution. Invert the tube several times to agitate the cell suspension.
6. Centrifuge at 1500 rpm for 5 min.
7. Count the total number of cells using hemocytometer.
8. Transfer the 500 μl of cell solution (10^6 cells/kg) to a polycarbonate syringe.
9. Anesthetize the rabbit with ketamine–xylazine mixture (*see* **Note 11**).
10. Apply ointment to the rabbit eye to prevent irritation and drying out.
11. Place the rabbit in supine position with the tongue pulled aside to widen the opening of the mouth.
12. Apply KY Jelly onto the tip of the endotracheal tube to smooth out the insertion procedure.

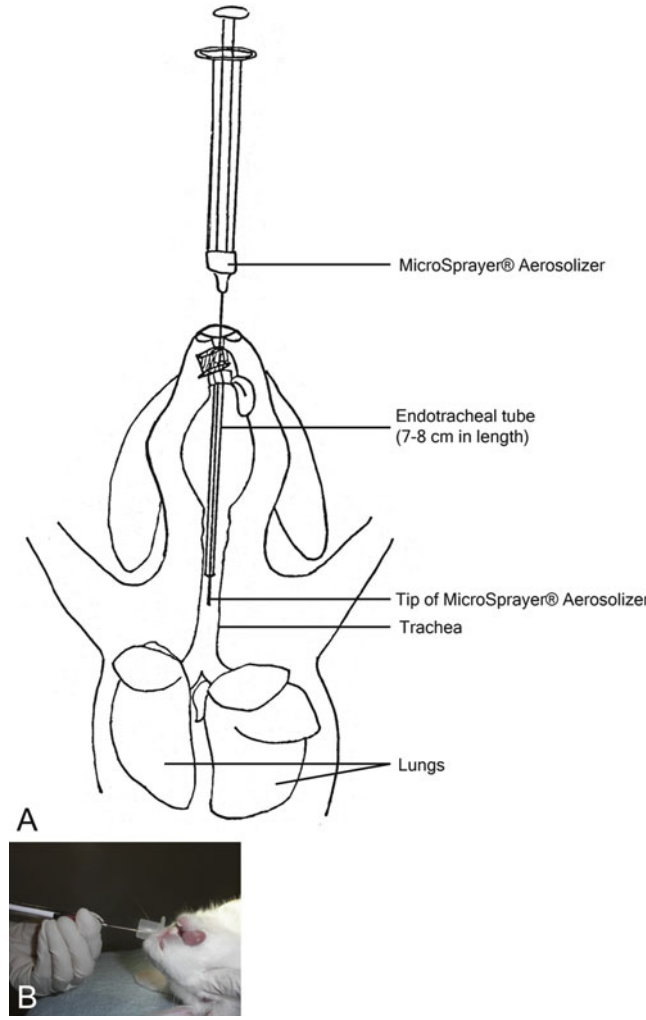

Fig. 6 (**a**, **b**) Schematic diagram of in vivo aerosolization. The tubing of MicroSprayer was inserted into the mouth of the rabbit to deliver the cells into the airway

13. Insert the endotracheal tube into the mouth and breathing should be heard through the tube.
14. Insert the tubing of MicroSprayer into mouth until it reached the appointed length and push the plunger with a firm constant pressure (*see* **Note 12** and Fig. 6).
15. Return the rabbit into the cage after transplantation
16. Monitor rabbit weight, food and drink intake on daily basis along with physical and behavior assessments as to monitor any symptoms of cell rejection such as blood in feces, diarrhea, swelling, depression, and fever (*see* **Note 13**).

4 Notes

1. For airway epithelial cell culture, large rabbits may be used to ensure a large quantity of epithelial cells harvested from each animal.
2. To prepare 1 μl $Fe(NO_3)_3$, mix 0.001 g $Fe(NO_3)_3.9H_2O$ with 1 ml dH_2O.
3. BEGM™ is light sensitive, must be kept in a dark bottle or cover the bottle with aluminum foil.
4. All animal procedures should be conducted in accordance with animal care policies and ethical approval must be obtained prior the experimental procedure.
5. Use the following dose: 1 ml/kg by intravenous injection.
6. Prepare 1 day before cell seeding. After overnight air-drying, remove traces of liquid collagen. Residual liquid collagen can be toxic to cells.
7. MACSmix™ tube rotator setting: operate the tube rotator on permanent run at a speed of $2.4 \times g$.
8. Gently scrape the epithelial cell layer 2–3 times until a layer is detached from the cartilage.
9. Cells with beating cilia are expected to be in the culture right after isolation.
10. Under the conditions described above, cultures usually remain morphologically heterogeneous with a mix of epithelial and fibroblast cells. The proportion of fibroblast cells will increase gradually starting from passage 2. Fibroblasts can attach more quickly, to prevent fibroblast overgrowth, when subculturing the cells, allow fibroblast to adhere first (about 15–20 min) and then replate the culture into a new culture flask.
11. Use the following dose: ketamine 35 mg/kg and xylazine 4 mg/kg by intramuscular injection.
12. Measure and mark 9 cm length from the tip of the MicroSprayer.
13. During first 24 h after transplantation, animals should be closely monitored as cell rejection can happen at any time after transplantation.

Acknowledgement

This work was supported by grants from the Universiti Sains Malaysia (USM) Short Term Grant Scheme (304/CIPPT/61312001) and the Universiti Sains Malaysia (USM) Research University Grant (1001/CIPPT/813059).

References

1. Kardia E, Yusoff NM, Zakaria Z, Yahaya B (2014) Aerosol-based delivery of fibroblast cells for treatment of lung diseases. J Aerosol Med Pulm Drug Deliv 27(1):30–34. doi:10.1089/jamp.2012.1020
2. Ten Hallers E, Rakhorst G, Marres H, Jansen J, Van Kooten T, Schutte H, Van Loon J-P, Van Der Houwen E, Verkerke G (2004) Animal models for tracheal research. Biomaterials 25 (9):1533–1543
3. Kamaruzaman NA, Kardia E, Kamaldin N, Latahir AZ, Yahaya BH (2013) The rabbit as a model for studying lung disease and stem cell therapy. BioMed Res Int 2013:691830. doi:10.1155/2013/691830
4. Fischer UM, Harting MT, Jimenez F, Monzon-Posadas WO, Xue H, Savitz SI, Laine GA, Cox CS Jr (2009) Pulmonary passage is a major obstacle for intravenous stem cell delivery: the pulmonary first-pass effect. Stem Cells Dev 18(5):683–692
5. Gupta N, Su X, Popov B, Lee JW, Serikov V, Matthay MA (2007) Intrapulmonary delivery of bone marrow-derived mesenchymal stem cells improves survival and attenuates endotoxin-induced acute lung injury in mice. J Immunol 179(3):1855–1863, Doi:179/3/1855 [pii]
6. Kichler A, Chillon M, Leborgne C, Danos O, Frisch B (2002) Intranasal gene delivery with a polyethylenimine–PEG conjugate. J Control Release 81(3):379–388

Methods in Molecular Biology (2016) 1516: 257–267
DOI 10.1007/7651_2016_328

Published online: 01 April 2016

Induction of Inner Ear Hair Cells from Mouse Embryonic Stem Cells In Vitro

Masahide Yoshikawa and Yukiteru Ouji

Abstract

Inner ear hair cells (HCs) function as the primary transducers for perception of sound and balance, while a defect in their formation or their loss results in sensory deficits. In mammals, once HCs are lost, they are not regenerated, and thus, various medical strategies have been proposed for their reproduction. Although embryonic stem (ES) cells are a promising source for cell therapy, little is known about efficient generation of hair cell-like cells (HCLs) from mouse ES cells. In the present protocol, we describe a simple method for obtaining ES-derived murine HCLs (HIST2 method).

Keywords: Embryonic stem cell, Differentiation, Inner ear, Hair cells, In vitro culture, HIST2 method

1 Introduction

Hearing loss is mainly caused by loss of sensory hair cells (HCs) in the organ of Corti or cochlea [1–3]. Although embryonic stem (ES) cells are a promising source for cell therapy [4, 5], few investigations have documented in vitro differentiation of ES cells into HCs [6–8]. In our previous study, we reported a single medium culture method for growing embryoid bodies (EBs), in which conditioned media from cultures of ST2 stromal cells (ST2-CM cells) were used for 14-day cultures of 4-day EBs [9]. At the end of the 14-day cultures, up to 20 % of the cells in EB outgrowths expressed HC-related markers, while they also showed formation of stereocilia-like structures. Here, we describe our method of inner ear hair cell induction using ST2-CM cells (HIST2 method).

2 Materials

All reagents and materials used for cell culturing are confirmed to be sterile.

2.1 ES Cell Culture

2.1.1 ES Cell Line

The ES cell lines most commonly used in our laboratory are EB3 and G4-2 cells, kindly gifted from Dr. Hitoshi Niwa (RIKEN CDB, Kobe, Japan) [10]. These lines are able to maintain growth in an undifferentiated state without the use of feeder cells (*see* **Note 1**) [11].

2.1.2 ES Cell Maintenance Medium

1. Dulbecco's modified Eagle's medium including 4.5 g/L of D-glucose (DMEM) (Invitrogen, Grand Island, N.Y., cat. no. 11960-044).
2. Fetal bovine serum (FBS) (10 %) for ES cell culture (Invitrogen, cat no. 16141-079).
3. Sodium pyruvate (100 mM) (Invitrogen, cat. no. 11360-50).
4. 2-mercaptoethanol (0.1 mM) (Sigma, St. Louis, MO, cat. no. M3148).
5. Nonessential amino acids (0.1 mM) (Invitrogen, cat. no. 11140-50).
6. Leukemia inhibitory factor (LIF) (1000 U/ml) (Millipore, Billerica, MA, cat. no. ESG1107).
7. Penicillin and streptomycin (Wako, Osaka, cat. no. 168-23191).

2.1.3 Growth and Maintenance of ES Cells

1. Phosphate-buffered saline (PBS), pH 7.4 (Wako, cat. no. 048-29805).
2. Gelatin (0.1 %) in PBS (Sigma; cat. no. G1890).
3. Trypsin–EDTA (0.25 %) (Invitrogen, cat. no. 25200-056).
4. ES cell maintenance medium (*see* Section 2.1.2).
5. Plastic cell culture dishes (10 cm) (BD, Bedford, MA, cat. no. 353003).

2.2 Differentiation into HCLs

2.2.1 Differentiation Medium

Various differentiation media are prepared by adding supplements (shown in Table 1) to ES cell maintenance medium without LIF (*see* Section 2.1.2. and **Note 2**).

1. Knockout serum replacement (KOS) (Invitrogen, cat. no. 10828).
2. B27 supplement (Invitrogen, cat. no. 17504).
3. N2 supplement (Invitrogen, cat. no. 17502).
4. bFGF (Sigma, cat. no. SRP4038).

2.2.2 Conditioned Medium (CM)

ST2 cells and PA6 cells were used to prepare conditioned medium (CM). These cell lines were purchased from BRC (RIKEN Cell Bank, BioResource Center, Tsukuba, Japan) and maintained in DMEM supplemented with 10 % FBS (Sigma, cat. no. A15002).

1. Plastic cell culture dishes (10 cm).
2. PBS.

Table 1
Differentiation medium types used in the present study

	FBS	KOS	N2, B27	bFGF	PA6[a]	ST2[a]
ES-M	+	–	–	–	–	–
KOS-M	–	+	–	–	–	–
N2-M	–	–	+	–	–	–
N2-Mb	–	–	+	+	–	–
PA6-CM[b]	+	–	–	–	+	–
ST2-CM[b]	+	–	–	–	–	+

[a]Medium conditioned for 48 h (*see* Section 3.2.1)
[b]*CM* conditioned medium

3. ES cell maintenance medium without LIF (*see* Section 2.1.2).
4. Plastic tubes (50 mL) (BD, cat. no. 352070).
5. Filter membrane (0.22 μm) (TPP, Switzerland, cat. no. 99522).

2.2.3 Induction of Embryoid Bodies (EBs)

1. PBS.
2. Trypsin–EDTA (0.25 %).
3. ES cell maintenance medium without LIF (*see* Section 2.1.2).
4. Trypan blue (Invitrogen, cat. no. 15250061).
5. Hemocytometer (Waken-Btech, Kyoto, Japan, cat. no. WC2-100).
6. Plastic tubes (15 mL) (BD, cat. no. 352096).
7. Bacterial dishes (Sigma, cat. no. SIAL506CC0SnV).

2.2.4 Induction of Hair Cell-Like Cells (HCLs)

1. Plastic cell culture dishes (10 cm).
2. Gelatin (0.1 %) in PBS.
3. Various differentiation media (*see* Table 1 and Sects. 2.2.1 and 2.2.2).

2.3 Characterization of HCLs

2.3.1 RT-PCR

1. PBS.
2. TRIzol (Invitrogen, cat. no. 15596-026).
3. Random primer (Takara, Otsu, Japan, cat. no. 3801).
4. DNase (Takara, cat. no. 2215A).
5. M-MLV reverse transcriptase (Promega, Madison, WI, cat. no. M1861).
6. PCR primers (*see* Table 2).
7. PCR rTaq enzyme (Takara, cat. no. R001A).

Table 2
List of gene-specific primers

Genes	Forward primer sq.	Reverse primer sq.	Size of product (bp)	GeneBank accession no.	Cycle number
Brn3c	ccatgcgccgagtttgtctcc	ctccacatcgctgagacacgc	455	S69352	25
Myosin6	tcagaagacatcagggagaagc	tgttcttcagattgcagccacc	334	NM_001039546	29
Myosin7a	ctttaacaagcgtggtgccatc	gattgctgcgttgatcttctcc	655	U81453	25
α9AchR	aagccgtagagacagcaaatgg	ttcccattgtaggtccaggaac	481	NM_001081104	30
Gapdh	accacagtccatgccatcac	tccaccaccctgttgctgta	452	NM_008084	25

8. Thermal cycler (MJ Research; model no. PTC-200).
9. Agarose (Nakarai Tesque, Osaka, cat. no. 011-53).
10. Tris–acetate–EDTA (TAE) electrophoresis buffer (Nippon Gene, Toyama, Japan, cat. no. 313-90035).
11. DNA molecular weight markers (Takara, cat. no. 3407A).
12. Ethidium bromide (Bio-Rad, Hercules, CA, cat. no. 161-0433).
13. Horizontal gel electrophoresis apparatus (COSMO BIO, model no. MyRun system).

2.3.2 Phalloidin Staining

1. PBS.
2. Paraformaldehyde (PFA) (4 %) (Wako, cat. no. 163-20145).
3. Triton X-100 (0.3 %, diluted in PBS) (Sigma, cat. no. T8787).
4. TRITC labeled-phalloidin (diluted 1:100 in PBS, Sigma, cat. no. P1951).
5. 4′,6-diamidino-2-phenylindole, dihydrochloride, solution (DAPI) (Dojin Kagaku, Kumamoto, Japan, cat. no. D523).
6. Mounting medium (Dako, Carpinteria, CA, cat. no. S1964).
7. Fluorescent microscope, equipped for fluorescent detection (Carl Zeiss; model no. Axiovert 40CFL).

2.3.3 Immunocyto-chemistry

1. PBS.
2. PFA (4 %).
3. Triton X-100 (0.1 %) in PBS containing 1 % BSA (TPBS) (BSA; Sigma, cat. no. A1470).
4. Mouse anti-$p27^{Kip1}$ monoclonal antibody (1:200, BIOSOURCE, Camarillo, CA, cat. no. AHZ0452).
5. Goat anti-calretinin polyclonal antibody (1:1000, CHEMICON, cat. no. AB1550).

6. Alexa Fluor 488 conjugated rabbit anti-goat secondary antibodies (1:200, Molecular Probes, cat. no. A11078).
7. Alexa Fluor 546 conjugated rabbit anti-mouse secondary antibodies (1:200, Molecular Probes, cat. no. A11060).
8. DAPI.
9. Mounting medium.
10. Fluorescent microscope.

3 Methods

3.1 Maintenance of ES Cells

1. Change ES cell medium until subconfluence is reached.
2. Treat 10-cm plastic cell culture dishes with 0.1 % gelatin.
3. Aspirate medium, wash cells with PBS twice and treat with trypsin–EDTA solution at 37 °C for 3 min.
4. Add new maintenance medium and dissociate ES cell clumps by pipetting.
5. Centrifuge at 250 × *g* for 5 min and resuspend pellets in new-culture medium.
6. Seed cells into 10-cm plastic cell culture dishes (1×10^5 cells/dish).

3.2 Differentiation into HCLs

3.2.1 Preparation of Various Differentiation Media

We prepared differentiation media, including ES-M, KOS-M, N2-M, and N2Mb, by adding supplements (e.g., KOS, B27, N2, bFGF) to ES cell maintenance medium without FBS or LIF, as shown in Table 1 (*see* Section 2.1.2). PA6-CM and ST2-CM media were prepared using the following protocol.

1. Culture PA6 or ST2 cells with DMEM containing 10 % FBS until reaching subconfluence.
2. Harvest PA6 or ST2 cells using trypsin–EDTA.
3. Seed PA6 or ST2 cells into 10-cm dishes at a density of 2×10^5 cells/cm^2.
4. The next day, confirm confluent cell growth in the dishes. To prepare conditioned medium, irradiate cells by X-ray (40 Gy), then rinse with PBS and add 20 mL of new ES cell maintenance medium without LIF (*see* Section 2.1.2).
5. After 48 h, collect supernatants.
6. Centrifuge samples at 250 × *g* for 5 min and collect supernatants.
7. Filtrate supernatants with 0.22-μm filter membrane and add 10-mL aliquot samples to 15-mL tubes (*see* **Note 3**).

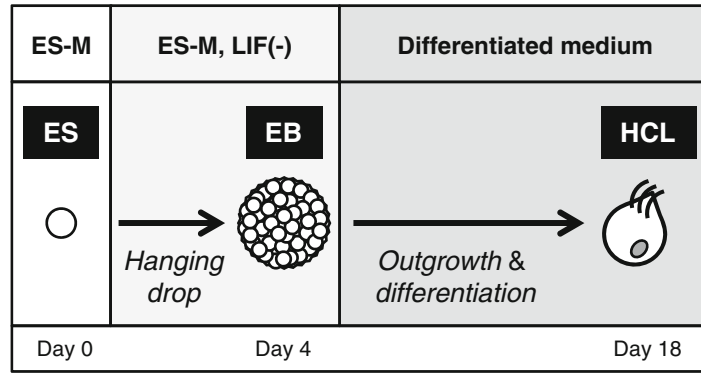

Fig. 1 Schema for induction of hair cell-like cells (HCLs). Following embryoid body (EB) formation, EBs were cultured with various differentiation media (*see* Table 1) for 2 weeks

3.2.2 Procedure for HCL Induction

We used a simple culture method to induce hair cell-like cells (HCLs) from ES cells, and found it to be very useful for studies of hair cell differentiation and inner ear development. Figure 1 shows the differentiation protocol used to produce HCLs from undifferentiated ES cells. In the first step, embryoid bodies (EBs) are prepared using a hanging drop method [12]. In the second step, EBs are cultured in differentiation media on gelatin-coated dishes for 2 weeks, resulting in effective induction of HCLs.

Induction of EBs

1. Culture undifferentiated ES cells in ES cell maintenance medium (*see* Section 2.1.2) until reaching subconfluence.
2. Aspirate medium, then wash twice with PBS and treat with trypsin–EDTA solution at 37 °C for 3 min.
3. Add new maintenance medium and dissociate ES cell clumps by pipetting.
4. Centrifuge at 250 × *g* for 5 min, then resuspend pellets in ES cell maintenance medium without LIF.
5. Determine cell number using trypan blue exclusion method and prepare cell suspension (2.5×10^4 cells/mL) in ES maintenance medium without LIF.
6. Drop 20 μL of ES cell suspension onto the inside of the cover of a bacterial plastic dish and allow hemisphere to form by surface tension, resulting in a cell density of 500 cells/20 μL in each drop.
7. Place dishes inside humidified chamber for 4 days.

Induction of HCLs

1. Treat 10-cm plastic cell culture dishes with 0.1 % gelatin.
2. Remove gelatin solution and add various differentiation media (*see* Section 3.2.1 and Table 1) into dishes.

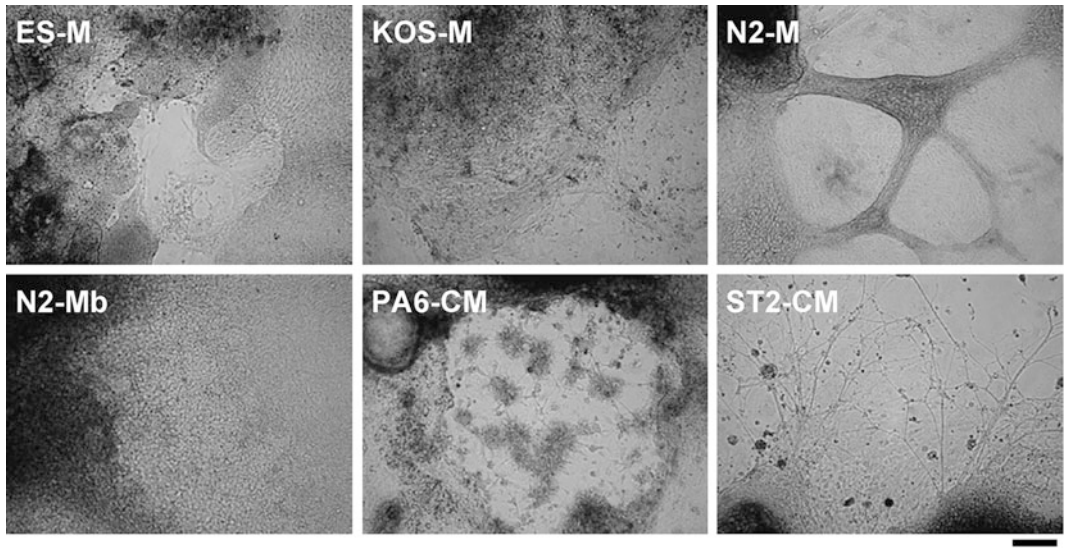

Fig. 2 Morphology of EB outgrowths. Differentiation of EBs was induced using various media, as listed in Table 1. Images show EB outgrowths after 2 weeks of cultivation. Scale bar = 100 μm

3. Collect 4-day EBs (*see* Section 3.2.2.1) using a pipette.
4. Gently transfer 20 EBs per dish, and allow them to attach and grow.
5. On the next day, exchange all culture media with fresh medium.
6. Thereafter, exchange half of each culture medium sample with fresh medium every 2 days during 2-week EB outgrowth culture period (*see* Fig. 2, **Notes 2**, and **4**).

3.3 Characterization of HCLs

Extract total RNA and perform RT-PCR at 2 weeks after plating EBs using the following procedure.

3.3.1 Analysis of Gene Expression in HCLs

1. Wash cells with PBS twice, add 1.0 mL of TRIzol to cultures of attached DPCs to extract total RNA and purify using the protocol recommended by the manufacturer.
2. Prepare cDNA by reaction with a random primer and M-MLV reverse transcriptase with 1 μg of DNase-treated total RNA.
3. For PCR analysis, use 0.5 μg of cDNA as a template and perform amplification using the primer sequences shown in Table 2. General PCR conditions: 25–30 cycles at 94 °C for 2 min, 94 °C for 30 s, 52–62 °C for 30 s, and 72 °C for 1 min.
4. Run PCR products on 1.5 % agarose gels and visualize by ethidium bromide staining (*see* **Note 5** and Fig. 3).

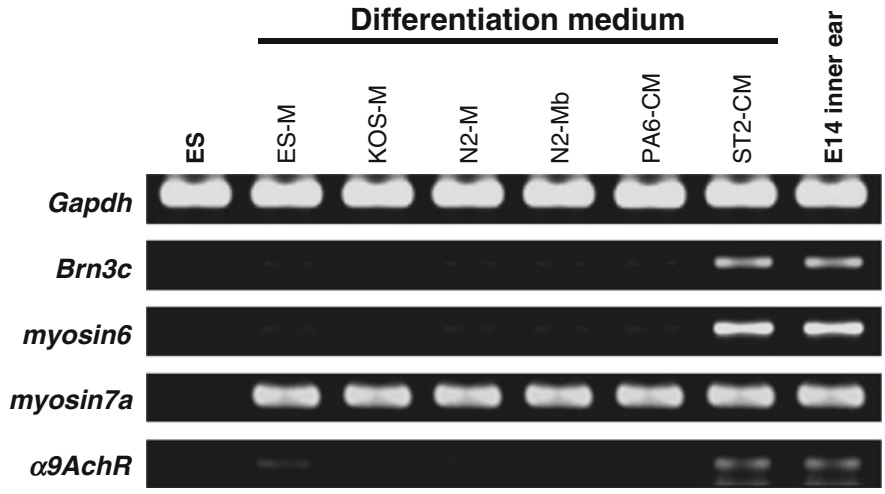

Fig. 3 Gene expressions of hair cell (HC)-related markers in EB outgrowths. Gene expressions of HC-related markers (Brn3c, myosin 6, myosin 7a, α9AchR) in EB outgrowths cultured in various media (*see* Table 1) were analyzed using an RT-PCR method. Samples from day 14 embryonic (E14) mouse inner ears served as a positive control

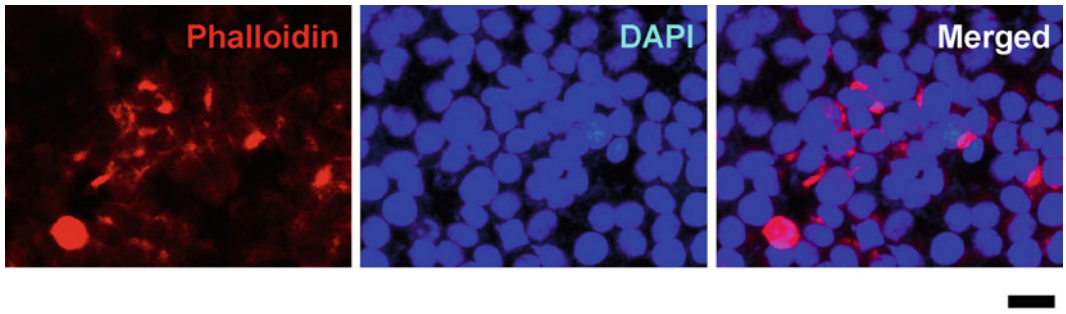

Fig. 4 Phalloidin-positive cells in EB outgrowths cultured with ST2-CM for 14 days. EB outgrowths were cultured with ST2-CM for 2 weeks and examined following phalloidin staining. Some cells showed phalloidin-labeled protrusions, which was highly suggestive of actin-rich hair bundles. Scale bar = 10 μm

3.3.2 Phalloidin Staining of HCLs

1. Induce HCLs by cultivation in differentiation medium for 2 weeks (*see* Section 3.2).
2. Wash cells with PBS twice, then fix in 4 % PFA solution at room temperature for 30 min.
3. Remove PFA solution and permeabilize with 0.3 % Triton X-100 in PBS for 10 min.
4. Remove Triton solution and wash with PBS.
5. Remove PBS, then add TRITC-labeled phalloidin solution and allow reaction for 30 min.
6. Remove phalloidin solution and wash with PBS three times.
7. Remove PBS and stain nuclei with DAPI.
8. Rinse cells with PBS three times and observe under a fluorescence microscope (*see* **Note 6** and Fig. 4).

3.3.3 Immunocytochemical Analysis of HCLs

1. Induce HCLs by cultivation in differentiation medium for 2 weeks (*see* Section 3.2).
2. Wash cells with PBS twice, then fix in 4 % PFA solution at room temperature for 30 min.
3. Remove PFA solution and permeabilize with 0.1 % Triton X-100 in PBS containing 1 % BSA (TPBS) for 10 min.
4. Remove Triton solution and wash with TPBS.
5. Remove TPBS, then add primary antibodies (anti-calretinin and anti-$p27^{Kip1}$, diluted in TPBS) and allow reaction at 4 °C overnight.
6. Remove primary antibodies and wash with TPBS three times.
7. Remove TPBS, add secondary antibodies (Alexa Fluor 488 or 546 conjugated anti-goat or anti-mouse, diluted in TPBS) and allow reaction at room temperature for 1 h.
8. Remove secondary antibodies and wash with TPBS three times.
9. Remove TPBS and stain nuclei with DAPI.
10. Rinse cells with TPBS 3 times and observe under a fluorescence microscope (*see* **Note** 7 and Fig. 5).

4 Notes

1. EB3 and G4-2 cells are sublines derived from E14tg2a ES cells, which carry the blasticidin S-resistant selection marker gene driven by the Oct-3/4 promoter (active in undifferentiated state) [10]. G4-2 ES cells are derived from EB3 ES cells and carry the enhanced green fluorescent protein (EGFP) gene under control of the CAG expression unit.
2. We developed a simple single-medium culture method for differentiation of ES cells into hair cell-like cells (HCLs) by screening several types of culture media including stromal cell-conditioned medium. The differentiation protocol using conditioned medium from ST2 cells was able to efficiently induce HCLs and we designated it as an inner ear hair cell induction method using ST2-CM, or the HIST2 method. Our HIST2 method is quite simple to perform and highly efficient for obtaining ES-derived HCLs within a relatively short cultivation period.
3. Culture supernatants from PA6 or ST2 cells contain various differentiation factors. Aliquots may be stored for up to 1 week at 4 °C or at −80 °C for a longer period.
4. Figure 2 shows representative morphologies of EB outgrowths cultured in various differentiation media. Prominent neurite-like outgrowths emerging from the aggregates were observed in cultures with ST2-CM.

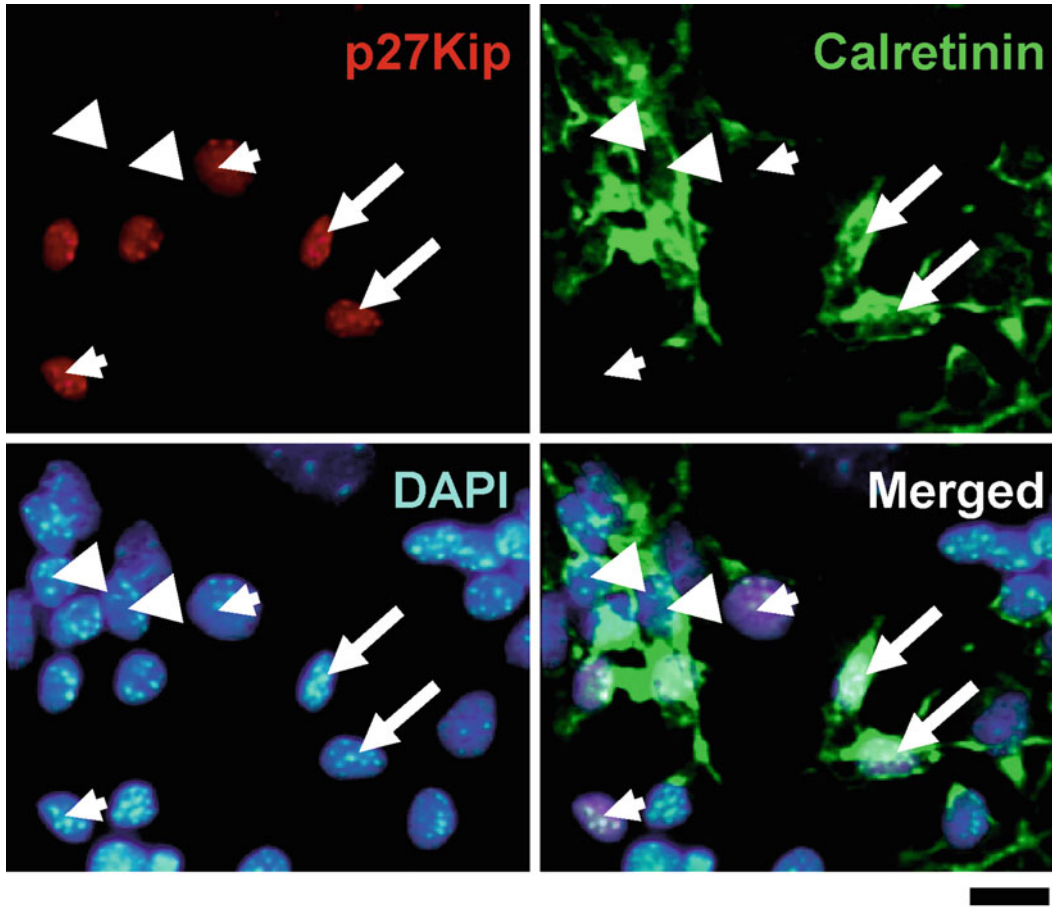

Fig. 5 Immunocytochemical analysis of p27kip1 and calretinin in EB outgrowths cultured with ST2-CM for 14 days. Three expression patterns were observed; $p27^{kip1}$-positive and calretinin-negative cells (*short arrow*), $p27^{kip1}$-negative and calretinin-positive cells (*arrowhead*), and $p27^{kip1}$-positive and calretinin-positive cells (*long arrow*). Scale bar = 10 μm

5. Gene expressions of the hair cell-related markers Brn3c, myosin6, myosin7a, and α9AchR were analyzed using an RT-PCR method after cultivating EBs in various media for 2 weeks (*see* Fig. 3). Samples taken from the inner ears of embryonic day 14 (E14) mice were used as a positive control. No expression was observed in undifferentiated ES cells. Expressions of the target genes were only observed in EB outgrowths cultured with ST2-CM.
6. Some EB outgrowths allowed to differentiate in ST2-CM for 2 weeks had phalloidin-labeled protrusions (*see* Fig. 4).
7. Immunocytochemical analysis of EB outgrowths cultured in ST2-CM for 18 days revealed cells immuno-positive for $p27^{kip1}$, a marker of supporting cells, as well as cells immuno-positive for calretinin, a marker for HCs (*see* Fig. 5).

The following 3 expression patterns were observed; $p27^{kip1}$-positive and calretinin-negative cells (Fig. 5c, short arrow), $p27^{kip1}$-negative and calretinin-positive cells (Fig. 5c, arrowhead), and p27kip1-positive and calretinin-positive cells (Fig. 5c, long arrow), suggesting the possibility that HC-like cells had differentiated from supporting cells.

References

1. Raphael Y (2002) Cochlear pathology, sensory cell death and regeneration. Br Med Bull 63:25–38
2. Fekete DM (1996) Cell fate specification in the inner ear. Curr Opin Neurobiol 6(4):533–541, doi: S0959-4388(96)80061-4 [pii]
3. Carey J, Amin N (2006) Evolutionary changes in the cochlea and labyrinth: solving the problem of sound transmission to the balance organs of the inner ear. Anat Rec A: Discov Mol Cell Evol Biol 288(4):482–489. doi:10.1002/ar.a.20306
4. Wobus AM (2001) Potential of embryonic stem cells. Mol Aspects Med 22(3):149–164, doi: S0098-2997(01)00006-1 [pii]
5. Wobus AM, Boheler KR (2005) Embryonic stem cells: prospects for developmental biology and cell therapy. Physiol Rev 85(2):635–678. doi:10.1152/physrev.00054.2003, 85/2/635 [pii]
6. De Silva MG, Hildebrand MS, Christopoulos H, Newman MR, Bell K, Ritchie M, Smyth GK, Dahl HH (2006) Gene expression changes during step-wise differentiation of embryonic stem cells along the inner ear hair cell pathway. Acta Otolaryngol 126(11):1148–1157. doi:10.1080/00016480600702118, Q1L63216X1671V13 [pii]
7. Rivolta MN, Li H, Heller S (2006) Generation of inner ear cell types from embryonic stem cells. Methods Mol Biol 330:71–92. doi:10.1385/1-59745-036-7:71
8. Oshima K, Shin K, Diensthuber M, Peng AW, Ricci AJ, Heller S (2010) Mechanosensitive hair cell-like cells from embryonic and induced pluripotent stem cells. Cell 141(4):704–716. doi:10.1016/j.cell.2010.03.035, S0092-8674(10)00353-3 [pii]
9. Ouji Y, Ishizaka S, Nakamura-Uchiyama F, Yoshikawa M (2012) In vitro differentiation of mouse embryonic stem cells into inner ear hair cell-like cells using stromal cell conditioned medium. Cell Death Dis 3, e314. doi:10.1038/cddis.2012.56
10. Niwa H, Miyazaki J, Smith AG (2000) Quantitative expression of Oct-3/4 defines differentiation, dedifferentiation or self-renewal of ES cells. Nat Genet 24(4):372–376. doi:10.1038/74199
11. Nishimura F, Yoshikawa M, Kanda S, Nonaka M, Yokota H, Shiroi A, Nakase H, Hirabayashi H, Ouji Y, Birumachi J, Ishizaka S, Sakaki T (2003) Potential use of embryonic stem cells for the treatment of mouse parkinsonian models: improved behavior by transplantation of in vitro differentiated dopaminergic neurons from embryonic stem cells. Stem Cells 21(2):171–180. doi:10.1634/stemcells.21-2-171
12. Keller GM (1995) In vitro differentiation of embryonic stem cells. Curr Opin Cell Biol 7(6):862–869, doi:0955-0674(95)80071-9 [pii]

Methods in Molecular Biology (2016) 1516: 269–277
DOI 10.1007/7651_2016_319

Published online: 01 April 2016

Maintenance of Dermal Papilla Cells by Wnt-10b In Vitro

Yukiteru Ouji and Masahide Yoshikawa

Abstract

Dermal papilla cells (DPCs) are associated with development of hair follicles (HFs) and regulation of the hair cycle. However, primary DPCs are known to lose their ability to induce HFs after culture in standard media for fibroblasts. We examined a new culture condition for DPCs including addition of Wnt-10b, which promoted proliferation and maintained their HF induction ability for more than ten passages. These results suggest that Wnt-10b plays a pivotal role in proliferation and maintenance of DPCs in vitro.

Keywords: Dermal papilla, Wnt signaling, Wnt-10b, Cell proliferation, Cell culture

1 Introduction

Dermal papilla cells (DPCs), specialized fibroblasts located in hair follicles (HFs), are deeply associated with HF development and regulation of the hair cycle, and known to be an important target for elucidating the mechanism of HF induction and hair growth [1–3]. Technical advances in isolation of DPCs from HFs and subsequent in vitro cultures have made it possible to investigate the ability of these cells to induce HFs and promote hair growth [4–6].

DPCs lose their ability for HF induction and do not promote hair growth after being cultured in standard medium for fibroblasts [4, 6, 7], thus establishment of an effective culture method by which the functions of DPCs are maintained is considered to be important. Previously, DPCs cocultured with Wnt-3a-producing cells were shown to sustain their ability to induce HFs [5], suggesting that canonical Wnts may be important for DPC growth. Another study provided supportive evidence concerning the role of Wnts, as it found that a GSK inhibitor (BIO) acted favorably for maintaining DP function [8]. However, there are no reports documenting the direct effects of Wnt proteins on DPCs. In our previous study, we investigated the effects of Wnt-10b on primary DPCs prepared from DP cultures and DPCs after serial passages, and found that Wnt-10b promoted their proliferation and maintained HF induction ability [9]. In the present protocol, we describe more detail of the culture method, by which DPCs can be maintained over several passages with their sustained function.

2 Materials

2.1 Isolation of DPCs

1. Inbred 4-week-old C3H/HeN mice.
2. Dissection instrument (micro-scissors, fine forceps).
3. Stereo microscope.
4. Saline (Otsuka, Tokyo, cat. no. D05352).
5. Plastic petri dishes.
6. Dulbecco's modified Eagle's medium (DMEM; Wako, Osaka, cat. no. 043-30085) containing 10 % fetal bovine serum (FBS; PAA Laboratory, Morningside QLD, cat. no. A15002).

2.2 Preparation of Wnt-10b

1. Wnt-10b-secreting COS cell line (Wnt-COS cells) (*see* **Note 1**).
2. Plastic cell culture dishes (10 cm) (BD, Bedford, MA, cat. no. 353003).
3. Phosphate-buffered saline (PBS), pH 7.4 (Wako, cat. no. 048-29805).
4. DMEM medium containing 10 % FBS.
5. Penicillin and streptomycin (Wako, cat. no. 168-23191).
6. Plastic tubes (50 mL) (BD, cat. no. 352070).
7. Filter membrane (0.22 μm) (TPP, Switzerland, cat. no. 99522).

2.3 DPC Culture

1. Plastic cell culture dishes (6 cm) (BD, cat. no. 353002).
2. PBS.
3. DMEM medium containing 10 % FBS.
4. Penicillin and streptomycin.
5. Trypsin–EDTA (0.25 %) (Invitrogen, Burlington, ON, Canada, cat. no. 25200-056).
6. Wnt-COS supernatant prepared from Wnt-COS cells (*see* Subheading 3.2).

2.4 Characterization of DPCs

2.4.1 ALP staining

1. PBS.
2. Alkaline phosphatase kit (Sigma, St Louis, MO, cat. no. 85L3R).
3. Distilled water.
4. Light microscope (CarlZeiss; model no. Axivert 40CFL).

2.4.2 Cell Proliferation Assay

1. Flat-bottom 96-well plastic plates (BD, cat. no. 353072).
2. PBS.
3. Trypsin–EDTA (0.25 %).

4. Trypan blue (Invitrogen, cat. no. 15250061).
5. Hemocytometer (Waken Btech, Kyoto, Japan, cat. no. WC2-100).
6. Light microscope.

2.4.3 RT-PCR

1. PBS.
2. TRIzol (Invitrogen, cat. no. 15596-026).
3. Random primer (Takara, Otsu, Japan, cat. no. 3801).
4. DNase (Takara, cat. no. 2215A).
5. M-MLV reverse transcriptase (Promega, Madison, WI, cat.no. M1861).
6. PCR primers (*see* Table 1).
7. PCR rTaq enzyme (Takara, cat. no. R001A).
8. Thermal cycler (MJ Research; model no. PTC-200).
9. Agarose (Nacalai Tesque, Osaka, cat. no. 011-53).
10. Tris–acetate–EDTA (TAE) electrophoresis buffer (Nippon Gene, Toyama, Japan, cat. no. 313-90035).
11. DNA molecular weight markers (Takara, cat. no. 3407A).
12. Ethidium bromide (Bio-Rad, cat. no. 161-0433).
13. Horizontal gel electrophoresis apparatus (COSMO BIO, model no. MyRun system).

Table 1
Gene-specific primers used in the present study

Genes	Primer sequences	Product size (bp)	GenBank accession No.	Temp. (°C)
Versican	Forward: 5′- gacgactgtcttggtgg Reverse: 5′- atatccaaacaagcctg	285	NM_001081249	58
Lef-1	Forward: 5′- actgtcaggcgacacttcc Reverse: 5′- tgcacgttgggaaggagc	541	NM_010703	58
Ptc-1	Forward: 5′- tcctcatatttggggccttc Reverse: 5′- ctgatccatgtaacctgtctcc	338	NM_008957	58
Gli-1	Forward: 5′- tccaatgactccaccacaag Reverse: 5′- cattgaaccccgagtagagtc	493	NM_010296	58
Gapdh	Forward: 5′-accacagtccatgccatcac Reverse: 5′-tccaccaccctgttgctgta	452	NM_008084	58

Lef-1 lymphoid enhancer binding factor 1, *Ptc-1* patched homolog 1, *Gli-1* GLI-Kruppel family member GLI1, *Gapdh* glyceraldehyde-3-phosphate dehydrogenase

3 Methods

3.1 Isolation of DPCs

1. Isolate dermal papilla (DP) from vibrissa of 4-week-old mice using microdissection method. Cut open the mystacial pad, invert the skin, and remove follicles using micro-scissors (Fig. 1a).
2. Remove collagen capsules surrounding vibrissae follicles to expose the follicle base and dissect DP using fine forceps (Fig. 1b).
3. Place DP specimens into 6-cm dishes and culture quietly for 4 days in DMEM containing 10 % FBS (Fig. 1c).

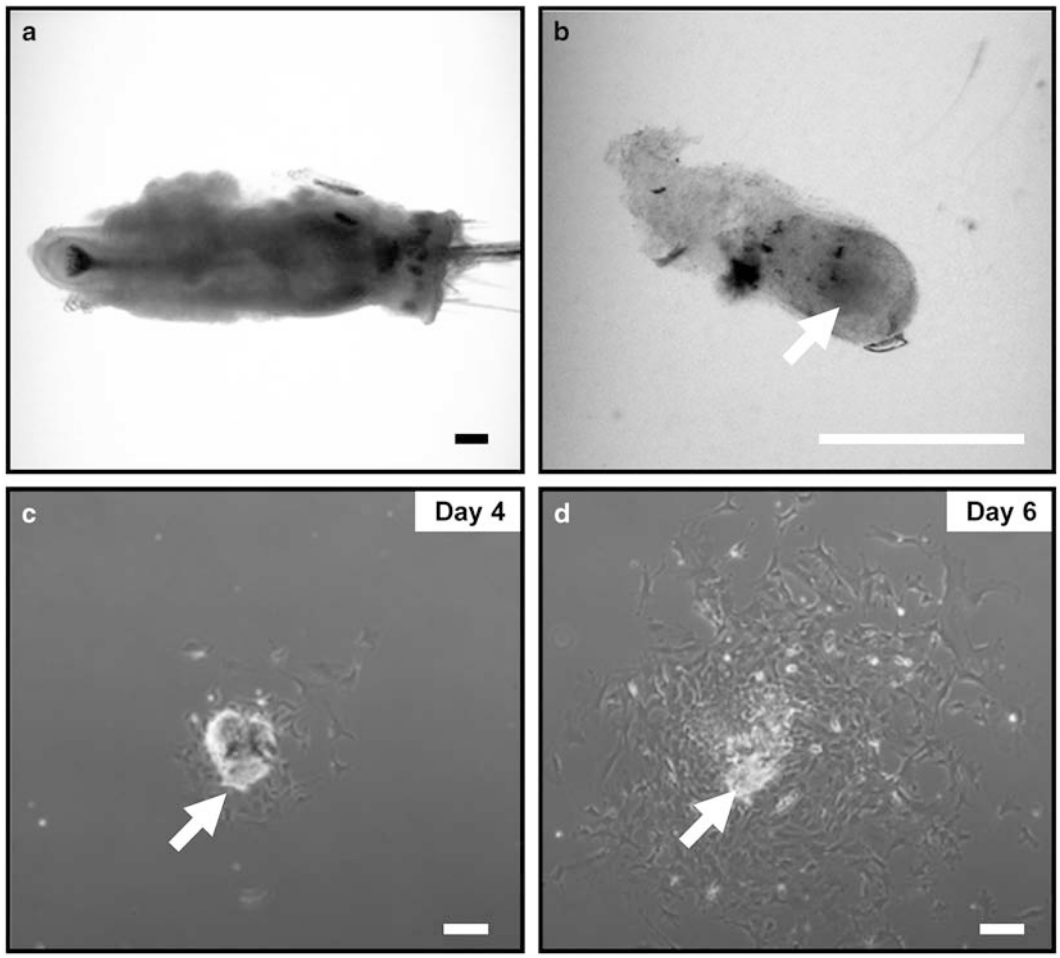

Fig. 1 Isolation and cultivation of DP cells. (**a**) Vibrissa follicles isolated from 4-week-old C3H/HeN mice. Scale bar = 100 μm (**b**) The collagen capsule surrounding each follicle was removed to expose the follicle base, then the DP (arrow) was dissected. Scale bar = 250 μm (**c**) On day 4, DPCs appeared only around the DP specimens (*arrow*). Scale bar = 100 μm (**d**) During the following 2 days, DP cells showed rapid outgrowth. Scale bar = 100 μm

4. DP cells (DPCs) appear only around the DPs and begin to show rapid outgrowth over the following 2 days (Fig. 1d). By day 10, DPCs show spreading throughout all areas of the dishes.

3.2 Preparation of Wnt-10b

1. Collect Wnt-COS cells cultured in DMEM containing 10 % FBS using trypsin–EDTA.
2. Seed Wnt-COS cells into 10-cm dishes at a density of 2×10^5 cells/cm^2.
3. The next day, confirm confluent cell growth in the dishes. To prepare conditioned medium, irradiate the cells using X-ray (40 Gy) and rinse with PBS, then add 20 mL of fresh DMEM medium containing 10 % FBS.
4. After 48 h, collect the supernatants.
5. Centrifuge samples at $250 \times g$ for 5 min and collect the supernatants.
6. Filtrate supernatants with 0.22-μm filter membrane and aliquot 10-mL samples into 15-mL tubes (*see* **Note 2**).

3.3 DPC Cultures

Figure 2 shows outlines of the DP and DPC culture protocols.

1. Culture primary DPCs from DPs in DMEM medium containing 10 % FBS for 10 days to allow for proliferation (*see* Subheading 3.1).
2. Wash DPCs with PBS and harvest with 0.25 % trypsin–EDTA.

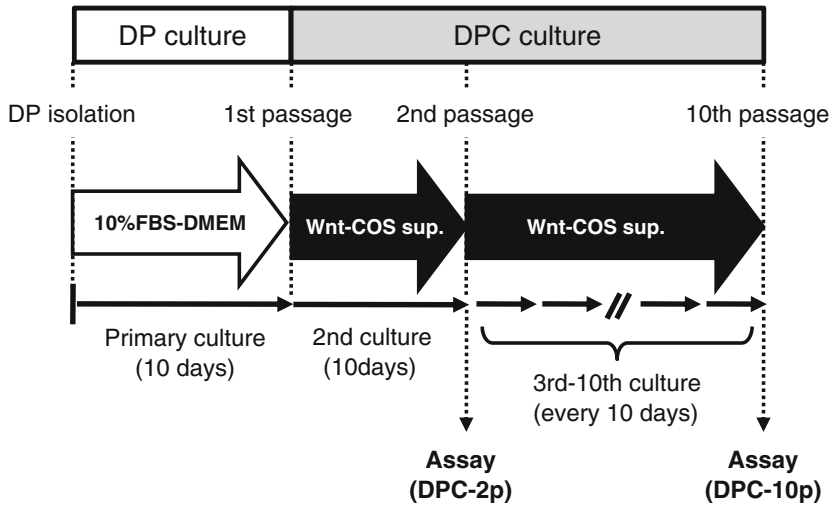

Fig. 2 Experimental design and procedures. DP culture: DPs were isolated from vibrissa of C3H/HeN mice, then placed in 6-cm dishes and quietly cultured in DMEM containing 10 % FBS. DPC cultures: Primary DPCs harvested from DP cultures were seeded into 6-cm culture dishes and cultured in Wnt-COS supernatant (Wnt-COS sup), then harvested on day 10. DPCs cultured in Wnt-COS sup underwent passaging every 10 days until the end of the tenth culture

3. Subject samples to centrifuging at 250 × *g* for 5 min and collect DPCs.
4. Seed 1×10^3 DPCs into 6-cm culture dishes with Wnt-COS supernatant (*see* Subheading 3.2).
5. Change medium every 4 days.
6. DPCs cultured in Wnt-COS supernatant undergo passaging every 10 days (*see* **Note 3**)
7. Harvest DPCs on day 10 using 0.25 % trypsin–EDTA and use for various experiments (e.g., transplantation).

3.4 Characterization of DPCs

1. Culture DPCs with Wnt-COS supernatant for 10 days to allow for proliferation (*see* Subheading 3.3).

3.4.1 ALP Staining

2. Wash cells twice in PBS and fix in fixation solution at room temperature for 30 s.
3. Remove fixation solution and wash with water.
4. Remove water and add dye solution, then incubate for 30 min at room temperature.
5. Rinse cells with water 3–4 times and observe under a light microscope (*see* **Note 4** and Fig. 3a).

3.4.2 Cell Proliferation Assay

1. Culture DPCs with Wnt-COS supernatant to allow for proliferation (*see* Subheading 3.3.).
2. Wash DPCs with PBS and harvest with 0.25 % trypsin–EDTA.
3. Centrifuge samples at 250 × *g* for 5 min and collect DPCs.
4. Seed DPCs into flat-bottom 96-well plastic plates at a density of 50 cells per well with Wnt-COS supernatant.
5. Change medium every 4 days.
6. Harvest DPCs on day 10 using 0.25 % trypsin–EDTA and resuspend pellets with DMEM.
7. Transfer 100 μL of cells into new 1.5-mL tubes and add 400 μL of 0.4 % trypan blue (final concentration 0.08 %). Mix gently.
8. Using a pipette, take 100 μL of the trypan blue-treated cell suspensions and examine with hemocytometer.
9. Using a hand tally counter, count live (unstained) cells (live cells do not take up trypan blue) in a single set of 16 squares (*see* **Note 5** and Fig. 3b).

3.4.3 RT-PCR

1. Culture DPCs with Wnt-COS supernatant to allow for proliferation (*see* Subheading 3.3).
2. Wash DPCs with PBS twice, add 1.0 mL of TRIzol to attached DPCs to extract total RNA, and purify using the protocol recommended by the manufacturer.
3. Prepare cDNA by reaction of random primer and M-MLV reverse transcriptase with 1 μg of DNase-treated total RNA.

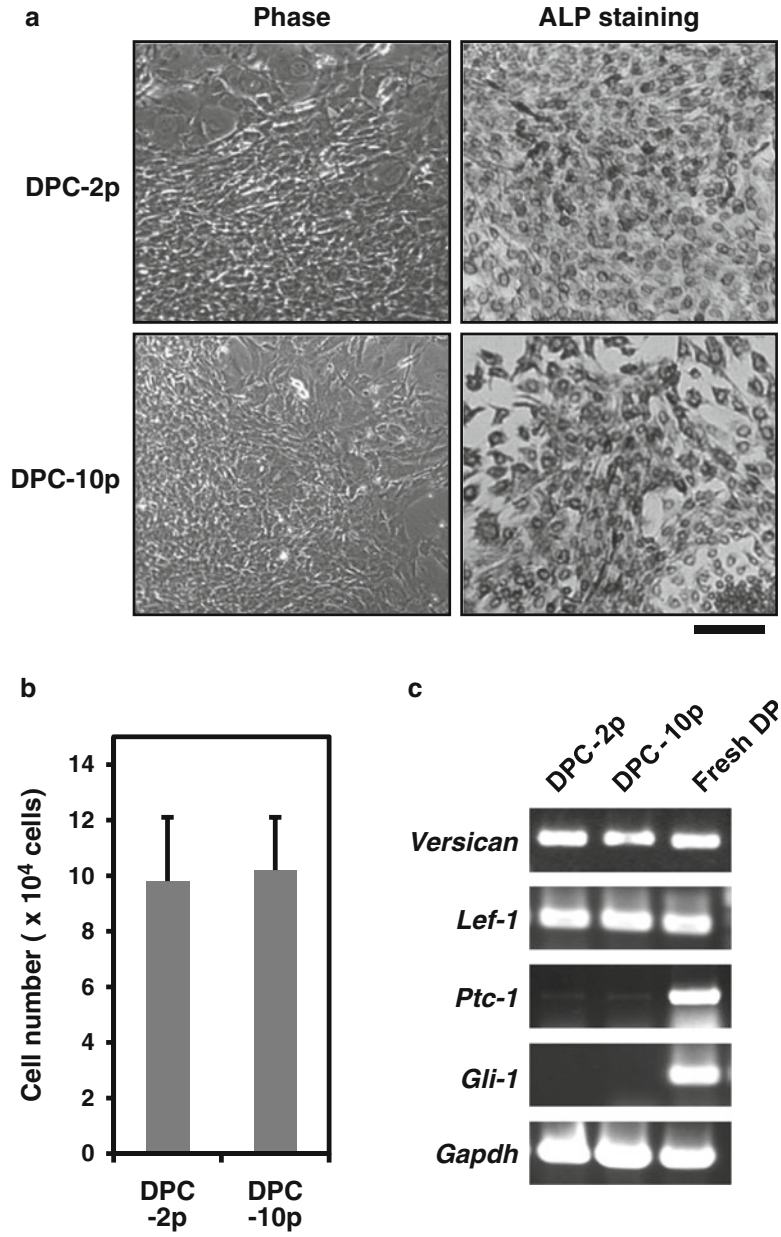

Fig. 3 Properties maintained by Wnt-10b in serially passaged DP cells. (**a**) DPC-10p formed multilayered clumps and retained ALP activity in a manner similar to DPCs after two passages in Wnt-COS supernatant (DPC-2p). Scale bar = 100 μm (**b**) DPC-10p proliferated in a manner similar to DPC-2p in regard to cell number. (**c**) RT-PCR findings showed clear expressions of *Lef-1* and *versican*, and slight expression of *Ptc-1*

4. For PCR analysis, use 0.5 μg of cDNA as a template and perform amplification using primer sequences shown in Table 1. General PCR conditions: 25–30 cycles at 94 °C for 2 min, 94 °C for 30 s, 52–62 °C for 30 s, and 72 °C for 1 min.
5. Run PCR products on 1.5 % agarose gels and visualize by ethidium bromide staining. (*see* **Note 6** and Fig. 3c)

4 Notes

1. In order to obtain Wnt-10b protein, we constructed a plasmid carrying the Wnt-10b cDNA gene and transfected it into COS-7 cells [10]. The clone that produced recombinant Wnt-10b protein most abundantly was selected and termed Wnt-COS. Supernatant from cultures of Wnt-COS cells contained secreted recombinant Wnt-10b, which inhibited the differentiation of a pre-adipocyte cell line (3 T3-L1) into lipid-carrying adipocytes.
2. The culture supernatant of Wnt-COS cells (Wnt-COS supernatant) contains bioactive Wnt-10b protein. The aliquots may be stored at 4 °C for up to 1 week or at −80 °C for a much longer period.
3. We examined DPCs after ten passages in cultures with Wnt-COS supernatant (DPC-10p). DPC-10p cells proliferated in a manner similar to DPCs after two passages in Wnt-COS supernatant (DPC-2p), and retained their ALP activity and gene expressions (*see* Subheading 3.4 and Fig. 3). It was shown possible that growth can continue for more than ten passages [9].
4. DPC-10p cells retained ALP activity in a manner similar to DPCs after two passages in cultures with Wnt-COS supernatant (DPC-2p) (*see* Fig. 3a).
5. DPC-10p cells proliferated in a manner similar to DPCs after two passages in cultures with Wnt-COS supernatant (DPC-2p) (*see* Fig. 3b).
6. Isolated DPs expressed all of the target genes (*Versican*, *Lef-1*, *Ptc-1*, *Gli-1*). Both DPC-10p and DPC-2p cells cultured with Wnt-COS supernatant distinctly expressed *Versican* and *Lef-1*, while they showed faint *Ptc-1* expression and none of *Gli-1* (*see* Fig. 3c).

References

1. du Cros DL, LeBaron RG, Couchman JR (1995) Association of versican with dermal matrices and its potential role in hair follicle development and cycling. J Invest Dermatol 105(3):426–431
2. Millar SE (2002) Molecular mechanisms regulating hair follicle development. J Invest Dermatol 118(2):216–225. doi:10.1046/j.0022-202x.2001.01670.x, 1670 [pii]
3. Botchkareva NV, Ahluwalia G, Shander D (2006) Apoptosis in the hair follicle. J Invest Dermatol 126(2):258–264. doi:10.1038/sj.jid.5700007, 5700007 [pii]
4. Jahoda C, Oliver RF (1981) The growth of vibrissa dermal papilla cells in vitro. Br J Dermatol 105(6):623–627
5. Kishimoto J, Burgeson RE, Morgan BA (2000) Wnt signaling maintains the hair-inducing activity of the dermal papilla. Genes Dev 14(10):1181–1185
6. Osada A, Iwabuchi T, Kishimoto J, Hamazaki TS, Okochi H (2007) Long-term culture of mouse vibrissal dermal papilla cells and de novo hair follicle induction. Tissue Eng 13 (5):975–982. doi:10.1089/ten.2006.0304

7. Inamatsu M, Matsuzaki T, Iwanari H, Yoshizato K (1998) Establishment of rat dermal papilla cell lines that sustain the potency to induce hair follicles from afollicular skin. J Invest Dermatol 111(5):767–775. doi:10.1046/j.1523-1747.1998.00382.x
8. Yamauchi K, Kurosaka A (2009) Inhibition of glycogen synthase kinase-3 enhances the expression of alkaline phosphatase and insulin-like growth factor-1 in human primary dermal papilla cell culture and maintains mouse hair bulbs in organ culture. Arch Dermatol Res 301(5):357–365. doi:10.1007/s00403-009-0929-7
9. Ouji Y, Ishizaka S, Yoshikawa M (2012) Dermal papilla cells serially cultured with Wnt-10b sustain their hair follicle induction activity after transplantation into nude mice. Cell Transplant. doi:10.3727/096368912X636867
10. Ouji Y, Yoshikawa M, Shiroi A, Ishizaka S (2006) Wnt-10b promotes differentiation of skin epithelial cells in vitro. Biochem Biophys Res Commun 342(1):28–35. doi:10.1016/j.bbrc.2006.01.104, S0006-291X(06)00177-X [pii]

Methods in Molecular Biology (2016) 1516: 279–288
DOI 10.1007/7651_2016_320

Published online: 01 April 2016

Maintenance of Skin Epithelial Stem Cells by Wnt-3a In Vitro

Yukiteru Ouji and Masahide Yoshikawa

Abstract

CD49f+ CD34+ cells, a population rich in skin epithelial stem cells (EpSCs), were obtained from adult mouse skin and cultured with Wnt-3a for 10 days. On day 10, CD49f+ CD34+ cells were sorted and subjected to a second 10-day culture with Wnt-3a. The same procedures were repeated until fifteenth 10-day culture. CD49f+ CD34+ cells obtained from each 10-day culture retained the same EpSC-characteristics as seen in the original EpSCs from adult mouse skin. Here, wedescribe the culture protocol using Wnt-3a for successful maintenance of EpSCs.

Keywords: Skin, Epithelial cells, Stem cells, Wnt signaling, Wnt-3a, Cell proliferation

1 Introduction

Wnt signaling is critical for regulation of a number of basic cell functions, such as cell proliferation, fate, polarity, and differentiation [1–3], and is also considered to be deeply involved in maintenance of stem cells including embryonic, neural, hematopoietic, mammary, hepatic, and skin epithelial stem cells [4–8]. Recently, the cell surface protein CD34 was shown to be uniquely expressed in stem cells from the mouse hair follicle bulge region (HFSCs) and an isolation method for living skin epithelial stem cells (EpSCs) from adult mouse-derived primary skin epithelial cells (MPSECs) was established by fluorescent activated cell sorting (FACS) using two selective surface markers, CD49f (α6 integrin) and CD34 [9, 10]. The population of CD49f+ CD34+ cells is considered to be an EpSC-rich fraction containing HFSCs. In our previous study, we reported successful maintenance of EpSCs in vitro for a prolonged period (at least 150 days) using Wnt-3a and FACS [11]. In this chapter, we show our culture method protocol used to maintain EpSCs with sustained characteristics.

2 Materials

2.1 Isolation of EpSCs

1. Inbred 8-week-old mice (Japan SLC, Shizuoka, Japan, C3H/HeN Slc).
2. Dissection instruments (micro-scissors, fine forceps).
3. Stereo microscope (Leica, model no. MS5).
4. Saline (Otsuka, Tokyo, Japan, cat. no. D05352).
5. Trypsin (0.25 %) (Invitrogen, Grand Island, NY, cat. no. 15050).
6. Plastic petri dishes (Sigma, cat. no. SIAL506CC0SnV).
7. Dulbecco's modified Eagle's medium (DMEM; Wako, Osaka, Japan, cat. no. 043-30085) containing 10 % fetal bovine serum and FBS (PAA Laboratory, Morningside QLD, cat. no. A15002).
8. Phosphate-buffered saline (PBS), pH 7.4 (Wako, cat. no. 048-29805).
9. Rat anti-α6 integrin (CD49f) directly coupled to PE (R&D Systems, Inc., Minneapolis, MN, cat. no. FAB13501P).
10. Rat IgG2a isotype directly coupled to PE (R&D Systems, Inc, cat. no. IC006P).
11. Rat anti-CD34 directly coupled to FITC (AbD Serotec, Oxford, UK, cat. no. MCA1825F).
12. Rat IgG2a isotype directly coupled to FITC (eBioscience, San Diego, CA, cat. no. 11-4321-73).
13. Polystyrene round-bottom tubes (BD, Bedford, MA, cat. no. 352235 or 352003).
14. Cell strainer (40 μm) (BD, cat. no. 352340).
15. Epilife™ serum-free culture medium kit (Thermo Fisher, Waltham, MA, cat. no. M-EPICF-500).
16. FACSAria system equipped with FACS DiVa software (BD Biosciences, San Jose, CA).
17. Trypan blue (Invitrogen, cat. no. 15250061).
18. Hemocytometer (Waken-Btech, Kyoto, Japan, cat. no. WC2-100).
19. Plastic cell culture dishes (6 cm) (BD, Bedford, MA, cat. no. 353002).
20. Light microscope (Carl Zeiss; model no. Axiovert 40CFL).

2.2 EpSCs Sequential Culture

1. Plastic cell culture dishes (6 cm).
2. Collagen type I (Nippon Ham, Tsukuba, Japan).
3. PBS.

4. Trypsin–EDTA (0.25 %) (Invitrogen, Burlington, ON, Canada, cat. no. 25200-056).
5. Rat anti-α6 integrin (CD49f) directly coupled to PE.
6. Rat IgG2a isotype directly coupled to PE.
7. Rat anti-CD34 directly coupled to FITC.
8. Rat IgG2a isotype directly coupled to FITC.
9. Polystyrene round-bottom tubes.
10. Epilife™ serum-free culture medium kit.
11. Wnt-3a recombinant protein (R&D Systems Inc., cat. no. 1324-WN/CF).
12. FACSAria system equipped with FACS DiVa software.
13. Trypan blue.
14. Hemocytometer.
15. Light microscope.

2.3 Characterization of EpSCs

1. PBS.
2. Trypsin–EDTA (0.25 %).

2.3.1 Flow Cytometry

3. Rat anti-α6 integrin (CD49f) directly coupled to PE.
4. Rat IgG2a isotype directly coupled to PE.
5. Rat anti-CD34 directly coupled to FITC.
6. Rat IgG2a isotype directly coupled to FITC.
7. Polystyrene round-bottom tubes.
8. PFA (1 %) solution (prepared by dilution of 4 % PFA solution, Wako, cat. no. 163-20145).
9. FACSCalibur (BD Biosciences).

2.3.2 Hair Reconstitution Assay

1. EpSCs (CD34+ CD49f+ cells sorted following serial cultivations) (*see* Sect. 3.2).
2. Newborn (day 2) mice (from C3H/HeN Slc).
3. Nude mice (BALB/c Slc-*nu/nu*, Japan SLC).
4. PBS.
5. Dispase (diluted in PBS, Godo Shusei Co. Ltd., Tokyo, Japan, cat. no. GD81020).
6. Collagenase (diluted in PBS, Wako, cat. no. 034-10533).
7. Cell strainer (40 μm).
8. Isoflurane (final concentration 2–4 %, Wako, cat. no. 099-06571).
9. Silicon transplantation chamber (kindly gifted by Dr. J. Kishimoto of Shiseido Co. Ltd.).
10. Dissection instruments (micro-scissors, fine forceps).
11. Animal clipper (Natsume Seisakusho, Tokyo, Japan, cat. no. C-29-8).

3 Methods

3.1 Isolation of EpSCs

1. Shave dorsal skin areas of adult mice.
2. Isolate dorsal skin tissues using forceps and scissors, and place in petri dishes.
3. Wash isolated skin samples several times with PBS.
4. Remove PBS and incubate skin tissues in 0.25 % trypsin at 4 °C overnight.
5. Add same volume of DMEM containing 10 % FBS into dishes.
6. Detach dermis from epidermis using fine forceps.
7. Collect whole epithelial cells by scrubbing epidermis-facing surface of dermis using belly of the forceps. These cells were designated as mouse-derived primary skin epithelial cells (MPSECs).
8. Filtrate whole cells using 40-μm cell strainer.
9. Centrifuge cell suspension at 250 × *g* for 5 min, then wash cells three times with PBS.
10. Prepare MPSECs as single cells by addition of PBS to pellets and determine cell number using trypan blue exclusion method.
11. Add antibodies directly coupled with a fluorochrome and expose cells for 30 min on ice (*see* **Note 1**).
12. After washing twice with PBS, resuspend cells in Epilife™ serum-free culture medium.
13. Sort CD34+ CD49f+ cells (EpSCs) from MPSECs using FACSAria system (*see* Fig. 1).

3.2 EpSC Sequential Cultures

Figure 2 shows the outline of the protocol for sequential culturing of EpSCs.

1. Treat 60-mm dishes with collagen type I and wash with PBS three times.
2. Resuspend CD49f+ CD34+ cells (EpSCs) sorted from MPSECs in Epilife™ serum-free culture medium and confirm their viability by trypan blue staining.
3. Seed EpSCs at a density of 5×10^4 cells per dish and culture in the presence of 200 ng/ml of Wnt-3a for 10 days.
4. Change to fresh medium containing Wnt-3a every 2 days.
5. On day 10, collect all cells by trypsin treatment and centrifuge cell suspensions at 250 × *g* for 5 min, then wash with PBS three times.

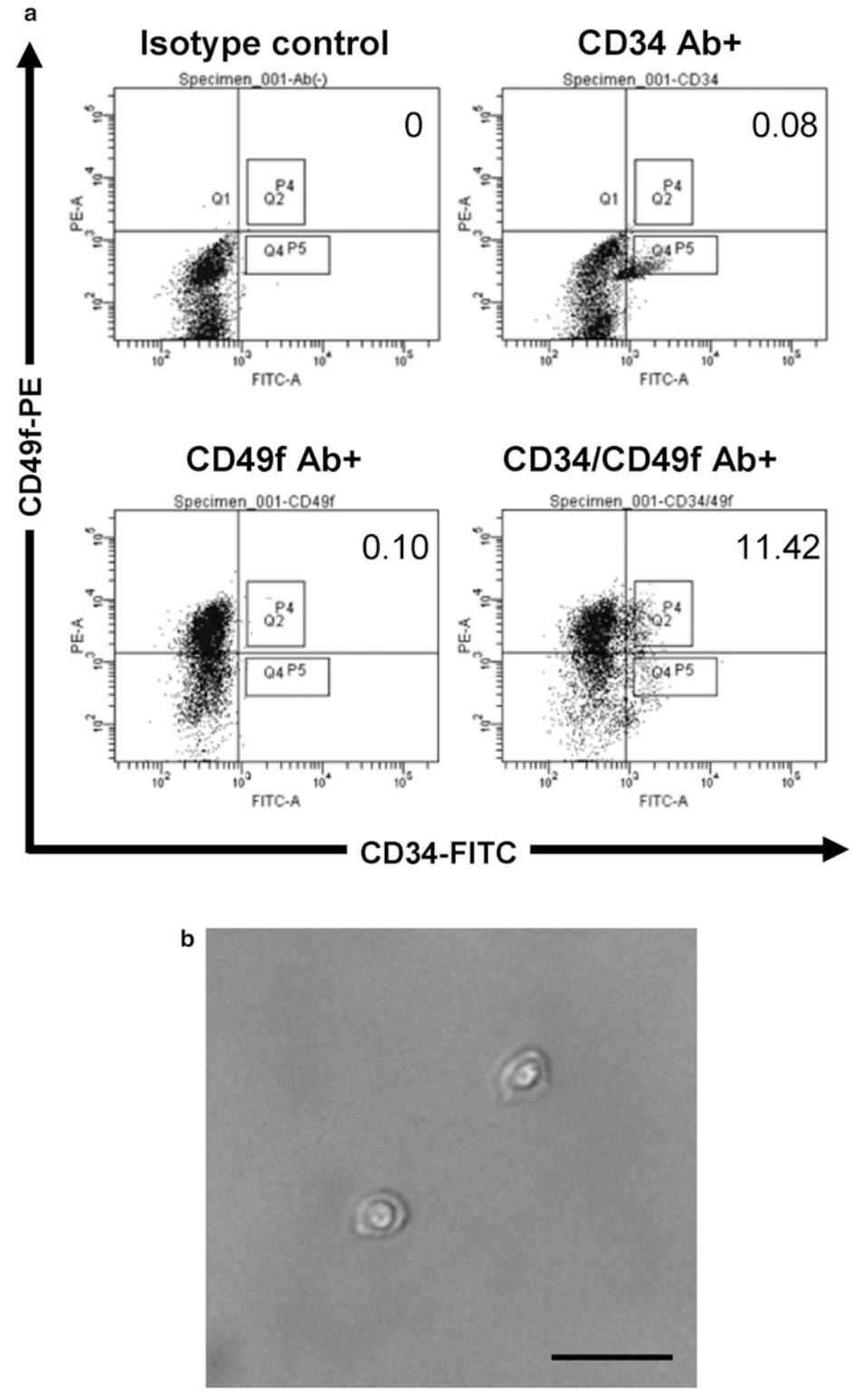

Fig. 1 Isolation of EpSCs. (**a**) MPSECs were stained with the isotype control, anti-CD34-FITC, or anti-CD49f-PE antibodies (isotype control Ab, CD34 Ab, CD49f Ab, respectively). EpSCs were collected from the MPSECs as CD34 and CD49f double-positive cells. (**b**) Bright microscopic field showing morphology of sorted EpSCs after attachment to culture plate. Scale bar = 50 μm

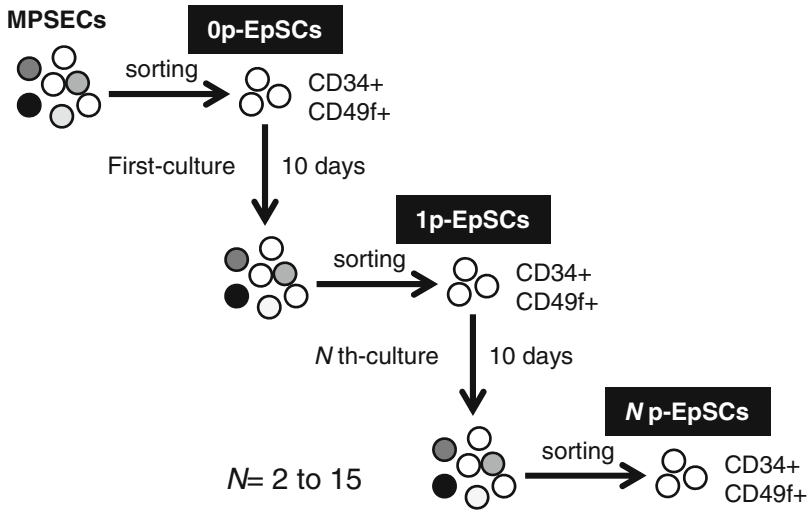

Fig. 2 Experimental design and procedures. 0p-EpSCs (primary sorted cells) were cultured in the presence of Wnt-3a for 10 days. At the end of the first 10-day culture, CD49f+ CD34+ cells were collected as 1p-EpSCs and subjected to the second 10-day culture with Wnt-3a. By repeating this process, cultures of CD49f+ CD34+ cells were sequentially performed up to 15 passages

6. Make single cell preparations into pellets by addition of PBS and determine the cell numbers using trypan blue exclusion method.
7. Add antibodies with a fluorochrome and expose cells for 30 min on ice.
8. After washing twice with PBS, resuspend cells in Epilife™ serum-free culture medium.
9. Sort EpSCs using FACSAria system (*see* **Note 2**).
10. Repeat **steps 5–9** for each experiment (*see* **Note 3**).

3.3 Characterization of EpSCs

3.3.1 Flow Cytometry

1. Culture EpSCs with or without Wnt-3a for 10 days (*see* Sect. 3.2.).
2. Wash EpSCs with PBS and harvest with 0.25 % trypsin–EDTA.
3. Centrifuge samples at 250 × *g* for 5 min, then wash with PBS and collect EpSCs.
4. Make single cell preparations into pellets by addition of PBS and determine cell numbers using trypan blue exclusion method.
5. Add antibodies with a fluorochrome and expose cells for 30 min on ice (*see* Sect. 3.2).
6. After washing twice with PBS, resuspend cells in 1 % PFA solution.
7. Analyze whole cells using FACSCalibur (*see* **Note 4**).

3.3.2 Hair Reconstitution Assay

A hair reconstitution experiment was performed as previously described by J. Kishimoto et al., with minor modifications.

Preparation of Dermal Cells

1. Isolate dorsal skin tissues from dorsal skin areas of newborn (day 2) mice using forceps and scissors, and place into petri dishes.
2. Wash isolated skin samples with PBS several times.
3. Incubate skin tissues in 500 units/ml dispase at 4 °C overnight.
4. Transfer skin tissues into dishes containing PBS and detach dermis samples from epidermis using fine forceps.
5. Incubate skin dermis in 0.25 % collagenase at 37 °C for 1 h.
6. Collect whole cells, then centrifuge and resuspend with PBS.
7. Allow tubes to stand for 20 min (*see* **Note 5**).
8. Collect all cells in supernatant and filtrate using 40-μm cell strainer.
9. Centrifuge cell suspension at 250 × *g* for 5 min and wash cells with PBS three times.
10. Add PBS to pellet samples and determine cell number using trypan blue exclusion method. Next, use dermal cell population containing dermal fibroblasts and papilla cells for transplantation (*see* **Note 6**).

Preparation of EpSCs as Epithelial Cells

On the day of transplantation, prepare cell population containing EpSCs cultured in serum-free medium with Wnt-3a.

1. Collect all cells cultured in Epilife™ serum-free culture medium with Wnt-3a using trypsin treatment.
2. Centrifuge cell suspensions at 250 × *g* for 5 min and wash with PBS three times.
3. Check cell viability and determine numbers using trypan blue staining.
4. Add antibodies with a fluorochrome and expose to cells for 30 min on ice (*see* Sect. 3.2.).
5. After washing twice with PBS, resuspend cells in Epilife™ serum-free culture medium.
6. Sort CD49f+ CD34+ cells as EpSCs using FACSAria system.
7. After washing with PBS, use EpSCs as epithelial cells for transplantation.

Transplantation

1. Prepare a mixed solution containing EpSCs (2.5×10^7/ml) and dermal cells (2.5×10^7/ml) to transplant into nude mice. Store on ice until transplantation.
2. Anesthetize nude mice with an inhalation of isoflurane.
3. Sterilize back skin of each mouse with 70 % ethanol.

4. Remove a section of back skin tissue with a diameter of 10 mm using scissors.
5. Implant silicon transplantation chambers into dorsal site of nude mice and fix using animal clipper.
6. Inject 200-μl mixture of EpSCs (2.5×10^6) and dermal cells (2.5×10^6) into each chamber by pipette.
7. Cut off the roof of the chamber at 1 week after transplantation.
8. Remove chamber at 2 weeks after transplantation.
9. Observe new hairs in graft sites at 3 weeks after removing chambers (*see* Fig. 4. and **Note** 7).
10. Harvest skin tissues for assessment of reconstituted skin, if required.

4 Notes

1. The following antibodies and dilutions were used: rat anti-α6 integrin (CD49f) labeled PE; 1:100; rat IgG2a isotype labeled PE; 1:100; rat anti-CD34 labeled FITC, 1:100; rat IgG2a isotype labeled FITC, 1:100.
2. We termed CD49f+ CD34+ cells isolated from MPSECs as 0p-EpSCs, then those from the first culture as 1p-EpSCs and those from the second culture as 2p-EpSCs, with the same naming protocol used for CD49f+ CD34+ cells from each successive passaged culture.
3. By repeating the procedure for CD49f+ CD34+ cell sorting on day 10 and subsequent passage to the next 10-day culture with Wnt-3a, sequential cultures were performed for up to 15 cultures.
4. EpSCs were gated for single events and sorted according to their expressions of CD49f and CD34. The purity of sorted cells was determined using post-sort FACS analysis and typically exceeded 95 %. Representative results for 2p- and 15p-EpSCs are presented (*see* Fig. 3).
5. The process utilized resulted in a sediment composed of large cells, debris, and follicles.
6. The dermal fibroblast fraction contained unavoidable contamination by non-dermal cells such as melanocytes.
7. The CD49f+ CD34+ population in sequential cultures with Wnt-3a showed an ability to reconstitute skin. Results from 2p- and 15p-EpSCs are presented (*see* Fig. 4).

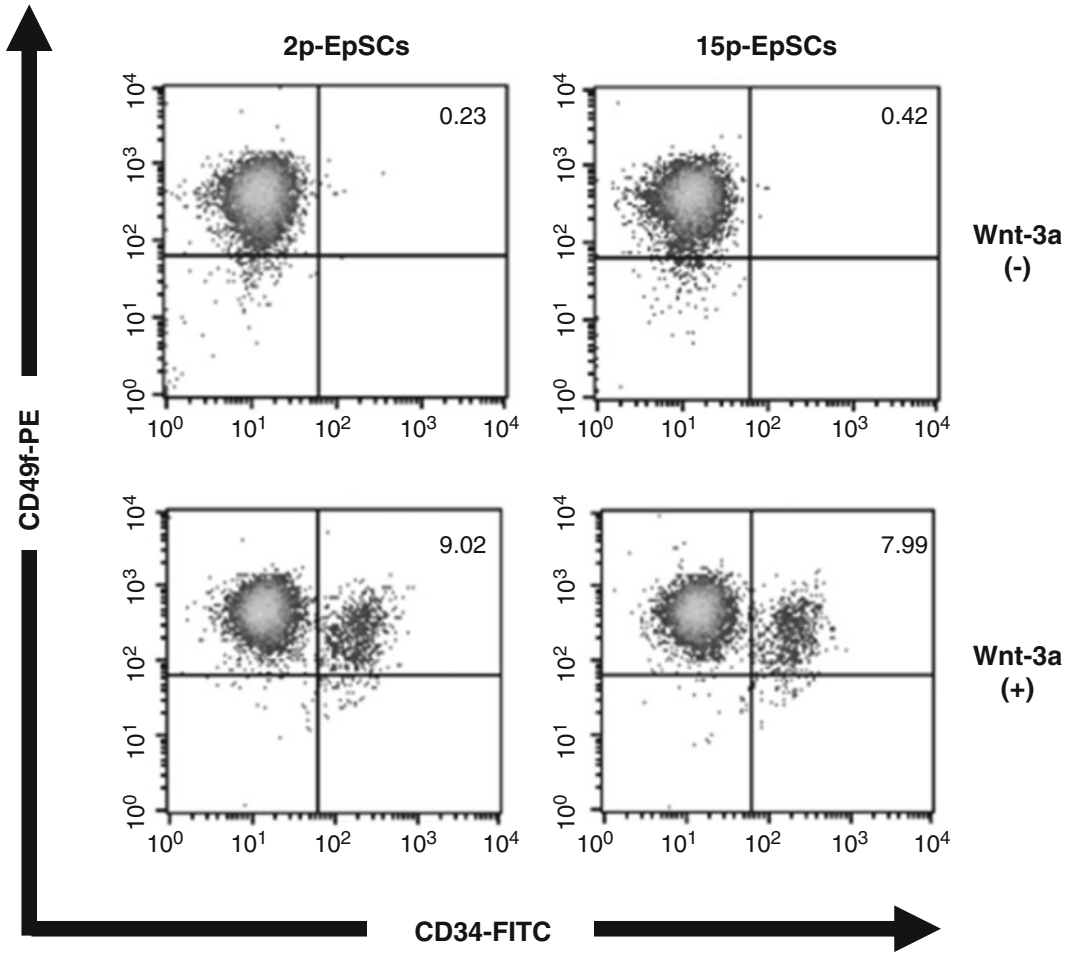

Fig. 3 Long-term maintenance of EpSCs by Wnt-3a in sequential cultures. The CD49f+ CD34+ population comprised approximately 8–10 % of all cells on day 10 in cultures with Wnt-3a, while there were few CD49f+ CD34+ cells in cultures without Wnt-3a. Representative results for 2p- and 15p-EpSCs are shown

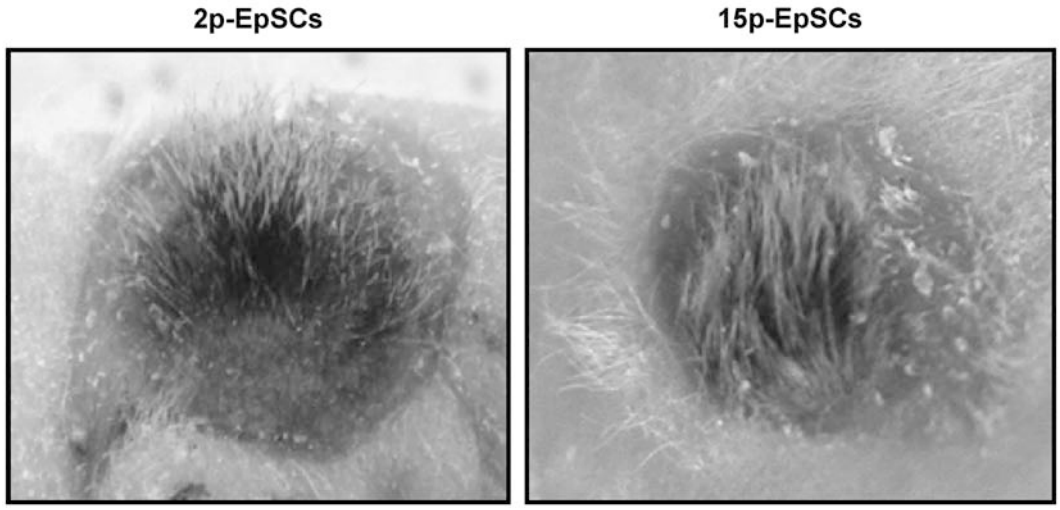

Fig. 4 EpSCs maintained in serial cultures showed sustained hair reconstitution ability. The CD49f+ CD34+ population in sequential cultures with Wnt-3a was able to reconstitute skin. Representative results from 2p- and 15p-EpSCs are presented

References

1. Peifer M, Polakis P (2000) Wnt signaling in oncogenesis and embryogenesis – a look outside the nucleus. Science 287(5458):1606–1609
2. Nusse R (2008) Wnt signaling and stem cell control. Cell Res 18(5):523–527. doi:10.1038/cr.2008.47
3. Moon RT, Bowerman B, Boutros M, Perrimon N (2002) The promise and perils of Wnt signaling through beta-catenin. Science 296 (5573):1644–1646. doi:10.1126/science.1071549
4. Watt FM, Collins CA (2008) Role of beta-catenin in epidermal stem cell expansion, lineage selection, and cancer. Cold Spring Harb Symp Quant Biol 73:503–512. doi:10.1101/sqb.2008.73.011
5. Hu M, Kurobe M, Jeong YJ, Fuerer C, Ghole S, Nusse R, Sylvester KG (2007) Wnt/beta-catenin signaling in murine hepatic transit amplifying progenitor cells. Gastroenterology 133(5):1579–1591. doi:10.1053/j.gastro.2007.08.036
6. Singla DK, Schneider DJ, LeWinter MM, Sobel BE (2006) wnt3a but not wnt11 supports self-renewal of embryonic stem cells. Biochem Biophys Res Commun 345(2):789–795. doi:10.1016/j.bbrc.2006.04.125
7. Nguyen H, Merrill BJ, Polak L, Nikolova M, Rendl M, Shaver TM, Pasolli HA, Fuchs E (2009) Tcf3 and Tcf4 are essential for long-term homeostasis of skin epithelia. Nat Genet 41(10):1068–1075. doi:10.1038/ng.431
8. Kleber M, Lee HY, Wurdak H, Buchstaller J, Riccomagno MM, Ittner LM, Suter U, Epstein DJ, Sommer L (2005) Neural crest stem cell maintenance by combinatorial Wnt and BMP signaling. J Cell Biol 169(2):309–320. doi:10.1083/jcb.200411095
9. Trempus CS, Morris RJ, Bortner CD, Cotsarelis G, Faircloth RS, Reece JM, Tennant RW (2003) Enrichment for living murine keratinocytes from the hair follicle bulge with the cell surface marker CD34. J Invest Dermatol 120 (4):501–511. doi:10.1046/j.1523-1747.2003.12088.x
10. Blanpain C, Lowry WE, Geoghegan A, Polak L, Fuchs E (2004) Self-renewal, multipotency, and the existence of two cell populations within an epithelial stem cell niche. Cell 118 (5):635–648. doi:10.1016/j.cell.2004.08.012
11. Ouji Y, Ishizaka S, Nakamura-Uchiyama F, Okuzaki D, Yoshikawa M (2015) Partial maintenance and long-term expansion of murine skin epithelial stem cells by Wnt-3a in vitro. J Invest Dermatol 135(6):1598–1608. doi:10.1038/jid.2014.510

Methods in Molecular Biology (2016) 1516: 289–297
DOI 10.1007/7651_2016_348

Published online: 05 April 2016

Enzyme-Free Dissociation of Neurospheres by a Microfluidic Chip-Based Method

Ching-Hui Lin, Hao-Chen Chang, Don-Ching Lee, Ing-Ming Chiu, and Chia-Hsien Hsu

Abstract

Neurosphere assay is a common and robust method for identification of neural stem/progenitor cells, but obtaining large numbers of live single cells from dissociated neurospheres is difficult using nonenzymatic methods. Here, we present an enzyme-free method for high-efficiency neurosphere dissociation into single cells using microfluidic device technology. This method allows single cell dissociation of DC115 and KT98 cells with high cell viabilities (80–85 %), single-cell yield (91–95 %), and recovery (75–93 %).

Keywords: Enzyme-free dissociation, Neurospheres, Single cells, Microfluidics, BioMEMS, Lab-on-a-chip

1 Introduction

Neurosphere dissociation—the separation of a cluster of cultured neural stem/progenitor cells into single cells—is a routine procedure in the fields of neurobiology and neural stem cell research [1, 2]. Neurosphere dissociations are commonly performed by using enzymatic methods which can generate high yields of single dissociated cells with reproducible results. However, to avoid protease and collagenolytic activities, which degrade cell membrane proteins [3], mechanical methods including trituration [4], manual cutting with scalpel [5], micro-scissors [6], tissue chopper [7], and microfabricated filter are used [8]. We have developed a microfluidic chip-based mechanical method to dissociate neurospheres [9]. Using this method we were able to obtain high single cell yield and cell recovery results of DC155 and KT98 neurospheres. The dissociated cells were highly viable and could subsequently regrow neurospheres and differentiate into the three central neural lineages. Typical results are also included in this chapter (Fig. 1 and Table 1).

The original version of this chapter was revised: Two author names were added to the chapter. The erratum to this chapter is available at 10.1007/978-1-4939-6550-2_327

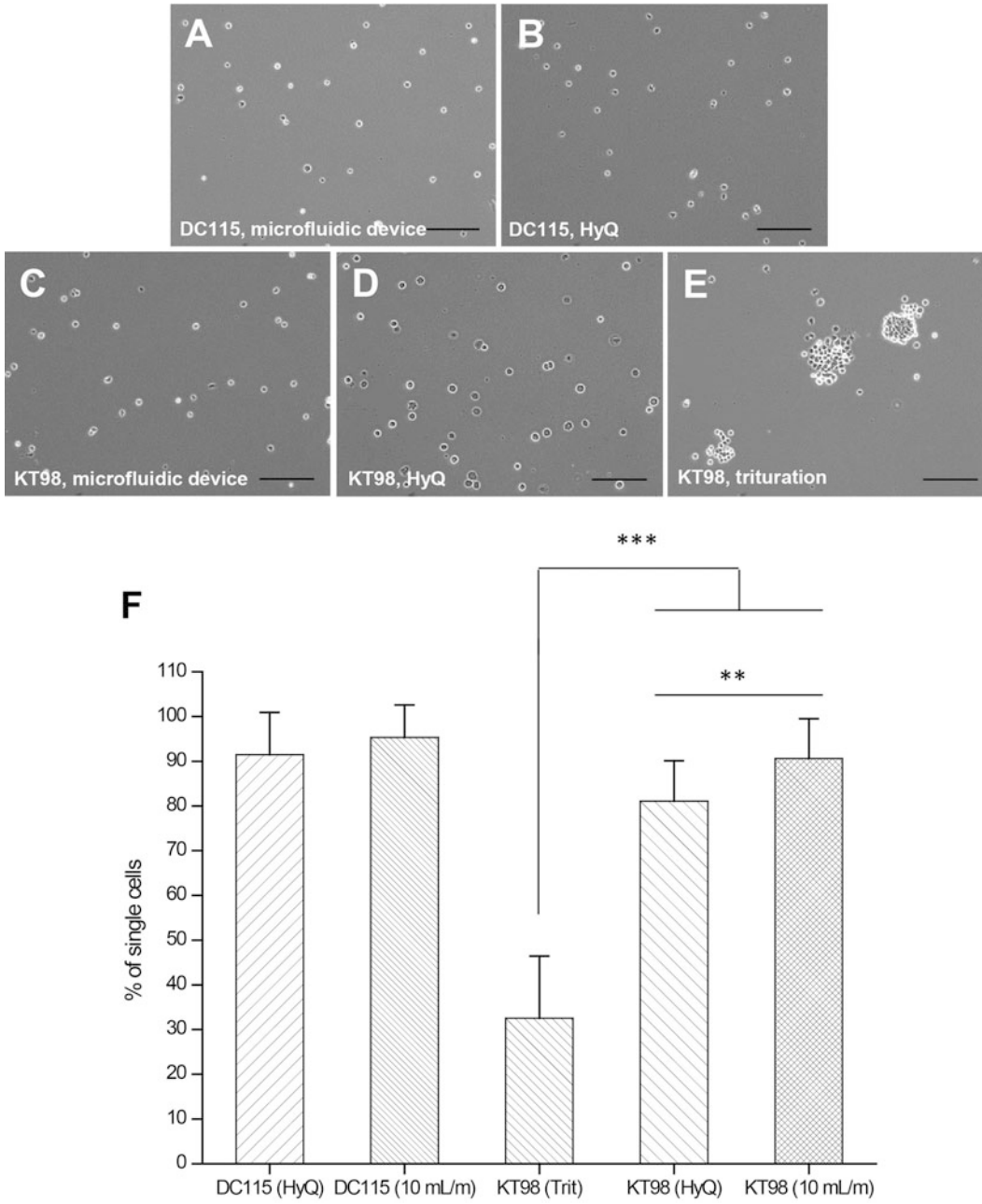

Fig. 1 Comparison of single cell dissociation efficiency of DC115 and KT98 neurospheres using the enzyme-free microfluidic device, HyQTase and mechanical trituration. Micrograph of single DC115 cells obtained from dissociated neurospheres by (**a**) microfluidic device and (**b**) HyQTase. Note that the majority of the cells are single cells. Micrograph of single KT98 cells obtained from dissociated neurospheres by (**c**) microfluidic device, (**d**) HyQTase, and (**e**) mechanical trituration method. Note large cell clusters were found in dissociated cell suspension after used of mechanical trituration method. Scale bar: 200 μm. (**f**) Single cell ratios from neurosphere dissociation using the microfluidic device, HyQTase and mechanical trituration dissociation methods. The microfluidic device could result in high ratios of single cells similar to that of enzymatic dissociation methods. Mechanical trituration resulted in a low number of single cells and many clusters

Table 1
Cell viability of dissociated cells after microfluidic device, HyQTase, and trituration dissociation

Traditional methods	Cell viability (%)	Microfluidic device	Cell viability (%)
DC115 (HyQTase)	94.22 ± 0.78	DC115 (10 mL/min)	84.52 ± 3.87
KT98 (HyQTase)	85.39 ± 1.97	KT98 (10 mL/min)	79.37 ± 3.77
KT98 (Trituration)	52.74 ± 5.69		

2 Materials

The production of the microfluidic PDMS device was utilized the soft lithography technique [10]. First of all, photomask designs were drawn by using AutoCAD software and then used for chrome masks to microfabricate master molds.

2.1 Fabrication of Master Molds

1. Chrome photomasks with the designed pattern.
2. 4-in. silicon wafers.
3. Conventional oven for dehydration of silicon wafers.
4. Plasma cleaner: a bench-top plasma treatment system for cleaning silicon wafers after dehydration.
5. Negative photoresists: using high viscosity photoresist SU-8 100 to make the high aspect ratio structures of micropillars.
6. Spin coater: for spin coating photoresists on the plasma cleaned silicon wafers.
7. Hot plate: to control the temperature of soft-baking and post-baking steps during the photolithography process.
8. Mask aligner: for aligning the photomasks to photoresist coated silicon wafers.
9. SU-8 developer: using propylene glycol monomethyl ether acetate (PGMEA) to wash off uncross-linked SU-8 photoresist to develop the master mold patterns.
10. Pure nitrogen gas (purity >99 %).

2.2 Microfluidic PDMS Device Fabrication

1. Trichlorosilane: to coat the surface of master molds before PDMS casting to create a hydrophobic surface for easier peeling of poly-dimethylsiloxane (PDMS) replicas from the master molds.
2. Desiccator: for creating a vacuum condition for vaporizing trichlorosilane solution during the silanization process of master molds.
3. Poly-dimethylsiloxane kit: a kit containing a PDMS base and a curing agent.

4. Plasma cleaner: a bench-top plasma treatment system to make the surface of PDMS replicas and 1" × 3" glass slides hydrophilic.
5. 3 M tapes: for removing the debris on PDMS surface.
6. Puncher with plunger with 0.75 mm inner diameter: for making the inlet and outlet holes of the microfluidic channels.
7. Hot plate: the temperature was set at 75 °C to enhance permanent bonding between PDMS replicas and glass slides.
8. Bovine serum albumin (BSA) solution: 5 % in phosphate-buffered saline (PBS).

2.3 Cell Culture

1. Cell lines: neural stem cells and brain tumor cell lines were used in this experiment.
2. Neurosphere medium: DMEM/F12 basal medium supplemented with 1 % N-2, 2 % B27, 20 ng/mL hFGF2, 20 ng/mL hEGF, and 2 μg/mL heparin.
3. Culture dish: 60 mm or 100 mm petri dish.

2.4 Enzyme-Free Dissociation of Neurosphere by a Microfluidic Chip

1. Plastic syringe: 1 mL for loading neurosphere suspension.
2. Connecter: 21 Gauge stainless steel blunt needle.
3. Teflon (polytetrafluorethylene) tubing: for connecting the inlet holes of the microfluidic device to plastic syringe; the inner diameter was 0.51 mm and the outer diameter was 0.82 mm.
4. Syringe pump: For driving neurosphere suspension and PBS buffer at controlled speed.

3 Methods

3.1 Master Mold Fabrication by Photolithography Technique

1. Preheat one hot plate to 65 °C and another hot plate to 95 °C.
2. Dehydrate a 4-in. silicon wafers at 120 °C for 10 min in a conventional oven, then clean the silicon wafers by oxygen plasma treatment for 30 s (*see* **Note 1**).
3. Place the cleaned silicon wafer on the scale and dispense 5 g of SU-8 100 photoresist onto the wafer, and coat the dropped PR by a spin coater for the expect thickness (please see the datasheet provided by MicroChem) (*see* **Note 2**). After coating, transfer the PR coated wafer onto the hot plate at 65 °C for 25–30 min, then transfer the wafer to the other hot plate at 95 °C for 70–80 min for the soft-baking process, followed by turning the hot plate off to allow the wafer to cool down to room temperature.
4. Place the wafer on the chuck stage of the mask aligner, align the chrome photomask to the PR coated wafer and expose the wafer to UV light (365 nm) at a dose of 600 mJ/cm^2 to photolithographically pattern the PR coated silicon wafer.

5. Transfer the wafers from the aligner to a hot plate at 95 °C for the post-baking process, followed by turning off the hot plate to allow the wafer to cool down to room temperature (*see* **Note 3**). Once cooled, soak the PR coated wafer in the developer solution (PGMEA) (*see* **Note 4**) to wash away the uncross-linked photoresist and followed by drying the wafer with pure nitrogen gas (*see* **Note 5**).

3.2 PDMS Device Assembling

1. Silanize the master mold with trichlorosilane by chemical vapor deposition (CVD) method to create a hydrophobic surface for easier removing of PDMS replicas from the master mold.
2. Drop 200 μL of trichlorosilane in a small weighting boat and place it and the oxygen plasma cleaned master mold together in a desiccator. Connect the desiccator to a vacuum source (−85 kPa) for 15 min. Close the valve of the desiccator and allow the CVD process to go for at least 1 h. Finally, devacuum the desiccator and remove the master mold from the desiccator to a 150 mm petri dish (*see* **Note 6**).
3. Prepare 17.6 g of PDMS prepolymer by mixing 16 g of PDMS base with 1.6 g of PDMS curing agent. Pour the mixture into a 150 mm petri dish containing the master mold. Then place the petri dish in a desiccator and apply vacuum to remove air bubbles from the PDMS. Finally, stop vacuum and transfer the petri dish to a conventional oven to cure the PDMS at 65 °C overnight (*see* **Note 7**).
4. Peel off the cured PDMS replica from the master mold and make two holes as fluid inlet and outlet at the two ends of the microchannel by a puncher with 1.0 mm inner-diameter (*see* **Note 8**).
5. Use 3 M tape to remove particles and debris on the surface of the PDMS replica. Clean a 1" × 3" glass slide with 75 % ethanol and followed by deionized (DI)-water. Treat the PDMS replica and glass slide with a brief oxygen plasma treatment (100 W for 14 s) in a plasma cleaner and then remove them from the oxygen plasma machine (*see* **Note 9**).
6. Use hands and bare eyes to align the PDMS replica to the glass slide and bring them into contact. Then place the PDMS device on a hot plate at 75 °C to enhance the bonding process for 10 min. The resulted PDMS device is shown in Fig. 2a.
7. Inject DI water into the PDMS device and leave the device inside a tissue culture hood to sterilize the device by using UV light (wavelength of light: 254 nm) for 30 min.
8. Replace the DI water in the PDMS device with a 5 % BSA solution and incubate the device at 37 °C for 30 min to prevent neurospheres sticking to the PDMS surface (*see* **Note 10**).

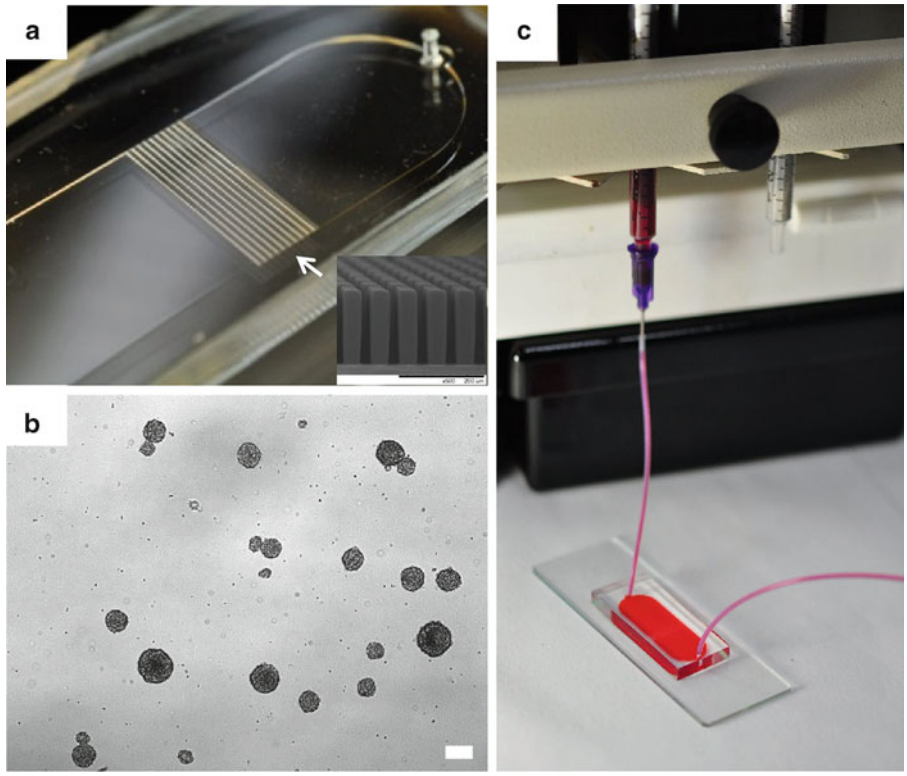

Fig. 2 Pictures of the microfluidic enzyme-free dissociation device and neurospheres. (**a**) Enzyme-free microfluidic device containing a cell aggregate dissociation micropillar array. (**b**) Micrograph of DC115 neurospheres after 7 days of culture in neurosphere culture medium. Scale bar: 100 μm. (**c**) The experiment setup showing the PDMS device contains a single inlet (*upper left*) and outlet (*lower right*)

3.3 Neurosphere Culture and Dissociation

1. Floating culture of neural stem cell (DC115) or brain tumor isolated cell (KT98) was performed with 100 mm petri dish containing 10 mL of neurosphere with seeding density of 10 cells per μL. The cells were cultured in a 5 % CO_2 humidified incubator at 37 °C for 7 days (*see* **Note 11**).
2. Collect the neurospheres from the petri dish into a 50 mL conical tube at day 7. Pass the cells through a 40 μm cell-strainer to remove small spheres and single cells (*see* **Note 12**).
3. Centrifuge the neurospheres at 300 × *g* for 3 min then discard the supernatant followed by resuspending the cells in 1 mL PBS. Load the neurosphere suspension into a 1 mL plastic syringe and cap the syringe with a connecter (Fig. 3).
4. Connect the neurosphere loaded 1 mL plastic syringe to the microfluidic chip inlet hole of the PDMS device via a Teflon tubing. Insert another Teflon tubing into microfluidic chip outlet hole for collecting the dissociated cells to a conical tube.

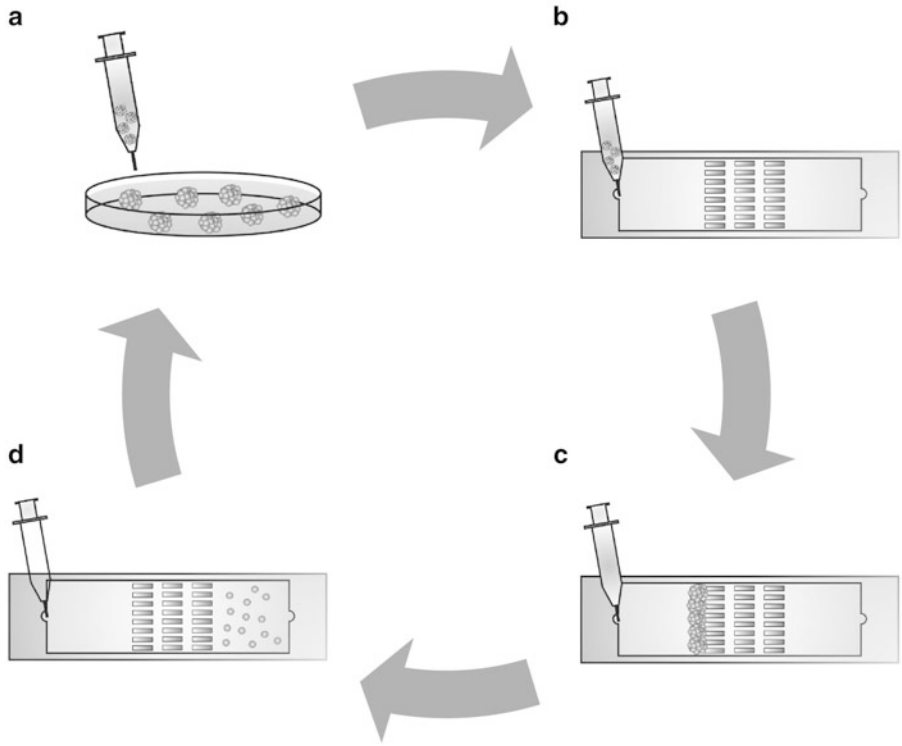

Fig. 3 Schematics of the operation procedure of the microfluidic PDMS device. (**a**) Neurosphere preparation and loading (initial cell number: 1×10^5/dish). (**b**) Cell loading into the microfluidic device. (**c**) Mechanical dissociation of neurospheres by flowing the neurospheres through micropillars with 20 μm gaps. (**d**) Neurospheres are dissociated into single cells which can be collected from the outlet of the device

5. Setup the neurosphere suspension loaded syringe on a syringe pump to drive the neurosphere suspension into the microchannel (Fig. 2c).
6. Load 800 μL of neurosphere suspension into the PDMS device at flow rate of 500 μL/min by the syringe pump. Replace the cell suspension syringe with a PBS loaded syringe, and use a flow rate of 10 mL/min to drive 10 mL of PBS into the microchannel (*see* **Note 13**).
7. Collect the microfluidic chip dissociated cells into a 15 mL conical tube from the Teflon tubing inserted in the outlet hole of the PDMS device. The collected cells can be used for further subculture or experiment.

4 Notes

1. Oxygen plasma treatment can enhance the adhesion and uniform-distribution of photoresist to silicon wafer.

2. To obtain uniform coating of photoresist, the photoresist should be dispensed as close to the center of the wafer as possible. The spin speed should be ramped up and down.
3. Cooling down the wafer before soaking it into the developer solution to avoid rapid temperature change of the wafer which could cause the patterned PR to peel off from the wafer.
4. During PR development, gently shake the container could accelerate the process. If PR structure peeling off from the wafer is observed, it is an indication that an insufficient exposing time or baking time was used.
5. When drying the wafer with nitrogen gas, strong gas stream should be avoided collapsing the high aspect ratio PR structures (e.g., the micropillars) on the wafer. To increase the mechanical strength of the SU-8 structure of the master mold, the developed wafer can be treated with an addition UV-exposure and hard bake step.
6. Store trichlorosilane in a desiccator and avoid expose it to humid environment as trichlorosilane is highly reactive to moisture. Note that trichlorosilane toxic, so the silanization process must be done in a chemical hood.
7. Thorough mixing of PDMS base and curing agent is necessary to obtain full curing of the PDMS. The standard ratio of PDMS base to its curing agent is 10:1. The ratio could be adjusted to obtain different rigidities of the cured PDMS product. The oven needs to be leveled to make the thickness of the cured PDMS uniform.
8. Carefully remove the PDMS replica from the master mold to avoid destructing thin PDMS and SU-8 structures of PDMS replica and master mold, respectively.
9. Do not touch the plasma treated PDMS and glass surface. This will damage the activated surface chemistry resulting in compromised bonding between the PDMS replica and glass slide.
10. The 5 % of BSA solution was prepared by dissolving 5 g of BSA powder into 100 mL of DI water, followed by passing the 5 % BSA solution through a 0.22 μm filter to sterilize microbially. The filtered 5 % BSA solution was stored at 4 °C before use.
11. Do not shake the petri dish at all times during cell culture to avoid forced-the aggregation of neurosphere cells.
12. Removing small spheres and single cells could increase the growth curve of the subcultured neurospheres.
13. The syringe pump should be placed vertically to avoid neurospheres settling and trapping in the syringe during cell loading. The cell loading step is used to position the neurospheres at the entrance area of the micropillars where as the PBS solution is used to push the neurospheres to pass through the micropillars.

References

1. Ahmed S (2009) The culture of neural stem cells. J Cell Biochem 106:1–6
2. Campos LS (2004) Neurospheres: insights into neural stem cell biology. J Neurosci Res 78:761–769
3. Delcroix GJR, Jacquart M, Lemaire L, Sindji L, Franconi F, Le Jeune JJ, Montero-Menei CN (2009) Mesenchymal and neural stem cells labeled with HEDP-coated SPIO nanoparticles: In vitro characterization and migration potential in rat brain. Brain Res 1255:18–31
4. Jensen PS, Lyck L, Jensen P, Zimmer J, Meyer M (2012) Characterization of porcine ventral mesencephalic precursor cells following long-term propagation in 3D culture. Stem Cells Int 2012:761843
5. Lin CH, Lee DC, Chang HC, Chiu IM, Hsu CH (2013) Single-cell enzyme-free dissociation of neurospheres using a microfluidic chip. Anal Chem 85:11920–11928
6. Lindvall O, Kokaia Z (2006) Stem cells for the treatment of neurological disorders. Nature 441:1094–1096
7. Serra M, Leite SB, Brito C, Costa J, Carrondo MJ, Alves PM (2007) Novel culture strategy for human stem cell proliferation and neuronal differentiation. J Neurosci Res 85:3557–3566
8. Wallman L, Akesson E, Ceric D, Andersson PH, Day K, Hovatta O, Falci S, Laurell T, Sundstrom E (2011) Biogrid—a microfluidic device for large-scale enzyme-free dissociation of stem cell aggregates. Lab Chip 11:3241–3248
9. Wolfe DB, Qin D, Whitesides GM (2010) Rapid prototyping of microstructures by soft lithography for biotechnology. Methods Mol Biol 583:81–107
10. Ziegler L, Segal-Ruder Y, Coppola G, Reis A, Geschwind D, Fainzilber M, Goldstein RS (2010) A human neuron injury model for molecular studies of axonal regeneration. Exp Neurol 223:119–127

Methods in Molecular Biology (2016) 1516: 299–308
DOI 10.1007/7651_2016_344

Published online: 05 April 2016

Automated Cell-Based Quantitation of 8-OHdG Damage

Bilge Debelec-Butuner, Aykut Bostancı, Lisa Heiserich, Caroline Eberle, Filiz Ozcan, Mutay Aslan, Dirk Roggenbuck, and Kemal Sami Korkmaz

Abstract

Detection of 8-OHdG-base damage has been a big challenge for decades, though different analytical methods are developed. The recent approaches that are used for quantitating either the total amount of base damage or the amount of base damage per cell from different sources of samples are not automated. We have developed a method for automated damage detection from a single cell and applied it to 8-OHdG quantitation.

Keywords: 8-OHdG, DNA damage, ROS, Oxidative stress, Base excision repair

1 Introduction

It is widely recognized that high levels of reactive oxygen species (ROS) might result in structural and/or genetic changes in cells modulating especially initial steps of carcinogenesis. As the accumulation of ROS and subsequent oxidative damage is commonly observed and widely studied in inflammatory diseases [1–3], recent reports supported the concern to inflammation induced carcinogenesis [4–6] and exercise-induced DNA damage [7–10]. Thus, inflammation induced ROS are linked to mutations in proto-oncogenes and tumor suppressors resulting in genomic heterogeneity during cancer progression.

Although continuously repaired in a cell by base excision repair (BER), 8-hydroxy-2′-deoxyguanosine (8-OHdG) is a single nucleotide base lesion and recognized as a biomarker of oxidative DNA damage [11, 12]. The quantitation of 8-OHdG is performed with a wide range of methodologies including immunofluorescence labeling with subsequent density analysis. This technique has been mostly carried out in deterministic studies on both cells and tissue samples [13–15]. However, the readout is usually given as average signal intensity with dense background due to cytoplasmic RNA staining interfering with DNA specific quantitation.

Although other methodologies such as IHC [3, 4] and ICC [16] may be used too, these methods produce uneven and

semiquantitative data. Thus, LC-MS/MS quantitation is preferred where applicable. Beside the huge advantages of producing highly precise and sensitive data at femtomolar amounts of genomic DNA from various samples including tissue, plasma, and urine [1, 5, 6, 17], the LC-MS/MS analysis also encompasses a common disadvantage of quantitating the cell-based damage in oxidative conditions. In this method, a pool of DNA isolated from any source is used. HPLC as an alternative method is applied to measure the amount of 8-OHdG from small amounts of samples [18]. In contrast, the immunofluorescence method has certain benefits such as being performed with low amounts/numbers of samples/cells in comparison to the analytical methods, in which more cells or the material is required to isolate relatively higher amounts of DNA for reliable quantitation of the damaged base.

In immunofluorescence-based methods, the data is quantitated by different methods/algorithms involving simple image analysis with criteria's like size, intensity, or distribution where the limitation might be the high throughput analysis. Therefore, we aimed to combine the conventional immunostaining of 8-OHdG-base damage with an automated immunofluorescence-based analysis system, where the platform is equipped with a high-resolution semi-confocal immunofluorescence microscope controlled by a sophisticated image-analysis software. The system was initially designed to quantitate the analysis of double strand DNA breaks (γ-H2AX$^{(S139)}$ foci) in cells. As a fact, automated analysis of γ-H2AX$^{(S139)}$ foci with AKLIDES Nuk has been demonstrated as a reliable, rapid, and efficient method enabling the detection of DNA damage in various cell lines [19, 20]. It has been consistently used for clinical purposes such as to measure drug resistance and radiotherapy sensitivity [21–23].

Here, we implemented the improved method of 8-OHdG labeling with automatic counting of cells using the AKLIDES Nuk system and defined the amount of oxidative damage as foci per cell. Methodologically, first, we treated cells with 2 M HCl before labeling the 8-OHdG with specific antibodies to facilitate the access of the antibody to damaged sites. This treatment resulted a lower RNA labeling and, thus, a lower background staining in the cytoplasm [24] (Fig. 1a, b). Second, we performed the foci counting on IF-labeled cells at 5 confocal planes to define foci related to the DNA damage by using the AKLIDES Nuk system, which was developed at Medipan GmbH (Germany). When the cells were detected by the system, defined object criteria were applied to determine parameters such as number of cells analyzed, number of foci per cell, their sizes, volumes and the number of cells having or not having foci. Subsequently, data were transferred into Excel files automatically. Finally, the same samples of treatments were validated at LC-MS/MS analysis. We observed that the 8-OHdG levels obtained by LC-MS/MS and AKLIDES Nuk methods were

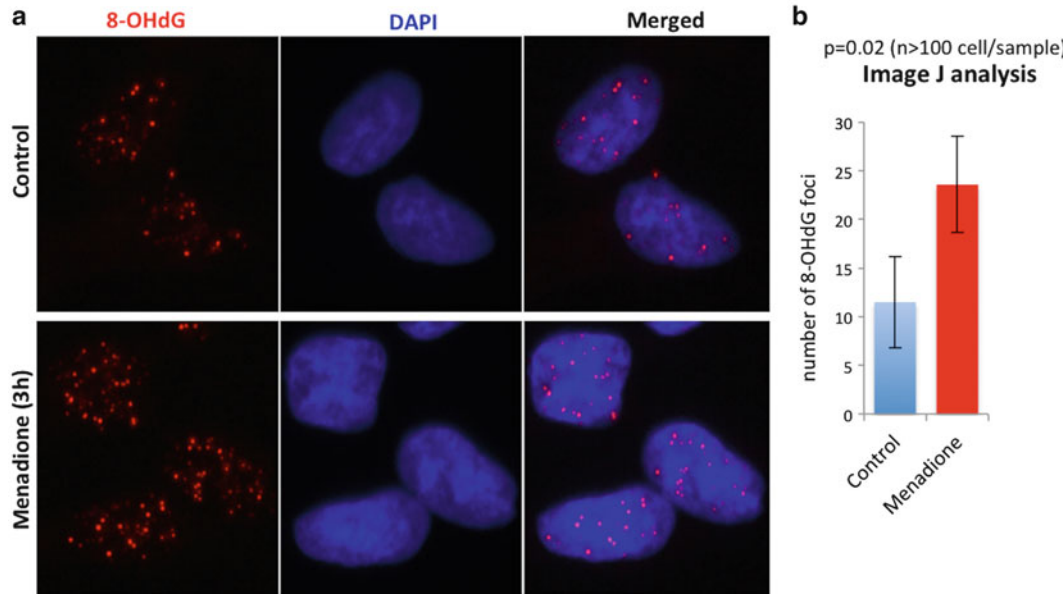

Fig. 1 (**a**) LNCaP cells were treated wi th 0.1 mM menadione for 3 h to induce 8-OHdG DNA damage and foci were detected by immunofluorescence labeling. Microscopic images were taken with 60× magnification. (**b**) Foci counting was performed by using Image J and results were graphed

correlated and associated with the amount of base damage before and after oxidant, menadione treatments. Thus, a cell-based method was developed for the quantitation of oxidative menadione-mediated 8-OHdG foci in the prostate cancer cell line LNCaP. The data are presented as average damage/cell; the number of cells having more than three foci; and total damage/100 cells in comparison to 8-OHdG/dG ratio from LC-MS/MS analysis (Fig. 2a–d).

2 Materials

Materials required for quantitation of 8-OHdG are listed below. Prepare all solutions using ultrapure water and molecular biology grade reagents.

1. PBS: Add 100 ml water to a 1 l graduated cylinder. Weigh 1.24 g Na_2HPO_4, 8 g NaCl, and 0.2 g KCl. Transfer chemicals to the cylinder and add water to the volume of 900 ml. Mix and adjust pH to 7.4 with 1 M HCl (*see* **Note** 7). Make up to 1 l with water. Autoclave for 45 min at liquid mode and store at room temperature.
2. 2 M HCl preparation; Add 250 ml water into a glass bottle (suitable for the 300 ml final volume). Under hood, add 50 ml

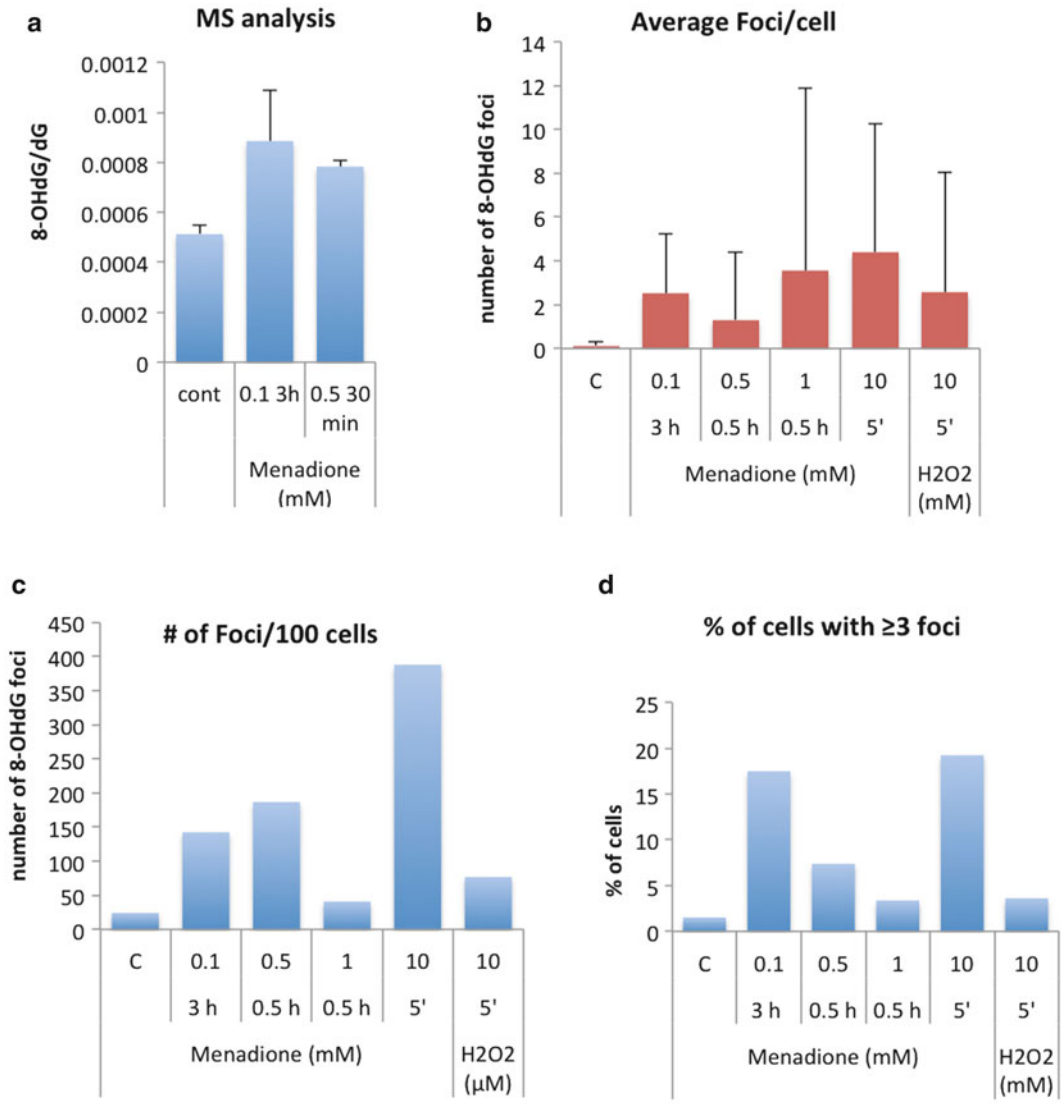

Fig. 2 8-OHdG DNA damage was induced with menadione for 3 h (0.1 mM), 30 min (0.5 mM, 1 mM), 5 min (10 mM) and with H_2O_2 for 5 min (10 mM). (**a**) DNA isolations were performed and samples were subjected to MS analysis. Results are presented indicating changes in 8-OHdG/dG ratio due to menadione treatments by LC/MS/MS analysis. (**b**) Foci were labeled by immunofluorescence and counted by AKLIDES Nuk and results were presented as graph showing average foci number for each cell. (**c**) Total number of foci in 100 cells. (**d**) % of cells having more than three foci. Error bars indicate standard deviation of two independent experiments

of 12 M HCl stock solution to the bottle. Mix and store at room temperature.

3. 0.1 M pH: 8.5 sodium borate: Weigh 9.1 g sodium borate ($Na_2B_4O_7.10H_2O$) and transfer to a glass bottle (suitable for the 300 ml final volume). Add 250 ml water and mix. Adjust

pH to 8.5 with 1 M HCl and make up to 300 ml with water (*see* **Note 9**). Store at 4 °C.

4. 0.2 % Triton X-100/PBS: Add 300 ml PBS into a glass bottle (suitable for the 300 ml final volume). Add 600 μl Triton X-100 into the solution by slow pipetting and mix (*see* **Note 8**). To ensure complete dissolution, incubate the solution at 37 °C water bath for 10 min and mix again. Store at 4 °C.
5. 3 % bovine serum albumin (BSA)/PBS: Add 250 ml PBS into a glass bottle (suitable for the 300 ml final volume). Weigh 9 mg BSA and transfer to the bottle. Mix until complete dissolution. Make up to 300 ml with PBS and store at 4 °C.
6. 70 % ethanol: Add 90 ml water into a glass bottle (suitable for the 300 ml final volume). Add 210 ml pure ethanol and mix. Store at −20 °C.
7. Mounting solution: Add 3.5 ml PBS into a 15 ml falcon tube. Add 1.5 ml glycerol by slow pipetting (*see* **Note 8**) and mix by vortexing. Add 50 μl of 100 μg/ml 4′,6-diamidino-2-phenylindole (DAPI) and vortex for 10 s. Store at −20 °C.

3 Methods

3.1 Immunofluorescence Labeling of 8-OHdG Foci

Cell Preparation

1. Split adherent cells onto coverslips in cell culture plates. Optimize cell number according to the cell type and cell culture plate.
2. Perform appropriate treatments if necessary to induce 8-OHdG foci formation.

Fixation

3. Discard the medium and wash with PBS.
4. Add 100 % methanol (stored at −20 °C) and incubate at −20 °C for 30 min.

   Wash with PBS.

Antibody Accession Treatment

5. Add 2 M HCl and incubate on an orbital shaker at room temp for 20 min and discard HCl.
6. Add 0.1 M pH 8.5 sodium borate ($Na_2B_4O_7{\cdot}10H_2O$) and incubate on an orbital shaker at room temp for 2 min and discard sodium borate.
7. Wash with PBS.

Antibody Incubation

8. Permeabilization: Add 0.2 % Triton X-100/PBS and incubate on an orbital shaker at room temperature for 5 min and discard.
9. Wash with PBS.
10. Blocking: Add 3 % BSA/PBS and incubate on an orbital shaker at room temp for 5 min and discard.
11. Wash with PBS.
12. Primary antibody incubation: Prepare the primary antibody at 1/3000 dilution in 3 % BSA/PBS. Add 50 μl onto each coverslip and cover the cells with Parafilm to ensure the cells do not dry out. Incubate at 4 °C overnight (16 h).
13. Remove Parafilm and wash with PBS four times.
14. Secondary antibody incubation: Prepare the secondary antibody (Alexa Fluor etc.) at 1/1000 dilution in 3 % BSA/PBS. Add 50 μl onto each coverslip and cover the cells with Parafilm to ensure the cells do not dry out. Incubate at room temp for 1 h.
15. Remove Parafilm and wash with PBS four times.
16. Add 70 % ethanol (stored at −20 °C) and incubate at room temp for 1 min.
17. Add 100 % ethanol (stored at −20 °C) and incubate at room temp for 1 min.
18. Remove coverslips from the plate, put on a drying paper, and let them to air-dry.
19. Add mounting solution including DAPI (Fig. 1a, b).

3.2 Measurement by AKLIDES Nuk

1. Place coverslips onto the AKLIDES Nuk slide holder.
2. Adjust the parameters for detection of cell and the foci type (parameters for nucleus definition such as diameter, height–-width ratio, and foci diameter, intensity, and confocality)
3. Count foci according to the adjusted parameters.
4. Analyze results to quantitate 8-OHdG damage level for each cell or cell population (Total foci number in 100 cells for each sample, average foci number for each cell, and number of cells with more than three foci).

3.3 Electrospray Ionization Mass Spectrometry (Used as the Validation Method)

Standards for 2′-deoxyguanosine (dG) and 8-hydroxy-2′-deoxyguanosine (8-OHdG) were purchased from Sigma-Aldrich (St. Louis MO, USA). Labeled [15N5] 2′-deoxyguanosine and [15N5] 8-hydroxy-2′-deoxyguanosine internal standards were obtained from Cambridge Isotope Laboratories (Andover, MA, USA). Solutions of dG, 8-oxo-dG, [15N5] dG and [15N5] 8-oxo-dG standards were prepared in dimethyl sulfoxide (DMSO; Calbiochem, EMD Bioscience, La Jolla, CA, USA). An optimized

multiple reaction monitoring (MRM) method was developed using ultrafast liquid chromatography (UFLC) coupled with tandem mass spectrometry (MS/MS) as previously described [6]. A UFLC system (LC-20AD UFLC XR, Shimadzu Corporation, Japan) was coupled to a LCMS-8040 triple quadrupole mass spectrometer (Shimadzu Corporation, Japan). Chromatographic separations were carried out using an HPLC column (Atlantis dC18, 2.1 × 150 mm, 5 μm; Waters, Massachusetts, USA) maintained at 25 °C. 2′-deoxyguanosine, 8-oxo-dG, [15N5] dG and [15N5] 8-oxo-dG were separated using a gradient elution with a flow rate of 0.2 ml/min. Mobile phase solvent A was 10 mM ammonium acetate (Sigma-Aldrich, St. Louis, MO, USA) adjusted to pH 3.75 with acetic acid in water and solvent B was methanol (Sigma-Aldrich, St. Louis, MO, USA). Gradient program was solvent B, 5 % (0–3 min), 50 % (3.01–4 min) and 5 % (4.01–13 min). MRM transitions and responses were automatically optimized for individual compounds in positive electrospray ionization (ESI). In the positive ESI-MS mode the precursor and product m/z values were as follows: dG, precursor ion 268.1 and product ions 152.2/135.1; 8-oxo-dG, precursor ion 283.8 and product ions 168.2/139.9; [15N5] dG, precursor ion 272.8 and product ion 157.0; [15N5] 8-oxo-dG, precursor ion 288.8 and product ion 173.2. Retention time of dG, 8-oxo-dG, [15N5] dG, [15N5] 8-oxo-dG, was 6.34, 6.38, 6.39 and 6.40 min, respectively. Responses to dG, 8-oxo-dG, [15N5] dG and [15N5] 8-oxo-dG were optimized to a linear calibration range from 0.78 ng/ml to 1 μg/ml and a sample analysis time of 13 min.

3.4 Preparation of Samples for Mass Spectrometric Analysis

DNA was isolated using the High Pure PCR Template Preparation Kit (Roche Diagnostics, Mannheim, Germany) according to manufacturer's instructions. Preparation and hydrolysis of nucleic acids was done as previously described with minor modifications [6]. DNA was dissolved in 100 μl TE buffer (10 mM Tris–HCl, pH 8.0, 1 mM EDTA). Ten microliters of dissolved DNA was added to 990 μl TE buffer (1:100 dilution). Diluted DNA samples were measured at absorbances of 260 and 280 nm, using TE buffer as a blank. One absorbance unit at 260 nm is equal to 50 μg/ml dsDNA. 20 μg of DNA was dissolved in 85 μl of 0.1 mM deferoxamine mesylate (DFOM) (Sigma-Aldrich, St. Louis MO, USA) solution and denatured by heating at 100 °C for 3 min, followed by rapid chilling. To the DNA solution, 1 μl of 100 ng/ml [15N5] 8-oxo-dG and 1 μl of 1 μg/ml [15N5] dG were added as internal standards for subsequent mass analysis. The DNA was hydrolyzed to nucleosides by incubation with nuclease P1 (Sigma-Aldrich, St. Louis MO, USA) dissolved in 0.3 M sodium acetate, 1 mM ZnSO4 at pH 5.3. 1 U/μl of nuclease P1 was added to samples and samples were incubated at 50 °C for 1 h. This incubation was followed by incubation with alkaline phosphatase (1 U/μl) at 37 °C

for 1 h. The DNA hydrolysate in a total volume of 100 μl was centrifuged at 12,000 × *g* for 10 min at 4 °C, and 80 μl of the supernatant was used for the LC-MS/MS analysis.

4 Hints

1. We use coverslips indicated as #1.
2. Solution volume needs to be adjusted according to the plate surface. We use 2 ml for 6-well plates.
3. 2 M HCl, 0.1 M pH 8.5 Sodium borate, 0.2 % Triton X-100/PBS and 3 % BSA/PBS should be prepared freshly before use.
4. Store 100 % methanol, 70 %, and 100 % ethanol at −20 °C until use.
5. Fixed cells can be stored at 70 % ethanol at 4 °C for 1 day if necessary but not preferred.
6. Labeled cells can be stored at 70 % ethanol at 4 °C for 1 day if necessary but not preferred.
7. 6 M HCl can be used for titrating at first to use less volume of HCl to reach the required pH value. When reaching at closer pH, it would be better to use 1 M HCl to avoid a sudden drop in pH.
8. Pipetting Triton X-100 and glycerol are needed to be careful for correct dispensing of volume.
9. To complete dissolution of sodium borate, pH needs to be adjusted at 8.5.
10. Antibodies experienced are: 8-OHdG (SCBT, sc-66036 [15A3], 1/3000 dilution), (Abcam, ab62623 [15A3], 1/3000 dilution). In addition, higher antibody concentrations are detected to give higher background and lower control/treatment difference.
11. Addition of the solutions into the well should be done without disturbing the cells.
12. Washing with PBS should be done as pipetting PBS into the well without disturbing the cells, incubating 30 s. and discarding the solution.
13. Optimization of HCl treatment can be performed by using 0.5, 1, and 2 M HCl for 10 min and 20 min. Best results are taken with 2 M concentration and 20 min. However, more optimization can be performed for different cell types.
14. Double labeling with 8-OHdG and another primary antibody (pAb) can be performed though resulting in less performance compared to mono labeling of 8-OHdG. Since the labeling of pAb is negatively effected by HCl treatment, simultaneous

double labeling could not be achieved. Therefore, sequential labeling can be performed. pAb labeling is performed by using its own protocol and then 8-OHdG labeling is performed starting from fixation step.

15. For suspension cells; cells are collected into 1.5 ml dolphin nose tubes and solutions are added at 1 ml volumes onto cells. Shaking is performed on a rotator. To discard solutions, cells are centrifuged at 4000 $\times$ *g* for 3 min to collect cells at the bottom of the tube and the solution is discarded by using micropipette. For mounting, cells are resuspended in mounting solution and transferred onto coverslip for immunofluorescence imaging.

Acknowledgement

This research was supported by TUBITAK grant 113S044 to KSK.

References

1. Kurgan S, Onder C, Altingoz SM, Bagis N, Uyanik M et al (2015) High sensitivity detection of salivary 8-hydroxy deoxyguanosine levels in patients with chronic periodontitis. J Periodontal Res 50:766–774
2. Nakamura A, Osonoi T, Terauchi Y (2010) Relationship between urinary sodium excretion and pioglitazone-induced edema. J Diabetes Investig 1:208–211
3. Ding X, Hiraku Y, Ma N, Kato T, Saito K et al (2005) Inducible nitric oxide synthase-dependent DNA damage in mouse model of inflammatory bowel disease. Cancer Sci 96:157–163
4. Murata M, Thanan R, Ma N, Kawanishi S (2012) Role of nitrative and oxidative DNA damage in inflammation-related carcinogenesis. J Biomed Biotechnol 2012:623019
5. Gan W, Nie B, Shi F, Xu XM, Qian JC et al (2012) Age-dependent increases in the oxidative damage of DNA, RNA, and their metabolites in normal and senescence-accelerated mice analyzed by LC-MS/MS: urinary 8-oxoguanosine as a novel biomarker of aging. Free Radic Biol Med 52:1700–1707
6. Nie B, Gan W, Shi F, Hu GX, Chen LG et al (2013) Age-dependent accumulation of 8-oxoguanine in the DNA and RNA in various rat tissues. Oxid Med Cell Longev 2013:303181
7. Yasuda N, Bolin C, Cardozo-Pelaez F, Ruby BC (2015) Effects of repeated bouts of long-duration endurance exercise on muscle and urinary levels of 8-hydroxy-2′-deoxyguanosine in moderately trained cyclists. J Sports Sci 33:1692–1701
8. Fogarty MC, Devito G, Hughes CM, Burke G, Brown JC et al (2013) Effects of alpha-lipoic acid on mtDNA damage after isolated muscle contractions. Med Sci Sports Exerc 45:1469–1477
9. Soares JP, Silva AM, Oliveira MM, Peixoto F, Gaivao I et al (2015) Effects of combined physical exercise training on DNA damage and repair capacity: role of oxidative stress changes. Age (Dordr) 37:9799
10. Villano D, Vilaplana C, Medina S, Cejuela-Anta R, Martinez-Sanz JM et al (2015) Effect of elite physical exercise by triathletes on seven catabolites of DNA oxidation. Free Radic Res 49:973–983
11. Kryston TB, Georgiev AB, Pissis P, Georgakilas AG (2011) Role of oxidative stress and DNA damage in human carcinogenesis. Mutat Res 711:193–201
12. Cadet J, Loft S, Olinski R, Evans MD, Bialkowski K et al (2012) Biologically relevant oxidants and terminology, classification and nomenclature of oxidatively generated damage to nucleobases and 2-deoxyribose in nucleic acids. Free Radic Res 46:367–381
13. Kim J, Kim NH, Sohn E, Kim CS, Kim JS (2010) Methylglyoxal induces cellular damage by increasing argpyrimidine accumulation and oxidative DNA damage in human lens

epithelial cells. Biochem Biophys Res Commun 391:346–351

14. Cafueri G, Parodi F, Pistorio A, Bertolotto M, Ventura F et al (2012) Endothelial and smooth muscle cells from abdominal aortic aneurysm have increased oxidative stress and telomere attrition. PLoS One 7:e35312
15. Puente BN, Kimura W, Muralidhar SA, Moon J, Amatruda JF et al (2014) The oxygen-rich postnatal environment induces cardiomyocyte cell-cycle arrest through DNA damage response. Cell 157:565–579
16. Thompson CM, Fedorov Y, Brown DD, Suh M, Proctor DM et al (2012) Assessment of Cr (VI)-induced cytotoxicity and genotoxicity using high content analysis. PLoS One 7: e42720
17. Dizdaroglu M, Jaruga P, Rodriguez H (2001) Measurement of 8-hydroxy-2′-deoxyguanosine in DNA by high-performance liquid chromatography-mass spectrometry: comparison with measurement by gas chromatography-mass spectrometry. Nucleic Acids Res 29:E12
18. Kondo S, Toyokuni S, Tanaka T, Hiai H, Onodera H et al (2000) Overexpression of the hOGG1 gene and high 8-hydroxy-2′-deoxyguanosine (8-OHdG) lyase activity in human colorectal carcinoma: regulation mechanism of the 8-OHdG level in DNA. Clin Cancer Res 6:1394–1400
19. Runge R, Hiemann R, Wendisch M, Kasten-Pisula U, Storch K et al (2012) Fully automated interpretation of ionizing radiation-induced gammaH2AX foci by the novel pattern recognition system AKLIDES(R). Int J Radiat Biol 88:439–447
20. Willitzki A, Lorenz S, Hiemann R, Guttek K, Goihl A et al (2013) Fully automated analysis of chemically induced gammaH2AX foci in human peripheral blood mononuclear cells by indirect immunofluorescence. Cytometry A 83:1017–1026
21. Leifert WR, Siddiqui SM (2015) gammaH2AX is a biomarker of modulated cytostatic drug resistance. Cytometry A 87:692–695
22. Reddig A, Lorenz S, Hiemann R, Guttek K, Hartig R et al (2015) Assessment of modulated cytostatic drug resistance by automated gammaH2AX analysis. Cytometry A 87:724–732
23. Menegakis A, von Neubeck C, Yaromina A, Thames H, Hering S et al (2015) gamma-H2AX assay in ex vivo irradiated tumour specimens: A novel method to determine tumour radiation sensitivity in patient-derived material. Radiother Oncol 116:473–479
24. Moiseeva O, Bourdeau V, Roux A, Deschenes-Simard X, Ferbeyre G (2009) Mitochondrial dysfunction contributes to oncogene-induced senescence. Mol Cell Biol 29:4495–4507

Methods in Molecular Biology (2016) 1516: 309–317
DOI 10.1007/7651_2016_350

Published online: 07 April 2016

$CoCl_2$ Administration to Vascular MSC Cultures as an In Vitro Hypoxic System to Study Stem Cell Survival and Angiogenesis

Carmen Ciavarella*, Silvia Fittipaldi*, and Gianandrea Pasquinelli

Abstract

Mesenchymal stem cells (MSCs) possess well-known reparative properties, among which the ability to form neovessels; in vivo, this characteristic is carried out both in a normal and in a pathological setting. Hypoxia, a condition common to many human diseases, is known to promote angiogenesis and to improve stem cell proliferation and differentiation. For this purpose, we provide an experimental protocol to test stem cell viability and angiogenesis under hypoxic conditions, comparing a vascular model of MSCs with stable cell lines. In order to avoid the use of expensive facilities, we propose the application of a chemical hypoxia inducer, cobalt chloride.

Keywords: Mesenchymal stem cells, Heterogeneity, Hypoxia, $CoCl_2$, Survival, Angiogenesis

1 Introduction

Mesenchymal stem cells (MSCs) are adult stem cells obtained from several human tissues (i.e., bone marrow, bone, fat, peripheral blood, synovium, vascular wall), representing a promising cell reservoir for clinical applications [1]. According to the International Society for Cellular Therapy, MSCs are defined by an immunophenotype positive to CD73, CD90, CD105 and negative to CD45, CD34, CD14 or CD11b, CD79α or CD19 and HLA-DR antigens [2]. The adherence to plastic and the ability to differentiate into mesodermal lineages (osteogenesis, adipogenesis, chondrogenesis) under appropriate culture conditions, complete the triad for the MSC characterization [2]. Despite the adherence to these criteria, the MSC population displays an elevate grade of heterogeneity in terms of differentiation efficiency and regenerative potential. Indeed, depending on the source and the donor age, MSCs comprise subsets of cells at distinct differentiation levels [3].

*Author contributed equally with all other contributors.

Our protocol is aimed to mimic the stem cell microenvironment, keeping low oxygen levels, in order to preserve the stem cell properties. In fact, stem cells are able to survive under stressful conditions as low and high oxygen tension. For instance, the standard laboratory in vitro culture exposes cells to 21 % O_2 tension, which is a very high percentage considering the normal in vivo tissue O_2 values are comprised between 1 and 12 % [4].

In this protocol, cells were cultured under hypoxic conditions, by using a chemical inducer of hypoxia—cobalt chloride [5]; after evaluating the cell survival, we observed the angiogenic potential (formation of neovessels) as it represents a common response to hypoxia and oxidative stress exposure [6].

Each cell model used in our study represents a specific in vitro system with distinct characteristics. Human aortic MSCs represent a primary vascular cell model, isolated from healthy and pathological conditions, previously characterized and tested for their resistance under stress [7].

In order to optimize the use of $CoCl_2$ also in other common in vitro cell models, two additional cell lines were tested: a tumorigenic model, the U2OS cell line, and a non-tumorigenic cell line WPMY-1.

U2OS derives from a human osteosarcoma and shows an epithelioid morphology with a doubling time of 24 h. WPMY-1 is a reactive mesenchymal cell line isolated from the stroma of a non-neoplastic prostate usually used to study the stromal-epithelial interactions, defined as healthy myofibroblasts with a doubling time of 37 h [8].

Briefly, cells were exposed to $CoCl_2$ at different doses and time intervals; after that we selected the $CoCl_2$ concentration eligible for the angiogenic assay, with less drastic effects on cell proliferation. The capillary-like structure formation was performed on a three-dimensional Matrigel matrix [9] followed by the mRNA analysis of the angiogenic and stress responsive genes by real-time PCR: the Vascular Endothelial Growth Factor (VEGF); NESTIN, a documented marker of stemness and neoangiogenesis active progression [10, 11]; the receptor tyrosine kinase insulin-like growth factor 1 (IGF1R) and the transforming growth factor-1β (TGF-1β), considered two other promising markers recently studied in both human cancerogenesis and neoangiogenesis [10].

In the first step, we observed that all the cell models survived at 500 μM $CoCl_2$ for 24 h and, at these conditions, the angiogenesis resulted improved in MSCs, especially in the pathological model. U2OS did not form neovessels. WPMY-1 displayed a clear angiogenic capacity, started to form stable vessels at 2 h from seeding in the Matrigel in all the culture conditions and these structures were kept at each time lapse.

According to data obtained in our primary vascular cell cultures, hypoxia $CoCl_2$-induced may represent a good in vitro system to mimic stem cell microenvironment, to be considered for future studies on stem cell clinical applications.

2 Materials

2.1 Cell Cultures

1. Incubator at 37 °C with an atmosphere of 5 % CO_2.
2. Primary cultures of mesenchymal stromal cells (MSCs) isolated from healthy thoracic aorta (hMSCs) and from aneurysm-affected abdominal aorta (AAA-MSCs).
3. Immortalized cell lines: U2OS and WPMY-1 (*see* **Note 1**).
4. Dulbecco's modified Eagle's medium (DMEM, Sigma-Aldrich) enriched with 1 % antibiotics and 0.5 % essential amino acids (*see* **Note 2**).
5. Phosphate Buffered Solution pH 7.4 (PBS)
6. Trypsin–EDTA 10× solution: add 10 mL of 10× trypsin to 90 mL of sterile PBS to obtain the 1× working solution.

2.2 Enzymatic Digestion Reagents

1. Liberase type II 50 mg, 260 U (Liberase TM Research Grade, Roche). Work under laminar flow cabinet to ensure sterility and keep the Liberase II on ice (*see* **Note 3**). The lyophilized stock contains 50 mg of enzyme to be suspended in 10 mL of sterile water to obtain the final stock concentration of 5 mg/mL. The whole solution can be stocked at −20 °C, in aliquots of 1 mL each.

2.3 Cobalt (II) Chloride Hexahydrate ($CoCl_2$)

1. Chloride hexahydrate ($CoCl_2 \cdot 6H_2O$; mw: 237.9 g/mol; Sigma-Aldrich). Dilute the 25 mM stock solution in sterile ddH_2O to obtain a final concentration of 100 μM (*see* **Note 4**).

2.4 Cell Viability Assay Components: Cell Fixation and Staining

1. Buffered Formalin 10 %.
2. Crystal Violet (CV) (*see* **Note 4**): Under the chemical hood, dissolve 1 g of CV powder in 100 mL of dH_2O to obtain the CV 1 %. Add 20 mL of MetOH in 80 mL of dH_2O to obtain 20 % MetOH. Add 10 mL of the CV at 1 % to 90 mL of 20 % MetOH.
3. Acetic acid 10 % in dH_2O.
4. Microplate Reader (Bio-Rad Model 3350-UV).

2.5 Angiogenic Induction Media

1. Vascular Endothelial Growth Factor (V2759, 10 μg; mw: 38.2 kDa; Sigma-Aldrich). The lyophilized protein needs to be stored at −20 °C. The vial content can be diluted in sterile water at a concentration between 0.1 and 1 mg/mL.
2. DMEM 2 % FBS (*see* **Note 2**).

2.6 Tubule-Formation Assay

1. BD Matrigel Basement Membrane Matrix (354234, BD Biosciences) is stable at −20 °C (*see* **Note 5**). Dispense the Matrigel stock solution into one-time aliquots and store them at −20 °C until use.
2. Serum-free DMEM.
3. Precooled tips and 96-well plates.

2.7 RNA Extraction, cDNA Synthesis and Real-Time PCR

1. TRIzol reagent solution (Invitrogen, Italy).
2. Ethanol 75 %, chloroform, isopropanol, glycogen (Stock 20 μg/μL, use diluted 10×).
3. RNAse free water.
4. ND-1000 spectrophotometer (NanoDrop, Fisher Thermo, Wilmington, DE, USA).
5. High Capacity Reverse Transcription Kit (Life Technologies).
6. TaqMan Univ PCR MasterMix (Life Technologies).
7. Specific probes for NESTIN, TGF1β, IGF1R and GUSB (housekeeping gene in our assay) in the RT-PCR mix.
8. ABI PRISM 7900HT Sequence Detection System (Life Technologies).

3 Methods

Where not specified, warm up at 37 °C all the reagents before using on living cell cultures.

3.1 MSC Isolation from Healthy and Aneurysm-Affected Aorta

3.1.1 Enzymatic Digestion of Fresh Aortic Tissues

As showed in a previous study [12] the Liberase II is used for aortic wall digestion at a final concentration of 0.3 mg/mL.

Use warm serum-free DMEM (*see* **Note 2**), enriched with essential amino acids, L-glutamine, and penicillin–streptomycin to prepare the Liberase II working solution: add 19 mL of DMEM to 1 mL of thawed stock solution 0.3 mg/mL to obtain the 20 mL of Liberase II working solution. One aliquot (1 mL) of Liberase II can be used to digest vascular tissue with a 2–4 cm^2 total area. Warm the working solution at 37 °C to allow enzyme activation.

Meanwhile, prepare scalpel, scissors, and emesis basin under sterile flow.

Wash the tissue with fresh physiologic solution in the sterile emesis basin. Cut the tissue into small pieces measuring 2 cm^2 and incubate with the Liberase II working solution into a rotor apparatus at 37 °C to allow the continuous enzymatic activity. Leave the tissues to digest overnight (o/n).

3.1.2 Cell Count and Seeding

Prepare DMEM enriched with essential amino acids, L-glutamine, and penicillin–streptomycin and FBS at 20 % and warm up at 37 °C.

After the o/n digestion with Liberase II solution, the tissue will be almost entirely homogenous; filter the digested tissue through cell strainers with decreasing diameter (100 μm; 70 μm; 40 μm) and use PBS to facilitate the passage of the digested tissue through the sieve. Centrifuge at 300 × *g* for 10 min and after cell counting seed the cell suspension according the proper density seeding on sterile flasks in 20 % FBS DMEM (*see* **Note 2**).

3.1.3 Cell Cultures

MSCs isolated from the vascular wall (VW-MSCs) can be expanded in culture using 20 % FBS DMEM until passage 3 and reducing the FBS concentration to 10 % from the passage 4. VW-MSCs can be frozen with FBS and 10 % DMSO.

3.2 Cell Exposure to $CoCl_2$

3.2.1 Cell Seeding for the Viability Assay

For each cell model, plate 10,000 cells/well in three different 48 well plates in 0.5 mL of DMEM/well). Use one plate for each time lapse.

After 24 h add 2 μL of $CoCl_2$ (100 μM) and 10 μL of $CoCl_2$ (500 μM) in 0.5 mL culture media in all wells, except for the control. After 24 h, remove plate from the incubator, wash once with PBS and fix with 500 μL formalin under a biochemical hood. Repeat fixation at 48 and 72 h for the two remaining plates. After fixation, store the plates at 4 °C, until use.

3.3 Crystal Violet Staining

1. Aspirate formalin and wash two times with dH_2O. Stain with 0.5 mL CV for 30 min, shaking at room temperature.
2. Wash four times with dH_2O and leave the plates to air dry for 20 min (*see* **Note 4**).
3. Add 1 mL of acetic acid 10 % in dH_2O in each well and shake for 15 min at RT.
4. Recover liquid and transfer 100 μL/well in a 96-well plate in triplicate. Use the acetic acid 10 % as blank. Read the absorbance at wavelength 595 nm (*see* **Note 4**).

3.4 Cell Seeding for the Angiogenic Differentiation Assay

Trypsinize hMSCs, AAA-MSCs, U2OS and WPMY-1 and, for each cell model, seed 100,000 cells/well in a 12-well plate in 1 mL DMEM 10 % for each well. According to the viability assay results, select the $CoCl_2$ concentration and exposure time that does not induce cell death. Considering our cell models, the 24 h treatment with 500 μM of $CoCl_2$ did not significantly influence the cell viability (Fig. 1). For this assay, use DMEM at low concentrations to avoid interference between serum growth factors and exogenous VEGF. After 24 h, add $CoCl_2$ to cells in 2 % FBS DMEM. After 24 h exposure to $CoCl_2$, remove the cell media and add 50 ng/mL VEGF in 2 % FBS DMEM; cells not treated with $CoCl_2$ and VEGF will be controls. The treatment will be performed for 7 days; add fresh media to cell cultures every 2 days.

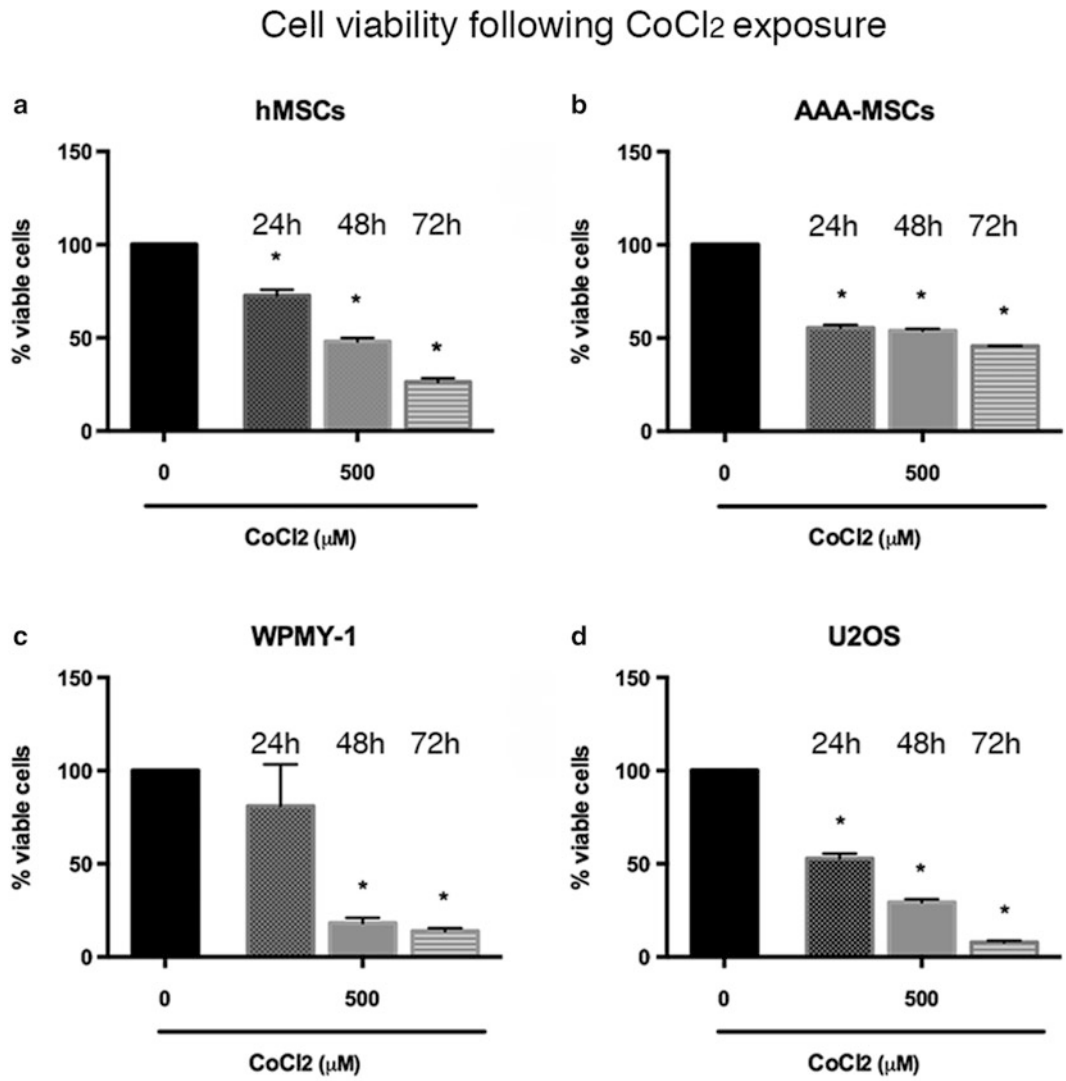

Fig. 1 Cell viability following $CoCl_2$ exposure. Cell viability was assayed through crystal violet staining on (**a**) healthy vascular MSCs, (**b**) AAA-MSCs, (**c**) WPMY-1 and (**d**) U2OS. The $CoCl_2$ concentration with less deleterious effects on cell viability was 500 μM at 24 h for most of the cell models tested in this protocol. Statistical analysis was performed by means of Prism 6 software (GraphPad Software), unpaired multiple *T* tests was used to evaluate significant differences among treatment groups and untreated control, with the False Discovery Rate approach set at 1 %. * = $p < 0.05$

Always keep sterility and work on ice. Thaw the Matrigel at 4 °C overnight. Use precooled tips and plates (*see* **Note 5**). Dispense 50 μL of Matrigel for each well, according to the experimental design. Then, place the plate in incubator, at 37 °C.

During this step, start to detach the cells. After cell count, seed 15,000 cells for each well and incubate at 37 °C. Follow the tube-formation process under the light microscope every 2 h and take photography at each time lapse (every 2 h, Fig. 2a).

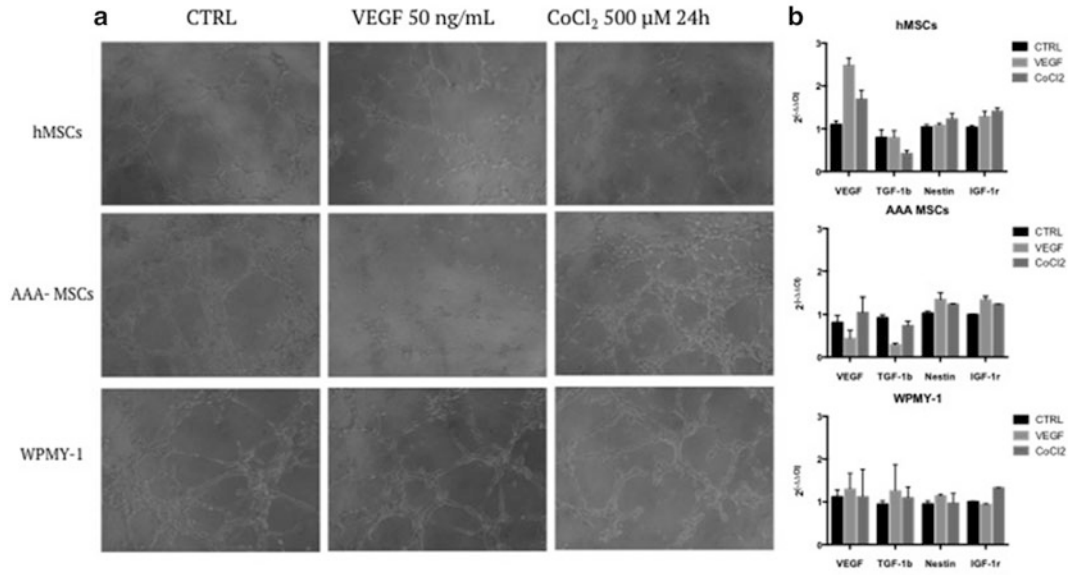

Fig. 2 Angiogenesis following $CoCl_2$ exposure. (**a**) Tubule-formation after 6 h and (**b**) angiogenic-associated genes after 7-days induction. Angiogenesis was analyzed on hMSCs, AAA-MSCs and WPMY-1 treated with CoCl2 500 µM, for 24 h, compared to unexposed controls and VEGF-induced cells. The evolution of tubule structures was followed 6 h from seeding on the Matrigel under the light microscopy. All cell models spontaneously form neovessels, more intensely in AAA-MSCs and WPMY-1. VEGF, normally used for the induction media, stimulates angiogenesis in all the cell models, except in AAA-MSCs. In presence of $CoCl_2$, angiogenesis was not disturbed, even resulting enhanced in the pathological model AAA-MSCs. Matrigel results were confirmed by PCR analysis of angiogenic and stress genes: no significant variations on gene expression were observed, concluding that angiogenic potential is not compromised by $CoCl_2$

3.5 Evaluation of Angiogenic Response Genes

IGF1R, NESTIN, VEGF, and TGF1beta genes were chosen to analyze the stem cell angiogenic activity under low oxygen levels at the mRNA level (Fig. 2b). For this purpose, recover the remaining part of cells exposed to angiogenic induction medium and resuspend in TRIzol to allow the cell lysis.

Perform RNA extraction, reverse transcription into cDNA and real-time PCR according to the protocol in use in the laboratory.

4 Notes

1. WPMY-1: careful attention should be given by operators when using WPMY-1 cells as it contains SV40 viral DNA sequence. Use class II biological safety cabinets.
2. DMEM at different FBS percentage, according to the intended use: 20%FBS for primary cultures (MSCs) at the early passages [1–3] to enhance and stimulate cell growth and expansions; 10 % FBS for primary cultures (MSCs) once established (from 4^{th} passage and so on), cell lines (WPMY-1, U2OS) and for

$CoCl_2$ treatment (it needs to keep the normal cell culture condition); 2 % FBS for angiogenic induction media, because FBS contains additional growth factors that may interfere with VEGF during the differentiation process (7 days long); serum-free to reconstitute enzymes (Libearase II), because FBS has an inhibitory property on enzyme activity.

For MSC at the first passage, just in case of huge bacterial contamination add 1 % antibiotics to the complete DMEM culture media.

3. Liberase reconstitution: Always keep sterility and work on ice, to prevent enzyme activation and protein denaturation.
4. Cobalt chloride hexahydrate ($CoCl_2 \cdot 6H_2O$) is lyophilized and is soluble in water at 100 mg/mL, becoming a red solution. Always wear protective gear when managing $CoCl_2$ because it is toxic and cancerous.

   Crystal violet is carcinogenic and it must be held under the chemical hood. Weight with care. During staining, you can stop at point 2. After staining, read the absorbance at 595 nm, the range of readings should be 0.1–1 Abs. If Abs >1, dilute the samples in acetic acid. Calculate the mean abs for each triplicate and subtract the mean of the blank. To compare values transform values in percentage of controls.
5. Matrigel: in order to avoid Matrigel polymerization, use pre-cooled tips, tubes and plates. The day before angiogenic assay, place p200 clear tips and the 96-well plates at 4 °C, thaw overnight an aliquot of the Matrigel working solution at 4 °C. When dispensing Matrigel, always keep the plate on ice and avoid bubble formation. Place the plate in incubator, at 37 °C, for 1 h to allow Matrigel polymerization. Always use safety clothing, because it is carcinogenic.

References

1. Deans RJ, Moseley AB (2000) Mesenchymal stem cells: biology and potential clinical uses. Exp Hemat 28:875–884
2. Dominici M, Le Blanc K, Mueller I et al (2006) Minimal criteria for defining multipotent mesenchymal stromal cells. The International Society for Cellular Therapy position statement. Cytotherapy 8(4):315–317
3. Fischer MP, Levin S, Zipori D (2011) The origins of mesenchymal stromal cell heterogeneity. Stem Cell Rev and Rep 7:560–568. doi:10.1007/s12015-011-9229-7
4. Liu J, Hao H, Xia L et al (2015) Hypoxia pretreatment of bone marrow mesenchymal stem cells facilitates angiogenesis by improving the function of endothelial cells in diabetic rats with lower ischemia. Plos One 10(5):e0126715. doi:10.1371/journal.pone.0126715
5. Wu D, Yotnda P (2011) Induction and testing of hypoxia in cell culture. JoVE 54:2899. doi:10.3791/2899
6. Krock BL, Skuli N, Simon MC (2011) Hypoxia-induced angiogenesis: good and evil. Genes Cancer 2:1117–1133. doi:10.1177/1947601911423654
7. Ciavarella C, Fittipaldi S, Pedrini S et al (2015) In vitro alteration of physiological parameters do not hamper the growth of human multipotent vascular wall-mesenchymal stem cells. Frontiers. 3. doi: 10.3389/fcell.2015.00036
8. Webber MM, Trakul N, Thraves PS et al (1999) A human prostatic stromal myofibroblast cell line WPMY-1: a model for stromal-

epithelial interactions in prostatic neoplasia. Carcinogenesis 20:1185–1192

9. Arnaoutova I, George J, Kleinman HK, Benton G (2009) The endothelial cell tube formation assay on basement membrane turns 20: state of the science and the art. Angiogenesis 12:267–274. doi:10.1007/s10456-009-9146-4
10. Fittipaldi S, Vasuri F, Degiovanni A et al (2014) Nestin and WT1 expression in atheromatous plaque neovessels: association with vulnerability. Histol Histopathol 29:1565–1573
11. Vasuri F, Fittipaldi S, Giunchi F et al (2015) Facing the enigma of the vascular network in hepatocellular carcinomas in cirrhotic and non-cirrhotic livers. J Clin Path. 0:1–7. doi: 10.1136/jclinpath-2015-203028 [Epub ahead of print]
12. Valente S, Alviano F, Ciavarella C et al (2014) Human cadaver multipotent stromal/stem cells isolated from arteries stored in liquid nitrogen for 5 years. Stem Cell Res Ther 5:8. doi:10.1186/scrt397

Methods in Molecular Biology (2016) 1516: 319–333
DOI 10.1007/7651_2016_360

Published online: 25 May 2016

Reporter Systems to Study Cancer Stem Cells

Caner Saygin, Mohamed Samour, Anastasia Chumakova, Awad Jarrar, Justin D. Lathia, and Ofer Reizes

Abstract

Cancer stem cells have been identified in primary tumors, patient derived xenografts, and established cancer cell lines. The development of reporters has enabled investigators to rapidly enrich for these cells and more importantly track these cells in real time. Here we describe the current state of the reporter field and their use and limitations in multiple cancers.

Keywords: Tumor heterogeneity, Cancer stem cells, NANOG, Reporter, Pluripotency transcription factor

1 Introduction

1.1 Tumor Heterogeneity and Cancer Stem Cells

Tumors are composed of heterogeneous populations of cells, which differ in their phenotypic and genetic features [1]. This multifaceted heterogeneity accounts for the differences in tumor biology and treatment sensitivity, not only amongst different individuals with same tumor types, but also between primary cancers and metastases [2]. Originating from this concept of tumor heterogeneity, a distinct subpopulation of self-renewing cells termed cancer stem cells (CSCs) has been shown to be present in both solid and hematopoietic tumors [3–7]. CSC are defined as a cell within a tumor, which has the capacity to give rise to the heterogeneous lineages of cancer cells that constitute the tumor and also undergoes self-renewal to maintain its reservoir [8]. Because of their intrinsic ability to repopulate tumor heterogeneity, CSCs are also known as "tumor-initiating cells" [1]. Additionally, CSCs have been shown to be more resistant to chemotherapy and radiotherapy as compared to non-CSCs [9–11]. Therefore, the residual pool of CSCs after initial cancer therapy has been postulated to be responsible for tumor recurrence [12]. Due to their cardinal roles in tumor initiation, maintenance, progression, and treatment-resistance, various drugs targeting critical CSC pathways are being extensively investigated in clinical trials [13–15].

1.2 Isolation of CSCs by Surface Markers

To date, the isolation and characterization of CSCs have largely been through the differential expression of surface markers between CSCs and non-CSCs [16]. Since the first prospective identification of $CD34^+CD38^-$ CSCs in acute myelogenous leukemia [17], various other markers shared between CSCs and normal human stem cells have been used to isolate self-renewing CSCs in solid tumors. These include CD133, a human hematopoietic progenitor cell marker, which is highly expressed in CSCs of lung [18], colon [19], brain [20], liver [21], ovarian [22], and breast [23] cancers. Moreover, certain adhesion molecules can reliably enrich CSCs within a mixed population of tumor cells. The cell surface glycoprotein CD44 is a well-characterized CSC marker used to isolate CSCs in tumors of breast [5], colon [24], prostate [25], pancreas [26], ovary [27], lung [28], and stomach [29]. Likewise, CD49f (integrin α6) and CD166 were reported to be reliable surface markers for CSC isolation [30, 31]. Other surface markers that were used to isolate CSCs include CD24 [32], CD117 [33], CD138 [34], EpCAM [24], CXCR4 [35], CD66c [36], and CA125 [37].

In order to isolate CSCs from a heterogenous population of tumor cells, two methods are commonly used: fluorescence-activated cell sorting (FACS) and antibodies conjugated to magnetic beads (MACS). The purity of isolation is typically higher with FACS but the survival of the cells is higher with the magnetic beads separation methods [1].

1.3 Reporter Systems to Identify CSCs

Despite the common use of cell surface markers to enrich CSCs in various tumors, this approach has limitations due to the inter-patient heterogeneity and fluctuation of the expression of these markers at different points of cell cycle. The CSC state is dynamic with rapid transitions between CSC to non-CSC states. As sorting/isolation approaches are limited in their ability to track changes in the stem cell state in real time, efforts have been made towards developing reporter systems that can actively monitor certain intracellular markers [38].

The pluripotent stem cell transcription factors NANOG, SOX2, OCT4 are highly expressed in CSCs and have been used to develop reporter systems based on their promoters. The utility of promoter reporter systems allows interrogation of the CSC state in real time [39–41]. Certain CSC-related signaling pathways have also been explored to generate reporters, of which Notch pathway is particularly useful in breast cancer models [42]. Moreover, telomerase reverse-transcriptase (TERT) promoter-driven green fluorescence protein (GFP) reporter was successfully utilized to enrich human osteosarcoma stem cells [38]. The major reporter systems used to isolate CSCs are summarized in Table 1, together with the types of tumors that they have been useful.

Table 1
Reporter systems validated for CSC enrichment

Reporter gene	Gene function	Cancers in which the reporter has been validated
NANOG	Transcription factor, expressed in embryonic stem cells maintaining pluripotency, oncogene	Breast [41], prostate [40], nasopharynx [51], liver [43], ovary [52]
SOX2	Transcription factor, expressed in embryonic stem cells maintaining pluripotency, oncogene	Breast [54], glioma [56], skin [53], cervix [55]
OCT4	Transcription factor, expressed in embryonic stem cells maintaining pluripotency, oncogene	Liver [58], melanoma [57], sarcoma [59]
SOX2-OCT4	Transcription factors, expressed in embryonic stem cells maintaining pluripotency, oncogene	Breast [39]
NOTCH	Maintenance of stem cell state by inhibiting differentiation, oncogene	Breast [42], lung [64]
Telomerase reverse transcriptase (TERT)	Catalytic subunit of the enzyme, telomerase	Osteosarcoma [38]
stem-SH2-domain-containing 5′-inositol phosphatase (s-SHIP)	Regulation of growth factor receptor mediated signaling	Prostate [66]
LGR5	Wnt signaling pathway	Colon [68]
Alpha-fetoprotein (AFP)	Fetal plasma protein	Cholangiocarcinoma [67]

In this chapter, various reporter systems used to enrich CSCs from a heterogenous population of tumor cells are discussed with a special focus on NANOG-GFP reporter system that we have successfully employed to study CSCs in breast and ovarian cancers.

2 Materials

1. PureLink HiPure Plasmid DNA Purification Kit for Maxiprep
2. HEK293T/17 cells at low passage number (ideally <10) (**Note 1**)
3. 2× BBS solution
   (a) For 250 mL 2×BBS solution, prepare:

2.665 g	BES (Sigma, B6266)
4.091 g	NaCl (Chemika Fluka, 71380)
100.52661 mg	$NA_2HPO_4 \times 7H_2O$

Add distilled water up to 250 mL. Dissolve and titrate to pH 6.95 with 1 M NaOH. Efficiency of transfection is highly dependent on pH. Filter, sterilize, and store 50 mL aliquots at 4 °C

4. 0.25 M $CaCl_2$ solution
   (a) For 250 mL 0.25 M $CaCl_2$ solution, prepare:

9.8175 g	$CaCl_2$ (Sigma C 7902)

Add distilled water up to 250 mL. Dissolve, filter, sterilize, and store 50 mL aliquots at 4 °C (**Note 2**)

5. DNA packaging vectors
   (a) For two vectors system, prepare:

pMD2G	4 μg
psPAX	7 μg

These vectors are compatible with non-inducible pCDH, pLKO, pGIPZ vectors (**Note 3**)

6. PEG-it virus precipitation solution (System Biosciences, LV810A-1)
7. Polybrene (**Note 4**)
8. Puromycin

3 Methods

3.1 NANOG Promoter-Driven GFP Reporter

3.1.1 NANOG Is a Pluripotency Gene Involved in Oncogenesis

NANOG is a transcription factor expressed in embryonic stem cells, and together with SOX-2 and OCT-4, the so called "core triad," maintains the pluripotent state [43]. Several studies have demonstrated that NANOG mRNA and protein are expressed in various cancers and its expression is positively correlated with poor clinical outcome [43, 44]. Therefore, it has been suggested as a prognostic biomarker. Based on a search of the cBioPortal database, the NANOG gene is frequently amplified in cancers of breast (17.2 %), peripheral nerve sheath (13.3 %), ovary (8.4 %), lung (6.7 %), and brain (4.9 %) (Fig. 1) [45]. NANOG expression also correlates with poor differentiation and vascular invasion in primary tumor samples [43].

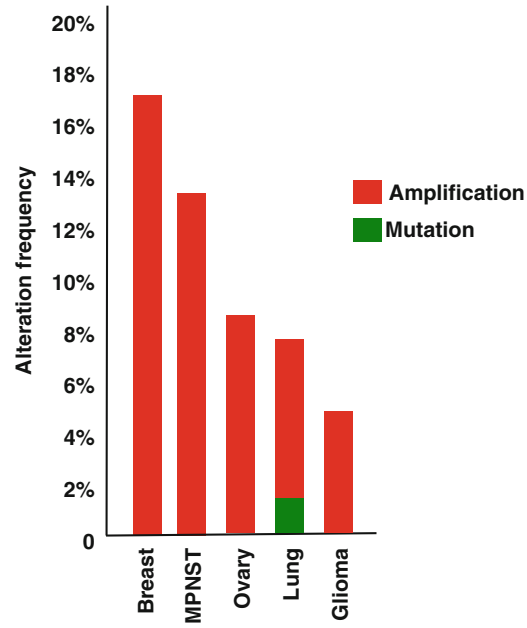

Fig. 1 NANOG alterations in various cancers

In support of these observations, embryonic stem cell-like gene expression signatures were found to be enriched in most aggressive tumors [46]. Myeloid leukemia stem cells have been shown to employ a transcriptional program similar to embryonic rather than adult stem cells [47]. Moreover, increased levels of NANOG protein has been demonstrated in CSCs of various tumor types, which were isolated by differential expression of surface markers [28, 48, 49]. Consistent with these association studies, NANOG knockdown is sufficient to decrease tumorigenicity and clonogenic growth of several breast, prostate, and colon cancer cell lines [50]. Whereas overexpression of NANOG is sufficient to induce self-renewal, tumor initiation, and drug resistance in prostate and breast cancer cell lines [40]. This change in cell behavior is also accompanied by a more stem-like phenotype with increased expression of CD133, CD44, and ABCG2 [40].

These findings indicate that NANOG is expressed in CSCs and confers pluripotency similar to observed effects in embryonic stem cells. Moreover, NANOG expression promotes malignant transformation and tumor progression.

3.1.2 NANOG-GFP Reporter Enriches CSCs

Originating from the abundant expression and importance of NANOG in cancer, a novel reporter system was developed using the NANOG promoter to control green fluorescent protein expression to track CSCs in established cancer lines [40, 41, 51]. Under this paradigm, cells expressing bright green signal by green fluorescence imaging or flow cytometry are presumed as putative CSCs,

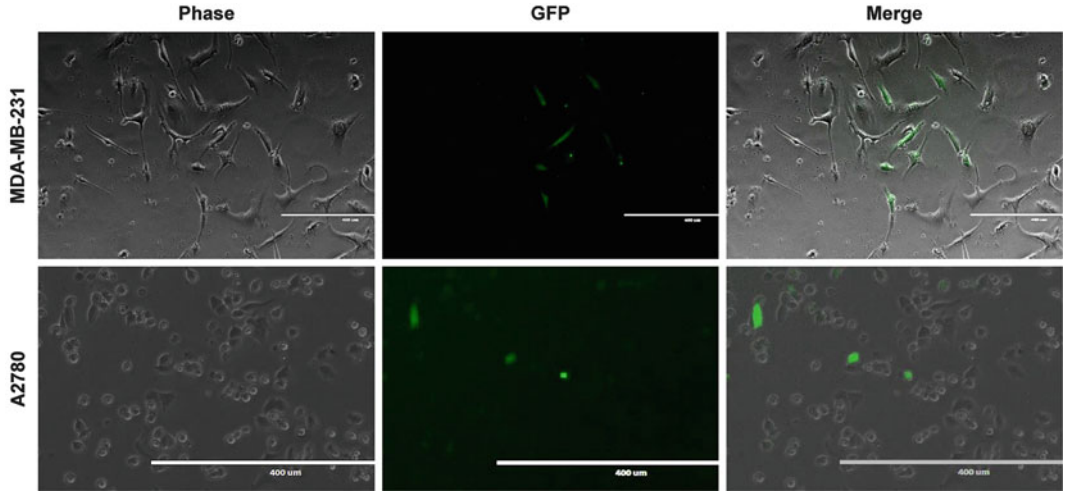

Fig. 2 Transduction of breast and ovarian cancer cells with NANOG promoter-driven GFP reporter

whereas cells expressing dim green fluorescence are considered nonCSCs.

To generate stable cell lines harboring NANOG-GFP reporter, MDA-MB-231 and HCC70 breast cancer cells [41], and A2780/CP70 ovarian cancer cells (data not published) were transduced with recombinant lentiviruses and monitored for green fluorescence (Fig. 2). Lentivirus production was generated using established methods.

1. Genetically engineered plasmid containing reporter gene (i.e., GFP) under the control of human NANOG promoter, and puromycin resistance gene under the control of EF-1α promoter were purified from *E. coli*.
2. Low-passage HEK293T/17 cells were transfected with this plasmid and the lentivirus packaging plasmids (psPAX2 and pMD2.G). HEK293T/17 cell line, which is a derivative of 293T cell line, is known for its high transfectability.
3. After transfection, cells should be incubated at 3 % CO_2, 37 °C overnight (16–20 h). Incubation at 3 % CO_2 is absolutely required as $CaPO_4$ precipitation (and therefore transfection efficacy) is highly dependent on media pH.
4. Then, media were removed and cells were incubated with 6 mL PBS (37 °C) per dish for 10 min. After that, 10 mL medium was added and cells are incubated at 5 % CO_2 incubator.
5. On the following day, cells were reaching confluency. More than half of the cells were expressing GFP.
6. Cell medium from HEK293T/17 was collected and centrifuged at 3000 × *g* for 15 min to remove debris. Then, supernatant was transferred to a sterile vessel and recombinant

lentivirus was precipitated from culture medium by using PEG-it virus precipitation solution (**Note 5**).

7. Supernatant/PEG-it mixture was centrifuged at 1500 × *g* for 30 min at 4 °C. After this centrifugation, lentiviral particles appeared as a beige pellet at the bottom of the vessel. Supernatant was aspirated off and lentiviral pellet was resuspended in 400 μL cold and sterile 1× PBS.
8. Breast and ovarian cancer cells were infected with the virus and 5 μg/mL Polybrene was used to enhance viral entry into cells.
9. After 2 days, transduction efficacy was >80 % and cultures were selected with puromycin in 4 μg/mL concentration for 3 days.
10. Transduced cell cultures were flow sorted and GFP+ cells were enriched. Upon 1–2 weeks of culture, GFP+ cells repopulated the culture heterogeneity and stably transduced cancer cell lines were subsequently expanded up to 20 passages.

Once the GFP reporter construct is incorporated, cancer cells can readily be sorted to obtain GFP+ CSCs and GFP− non-CSCs. Ideally, the histograms should demonstrate an even distribution or two peaks of GFP− and GFP+ ends. In the latter, the difference is usually clear and isolation of GFP+ and GFP− is simple. However, in case of a Gaussian distribution, GFP− population can be discriminated by using non-transduced parental cell line as negative control. For example, assuming that 30 % of all events have GFP signal overlapping with parental cells and hence sorted as GFP− cells, one can take the upper 30 % with bright GFP signal and designate as GFP+ population. It is good practice to eliminate cells with intermediate GFP signal. However, the optimal way to determine a cutoff percentage point is to divide the histogram into ten columns from the dimmest to brightest end with each having 10 % of cells, and sort these cells for in vitro self-renewal assay. This critical percentage point should demonstrate a significant difference in self-renewal between GFP high vs. low populations. Further validation requires demonstration of a difference in expression of pluripotency markers, including NANOG, SOX2, and OCT4.

In our experience, GFP+ cells isolated from both triple negative breast cancer (TNBC) [41] and ovarian cancer cell lines (unpublished data) had higher expression of NANOG, SOX2, and OCT4 as well as GFP as compared to their GFP− counterparts. Moreover, we compared the power of NANOG-GFP reporter system with other markers used to enrich CSCs. The reporter was more efficient than CD44, CD49f, and ALDH in isolation of self-renewing population in TNBC [41].

3.1.3 NANOG-GFP Reporter Is a Dynamic System

The novel NANOG-GFP reporter system provides a facile method to isolate CSCs and eliminates the need for antibodies, thus is free of antibody specific-related biases. At the same time, it is also a

functional imaging approach for CSC identification and enables visual tracking of putative CSCs within a population of cultured cancer cells. This system has a range of applications, including but not limited to migration and invasion assays, time lapse imaging to study CSC biology, and monitoring changes in CSC state upon treatment with cytokines, drugs, or inhibitors. We have also taken advantage of NANOG-GFP reporter system to identify CSC-specific molecular pathways by using high-throughput flow cytometry screen in TNBC [41]. This enabled us to discover a novel CSC marker, junctional adhesion molecule (JAM)-A, in TNBC [41]. Similarly, we utilized the reporter system to study the differential effects of cisplatin and certain targeted therapies on CSCs compared to non-CSCs with visual tracking of changes via time-lapse imaging (unpublished data). Therefore, the NANOG-GFP reporter system is a dynamic tool that enables interrogation of CSC state in real time.

3.2 Other Reporter Systems

3.2.1 SOX2

Sex determining region Y box 2 (SOX2) is a transcription factor and expressed in various cancers including gastric cancer, small cell lung cancer, melanoma, esophageal squamous cell carcinoma, and breast cancer [53, 54]. SOX2 is known to be an essential factor for inducing and maintaining stemness, namely pluripotency and self-renewal [54]. SOX2 promoter-driven reporter system has first been used in breast cancer [54]. Liang et al. demonstrated that cells with high SOX2 promoter activity had higher expression of stemness-related genes including CD44, ABCB1, NANOG and TWIST1 [54]. Subsequently, the efficacy of this reporter in enriching CSCs has also been shown in cervical cancer [55], glioma [56], and squamous cell carcinoma (SCC) of skin [53]. In a mouse model of glioblastoma, Stoltz, et al. showed that Sox2-EGFP reporter successfully isolated CSCs, which were phenotypically similar to patient-derived tumor initiating cells with respect to modes of cell division, self-renewal, niche location, and differentiation [56].

Of interest, SOX2 has been shown to be upregulated in pre-neoplastic skin tumors and it is much highly expressed in human SCC. Using a SOX2-GFP knock-in mice, Boumahdi, et al. demonstrated that SOX2-high SCC cells were greatly enriched in tumor-propagating cells, and they elucidated the role of SOX2 in initiation and progression of primary skin tumors [53].

Taken together, SOX2 promoter-driven reporter constructs have been shown to enrich CSCs in different solid tumors and utilized as a powerful tool to track CSCs real time with both in vitro and in vivo models.

3.2.2 OCT4

Similar to NANOG and SOX2, OCT4 is a master regulator of pluripotency and is upregulated in human solid tumors [57]. OCT4-promoter activity-dependent CSC enrichment strategy has been validated in melanoma [57], hepatocellular carcinoma [58],

and soft tissue sarcomas [59]. This reporter system was used in two studies to investigate the preclinical activity of patient-derived cytokine-induced killer (CIK) cells against CSCs and non-CSCs of melanoma and soft tissue sarcoma cells [57, 59]. In hepatocellular carcinoma, OCT4+ cells demonstrated classical CSC features including higher expression of stemness associated transcription factors, in vitro sphere formation, tumor initiation in immunocompromised mice, and resistance to sorafenib [58]. Therefore, OCT4 promoter-driven reporter system is a promising novel way to isolate CSCs in solid tumors.

3.2.3 SORE6

SORE6 is a novel reporter system generated by Tang, et al. which is a flexible CSC reporter system in which six tandem repeats of a composite OCT4/SOX2 response element were used to drive expression of a fluorescent protein [39]. This reporter is special as it responds to two core stem cell transcription factors. Breast cancer stem cells enriched by SORE6 reporter exhibited higher self-renewal, tumor initiating capability, and resistance to chemotherapeutics [39]. Tumor cell subpopulation selected by SORE6 reporter could generate a heterogeneous offspring, which is a cardinal characteristic of CSCs. Utility of this reporter in other solid tumors is under investigation.

3.2.4 NOTCH

NOTCH signaling pathway is involved in the development of many multicellular organisms. In humans and other mammals, four distinct receptors (NOTCH 1–4) are involved in a downstream proteolysis pathway that eventually releases the Notch Intracellular Domain (NICD) protein, which enhances gene transcription [60]. In addition to its critical role in embryogenesis and fate decision of various cellular systems, NOTCH pathway has also been implicated in a wide variety of malignancies [61]. For example, overexpression of NOTCH has been shown in non-small-cell lung cancer (NSCLC) and blockade of this signaling pathway had direct effects on tumor growth, apoptosis, and cellular proliferation [62, 63].

NOTCH-GFP reporter construct has been used to enrich for self-renewing cell population in non-small-cell lung cancer [64]. NOTCH 2 and 4 receptor expressions were higher in the GFP-bright population, while the GFP-dim population showed higher expression of NOTCH-1 and NOTCH-3 receptors. GFP-bright cells had higher tumor initiation capacity as assessed by serial in vivo xenotransplantation assays in NOD/SCID mice. Cells with high NOTCH activity were more resistant to chemotherapy and NOTCH activity correlated with poor clinical outcome. NOTCH reporter system has also been used in breast cancer cell lines and successfully enriched CSCs with higher tumor initiating capacity [42].

3.2.5 TERT

Telomerase is known to be essential in maintaining cancer stem/progenitor cells. Human telomerase reverse transcriptase (hTERT) is the catalytic subunit of the telomerase enzyme and hTERT reporter has been used to enrich CSCs in osteosarcoma [38]. It was found that a subpopulation of osteosarcoma cells expressed higher levels of telomerase, which was read out by bright GFP expression linked to the hTERT promoter. Telomerase-positive cells had enhanced ability to form sarcospheres and demonstrated higher levels of epithelial–mesenchymal transition marker expressions.

3.2.6 s-SHIP

Stem-SH2-domain-containing 5′ inositol phosphatase (s-SHIP) expression has been previously shown to be linked to stem/progenitor cell activity [65]. In the context of cancer stem cells, the role of s-SHIP has been studied in human prostate cancer cell lines [66]. An s-SHIP promoter linked GFP reporter has been used to isolate a stem-cell like subpopulation of cells in the RWPE-1 cell line. Cells with high s-SHIP activity demonstrated the ability of anchorage-independent growth (i.e., forming spheres) and had higher expression of pluripotency transcription factors (OCT4, SOX2) and stem cell surface markers (TROP2, CD44, CD166).

3.2.7 AFP

Alpha-fetoprotein is a well-known marker for hepatic progenitor cells, but it has also been studied as a marker for CSCs in cholangiocarcinoma [67]. Four cholangiocarcinoma cell lines were transfected with AFP enhancer/promoter-driven EGFP gene and one out of four cell lines showed a population of cells expressing both AFP and EGFP. EGFP-positive cells had higher tumorigenic potential and Notch1 expression, which supported the role of Notch pathway in maintaining CSC characteristics.

3.3 Caveats of Using Reporters

The reporter systems are extremely useful tools to isolate CSCs and in the design of continuous functional experiments to monitor the CSC state in real time. However, there are some potential limitations. First, a limitation of the process is efficacy in transduction that may differ between different cell lines. Second, tumor heterogeneity might not be repopulated after initial enrichment of GFP high cells. Third, long promoter sequences might contain binding sites for various different transcription factors, which may adversely affect the specificity of reporter. Therefore, meticulous validation of sorted cells for differential self-renewal capability (both in vitro and in vivo) and expression of CSC markers (i.e., “core triad” of pluripotency markers) is imperative. Fourth, certain cells with aggressive phenotypes (e.g., chemotherapy resistant cell lines) might not be efficiently enriched for CSCs based on reporter systems. For example, although the NANOG-GFP reporter was very useful in isolating CSCs in cisplatin-naïve A2780 ovarian cancer cell line, it could not enrich CSCs in its isogenic cisplatin-resistant derivative,

CP70 (unpublished data). We later found out that CP70 cells had higher baseline expression of CSC markers and self-renewing capability than their cisplatin-naïve counterparts. In addition, GFP is a stable molecule and its half life may exceed 24 h. Therefore, there might be a time period between the onset of loss of CSC gene expression, and visualization of this by reporter read-outs. Finally, experiments incorporating fluorescent dyes should be designed carefully in order to prevent cross talk between GFP signal and other fluorophores. This is a common problem while comparing GFP+ and GFP− cells with commercially available assays (e.g., annexin V-FITC staining, BCECF-based assays).

3.4 Conclusions

The cancer stem cell model proposes that tumors contain a heterogeneous population of cells, which are hierarchically organized [1]. CSCs are at the highest level of this organization, and are important for tumor formation, maintenance, invasion, metastasis, and drug resistance [8]. Therefore, isolation of CSCs is critically important to discover drivers of tumorigenic properties and target them effectively. Reporter systems depend on CSC-specific pathways and transcriptomes, enable segregation of CSCs easily, and are dynamic tools that can track CSCs with functional imaging approaches. In our experience, they isolated CSCs with higher fidelity compared to conventional methods (i.e., surface markers, ALDH enzyme activity assays) and were utilized in screening approaches to identify CSC-specific markers as promising future therapeutic targets [41, 56].

4 Notes

1. Split HEK293T/17 cells to the 10 cm dishes, swirl the cells thoroughly as you seed them in order to obtain even distribution across the surface of the dish. Incubate at 37 °C overnight. Cells should preferably be of low passage number and their use is not recommended after passage 20 or if growth is slow. The cells should be 80–90 % confluent at the time of transfection.
2. For each 10 cm dish, prepare 2 eppi tubes with 0.5 mL 0.25 M $CaCl_2$ solution and 0.5 mL 2×BBS solution.
3. An alternative might be 3 vectors system (pPACKH1 Lentiviral packaging kit, System Biosciences) which is compatible with inducible pLVX vectors (Clontech).

pMDL/GAG	5.6 μg
VSU-G	3 μg
REV	2.13 μg

The amount of expression vector DNA to add in this setting is 9.27 μg.

4. Polybrene increases the efficacy of transfection by changing surface potential.
5. Lentivector-containing supernatants mixed with PEG-it virus precipitation solution are stable for up to 2 days at 4 °C

References

1. Ajani JA, Song S, Hochster HS, Steinberg IB (2015) Cancer stem cells: the promise and the potential. Semin Oncol 42 Suppl 1:S3–S17
2. Wang A, Chen L, Li C, Zhu Y (2015) Heterogeneity in cancer stem cells. Cancer Lett 357 (1):63–68
3. Dg T (2012) Understanding cancer stem cell heterogeneity and plasticity. Cell Res 22 (3):457–472
4. Huntly BJ, Gilliland DG (2005) Leukemia stem cells and the evolution of cancer-stem-cell research. Nat Rev Cancer 5(4):311–321
5. Al-Hajj M, Wicha MS, Benito-Hernandez A, Morrison SJ, Clarke MF (2003) Prospective identification of tumorigenic breast cancer cells. Proc Natl Acad Sci U S A 100 (7):3983–3988
6. Singh SK, Hawkins C, Clarke ID, Squire JA, Bayani J, Hide T, Henkelman RM, Cusimano MD, Dirks PB (2004) Identification of human brain tumor initiating cells. Nature 432 (7015):396–401
7. O'Brien CA, Pollett A, Gallinger S, Dick JE (2007) A human colon cancer cell capable of initiating tumour growth in immunodeficient mice. Nature 445(7123):106–110
8. Adorno-Cruz V, Kibria G, Liu X, Doherty M, Junk DJ, Guan D, Hubert C, Venere M, Mulkearns-Hubert E, Sinyuk M, Alvarado A, Caplan AI, Rich J, Gerson SL, Lathia J, Liu H (2015) Cancer stem cells: targeting the roots of cancer, seeds of metastasis, and sources of therapy resistance. Cancer Res 75(6):924–929
9. Hoofd C, Wand X, Lam S, Jenkins C, Wood B, Giambra V, Weng AP (2016) CD44 promotes chemoresistance in T-ALL by increased drug efflux. Exp Hematol 44(3):166. e17–171.e17
10. Yoon C, Cho SJ, Aksoy BA, Park DJ, Schultz N, Ryeom SW, Yoon SS (2016) Chemotherapy resistance in diffuse-type gastric adenocarcinoma is mediated by RhoA activation in cancer stem-like cells. Clin Cancer Res 22(4):971–83
11. Fong CY, Gilan O, Lam EY, Rubin AF, Ftouni S, Tyler D, Stanley K, Sinha D, Yeh P, Morison J, Giotopoulos G, Lugo D, Jeffrey P, Lee SC, Carpenter C, Gregory R, Ramsay RG, Lane SW, Abdel-Wahab O, Kouzarides T, Johnstone RW, Dawson SJ, Huntly BJ, Prinjha RK, Papenfuss AT, Dawson MA (2015) BET inhibitor resistance emerges from leukaemia stem cells. Nature 525(7570):538–542
12. Wicha MS, Liu S, Dontu G (2006) Cancer stem cells: an old idea—a paradigm shift. Cancer Res 66(4):1883–1890
13. Basset-Seguin N, Hauschild A, Grob JJ, Kunstfeld R, Dréno B, Mortier L, Ascierto PA, Licitra L, Dutriaux C, Thomas L, Jouary T, Meyer N, Guillot B, Dummer R, Fife K, Ernst DS, Williams S, Fittipaldo A, Xynos I, Hansson J (2015) Vismodegib in patients with advanced basal cell carcinoma (STEVIE): a pre-planned interim analysis of an international, open-label trial. Lancet Oncol 16(6):729–736
14. Berlin J, Bendell JC, Hart LL, Firdaus I, Gore I, Hermann RC, Mulcahy MF, Zalupski MM, Mackey HM, Yauch RL, Graham RA, Bray GL, Low JA (2013) A randomized phase II trial of vismodegib versus placebo with FOLFOX or FOLFIRI and bevacizumab in patients with previously untreated metastatic colorectal cancer. Clin Cancer Res 19(1):258–267
15. Robinson GW, Orr BA, Wu G, Gururangan S, Lin T, Qaddoumi I, Packer RJ, Goldman S, Prados MD, Desjardins A, Chintagumpala M, Takebe N, Kaste SC, Rusch M, Allen SJ, Onar-Thomas A, Stewart CF, Fouladi M, Boyett JM, Gilbertson RJ, Curran T, Ellison DW, Gajjar A (2015) Vismodegib exerts targeted efficacy against recurrent sonic hedgehog-subgroup medulloblastoma: results from phase II pediatric brain tumor consortium studies PBTC-025B and PBTC-032. J Clin Oncol 33 (24):2646–2654
16. Visvader JE, Lindeman GJ (2008) Cancer stem cells in solid tumours: accumulating evidence and unresolved questions. Nat Rev Cancer 8 (10):755–768
17. Lapidot T, Sirard C, Vormoor J, Murdoch B, Hoang T, Caceres-Cortes J, Minden M, Paterson B, Caligiuri MA, Dick JE (1994) A

cell initiating human acute myeloid leukaemia after transplantation into SCID mice. Nature 367(6464):645–648

18. Eramo A, Lotti F, Sette G, Pilozzi E, Biffoni M, Di Virgilio A, Conticello C, Ruco L, Peschle C, De Maria R (2008) Identification and expansion of the tumorigenic lung cancer stem cell population. Cell Death Differ 15 (3):504–514
19. Ricci-Vitiani L, Lombardi DG, Pilozzi E, Biffoni M, Todaro M, Peschle C, De Maria R (2007) Identification and expansion of human colon-cancer-initiating cells. Nature 445 (7123):111–115
20. Singh SK, Clarke ID, Terasaki M, Bonn VE, Hawkins C, Squire J, Dirks PB (2003) Identification of a cancer stem cell in human brain tumors. Cancer Res 63(18):5821–5828
21. Ma S, Chan KW, Hu L, Lee TK, Wo JY, Ng IO, Zheng BJ, Guan XY (2007) Identification and characterization of tumorigenic liver cancer stem/progenitor cells. Gastroenterology 132 (7):2542–2556
22. Baba T, Convery PA, Matsumura N, Whitaker RS, Kondoh E, Perry T, Huang Z, Bentley RC, Mori S, Fujii S, Marks JR, Berchuck A, Murphy SK (2009) Epigenetic regulation of CD133 and tumorigenicity of CD133+ ovarian cancer cells. Oncogene 28(2):209–218
23. Santilli G, Binda M, Zaffaroni N, Daidone MG (2011) Breast cancer-initiating cells: insights into novel treatment strategies. Cancers (Basel) 3(1):1405–1425
24. Dalerba P, Dylla SJ, Park IK, Liu R, Wang X, Cho RW, Hoey T, Gurney A, Huang EH, Simeone DM, Shelton AA, Parmiani G, Castelli C, Clarke MF (2007) Phenotypic characterization of human colorectal cancer stem cells. Proc Natl Acad Sci U S A 104 (24):10158–10163
25. Collins AT, Berry PA, Hyde C, Stower MJ, Maitland NJ (2005) Prospective identification of tumorigenic prostate cancer stem cells. Cancer Res 65(23):10946–10951
26. Li C, Heidt DG, Dalerba P, Burant CF, Zhang L, Adsay V, Wicha M, Clarke MF, Simeone DM (2007) Identification of pancreatic cancer stem cells. Cancer Res 67(3):1030–1037
27. Zhang S, Balch C, Chan MW, Lai HC, Matei D, Schilder JM, Yan PS, Huang TH, Nephew KP (2008) Identification and characterization of ovarian cancer-initiating cells from primary human tumors. Cancer Res 68 (11):4311–4320
28. Leung EL, Fiscus RR, Tung JW, Tin VP, Cheng LC, Sihoe AD, Fink LM, Ma Y, Wong MP (2010) Non-small cell lung cancer cells expressing CD44 are enriched for stem cell-like properties. PLoS One 5(11), e14062
29. Takaishi S, Okumura T, Tu S, Wang SS, Shibata W, Vigneshwaran R, Gordon SA, Shimada Y, Wang TC (2009) Identification of gastric cancer stem cells using the cell surface marker CD44. Stem Cells 27(5):1006–1020
30. Lathia JD, Gallagher J, Heddleston JM, Wang J, Eyler CE, Macswords J, Wu Q, Vasanji A, McLendon RE, Hjelmeland AB, Rich JN (2010) Integrin alpha 6 regulates glioblastoma stem cells. Cell Stem Cell 6(5):421–432
31. Zhang WC, Shyh-Chang N, Yang H, Rai A, Umashankar S, Ma S, Soh BS, Sun LL, Tai BC, Nga ME, Bhakoo KK, Jayapal SR, Nichane M, Yu Q, Ahmed DA, Tan C, Sing WP, Tam J, Thirugananam A, Noghabi MS, Pang YH, Ang HS, Mitchell W, Robson P, Kaldis P, Soo RA, Swarup S, Lim EH, Lim B (2012) Glycine decarboxylase activity drives non-small cell lung cancer tumor-initiating cells and tumorigenesis. Cell 148(1–2):259–272
32. Burgos-Ojeda D, Wu R, McLean K, Chen YC, Talpaz M, Yoon E, Cho KR, Buckanovich RJ (2015) CD24+ ovarian cancer cells are enriched for cancer-initiating cells and dependent on JAK2 signaling for growth and metastasis. Mol Cancer Ther 14(7):1717–1727
33. Luo L, Zeng J, Liang B, Zhao Z, Sun L, Cao D, Yang J, Shen K (2011) Ovarian cancer cells with the CD117 phenotype are highly tumorigenic and are related to chemotherapy outcome. Exp Mol Pathol 91(2):596–602
34. Van Valckenborgh E, Matsui W, Agarwal P, Lub S, Dehui X, De Bruyne E, Menu E, Empsen C, van Grunsven L, Agarwal J, Wang Q, Jernberg-Wiklund H, Vanderkerken K (2012) Tumor-initiating capacity of CD138- and CD138+ tumor cells in the 5T33 multiple myeloma model. Leukemia 26(6):1436–1439
35. Hermann PC, Huber SL, Herrler T, Aicher A, Ellwart JW, Guba M, Bruns CJ, Heeschen C (2007) Distinct populations of cancer stem cells determine tumor growth and metastatic activity in human pancreatic cancer. Cell Stem Cell 1(3):313–323
36. Gemei M, Mirabelli P, Di Noto R, Corbo C, Iaccarino A, Zamboli A, Troncone G, Galizia G, Lieto E, Del Vecchio L, Salvatore F (2013) CD66c is a novel marker for colorectal cancer stem cell isolation, and its silencing halts tumor growth in vivo. Cancer 119(4):729–738
37. Janzen DM, Tiourin E, Salehi JA, Paik DY, Lu J, Pellegrini M, Memarzadeh S (2015) An apoptosis-enhancing drug overcomes platinum resistance in a tumour-initiating subpopulation of ovarian cancer. Nat Commun 6:7956

38. Yu L, Liu S, Zhang C, Zhang B, Simões BM, Eyre R, Liang Y, Yan H, Wu Z, Guo W, Clarke RB (2013) Enrichment of human osteosarcoma stem cells based on hTERT transcriptional activity. Oncotarget 4(12):2326–2338
39. Tang B, Raviv A, Esposito D, Flanders KC, Daniel C, Nghiem BT, Garfield S, Lim L, Mannan P, Robles AI, Smith WI Jr, Zimmerberg J, Ravin R, Wakefield LM (2015) A flexible reporter system for direct observation and isolation of cancer stem cells. Stem Cell Reports 4 (1):155–169
40. Jeter CR, Liu B, Liu X, Chen X, Liu C, Calhoun-Davis T, Repass J, Zaehres H, Shen JJ, Tang DG (2011) NANOG promotes cancer stem cell characteristics and prostate cancer resistance to androgen deprivation. Oncogene 30(36):3833–3845
41. Thiagarajan PS, Hitomi M, Hale JS, Alvarado AG, Otvos B, Sinyuk M, Stoltz K, Wiechert A, Mulkearns-Hubert E, Jarrar AM, Zheng Q, Thomas D, Egelhoff TT, Rich JN, Liu H, Lathia JD, Reizes O (2015) Development of a fluorescent reporter system to delineate cancer stem cells in triple-negative breast cancer. Stem Cells 33(7):2114–2125
42. D'Angelo RC, Ouzounova M, Davis A, Choi D, Tchuenkam SM, Kim G, Luther T, Quraishi AA, Senbabaoglu Y, Conley SJ, Clouthier SG, Hassan KA, Wicha MS, Korkaya H (2015) Notch reporter activity in breast cancer cell lines identifies a subset of cells with stem cell activity. Mol Cancer Ther 14(3):779–787
43. Shan J, Shen J, Liu L, Xia F, Xu C, Duan G, Xu Y, Ma Q, Yang Z, Zhang Q, Ma L, Liu J, Xu S, Yan X, Bie P, Cui Y, Bian XW, Qian C (2012) Nanog regulates self-renewal of cancer stem cells through the insulin-like growth factor pathway in human hepatocellular carcinoma. Hepatology 56(3):1004–1014
44. Badeaux MA, Jeter C, Gong S, Liu B, Suraneni MV, Rundhaug J, Fischer SM, Yang T, Kusewitt D, Tang DG (2013) In vivo functional studies of tumor-specific retrogene NanogP8 in transgenic animals. Cell Cycle 12 (15):2395–2408
45. http://www.cbioportal.org
46. Ben-Porath I, Thomson MW, Carey VJ, Ge R, Bell GW, Regev A, Weinberg RA (2008) An embryonic stem cell-like gene expression signature in poorly differentiated aggressive human tumors. Nat Genet 40(5):499–507
47. Somervaille TC, Matheny CJ, Spencer GJ, Iwasaki M, Rinn JL, Witten DM, Chang HY, Shurtleff SA, Downing JR, Cleary ML (2009) Hierarchical maintenance of MLL myeloid leukemia stem cells employs a transcriptional program shared with embryonic rather than adult stem cells. Cell Stem Cell 4(2):129–140
48. Cioffi M, D'Alterio C, Camerlingo R, Tirino V, Consales C, Riccio A, Ieranò C, Cecere SC, Losito NS, Greggi S, Pignata S, Pirozzi G, Scala S (2015) Identification of a distinct population of CD133(+)CXCR4(+) cancer stem cells in ovarian cancer. Sci Rep 5:10357
49. Meyer MJ, Fleming JM, Lin AF, Hussnain SA, Ginsburg E, Vonderhaar BK (2010) CD44posCD49fhiCD133/2hi defines xenograft-initiating cells in estrogen receptor-negative breast cancer. Cancer Res 70 (11):4624–4633
50. Jeter CR, Badeaux M, Choy G, Chandra D, Patrawala L, Liu C, Calhoun-Davis T, Zaehres H, Daley GQ, Tang DG (2009) Functional evidence that the self-renewal gene NANOG regulates human tumor development. Stem Cells 27(5):993–1005
51. Wei F, Rong XX, Xie RY, Jia LT, Wang HY, Qin YJ, Chen L, Shen HF, Lin XL, Yang J, Yang S, Hao WC, Chen Y, Xiao SJ, Zhou HR, Lin TY, Chen YS, Sun Y, Yao KT, Xiao D (2015) Cytokine-induced killer cells efficiently kill stem-like cancer cells of nasopharyngeal carcinoma via the NKG2D-ligands recognition. Oncotarget 6(33):35023–35039
52. Wiechert A, Saygin C, Thiagarajan C, Rao VS, Hale JS, Gupta N, Hitomi M, Nagaraj AB, DiFeo A, Lathia JD, Reizes O (2016). Cisplatin induces stemness in ovarian cancer. Oncotarget, in press
53. Boumahdi S, Driessens G, Lapouge G, Rorive S, Nassar D, Le Mercier M, Delatte B, Caauwe A, Lenglez S, Nkusi E, Brohée S, Salmon I, Dubois C, del Marmol V, Fuks F, Beck B, Blanpain C (2014) SOX2 controls tumour initiation and cancer stem-cell functions in squamous-cell carcinoma. Nature 511 (7508):246–250
54. Liang S, Furuhashi M, Nakane R, Nakazawa S, Goudarzi H, Hamada J, Iizasa H (2013) Isolation and characterization of human breast cancer cells with SOX2 promoter activity. Biochem Biophys Res Commun 437(2):205–211
55. Liu XF, Yang WT, Xu R, Liu JT, Zheng PS (2014) Cervical cancer cells with positive Sox2 expression exhibit the properties of cancer stem cells. PLoS One 9(1), e87092
56. Stoltz K, Sinyuk M, Wu Q, Otvos B, Walker K, Vasanji A, Rich JN, Hjelmeland AB, Lathia JD (2015) Development of a Sox2 reporter system modeling cellular heterogeneity in glioma. Neuro Oncol 17(3):361–371
57. Gammaitoni L, Giraudo L, Leuci V, Todorovic M, Mesiano G, Picciotto F, Pisacane A,

Zaccagna A, Volpe MG, Gallo S, Caravelli D, Giacone E, Venesio T, Balsamo A, Pignochino Y, Grignani G, Carnevale-Schianca F, Aglietta M, Sangiolo D (2013) Effective activity of cytokine-induced killer cells against autologous metastatic melanoma including cells with stemness features. Clin Cancer Res 19(16):4347–4358

58. Wu G, Wilson G, Zhou G, Hebbard L, George J, Qiao L (2015) Oct4 is a reliable marker of liver tumor propagating cells in hepatocellular carcinoma. Discov Med 20(110):219–229
59. Sangiolo D, Mesiano G, Gammaitoni L, Leuci V, Todorovic M, Giraudo L, Cammarata C, Dell'Aglio C, D'Ambrosio L, Pisacane A, Sarotto I, Miano S, Ferrero I, Carnevale-Schianca F, Pignochino Y, Sassi F, Bertotti A, Piacibello W, Fagioli F, Aglietta M, Grignani G (2014) Cytokine-induced killer cells eradicate bone and soft-tissue sarcomas. Cancer Res 74 (1):119–129
60. Yahyanejad S, Theys J, Vooijs M (2016) Targeting notch to overcome radiation resistance. Oncotarget 7(7):7610–28
61. Ranganathan P, Weaver KL, Capobianco AJ (2011) Notch signalling in solid tumours: a little bit of everything but not all the time. Nat Rev Cancer 11(5):338–351
62. Dang TP, Gazdar AF, Virmani AK, Sepetavec T, Hande KR, Minna JD, Roberts JR, Carbone DP (2000) Chromosome 19 translocation, overexpression of Notch3, and human lung cancer. J Natl Cancer Inst 92(16):1355–1357
63. Konishi J, Kawaguchi KS, Vo H, Haruki N, Gonzalez A, Carbone DP, Dang TP (2007) Gamma-secretase inhibitor prevents Notch3 activation and reduces proliferation in human lung cancers. Cancer Res 67(17):8051–8057
64. Hassan KA, Wang L, Korkaya H, Chen G, Maillard I, Beer DG, Kalemkerian GP, Wicha MS (2013) Notch pathway activity identifies cells with cancer stem cell-like properties and correlates with worse survival in lung adenocarcinoma. Clin Cancer Res 19(8):1972–1980
65. Bai L, Rohrschneider LR (2010) s-SHIP promoter expression marks activated stem cells in developing mouse mammary tissue. Genes Dev 24(17):1882–1892
66. Bauderlique-Le Roy H, Vennin C, Brocqueville G, Spruyt N, Adriaenssens E, Bourette RP (2015) Enrichment of human stem-like prostate cells with s-SHIP promoter activity uncovers a role in stemness for the long non-coding RNA H19. Stem Cells Dev 24 (10):1252–1262
67. Ishii T, Yasuchika K, Suemori H, Nakatsuji N, Ikai I, Uemoto S (2010) Alpha-fetoprotein producing cells act as cancer progenitor cells in human cholangiocarcinoma. Cancer Lett 294(1):25–34
68. Hirsch D, Hu Y, Ried T, Moll R, Gaiser T (2014) Transcriptome profiling of LGR5 positive colorectal cancer cells. Genom Data 2:212–215

Methods in Molecular Biology (2016) 1516: 335–346
DOI 10.1007/7651_2016_346

Published online: 05 April 2016

Agent-Based Modeling of Cancer Stem Cell Driven Solid Tumor Growth

Jan Poleszczuk, Paul Macklin, and Heiko Enderling

Abstract

Computational modeling of tumor growth has become an invaluable tool to simulate complex cell–cell interactions and emerging population-level dynamics. Agent-based models are commonly used to describe the behavior and interaction of individual cells in different environments. Behavioral rules can be informed and calibrated by in vitro assays, and emerging population-level dynamics may be validated with both in vitro and in vivo experiments. Here, we describe the design and implementation of a lattice-based agent-based model of cancer stem cell driven tumor growth.

Keywords: Agent-based model, Tumor growth, Cancer stem cell, Calibration, Domain, Search order, High performance, Digital cell line

1 Introduction

Agent-based modeling has a long history in quantitative oncology [1–3], including stem cell dynamics [4–9], and heterogeneity [10–12]. Such models can help predict disease progression and make invaluable recommendations for therapeutic interventions [13, 14]. Agent-based models simulate the behavior and interaction of individual cells. Behavioral rules can be dependent on environmental conditions, which include chemicals in the extracellular environment [15–17], supporting structures in the extracellular matrix [18, 19], fluid dynamics [20], physical forces [21], or presence and interactions with other cells [22, 23]. Computer simulations are usually initialized with a single cell or a cluster of individual cells, and the status and behavior of each cell are typically updated at discrete time points based on their internal rules and current environmental conditions. Such models may help identify if cancer stem cells comprise a subpopulation of specific proportion in a tumor [24], and how to deliver radiotherapy doses efficiently to eradicate cancer stem cells [25].

2 Materials

Implement all classes and functions in a concurrent version system to allow shared programming and efficient debugging.

2.1 Lattice

A finite 2D (or 3D if necessary) lattice, where each site can be occupied by a single or a population of cells (crowding).

1. Lattice size. Simulations are commonly initialized with either (a) a small number of cells to observe emergent population-level behavior, or (b) a populated tissue architecture. Define lattice size to accommodate anticipated final cell number. Account for possible boundary effects in case of a growing population. Set the size of a single lattice site to the size of a cell.
2. Neighborhood. Determine if cells interact with their four orthogonal neighbors (north, south, east, west; von Neumann neighborhood), or with the adjacent eight neighboring lattice points (northwest, north, northeast, east, west, southeast, south, southwest; Moore neighborhood) (Fig. 1).
3. Boundary conditions. Define behavior of cells on the boundary of the lattice, set to either periodic (the boundary "wraps", so cells on the left edge interact with cells on the far right edge) or no-flux reflective (cells on the edge of the lattice only interact with interior and edge cells). Note that simulations with no-flux boundary conditions may introduce boundary effects, i.e., accumulation of cells near the boundary. For dynamically expanding arrays no boundary conditions are necessary.

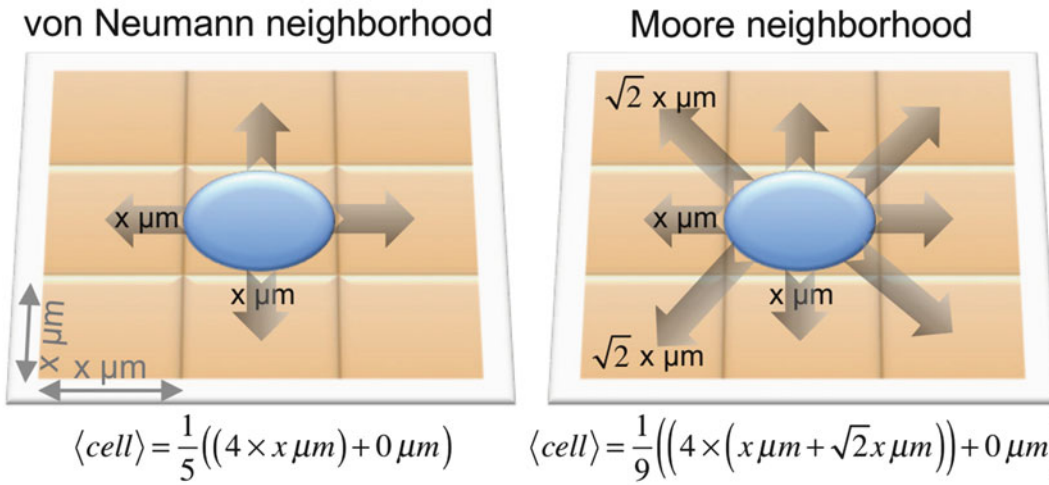

Fig. 1 Schematic of expected cell displacement, *cell*, in the von Neumann (*left*) and Moore (*right*) neighborhoods on a two-dimensional lattice with lattice sizes of x^2 μm^2

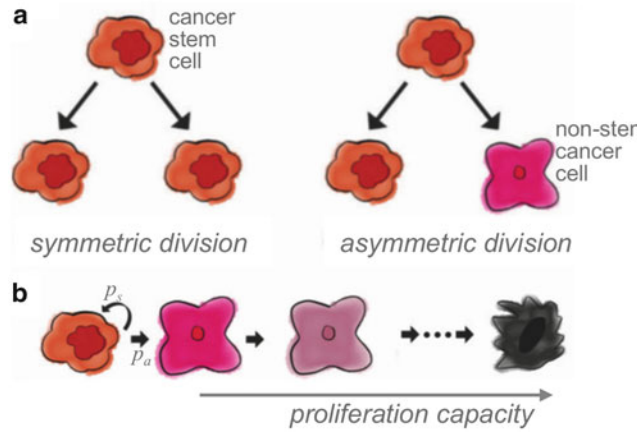

Fig. 2 (**a**) Schematic of cancer stem cell symmetric and asymmetric division. (**b**) Schematic representation of cancer stem cell symmetric (p_s) and asymmetric division (p_a) and non-stem cancer cell proliferation capacity. Adapted from [24]

2.2 Cell

Each cell is an individual entity with the following basic attributes:

1. Time to next division event (t_c).
2. Type of the cell—stem/non-stem (isStem).
3. Probability of symmetric division (p_s). Cancer stem cells divide either symmetrically to produce two identical cancer stem cells, or asymmetrically to produce a cancer stem cell and a non-stem cancer cell [26]. In the case of cancer stem cell define probabilities of symmetric division, $0 < p_s \leq 1$, and asymmetric division $p_a = 1 - p_s$ (Fig. 2).
4. Telomere length (p). Set the telomere length of the initial cell or cell population as a molecular clock [27–29], which is a quantification of the Hayflick limit [30].
5. Current cell cycle phase (if required). If information about specific cell cycle phases is required (such as for simulations of cell cycle specific chemotherapeutics) define cell cycle phases. Cell cycle length can be divided into fractions comparable to experimentally measured cell cycle distributions.
6. Probability of spontaneous death (α). Cancer cells (isStem = false) accumulate mutations that introduce genomic instability which may lead to premature cell death. Define a probability of spontaneous cell death, $\alpha \geq 0$, at which rate cells may die during cell division attempts. Cancer stem cells (isStem = true) have a superior DNA damage repair machinery [31–33] and, thus, the probability of spontaneous cell death can be set to zero. For more biological realism, define a cell death rate that is larger than zero, but less than the self-renewal rate to ensure net population growth.

Each cell is equipped with a set of basic functions:

1. Procedure *advance time* (input arguments = time increment Δt, list of available sites in the direct neighborhood).
   - Decrease time to next division (t_c) by Δt. If $t_c < 0$ set $t_c = 0$.
   - Update current cell cycle phase (if necessary).
   - If $t_c \leq 0$ and there is available space, then perform *division* and *generate new times to next division* for both resulting cells.
2. Procedure *divide* (input argument = list of available sites in the direct neighborhood).

   Choose a random number $0 \leq n \leq 1$ from the uniform distribution. If $n < \alpha$, then simulate cell death, i.e., remove cell from the simulation and instantaneously make a corresponding lattice point available. If required, instead of instantaneous cell removal, site on the lattice can be made available for new cells after specified amount of time, e.g., in order to simulate duration of apoptosis process. Otherwise:
   - If the cell is not-stem (isStem = false) then decrease the proliferation capacity (p) by one, as non-stem cancer cells do not upregulate telomerase and are thus not long-lived and cannot initiate, retain, and reinitiate tumors [34, 35]. Simulate cell death by removing the cell from the simulation if the proliferation capacity is exhausted, i.e., less or equal to zero. Otherwise, new cell is a clone of the mother cell, i.e., non-stem cancer cell only produces non-stem cancer cell and decremented proliferation capacity is inherited by the daughter cell. Place new cell at vacant neighboring lattice point at random.
   - If the cell is cancer stem cell (isStem = true), then draw a number from uniform distribution to decide if the division is symmetric based on the probability p_s. If division is symmetric, new cell is a perfect clone of the mother cell; that is a cancer stem cells do not erode telomeres and retain identical proliferation capacity after mitosis. Otherwise, non-stem cancer cell offspring of a cancer stem cell inherit the current telomere length and determined proliferation capacity, i.e., new cell is identical except for attribute isStem, which set to false. Place new cell at vacant neighboring lattice point at random.
3. Procedure *generate time to next division*. Cells divide on average every 24 h. Derive specific cell cycle times t_c (hours), averages and standard deviations from proliferation rate calculations from clonogenic assays or live microscopy imaging [36].

4. Procedure *random migration* (input argument = list of available sites in the direct neighborhood). Cells may perform a random walk, and probabilities of migrating into adjacent lattice points can be obtained from a discretized diffusion equation [37, 38]. Assuming Moore neighborhood (*see* Sect. 2.1 above) and a cell at position (x_0,y_0): at time t can move based on available lattice points in the immediate eight-cell Moore neighborhood $N_{(x0,y0)}$ with probabilities

$$P\left(x_i^{t+1}, y_i^{t+1}\right) = \frac{\Gamma\left(x_i^t, y_i^t\right)}{1 + \sum_{N\left(x_0,y_0\right)} \Gamma\left(x_i^t, y_i^t\right)}, \quad i = 1, \ldots, 8.$$

With

$$\Gamma\left(x_i^t, y_i^t\right) = \begin{cases} 1, \text{ if lattice point } x_i, y_i \text{ is unoccupied at time } t \\ 0, \text{ otherwise} \end{cases}.$$

With probability 1/(1+number of unoccupied neighboring lattice points) the cell remains temporarily stationary, and a cell that completely surrounded by other cells is not moving. Note that in this implementation, movement to all adjacent lattice points is equally weighted. This can be modified to account for increased distance to diagonal lattice points.

5. Procedure *directed migration* (if required) (input arguments = list of available sites in the direct neighborhood, function F whose gradient ∇F describes the migration stimulus, such as chemoattractant or chemorepellant). Vector $\vec{n}$ describes the vector connecting the current cell position (x_0, y_0) to the center of one of the adjacent lattice points (x_i, y_i). Directed migration only occurs towards available lattice sites (S) when $\nabla F \cdot \vec{n} > 0$. Weight each available site S by the factor $\cos(\theta)$, where θ is the angle between the gradient ∇F and the movement direction $\vec{n}$ for each possible movement). (Notice that $\cos(\theta) = 1$ when ∇F and $\vec{n}$ are parallel, and $\cos(\theta) = 0$ when they are perpendicular, to give greatest weight to travel along the chemoattractant gradient direction.)

Sum each $\cos(\theta)$ over the S available sites to get the averaged cosine value AS. Define the probability of mobilization G through an arbitrary chemotactic/haptotactic responsiveness function via $G = H(|\nabla F|\mathrm{AS}/(\mathrm{AS}+1))$, where H has the properties:

- $H(0) = 0$ (no directed motion when no lattice sites are available or the chemical gradient is zero),
- H is a (monotonically) increasing function (directed motility increases with the magnitude chemotactic signal and alignment with the lattice), and

- H tends to 1 as $|\nabla F|\mathrm{AS}/(\mathrm{AS}+1)$ approaches ∞ (directed motility increases with the chemotactic signal, but saturates at a maximal level scaled to 1).

If a cell moves, its direction is weighted by the respective cosines for movement, so that $\cos(\theta)G/(\mathrm{AS})$ is the probability of movement to the available site at angle θ. This method is explained in detail elsewhere [39].

3 Methods

3.1 Programming Environment

1. Define programming language. Agent-based models can be implemented and simulated in any programming language; most prominent languages including C++, Java, Julia, Python, and Matlab. Each of these languages offers different computational speed and coding feasibility. C++ is considered as the environment offering the best performance, but has a high programming complexity. Matlab offers a great number of built-in functions and is easy to code in, but has significantly lower performance (e.g., when using nested loops).
2. Define graphical output. Visualize simulation solutions of agent-based models using existing implementations of graphical programming or implement specific visualization tools.
3. Agent-based software packages. Utilize predeveloped agent-based software packages; most prominent include Netlogo [40, 41], CompuCell3D [36, 42], Chaste [43], or Swarm [44].

3.2 Simulation Procedure

1. Time step. Define the simulation time step, Δt, such that Δt is smaller than the fastest biological process that is being considered in the model. In a model of cell proliferation (~1/day) and cell migration (~1 cell width/h), set $\Delta t \leq 1$ h.
2. Develop a simulation flowchart to conceptualize and visualize the simulation procedure. At each defined discrete simulation time step, consider mutually exclusive processes that occur with lowest rate constant first. Let us assume that cell migration and cell proliferation are mutually exclusive (e.g., cells could migrate through most of G1, S, G2 phases). Check if maturation age is reached; if not, check if migration time is reached (Fig. 3).
3. Lattice update sequence. Update cells in random order to avoid lattice geometry effects. Maintain a list of "live" cell agents and select cells for update from this list at random.
4. Cell update sequence. Consider vacancy in cell neighborhood in random order to avoid lattice geometry effects. Maintain a list of vacant adjacent lattice sites for each cell agent and select for update from this list at random.

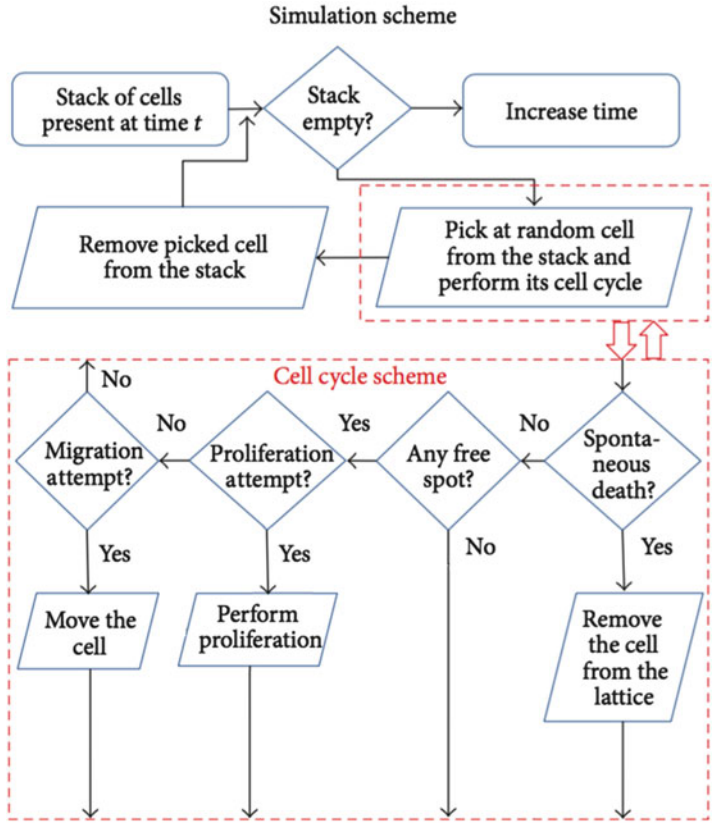

Fig. 3 Sample simulation flowchart with cell cycle scheme

4 Notes

1. Homogenous populations. The presented model produces a heterogeneous population of stem and non-stem cancer cells. If $p_s = 1$, the population remains (if only initialized with cancer stem cells) or will become (if initialized with both stem and non-stem cancer cells) homogenous comprised of only cancer stem cells. If $p_s = 0$, only non-stem cancer cells are produced and the resulting population size oscillates around a dynamic equilibrium or, if the probability of cancer stem cell death is positive and non-zero, the population will inevitably die out [45].
2. Plasticity. The presented model considers cancer stemness a cell *phenotype*, whereas recent literature may suggest stemness to be a reversible *trait* [46, 47]. The model can be extended to simulate phenotypic plasticity through cancer stem cell differentiation (that is, the cancer stem cell phenotype is set to non-stem cancer cell) and non-stem cancer cell

de-differentiation (that is, the non-stem cancer cell phenotype is set to cancer stem cell) [48].

3. Senescence. The presented model considers cell death after exhaustion of proliferation potential. Alternatively, cells may enter senescence [49] and, although mitotically inactive, continue to consume resources that influence the behavior of remaining cancer cells [50].
4. Evolution. The presented model considers fixed parameters or rate constants for each cell trait. Rate constants can change due to mutations and genetic drift [51], which allows for simulations of the evolution of cancer stem cell traits under different environmental conditions [12, 52].
5. Carcinogenesis. Such modeling framework can be adapted to model tissue homeostasis and mutation/selection cascades during cancer development [16, 53].
6. To ensure model results are reproducible, simulation inputs (parameters) and outputs should be recorded using open, standardized data formats, using biologically driven data elements that can be reused in independent models. The MultiCellDS (multicellular data standard) Project assembled a cross-disciplinary team of biologists, modelers, data scientists, and clinicians to draft a standard for *digital cell lines*, which record phenotype parameters such cell cycle time scales, apoptosis rates, and maximum proliferative capacity. Separate digital cell lines can represent cancer stem cells and non-stem cells. Similarly, standardized simulation outputs can record the position, cell cycle status, and other properties of simulated cells. Using standards will allow better software compatibility, facilitate cross-model validation, and streamline development of user-friendly software to start, modify, visualize, and analyze computational models. See MultiCellDS.org for further details.
7. Model assumptions (e.g., Fig. 3) should also be recorded with standardized data formats. The Cell Behavior Ontology (CBO) [54] provides a "dictionary" (ontology) of applicable stem cell behaviors, but it may not be able to fully capture the entire model logic in its present form. Extensions to the Systems Biology Markup Language (SBML) [55], such as SBML-Dynamic [56], are currently being developed to leverage the model structure of SBML and the ontology of CBO to annotate the mathematical structure of agent-based models, but the standards are not yet complete.
8. Treatment. The presented agent-based model can be extended to account for the effects of cancer therapy including radiation [57–59], chemotherapy [60], oncolytic viruses [61], or immunotherapy [62].

9. Analysis. Agent-based models can be rigorously analyzed for sensitivity and stability [63, 64]. Comparison of coarse-grained model behavior (e.g., growth curves) with known analytical results can quality-check calibration protocols and the computational implementation.
10. Dynamically expanding domains. Tradeoffs between lattice size and computing speed can be avoided using dynamically growing domains [65].
11. Hybrid models. The discussed model setup can be extended to a hybrid discrete-continuous framework where single cells are modeled as discrete agents, and environmental chemicals diffuse on a mapped continuum layer [66–68]. In those models cell cycle time may vary with environmental conditions (e.g., [16] and [69]).
12. Cell neighborhood. In more complex cases daughter cells can populate empty lattice sites within a given distance to approximate tissue deformability.

Acknowledgments

JP and HE were partially supported by the Personalized Medicine Award 09-33000-15-03 from the DeBartolo Family Personalized Medicine Institute Pilot Research Awards in Personalized Medicine (PRAPM). PM was supported by the Breast Cancer Research Foundation and the National Institutes of Health [1R01CA180149].

References

1. Anderson A, Chaplain MAJ, Rejniak K (2007) Single-cell-based models in biology and medicine. Springer Science & Business Media, Birkhäuser Basel, ISBN 978-3-7643-8101-1
2. Enderling H, Rejniak KA (2013) Simulating cancer: computational models in oncology. Frontiers Oncol 3:233
3. Wang Z, Butner JD, Kerketta R et al (2015) Simulating cancer growth with multiscale agent-based modeling. Semin Cancer Biol 30:70–78
4. d'Inverno M, Saunders R (2004) Agent-based modelling of stem cell self-organisation in a niche. In: Engineering Self-Organising Systems. Springer, Berlin, pp 52–68
5. Mallet DG, de Pillis LG (2006) A cellular automata model of tumor-immune system interactions. J Theor Biol 239:334–350
6. Chao DL, Eck JT, Brash DE et al (2008) Preneoplastic lesion growth driven by the death of adjacent normal stem cells. Proc Natl Acad Sci U S A 105:15034–15039
7. Enderling H, Hlatky L, Hahnfeldt P (2009) Migration rules: tumours are conglomerates of self-metastases. Br J Cancer 100:1917–1925
8. Enderling H, Anderson ARA, Chaplain MAJ et al (2009) Paradoxical dependencies of tumor dormancy and progression on basic cell kinetics. Cancer Res 69:8814–8821
9. Norton K-A, Popel AS (2014) An agent-based model of cancer stem cell initiated avascular tumour growth and metastasis: the effect of seeding frequency and location. J R Soc Interface 11, pii: 20140640
10. Gerlee P, Anderson ARA (2008) A hybrid cellular automaton model of clonal evolution in cancer: the emergence of the glycolytic phenotype. J Theor Biol 250:705–722
11. Sottoriva A, Verhoeff JJC, Borovski T et al (2010) Cancer stem cell tumor model reveals

invasive morphology and increased phenotypical heterogeneity. Cancer Res 70:46–56

12. Poleszczuk J, Hahnfeldt P, Enderling H (2015) Evolution and phenotypic selection of cancer stem cells. PLoS Comput Biol 11: e1004025
13. Anderson ARA, Quaranta V (2008) Integrative mathematical oncology. Nat Rev Cancer 8:227–234
14. Yankeelov TE, Quaranta V, Evans KJ et al (2015) Toward a science of tumor forecasting for clinical oncology. Cancer Res 75:918–923
15. Xavier JB, Foster KR (2007) Cooperation and conflict in microbial biofilms. Proc Natl Acad Sci U S A 104:876–881
16. Gatenby RA, Smallbone K, Maini PK et al (2007) Cellular adaptations to hypoxia and acidosis during somatic evolution of breast cancer. Br J Cancer 97:646–653
17. Enderling H, Hlatky L, Hahnfeldt P (2012) The promoting role of a tumour-secreted chemorepellent in self-metastatic tumour progression. Math Med Biol 29:21–29
18. Enderling H, Alexander NR, Clark ES et al (2008) Dependence of invadopodia function on collagen fiber spacing and cross-linking: computational modeling and experimental evidence. Biophys J 95:2203–2218
19. Schlüter DK, Ramis-Conde I, Chaplain MAJ (2012) Computational modeling of single-cell migration: the leading role of extracellular matrix fibers. Biophys J 103:1141–1151
20. Rejniak KA (2007) An immersed boundary framework for modelling the growth of individual cells: an application to the early tumour development. J Theor Biol 247:186–204
21. Drasdo D, Höhme S (2005) A single-cell-based model of tumor growth in vitro: monolayers and spheroids. Phys Biol 2:133–147
22. Ramis-Conde I, Drasdo D, Anderson ARA et al (2008) Modeling the influence of the E-cadherin-beta-catenin pathway in cancer cell invasion: a multiscale approach. Biophys J 95:155–165
23. Schlüter DK, Ramis-Conde I, Chaplain MAJ (2015) Multi-scale modelling of the dynamics of cell colonies: insights into cell-adhesion forces and cancer invasion from in silico simulations. J R Soc Interface 12, piii: 20141080
24. Enderling H (2014) Cancer stem cells: small subpopulation or evolving fraction? Integr Biol 7:14–23
25. Alfonso JCL, Jagiella N, Núñez L et al (2014) Estimating dose painting effects in radiotherapy: a mathematical model. PLoS One 9: e89380
26. Dingli D, Traulsen A, Michor F (2007) (A) symmetric stem cell replication and cancer. PLoS Comput Biol 3:e53
27. Olovnikov AM (1973) A theory of marginotomy. The incomplete copying of template margin in enzymic synthesis of polynucleotides and biological significance of the phenomenon. J Theor Biol 41:181–190
28. Blackburn EH, Gall JG (1978) A tandemly repeated sequence at the termini of the extrachromosomal ribosomal RNA genes in Tetrahymena. J Mol Biol 120:33–53
29. Harley CB (1991) Telomere loss: mitotic clock or genetic time bomb? Mutat Res DNAging 256:271–282
30. Hayflick L (1965) The limited in vitro lifetime of human diploid cell strains. Exp Cell Res 37:614–636
31. Bao S, Wu Q, McLendon RE et al (2006) Glioma stem cells promote radioresistance by preferential activation of the DNA damage response. Nature 444:756–760
32. Maugeri-Saccà M, Bartucci M, De Maria R (2012) DNA damage repair pathways in cancer stem cells. Mol Cancer Ther 11:1627–1636
33. Skvortsov S, Debbage P, Lukas P et al (2015) Crosstalk between DNA repair and cancer stem cell (CSC) associated intracellular pathways. Semin Cancer Biol 31:36–42
34. Allsopp RC, Morin GB, DePinho R et al (2003) Telomerase is required to slow telomere shortening and extend replicative lifespan of HSCs during serial transplantation. Hematopoiesis 102:517–520
35. Shay JW, Wright WE (2010) Telomeres and telomerase in normal and cancer stem cells. FEBS Lett 584:3819–3825
36. Gao X, McDonald JT, Hlatky L et al (2013) Acute and fractionated irradiation differentially modulate glioma stem cell division kinetics. Cancer Res 73:1481–1490
37. Anderson ARA, Chaplain MAJ, Newman EL et al (2000) Mathematical modelling of tumour invasion and metastasis. Comput Math Methods Med 2:129–154
38. Anderson ARA, Weaver AM, Cummings PT et al (2006) Tumor morphology and phenotypic evolution driven by selective pressure from the microenvironment. Cell 127:905–915

39. Enderling H, Hlatky L, Hahnfeldt P (2010) Tumor morphological evolution: directed migration and gain and loss of the self-metastatic phenotype. Biol Direct 5:23
40. Kareva I (2015) Immune evasion through competitive inhibition: the shielding effect of cancer non-stem cells. J Theor Biol 364:40–48
41. Bravo R, Axelrod DE (2013) A calibrated agent-based computer model of stochastic cell dynamics in normal human colon crypts useful for in silico experiments. Theor Biol Med Model 10:66
42. Swat MH, Thomas GL, Belmonte JM et al (2012) Multi-scale modeling of tissues using CompuCell3D. Methods Cell Biol 110:325–366
43. Mirams GR, Arthurs CJ, Bernabeu MO et al (2013) Chaste: an open source C++ library for computational physiology and biology. PLoS Comput Biol 9:e1002970
44. Minar N, Burkhart R, Langton C et al (1996) The swarm simulation system: a toolkit for building multi-agent simulations. Working Paper 96-06-042, Santa Fe Institute, Santa Fe
45. Enderling H (2013) Cancer stem cells and tumor dormancy. Adv Exp Med Biol 734:55–71
46. Marjanovic ND, Weinberg RA, Chaffer CL (2013) Cell plasticity and heterogeneity in cancer. Clin Chem 59:168–179
47. Schwitalla S (2014) Tumor cell plasticity: the challenge to catch a moving target. J Gastroenterol 49:618–627
48. Poleszczuk J, Enderling H (2016) Cancer stem cell plasticity as tumor growth promoter and catalyst of population collapse. Stem Cells Int. 2016:3923527
49. Campisi J, Kim SH, Lim CS et al (2001) Cellular senescence, cancer and aging: the telomere connection. Exp Gerontol 36:1619–1637
50. Poleszczuk J, Hahnfeldt P, Enderling H (2014) Biphasic modulation of cancer stem cell-driven solid tumour dynamics in response to reactivated replicative senescence. Cell Prolif 47:267–276
51. Sottoriva A, Vermeulen L, Tavaré S (2011) Modeling evolutionary dynamics of epigenetic mutations in hierarchically organized tumors. PLoS Comput Biol 7:e1001132
52. Scott JG, Hjelmeland AB, Chinnaiyan P et al (2014) Microenvironmental variables must influence intrinsic phenotypic parameters of cancer stem cells to affect tumourigenicity. PLoS Comput Biol 10:e1003433
53. Carulli AJ, Samuelson LC, Schnell S (2014) Unraveling intestinal stem cell behavior with models of crypt dynamics. Integr Biol 6:243–257
54. Sluka JP, Shirinifard A, Swat M et al (2014) The cell behavior ontology: describing the intrinsic biological behaviors of real and model cells seen as active agents. Bioinformatics 30:2367–2374
55. Hucka M, Finney A, Sauro HM et al (2003) The systems biology markup language (SBML): a medium for representation and exchange of biochemical network models. Bioinformatics 19:524–531
56. Myers C, Myers C (2011) Dynamic structures in SBML. Nat Precedings, http://dx.doi.org/10.1038/npre.2011.6342.1
57. Enderling H, Park D, Hlatky L et al (2009) The importance of spatial distribution of stemness and proliferation state in determining tumor radioresponse. Math Model Nat Phenom 4:117–133
58. Powathil GG, Kohandel M, Sivaloganathan S et al (2007) Mathematical modeling of brain tumors: effects of radiotherapy and chemotherapy. Phys Med Biol 52:3291–3306
59. Kempf H, Hatzikirou H, Bleicher M et al (2013) In silico analysis of cell cycle synchronisation effects in radiotherapy of tumour spheroids. PLoS Comput Biol 9:e1003295
60. Powathil GG, Gordon KE, Hill LA et al (2012) Modelling the effects of cell-cycle heterogeneity on the response of a solid tumour to chemotherapy: biological insights from a hybrid multiscale cellular automaton model. J Theor Biol 308:1–19
61. Wodarz D, Hofacre A, Lau JW et al (2012) Complex spatial dynamics of oncolytic viruses in vitro: mathematical and experimental approaches. PLoS Comput Biol 8:e1002547
62. Shengjun W, Yunbo G, Liyan S et al (2012) Quantitative study of cytotoxic T-lymphocyte immunotherapy for nasopharyngeal carcinoma. Theor Biol Med Model 9:6
63. Gerlee P, Anderson ARA (2007) Stability analysis of a hybrid cellular automaton model of cell colony growth. Phys Rev E Stat Nonlin Soft Matter Phys 75:051911
64. Gerlee P, Anderson ARA (2010) Diffusion-limited tumour growth: simulations and analysis. Math Biosci Eng 7:385–400
65. Poleszczuk J, Enderling H (2014) A high-performance cellular automaton model of

tumor growth with dynamically growing domains. Appl Math 5:144–152

66. Anderson ARA (2005) A hybrid mathematical model of solid tumour invasion: the importance of cell adhesion. Math Med Biol 22:163–186
67. Gerlee P, Anderson ARA (2007) An evolutionary hybrid cellular automaton model of solid tumour growth. J Theor Biol 246:583–603
68. Enderling H, Hlatky L, Hahnfeldt P (2012) Immunoediting: evidence of the multifaceted role of the immune system in self-metastatic tumor growth. Theor Biol Med Model 9:31
69. Macklin P, Edgerton ME, Thompson AM et al (2012) Patient-calibrated agent-based modelling of ductal carcinoma in situ (DCIS): from microscopic measurements to macroscopic predictions of clinical progression. J Theor Biol 301:122–140

Methods in Molecular Biology (2016) 1516: 347–360
DOI 10.1007/7651_2016_323

Published online: 01 April 2016

Induction of a Tumor-Metastasis-Receptive Microenvironment as an Unwanted Side Effect After Radio/Chemotherapy and In Vitro and In Vivo Assays to Study this Phenomenon

Gabriela Schneider, Zachariah Payne Sellers, and Mariusz Z. Ratajczak

Abstract

Besides surgical removal of tumor tissue, chemotherapy and radiotherapy are the most important and efficient treatment modalities employed to treat therapy-susceptible malignancies. The main aim of this treatment—to destroy tumor cells—is unfortunately usually associated with toxicity to nontumor cells and different degrees of tissue and organ damage. In damaged tissues several chemoattractants are upregulated and released that may attract tumor cells. Moreover, highly migratory radio/chemotherapy treatment may endow cells with several properties of cancer stem cells which survive and respond to these chemoattractants upregulated in collateral tissues. Based on this, one of the unwanted and underappreciated side effects of chemotherapy or radiotherapy is the creation of a metastasis-receptive microenvironment in bones as well as in other organs of the body. Herein we describe methods and assays that can be employed to study migratory properties of cancer cells in in vitro (chemotaxis) and in vivo (seeding efficiency assay) conditions in response to the induction of pro-metastatic microenvironments in various organs and tissues.

Keywords: Chemotaxis, Seeding efficiency

1 Introduction

There are several mechanisms that may lead to cancer development, but it is presently unclear whether cancer originates in mutated normal stem cells (SCs), progenitor cells, or more differentiated somatic cells [1, 2]. Some recent evidence suggests that malignancy arises from the accumulation of mutations and maturation arrest of normal SCs or progenitor cells rather than by the dedifferentiation of already differentiated somatic cells [3, 4]. It has been postulated that normal SCs acquire mutations and give rise to cancer stem cells (CSCs), which are subsequently responsible for tumor growth, tumor recurrence after unsuccessful radio/chemotherapy, and establishing distant metastases. Thus, this SCs origin of cancer hypothesis is based on the assumption that long-living SCs residing in organs and tissues, and not mature short-living differentiated somatic cells such as those lining the bronchial or stomach mucosa,

may acquire and accumulate mutations during a life time and pass them to daughter SCs [1, 2]. These daughter stem cells may subsequently be subjected to additional mutations and epigenetic changes to the point where the genome is destabilized and uncontrolled, initiating neoplastic proliferation. In addition to those hypothetical considerations, recent research from several laboratories have provided direct evidence that several neoplasms (e.g., brain tumors, prostate cancer, melanomas, colon and lung cancer) may in fact originate in the stem cell compartment [5–9].

Surgical removal of tumor tissue, chemotherapy and radiotherapy are the most important treatment modalities employed to treat malignancies. However radio/chemotherapy is associated with significant toxicity to vital organs. Moreover, recent evidence indicates that another unwanted side effect of radio/chemotherapy is the induction of a pro-metastatic environment due to the upregulation of different chemotactic/chemokinetic factors in collateral tissues [10–12]. Furthermore, chemotherapy- or radiotherapy-associated tissue and organ damage also activates developmentally early proteolytic cascades, such as the complement cascade (ComC), coagulation cascade (CoaC), and fibrinolytic cascade (FibC). It is well known that some of the activated proteolytic cleavage products of these cascades, such as C3a, C5a, thrombin, urokinase, and uPAR [13–16], are directly or indirectly involved in cancer metastasis. An important mechanism related to chemotherapy- or radiotherapy-mediated activation of CoaC and ComC is the activation of blood platelets and the release of platelet-derived microvesicles [17–20]. These small circular membrane fragments may transfer several platelet–endothelium cell adhesion receptors, such as glycoprotein IIb/IIIa (CD41), Ib, IaIIa, and P-selectin (CD62P), to the surface of circulating tumor cells and thus facilitate the attachment of CSCs or disseminated tumor cells (DTCs) to the endothelium at the site of a future metastasis [17, 18]. In addition to this pro-metastatic, adhesion-mediated effect, it has also been reported that some cytostatics (e.g., cyclophosphamide) exert direct toxicity to the endothelial wall, which affects the integrity of the endothelial barrier and may facilitate the seeding of cancer cells into damaged organs through the disrupted endothelium [21].

Figure 1 depicts our concept postulating the creation of a radio/chemotherapy mediated pro-metastatic microenvironment in the bone marrow (BM) and other organs. This unwanted side effect is mainly involved in the metastasis of tumor cells to tissues that are highly sensitive to damage by both chemotherapeutics and toxic doses of radiation (e.g., BM, liver, and lungs). Since BM tissue is highly sensitive to radio/chemotherapy, its damage facilitates the creation of a metastasis-receptive microenvironment and is responsible for the occurrence of frequent bone metastases that are often seen in the clinical setting. Upregulation of several chemokines,

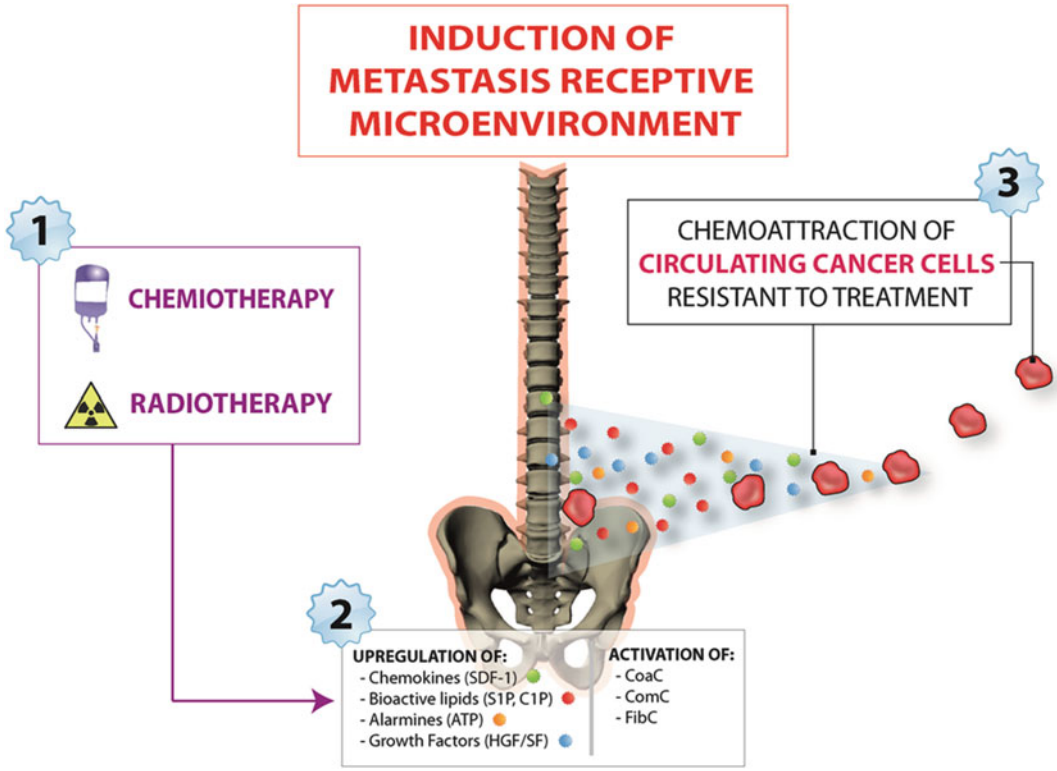

Fig. 1 Radio/chemotherapy induce the formation of pro-metastatic microenvironments via the upregulation of several chemoattractants and the activation of different pathways, resulting in the increased migration of cancer cells that survive the initial treatment

growth factors, alarmines, bioactive phosphosphingolipids as well as the activation of the complement cascade, coagulation cascade, fibrinolytic cascade, and metalloproteinases, in toto, enhances and modulates trafficking and survival of CSCs and that survived treatment. This implies a challenge for modern pharmacology to develop powerful antimetastatic compounds that can be combined with standard chemotherapy and radiotherapy protocols or applied as a follow-up to these protocols. The targeting of CSCs, which are reported to resist chemotherapy and be responsible for the recurrence of cancer, along with cancer cells is an appropriate approach to treat cancer and prevent the more deadly especially recurrence of cancers.

In this chapter we describe several experimental approaches in vitro and in vivo that could be employed to better characterize the metastatic properties of cancer cells that arise in response to a radio/chemotherapy-induced pro-metastatic microenvironment. We focus on assays that assess the effects of pro-metastatic chemokines, growth factors, and bioactive lipids.

2 Materials

2.1 In Vitro Chemotaxis/ Chemokinesis Assay for Adherent and Non-adherent Cells

1. For adherent cells: prepare a 0.5 % gelatin solution by weighting 0.5 g of gelatin and adding 100 ml of PBS. Incubate the mixture at 56 °C until all gelatin dissolves. Filter the mixture through a 0.22 μm filter to obtain a sterile solution. Store the solution at 4 °C and warm it up to 37 °C at least 1 h before running the assay (*see* **Note 1**).
2. For adherent cells: Hema 3 stains solution (Fisher Scientific) and cotton swabs.
3. For non-adherent cells: Neubauer chamber
4. 6.5 mm Transwell® (Corning) with 8 μm pore polycarbonate membrane insert, sterile (Corning #3422) or equivalent; 24 well plate (*see* **Note 2**).
5. Appropriate medium used for cell culture without FBS but supplemented with 0.5 % BSA (*see* **Note 3**).
6. Chemotactic/chemokinetic factors induced by radio/chemotherapy or conditioned medium harvested from organs damaged by radio/chemotherapy.

2.2 In Vivo Seeding Efficiency Assay (Detection of Human–Murine Chimerism)

1. Immunodeficient mice (e.g., SCID-beige CBSCBG; Taconic) (*see* **Note 4**).
2. Sterile PBS or 0.9 % NaCl.
3. 1 cc U-100 28 G ½ insulin syringes.
4. 3 and 5 ml syringes with 25 G 5/8 needles.
5. SYBR Green PCR Master Mix (Life Technologies)
6. Primers α-satellite-F 5′-ACC ACT CTG TGT CCT TCG TTC G-3′, α-satellite-R 5′-ACT GCG CTC TCA AAA GGA GTG T-3′, β-actin-F 5′-TTC AAT TCC AAC ACT GTC CTG TCT -3′ β-actin-R 5′-CTG TGG AGT GAC TAA ATG GAA ACC-3′.
7. Kit for genomic DNA purification (e.g., Qiagen DNeasy Blood and Tissue Kit)

2.3 Preparation of Conditioned Medium for Organs Damaged by Radio/ Chemotherapy

1. C57BL/6 J mice (or another strain of mice used for studies).
2. Irradiator.
3. Chemotherapeutic (e.g., Vincristine).
4. 1 cc U-100 28 G ½ insulin syringes.
5. 3 and 5 ml syringes with 25 G 5/8 needles.
6. Medium (e.g., RPMI), antibiotics (100 U/ml penicillin, and 10 μg/ml streptomycin), plastic dishes.
7. Optional, to prepare samples for quantification of small molecules (e.g., nucleotides): deproteinizing Sample Preparation Kit (BioVision Inc).

3 Methods

Carry out all procedures at room temperature unless otherwise specified.

3.1 Chemotaxis of Adherent Cells (Fig. 2)

1. Trypsinize cells, centrifuge them at 300 × *g* for 5 min, resuspend the pellet in medium with 0.5 % BSA and count the cells. Prepare the solution of cells in medium with 0.5 % BSA to get a final concentration of 3.5–12 × 10^5 cells per 1 ml (*see* **Note 5**). For 1 well 100 μl of cell suspension will be used, so the final volume of cell solution is based on the number of conditions/inserts used for chemotaxis. Quiesce the cells by incubating them at 37 °C, 5 % CO_2 for 4 h (*see* **Note 6**). If the effect of an inhibitor on chemotaxis is being studied, it should be added to cells 30 min to 1 h prior to seeding cells on the membrane (*see* **Note 7**).
2. At 30 min–1 h before chemotaxis coat the membrane of Transwell® inserts with 70 μl/insert of 0.5 % gelatin solution. Remove any air bubbles that could affect coating. Incubate the inserts in 37 °C and 5 % CO_2.
3. Add 650 μl of medium to the desired wells on 24-well plate and supplement each with the desired chemoattractant(s). Medium alone is the negative control and the positive control will be the known chemoattractant or medium supplemented with 10 % serum (e.g., FBS).
4. Remove the gelatin from the inserts and seed the cells (100 μl) onto the membrane (*see* **Note 8**). Immediately transfer each insert into the well with appropriate medium. Remove any air bubbles trapped between the membrane and medium in the lower chamber because their presence affects the results of chemotaxis (*see* **Note 9**). Incubate the plate with inserts at 37 °C and 5 % CO_2 for 24 h.
5. To visualize the migrated cells, place the inserts into 800 μl (per well of 24 well plate) of fixative solution (Hema 3 staining kit) for 6 min, followed by staining in Solution I (6 min) and then solution II (2 min). Wash the inserts twice in water and then use a cotton swab to gently remove cells from the top side of the membrane (cells that did not migrate). During the whole procedure avoid touching the bottom of the membrane.
6. Let the membrane dry and count the cells on the bottom side of the membrane under an inverted microscope. Calculate the data in comparison to the negative control. The experiment should be run at least in duplicates. On Fig. 3 there are examples of microscope images of cells migrating to different chemoattractants.

3.2 Chemotaxis of Non-adherent Cells

1. Centrifuge the cells, resuspend the pellet in medium with 0.5 % BSA and count the cells. Prepare the solution of cells in medium with 0.5 % BSA to get final concentration of

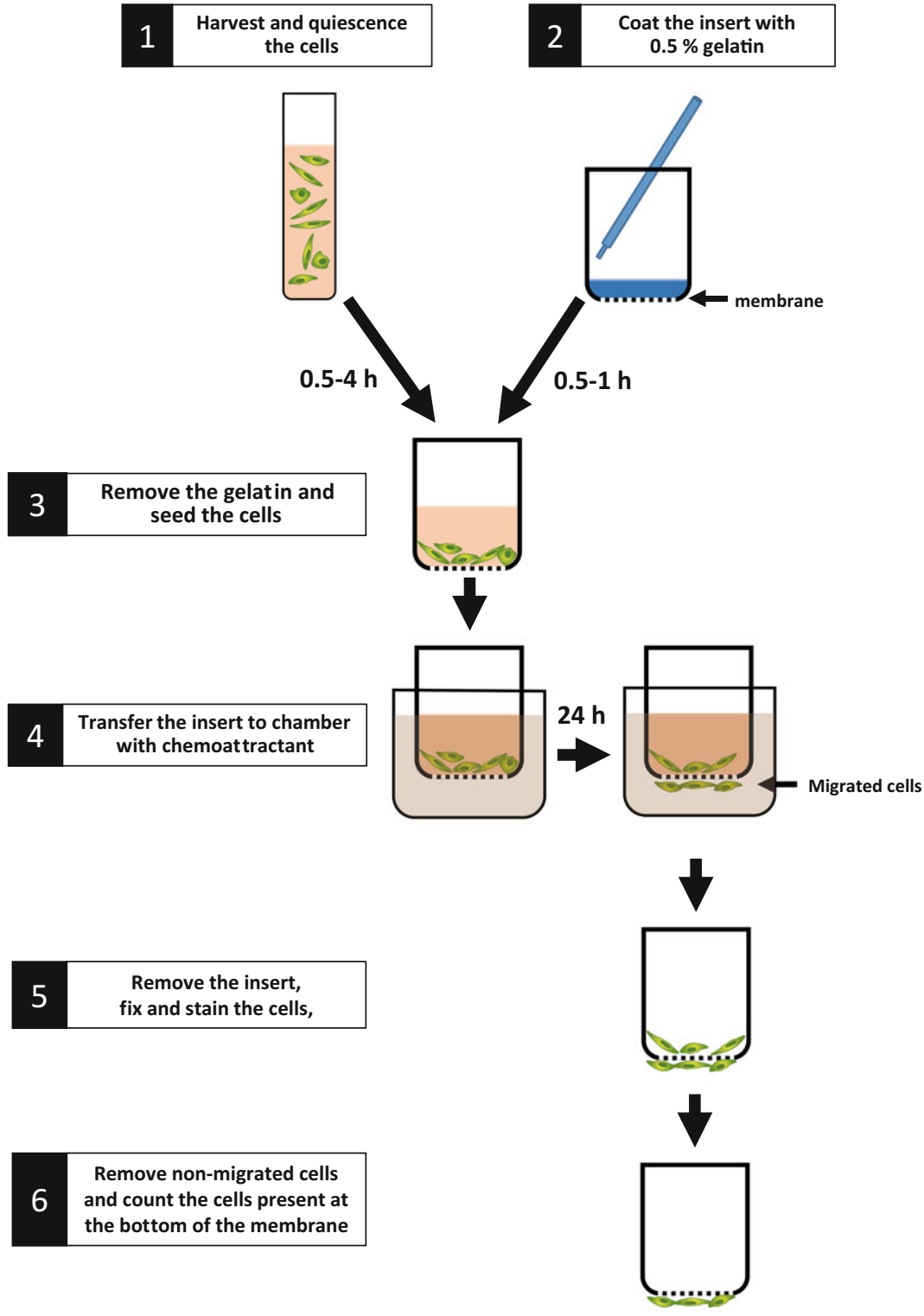

Fig. 2 The overall scheme of chemotactic assays performed in the trans-well system used to evaluate the migration of cells towards different chemoattractants

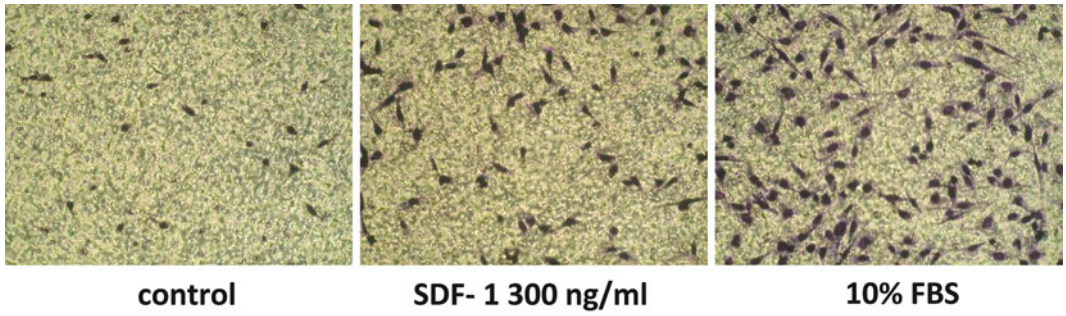

Fig. 3 Migration of RH30 (rhabdomyosarcoma) cells towards control medium (no chemoattractant), stromal cell-derived factor 1 (SDF-1) and medium with 10 % FBS. Cells present on the bottom side of the insert membrane were fixed and stained using HEMA 3

1×10^6 cells per 1 ml (*see* **Note 5**). For 1 well 100 μl of cell suspension will be used, so the final volume of cell solution is based on the number of conditions/inserts used for chemotaxis. Quiesce the cells by incubating them in 37 °C and 5 % CO_2 for 5 h (*see* **Note 6**). If the effect of a particular inhibitor on chemotaxis is being studied, it should be added to the cells 30 min to 1 h prior to seeding cells onto the membrane (*see* **Note 7**).

2. Add 650 μl of medium to each well and supplement with the desired chemoattractant (s). Medium alone is the negative control and the positive control will be the known chemoattractant or medium supplemented with 10 % serum (e.g., FBS).
3. Seed cells (100 μl) onto the membranes of the inserts and immediately transfer the inserts immediately into well with appropriate medium. Remove any air bubbles trapped between the membrane and medium in the lower chamber because their presence affects the results of chemotaxis (*see* **Note 9**). Incubate the plate with inserts at 37 °C and 5 % CO_2 for 4 h.
4. After incubation, gently remove the inserts and count the cells that migrated to the lower chamber. This can be done by transferring the medium with cells from the bottom chamber to 1.5 ml tubes, centrifuging the cells and resuspending the cells in a small volume (50–100 μl) of Trypan Blue. Count the cells using Neubauer chamber. Alternatively, the cells can be counted directly in the medium using an automatic cell counter or using a flow cytometer in which number of cells will be analyzed during a fixed amount of time (e.g., 1 min).

3.3 Chemotaxis vs. Chemokinesis

1. Run the chemotaxis as usual. To analyze whether a particular factor acts as a chemoattractant or chemokinetic factor, compare the migration of cells in the presence of the analyzed

molecule in the lower chamber only vs. conditions when the analyzed molecule is present in the upper and lower chambers at the same concentration. Chemotaxis occurs only when there is a gradient, so the presence of an analyzed chemoattractant in both the upper and lower chambers will inhibit the migration of cells as compared to the conditions when it is present only in bottom chambers. Chemokinetic factors will increase the migration of cells to the lower chamber even when there is a lack of a gradient. Please note that many factors possess both chemokinetic and chemotactic properties.

3.4 In Vivo Seeding Efficiency Assay (Detection of Human–Murine Chimerism)

This method is based on the detection of human–murine chimerism. Therefore only human cancer/cancer stem cells can be used in this study. For studies of murine cancer/cancer stem cells, this method has to be modified to use another species of animal (e.g., rat) and another set of primers.

Carry out all the procedures at room temperature unless otherwise specified.

3.4.1 Preparation of Standard Curve

1. Isolate murine bone marrow cells by flushing the bone marrow from tibias and femurs into PBS using 3 ml syringe and 25 G 5/8 needle. It is recommended to use the same strain of mice as will be used for seeding efficiency assay. Count the cells and prepare aliquots containing 1×10^6 cells. Add a different number of human cells that will be used in studies (e.g., 1×10^6, 0.5×10^6, 1×10^5, 0.5×10^5, 1×10^4, 1×10^3, 0.5×10^3, 1×10^2, 0.5×10^2, 100, 50, 10, 1). Centrifuge the cell mixture ($350 \times g$, 10 min), remove the supernatant and purify DNA from the cell pellet (e.g., using the DNeasy Kit, Qiagen) according to manufacturer's instruction.
2. Analyze human α-satellite and murine β-actin DNA levels using quantitative real-time PCR (qRT-PCR). For each 25-μl reaction mixture use 12.5 μl of SYBR Green PCR Master Mix (Life Technologies), 100 ng of DNA template (*see* **Note 10**) and the appropriate set of primers. Real-time PCR conditions are as follows: 95 °C (15 s), 40 cycles at 95 °C (15 s), and 60 °C (1 min). According to the melting point analysis, only one PCR product should be amplified under these conditions. Calculate ΔCt for each sample where ΔCt = (Ct of α-satellite) − (Ct of β-actin).
3. Prepare a standard curve using the ΔCt values and the number of human cells in sample. Use a logarithmic scale for the number of cells. An example of a standard curve is presented in Fig. 4.

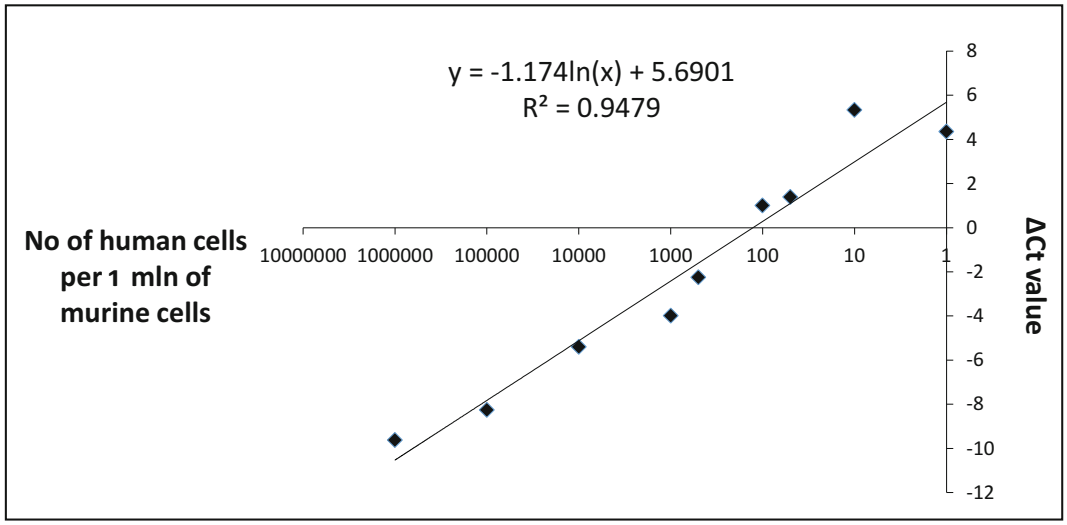

Fig. 4 An example of a standard curve used for the calculation of human–murine chimerism

3.4.2 Detection of Human–Murine Chimerism (Fig. 5)

1. Inject the suspension of cells (3×10^6 of human cells in 100 μl of sterile 0.9 % NaCl or PBS per mouse) intravenously into the tail vain of severe combined immunodeficient SCID-Beige mice (*see* **Note 11**) using 1 cc U-100 28 G ½ insulin syringes. Try to avoid repeated movements of cells through the syringe because that can lyse the cells. Remove any air bubbles from the syringe before injection. If the effect of radiotherapy and/or chemotherapy is being analyzed, animals should receive the treatment prior to the injection of cells (e.g., 24 h before).
2. Isolate marrows, livers, and lungs (and other organs of interest) 48 h after injection of the cells. Isolate DNA from organs (e.g., using DNeasy Kit, Qiagen) according to the manufacturer's instruction.
3. Analyze human α-satellite and murine β-actin DNA levels using qRT-PCR as described in Section 3.4.1.
4. Base on the standard curve, calculate the level of human–murine chimerism in all analyzed samples.

3.5 Harvesting of Conditioned Medium from Organs

Conditioned medium can be used in chemotaxis, proliferation assays etc. Similarly, as it is for detection of human–murine chimerism, when the effect of radiotherapy and/or or chemotherapy is being studied, samples should be collected several hours (e.g., 24 h) after irradiation or chemotherapeutic drug administration. C57BL/6J or another wild type strain of mice should be used for these studies. If conditioned medium is not used immediately, store it in −80 °C in small aliquots. Avoid repeated freezing/thawing cycles.

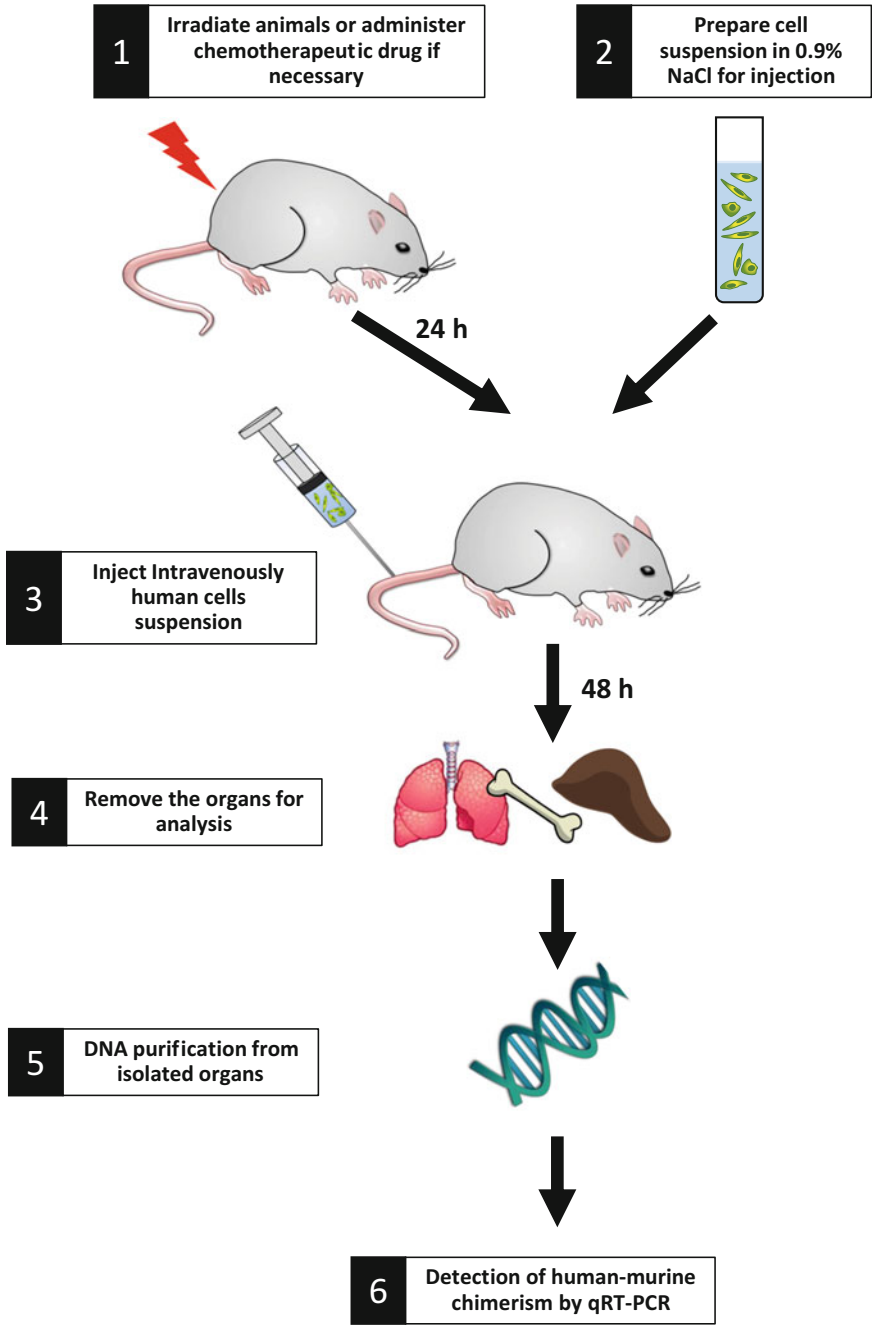

Fig. 5 The overall scheme of a seeding efficiency assay

1. Bone marrow conditioned medium: isolate murine bone marrow cells by flushing bone marrow from both tibias and femurs into 3 mL of RPMI supplemented with penicillin and streptomycin using 3 ml syringed and 25 G 5/8 needles. Centrifuge samples at 850 × *g*, 4 °C for 10 min and collect supernatants.

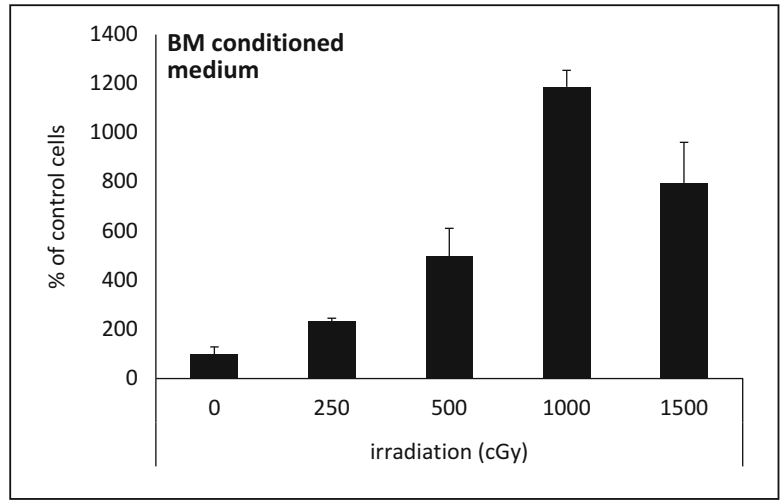

Fig. 6 Results of the chemotaxis of the HTB177 cell line (lung cancer) across transwell membranes to bone marrow conditioned medium harvested from control or irradiated animals

Measure the volumes of remaining medium and count the cells (*see* **Note 12**). This type of medium can be used directly for chemotaxis (*see* example results presented in Fig. 6), however it might be required to be diluted for some of the cells—this should be tested experimentally.

2. Conditioned medium from liver, lung, brain, and other organs: isolate organs, wash them with PBS and weigh the tissues (*see* **Note 13**). Next, transfer the organs into sterile RPMI (5 ml) supplemented with penicillin and streptomycin and cut the tissue into small pieces using scalpel. Additionally homogenize tissue by repeatedly passaging it through a syringe without any needle (*see* **Note 14**). Transfer the mixture to tubes, centrifuge at 850 × *g* and 4 °C for 10 min, and collect supernatants. This type of conditioned medium is concentrated and should be (e.g., for chemotaxis) in diluted (2–10 %) form. The final concentration used in experiments should be determined experimentally.

Optional, for samples that will be used for quantification of small molecules (e.g., ATP, cAMP, glutathione, glycogen), proteins removal from sample prior to analysis might be necessary. Deproteinizing Sample Preparation Kit (BioVision Inc)) utilize perchloric acid (PCA) precipitation method. PCA was shown to not only removes most of the protein present in samples but also stabilize some of small molecules analytes. Samples should be prepared according to the manufacturer's instruction and can be used for ATP measurements (e.g., ATP Colorimetric/Fluorometric Assay Kit, BioVision Inc), adenosine (e.g., adenosine Assay Kit Fluorometric, BioVision Inc) or UTP (ELISA Kit for Uridine

Triphosphate (UTP), USCN Business Co, Ltd). Deproteinized samples can be stored at −80 °C up to a month.

3.6 Conclusions

We have proposed a novel concept whereby the unwanted and underappreciated side effects of radio/chemotherapy create a metastasis-receptive microenvironment in several organs in the body. Upregulation of pro-migratory chemokines, growth factors, alarmines, bioactive phosphosphingolipids as well as the activation of CoaC, ComS, FibC, and metalloproteinases, in toto, enhances and modulates the trafficking and survival of cancer cells (and CSCs?) that survived treatment. This implies a challenge for modern pharmacology to develop powerful antimetastatic compounds that can be combined with standard radio/chemotherapy protocols to ameliorate the pro-metastatic microenvironments induced by anticancer treatment. The protocols described in this chapter will be helpful for developing strategies to ameliorate this unwanted effect of anticancer treatment.

4 Notes

1. Different adherent cells might need different substrates to migrate. Besides gelatin (in concentrations of 0.5–1 %), other coatings include fibronectin (5–50 μg/ml), laminin (20 μg/ml) or Matrigel® (50 μg/ml).
2. Use of appropriate Transwell® pore sizes is necessary for optimal results. Smaller cells might require a smaller pore size (e.g., 6 μm) whereas larger cells or cells with low migratory properties might require a larger pore size (e.g., 12 μm).
3. Concentration of BSA can be between 0.1 and 0.5 % depending on the sensitivity of cells used in the chemotaxis assay.
4. The use of immunodeficient mice is necessary to prevent immune reactions after injection of human cells.
5. The number of cells depends on their size and type. Too many cells (especially non-adherent) can clog the pores of the insert.
6. Quiescence time differs between cell types and it varies from 0.5 to 5 h of incubation. Some already publish protocols suggest to use FBS in low concentration (e.g., 1 %) however we have found that such doses possess remarkably high chemotactic/chemokinetic activity [22] and therefore might affect results of the assay by indicating that there is no effect of studied chemoattractant, or that a higher concentration must be used to see any effect at all. This could also lead to incorrect conclusions (e.g., the effective concentrations of studied chemoattractant are supraphysiological whereas in fact under the appropriate assay conditions cells can react to physiological concentrations).

7. Since chemotaxis of adherent cells is run for 24 h, for studies where the effect of inhibitors is analyzed, not only pretreatment of cells but also the addition of inhibitors to the lower chamber should be considered in order to expose the cells to their presence throughout the whole process. Such decisions should be made based on the known receptor turnover as well as the stability of inhibitors and their binding kinetics. For non-adherent cells, the time of chemotaxis is much shorter, so it is enough to pretreat cells only and there is no need for the addition of inhibitors to the lower chamber.
8. After gelatin removal, cells should be seeded onto inserts within 5–10 min. Be careful to not puncture the membrane during gelatin removal.
9. To avoid air bubbles between the membrane and medium in the prefilled lower chamber, gently place the insert at a slight angle. This will allow any air bubbles to move upwards across the membrane.
10. 100–300 ng of genomic DNA is sufficient for the qRT-PCR reaction; however, the same amount should be used for all analyzed samples.
11. Cell suspension cannot exceed 150 μl and it should be injected very slowly. The number of cells depends on their size and adhesion properties, however it should not be too high since cells can obstruct lung vessels and possibly result in animal death. Animals should be monitored throughout the whole experiment according to the regulations provide by Institutional Animal Care and Use Committee.
12. The number of cells (BM)/organ weight (liver, lung, brain, etc.) and the volume of obtained conditioned medium is necessary to calculate final concentration of chemotactic factors present in this medium. For bone marrow this also allows for the efficiency of bone flushing to be monitored (similar cell number should be isolated from similar age/gender/size mice undergoing the same treatment). Please remember that the number of bone marrow cells decreases with increasing doses of irradiation and/or chemotherapy [12].
13. It is necessary to wash the organs to remove excess of blood. Weighing the tissue allows for later calculation of the concentration of different chemoattractants per μg of tissue.
14. This method unfortunately results with the lysis of part of the cells, so each sample obtained for the same tissue (but after different treatments) should be processed in the same manner. It is recommended to make analyses (e.g., ELISA, chemotaxis, proliferation, etc.) for at least two separate isolations of conditioned medium or to combine conditioned medium (the same organ and the same conditions) that were harvested from several animals.

Acknowledgment

We would like to thank Tomasz Jadczyk, M.D. for preparing a scheme for Figure 1.

References

1. Houghton J, Stoicov C, Nomura S, Rogers AB, Carlson J, Li H et al (2004) Gastric cancer originating from bone marrow-derived cells. Science 306:1568–1571
2. Kim CF, Jackson EL, Woolfenden AE, Lawrence S, Babar I, Vogel S et al (2005) Identification of bronchioalveolar stem cells in normal lung and lung cancer. Cell 121:823–835
3. Reya T, Morrison SJ, Clarke MF, Weissman IL (2001) Stem cells, cancer, and cancer stem cells. Nature 414:105–111
4. Sell S (2004) Stem cell origin of cancer and differentiation therapy. Crit Rev Oncol Hematol 51:1–28
5. Singh SK, Hawkins C, Clarke ID, Squire JA, Bayani J, Hide T et al (2004) Identification of human brain tumour initiating cells. Nature 432:396–401
6. Fang D, Nguyen TK, Leishear K, Finko R, Kulp AN, Hotz S et al (2005) A tumorigenic subpopulation with stem cell properties in melanomas. Cancer Res 65:9328–9337
7. Mikhail S, Zeidan A (2014) Stem cells in gastrointestinal cancers: the road less travelled. World J Stem Cells 6:606–613
8. Jaworska D, Krol W, Szliszka E (2015) Prostate cancer stem cells: research advances. Int J Mol Sci 16:27433–27449
9. Nguyen N, Couts KL, Luo Y, Fujita M (2015) Understanding melanoma stem cells. Melanoma Manag 2:179–188
10. Schneider G, Bryndza E, Abdel-Latif A, Ratajczak J, Maj M, Tarnowski M et al (2013) Bioactive lipids S1P and C1P are prometastatic factors in human rhabdomyosarcoma, and their tissue levels increase in response to radio/chemotherapy. Mol Cancer Res 11:793–807
11. Schneider G, Sellers ZP, Abdel-Latif A, Morris AJ, Ratajczak MZ (2014) Bioactive lipids, LPC and LPA, are novel prometastatic factors and their tissue levels increase in response to radio/chemotherapy. Mol Cancer Res 12:1560–1573
12. Schneider G, Glaser T, Lameu C, Abdelbaset-Ismail A, Sellers ZP, Moniuszko M et al (2015) Extracellular nucleotides as novel, underappreciated pro-metastatic factors that stimulate purinergic signaling in human lung cancer cells. Mol Cancer 14:201
13. Hu L, Lee M, Campbell W, Perez-Soler R, Karpatkin S (2004) Role of endogenous thrombin in tumor implantation, seeding, and spontaneous metastasis. Blood 104:2746–2751
14. Shi X, Gangadharan B, Brass LF, Ruf W, Mueller BM (2004) Protease-activated receptors (PAR1 and PAR2) contribute to tumor cell motility and metastasis. Mol Cancer Res 2:395–402
15. Wysoczynski M, Liu R, Kucia M, Drukala J, Ratajczak MZ (2010) Thrombin regulates the metastatic potential of human rhabdomyosarcoma cells: distinct role of PAR1 and PAR3 signaling. Mol Cancer Res 8:677–690
16. LeBeau AM, Duriseti S, Murphy ST, Pepin F, Hann B, Gray JW et al (2013) Targeting uPAR with antagonistic recombinant human antibodies in aggressive breast cancer. Cancer Res 73:2070–2081
17. Scholz T, Temmler U, Krause S, Heptinstall S, Losche W (2002) Transfer of tissue factor from platelets to monocytes: role of platelet-derived microvesicles and CD62P. Thromb Haemost 88:1033–1038
18. Janowska-Wieczorek A, Wysoczynski M, Kijowski J, Marquez-Curtis L, Machalinski B, Ratajczak J et al (2005) Microvesicles derived from activated platelets induce metastasis and angiogenesis in lung cancer. Int J Cancer 113:752–760
19. Janowska-Wieczorek A, Marquez-Curtis LA, Wysoczynski M, Ratajczak MZ (2006) Enhancing effect of platelet-derived microvesicles on the invasive potential of breast cancer cells. Transfusion 46:1199–1209
20. Liang H, Yan X, Pan Y, Wang Y, Wang N, Li L et al (2015) MicroRNA-223 delivered by platelet-derived microvesicles promotes lung cancer cell invasion via targeting tumor suppressor EPB41L3. Mol Cancer 14:58
21. Park SI, Liao J, Berry JE, Li X, Koh AJ, Michalski ME et al (2012) Cyclophosphamide creates a receptive microenvironment for prostate cancer skeletal metastasis. Cancer Res 72:2522–2532
22. Schneider G, Serwin K, Bryndza E, Kucia M, Ratajczak J, Ratajczak MZ (2012) Studies with diluted plasma reveal the presence of a remarkably potent factor that enhances the motility of cancer cells and is quenched by fibrinogen – a novel view of cancer metastasis. Blood 120: abstr. 3431

Methods in Molecular Biology (2016) 1516: 361–369
DOI 10.1007/7651_2016_342

Published online: 05 April 2016

Isolation and Propagation of Glioma Stem Cells from Acutely Resected Tumors

Jinkyu Jung, Mark R. Gilbert, and Deric M. Park

Abstract

Gliomas are characterized by striking intratumoral cellular heterogeneity. A consistent method to isolate undifferentiated GSC fraction from clinical specimens provides an opportunity to establish in vitro models that more closely mirror the in vivo state compared to traditional serum containing culture methods. Here we describe techniques involved with isolation, identification, and expansion of human malignant glioma-derived stem cells using a serum-free growth condition.

Keywords: Glioma stem cell, Glioblastoma multiforme, GBM, Neural stem cell, N2 medium, Serum-free cell culture

1 Introduction

The suggestion that cancers have properties of stemness (undifferentiated, high capacity for self-renewal) dates back many years [1]. This hypothesis driven by histopathologic similarities between undifferentiated developing tissue and poorly differentiated cancers was extended by subsequent investigators who proposed that cancer represents a disrupted developmental program in which tissues fail to appropriately differentiate to instructive specification [2, 3]. Benefiting from improved understanding of development and technical improvements, leukemic stem cells were identified [4]. Subsequently, the presence of the so-called "cancer stem cell" or "cancer initiating cell" has been identified in a variety of solid tumors [5–11]. Although some investigators take issue with the term "cancer stem cell," and suggest alternative names such as cancer recapitulating cell, cancer initiating cell, or stem-like cell, the argument is mostly semantic since the cancer stem cell hypothesis does not necessarily imply that all cancers originate from stem cells, nor does it assert that even some cancers are derived from the direct malignant transformation of stem cells. The conceptual importance may be that certain cancers are maintained by a population of malignant cells that exhibit stem-like properties of self-renewal and capacity to differentiate into specialized lineage(s),

irrespective of the cell of origin which may be a progenitor cell or a differentiated somatic cell that has reacquired the stem-like properties.

Ideal culture system should be able to preserve the functional capacities and self-renewal activity of the parental tumor cells. Standard serum-dependent cell culture techniques alter the cellular phenotype by inducing artificial genetic and epigenetic changes. The N2 medium based serum-free method is largely adopted from techniques used for the study of in vitro rodent neural stem cells [12, 13]. Also, the strictly defined condition of the medium excludes all uncharacterized additives. We discuss methods to establish initial primary culture from tissue, composition of the N2 medium, protocols to identify GSC, techniques to passage and freeze cells for storage, and preparation for in vivo implantation into immunodeficient hosts.

2 Materials

2.1 Plate Preparation for Propagation as Monolayer

- 100 mm tissue culture dishes.
- Poly-L-ornithine (Sigma-Aldrich, cat. no. P-3655).
  (a) Prepare 5 mg/mL stock solution in sterile water and store at −20 °C for up to 6 months.
  (b) For working solution, dilute stock solution to 0.5 mg/mL with water and filter sterilize. Prepare 6 mL solution per 100 mm tissue culture dish.
  (c) This diluted solution can be stored at 4 °C for up to 4 weeks.
    - Fibronectin (R&D Systems, cat. no. 1030-FN).

2.2 Dissection of Glioma Patient Tissue

Dissection-related general instruments such as blade, forceps, clean tissue culture hood, and occasionally dissection microscopy.

- N2 medium: Combine N2 supplements, which are 50 mg apo-transferrin (Sigma-Aldrich, cat. no. T-2036), 12.5 mg insulin (Sigma-Aldrich, cat. no. I-0516), 50 μL putrescine (Sigma-Aldrich, cat. no. P-5780), 30 μg sodium selenite (Sigma-Aldrich, cat. no. S-5261), 100 μL progesterone (Sigma-Aldrich, cat. no. P-8783), and penicillin/streptomycin/Fungizone antibiotic/antimycotic in 500 mL of DMEM/F12 (Thermo Fisher Scientific, cat. no. 11320-033; including high glucose, L-glutamine, and phenol red). Adjust pH to 7.2. Filter the medium through a 0.2 μm filter. The medium can be stored up to 4 weeks at 4 °C.
- Sterile EBSS (Earle's Balanced Salt Solution; Thermo Fisher Scientific, cat. no. 14155063) with bicarbonate and phenol red. Refrigerate between each use (*see* **Note 1**).

- Papain solution containing L-cysteine and EDTA (Worthington Biochemical Cooperation, papain dissociation system, cat. no. LK003150). 5 mL EBSS solution should contain 20 units of papain per mL, 1 mM L-cysteine, and 0.5 mM EDTA. Short incubation is necessary for full solubility and activity.
- DNase (Deoxyribonuclease I; Worthington Biochemical Cooperation, papain dissociation system, cat. no. LK003150). Reconstitute with 0.5 mL of EBSS at 2000 units of DNase per mL. Avoid vigorous vortexing.
- Ovomucoid protease inhibitor with bovine serum albumin (Worthington Biochemical Cooperation, papain dissociation system, cat. no. LK003150). Prepare to 10 mg/mL with EBSS.
- Cell strainer (70 μm filter; Falcon, cat. no. 352350).
- PBS (phosphate buffered saline; HyClone, cat. no. SH3002802) without calcium and magnesium.
- Incubator preset for 95 % O_2: 5 % CO_2 equilibration for EBSS solution.

2.3 Identification of GSC

- CD133 MicroBeads kit (Miltenyi Biotec, cat. no. 130-050-801).
- Magnetic-activated cell sorting (MACS) separator and column (*refer* **Miltenyi Biotec homepage**; http://www.miltenyibiotec.com/).
- Basic F12/DMEM (Thermo Fisher Scientific, cat. no. 11320-033).

2.4 Passaging

- HBSS (Hank's balanced salt solution; HEPES buffer, Media-Tech, cat. no. 20-021-CV). Mix 700 mL water with 100 mL of 10× Ca^{2+} and Mg^{2+}-free (CMF) HBSS. Weigh 3.7 g $NaHCO_3$ and 3.9 g HEPES and transfer to mixture. Adjust pH to 7.1–7.2 with 1 N HCl. Make up to 1 L with water. Sterilize with filter.
- Stock solution for EGF (20 μg/mL, epidermal growth factor; R&D Systems, cat. no. 236-EG) and (20 μg/mL, bFGF, basic fibroblast growth factor; R&D Systems, cat. no. 233-FB). Final working concentration should be 20 ng/mL.
- N2 medium (*see* Sect. 2.2).

2.5 Freezing Cell Stocks in 10 % DMSO Plus N2 Medium Without Serum

- DMSO (Dimethyl sulfoxide; Sigma-Aldrich, cat. no. D-2650).
- Cryo-freezing vials (Corning Life Sciences, cat. no. 430487).
- Propanol.
- Liquid nitrogen tank for cell storage.

2.6 Induction of Differentiation Using Serum or CNTF

- CNTF (Ciliary neurotrophic factor; R&D Systems, cat. no. 557-NT/CF).
- FBS (Fetal bovine serum; Gibco, cat. no. 10437-028).

2.7 Neurosphere Culture and Daily Maintenance with EGF and bFGF

- Non-treated tissue culture dishes (100 mm dish).
- Accutase (Sigma-Aldrich, cat. no. A6964).
- N2 medium, EGF, bFGF, and HBSS (*please see* Sects. 2.2 and 2.4).
- Cell counter.

2.8 Preparation of Cells for Establishing Animal Models

- Cell counter.
- PBS (*please see* Sect. 2.2) and ice.

3 Methods

3.1 Plate Preparation for Propagation as Monolayer

1. Coat 100 mm dish with 6 mL of poly-L-ornithine overnight in cell culture incubator. This should be done at least 2 days before day of tissue processing.
2. On the following day, aspirate poly-L-ornithine and wash twice for 5 min with 10 mL PBS.
3. Coat the surface of the dish with fibronectin (1:250, in PBS) and incubate overnight (or at least 2 h if urgent).
4. Aspirate fibronectin next day (day of tissue processing), and wash with PBS twice. Incubate the fibronectin-coated dish coated with PBS used in washing step in the cell culture incubator until dissociated cells from the tumor tissue is ready for plating.
5. Dish coated with poly-L-ornithine can be stored in the incubator for up to 2 weeks. The dish double-coated with poly-L-ornithine and fibronectin can be stored for up to 1 week (*see* **Note 2**).

3.2 Disassociation of Human Glioma Tissue

1. Place acutely resected tumor tissue in 100 mm dish with ~5 mL of N2 medium containing EGF and bFGF (20 ng/mL) in tissue culture hood (*see* **Note 3**).
2. Aspirate medium and then wash several times with N2 medium.
3. Chop and mince tissue using forceps and scalpel, removing membranes, blood vessels, and necrotic portions of the tumor.
4. Prepare a premixture of DNase (350 μL) and papain solution containing L-cysteine and EDTA. Add this solution and gently disassociate with 10 mL pipette until a homogenous suspension is formed. Keep remaining solution of DNase on ice for later use.

5. Incubate the dish at 37 °C. Approximately every 10 min, blend the suspension with 5 mL pipette, and then inspect with inverted microscope for presence of single cells. Repeat this step until single cells are visualized. This step should not exceed 60 min. Total time is dependent on density and tumor size. (*see* **Note 4**).
6. Prepare two 50 mL conical tubes with 70 μm cell strainer while tumor cells are in incubator.
7. Transfer the slurry onto the filter in the conical tube. Rinse plate with N2 medium and continue to filter.
8. Repeatedly triturate the slurry mixture on filter and continue to wash with N2 medium.
9. Centrifuge at 300 relative centrifugal force (RCF) for 5 min.
10. During centrifugation, prepare a mixture containing 2.7 mL EBSS with ~300 μL ovomucoid protease inhibitor with albumin, and 150 μL DNase.
11. Gently aspirate the supernatant and resuspend the cell pellet in above solution (**step 10**).
12. Layer the cell suspension in 5 mL of the remaining ovomucoid protease inhibitor plus albumin, and then centrifuge at 200 RCF for 5 min. The interface between the two gradient layers should be clearly visible. Dissociated cells remain at the bottom of the tube and membrane fragments at the interface.
13. Resuspend the cells with 10 mL of N2 medium, and incubate overnight at 37 °C.
14. Next day, centrifuge the cells at 300 RCF for 3 min.
15. Wash the cells with 10 mL PBS and centrifuge at 300 RCF for 3 min.
16. Resuspend the collected cells in N2 medium containing EGF and bFGF, and incubate at 37 °C (*see* **Note 5**).

3.3 Selection of CD133 Expressing GSC

1. This section concerns isolation of GSC positive for expression of CD133 surface marker.
2. Centrifuge collected cells from above, at 300 RCF for 5 min.
3. Remove supernatant and wash with basic F12/DMEM medium.
4. Count number of cells (*see* **Note 6**).
5. Centrifuge at 300 RCF for 5 min.
6. Remove supernatant and resuspend with N2 medium (up to 3×10^7 cells per 300 μL).
7. Turn off light source in cell culture hood and add 100 μL of blocking reagent per 3×10^7 cells.

8. Label the cells with 100 μL of the CD133 microbeads per 3×10^7 cells (Total volume is 500 μL per 3×10^7 cells).
9. Suspend the mixture and incubate for 1 h in dark at room temperature.
10. Invert mixture every 10 min.
11. Wash with medium.
12. Centrifuge at 200 RCF for 5 min.
13. Aspirate supernatant and resuspend cell pellet in 500 μL of medium per 1×10^7 cells.
14. Place column on magnet with a 50 mL conical tube under the column to collect CD133-negative cells.
15. Equilibrate the column by rinsing with 3 mL DMEM/F12 (*see* **Note 7**).
16. Wash the column with 1 mL DMEM/F12 and collect in the same tube as prior step. Label these as first pass CD133-negative cells.
17. Place a fresh 50 mL conical tube under the magnet and wash the column with 3 mL DMEM/F12 three times (*see* **Note 8**).
18. Firmly flush out the CD133-positive fraction containing the magnetically labeled cells using the supplied plunger into CD133-positive conical tube.
19. Collect CD133-positive cell in N2 medium.
20. Send the first pass CD133-negative cells through a new column and keep only the cells that pass through the column initially. Keep these cells as CD133-negative fraction (*see* **Note 9**).

In our hands, we are unable to maintain and propagate pure population of CD133-positive cells. A fraction of this pool appears to revert to CD133-negative state. Nevertheless, this method may be useful for short-term experiments that call for CD133-positive cells.

3.4 Passaging

1. After several days in culture, cells should begin to form distinct colonies with cell-free space between spheres. At 80 % confluency, cells should be passaged.
2. Place the culture dish under cell culture hood and wash twice with 10 mL of prewarmed HBSS (*see* **Note 10**). Incubate for 5 min at 37 °C with 5 mL HBSS containing EGF (20 ng/mL) and bFGF (20 ng/mL).
3. Gently pipet HBSS over the surface of the culture dish to lift the colonies off.
4. Collect the HBSS solution including the cells in a 15 mL conical tube, and centrifuge at 300 RCF for 5 min. Remove the supernatant.

5. Resuspend the cells in 1 mL N2 medium and count the viable cells. Inoculate 1.5 million cells per 100 mm precoated dish in 10 mL N2 medium containing recombinant growth factors.

3.5 Freezing Cell Stocks in 10 % DMSO Plus N2 Medium Without Serum

1. Cells can be frozen in liquid nitrogen for long-term storage. Prepare cell freezing container with 250 mL propanol.
2. Centrifuge the cells and remove the supernatant. Harvest and count cells.
3. Redilute to final concentration of greater than 3×10^6 cells per mL.
4. Add 100 μL of DMSO in cryo freezing vial and add 900 μL of cells in the vial. Invert twice and store in freezing container overnight at −80 °C (at least 4 h). Transfer to liquid nitrogen tank for long term storage.

3.6 Induction of Differentiation

Differentiation of GSC can be induced by addition of serum, cytokine such as CNTF, or growth factor withdrawal.

1. Add 10 % FBS or 20 ng/mL CNTF.
2. Replace with medium containing FBS or CNTF every day for 3–5 days.
3. Confirm extent of differentiation by immunocytochemistry for expression of stem and lineage markers.

3.7 Neurosphere Culture and Daily Maintenance with EGF and bFGF

GSC can be maintained in sphere form without use of precoated culture dishes. EGF signaling promotes sphere formation capacity [13]. In our experience, daily addition of growth factors appears critical in maintaining the stem state.

1. For sphere propagation, use uncoated dishes.
2. Count cell number and plate 1×10^6 cells (100 mm dish) with N2 medium containing growth factors.
3. Add 20 ng/mL EGF and bFGF every day.
4. When ready to passage or store, collect the culture medium including tumor spheres. Rinse with 5 mL of warm HBSS.
5. Centrifuge the cells for 5 min at 200 RCF and aspirate supernatant.
6. Resuspend cells with 1 mL of Accutase at 37 °C during 2 min to dissociate the cells. Mechanical trituration can be used in lieu of Accutase.
7. Centrifuge the cells for 5 min at 200 RCF and collect the cell pellet.
8. Inoculate 1×10^6 cells (100 mm dish) in N2 medium or freeze for storage.

3.8 Preparation of Cells for Establishing Animal Models

Acutely dissociated tumor cells and primary culture cells can also be used to establish orthotopic xenograft models in immunodeficient hosts.

1. We found most GSC lines to be capable of forming infiltrative tumors with 1×10^3 to 1×10^4 cells per mice.
2. Centrifuge and wash with PBS. Dissociate (Accutase or trituration) and collect cells by centrifugation.
3. Count cells and resuspend in 8 μL of PBS per each mice. Keep on ice until transplantation.

4 Notes

1. EBSS includes a pH-sensitive dye. Color purple indicates alkaline state. Incubation medium should be well buffered at physiological pH.
2. Fibronectin is susceptible to denaturation. Care should be taken to prevent drying of tissue culture dishes.
3. Only one tumor sample should be processed at a time to avoid cross-contamination.
4. Trituration is a critical process. Too vigorous manipulation will result in damaged cells; too weak and tissue fragments will be left intact. Gentle trituration is needed using 5 mL pipette.
5. Cells should be maintained with daily addition of growth factors.
6. Dead cell should be removed to improve efficiency of the magnetic beads.
7. Do not allow column to dry out.
8. Do not use culture these cells for the following step.
9. Do not collect any other cells.
10. Do this step one dish at a time to avoid cell loss.

References

1. Virchow R (1858) Die Cellularpathologie in ihrer Begründung auf physiologische und pathologische Gewebelehre. In: Hirschwald A (ed) Berlin
2. Conheim V (1875) Congenitales, quergestreiftes muskelsarkom der nieren. Virchows Arch Pathol Anat Physiol Klin Med 65:64–69
3. Harris H (2005) A long view of fashions in cancer research. Bioessays 27(8):833–838
4. Lapidot T et al (1994) A cell initiating human acute myeloid leukaemia after transplantation into SCID mice. Nature 367 (6464):645–648
5. Al-Hajj M et al (2003) Prospective identification of tumorigenic breast cancer cells. Proc Natl Acad Sci U S A 100(7):3983–3988
6. Bonnet D, Dick JE (1997) Human acute myeloid leukemia is organized as a hierarchy that

originates from a primitive hematopoietic cell. Nat Med 3(7):730–737

7. Collins AT et al (2005) Prospective identification of tumorigenic prostate cancer stem cells. Cancer Res 65(23):10946–10951
8. Hemmati HD et al (2003) Cancerous stem cells can arise from pediatric brain tumors. Proc Natl Acad Sci U S A 100(25):15178–15183
9. Kim CF et al (2005) Identification of bronchioalveolar stem cells in normal lung and lung cancer. Cell 121(6):823–835
10. O'Brien CA et al (2007) A human colon cancer cell capable of initiating tumour growth in immunodeficient mice. Nature 445(7123): 106–110
11. Singh SK et al (2003) Identification of a cancer stem cell in human brain tumors. Cancer Res 63(18):5821–5828
12. Androutsellis-Theotokis A et al (2008) Generating neurons from stem cells. Methods Mol Biol 438:31–38
13. Soeda A et al (2009) Hypoxia promotes expansion of the CD133-positive glioma stem cells through activation of HIF-1alpha. Oncogene 28(45):3949–3959

Methods in Molecular Biology (2016) 1516: 371–388
DOI 10.1007/7651_2016_326

Published online: 01 April 2016

Isolation and Characterization of Cancer Stem Cells of the Non-Small-Cell Lung Cancer (A549) Cell Line

Noor Hanis Abu Halim, Norashikin Zakaria, Nazilah Abdul Satar, and Badrul Hisham Yahaya

Abstract

Cancer is a major health problem worldwide. The failure of current treatments to completely eradicate cancer cells often leads to cancer recurrence and dissemination. Studies have suggested that tumor growth and spread are driven by a minority of cancer cells that exhibit characteristics similar to those of normal stem cells, thus these cells are called cancer stem cells (CSCs). CSCs are believed to play an important role in initiating and promoting cancer. CSCs are resistant to currently available cancer therapies, and understanding the mechanisms that control the growth of CSCs might have great implications for cancer therapy. Cancer cells are consist of heterogeneous population of cells, thus methods of identification, isolation, and characterisation of CSCs are fundamental to obtain a pure CSC populations. Therefore, this chapter describes in detail a method for isolating and characterizing a pure population of CSCs from heterogeneous population of cancer cells and CSCs based on specific cell surface markers.

Keywords: Cancer stem cells (CSCs), Method, Sorting, Characterization

1 Introduction

Emerging evidence shows that cancer growth is driven by a rare subpopulation of cancer cells called cancer stem cells (CSCs) [1–3]. CSCs, or so-called cancer-initiating cells, share several characteristics with normal stem cells, including the self-renewal and expression of specific cell markers and genes [4]. The failure of current cancer therapies is thought to be at least partially due to the failure of the treatments to target CSCs. Surviving CSCs can proliferate and generate secondary tumors. Conventional chemotherapy works by eliminating proliferative tumor cells. However, there is evidence that chemotherapy agents increase the proportion of drug-resistant CSCs, which can restore tumor growth [5].

The origin of CSCs can be explained by the CSC hypotheses [6]. The first hypothesis states that cancer arises from either mutated stem cells or mutated stem progenitor cells, which naturally have self-renewal and differentiation characteristics. The second hypothesis postulates that tumor progression is driven by a

subpopulation of tumor cells with self-renewal ability. This hypothesis is supported by well-documented observations that most tumors consist of cell subpopulations that have heterogeneous functions, including a group of cells with limitless proliferative potential and repopulation ability. Such CSCs were first identified in acute myeloid leukemia (AML) [7]. Dick (1997) found that most subtypes of AML could be engrafted in immunodeficient mice, but leukemic engraftment could only be initiated from the $CD43^{+}CD38^{-}$ fractions. This concept and experimental approach were then applied to solid breast cancer tumors for the first time by Clarke and colleagues [2]. They showed that as few as 100 $CD44^{+}CD24^{-/low}$ cells were tumorigenic, whereas other cell phenotypes were not. In addition, the tumorigenic $CD44^{+}CD24^{-/low}$ cells could be serially passaged and then generate new tumors containing cell fractions similar to those present in the initial tumor. Since then, other studies of different solid tumors, including brain [1], colon [3, 8], and lung [9], have been conducted.

CSCs can be identified and isolated from heterogeneous population of cancer cells using several approaches, including surface markers, side populations, and Aldehyde Dehydrogenase (ALDH) activity (Table 1). Further characterizations of CSCs are based on their stemness characteristics, including self-renewal, differentiation capabilities, and expression of stem cell-related genes. This chapter describes in detail a method for isolating CSCs using surface markers, i.e., CD44, CD166, and CD326. The cell lines used in this method are derived from non-small-cell lung cancer.

Table 1
Biomarkers for identification and isolation of CSCs

Approach	Tumor types	Markers	References
Surface marker	Breast cancer	$CD44^{+}CD24^{-}$	[2]
		$CD133^{+}$	[11]
	Colon cancer	$CD133^{+}$	[3]
		$EpCAM^{+}CD44^{+}CD166^{+}$	[12]
	Pancreatic cancer	$EpCAM^{+}CD44^{+}CD24^{+}$	[13]
		$CD133^{+}$	[14]
	Lung cancer	$CD166^{+}CD44^{+}$, $CD166^{+}EpCAM^{+}$	[9]
		$CD133^{+}$, $CXCR4^{+}$	[15]
Side population	Glioma		[16]
	AML		[17]
	Lung cancer		[18]
ALDH activity	Breast cancer	$ALDH\text{-}1^{+}$	[19]
	Pancreatic cancer	$ALDH\text{-}1^{+}$	[20]
	Liver cancer	ALDH	[21]
	Lung cancer	$ALDH\text{-}1^{+}$	[22]

However, the methods can also be applied to others types of cell lines for isolating and characterization of CSCs from heterogeneous population of cancer cells.

2 Materials

2.1 Cell Line

Purchase lung cancer cell lines (A549 and NCI-H2170) and human bronchial/tracheal epithelial cells (PCS-300-010) from the American Type Culture Collection (ATCC, Manassas, VA, USA).

2.2 Cell Culture Media

2.2.1 Cancer Cell Medium

Supplement the RPMI-1640 medium (Gibco, Thermo Scientific, Grand Island, NY, USA) with 10 % fetal bovine serum (FBS) (Gibco) and 1 % penicillin–streptomycin. Use 0.25 % trypsin–EDTA (Gibco) as the cell dissociation reagent (*see* **Note 1**).

2.2.2 Normal Cell Medium

Supplement the epithelial cell basal medium (ATCC® PCS-300-030) with the Bronchial/Tracheal Epithelial Growth Kit (ATCC® PCS-300-040), Gentamicin–Amphotericin B solution (ATCC® PCS-999-025), Penicillin–Streptomycin–Amphotericin B solution (ATCC® PCS-999-002), and Phenol Red (ATCC® PCS-999-001) (all from ATCC). Use 0.05 % trypsin–EDTA (Gibco) as the cell dissociation reagent (*see* **Note 1**).

2.3 Isolating CSCs

1. Antibody CD44-FITC (Clone: L178; Isotype: Mouse IgG1, κ), (BD Biosciences, San Jose, USA).
2. Antibody CD166-PE (Clone: 3A4; Isotype: Mouse IgG1, κ) (BD Biosciences).
3. Antibody CD326–FITC (Clone: 158206; Isotype: Mouse IgG_{2B}; Isotype: Mouse IgG1, κ) (EpCAM) (BD Biosciences).

2.4 Differentiation Assays

2.4.1 Osteogenic Assay

1. Osteogenic medium (PromoCell, Heidelberg, Germany). Store at –20 °C.
2. Alizarin Red S (Sigma-Aldrich, Munich, Germany) staining solution: pH 4.1–4.3. Add 100 mL of water to a 100 mL scotch bottle. Dissolve 2 g of Alizarin Red S in the water. Mix well and adjust pH to a 4.1–4.3 with 0.1 % ammonium hydroxide (NH_4OH). Filter the Alizarin Red S staining solution and store it in the dark at room temperature (*see* **Note 2**). Store at room temperature.
3. Phosphate buffered saline (PBS) (Gibco). Store at room temperature.
4. 10 % formalin: Add 27.03 mL of 37 % formalin to a 100 mL scotch bottle. Bring volume up to 100 mL with distilled water.

5. Alkaline phosphatase substrate solution: Dissolve one tablet of BCIP/NBT in 10 mL of distilled water. This substrate solution needs to be stored in the dark and used within 2 h. Washing buffer: Add 0.05 % Tween 20 to Dulbecco's PBS.

2.4.2 Adipogenic Assay

1. Adipogenic medium (PromoCell). Store at –20 °C.
2. Oil Red O (Sigma-Aldrich) staining solution: For stock solution of Oil Red O, dissolve 0.3 % Oil Red O in isopropanol. Store in the dark at room temperature. This stock solution is stable for 1 year. For working solution, dilute three parts of Oil Red O stock solution with two parts distilled water. Filter this mixture using a syringe filter. The solution needs to be used within 30 min (*see* **Note 3**). Store at room temperature.
3. 60 % isopropanol: Add 60 mL of absolute isopropanol and bring the volume up to 100 mL with distilled water.
4. Harris hematoxylin (Sigma-Aldrich). Store at room temperature.

2.4.3 Chondrogenic Assay

1. Chondrogenic medium (Promocell). Store at –20 °C.
2. Alcian Blue (Sigma-Aldrich) staining solution: Add 60 mL of ethanol (98–100 %) to a 100 mL scotch bottle. Mix ethanol with 40 mL of acetic acid (98–100 %). Weigh 10 mg of Alcian Blue 8GX and add to the mixture of ethanol and acetic acid. Mix well to achieve the Alcian Blue staining solution. The solution is stable for 1 year (*see* **Note 4**). Store at 4 °C.
3. Destaining solution: Mix 120 mL of ethanol (98–100 %) with 80 mL of acetic acid (98–100 %).
4. PBS. Store at room temperature.
5. Neutral buffered formalin. Store at room temperature.

2.5 Clonogenic Assay

1. Crystal Violet (BD Biosciences). Store at room temperature.

2.6 Spheroid Formation Assay

1. Dulbecco's Modified Eagle Medium–Nutrient Mixture F-12 (DMEM-F12K) (Gibco). Store at 4 °C.
2. Epidermal growth factor (EGF) (Life Technologies, Foster City, CA, USA). Store at –20 °C.
3. Basic fibroblast growth factor (bFGF) (Life Technologies). Store at –20 °C.
4. B27 supplement (Life Technologies). Store at –20 °C.
5. Penicillin–streptomycin (PenStrep) (Gibco). Store at –20 °C.
6. Matrigel (BD Biosciences). Store at –20 °C (*see* **Note 5**).

2.7 Microarray

1. Human GeneChip Gene 1.0 ST array (Affymetrix, Santa Clara, USA). Store at 4 °C. AllPrep DNA/RNA Isolation Kit (Qiagen, Limburg, Netherlands). Store at room temperature.
2. QIAshredder Homogenizer (Qiagen). Store at room temperature.
3. Applause™ WT-Amp ST System (NuGEN Technologies, Inc., San Carlos, USA). Store at –20 °C (*see* **Note 6**).
4. MinElute Reaction Cleanup Kit (Qiagen). Store at 4 °C/room temperature.
5. Encore Biotin Module (NuGEN Technologies). Store at –20 °C.
6. GeneChip® Hybridization, Wash, and Stain Kit (Affymetrix). Store at 4 °C/–20 °C.

2.8 In Vivo Tumorigenicity Studies

1. 4–7-week-old female NCR nude mice (InVivos, Perahu Road, Singapore) (*see* **Note 7**).
2. Matrigel (BD Biosciences). Store at –20 °C.
3. Hematoxylin (Sigma-Aldrich). Store at room temperature.
4. Eosin (Sigma-Aldrich). Store at room temperature.

2.9 Equipment and Plates

1. Inverted-phase contrast microscope (Olympus 1X70, Olympus Tokyo, Japan).
2. Ultra-low attachment plate (Corning, New York, USA).

3 Methods

3.1 Cell Culture

1. Culture lung cancer cell lines (A549 and NCI-H2170) in cancer cell medium (*see* Section 2.2.1) and normal human bronchial/tracheal epithelial cells (PHBEC) in normal cell medium (*see* Section 2.2.2).
2. Incubate both cells in a humidified incubator at 37 °C supplied with 5 % carbon dioxide (*see* **Note 8**).
3. Maintain the cells routinely in 75 cm^2 tissue culture flasks and harvest by trypsin treatment when the cells are in the logarithmic phase of growth or at 80 % confluence for flow cytometry analysis.

3.2 Analysis and Sorting of CSCs Using the Cell Sorter

1. Detach the lung cancer cells and normal cells with 0.25 % trypsin and wash with PBS/2 % FBS.
2. Label the cell suspensions with CD44-FITC, CD166-PE, and EpCAM–FITC antibodies.
3. Briefly resuspend the cells in 90 μL of PBS/2 % FBS.

4. Add 10 μL of each antibody to the cell suspension (1.0×10^6 cells/mL) and incubate for 30 min in the dark.
5. At the end of the incubation, wash away unbound antibodies with PBS/2 % FBS.
6. Resuspend each cell pellet in 300–500 μL of PBS/2 % FBS and filter it through a 40 μm cell strainer to obtain a single cell suspension before sorting.
7. Analyze the expression of CSC markers (CD166, CD44, and EpCAM), and sort the CSCs using the FACSAria III (BD Biosciences) (Fig. 1).
8. Sort the double positive cell population ($CD166^+/CD44^+$ and $CD166^+/EpCAM^+$) and double negative ($CD166^-/CD44^-$ and $CD166^-/EpCAM^-$) fractions.
9. The purity of the sorted populations is routinely >90 %. Evaluate aliquots of the sorted cell populations for post-sorting purity using the FACSAria III.
10. Culture the sorted cell populations in the standard medium and use them for subsequent assays, including the colony and sphere forming, differentiation, and microarray assays.

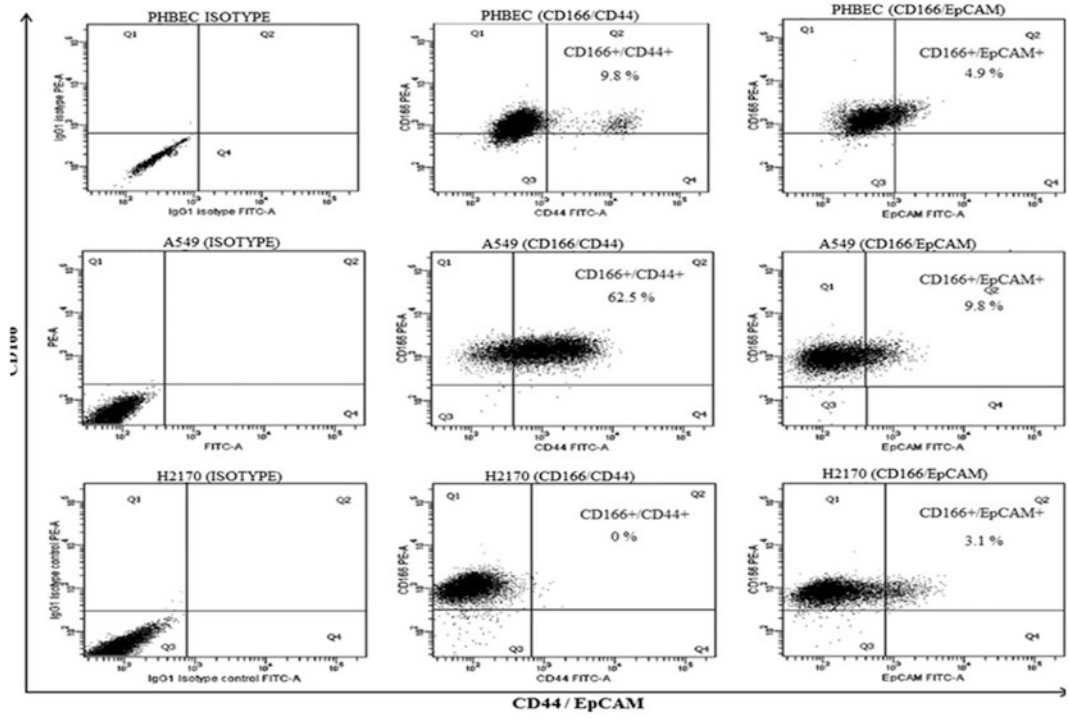

Fig. 1 Analysis of CD166/CD44 and CD166/EpCAM on lung cancer cells [9]

3.3 Differentiation Assay

3.3.1 Osteogenic Differentiation

1. Seed CSCs by plating 6×10^4 cells per well in 24-well tissue culture plates using growth medium. Seed the cells in two wells, one well for induction and the other well as the negative control.
2. Grow CSCs until they reach >100 % confluence within 24–72 h.
3. Induce CSC differentiation. Induce one of the samples with osteogenic differentiation medium; for the other (negative control), use growth medium.
4. Incubate cells for 21 days in osteogenic differentiation medium. Change the medium every third day (*see* **Note 9**). Extent osteogenic differentiation can be determined by deposition of calcium and alkaline phosphatase activity.

3.3.2 Osteoblast Detection (Calcium Deposits)

Differentiated osteoblasts will exhibit vast extracellular calcium deposits, whereas undifferentiated stem cells will not exhibit calcium deposits. Presence of calcium deposits can be determined by staining with Alizarin Red S.

1. Wash the cells: Take the cells from the incubator. Aspirate the induction and growth media from the cells carefully. Carefully wash the cells with Dulbecco's PBS, W/O Ca^{++}/Mg^{++} (*see* **Note 10**).
2. Fix the cells: Aspirate the PBS and transfer the cell culture plate to a fume hood. Add about 500 μL of 10 % neutral buffered formalin to the cellular monolayer. Make sure the cellular monolayer is covered by formalin. Incubate the cell monolayer for 30 min (*see* **Note 11**). Carefully aspirate the formalin (*see* **Note 12**), and add distilled water to the cells to wash them.
3. Stain the cells: Carefully remove the distilled water from the cell monolayer. Add about 500 μL Alizarin Red S staining solution to the cell monolayer. Make sure the cell monolayer surface is covered by Alizarin Red S; if not, add more staining solution. Incubate in the dark at room temperature for 45 min.
4. Wash the cells: Carefully aspirate the Alizarin Red S staining solution and wash the cell monolayer with 1 mL of distilled water. Repeat the washing step four times to remove excess stain. Remove the distilled water from the cell monolayer and add PBS.
5. Analyze the cells: Undifferentiated CSCs (without extracellular calcium deposits) are slightly reddish, whereas CSC-derived osteoblasts (with extracellular calcium deposits) are bright orange-red.

3.3.3 Osteoblast Detection (Alkaline Phosphatase)

Differentiated osteoblasts show high alkaline phosphatase (AP) activity whereas undifferentiated stem cells show weak AP activity. Presence of AP can be detected by using BCIP/NBT as a substrate where the AP-containing cell will stain blue-violet.

1. Wash the cells: Take the cells from the incubator. Aspirate the induction and growth media from the cells carefully. Carefully wash the cells with Dulbecco's PBS, W/O Ca^{++}/Mg^{++} (*see* **Note 10**).
2. Fix the cells: Aspirate the PBS and transfer the cell culture plate to a fume hood. Add about 500 μL of 10 % neutral buffered formalin to the cellular monolayer. Make sure the cellular monolayer is covered by formalin. Incubate the cell monolayer for 60 s (*see* **Note 11**). Carefully aspirate the formalin (*see* **Note 12**), and add Washing buffer to the cells to wash them.
3. Stain the cells: Carefully remove the Washing buffer from the cell monolayer. Add about 500 μL BCIP/NBT substrate solution to the cell monolayer. Make sure the cell monolayer surface is covered by substrate solution; if not, add more substrate solution. Incubate in the dark at room temperature for 2–3 min.
4. Wash the cells: Carefully aspirate the substrate solution and wash the cell monolayer with 1 mL of Washing buffer. Remove the Washing buffer from the cell monolayer carefully and add PBS to the cell.
5. Analyze the cells: Undifferentiated CSCs (without or weak AP activity) are colouroless or faintly bluish whereas CSC-derived osteoblasts (high AP activity) are stained dark blue-violet.

3.3.4 Adipogenic Differentiation

Mature adipocytes will exhibit large number of intracellular lipid vesicles whereas undifferentiated stem cells will not exhibit intracellular lipid vesicles. Presence of intracellular lipid vesicles can be determined by staining with Oil Red O than give the cell bright red color.

1. Seed CSCs by plating 6×10^4 cells per well in 24-well tissue culture plates using growth medium. Seed the cells in two wells, one well for induction and the other well as the negative control.
2. Grow cells until they reach >100 % confluence within 24–72 h.
3. Induce CSC differentiation. Induce one of the samples with adipogenic differentiation medium; for the other (negative control), use growth medium.
4. Incubate cells for 14 days in adipogenic differentiation medium. Change the medium every third day (*see* **Note 9**). Extent adipogenic differentiation can be determined by adipocyte formation.

3.3.5 Adipocyte Detection

1. Wash the cells: Take the cells from the incubator. Aspirate the induction and growth media from the cells carefully. Carefully wash the cells with Dulbecco's PBS, W/O Ca^{++}/Mg^{++} (*see* **Note 10**).
2. Fix the cells: Aspirate the PBS and transfer the cell culture plate to a fume hood. Add about 500 μL of 10 % neutral buffered

formalin to the cellular monolayer. Make sure the cellular monolayer is covered by formalin. Incubate the cell monolayer at room temperature for 30 min (*see* **Note 11**). While waiting for incubation, prepare the Oil Red O staining solution (*see* Section 2.4.2).

3. Wash the cells: Carefully aspirate the formalin and add distilled water to the cells to wash them. Carefully aspirate the water and add 500 μL of 60 % isopropanol to each well. Make sure the isopropanol fully covers the entire cell monolayer surface. Incubate at room temperature for 5 min.
4. Stain the cells: Carefully remove the isopropanol from the cell monolayer. Add about 500 μL of Oil Red O staining solution to the cell monolayer. Make sure the entire cell monolayer surface is covered; if not, add more staining solution. Incubate at room temperature for 15 min.
5. Wash the cells: Carefully aspirate the Oil Red O staining solution and wash the cell monolayer with distilled water to remove excess stain. Repeat the washing step several times until the water becomes clear. Remove the water from the cell monolayer. Blot the wells containing the stained cells upside down on a paper towel to remove as much water as possible.
6. Counterstain the cells: Add 500 μL of hematoxylin solution to cover the cellular monolayer. Incubate at room temperature for 1 min.
7. Wash the cells: Carefully aspirate hematoxylin solution, and wash the cell monolayer with distilled water to remove excess stain. Repeat the washing step until the water becomes clear. Remove the water from cell monolayer and add PBS.
8. Analyze the cells: Intracellular lipid vesicles in mature adipocytes stain bright red, whereas the hematoxylin-stained nuclei appear blue-violet.

3.3.6 Chondrogenic Differentiation

Differentiated chondrocyte will form cartilage with a typical extracellular matrix. This extracellular matrix contains a molecule named as proteoglycan aggrecan that can be used as indicator for cartilage formation. In differentiated chondrocytes, the aggrecan will be stained as dark-blue by staining with Alcian Blue, a dark-blue copper-containing dye whereas in undifferentiated cells, the cells are at most faintly bluish due to the absence of cartilage formation.

1. Generate micromass cultures by seeding 10 μL of 1.6×10^7 CSCs per well of 24-well tissue culture plates using growth medium. Seed the cells in two wells, one well for induction and the other well as the negative control.
2. Incubate the micromass cultures of CSCs at 37 °C and 5 % CO_2 for 2 h.

3. Induce CSC differentiation. Induce one of the samples with chondrogenic differentiation medium; for the other (negative control), use growth medium.
4. Incubate cells for 14 days in chondrogenic differentiation medium. Change the medium every third day (*see* **Note 8**). Extent chondrogenic differentiation can be determined by chondrocyte formation.

3.3.7 Chondrocyte Detection

1. Wash the cells: Take the cartilage spheroids from the incubator. Aspirate the induction and growth media from the spheroids carefully. Carefully wash the spheroids with Dulbecco's PBS, W/O Ca^{++}/Mg^{++} twice (*see* **Note 10**).
2. Fix the cartilage spheroids: Aspirate the PBS and transfer the tissue culture plate to a fume hood. Add about 500 μL of 10 % neutral buffered formalin to the cartilage spheroids. Make sure the cartilage spheroids are covered by formalin. Incubate the cartilage spheroids for 60 min (*see* **Note 11**).
3. Wash the cells: Carefully aspirate the formalin and wash the cartilage spheroids with 1 mL of distilled water. Repeat the washing step twice.
4. Stain the cells: Carefully remove the distilled water from cartilage spheroids. Add about 500 μL of Alcian staining solution to generously cover the cartilage spheroids. Make sure the entire cartilage spheroid surfaces have been covered by staining solution; if not, add more staining solution. Incubate cartilage spheroids overnight in the dark at room temperature.
5. Wash the cells: Carefully aspirate Alcian staining solution and wash the cartilage spheroids with 1 mL of destaining solution for 20 min. Repeat the washing step twice to remove excess stain. Remove the destaining solution from the cartilage spheroids and add PBS.
6. Analyze the cells: Cartilage stains an intense dark blue, whereas other tissue is at most faintly bluish.

3.4 Clonogenic Assay

The clonogenic assay tests the ability of the cells to maintain their clonogenic capacity and form colonies.

1. Seed CSCs by plating 1×10^3 cells per well of 6-well tissue culture plates using growth medium.
2. Grow cells for 14 days in a CO_2 incubator at 37 °C.
3. After 14 days, take the cell monolayer from the incubator. Aspirate the growth medium from the cell monolayer, and carefully wash the cells with Dulbecco's PBS, W/O Ca^{++}/Mg^{++} twice. Aspirate the PBS and transfer the cell culture plate to a fume hood. Add about 500 μL of 10 % neutral

buffered formalin to the cellular monolayer. Make sure the cellular monolayer is covered by formalin. Incubate the cell monolayer at room temperature for 30 min (*see* **Note 11**).

4. Carefully remove the formalin from the cell monolayer. Add about 500 μL of Crystal Violet staining solution to the cell monolayer. Make sure the entire cell monolayer surface is covered; if not, add more staining solution. Incubate at room temperature for 30–60 min.
5. Carefully aspirate the Crystal Violet staining solution, and wash the cell monolayer with distilled water to remove excess stain. Repeat the washing step several times until the water becomes clear. Remove the water from the cell monolayer and allow the culture plate to dry.
6. Evaluate the staining results. Count the colonies formed manually. A colony is defined as consisting of >50 cells.

3.5 Spheroid Formation Assay

1. Plate the CSCs at ~200 cells per well in low-ultra attachment plates in spheroid culture medium containing serum-free medium DMEM-F12K (1:1) supplemented with 20 ng/mL EGF, 10 ng/mL bFGF, 1 % B27 supplement, and 1 % PenStrep.
2. Add Matrigel to the culture medium at a ratio of 1:5 of Matrigel to spheroid culture medium.
3. Incubate cells at 37 °C for 21 days according to the published protocol [10].
4. At the end of the incubation period, count spheroids using an inverted microscope (Fig. 2).

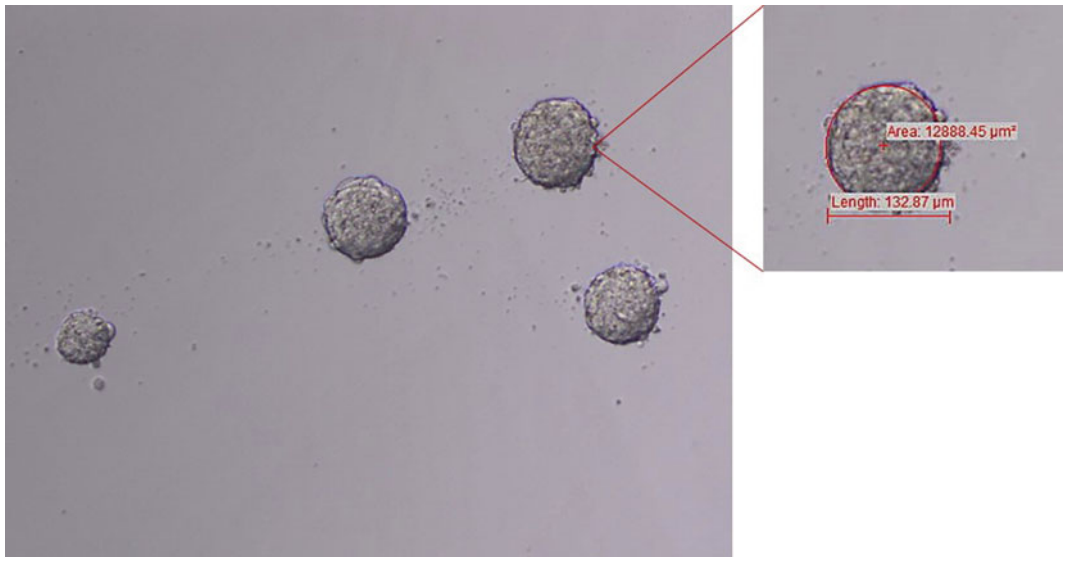

Fig. 2 CD166+/EpCAM+ show formation of spheroid capability (original magnification ×200)

3.6 Microarray Assay

3.6.1 RNA Extraction

1. Detach the cells with trypsin–EDTA.
2. Pellet the cells into 1.5 mL tubes and store at –80 °C until all cells are ready for extraction.
3. Extract total RNA from approximately 1×10^6 of cells using the AllPrep DNA/RNA Isolation Kit according to the manufacturer's protocol.
4. Lyse the cells with lysis buffer and homogenize the lysate using the QIAshredder Homogenizer. Add 70 % ethanol to the homogenized cell lysates and transfer the sample to an RNA spin column.
5. Elute the total RNA from the spin column using RNase free water and store the RNA at –80 °C for later use (*see* **Note 13**).

3.6.2 Determination of RNA Concentration and RNA Integrity

1. Determine the concentration and purity of the RNA were using a NanoDrop® ND1000 spectrophotometer (Agilent Technologies, Santa Clara, CA, USA) and Bioanalyzer 2100 (Agilent Technologies).
2. For the RNA to be subjected to microarray analysis, the concentration of RNA should range between 50 and 200 ng.
3. The A260:A280 ratio for RNA samples to be of acceptable purity should be in the range of 1.8–2.0, and the RNA integrity number (RIN) value should be >7.

3.6.3 cDNA Amplification

1. Use approximately 50–200 ng of total RNA for cDNA amplification using the Applause™ WT-Amp ST System.
2. Carry out the amplification based on the protocol provided by the manufacturer. The amplification system consists of several processes: first strand cDNA synthesis, second strand cDNA synthesis, post-second strand enhancement, SPIA® amplification, post-SPIA modification I, and post-SPIA modification II (Table 2).

3.6.4 cDNA Purification

1. Purify the synthesized ST-cDNA using the MinElute Reaction Cleanup Kit.
2. Measure the yield and purity of the purified ST-cDNA using the NanoDrop® ND1000 spectrophotometer.
3. The A260:A280 ratio must be >1.8, and the concentration must be in the range of 2–2.5 μg for the ST-cDNA to be hybridized to the array.

3.6.5 cDNA Fragmentation and Biotin Labeling

1. Label the purified ST-cDNA using the Encore Biotin Module following the standard protocol provided by the manufacturer.
2. Table 3 shows the thermal cycler program for conducting fragmentation and biotin labeling.

Table 2
Thermal cycling protocols

Program	Temperature
First strand cDNA synthesis	
Program 1: Primer annealing	65 °C—5 min, hold at 4 °C
Program 2: First strand synthesis	4 °C—1 min, 25 °C—10 min, 42 °C——10 min, 70 °C—5 min, hold at 4 °C
Second strand cDNA synthesis	
Program 3: Second strand synthesis	4 °C—1 min, 25 °C—10 min, 42 °C—10 min, 70 °C—5 min, hold at 4 °C
Post-second strand enhancement	
Program 4: Post-second strand enhancement	4 °C—1 min, 37 °C—15 min, 80 °C—20 min, hold at 4 °C
SPIA amplification	
Program 5: SPIA amplification	4 °C—1 min, 47 °C—90 min, 95 °C—5 min, hold at 4 °C
Post-SPIA modification	
Program 6: Post-SPIA modification I	4 °C—1 min, 37 °C—15 min, 95 °C—5 min, hold at 4 °C
Program 7: Post-SPIA modification II	4 °C—1 min, 30 °C—10 min, 42 °C—60 min, 75 °C—10 min, hold at 4 °C

Table 3
Thermal cycling program for cDNA fragmentation and biotin labeling

Program	Temperature
Program 8: cDNA fragmentation	37 °C—30 min, 95 °C—2 min, hold at 4 °C
Program 9: Biotin labeling	37 °C—60 min, 70 °C—10 min, hold at 4 °C

3.6.6 Hybridization

1. Before loading the labeled ST-cDNA to the microarray chip, assemble the labeled ST-cDNA with other components to form a hybridization cocktail (provided in the Affymetrix Wash and Stain Kit). The list of components is shown in Table 4.
2. The hybridization cocktail can be stored at –80 °C for long-term storage.
3. Prior to loading the sample into the array, heat the hybridization cocktail for 5 min at 45 °C, 3 min at 90 °C, and spin down for 1 min (10,000 rpm).
4. Load 90 μL of hybridization cocktail into the array by inserting a clean pipette tip into one of the array's septa to vent the array (*see* **Note 14**).

Table 4
Components needed for preparation of hybridization cocktail

Component	Volume	Final concentration
Fragmented, biotin-labeled amplified cDNA	25 μL	18.2—22.7 ng/μL
Control oligonucleotide B2 (3 nM)	1.8 μL	50 pM
20× Eukaryotic hybridization control (bioB, bioC, bioD, cre)	5.5 μL	1.5, 5, 25, and 100 pM, respectively
2× Hybridization buffer	55 μL	1×
100 % DMSO	11 μL	10 %
Water (nuclease free)	11.6 μL	–
Final volume	110 μL	–

5. Apply sealer on both septa to avoid condensation of the hybridization cocktail during the hybridization process.
6. Hybridize the chip for 17 h at 45 °C with rotation at 60 rpm.

3.6.7 Washing and Staining

1. Wash and stain the hybridized chips using the Affymetrix GeneChip® Hybridization, Wash, and Stain Kit, which consists of stain cocktail 1, stain cocktail 2, array holding buffer, and wash buffer A and B (*see* **Note 15**).
2. Perform the washing and staining procedures using the Affymetrix automated Fluidics station 450/250 operated using Affymetrix GeneChip Command Console (AGCC) software (*see* **Note 16**).

3.6.8 Scanning

1. Scan the chip using the Affymetrix GeneChip Scanner 3000. The scanner is controlled by the AGCC.
2. Before scanning, switch on the scanner and the scanner's laser. Let the scanner warm up for at least 10 min prior to scanning.
3. Register the chip on the AGCC portal by keying in the barcode number, sample name, and date of each array.
4. Load the chip into the autoloader and start scanning (*see* **Note 17**).

3.6.9 Microarray Statistical Data Analysis

1. Perform the microarray data analysis using GeneSpring GX 7.3.1 software (Agilent Technologies).
2. After normalization of all chips, filter the probes/genes based on expression to the 50th percentile. Exclude probes/genes with expressions <50th percentile.
3. Perform statistical analysis by comparing putative CSCs to normal counterparts using an independent *t*-test.

4. Filter the probes/genes based on p-value and fold change. Probes/genes with a p-value <0.05 and fold change >2.0 are assumed to be significantly regulated.

3.7 In Vivo Tumorigenicity Studies

1. Anesthetize mice using the anesthetizing reagent according to standard protocol.
2. Suspend approximately 2×10^4 cells in 200 μL of completed media–Matrigel (1:1), and subcutaneously inject the dose into the right flank of 4–7-week-old female NCR nude mice.
3. Monitor mice every 2 days for 2 weeks after inoculation (*see* **Note 18**).
4. Measure tumor size weekly using Vernier calipers and calculate tumor diameters.
5. Sacrifice the mice after 60 days or when the tumor diameter reaches 1 cm in size.
6. Collect all tumor tissues and fix them in formalin for histological and immunohistochemical analysis.
7. Perform hematoxylin and eosin staining to analyze tumor histology.
8. Conduct tumorigenicity assays in triplicate ($n = 3$).

4 Notes

1. The prepared growth medium needs to be filtered using a 0.22 μM syringe filter to prevent microbial growth in the cell culture.
2. During preparation of Alizarin Red S, wear gloves, lab coat, and mask to avoid direct contact and inhalation. It is crucial for the final pH of Alizarin Red S to be at 4.1–4.3 to ensure the effectiveness of this staining solution. Thus, pH adjustment needs to be done accurately.
3. During preparation of Oil Red O, work in a fume hood and wear gloves, lab coat, and mask to avoid direct contact and inhalation. This solution is a highly flammable liquid and vapor. Direct contact and inhalation can cause serious eye, skin, and respiratory irritation and may cause drowsiness and dizziness.
4. During preparation of Alcian Blue 8GX staining solution, work in a fume hood and wear gloves, lab coat, and mask to avoid direct contact and inhalation. This solution is corrosive. Direct contact and inhalation can cause serious eye, skin, and respiratory irritation.
5. Matrigel should be stored at –20 °C. Prior to use, thaw the Matrigel overnight at 4 °C to ensure that it is reliquefied. Keep

Matrigel on ice at all times when handling, and pipette Matrigel using precooled tips to ensure homogeneity.

6. The Applause WT Amplification Kit contains enzymes, and it should be stored in a –20 °C freezer without the auto-defrost function. All kit components must be keep on ice during the amplification process.
7. Mice should be maintained in individually ventilated cages (Allentown Inc., Allentown, NJ, USA). The experiments in this study were approved by the Universiti Sains Malaysia Animal Ethics Committee according to the institutional guidelines.
8. pH stability of the cell culture needs to be maintained throughout the entire process to ensure successful cell cultivation. pH can be affected by several parameters, including CO_2 concentration. Therefore, it is crucial for cell cultivation to be performed in a CO_2 incubator. Using 5 % CO_2 helps maintain the optimum pH for cell cultivation. Changes of the pH value might have negative consequences on cell growth.
9. Differentiation medium should be changed every third day to prevent drastic changes in the pH of the culture due to metabolic waste accumulation.
10. During the entire process of osteoblast, chondrocyte, and adipocyte detection, do not leave the cells for >30 s. All reagents need to be added to or removed from cells gently to avoid cell detachment. For example, to add a reagent, drip the reagent down the side of the culture well instead of dropping it directly onto the cell monolayer/spheroids.
11. Fixation by formalin need to be performed at room temperature, as this temperature is sufficient to maintain excellent morphological detail of cells.
12. After fixation is completed, aspirate the formalin from the cells. Remember to discard the formalin into the appropriate hazardous waste container inside the fume hood. Formalin should be discarded in the appropriate way and cannot be mixed with other wastes.
13. RNA should be stored and –80 °C to prevent degradation. It should be divided into small aliquots to avoid having to undergo the freeze–thaw process multiple times, which can cause degradation.
14. The array needs to be turned several times using a finger to make sure that there is a big bubble inside the sample chamber to allow sample movement during the hybridization process.
15. The staining kit components from 4 °C storage should be left to equilibrate at room temperature prior to use.

16. After the staining and washing process, the chip should be stored in the dark.
17. Before scanning, the stained chip can be stored at 4 °C by wrapping it with aluminum foil. Before scanning, equilibrate the chip at room temperature.
18. Cleaning practices should be monitored to ensure effective hygiene and sterile sanitation. The mice should be checked daily for evidence of illness.

References

1. Singh S, Hawkins C, Clarke I, Squire J, Bayani J, Hide T, Henkelman R, Cusimano M, Dirks P (2004) Identification of human brain tumor initiating cells. Nature 19:396–401
2. Al-Hajj M, Wicha MS, Benito-Hernandez A, Morrison SJ, Clarke MF (2003) Prospective identification of tumorigenic breast cancer cells. Proc Natl Acad Sci U S A 100(7):3983–3988. doi:10.1073/pnas.0530291100
3. O'Brien CA, Pollett A, Gallinger S, Dick JE (2007) A human colon cancer cell capable of initiating tumour growth in immunodeficient mice. Nature 445(7123):106–110. doi:10.1038/nature05372
4. Reya T, Morrison SJ, Clarke MF, Weissman IL (2001) Stem cells, cancer, and cancer stem cells. Nature 414(6859):105–111. doi:10.1038/35102167
5. Levina V, Marrangoni AM, DeMarco R, Gorelik E, Lokshin AE (2008) Drug-selected human lung cancer stem cells: cytokine network, tumorigenic and metastatic properties. PLoS One 3(8), e3077
6. Wicha MS, Liu S, Dontu G (2006) Cancer stem cells: an old idea—a paradigm shift. Cancer Res 66(4):1883–1890
7. Dick D (1997) Human acute myeloid leukemia is organized as a hierarchy that originates from a primitive hematopoietic cell. Nat Med 3:730–737
8. Ricci-Vitiani L, Lombardi DG, Pilozzi E, Biffoni M, Todaro M, Peschle C, De Maria R (2007) Identification and expansion of human colon-cancer-initiating cells. Nature 445 (7123):111–115. doi:10.1038/nature05384
9. Zakaria N, Yusoff NM, Zakaria Z, Lim MN, Baharuddin PJN, Fakiruddin KS, Yahaya B (2015) Human non-small cell lung cancer expresses putative cancer stem cell markers and exhibits the transcriptomic profile of multipotent cells. BMC Cancer 15(1):84
10. Leung EL-H, Fiscus RR, Tung JW, Tin VP-C, Cheng LC, Sihoe A, Fink LM, Ma Y, Wong MP (2010) Non-small cell lung cancer cells expressing CD44 are enriched for stem cell-like properties. PLoS One 5(11):e14062
11. Wright MH, Calcagno AM, Salcido CD, Carlson MD, Ambudkar SV, Varticovski L (2008) Brca1 breast tumors contain distinct CD44+/CD24-and CD133+ cells with cancer stem cell characteristics. Breast Cancer Res 10(1):R10
12. Dalerba P, Dylla SJ, Park I-K, Liu R, Wang X, Cho RW, Hoey T, Gurney A, Huang EH, Simeone DM (2007) Phenotypic characterization of human colorectal cancer stem cells. Proc Natl Acad Sci 104(24):10158–10163
13. Li C, Heidt DG, Dalerba P, Burant CF, Zhang L, Adsay V, Wicha M, Clarke MF, Simeone DM (2007) Identification of pancreatic cancer stem cells. Cancer Res 67(3):1030–1037. doi:10.1158/0008-5472.CAN-06-2030
14. Hermann PC, Huber SL, Herrler T, Aicher A, Ellwart JW, Guba M, Bruns CJ, Heeschen C (2007) Distinct populations of cancer stem cells determine tumor growth and metastatic activity in human pancreatic cancer. Cell Stem Cell 1(3):313–323
15. Bertolini G, Roz L, Perego P, Tortoreto M, Fontanella E, Gatti L, Pratesi G, Fabbri A, Andriani F, Tinelli S (2009) Highly tumorigenic lung cancer CD133+ cells display stem-like features and are spared by cisplatin treatment. Proc Natl Acad Sci 106(38):16281–16286
16. Kondo T, Setoguchi T, Taga T (2004) Persistence of a small subpopulation of cancer stem-like cells in the C6 glioma cell line. Proc Natl Acad Sci U S A 101(3):781–786
17. Feuring-Buske M, Hogge DE (2001) Hoechst 33342 efflux identifies a subpopulation of cytogenetically normal CD34+ CD38− progenitor cells from patients with acute myeloid leukemia. Blood 97(12):3882–3889
18. Ho MM, Ng AV, Lam S, Hung JY (2007) Side population in human lung cancer cell lines and tumors is enriched with stem-like cancer cells. Cancer Res 67(10):4827–4833

19. Ginestier C, Hur MH, Charafe-Jauffret E, Monville F, Dutcher J, Brown M, Jacquemier J, Viens P, Kleer CG, Liu S (2007) ALDH1 is a marker of normal and malignant human mammary stem cells and a predictor of poor clinical outcome. Cell Stem Cell 1(5):555–567
20. Feldmann G, Dhara S, Fendrich V, Bedja D, Beaty R, Mullendore M, Karikari C, Alvarez H, Iacobuzio-Donahue C, Jimeno A (2007) Blockade of hedgehog signaling inhibits pancreatic cancer invasion and metastases: a new paradigm for combination therapy in solid cancers. Cancer Res 67(5):2187–2196
21. Ma S, Chan KW, Lee TK-W, Tang KH, Wo JY-H, Zheng B-J, Guan X-Y (2008) Aldehyde dehydrogenase discriminates the CD133 liver cancer stem cell populations. Mol Cancer Res 6 (7):1146–1153
22. Ucar D, Cogle CR, Zucali JR, Ostmark B, Scott EW, Zori R, Gray BA, Moreb JS (2009) Aldehyde dehydrogenase activity as a functional marker for lung cancer. Chem Biol Interact 178(1):48–55

Methods in Molecular Biology
DOI 10.1007/978-1-4939-6550-2_327

Erratum to: Enzyme-Free Dissociation of Neurospheres by a Microfluidic Chip-Based Method

Ching-Hui Lin, Hao-Chen Chang, Don-Ching Lee, Ing-Ming Chiu, and Chia-Hsien Hsu

Methods in Molecular Biology (2016) 1516: 289–297
DOI 10.1007/7651_2016_348

Published online: 05 April 2016

DOI 10.1007/978-1-4939-6550-2_327

The publisher regrets that two authors were not mentioned in the chapter by mistake. The correct order of authors is provided below:

Ching-Hui Lin, Hao-Chen Chang, Don-Ching Lee, Ing-Ming Chiu, and Chia-Hsien Hsu

The updated original online version for this chapter can be found under http://dx.doi.org/10.1007/7651_2016_348

Methods in Molecular Biology (2016) 1516: 389–390
DOI 10.1007/978-1-4939-6550-2

INDEX

R

S

T

U

W

X